Design and direct synthesis of peptide-branched polysiloxane. Towards new generation of hybrid biomaterials

Julie Martin

THÈSE POUR OBTENIR LE GRADE DE DOCTEUR DE L'UNIVERSITÉ DE MONTPELLIER

En ingénierie biomoléculaire

École doctorale ED459 Sciences Chimiques Balard

Unité de recherche UMR5247 – Institut des Biomolécules Max Mousseron

Conception et synthèse directe de peptide-polysiloxane. Vers une nouvelle génération de matériaux hybrides pour des applications biologiques

Design and direct synthesis of peptide-branched polysiloxane. Towards new generation of hybrid biomaterials

Présentée par Julie MARTIN

Le 22 novembre 2019

Sous la direction de Gilles SUBRA

Devant le jury composé de

Sandra VAN VLIERBERGHE, Pr, Ghent University	Rapporteur
Sébastien LECOMMANDOUX, Pr, Université de Bordeaux	Rapporteur, Président du jury
Stéphanie DEVILLE-FOILLARD, Dr, Institut de Chimie des Substances Naturelles	Examinateur
Jean MARTINEZ, Pr, Université de Montpellier	Invité
Gilles SUBRA, Pr, Université de Montpellier	Directeur
Ahmad MEHDI, Pr, Université de Montpellier	Encadrant
Lubomir VEZENKOV, Dr, Université de Montpellier	Encadrant

UNIVERSITÉ DE MONTPELLIER

Design and direct synthesis of peptide-branched polysiloxane. Towards new generation of hybrid biomaterials

Remerciements

Ce travail de thèse est issu d'une collaboration entre l'équipe "Amino acides, Hétérocycles, Peptides et Protéines" (AHPP) de l'Institut des Biomolécules Max Mousseron (IBMM) et l'équipe "Chimie Moléculaire et Organisation du Solide" (CMOS) de l'Institut Charles Gerhardt (ICGM).

J'adresse mes remerciements au Pr. Sandra Van Vlierberghe et au Pr. Sébatsien Lecommandoux pour avoir accepté d'être les rapporteurs de ce manuscrit. Je remercie également le Dr. Stéphanie Deville-Foillard d'avoir accepté d'être examinatrice lors de ma soutenance de thèse.

Je remercie le Pr. Jean Martinez pour avoir initié la collaboration entre les équipes LAPP et CMOS sur le thème des peptides hybrides. Je remercie les Prs. Pascal Dumy et Jean-Marie Devoisselle, directeurs de l'IBMM et de l'ICGM pour m'avoir permis de réaliser ma thèse au sein de leur institut. Merci également aux Drs. Muriel Amblard et Hubert Mutin de m'avoir accueillie dans leur équipe respective.

Des remerciements particuliers vont à mon directeur de thèse. Un énorme merci au Pr. Gilles Subra, pour un encadrement exceptionnel, un investissement sans limite et une source d'idées infaillible. Merci de m'avoir gardée motivée et d'avoir animé ces trois années par ta bonne humeur et ton énergie. Merci pour ton implication impressionnante et tout particulièrement merci d'avoir été aussi efficace pour la rédaction de ce manuscrit. Merci aussi au Pr. Ahmad Mehdi, pour sa lumière sur les silicones mais surtout par sa disponibilité, sa bonne humeur contagieuse et ses précieux conseils. Merci de m'avoir fait une place au CMOS et d'avoir toujours été disponible quand j'en avais besoin. Un grand merci à mon encadrant Dr. Lubomir Vezenkov qui a toujours répondu avec entrain à mes questions, aussi bien pratiques que théoriques. Tes conseils et tes connaissances m'ont été très précieux. Merci d'avoir être disponible et de m'avoir accompagnée pendant ces trois années.

Je tenais également à remercier spécialement Sylvie Hunger, Audrey Bethry, Dr. Marie Morille, Dr. Laure-Anaïs Vincent, Dr. Nadir Betache et Franck Godiart pour leur participation à mes travaux de recherches, leurs conseils et leurs disponibilités. Je remercie aussi Aurélien Lebrun et Karine Parra pour les analyses RMN, Pierre Sanchez pour les analyses de spectrométrie de masse mais aussi sa disponiblitité et son aide quotidienne. Un grand merci à Luc Brunel, Nicolas Masurier, Jean-François pour leur bonne humeur quotidienne. Un merci à Jean-Alain pour ses cours particuliers d'HPLC analytique et préparative, grâce à toi je me sens l'âme d'une mécanicienne HPLC. Merci à Antoine et Pinar, mes deux stagiaires qui ont beaucoup apporté aux projets auquels ils ont participé. Une pensée pour Lyne-Rose et Emmanuelle, je vous remercie pour votre temps, vos sourires et vos aides précieuses.

Je tiens à remercier tout particulièrement Laurine et Titouan avec qui j'ai partagé mon bureau, mais également beaucoup plus que ça, du début à la fin de cette thèse. Merci d'avoir supporté mes humeurs de tous les jours, bonnes ou mauvaises, mes heures à me plaindre ou à râler, d'avoir tous les deux toujours été prêt à aider. Merci d'avoir été une aide et un soutien au quotidien, mais aussi un sacré divertissement, spécialement après les retours de week-end de certain. Ces trois années de thèse n'auraient pas été les mêmes sans vous.

Merci également à tous mes collègues qui ont fait ce bout de chemin avec moi : Bruno, Baptiste, Guillaume, Khoubaib, Mathieu, Bénédicte, Laurent, Youssef, Pascal, Séverine et Ludovic. Plus spécialement à Kévin, Laurent, Alex, Christophe et Barth pour ces bons moments passés ensemble, nos sorties et nos petites soirées. Un merci spécial pour Lisa et Alice, avec qui j'ai adoré passé tout ce temps à Montpellier. J'espère que ce n'est que le début. Et encore un merci à Alice, Kévin, Yohan et Prisca avec qui on forme une belle bande de bras cassés. Vous rendrez même cette fin d'aventure un peu triste, de devoir vous laisser.

Un merci aux doctorants du bâtiment 17, que ce soit du 2eme ou du 4eme. Vous avez animé ma vie à Montpellier, sans vous cela n'aurait pas été la même chose. Tout spécialement merci à François, Manon, Julien, Ryan et Justine. Merci d'avoir toujours répondu présent, de m'avoir suivi dans mes organisations douteuses et d'avoir rempli mon passage à Montpellier de tant d'aventures et de périples.

Merci à un collègue en particulier, qui m'a supporté bien plus que les autres, et qui est devenu bien plus que les autres. Merci de m'avoir autant fait rire au quotidien, de m'avoir soutenue et motivée quoi qu'il arrive. Merci d'arriver à me faire croire en moi. Et merci pour tes cours particuliers d'espagnol, ce n'est pas une cause perdue, je suis sure qu'un jour on arrivera à tenir une conversion. Merci d'être là.

Je n'oublie évidemment pas mes amis alsaciens ou bordelais qui ont su rythmer ma vie de moments forts, de tellement de joie et de rire. Rien ne vaut des amis comme vous pour garder le moral, quoi qu'il arrive. Vous avez toujours été là, et je compte bien que ça continue. Une dédicace spéciale aux filles, avec qui on a enfin réussi à s'organiser tellement de week-ends et même de vacances. Les années d'école ont beau être finies, on est toujours aussi proches et ça compte beaucoup pour moi que vous soyez encore là. Merci à Charbo d'avoir aidé à rendre la vie à Montpellier aussi géniale. T'avoir avec moi ici à été un bonheur. Et merci à Poche, d'avoir continué à être un rayon de soleil.

Enfin, je remercie fortement ma famille. Ça aura été un grand plaisir de rentrer à la maison pendant ces trois années, pour passer des week-ends ou des semaines en si bonne compagnie. Ça aura toujours été le meilleur moyen de me remonter le moral. Merci d'être ce que vous êtes, c'est comme ça que je vous aime. Et pour finir une pensée particulière à notre petit ange, qui ne le fait surement pas exprès, mais qui accueille toujours sa tata avec de grands sourires qui font chaud au cœur.

Table of Content

Table of Figures

Abbreviations

2D, 3D	two-dimensional, three-dimensional
ACN	acetonitrile
Alloc	allyloxycarbonyl
APTES	3-aminopropyltriethoxysilane
Boc	*tert*-butyloxycarbonyl
cat	catalyst
CPT	camptothecin
CTC	chloroTrityl chloride
CuAAC	copper(I)-catalyzed alkyne-azide cycloaddition
DCM	dichloromethane
DIEA	N,N-diisopropylethylamine
DMF	N-N'-dimethylformamide
DMSO	dimethylsulfoxide
DNA	deoxyribonucleic acid
DOPA	3,4-dihydroxyphenylalanine
DPBS	Dulbecco's phosphate-buffered saline
EDC	1-ethyl-3-(3-dimethylaminopropyl)-carbodiimide
eq	equivalent
ESI	electrospray ionization
FITC	fluorescein isothiocyanate
Fmoc	fluorenylmethoxycarbonyl
FPPS	fast parallel peptide synthesis
HA	hyaluronic acid
HATU	1-[Bis(dimethylamino)methylene]-1H-1,2,3-triazolo[4,5-b]pyridinium 3-oxid hexafluorophosphate
HBTU	N,N,N',N'-tetramethyl-O-(1H-benzotriazol-1-yl)uronium hexafluoro-phosphate
HPLC	high performance liquid chromatography
HRMS	high resolution mass spectrometry
ICPDMCS	3-isocyanatopropyldimethylchlorosilane
ICPTES	3-isocyanatopropyltriethoxysilane
LC/MS	tandem liquid chromatography/ mass spectrometry
MTX	methotrexate
Mw	molar mass
NCL	native chemical ligation
n. d.	non determined
NIPAM	poly(N-isopropylacrylamide)
NMP	N-methyl-2-pyrrolidone
NMR	nuclear magnetic resonance

NPs	nanoparticles
PA	polyacrylamide
Pbf	2,2,4,6,7-pentamethyldihydrobenzofuran-5-sulfonyl
PDI	Polydispersity
PDMS	polydimethylsiloxane
PEG	polyethylene glycol
pip	piperidine
PLA	poly(L,D-lactic acid)
PLGA	poly(lactic-co-glycolic acid)
PLL	poly-L-Lysine
PVA	poly(vinyl alcohol)
PS	polystyrene
RNA	ribonuleic acid
RP	reversed phase
RT	room temperature
siRNA	small interfering RNA
SPPS	solid phase peptide synthesis
TEM	transmission electron microscopy
TEOS	tetraethyl orthosilicate
Ter	terminal
TFA	trifluoroacetic acid
THF	tetrahydrofurane
TIC	Total Ion Current
TIS	triisopropylsilane
TMZ	temozolomide
Trt	trityl
UV	ultra-violet

Résumé

Résumé

L'utilisation des polymères synthétiques pour des applications biologiques s'est largement diversifiée depuis plusieurs années, en particulier pour la mise au point de systèmes de délivrance de médicaments, de biocapteurs, ou encore pour des applications en ingénierie tissulaire. En effet, les biopolymères tel que le polyéthylène glycol (PEG), Acide polylactique (PLA) ou encore le poly(méthacrylate de méthyle) (PMMA) sont régulièrement décrits pour ces applications biologiques et certains sont approuvés par les autorités de santé.

Dans le cadre de ce travail de thèse, nous nous sommes intéressés à un autre polymère synthétique très utilisé pour des applications biologiques : le polydimethylsiloxane (PDMS). Le PDMS est très répandu pour la préparation de revêtements hydrophobes ou comme lubrifiant mécanique mais il est aussi très largement utilisé dans le domaine des dispositifs médicaux en particulier comme cathéters, implants ou encore lentilles de contact. Biocompatible mais également bio inerte, le PDMS doit toutefois être modifié pour présenter des propriétés biologiques. Pour cela, deux stratégies sont possibles : la modification non-covalente, qui permet la fonctionnalisation par adsorption de biomolécules généralement pas des forces électrostatiques ; et/ou la modification covalente qui permet l'attachement des biomolécules de manière permanente par la création d'une liaison chimique mais qui nécessite souvent plusieurs étapes de traitement. Les modifications covalentes ont l'avantage de pouvoir mieux gérer la quantité de biomolécules attachés, de gagner en stabilité et surtout d'éviter un relargage anticipé. De nombreuses biomolécules ont été utilisées pour fonctionnaliser le PDMS comme des peptides, des protéines, des biopolymères ou des médicaments.

Le **premier chapitre** de cette thèse est consacré à la fonctionnalisation du PDMS par les peptides. A partir d'une analyse bibliographique, ce chapitre présente d'abord les différentes manières d'obtenir des peptides-polymères, c'est-à-dire des polymères modifiés de manière covalente avec des peptides. Les 3 stratégies pour y parvenir sont présentées et commentées : le *grafting to*, *grafting from* and *grafting through* (Figure 1).

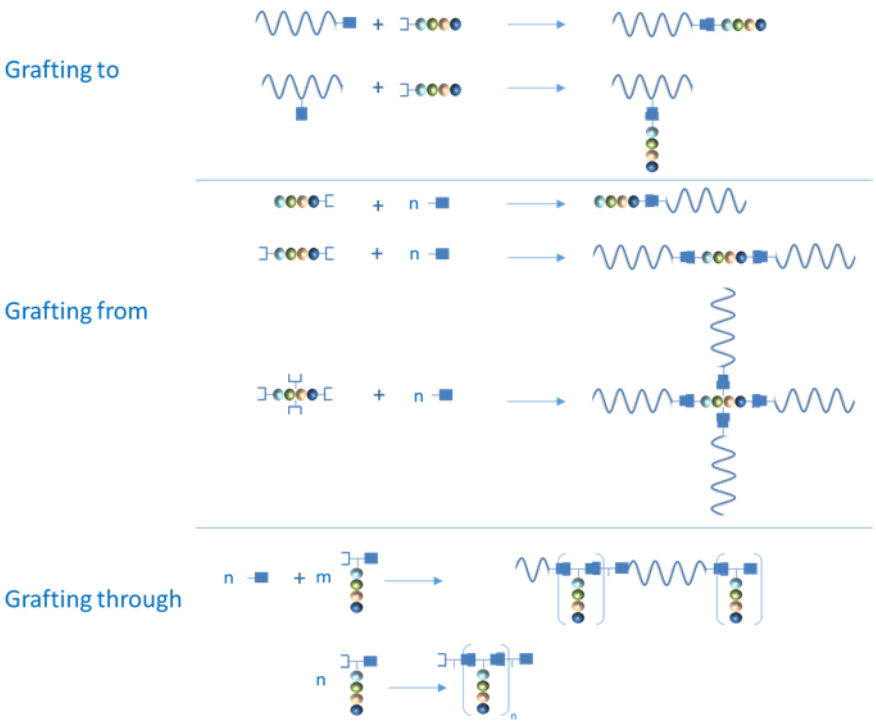

Figure 1. Différentes méthodes de synthèse de conjugués peptide-polymère.

Le *grafting to* est de loin la technique la plus fréquemment utilisée. Elle consiste à greffer le peptide sur un polymère déjà synthétisé. Ce polymère peut être préalablement activé pour générer des fonctions réactives permettant d'y attacher le peptide, directement ou via un bras espaceur. Les différentes stratégies chimiques de couplage trouvées dans la littérature sont détaillées et accompagnées d'un ou plusieurs exemples.

Le *grafting from* repose sur l'utilisation du peptide comme initiateur de polymérisation. Dans ce cas, le peptide n'est pas juste greffé sur un polymère déjà synthétisé mais prend part à la polymérisation. Les trois voies majeures de polymérisation sont décrites : polymérisation radicalaire par transfert d'atome (ATRP), polymérisation radicalaire par transfert de chaîne réversible par addition-fragmentation (RAFT) et polymérisation radicalaire en présence de nitroxydes (NMP).

Dans la technique du *grafting through*, le peptide est acteur principal de la polymérisation car il est utilisé comme un macromonomère. Le peptide doit être modifié pour porter au moins une fonction polymérisable et il est ensuite polymérisé seul ou avec d'autres monomères afin d'obtenir des squelettes de polymères variés. Plusieurs cas sont présentés : la polyaddition de peptide acrylate, la polymérisation par ouverture de cycle de peptides présentant un cycle activé, ou encore la polycondensation de peptides silylés ou la polycondensation de peptides diamine avec des chlorures d'acide.

La deuxième partie de ce chapitre est quant à elle centrée sur les modifications du PDMS par des peptides, et les applications qui en découlent (Figure 2). Les possibilités de modification non-covalente du PDMS sont présentées. Pour cela, le PDMS est généralement activé par un traitement plasma ou par des acides forts pour générer des fonctions SiOH en surface. Ensuite, les peptides s'adsorbent sur le PDMS par des interactions électrostatiques et liaisons hydrogène. Les modifications covalentes sont ensuite présentées en détail. Le PDMS peut être activé, puis modifié éventuellement par des bras espaceurs et finalement couplé au peptide par différents types de réactions, certaines étant chemosélectives. Ce chapitre est basé sur la publicaton : Martin, Julie, Jean Martinez, Ahmad Mehdi, et Gilles Subra. « Silicone Grafted Bioactive Peptides and Their Applications ». *Current Opinion in Chemical Biology,* 52 (octobre 2019): 125-35. https://doi.org/10.1016/j.cbpa.2019.06.012.

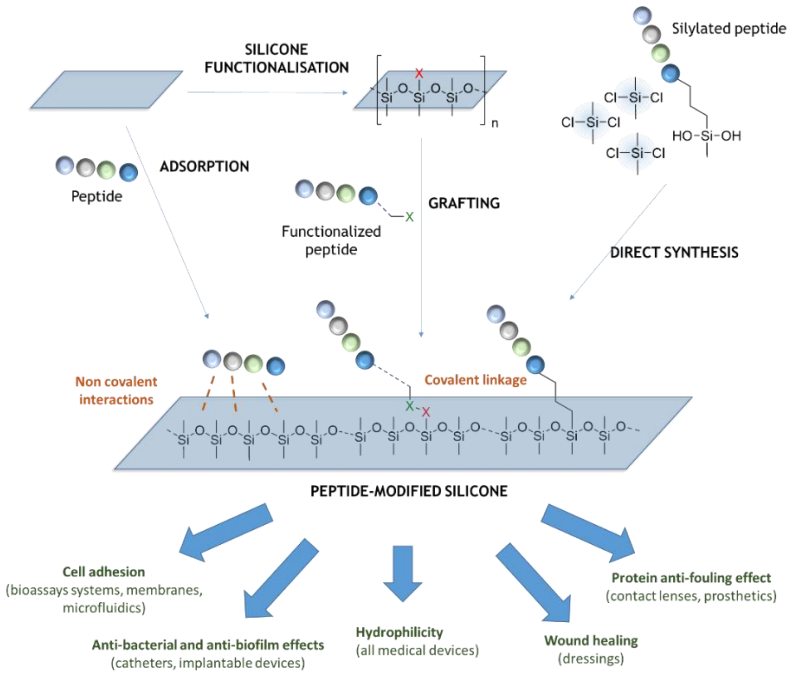

Figure 2. Les différentes méthodes de greffage de peptides sur du PDMS et leurs applications.[1]

A la fin de cette revue de la littérature, nous présentons notre stratégie pour la synthèse de polymères hybrides peptide-PDMS : des peptides possédant une fonction dihydroxysilane sont synthétisés comme macromonomères et éventuellement copolymérisés avec du dichlorodimethylsilane (DCDMS) pour obtenir un copolymère possédant un squelette polysiloxane avec des peptides en chaines pendantes.

De manière générale et en nous appuyant sur cette stratégie, l'objectif de cette thèse est la conception et la synthèse directe de nouveaux matériaux hybrides comportant des peptides ou d'autres biomolécules fonctionnalisant un squelette polysiloxane.

La **chapitre 2** expose une méthode de silylation que nous avons tenté d'optimiser pour l'appliquer aux peptides : l'hydrosilylation. Cette méthode est basée sur la formation d'une liaison carbone-silicium entre un alcène et un silane (SiH). Elle est généralement catalysée par des catalyseurs à base de platine comme le celui de Karstedt et peut être appliquée à la synthèse de matériaux solides par réticulation d'huiles silicone (i.e. polymères linéaires). Plusieurs conditions ont été testées comme, le solvant, la température, les équivalents de silane ou de catalyseur mais également les différents types de silanes et de peptides comportant une fonction insaturée, que ce soit en solution ou sur support solide. L'hydrosilylation du chlorodiméthylsilane sur l'AllylGlycine a servi de réaction témoin. En effet, que ce soit directement sur l'acide aminé protégé par un Fmoc ou sur un peptide modèle sur résine, AcPheAllylGly-résine, cette hydrosilylation a permis un taux de conversion de 95%. Cependant, l'utilisation d'autres silanes a révélé une réaction secondaire : la réduction de l'alcène. De même, l'utilisation d'autres acides aminés Lys(Alloc) et Glu(OAll) a conduit à la deprotection prématurés des groupements allyl de la chaine latérale.

Une étude supplémentaire a été effectués afin de déterminer l'origine de la réduction observée et de la limiter. Mais finalement cette méthode n'a pas été retenue pour la synthèse de nos peptide silylés. En effet, il s'est avéré difficile d'obtenir une hydrosilylation avec un trialkoxymethyl silane ou un dichloromethyl silane tous deux utiles pour la préparation de macromonomères peptidiques pour la préparation de peptide-PDMS hybride. Nous avons donc choisi d'utiliser le couplage d'un isocyanate silylé sur une amine primaire du peptide.

Le **chapitre 3** quant à lui, présente la synthèse de tous les peptides hybrides qui ont été choisis pour leur propriétés biologiques, silylés avec l'isocyanatopropyl dichloromethylsilane. D'autres types de biomolécules comme des médicaments ou encore des sondes pour l'imagerie, ont également été préparés. La silylation de ces biomolécules pour être silylées sélectivement ainsi que leurs propriétés biologiques et leur mode d'action pour les drogues, sont détaillés dans ce chapitre. Certaines silylations ont pu être effectuées sur résine, d'autres en solution. Parfois l'utilisation de protections sur des chaines latérales ou des groupements réactifs s'est avérée nécessaire.

Après avoir présenté les blocks silylés disponibles pour la synthèse des matériaux hybrides, le **chapitre 4** dévoile une première application. Ce chapitre présente la synthèse directe par copolymérisation, de polysiloxane contenant des peptides et des monomères fonctionnels : Si-H et Si-Vinyl. Ces deux monomères fonctionnels sont incorporés pour permettre la réticulation des huiles de polysiloxane par hydrosilylation catalysée par le catalyseur de Karstedt (Figure 3).

En modifiant leur pourcentage d'incorporation, nous avons ainsi pu faire varier la dureté des films de polysiloxane obtenu. De même, les deux types de peptides (un peptide antibactérien et un peptide favorisant l'adhésion cellulaire), ont été incorporés en différents pourcentages, pour étudier l'évolution des propriétés mécaniques et biologiques du matériau final. Ce chapitre est basé sur la publicatioin soumise : Martin Julie, Mohammad Wehbi, Cécile Echalier, Coline Pinese, Jean Martinez, Gilles Subra, et Ahmad Mehdi. « Direct synthesis of peptide-modified silicone. A new way for bioactive materials ». *Submitted*, 2019.

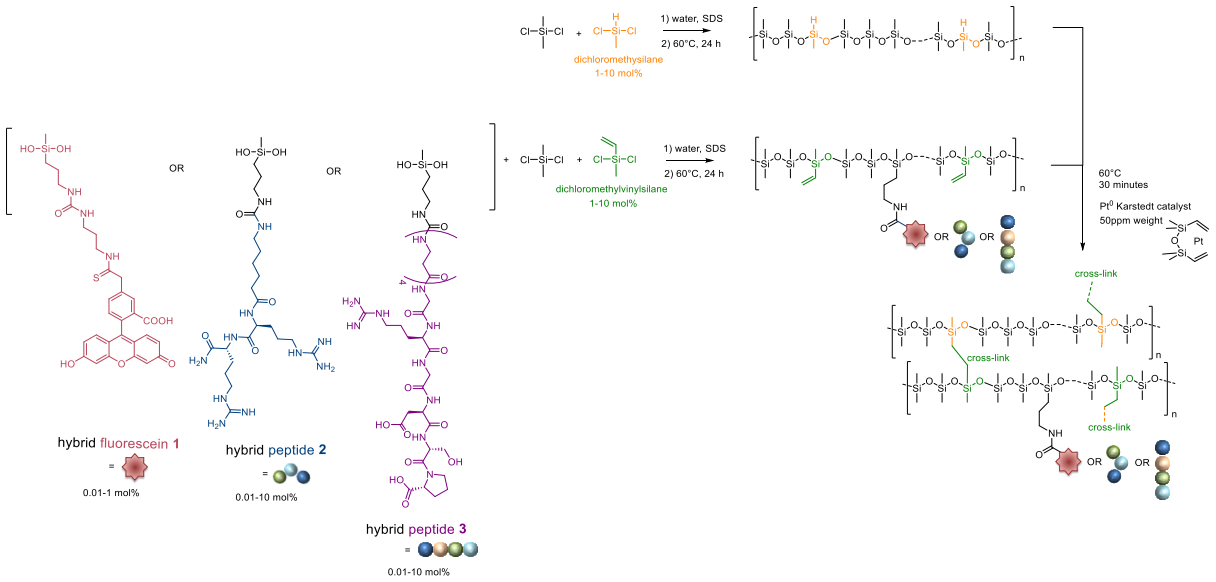

Figure 3. Synthèse directe de polysiloxanes fonctionnalisés par des biomolécules silylées et leur réticulation par hydrosilylation.

Le **chapitre 5** propose une autre application possible pour ces polysiloxanes fonctionalisés par des biomolécules silylées. En effet, plutôt que de synthétiser des films de PDMS multifonctionnels par réticulations, l'idée est de formée des nanoparticules (NPs). Le PDMS est complètement hydrophobe et il est difficile d'obtenir de manière directe des NPs de PDMS non modifié dans de l'eau. Pour pallier ce problème, le PDMS a été préalablement dissout dans le THF avant de subir une nano-précipitation dans l'eau. Les conditions de polymérisation et de précipitation ont été étudiées : concentration, usage d'un bain à ultrasons, filtration, lyophilisation.

Une fois le protocole mis en place pour obtenir des NPs présentant un diamètre aux alentours de 100-150 nm, la composition du PDMS a été modifiée en incorporant différentes quantités de macromonomère hydrophile : du PEG_{3000} silylé. La formation de NPs à partir de ce polymère amphiphile a été réalisée en suivant le protocole précédent mais également par ajout direct d'eau. La quantité optimale de PEG a été définie entre 0.5 et 1 mol% avec une concentration de finale de particule de 1 mg/mL.

Nous avons ensuite incorporé des biomolécules d'intérêt, à commencer par un ligand peptidique : le cyclo RGD. Pour garder les propriétés de ligand de ce peptide, il a été couplé à l'extrémité d'une chaine de PEG_{3000} dont l'autre extrémité portait un groupement silylé. Plusieurs quantités de ce ligand pegylé ont été testées : 0.2, 0.5 et 1 mol% en complétant à chaque fois avec du PEG silylé sans ligand pour obtenir un pourcentage final de PEG dans le polymère de 1 mol%. La taille de ces NPs s'est avérée cohérente avec les tailles obtenues précédemment, aux alentours de 120 nm. Enfin, des composés anticancéreux silylés ont été ajoutés. Le premier modèle a été le méthotrexate (MTX). Un polymère contenant le MTX modifié ainsi que plusieurs polymères servant de contrôles ont été synthétisés. Ensuite, les NPs multifonctionnelles ont été formées, selon le même protocole que celui du PEG-PDMS (Figure 4). Un test préliminaire de toxicité a été effectué et a montré que les NPs présentaient bien une activité cytotoxique *vs* une lignée cancéreuse sensible au MTX. D'autres polymères obtenus avec les autres molécules actives silylés au chapitre 3 pourront être synthétisés par la suite.

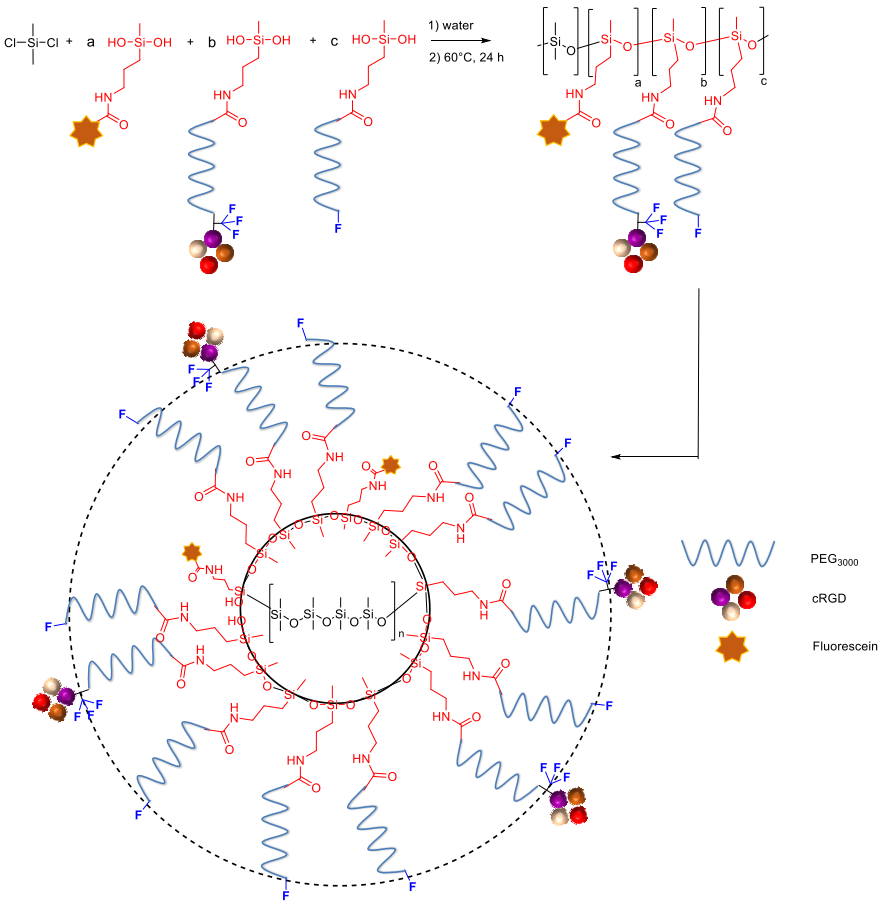

Figure 4. Synthèse de polysiloxane modifié par des macromonomères de PEG, cRGD-PEG et fluorescéine, et formation de NPs multifonctionnelles.

Le dernier chapitre de ce manuscrit (**Chapitre 6**) est consacré à une autre application possible du PDMS multifonctionnel : la vectorisation d'oligonucléotides (Figure 5). En effet, en choisissant des peptides capables d'interagir avec le siRNA grâce à leurs charges positives (i.e. His/Lys) et en les silylant, il s'est avéré possible de préparer des polyplexes. D'abord, en suivant le même protocole décrit dans le chapitre 5, nous avons obtenu des NPs de PDMS modifiés par des peptides théoriquement capables de complexer le siRNA chargé négativement. Malheureusement, la complexation n'a pas été observée, la charge globale des NPs étant restée négative, probablement dû à un phénomène de masquage des charges par les chaines de PEG.

Nous avons donc proposé une approche alternative plus ambitieuse n'utilisant que les peptides silylés. Deux méthodes ont alors été évaluées : la préformation du polymère peptidique suivi d'une complexation avec le siRNA ou la polymérisation des peptides macromonomères in situ, directement en présence du siRNA. La deuxième méthode, s'est avérée la plus efficace pour former des polyplexes bien définis et stables. Toutefois, les essais de dissociation de ces polyplexes, par compétition avec de l'héparine, se sont pour le moment avérés infructueux.

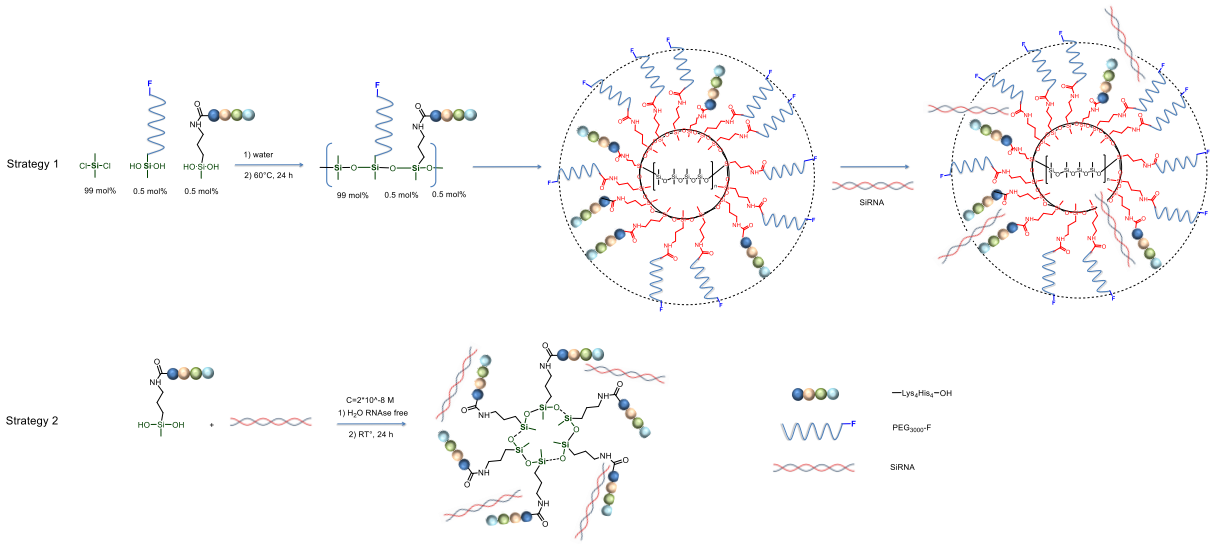

Figure 5. Les deux stratégies de synthèse de polyplexes à partir de peptide silylés.

Ces travaux de thèse ouvrent des perspectives très prometteuses. D'abord, la preuve de concept d'une synthèse bottom-up de silicones incorporant des peptides a été faite. A présent, nous pouvons envisager l'incorporation de nouveaux peptides biologiquement actifs. Ensuite, nous avons établi un protocole de préparation de NPs de polysiloxane multifonctionnelles reproductibles et stables dans le temps. Des tests biologiques plus approfondis sont nécessaires pour valider l'activité des NPs contenant le MTX et leur spécificité. D'autres médicaments, comme ceux synthétisés au chapitre 3, pourront être introduits dans les particules en fonction de l'activité souhaitée. Enfin, en ce qui concerne la préparation de polyplexes, la méthode de polymérisation *in situ* s'est montrée très efficace. La possibilité de synthétiser le polymère directement en présence du siRNA réduit les étapes de préparation des polyplexes et apporte une (trop) grande stabilité. Des tests complémentaires vont être effectués pour déterminer les conditions de dissociations des polyplexes et, si besoin, des modifications de composition du polymère seront envisagées pour diminuer stabilité du complex vecteur/siRNA.

Introduction

Introduction

The purpose of this PhD work is the design and synthesis of new hybrid biomaterials based on the silicone backbone. Several types of biomolecule-containing hybrid biomaterials were synthetized thanks to the sol-gel process. To do so, we first focused our attention on the synthesis of hybrid building blocks bearing a methyldihydroxysilane moiety. Those blocks were polymerized to get a siloxane backbone, very close to PDMS, with pendant covalently-bound biomolecules.

The **chapter 1** recapitulates the different strategies to synthesize peptide-polymers: *grafting to, grafting from and grafting through*. In each case, the role of the peptide is detailed. This overview of the literature is concluded by the use of functionalized peptide as macromonomers which is close to the bottom up strategy we wanted to develop in this PhD work. The second part of this chapter focused on a special type of polymer: the PDMS. The grafting strategies of peptides on PDMS are presented and justify the interest to develop a new method enabling the direct synthesis of peptide containing PDMS. Most of this chapter constitutes the publication: Martin Julie, Jean Martinez, Ahmad Mehdi, et Gilles Subra. « Silicone Grafted Bioactive Peptides and Their Applications ». *Current Opinion in Chemical Biology* 52 (octobre 2019): 125-35. https://doi.org/10.1016/j.cbpa.2019.06.012.

The **chapter 2** presents our attempt to prepare silylated peptides by hydrosilylation. Several reactants and conditions were essayed to synthesize hybrid silylated peptides on solid support. Different silanes were used with uneven conversion rates. During this study, we found out a side reaction leading to unwanted reduction of the unsaturated bond to be silylated. Hydrosilylation was finally not used in this PhD work. The silylation of biomolecules was then done by reaction with isocyanatopropyl silane derivatives on free amino groups of selected biomolecules.

The **chapter 3** discloses all the building blocks used in the design and synthesis of the hybrid biomaterials presented in this manuscript. Since this silylation method is not chemoselective, protections were used to avoid side reactions, especially in the case of peptide silylation. Besides peptides, small molecules drugs were also silylated.

The **chapter 4** details how to synthesize bioactive PDMS material. On one hand, hybrid fluorescein and two different bioactive silylated peptides have been successfully copolymerized, at different ratio, with dichlorodimethylsilane and vinyl silane yielding a functional PDMS polymer. In the other hand, silane modified PDMS have been synthesized. Combined together, the two linear polymers were reticulated to create cross-linked functional PDMS material by Pd-catalyzed hydrosilylation since it is the classic catalyst used in silicone industry. These materials exerted biological properties afforded by the bioactive peptide incorporated in them. Most of this chapter constitutes the submitted publication: Martin Julie, Mohammad Wehbi, Cécile Echalier, Coline Pinese, Jean Martinez, Gilles Subra, et Ahmad Mehdi. « Direct synthesis of peptide-modified silicone. A new way for bioactive materials ». *Submitted*, 2019.

The objective of the **chapter 5** is the preparation of hybrid polymeric NPs formed by nanoprecipitation. We elaborated a detailed protocol using non-functionalized PDMS as a model. Then, more hydrophilic PEG-PDMS was prepared by copolymerization of DCDMS and silylated PEG as macromonomer. This type of hybrid PEG PDMS enabled the NPs preparation. The next step was the introduction of bioactive silylated molecules. Hybrid peptide ligands and anticancer drugs were copolymerized with DCDMS and PEG macromonomer in order to prepare multifunctional NPs. The chapter is concluded by the presentation of preliminary cytotoxicity assays performed on cancer cell lines.

The last **chapter 6** explores another application of multifunctional hybrid silicone polymers. A peptide sequence has been selected for its ability to from complex with siRNA. This peptide sequence, Lys_4His_4 was silylated on solid support and copolymerized with silylated PEG and dichlorodimethylsilane to get NPs. Alternatively, the His/Lys hybrid peptide was polymerized alone and finally polymerized in the presence of siRNA. Polyplexes were obtained and was studied by DLS, TEM and gel electrophoresis.

Chapter 1.A: Bottom-up strategies for the synthesis of peptide-based polymers

Chapter 1.A: Bottom-up strategies for the synthesis of peptide-based polymers

I. Introduction: hybrid peptide-polymers

Synthetic polymers have been widely developed in life sciences for the design of medical devices, drug delivery systems, implants, biosensors or scaffolds for tissue engineering and regenerative medicine.[2–11] Some of them, like polyethylene glycol (PEG), poly(methylmethacrylate) (PMMA) or polylactic acid (PLA) have been extensively studied and used for medical devices approved by the Food and Drug Administration (FDA).

The polymer can be used as the only component (for example PDMS for the fabrication of soft prosthesis, PLA for stents, and PMMA for dental devices) or associated with other components to add functions or physical properties to the desired material. Combined to drugs or oligonucleotides, polymers can be used to form particles for gene[12] or drug[13] delivery. Polymers can be grafted on the surface of inorganic nanoparticles to yield hybrid organic-inorganic NP.[14] Polymers associated with cells, tissue inducing molecules (TIM) and porous three dimensional scaffolds are the main players to prepare hydrogels for tissue engineering.[15,16]

Although biocompatible, these synthetic polymers are bioinert, in a sense that they do not exhibit any particular activity by themselves. They have to be functionalized to get additional biological properties. This functionalization can be done by two main ways: either by non-covalent or covalent modification.
The non-covalent functionalization is usually done by adsorption on activated, or not, polymer. The adsorption can result from spray coating, dip-coating or incubation. Polymer surface can be treated to enhance the adsorption: for example, plasma treatment generating hydrophilic moieties on PDMS. Non-covalent functionalization of polymer by biomolecule is usually mediated through weak interactions (e.g. electrostatic, hydrogen bonding, aromatic, hydrophobic) or specific affinity (ligand-receptor pairing) interactions.[17] In the latter case, interaction may be really strong: like the one between biotin-adivin.[18] Non-covalent attachment leads to less stable functionalized polymer. The main advantage of the non-covalent functionalization over the covalent one is its simplicity and the easier delivery in the case of drug delivery system.

The covalent functionalization concerns a large number of polymers and biomolecules. Once conjugated with the desired biomolecule, polymers are then referred in literature as ‘hybrid polymers’ (‘bio hybrid polymers’ if the associated molecule is a biomolecule). For clarity purposes, it is worth to note that, in this PhD work, the term “hybrid” is reserved to hybrid inorganic/organic silylated molecules or materials.
The covalent attachment of biomolecule on a polymer surface can also be done by different ways: either by a direct grafting on the active group of the polymer, or by first an activation of the surface and then the grafting. Also, the biomolecule can be grafted directly onto the polymer surface or through a spacer (Figure 6).

Several types of biomolecules can be attached to polymer surfaces depending of the final application wanted. For example, enzyme and antibody can be conjugated to polymer surfaces in order to design biosensors; peptides and polysaccharides were commonly used for tissue engineering or the preparation of antimicrobial surfaces.[17,17,19,20]

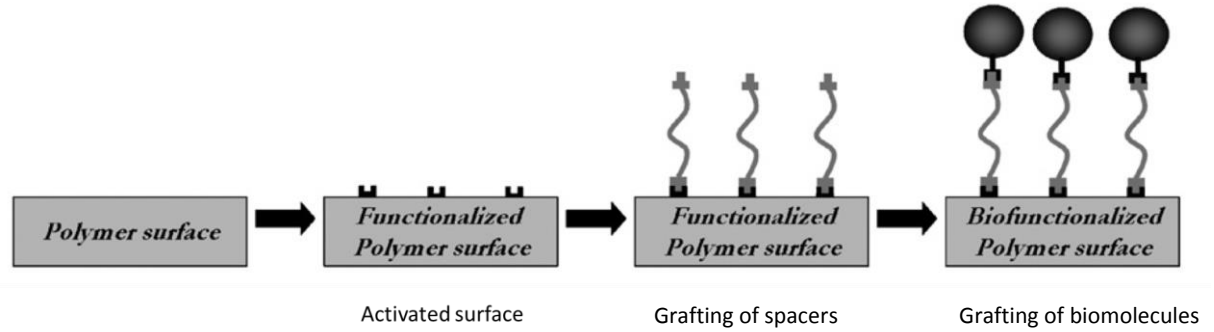

Figure 6. Multistep covalent biofunctionalization of polymer surface via (i) activation of a surface, (ii) grafting of spacers and iii conjugation with biomolecules.[17]

This chapter will focus on peptide-polymer: polymers functionalized covalently with peptides. Peptides are one of the most common biomolecules conjugated to polymers, mainly for their antimicrobial and cell adhesion properties. The preparation of peptides and analogues is well mastered thanks to efficient solid phase synthesis protocols (Solid Phase Peptide Synthesis: SPPS) widely spread among many laboratories. Combined to the numerous existing polymers, the huge diversity of structures and functions of peptides enables to design an unlimited range of peptide-polymers.[21] The diversity offered by each component and the structure of the polymer (i.e. linear, branched or even comb like) offers an additional level of adjustability.

Three different synthesis strategies are described for the preparation of covalent peptide polymer conjugates: *grafting to, grafting from and grafting through* (Figure 7).[22] The *grafting to* strategy is a multistep process in which the peptide is covalently coupled to the polymer after its synthesis. In the *grafting from* approach, the peptide is the initiator of the polymerization, which can be either Reversible Addition Fragmentation polymerization (RAFT), Atom Transfer Radical Polymerization (ATRP) or Nitroxide Mediated radical Polymerization (NMP). At last, the *grafting through* method is using a peptide containing macromonomer (PCM), leading to homopolymers (resulting from a single monomer), block copolymers (two different monomer polymerized one after the other) or alternating copolymers (two different monomer polymerized simultaneously).

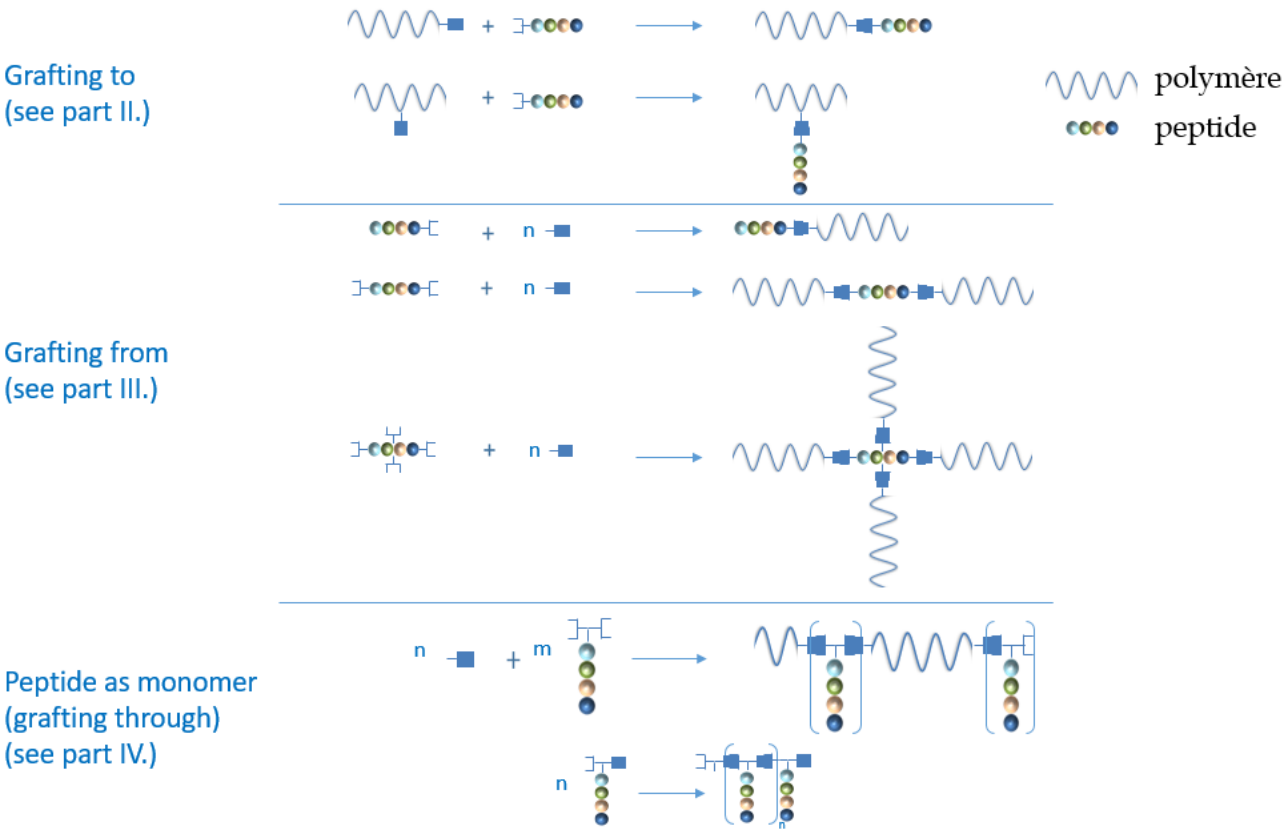

Figure 7. General strategies to obtain peptide-polymers.

II. *Grafting to* strategy: Post-functionalized polymers

a. *Grafting to strategy*

1. General strategy

Grafting to or post-functionalization, is the most common and the most used strategy to prepare peptide-polymers conjugates so far. This strategy is not a direct one to obtain functionalized polymer. Indeed, it requires two or more steps, depending on the activation and grafting chemistry required.

First, the polymer is prepared by classical polymerization methods, allowing the control of the wanted final structure. The polymer can be isolated, fully characterized and activated for the next step. Two situations are possible from here: either the polymer does contain reactive groups (e.g. on its backbone or at its ends) able to reacts for further grafting or it does not present any suitable reactive function to attach the peptide and have to be activated.

In the first case, the grafting is operated straightforwardly on the polymer resulting from the polymerization, eventually adding reagents for the conjugation between the peptide and the polymer. In the second case, the polymer has first to be activated in order to be able to be functionalized. Then the peptide can be grafted directly on the activated polymer or through a linker or spacer that will present the active group required for the grafting of the peptide (Figure 6).

Summing up, *grafting to* strategy leads to peptide-polymer conjugates based on well-controlled and

characterized polymer backbones. Besides, researchers can make a selection among the numerous conjugation strategies described so far that offer a good level of chemoselectivity when unprotected peptides displaying reactive side-chains are used.[23] Indeed, peptide may display several type reactive groups on its lateral side chains and its N and C termini. Therefore, in the case of unprotected peptide, the conjugation chemistry has to be chemoselective in order to avoid any side reactions.

To illustrate the different conjugation chemistries, some of the common biopolymer used for *grating to* strategy will be detailed as well as their application.

2. *Examples of common grafted polymers*

PEG has shown high interest in the synthesis of biomaterials mainly due to its biocompatibility, high hydrophilicity and antifouling properties. It is then widely used as a stealth agent for delivery systems.[24–27] PMMA was utilized in numerous encapsulation systems as shell material thanks to its high chemical stability and mechanical properties adapted to the formation of shell (high Young's modulus and low elongation at break).[28,29] As a biodegradable and nontoxic polymer, PLA is widely used for tissue engineering and medical devices such as implants.[30] Polydimethylsiloxane (PDMS) is probably one of the most use for soft prosthesis and catheters because of its notable mechanical properties that it is widely used to produce medical implants for example.[31] Besides its mechanical properties, it is biocompatible and shows stability over thermic and oxidative stress, great gas permeability and really good dielectric property.[32–34]

PEG is the most common polymer used for conjugation with peptides. The conjugation of a peptide on a single PEG chain results into PEGylated peptides. In some cases, the PEGylated peptide can be subsequently attached to various polymeric structure depending on the final application (e.g. micelles, nanotubes, hydrogel).[6,35–46] However, PEGylated peptides are closest to *modified peptides* than *peptide-modified polymers* and will not be covered in this chapter, which is devoted to the polymerization on peptides or peptide-initiated polymerization. The following description will focus on the other polymers coupled to peptide.

The key point of the *grafting to* strategy is the chemical reaction between the polymer ad the peptide (Figure 8) which involves two mutually reactive moieties present on the peptide and on the polymer. If one (or all) of these two types of functions is also present on the peptide (side chains or N or C-terminus) regioselectivity cannot be achieved except if suitable protecting groups are placed on peptide during conjugation. On the contrary, bioorthogonal reactions can be performed on unprotected peptides.

Besides the different possibilities of polymer applied to this *grafting to* technic, other parameters have to be fixed: the coupling chemistry or the polymer activation for example. The following scheme, Figure 8, presents the different coupling chemistries used for the synthesis of peptide-polymer by grafting that will be explained below.

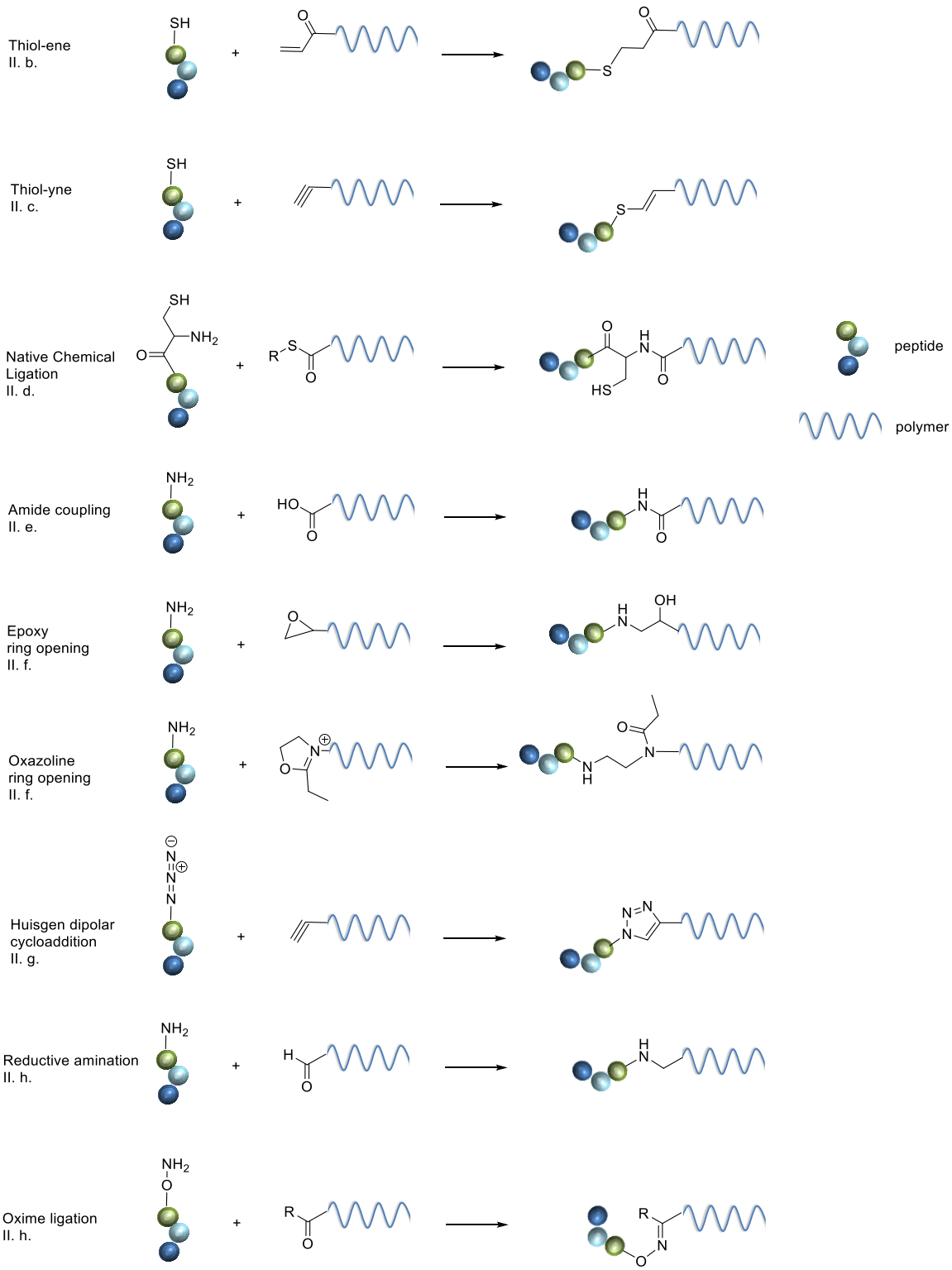

Figure 8. Examples of chemical reactions applied to peptide-polymer conjugates.

b. *Michael addition (non-radical thiol-ene chemistry)*

The most popular chemical reaction for the synthesis of peptide polymer conjugates is the Michael addition.[35,44,47,48] The Michael addition is based on the creation of a bond between a nucleophile, the donor, and an α,β

unsaturated system, the acceptor. The unsaturated bond is usually active nevertheless stable bond such as: acrylate, vinyl, maleimide group. In this case, it is mainly applied to thiol function as nucleophilic donor, so it is part of thiol-ene reactions however with nucleophilic attack mechanism (Figure 9). This reaction is chemoselective. When applied to peptide polymer conjugation, this reaction usually involve a thiol function, present on the peptide (unprotected Cys side chain), and an alkene function, displayed by the polymer.

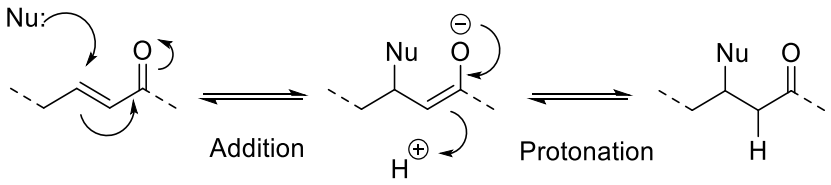

Figure 9. Mechanism of the thiol-ene Michael addition on an α,β unsaturated system.[49]

For example, Cys containing peptides with self-assembly properties (i.e. forming coiled coil dimers and tetramers) were coupled to both extremities of PEG chain modified at its extremities by maleimide. It leads to the formation of a physical viscoelastic hydrogel network.[50] Besides, peptides could be used as linker in addition to the biological properties that they bring to the material: for example to link polymeric nanoparticles, either organic[51] or inorganic.[47] Peptides can also be conjugated to star-PEG macromolecules to prepare hydrogels with biological properties.[52]

Besides PEG, several examples of bioconjugation by Michael addition with other polymers have been reported. For example, RGD based peptide have been conjugated to divinyl sulfone modified dextran in order to form a hydrogel for cell delivery.[53] Another example is detailing the bioconjugation of a peptide to a biopolymer: the PMAA-b-PHEMA-b-PMAA. The Cys containing peptide is attached to the acrylate group of the pendant chain of the PHEMA block of the copolymer, thanks to Michael addition.[54] Cys containing peptide were conjugated via Thiol-ene Michael addition to hyperbranched polyglycerol (HPG), through maleimide functionlaization,[55] or directly or hyperbranched polymer–peptide conjugates (PPC)[40]. In this last example, the peptide did not contain any Cys residue, neither thiol function. The Michael addition was done through the primary amine group on the N-ter.

Another example is describing a thiol-ene Michael addition with a thiol function at one extremity of a polystyrene (PS)[56]. The polymer was coupled to a cyclic peptide through the allyl oxycarbonyl (Alloc) protection present on the Lys residue.

c. *Thiol-yne chemistry*

In the same state of mind, the thiol-yne reaction has proven its efficiency for bioconjugation as well. This reaction is happening between a thiol function and an alkyne instead of an alkene like in thiol-ene reactions. Compared to thiol-ene Michael addition, thiol-yne offered the possibility of a double addition. Moreover, the alkyne function is less sensitive to its environment and so its reactivity is preserved. Indeed, for the thiol-yne radical reaction, the reactivity of the radical formed is depending on the alkene bond stability.[57] As thiol-ene conjugation, thiol-yne is also chemoselective.

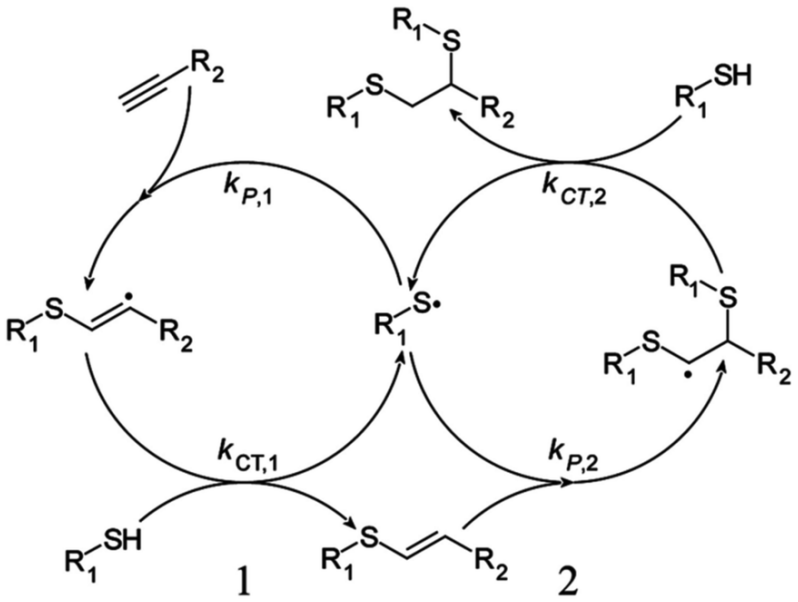

Figure 10. General scheme of the thiol-yne mechanism.[58]

As example fluorescent polymeric nanoparticles, issued from a dispersion polymerization, were wearing alkyne functions on their surfaces. Then a Cys-modified cRGD, was coupled to the surface of the NPs by thiol-yne reaction. The final cRGD decorated NPs have been used as fluorescent probe for imaging thanks to the ligand role of the peptide.[59]

d. *Native chemical ligation*

Another type of thiol-based conjugation used to conjugate peptides on polymers is the native chemical ligation. NCL was described by Kent et al. in 1994[60] and was originally developed for protein synthesis.[61] This reaction is chemoselective and thus enables the reaction of two unprotected peptides.

This reaction involves a thioester, which can be provided by the C-ter of a peptide for example, and a cysteine placed at the N-ter of another peptide. The first step is a transthioesterification between the carbonyl group of peptide 1 and the thiol group of peptide 2. Then a S-N acyl shift is occurring enabling the intramolecular rearrangement leading to a native amine bond along with a Cys residue (Figure 11). This reaction was applied to N-ter Cysteinyl peptides-polymer conjugates. As example, p(MeOx-b-DecOx) was synthesized by block copolymerization of a 2-methyl-2-oxazoline (MeOx) with 2-butenyl-2-oxazoline (BuOx) or 2-decenyl-2-oxazoline (DecOx). Then the alkene group of the side chain of the p(DecOx) block was functionalized by a cysteine derivative. The cysteine residue was conjugated with C-ter thioester peptides promoting cell adhesion for example. Advantageously, all these reactions were performed in water.

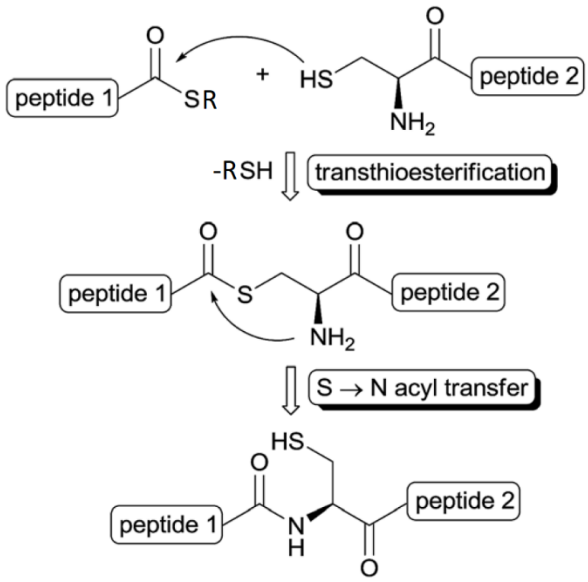

Figure 11. Principle of native chemical ligation, adapted from [61]

An acrylate-based polymer has been conjugated to C-ter thioester peptides through native chemical ligation. Polymer chains were modified at their extremities by RAFT single unit insertion of N-Boc allylamine moiety followed by aminolysis and then Boc deprotection.[62]

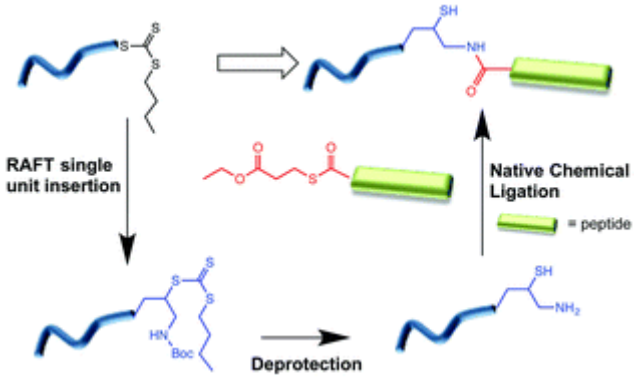

Figure 12. Example of NCL applied to acrylate-based polymer and peptide modified by Ethyl 3-mercaptopropionate.[62]

e. *Amide coupling*

Amide formation is commonly used to link peptide and polymer, involving a primary amine and a carboxylic acid. The carboxylic acid function has to be activated as an active ester, and undergoes a nucleophilic substitution by the amine. This activation can be done with a carbodiimide accompanied by an auxiliary nucleophile such as the EDC/NHS combination (1-éthyl-3-(3-dimethylaminopropyl)carbodiimide/N-hydroxysuccinimide). This recation can be performed both in water or organic solvent. Other activation methods are described such as the use of uronium activation (3-[Bis(dimethylamino)methyliumyl]-3H-benzotriazol-1-oxide hexafluorophosphate: HBTU or HATU) in the presence of a tertiary amine (e.g. DIEA, TEA) (Figure 13).

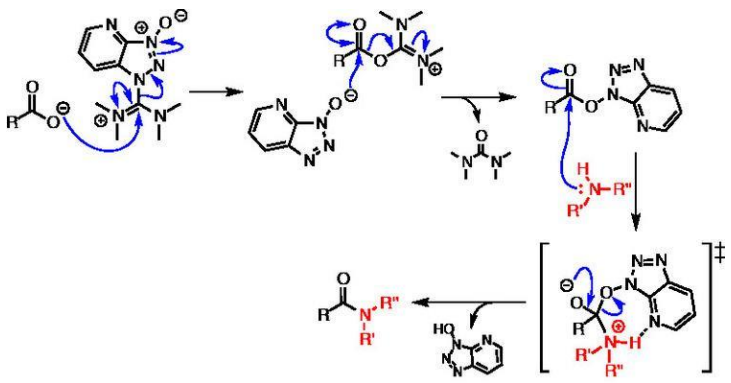

Figure 13. Amide coupling by HATU activation

The amine can be either on the polymer or the peptide, the carboxylic acid being on the other partner. This flexibility enlarges the scope of the possible polymers to be conjugated this way. As examples, it was applied on chitosan for the design of wound healing dressings[63] or dextran drug conjugates, using the peptide as a linker between the two components to design a tumor targeting system.[64,65] Also, acrylate-based polymers conjugate to peptide have been described such as HPMA for the design of tumor targeting and drug delivery systems.[66–69] Others examples of acrylate-based peptide-polymers have been detailed: the poly(N-vinyl-2-pyrrolidone-co-acrylic acid)-peptide (P(VPcoAA)) used as melanoma cancer vaccine prototype; and an acrylate based polymer conjugated with a peptide through NHS activation on monolith support for the immobilization of enzymes.[70,71] Finally, PS has also been used for peptide conjugation by amide coupling.[72] The PS is first treated with plasma to create acid functions at the surface and then coupling to nisin peptide, an antimicrobial peptide, by EDC/NHS activation in order to create antimicrobial surface.

Amide coupling is not chemoselective. Indeed, peptides may contain several free amino groups as well as other reactive groups such as alcohol or thiol functions, leading to ester or thioester linkage. Amines are more reactive than alcohols at physiological pH, but side reactions can still be observed if the alcohol function is not protected and the activated acid is in excess. Moreover, if the carboxylic acid is carried by the peptide, the other carboxylic acids should be protected during coupling reaction to insure regioselectivity.

f. *Other nucleophilic substitutions involving amines*

Besides amide forming, other nucleophilic substitutions involving primary amine functions of peptides have been used to modify polymers. Some examples of the ring opening reactions can be found in literature. They are all initiated by a primary amine function on the peptide and are non chemoselective since any free amine group of the peptide may reacts. The functionalization of the polymer can be operated by the ring opening of an epoxy function.[73] Another possibility is the direct conjugation on the terminal group at the extremity of a Pox via the ring opening of a 2-Ethyloxazoline by the primary amine at the N-ter of the peptide.[74] No ring opening polymerization (ROP) are observed since there is no initiator, catalyst or radical activation/propagation in these examples. All these examples used all a single conjugation.
Another single example of its kind: the primary amine of a peptide may also substitute halogen of poly(dichlorophosphazene) to lead to biodegradable polyphosphazene functionalized peptides.[75]

g. *Huisgen dipolar cycloaddition*

Huisgen dipolar cycloaddition, a type of click chemistry, is widely used for post-functionalization of polymer by peptides: usually the polymer bears the alkyne function while the peptide is display the azide one. It is a

chemoselective reaction between an azide and an alkyne functions forming a 1,2,3 triazole group linking the two components (Figure 15). In opposition of copper(I)-catalyzed alkyne-azide cycloaddition (CuAAC), the thermal Huisgen 1,3-dipolar cycloaddition leads to the formation of regiosiomers (Figure 14). The copper catalysis prevents this side reaction therefore leads to biorthogonal coupling. This type of chemistry could be performed on physiological conditions.

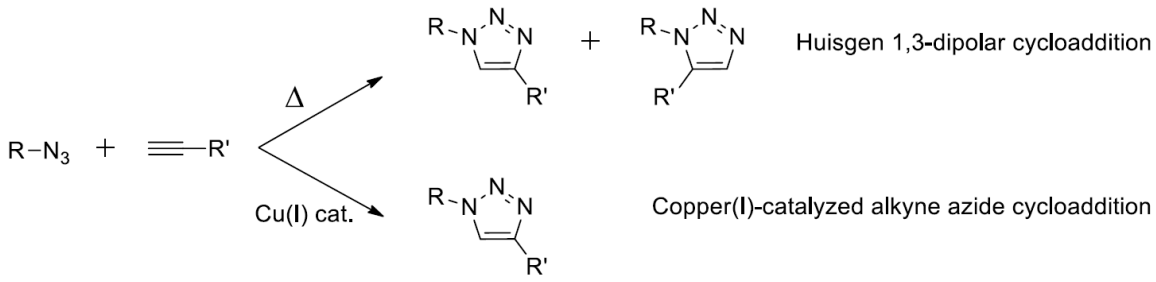

Figure 14. Comparison of catalyst for Huisgen cycloaddition.[76]

This chemical coupling reaction has been done on diverse polymers, mainly acrylate-based ones. As example, a cyclic peptide with self-assembly properties bearing an azide was conjugated with the alkyne functions of a poly(n-butyl acrylate) or poly(hydroxy ethyl acrylate).[77–80] In the same way, an azide modified peptide was conjugated to an alkyne functionalized PEG anchored on hyaluronic acid biopolymer leading to peptide-hyaluronan hydrogel.[81] Alternatively, an acrylate-based polymer with azide functions was conjugated to either alkyne-modified gramicidin S peptide or alkyne modified PEG.[82] The same authors reported also the use of cyclooctyne to replace simple alkyne function, which enables a copper-free coupling. However, due to the sterical hindered of the cyclooctyne, lower degree of grating was observed with the copper-free strategy.

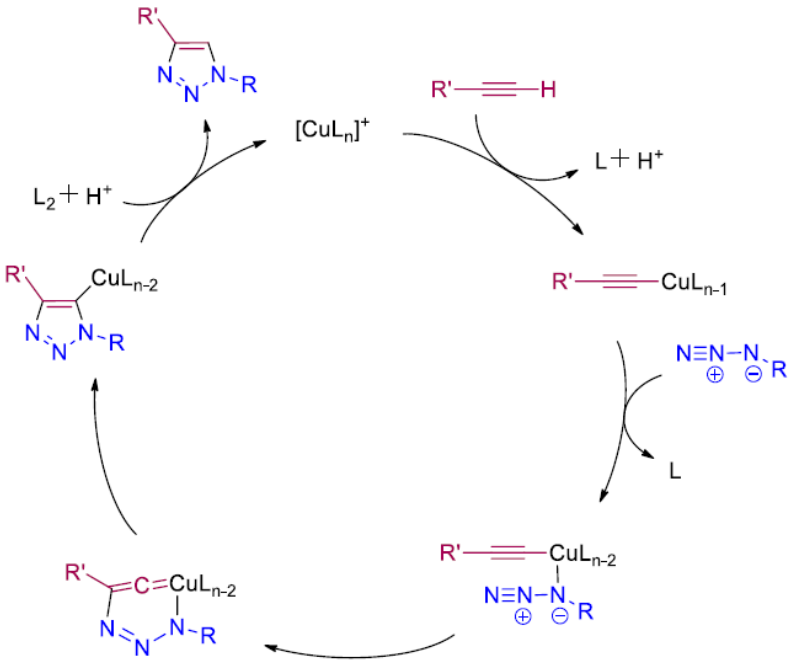

Figure 15. Huisgen dipolar copper catalyzed cycloaddition mechanism.[76]

A alkyne modified block copolymer PLA-PEG was coupled to an azido cRGD derivative.[83] The resulting peptide-polymer was able to form polymersomes with targeting properties.
This technic was also applied to Pox: two examples of alkyne modified Pox were conjugated with azide-modified

peptides as a polyTyrosine azide polypeptide leading to aqueous and non-aqueous stable micelles;[84] and cRGD derivative, giving radiotherapy targeting system.[85] In a similar way, superparamagnetic NPs were functionalized by hydroxymethylenebisphonates (HMBP) bearing an alkyne function. Then an azido cRGD peptide was grafted on the NPs resulting in integrin targeting NPs.[86]

h. *Aldehyde or Ketone-based ligation*

Last examples of coupling chemistry used for the synthesis of peptide-polymers is the oxime ligation and reductive amination. They represent a major interest due to the possibility to perform them in water, without copper catalyst and since they lead to chemoselective coupling.
The oxime ligation was applied to four different peptide vectors known as biomolecule carriers: such as AoaLeu$(Glu)_5$AlaTyrGlyTrpMetAspPhe-NH_2 for example.[87] They have been conjugated to two different block copolymers: polyvinylpyrrolidone-based polymers bearing pyruvoyl groups, at different composition. The oxime ligation kinetic have been studied and showed a rapid and complete conversion: up to 95% ligation in 2h.

The other conjugation technic enabling water as solvent is the reductive amination. It has been performed on a peptide, the oxytocin, conjugated to an acrylate-based polymer containing Pox pendant chain: p(OEtxMA) (Figure 16). The coupling chemistry is based on the direct reaction of the primary amine of the peptide that reacts with to the aldehyde function of the modified polymer, which is in this case at the extremity of the modified acrylate-based chain.[88]

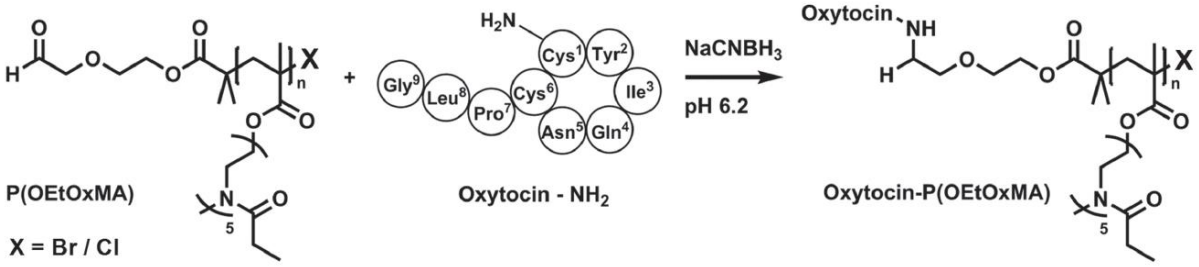

Figure 16. Reductive amination coupling of oxytocin at the extremity of p(OEtxMA).[88]

III. *Grafting from* strategy: Peptide as initiator of the polymerization

a. *Grafting from strategy*

Instead of being post-functionalized with peptides, the polymers can be generated *from* peptides, which take part in the polymerization as initiators. In other words, the difference between "*grafted to*" and "*grafted from*" techniques resides in the fact that the peptide is involved in the polymerization and is not added afterwards.[22] In this case, as the conjugation is done during the polymerization, purification or isolation of the polymer alone is impossible: it is directly obtained as a peptide conjugate.
Most of the polymerization reactions need a molecular initiator to start. It is the case for Atom Transfer Radical Polymerization (ATRP), Reversible Addition-Fragmentation chain Transfer polymerization (RAFT) and Nitroxide Mediated radical Polymerization (NMP). All of them being classified as Reversible Deactivation Radical Polymerization (RDRP). RDRP is gathering different radical polymerization methods that enable a good control of the final molar mass as well as the chain functionalities of the polymer.[89]

b. *Atom Transfer Radical Polymerization (ATRP)*

ATRP is a living radical polymerization catalyzed by a transition metal complex, which generate radicals from an initiator molecule containing one or several halogen atoms: the initiator is usually an alkyl halide (see Figure

17). Each halogen in the initiator structure is the seat of a polymer chain elongation. The main step of this polymerization process is the equilibrium between propagating radical and dormant species. This equilibrium is based on the formation of the radical through the dormant species and then the exchange of the radical with the transition metal complex. ATRP is well controlled and thus leading to polymers with low polydispersity index (~~Đ~~) meaning that the polymer chains obtained are about the same size. This polymerization method gives also access to high molar mass polymers.[90]

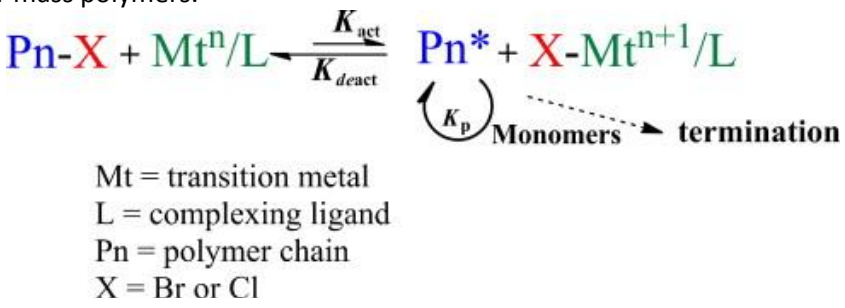

Figure 17. Equilibrium established during ATRP.[90]

The way for peptide to take part of this polymerization is to play the role of the initiator. Indeed, modified peptides bearing halogen at one or several positions (e.g. Br functionalization by 2-bromoisobutyric acid coupling on Lys side chains, Figure 18) have been successfully used as initiators for ATRP.[91–94] Then the geometry and the number of halogen atoms on the functionalized peptide is controlling the structure of the resulting polymer.

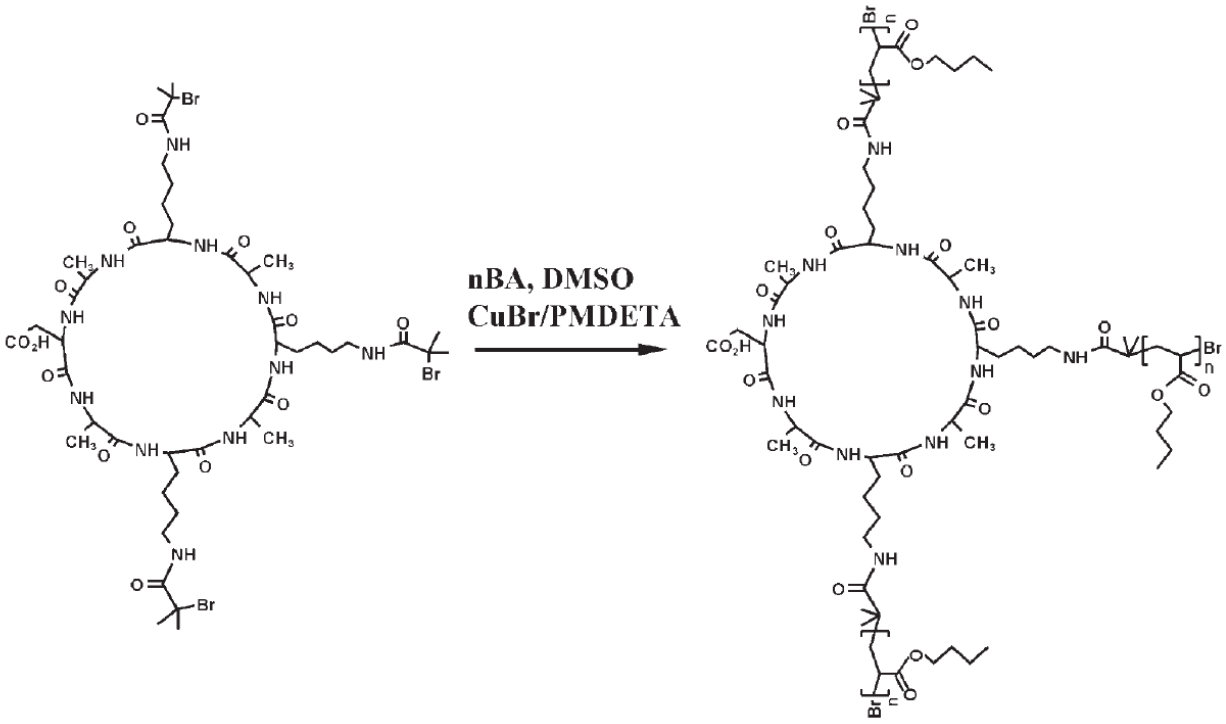

Figure 18. Example of cyclic peptide used as initiator for ATRP polymerization of acrylate based polymer.[94]

c. *Reversible Addition-Fragmentation chain Transfer polymerization (RAFT)*

RAFT is another radical polymerization method, which enables the synthesis of well controlled polymers in term of size (Mw), ~~Đ~~ ad even architecture.[95] RAFT polymerization needs a radical source, such as azobisisobutyronitrile (AIBN) and a chain transfer agent, such as thiocabornylthio or thiocarbamate. The radical initiates the polymerization by activating the monomer and thus enabling the growth of the chain by transfer of the radical from the chain to another monomer. The chain transfer agent is playing an important role in this process, as it ensures the propagation of the radical to activate another monomer (Figure 19). Peptides can be coupled to the chain transfer agent thus playing the role of initiator for the RAFT polymerization.[96–98]
Two cyclic peptides were modified by thiocabornylthio groups in order to become RAFT initiators. Then they enabled a *grafting from* polymerization on its modified side chain, in the same idea as the example of ATRP (Figure 18 and Figure 20). However, cyclic peptides are not the only possibility; GGRGDS-OH was also modified at its N-terminus with S-1-dodecyl-S'-(R,R'-dimethyl-R''-acetic acid) trithiocarbonate to initiate RAFT polymerization (Figure 20) and give linear peptide-polymer conjugate. This example is leading to a peptide-polymer conjugate with cell adhesion properties over fibronectin.

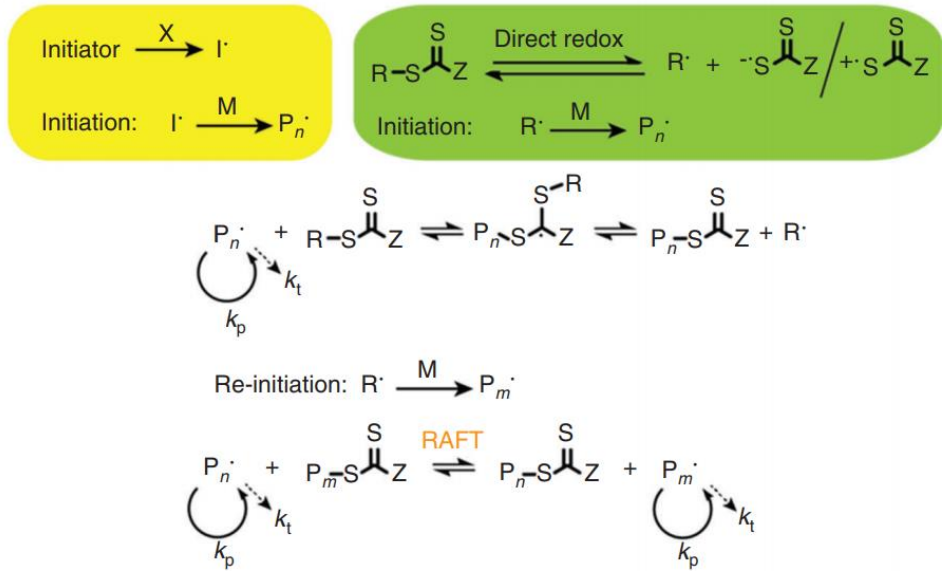

Figure 19. Mechanism of RAFT polymerization.[95]

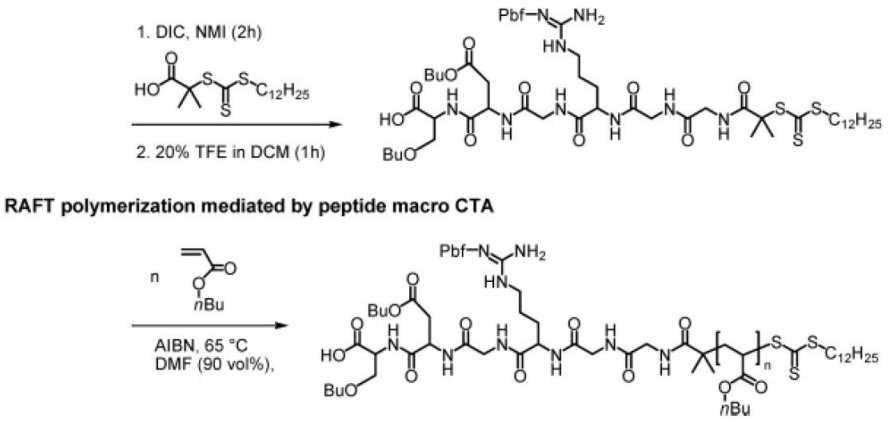

Figure 20. Example of peptide functionalization with S-1-dodecyl-S-(R,R-dimethyl-R-acetic acid) trithiocarbonateinitiator and RAFT *polymerization by grafting from strategy.[96]*

d. *Nitroxide-Mediated radical Polymerization (NMP)*

The last example of RDRP polymerization is the NMP polymerization. It is also based on propagating and dormant species, as in ATRP. However in this case, initiators are alkoxyamines that undergo homolysis into nitroxide and a radical active species: the initiating radical.[99] The initiating radical is responsible for the propagation. At some point, the radical species are captured again by the nitroxide species, and then an equilibrium is created with the resulting dormant polymer chain and the propagation (Figure 21). The most common initiator for NMP is 2,2,6,6-tetramethylpiperidinyloxy (TEMPO). The polymerization process has the advantage to be a metal free polymerization and to not need purification of the resulting polymer. However, this type of polymerization can be slower than the two first options.
These alkoxyamine groups can be introduced in the peptide sequences to enable them to be used as initiator of the polymerization.[100,101] Noteworthy, it is also possible to grow two different polymers on an unique peptide initiator still anchored on solid support (Figure 22).[100]

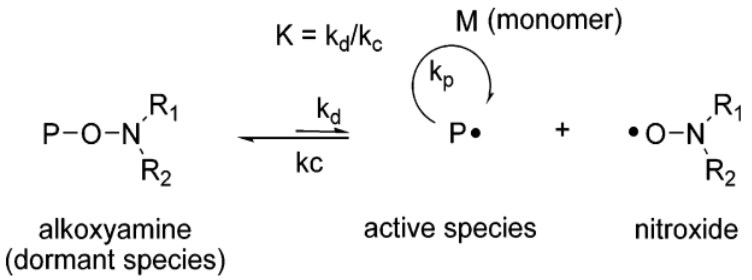

Figure 21. Nitroxide-Mediated radical Polymerization polymerization.[99]

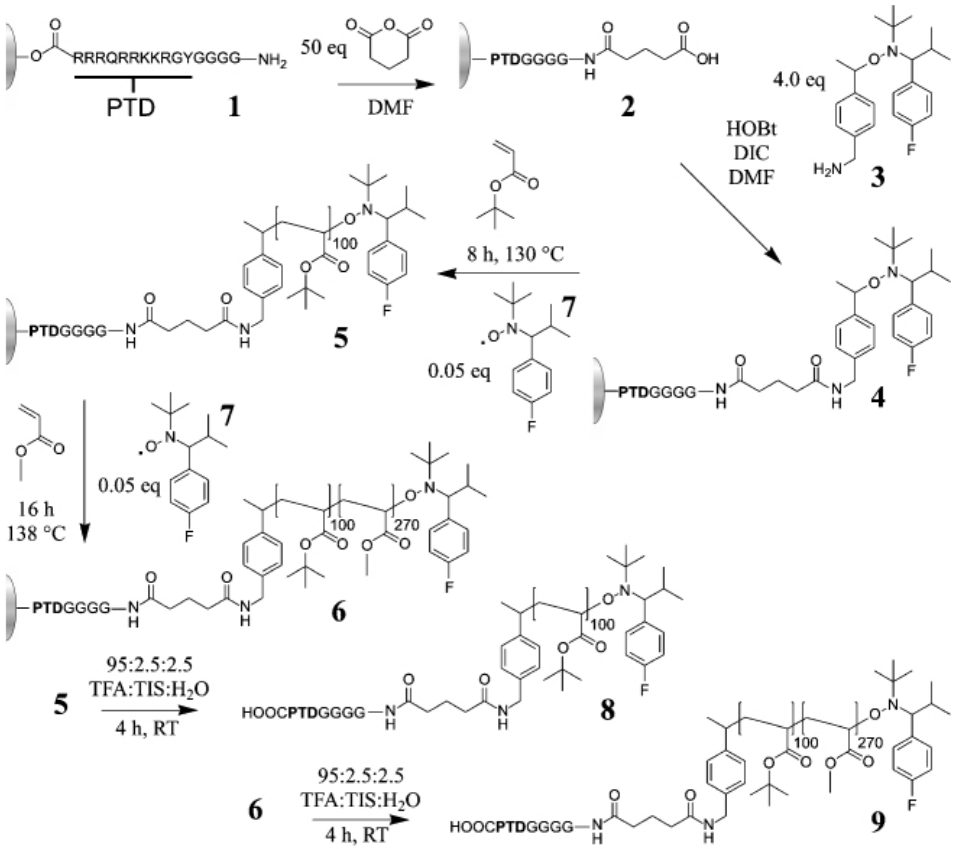

Figure 22. Example of peptide functionalization with fluorine-labeled alkoxyamine initiator and NMP polymerization by grafting from strategy.[100]

In all the cases, these three types of polymerization afford polymers (or copolymers) conjugated with a single peptide sequence. Interestingly, the peptides can contribute to the structure of the resulting polymer hybrid. Indeed, even when simple peptide-polymer blocks are obtained, the physicochemical properties of the peptides (ex: charge, polarity) or their inner self-assembling properties can yield to supramolecular arrangements such as core-shell cylinders, micelles or nanotubes.[93,94,97] In some cases, cyclic peptide may self-assemble, driving the global supramolecular arrangements into core-shell cylinder instead of polymeric micelles, that is the result of the basic block copolymer assembly (Figure 23).

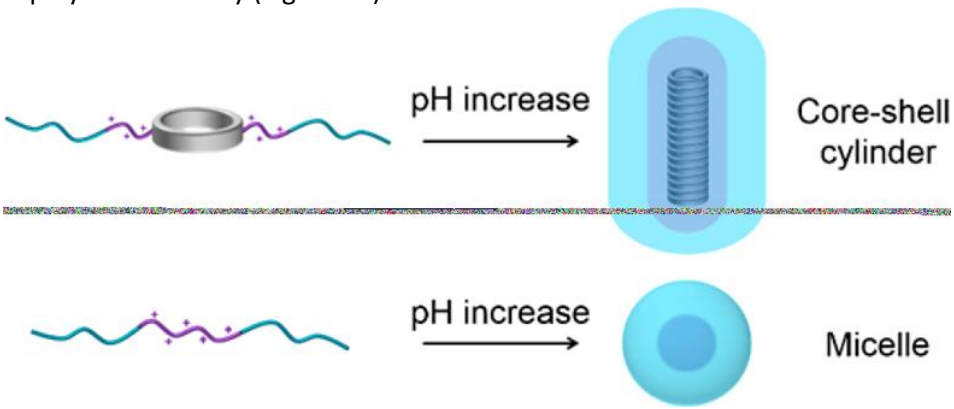

Figure 23. Example of supramolecular arrangement issued from peptide-polymer based of grafting from strategy.[97]

IV. *Grafting through* strategy: peptide as macromonomer (PCM)

Using a peptide as monomer is undoubtedly much more demanding in terms of chemical requirements than 'grafting' strategies. Indeed, the peptide needs to be functionalized with at least one 'polymerizable' moiety. This reactive group has to be introduced in the peptide sequence in order to let it (co)polymerize according to the chosen polymerization technic without interfering with the other functional groups of the biomolecules. PCM (peptide containing macromonomer) are usually called "macro-monomers" due to their relatively high molar mass. Using PCM is enabling the synthesis of polymers with higher level of peptide repetitions than *grafting from* approaches, yielding completely new characteristics coming from the peptide properties (i.e. structure, self-assembly, biological properties). The backbone of the final polymer is the result of the type of polymerizable moieties.

a. *Chain growth polymerization of acrylate-peptide macromonomer*

The most common reaction used with PCM is the poly-addition of acrylate or methacrylate peptide monomers, which is also the most common strategy for the *grafting to* method. Numerous research projects utilize biomolecules (saccharides[102–105], nucleotides[106–108] and peptides) modified with a methacrylate or acrylate group.[109]

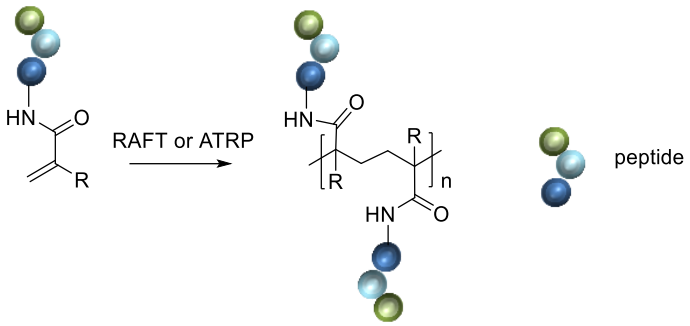

Figure 24. General scheme of acrylate and methacrylate functionalized peptide macromonomer polymerization by poly-addition either by RAFT or ATRP.

The acrylate modification of amino acids or peptides has to be done on protected peptides, otherwise more than one acrylate group would be anchored on the macromonomer and the polymerization would lead to 3D network instead of linear polymers.

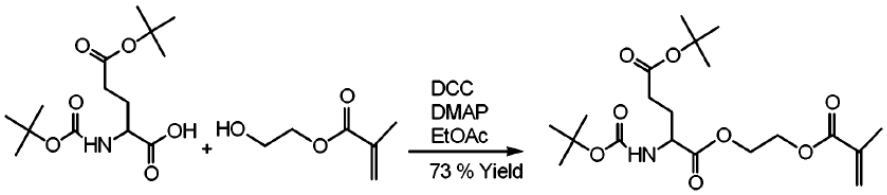

Figure 25. Example of amino acid modification at the C-terminus: synthesis of methacrylate functionalized protected glutamic acid.[110]

As examples, amino acids were functionalized at their C-ter in order to get an acrylate-based polymers with amino acids as pendant chains.[110] Acrylate-peptide monomers are able to react in the same way as Methyl methacrylate (MMA) do,[111] by RAFT or ATRP polymerization. Peptides are then incorporated as pendant chains along an aliphatic backbone (Figure 24). Noteworthy, this strategy is particularly useful to set up polymer-induced self-assembly (PISA) approaches (Figure 26).[112,113] Methacrylate or acrylate modified amino acids, (functionalized at the C-ter, e.g. cysteine, alanine[114]), and short peptides such as glutathione have been copolymerized with 2-hydroxypropyl methacrylate (HPMA) by RAFT. The resulting block copolymers comported a hydrophilic (the peptide) and hydrophobic (pHPMA) part. This amphiphilicity and the hydrophobic/hydrophilic balance was the driving force leading to supramolecular self-assembly into spheres, worms or vesicles as a function of the ratio of both parts of the resulting copolymer. Noteworthy, a linker is often introduced between the peptide and the polymerizable moiety that bring additional properties to the resulting material, favoring the self-assembly of the peptides[115] or bearing a cleavable bond (e.g. disulfide bridge) for potential peptide delivery applications. [116]

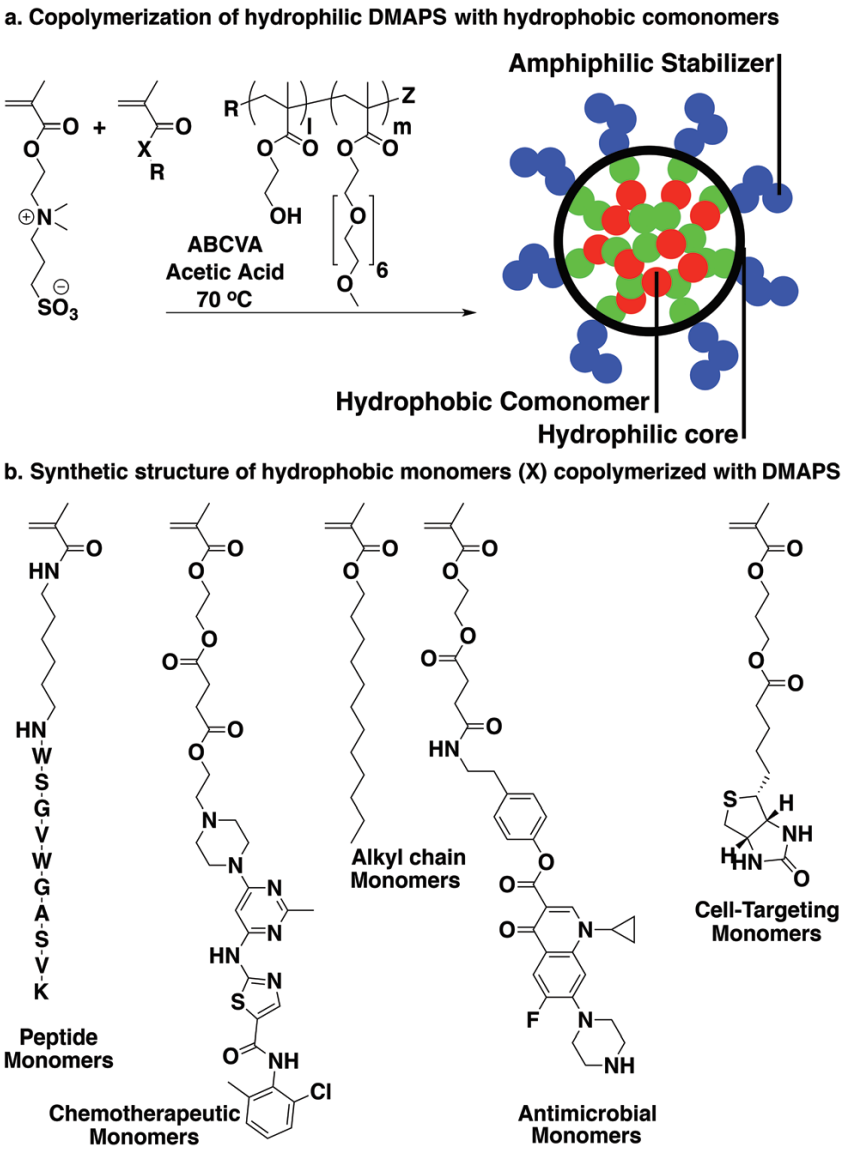

Figure 26. Example of acrylate functionalized macromonomers polymerized by RAFT and self-assembled into polymeric micelles by PISA.[113]

b. *Ring Opening Polymerization (ROP) of NCA-peptide macromonomers*

Besides ATRP and RAFT on acrylate PCM, ring-opening polymerization (ROP) was used to polymerize peptide sequences. ROP was initiated by a nucleophilic attack (e.g. amino group or primary alcohol) which in turn, unmask another nucleophilic function suitable for further chain elongation. It implies that this strategy is not suitable with some unprotected amino acid having nucleophilic groups as side chains or extremity. ROP of lactams was applied to the synthesis of Ser homopolymers [117] but was not used to polymerize peptide sequences. In a similar way, N-carboxyanhydride (NCA) modified amino acids,[118–120] were extensively used to obtain homo-oligomers as polyLys or polyMet.[121,122] Derivatives of polyglutamic acid such as poly(benzyl-L-glutamate) (pBLG) or poly(stearyl-L-glutamate) (pSLG) were also obtained by polymerization of side-chains modified Glu NCA.[123–125] ROP of two NCA modified amino acids, Lys and Val, have led to a direct grafting on hyperbranched polyamide amine NPs.[126]

The ROP of a Pox monomer lead to a polyamide whose structure is close to a peptide backbone. In order to obtain peptide-like polymer with amino acids as pendant chain, peptide sequences are functionalized by the oxazoline group at the N or C-terminus extremity, while all other reactive group remained protected (Figure 27).[127,128] The only example reported so far of PCM associated with Pox is issued from the ROP of NCA functionalized peptide or amino acids, copolymerized with oxazoline monomer. Indeed, different NCA aminoacids (e.g. Phenylalanine, protected Glutamic acid, glycosylated Serine) are copolymerized with Pox monomer in order to obtain block copolymer including a block with a peptide as pendant chain.[129,130] All the previously cited examples do not yield strictly speaking to peptide-polymers as defined in this introduction. Indeed, the peptide part is not a well-defined sequence but a polyamide formed by the random repetition of amino acids.

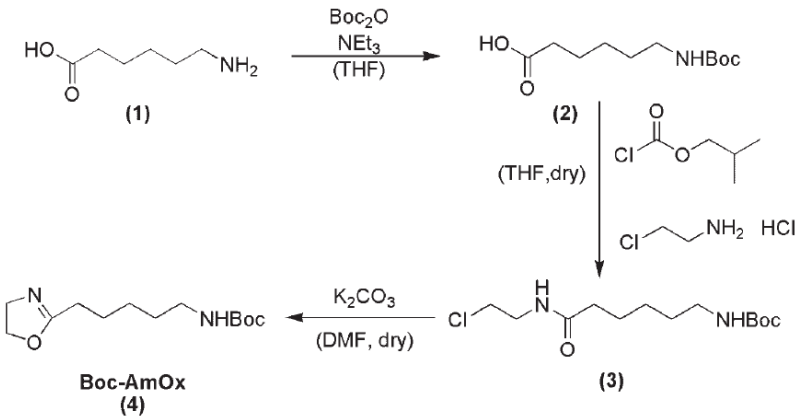

Figure 27. Example of preparation of an oxazoline modified macromonomer.[128]

More interestingly, NCA-peptide macromonomers were prepared. Their polymerization yielded to well defined comb-like peptide-polymers with a peptidic backbone.[131] In the case of peptide, the NCA modification can be done on solid support following the peptide synthesis. This enabled to keep the side chain protection of the peptide, in order to make sure no side reactions are possible since the modification is not chemoselective. The cleavage of the peptide from the resin was done after the cyclisation of the NCA modification. The macromonomer was then ready to polymerize. The polymerization of such macromonomer has also its limits, some amino acids, like Lys for example; have to still be protected during the polymerization to prevent any side reactions.

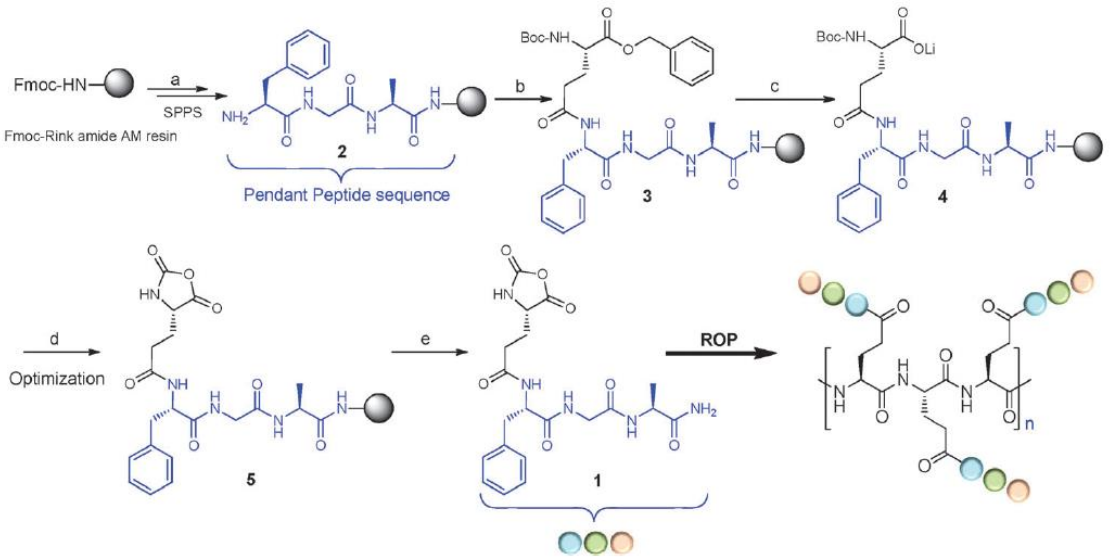

Figure 28. Example the synthesis and polymerization of an NCA modified peptide macromonomers: Synthesis of the Glu(Phe-Gly-Ala-NH_2)-NCA monomer on resin. Reagents and conditions: (a) SPPS: deprotection: piperidine–DMF (20/80), rt, 30 min; coupling: Fmoc-AA-OH (3 eq.), HBTU (3 eq.), DIEA (3 eq.), DMF, rt, 2 h; (b) (1) deprotection: piperidine–DMF (20/80), rt, 30 min; (2) Boc-Glu-OBzl (3 eq.), HBTU (3 eq.),DIEA (3 eq.), DMF, rt, 2 h; (c) 2 M LiOH aq.–THF (30/70), rt, 3 h; (d) cyanuric chloride (5 eq.), anhydrous DCM, rt, overnight; (e) TFA–anh. DCM (50/50), rt, 1.5 h.[131]

c. *Ring Opening Metathesis Polymerization (ROMP) of norbornene-peptide macromonomers*

Ring Opening Metathesis Polymerization (ROMP), a variant of ROP, relies on norbornene monomers and is catalyzed by ruthenium based Grubb's catalyst. The norbornene functional group contains an alkene function responsible for the ring opening and thus the polymerization (Figure 29). As ROP, ROMP was used to polymerize dipeptides such as GlyGly, LeuPhe or ValLeu.[132] More interestingly, ROMP was performed on norbornene modified peptide macromonomers whose polymerization resulted in a comb-like hybrid peptide polymer.[133] Norbornene modified cyclic peptides were used to obtain thermal and enzyme-responsive polymers by ROMP.

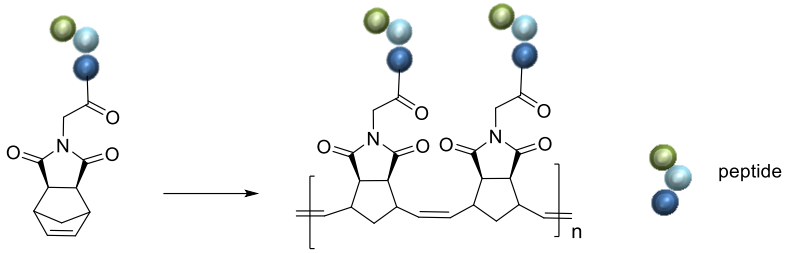

Figure 29. Norbornene functionalized peptide macromonomer polymerized by ROMP.

The peptide macromonomers were synthesized by coupling the N-ter of the peptide sequence with a norbornene carboxylic acid activated by oxalyl chloride, in the presence of trimethylamine (Figure 30). During functionalization, peptides have to be protected in order to avoid side reactions but the polymerization of norbornene macromonomer itself is chemoselective and could be performed on unprotected peptides.

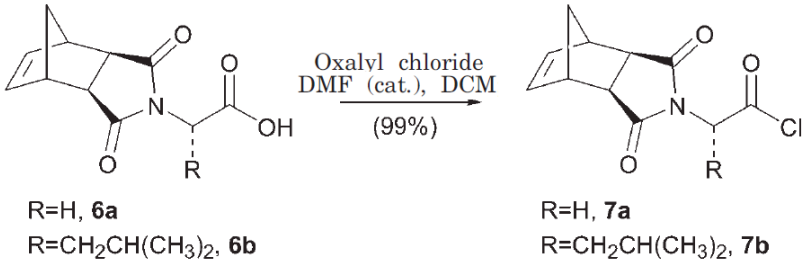

Figure 30. Preparation of the activated norbornene reactive block to be coupled on an amino group of a peptide. [132]

A norbornene-based polymer bearing a cyclic peptide (KVPGGGVPGLG, an elastin like polypeptide) as pendant chain was thermal-responsive: its thermal signature is directly linked to its crystallization. Enzymatic treatment of endopeptidase thermolysin opened the peptide cycle thus decreasing the thermal response and so the crystallization ability.[134] Copolymerization with norbornene-modified PEG monomers lead to interesting PEG-peptide-copolymer with higher water solubility.[135,136] Specific structures as spherical or cylindrical micelles, were obtained by copolymerization of norbornene PEGylated peptides with hydrophobic norbornene monomers.[137] These results paved the way to apply ROMP in PISA protocols (ROMPISA) to obtain amphiphilic polymer nanostructures such as micelles, worms or vesicles in function of the ratio of the peptide block over the PEG one.[138]

d. *Poly-condensation of diacid chloride with diamino-peptide macromonomer ('peptide-nylons')*

This type of peptide polymer has been developed by our research team. Polyamides peptide-polymers analogues of nylons were recently obtained by substituting the classical aliphatic diamine (e.g. diaminohexanoic) by peptides bearing two primary amino groups; one of them being the N-terminal amine and the other one afforded by a Lys side chain or by a diamino spacer placed on the C-terminus (Figure 31).[139] This technic enables the design of customable peptide nylons, resulting in either linear or comb-like polymers in function of the structure of the peptide macromonomer. Thus, the composition of the polymer is managed by the quantity of peptide macromonomer incorporated. Noteworthy, this strategy was not suitable for peptides bearing other unprotected amino groups than the two involved in the polymerization.

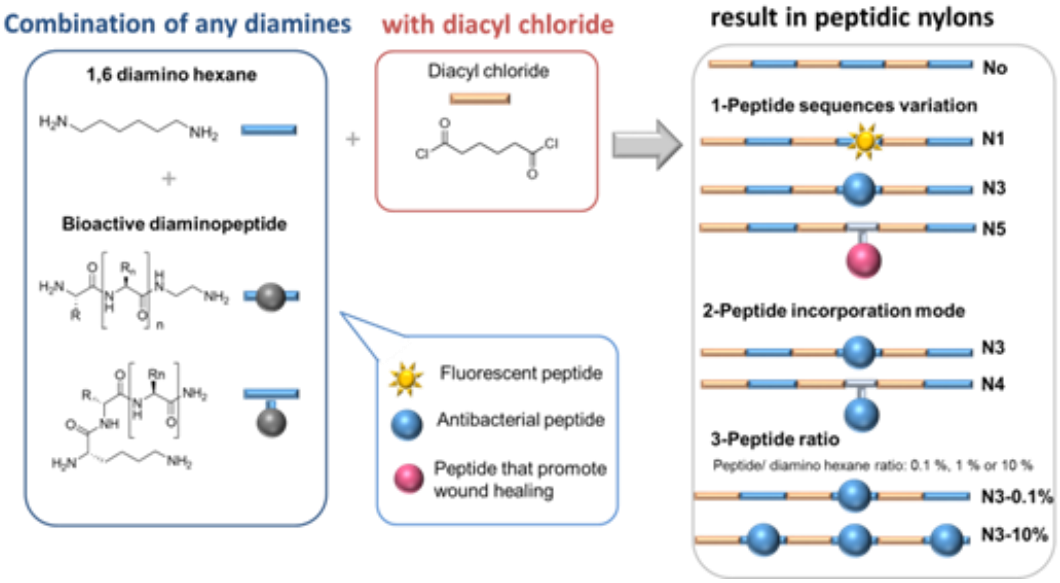

Figure 31. Poly-condensation of diacid chloride with diamino-peptide macromonomer.

e. *Nitroxide Mediated Polymerization (NMP) of peptide macromonomers*

NMP reaction was also performed with a peptide macromonomer. A cyclic peptide, opened by heat, leads to both a reactive carbon radical and a nitroxide radical respectively at the N-terminus and C-terminus of the peptide (Figure 32). The reactive carbon radical was able to initiate NMP while the nitroxide one was trapping radicals of growing polymer chain to terminate it but in a reversible way. Usually used as an additive, TEMPO was here directly incorporated into the peptide chain thanks to Fmoc/tBu SPPS, using Fmoc-TEMPO-COOH. A copolymerization by NMP with vinyl monomers yielded a hybrid block peptide-polymer.[140]

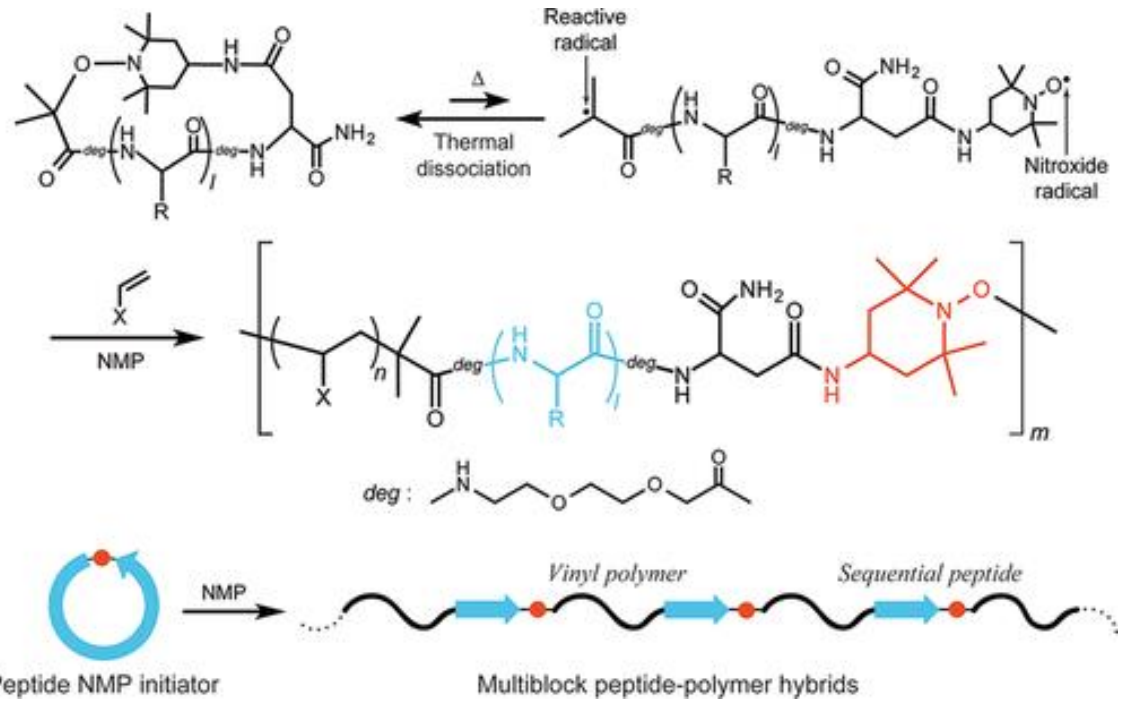

Figure 32. NMP polymerization of a cyclic peptide macromonomer.[140]

f. *Poly-condensation of silylated peptide macromonomers ('peptide-silicone')*

This last example of peptide macromonomer was developed by our research team and was at the origin of this PhD work. Versatility of silicon chemistry was utilized to synthesize polymerizable hybrid alkoxysilyl-modified peptides.

Monosilylated peptides were first successfully used for *grafting to* approach. As example, peptides were immobilized on silicone catheter after plasma activation in order to get antimicrobial properties.[141,142]

We also developed *grafting through* strategy using hybrid peptides as macromonomer. The first reported example concerned the hydrolysis and condensation of bi-functionalized dimethylcholorosilane peptides yielded Si-O-Si bridged polymerized peptide sequences.[143] This condensation proceeded chemoselectively towards AA side chains, thus enabling the use of unprotected peptides. Linear peptide polymers but also comb-like peptides polymers were obtained using an N-terminus bi-functionalized Lys.[88] On the other hand, by using mono functionalized dichloromethylsilane peptides, comb like polymers were obtained along a PDMS-like backbone (Figure 34)[143,144] The silylation of the peptide was done at the N-ter of the protected peptide sequence using isocyanatopropyl silane (Figure 33).

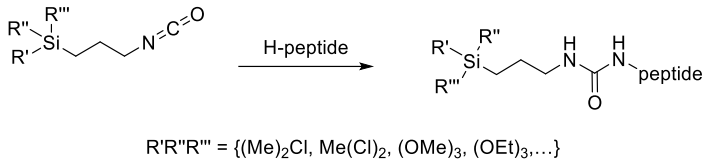

Figure 33. N-terminus peptide silylation by reaction with an isocyanate.

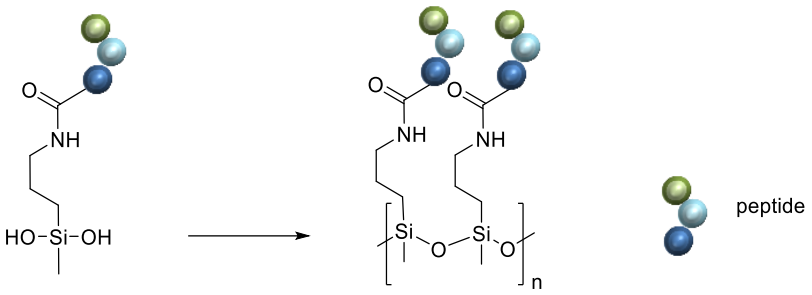

Figure 34. Sol-gel polymerization of dihydroxymethylsilyl peptide macromonomer.

This sol-gel polymerization constituted the basis for the syntheses of hybrid materials presented in this PhD. The synthesis of such silylated peptide, as well as other silylated biomolecules, will be detailed. Therefore, different hybrid macromonomers will eventually be combined and copolymerized with dichlorodimethylsilane to get modified PDMS multifunctional polymers.

V. Conclusion

A large choice of strategies to obtain peptide-polymers has been described. Firstly, often following a polymer modification, peptides can be grafted on the polymer by diverse conjugation techniques. On the other hand, peptides can take part of the polymerization as initiator. In that case, only single peptide sequence has to be functionalized to play the role of initiator. At last, the peptide may play an even more important role as a macromonomer, leading to polymers incorporating several copies of well-defined peptides along their backbone.

For a long time, peptides have been relegated to a second role in peptide-polymer conjugates, only considered as a way to improve the polymer properties, by post-functionalization for example. If the biological activity of peptides was extensively used to improve material properties, the exploitation of their structural and recognition features is in develpment. The recent literature demonstrates that peptides have to be considered as an attractive starting blocks for the design of novel macromolecular and biomimetic materials. Inspired by protein structural features and predictive weak interactions networks, the tremendous progress performed in the field self-assembling peptides will certainly fuels the research of well-defined functional peptide polymers.

Chapter 1.B: Silicone grafted bioactive peptides and their applications

NB: most of this chapter constitutes the publication : Martin Julie, Jean Martinez, Ahmad Mehdi, et Gilles Subra. « Silicone Grafted Bioactive Peptides and Their Applications ». *Current Opinion in Chemical Biology* 52 (octobre 2019): 125-35. https://doi.org/10.1016/j.cbpa.2019.06.012.

Chapter 1.B: Silicone grafted bioactive peptides and their applications

I. Introduction

Polydimethylsiloxane (PDMS) is a synthetic organic/inorganic polymer. Thanks to its interesting mechanical and chemical properties, such as high flexibility, thermal, electrical and chemical stability,[145] optical transparency and oxygen permeability,[146] it is widely use in industrial applications.[147] Besides, being a bio-compatible synthetic polymer,[148] it is one of the most used polymers for bio-applications especially for implants and other medical devices. Compared to other FDA-approved polymers like polyethylene glycol (PEG) or polylactic acid (PLA), the flexibility and the transparency of PDMS make it particularly suitable for the design of soft devices for ophthalmologic applications (contact lenses, artificial cornea) or blood contacting devices like catheters.[31]

PDMS can be used as silicone oil or can be cross-linked to yield a solid material. In the latter case, it requires functionalization of the silicone oils with vinyl (Si-CH=CH_2) and silane (Si-H) groups, which may react by hydrosilylation to create bridges between the PDMS polymer chains.[149]
Despite its huge popularity, PDMS suffers from some drawbacks. First, it is highly hydrophobic and this may lead to non-specific adhesion of biomolecules, in particular lipids and proteins.[150] The fouling of a PMDS device can be problematic by provoking unwanted biological reactions triggered by the adsorbed biomolecules[151]. It is thus desirable to improve the hydrophilicity of the surface, resulting in a reduced protein adsorption and improved biocompatibility.

Then, like most synthetic polymers, PDMS is bio-inert. Therefore, it has to be functionalized to reach the requirements of biological and therapeutic applications. PDMS surface can be functionalized by simple adsorption of relevant (bio)molecules or modified covalently generally using an activation step (e.g. plasma, UV) followed by multistep conjugation chemistries. These post-functionalization approaches were already performed with a wide range of compounds including simple organic molecules (e.g. fluorescein to study attachment of bacteria on silicone),[152] polymers like PEG to confer hydrophilic properties[153] and polysaccharides (e.g. oxidized dextran or hyaluronic acid)[154,155] which limit non-specific adsorption and enhance biocompatibility. Proteins were also immobilized on silicone surface. Collagen was used to get PDMS surfaces suitable for fibroblasts culture[156] and, trypsin-functionalized PDMS microchannels were used as enzymatic microreactors for proteomic MS analyses[157]

Peptides are good candidates for bio-functionalization of PDMS. Indeed, they exert a wide range of biological activities which improve the properties of silicone devices notably changing their hydrophilicity, cell-compatibility or adding antifouling behaviour. Moreover, their small size and their ease of synthesis, comparatively to proteins or biopolymers, allow the introduction of chemical functions enabling selective conjugation to the silicone material.

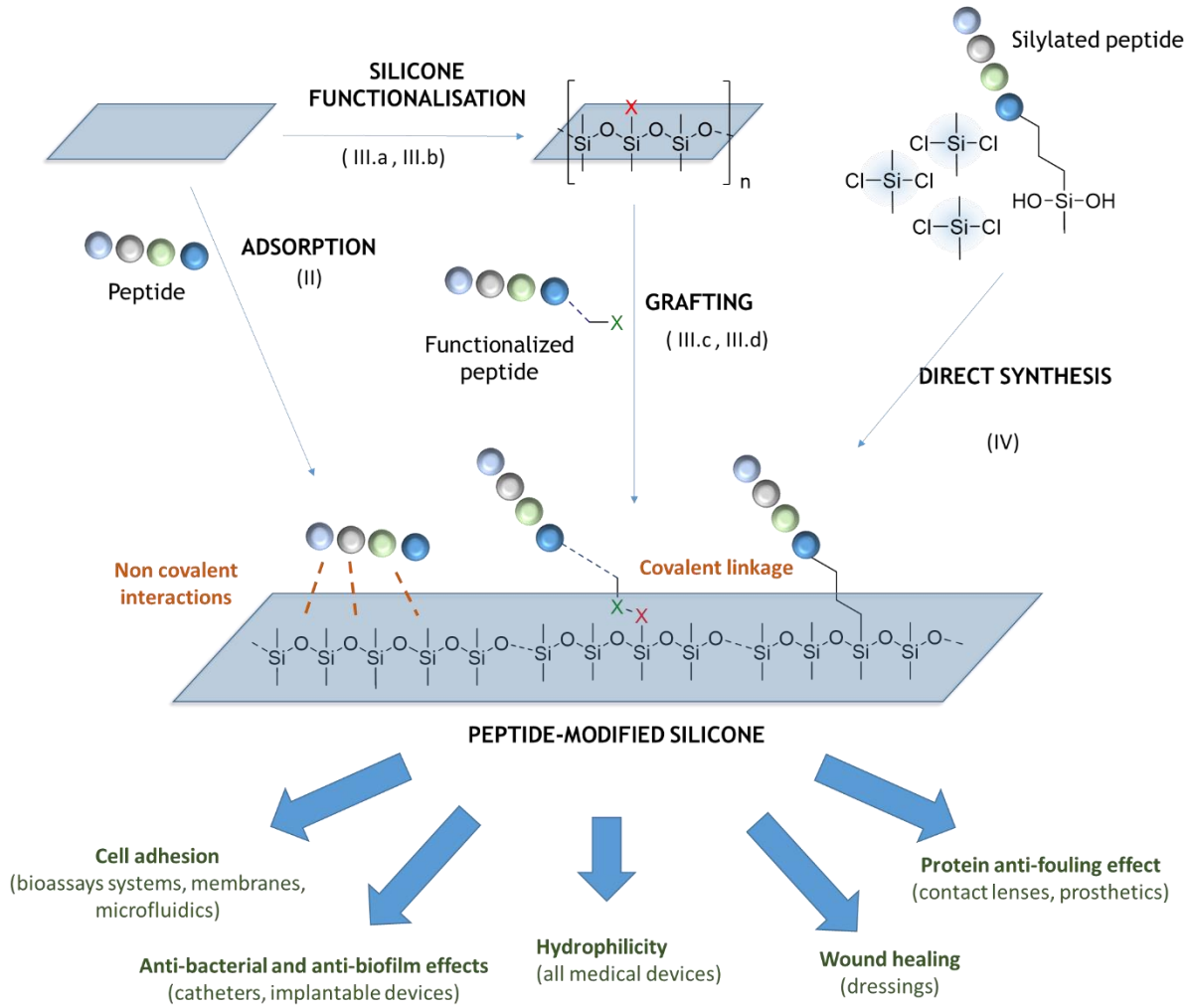

Figure 35.Peptide-modified silicone and its applications.

II. Peptide adsorption on silicone surface

It is possible to obtain bioactive PDMS without any chemical modification, by non-covalent adsorption of the biomolecule on the silicone surface. This simple process, generally performed by dip coating, is sufficient to change the PDMS properties. For example, hydrophobicity and consequently non-specific adsorption yield can be increased by adsorption of amino acid homo oligomers. Indeed, cationic PEG-DOPA-PolyLysine (DOPA: L-3,4-dihydroxyphenylalanine) conjugate was coated on untreated PDMS leading to a material with improved lubrication properties.[26] Due to numerous non-covalent interactions, macromolecules (e.g. biopolymers) can be adsorbed efficiently on bare PDMS surface. This is not the case with smaller molecules like peptides, which do not bind strongly on silicone surface and are quickly desorbed in biological media. In that case, the PDMS has to be previously modified to generate additional interactions. Oxidation is the most common modification of PDMS. Operated by air plasma, oxidation generates mainly Si-OH moieties from siloxane chain breakage or Si-CH_3 modification. Using this process, the peptide H-[(Ala-Glu-Ala-Glu-Ala-Arg-Ala-Arg)$_2$]-OH (EAR16-II) was adsorbed by dip coating, with the help of ionic interactions between the guanidine groups of Arginine side chains and silanolates (Si-O^-) on the PDMS surface. Adopting a β-sheet conformation, EAR16-II peptides self-assemble into parallel or anti-parallel fibers onto the PDMS surface because of the presence of both the positive as well as the negative charges from arginine and glutamic acid side chains respectively. Such peptide-modified silicone was used to prepare microfluidic devices with low non-specific adsorption of proteins.[158]

Plasma oxidation is also the first step of covalent modification of PDMS surfaces required for peptide adsorption. For instance, perfluorinated triethoxysilylalkanes are covalently grafted onto the silanols of PDMS plasma activated surface, by SiOSi condensation.[159,160] This new perfluorinated layer allows the selective and strong adsorption of fluorine-tagged-peptides, thanks to the hydrophobic nature of the perfluorinated alkyls moieties. In contrast, non-fluorinated peptides and proteins (e.g. insulin, ubiquitin) are much less adsorbed on these treated PDMS surfaces.

UV light activation of PDMS surfaces, generate radicals on the methyl groups (Si-CH_2·). This activation enables the immobilisation of acrylic acid (AA) by radical coupling. The resulting anionic surface (PDMS-COO^-) enables the self-assembly of a monolayer of poly(diallyldimethylammoniumchloride) (PDDA) by ionic interactions. Quaternary ammoniums from the PDDA layer are also used to create ionic interactions with the anionic groups of proteins. Trypsin, a serine protease, was immobilized on such PDDA-modified PDMS and used as active microfluidic device for on-line protein digestion and analysis.[157]
Alternatively, instead of coating a biomolecule on the PDMS surface, it is possible to load it into porous PDMS. This is an attractive strategy for controlled drug delivery applications, the biomolecule diffusing in a passive way through the porous PDMS layer. Porous PDMS nanoparticles (NPs) can be obtained by infiltration of the polymer into sacrificial silica porous NPs. Silica phase is then dissolved by HF treatment. To date, only doxorubicin has been loaded in such nanoparticles, which could also accommodate peptides.[161]

To favour a long-term biological effect and to avoid the release of the active moiety, the linkage between the peptides and the PDMS has to be covalent. While the simple coating of drugs and bioactive molecules on PDMS can be quite straightforward, their covalent anchoring is much more challenging.

III. Peptide grafted silicone

PDMS does not display any suitable function for further covalent modification. Consequently, the establishment of a covalent bond between PDMS and any other compound, including peptides, requires either generation of a reactive function on non-functionalized PDMS (e.g. Si-OH like in the case of non-covalent coatings), or the preparation of functional PDMS by copolymerization of functional monomers with non-functionalized monomers such as dimethyldichlorosilane and hexamethyl(cyclotrisiloxane).[149]
Theoretically, a peptide could be directly conjugated onto such functionalized PDMS, but all examples reported so far use an additional spacer, which can also be a polymer, to link the peptide to the PDMS surface. This spacer (Y-spacer-Z) is first coupled to the PDMS backbone and still presents a suitable organic (Z) function that allows the conjugation with the peptide.
First, we will present the methods to obtain PDMS displaying reactive functions by post-modification (III.a), and by direct preparation of functional-PDMS by copolymerization (III.b). Then, the functionalization by spacers adapted to each type of modified silicone will be presented (III.c). Finally, peptide-conjugation chemistries that are accessible to the spacer-modified PDMS will be described (III.d).

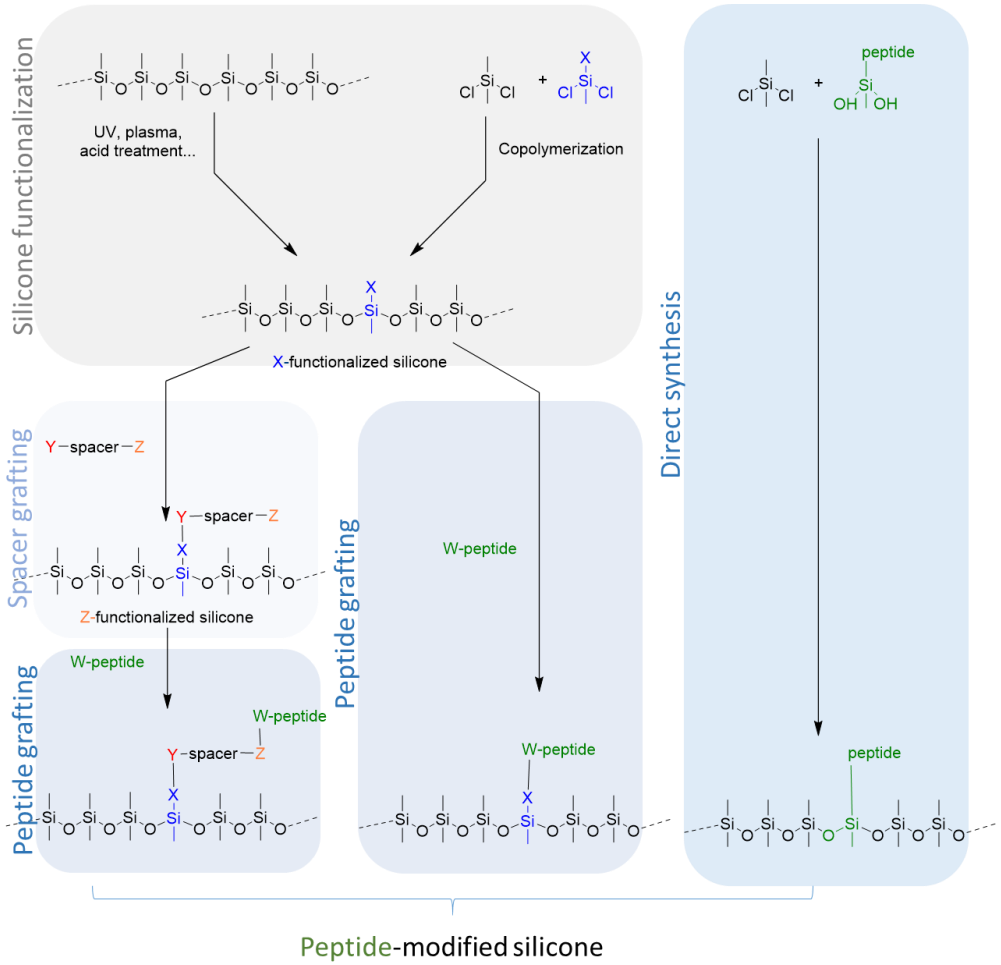

Figure 36. Different ways to obtain a peptide-modified PDMS. Most of the time, several step are needed for the synthesis of the peptide-modified silicone: (i) silicone surface functionalization, (ii) spacer grafting, (iii) peptide attachment. Noteworthy, the peptide can also be grafted directly of the functionalized silicone. Advantageously, a peptide monomer bearing a methyldihydroxysilyl moiety could be copolymerized with dimethyldichlorosilane to obtain peptide-functionalized PDMS material in one step.

a. PDMS activation to generate functions

1. Generation of Si-OH functions

As already stated, oxygen[154,158–160,162–166] and water plasma[167,168] or H_2O_2[169] oxidation lead to the formation of Si-OH groups at the surface of the PDMS, either by replacing one or two Si-Me group on the same silicon atom, or by cleaving a Si-O-Si bond of the silicone backbone.[170] This type of activation is fast (i.e. 30 s to a few minutes) and efficient, and may double the oxygen content of the silicone.[171] Si-OH functions may react readily with a range of organosilane reagents to fix a desired function on the surface by further condensation with organosilane derivatives, yielding a Si-O-Si bonds. Aminopropyltriethoxy or trimethoxysilane or (APTES or APTMS) are commonly used to generate a primary amine function at the surface of the PDMS (see III.c).

2. Generation of Si-H functions

Si-H functions can be generated by triflic acid (CF_3SO_3H) treatment of PDMS surfaces. This function may react with unsaturated compounds by hydrosilylation using Karstedt's Pt catalyst yielding Si-alkyl covalent bonds. Bifunctional PEGs bearing both an allyl and a N-hydroxysuccinimide (NHS) activated carboxylic acid, was used to obtain NHS-functionalized PDMS able to anchor amino functionalized peptides.[155,172–174]

3. Generation of radicals (Si-X=. Si-CH_2• or Si-O•)

Radicals can be generated on the backbone and surface PDMS, to react, for example, with allyl-containing compounds initiating free radical polymerization (FRP).[175] Free radicals can be generated either by direct argon plasma activation or with a photo-initiator.

3.1 Si-CH_2• radical generation by UV irradiation and photo-initiation

Acrylic acid was successfully polymerized by FRP on the surface of PDMS using benzophenone as radical initiator, yielding Si-CH_2• radicals.[176,177] The resulting polyacrylic acid (PAA) modified PDMS was further functionalized with peptides, thanks to the activation of carboxylic acids (cf. III.d.1). Noteworthy, Si-CH_2• radicals can be generated on PDMS directly by UV irradiation.[157,178] In this case, the PDMS was immersed into a solution containing acrylic acid for example, and then UV-irradiated to react with allyl monomers.

3.2. Si-CH_2• Radical generation by Argon plasma activation

Alternatively, argon plasma generates free radicals at the PDMS surface, which are converted into hydroxyl, carboxylic acid, C=O function or Si-O• radical when in contact with air.[175] It is also possible to use ionic argon plasma to activate the surface in order to gain more stability over time thanks to the ion-beam.[156,179] Then hydroxyl and radical modified PDMS can be functionalized by grafting allyl-containing monomers such as allyl glycidyl ether (AGE),[180] which can also be polymerized on the activated surface by FRP.[181] In the latest case, the epoxy groups were useful for subsequent peptide immobilization (cf. III.d.4).

b. Direct synthesis of functional PDMS by copolymerization

Copolymerization of dichlorodimethylsilane with methylsilane bearing a functional group yields PDMS chains displaying organic functions. Strictly speaking, these copolymers are not PDMS but functionalized polysiloxanes. Several functions have been introduced this way including azide for clic-chemistry reactions.[182] However, only thiol- and vinyl-modified PDMS obtained by copolymerization have been used for subsequent modification with peptides.

Copolymerization of dichloromethylmercaptopropylsilane with dichlorodimethylsilane affords poly[(3-mercaptopropyl)methylsiloxane-co-dimethylsiloxane].[152] This SH-containing polymer may undergo any thiol-ene reaction (either Michael or free radical addition). As example, glycidyl methacrylate (GMA), along with other acrylate-based monomers, has been polymerized on SH-modified PDMS by UV-catalyzed free radical thiol-ene polymerization. Therefore obtaining a vinyl-modified PDMS such as polystyrene-block-poly(dimethylsiloxane-vinylmethylsiloxane) (PS-b-P(DMS-VMS)[183] by copolymerization is also described. This polymer was further functionalized by thiol-ene addition with SH-containing peptides (e.g. Fmoc-[(Lys(PEG_3)-Lys(octanoate)]$_3$-Cys-OMe or Fmoc-[Lys(PEG_3)]$_3$-[Lys(octanoate)]$_3$-Cys-OMe, amphiphilic oligopeptides).

c. Post-functionalization of activated silicone by a spacer

Starting from a primary functional group (see III.a, X = OH, H or radical), bi functional spacers (Y-spacer-Z) of different lengths can be introduced. One function (Y) reacts with the silicone surface, while the other one (Z) constitutes the conjugation point for the peptides bearing a complementary reactive group (i.e. W-peptide, see Fig. 2)).

1. Reaction between Si-X = Si-OH and Y = Si(OR)

As already stated, silanols (Si-OH) react readily with functional alkoxysilanes such as sulfobetaine silane[164] or perfluorooctyltriethoxysilane.[159,160] The resulting functionalized PDMS material are popular for non-covalent binding of perfluorinated peptides. To achieve covalent modification of PDMS with biomolecules and biopolymers, the APTES spacer was preferred.[154,162,167,168] It affords primary amino groups on the silicone surface, which can react with activated carboxylic acid (e.g. NHS-ester) to form an amide bond, and with epoxides to yield secondary amines. However, no peptide grafting have been described do far on amine-modified silicone, although peptides have been straightforwardly grafted this way on silicon wafers[184] and silica NPs (Fig. 37, pathway A).[185,186]

2. Reaction between Si-X = Si-H and Y = vinyl

Allyl spacers can be grafted on Si-H containing PDMS by Karstedt's catalyst mediated hydrosilylation. In most cases, a bi functional vinyl PEG is bound to the PDMS surface to bring hydrophilicity, and to present a suitable functional group (Z) on the other end to enable further peptide coupling. For example, grafting of allyl-PEG-OH afforded PDMS-PEG-OH, which in turn can be further converted into PDMS-PEG-OCONHS by N,N-disuccinimidyl carbonate (NHSCONHS) treatment. These N-hydroxy-succinimidylcarbamate functions are suitable for peptide anchoring (Fig.37, pathway B).[173,174] Noteworthy, direct grafting of allyl-PEG-OCO-NHS on PDMS was also performed to give the same NHS-activated material.[172] Allyl-PEG-OH-Tosyl was also used to get PEG modified PDMS, and after Tosyl substitution by diethylenetriamine, PDMS-PEG-NH-$(CH_2)_2$-NH-$(CH_2)_2$-NH_2 is obtained.[155] The amine-functionalized PDMS was used to covalently immobilize hyaluronic acid after carboxylic acid activation, but no peptide was coupled this way so far.

3. Reaction with Si-X = Si-CH_2• radicals and Y = vinyl or Y= epoxy

Free radical polymerization of vinyl-containing monomers can be performed activated PDMS. Acrylic acid (AA) is polymerized on radical-activated PDMS to give a carboxylic acid (Z = CO_2H) functionalized PDMS[172–174,176] that can be further converted into a primary amine (Z = NH_2) functionalized PDMS by reacting with NH_2-PEG-NH_2 through carbodiimide activation (Fig.3, pathway C).[156,179] Another example shows a way to obtain HO-PDMS. Directly after the argon plasma treatment of the PDMS, a graft polymerization of allyl alcohol by microwave irradiation is operated.[187] Initiated by radicals, AGE polymerization afforded pendant epoxy groups on PDMS. Starting from that epoxy, two ways of introduction of a maleimide moiety on the PDMS were explored. It can be (i) a one-step addition of NH_2-PEG-Maleimide or (ii) a two-step modification using first diaminopropane, then reacting the resulting amino function with NHS-PEG-Maleimide[181] to finally obtain a Maleimide-PDMS, in both case (Fig.37, pathway D).

4. Reaction of unmodified PDMS with radicals, Y = N_3

Bifunctional azido-containing spacers can be advantageously grafted on unmodified PDMS by UV activation at 320 to 350 nm. For example, the azido function of sulfosuccinimidyl 6-(4'-azido-2'-nitrophenylamino)hexanoate (Sulfo-SANPAH)[178] turns into a nitrene upon UV treatment, which is able to react with PDMS. Finally, it gives a sulfoNHS-ester activated PDMS, which may react with any nucleophile function of peptides (Fig.3, pathway E). It is worth noting that NHS and sulfoNHS esters present the same reactivity, the later displaying a better water-solubility. In the same way, 4-azido-2,3,5,6-tetrafluoro-benzoic acid (AFB) was grafted on PDMS, and its carboxylic acid function was reacted with ethyl(dimethylaminopropyl)carbodiimide/NHS (EDC/NHS) to obtain another type of NHS ester functionalized PDMS.[176]

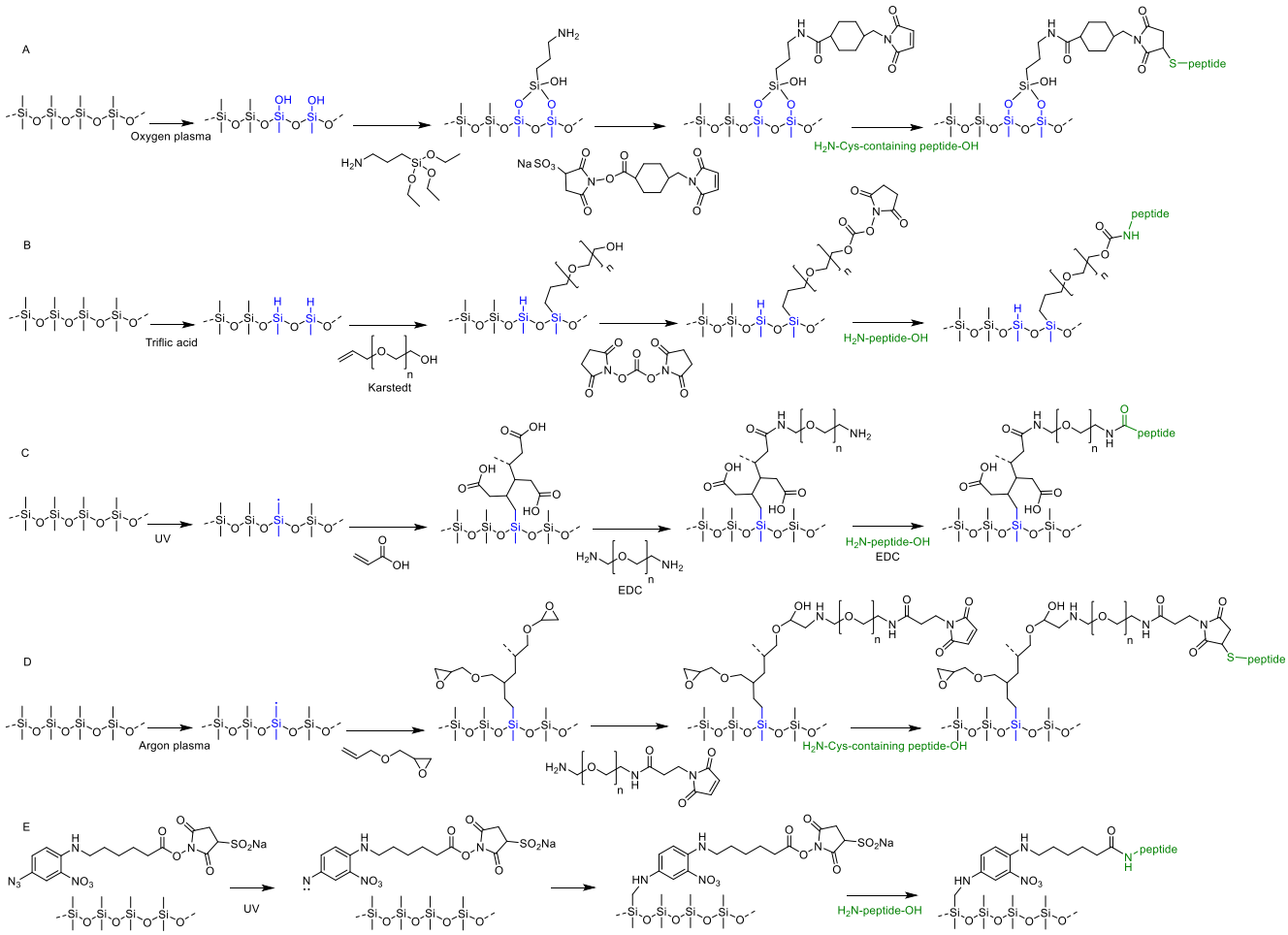

Figure 37.Examples of multistep preparation of peptide-grafted PDMS. A. PDMS activation by oxygen plasma followed by APTES grafting. Peptide is immobilized through one of its carboxylic acid after activation (III.c.1); B Si-H are generated on PDMS by triflic acid treatment. Hydrosilylation of allyl-PEG yields an alcohol function. Peptide is grafted through carbamate bond with one of its primary amine (III.c.2) using carbonyldimidazole; C. Radicals generated by UV irradiation reacted with acrylic acid. Peptide is grafted with one of its amino group via a diamino spacer using EDC activation; D. Radicals generated by plasma initiated the polymerization of allyl glycydyl ester. Pendant epoxy function reacted with amino maleimide bifunctional spacer which can handle a Cys-containing peptide by a Michael addition (III.c.3); E. Radicals generated by UV irradiation on azido function of a functional molecule reacted with methyl group of PDMS. Pendant NHS function reacted with primary amine function of peptide (III.c.4).

d. Grafting of peptides on functionalized silicones

Ideally, covalent immobilization of a peptide on functionalized PDMS should proceed in a controlled manner to guarantee the suitable orientation of the peptide on the material, and to avoid undesired reactions with peptide side chains, which could affect its bioactivity. This can be achieved in two ways: either by using chemoselective reactions involving two mutually reactive moieties present on the peptide and on the PDMS (i.e. chemoselective ligation between Z and W), or by using a peptide presenting a single unprotected reactive function. While the use of a temporary protection (e.g. on Lys side chains) is theoretically possible during the grafting step to control the regioselectivity of the covalent bond, in practice chemists prefer using unprotected peptides displaying a single reactive function (e.g. the N-terminus amine, the thiol of cysteine). Indeed, removal of protecting groups on a PDMS grafted peptide would probably raise coating and silicone stability issues depending on the pH, the solvents, and the reagents required.

Amide forming chemistries, whatever the amine or the carboxylic acid is present on the polymer (e.g. Z = NH_2 or Z = CO-NHS), fall in the first category and are mostly used when a single reactive function is present on the

peptide. If any 'click reaction' may theoretically be used for chemoselective immobilization of peptides, only Michael addition was employed so far to obtain peptide-grafted PDMSs. The last step of peptide grafting is preferentially performed in water, avoiding the used of any organic solvent, which could be detrimental to cell survival, but also facilitates the handling of unprotected water-soluble peptides.

1. *Active ester functionalized PDMS. Z = CO-NHS (or CO-Act, Act being electron attractor and leaving group), W = NH_2*

Any suitable nucleophile, including alcohols and phenols, may react with activated carboxylic acids such as NHS-esters. However, amines are much more reactive at pH close to neutrality resulting in a rather good chemoselectivity. Consequently, NHS ester-modified PDMS materials were reacted with a variety of primary amine-containing peptides (i.e. W = NH_2). Peptides derived from fibronectin promoting cell adhesion by interacting with integrin receptors are commonly used to enhance the cell-interacting properties of PDMS. For example, H-RGDS-OH and H-YIGDS-OH were coupled to PDMS-PEG-OCONHS.[172] H-RGDS-OH and H-GYRGDS-OH were reacted with PDMS displaying a sulfoNHS ester on PEG[173,174] and H-RGD-OH or H-GRGDSP-OH were reacted with sulfo-SANPAH treated PDMS.[178] Other antimicrobial peptides, Histatin 5 (H-DSHAKRHHGYKRKFHEKHHSHRGY-OH) and two of its derivatives Dhvar 4 (H-KRLFKKLLFSLRKY-OH) and Dhvar 5 (H-LLLFLLKKRKKRKY-OH), as well as polyLeu, polyHis and polyArg, were also grafted on PDMS-CO-NHS creating then an anti-biofilm surface used especially in Robbins device.[176]

Instead of using a pre-activated PDMS-CONHS, PDMS-COOH can be activated by a coupling reagent to generate *in situ* an active ester suitable for peptide coupling.
In the case of an amino acid modified PDMS surface, the grafting of an amino peptide is performed using a coupling reagent such as EDC, and an activating functional NHS group. This coupling chemistry has been applied using Histatin 5 and other derivatives on amino acid or AFB modified PDMS.[176] The final peptide silicone obtained can be used for the design of Robbins modified microfluidic devices, in order to avoid the formation of bacteria biofilm.
All these reactions have been performed by incubation of NHS-ester PDMS using peptides dissolved in aqueous buffers, for several hours at room temperature. Noteworthy, the authors have used peptides bearing a single primary amino group (i.e. the N-terminus). This trick allows avoiding the use of temporary protections, for example on lysine side chains, which should have been removed after the grafting step.

2. *Amine functionalized PDMS, Z = NH_2 W = carboxylic acid*

This reaction is similar to the one described in the previous paragraph (i.e. III.d.1), the reactive functions being switched between the partners. Here, PMDS bears the amino group instead of the peptide. This situation is not as straightforward as the previous one. Indeed, carboxylic acids present on the peptides have to be activated. This leads to uncontrolled peptide intermolecular cross-linking between unprotected side chains (mainly Lys, Ser, Thr and Tyr). Despite these drawbacks, EDC was used to activate carboxylic acids of type 1 collagen to react with PDMS-PEG-NH_2 yielding bio-compatible protein-grafted PDMS surface with improved adhesion of fibroblast cells.[156]

3. *Isocyanate functionalized PDMS, Z = N=C=O, W = NH_2*

PDMS functionalized with amino groups can be readily converted into reactive PDMS-isocyanates by triphosgen. This reaction has been performed on PDMS previously treated with APTMS. Isocyanates are highly reactive, and by reaction with amines and alcohols lead to ureas and carbamates respectively, thus being non-chemoselective. Peptides bearing a single primary amine function (e.g. H-RGD-OH) [169] are reacted with isocyanate functions of PDMS to obtain silicone micro channels suitable for cell immobilization.

4. *Alcohol functionalized PDMS, Z = OH, W = NH_2*

In the case of PDMS modified by polymerization of allyl alcohols, the resulting functions available at the surface are primary alcohols. The hydroxyl group can be converted to a leaving group by 2,2,2-trifluoroethanesulfonyl chloride.[187] Free amino N-terminus groups of H-YIGSR-OH, H-RGDS-OH, H-PDSGR-OH or H-PHSRN-OH, were then able to react with modified PDMS by nucleophilic substitution. The resulting material was designed for cornea replacement and the adhesion of corneal epithelial cells was improved with the grafting of some combination of peptides ligands derived from laminin and fibronectin.

5. *Alkene functionalized PDMS, Z = Maleimide or vinyl, W = SH*

The previous methods of immobilization of peptides on PDMS are not chemoselective and have to be used carefully, preferring peptides having a single unprotected amine function. In contrast, thiol-ene reactions (e.g. free-radical or Michael additions) are biorthogonal reactions. When no other thiol is present (i.e. when the peptide carries only one Cys residue), cysteine-containing peptides can be grafted chemoselectively on alkene-modified PDMS. Among these reactions, Michael addition involving maleimides as α,β-unsaturated carbonyl acceptors, are the most popular. As example, Ac-CGGEGYGEGRGDSPG-NH_2 peptide was immobilized on Maleimide-PDMS to get surface suitable for cardiac fibroblasts adhesion and study.[167,168] Antibacterial peptides were also grafted on maleimide-PDMS: a catheter was functionalized with CysLasioIII peptide (H-CVNWKKILGKIIKVVK-NH_2) [181] and peptide CRW11 (H-CWFWKWWRRRRR-NH_2)[180] was used to get an anti-biofilm PDMS surface. Interestingly, the same authors grafted CRW11 by nucleophilic addition on a polydopamine layer coated over PDMS.[188]

Radical thiol-ene reaction has been used to immobilize cysteine-containing peptides on a vinyl modified PDMS [i.e. PS-b-P(DMS-VMS)]. A solution containing a short oligolysine whose side chains are modified with diethylene glycol moieties [i.e. Fmoc-[Lys($COCH_2(OCH_2CH_2)_2OMe$)]$_6$Cys-OMe][183] was sprayed over the vinyl modified silicone. Upon heating, the peptide was covalently grafted, probably through the generation of thiyl radical RS•. As expected, the final peptide-modified silicone showed interesting anti-fouling and avoided non-specific protein adsorption.

6. *Direct hybrid peptide grafting on PMDS functionalized with silanol, Z = Si-OH, W = $Si(Me)_2OH$*

As already stated, the creation of silanol groups at the surface of PDMS can be achieved easily by oxygen plasma treatment. Thus, the most straightforward way to prepare peptide-grafted PDMS is to use hybrid silylated peptides, which may react by sol-gel hydrolysis and condensation on silanols to form Si-O-Si bonds at the silicone surface.[165,166] The key point of the strategy is the synthesis of the hybrid peptide, in solution or on solid support, silylated at a suitable position.[189,190] However, once it is prepared, this strategy is straightforward as it does require neither successive chemoselective reaction, nor spacer addition. The modified PDMS is simply immersed into a solution containing the hybrid biomolecule for several hours at room temperature. Interestingly, this reaction proceeds chemoselectively allowing the use of any unprotected peptide sequences. Antimicrobial catheters were obtained by grafting short amphipathic peptides [i.e. [$SiOH(Me)_2$-$(CH_2)_3$NHCO-AhxArg-Arg-NH_2]. These devices have shown a superior efficiency compared to commercially available Ag-doped catheters.[165] Using the same technique, wound-healing dressings were prepared, using silylated peptides whose sequences were derived from ECM proteins.[166]

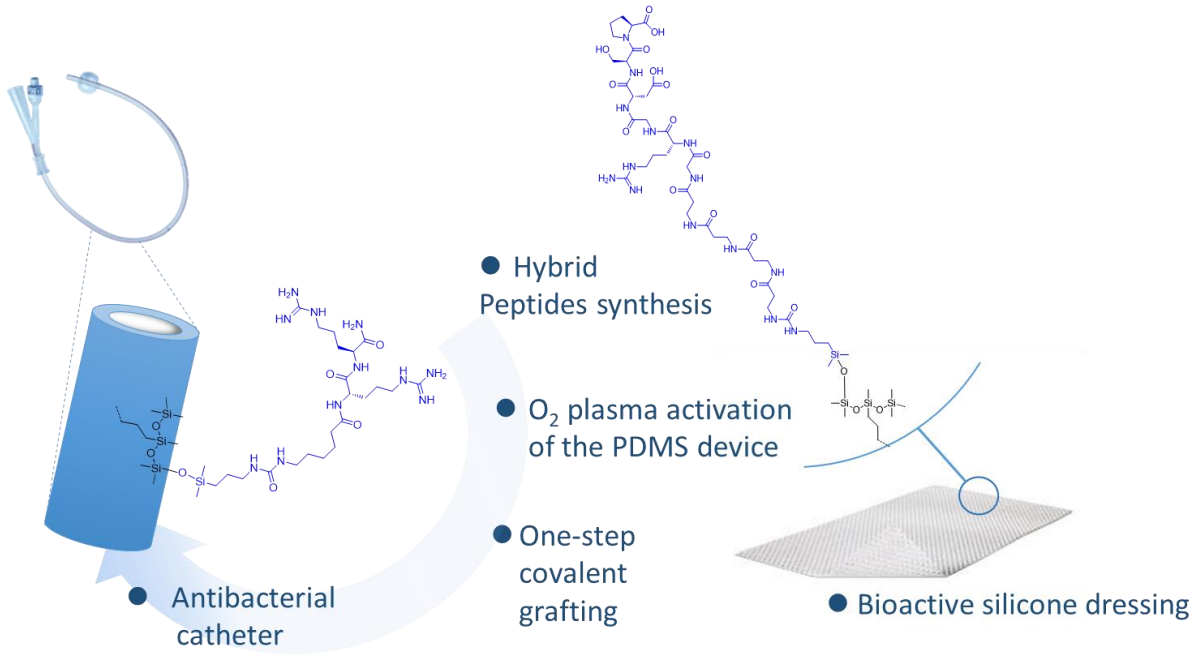

Figure 38. Direct grafting of hybrid silylated peptides on PMDS activated by O_2 plasma. The oxygen plasma generates Si-OH function at the surface of the PDMS. This enables the Si condensation of $Si(OH)Me_2$ silylated peptide. This functionalization method was applied to both silicone dressing[166] and catheter.[165]

Table 1. Summary of peptide sequences, functional groups on the activated PDMS (X), bi functional linker (Y, Z), on peptides (W), and applications of peptide modified-silicones.

Peptides	W	Z	Linkers	Y	X (*obtained by*)	Applications	Grafting density (pmol/cm^2)	ref
Silylated-Ahx-Arg-Arg-NH_2	$Si(Me)_2$-OH	/	/	/	Si-OH (*oxygen plasma)*	Antimicrobial silicone catheter	~30	[165]
Silylated peptides : H-(bAla)4-GRGDSP-OH, H-(bAla)4-EGLEPG-OH and Ac-Lys(H)-[Pro-Hyp-Gly]3-NH2	$Si(Me)_2$-OH	/	/	/	Si-OH (*oxygen plasma)*	Wound healing dressings	~60	[166]
Cystein-Oligopeptide modified by PEG or alkyl chain	SH	/	/	/	Vinyl *(functionalized PMDS obtained by copolymerization)*	Anti-fouling coating on glass slide	n.d.	[183]
H-RGD-OH	H_2N	S=C=N- (obtained from amine)	-APTMS-	$Si(OEt)_3$	Si-OH (*oxidation)*	Micro channel for cell immobilization	n.d.	[169]
Ac-CGGEGYGEGRGDSPG-NH_2	SH	Maleimide	-APTES-grafted with maleimide spacer	$Si(OEt)_3$	Si-OH (*water plasma)*	Flexible silicone membrane for cardiac fibroblast adhesion study	~30	[167,168]
H-YIGSR-OH, H-RGDS-OH, H-PDSGR-OH or H-PHSRN-OH	H_2N	HO-	-Poly(Allyl alcohol)-	Allyl	Si-OH *(microwave irradiation)*	Artificial cornea	~1	[187]
H-RGDS-OH, H-RDGS-OH and GYRGDS-OH	H_2N	NHS-CO	-PEG-	Allyl	Si-H (*triflic acid)*	Biomaterial for cell adhesion	~100	[173]
H-RGDS-OH and H-GYRGDS-OH	H_2N	NHS-CO-	-PEG-	Allyl	Si-H (*triflic acid)*	Biomaterial for cell adhesion	60	[174]
H-RGDS-OH, H-YIGSR-OH	H_2N	NHS-CO	-PEG-	Allyl	Si-H (*triflic acid)*	Biomaterial for cell adhesion	~30	[172]
H-RGD-OH	H_2N	sulfoNHS-CO-	-Azido hexanoic-	Azide	Si-CH_2• *(UV)*	Biomaterial for cell adhesion	~10	[178]
Dhvar 4 and 5, Histatin 5, poly(L, H or R)	H_2N	NHS-CO-	-Poly(AFB)-	Azide	Si-CH_2• *(UV)*	Anti-biofilm surface used in Robbins device (bioassays)	n.d.	[176]
Dhvar 4	H_2N	HOOC-	-PAA-	Allyl				
Collagen, type 1	COOH	H_2N-	-PEG-	Allyl	Si-CH_2• *(argon plasma)*	Biocompatible PEG- stabilized surface	n.d.	[156]
H-CVNWKKILGKIIKVVK-NH_2	SH	Maleimide	-PEG-	Allyl	Si-CH_2• (*argon plasma)*	Antimicrobial silicone catheter	~3500	[181]
H-CWFWKWWRRRRR-NH_2	SH	Maleimide	-PEG-	Allyl	Si-CH_2• *(argon plasma)*	Anti-biofilm surface	~400	[180]

n.d. non determined

IV. Conclusion and future developments

If protein can be adsorbed quite easily on bare PDMS surface, it is not the case of smaller peptides which are quickly once in contact with aqueous media. Therefore, to achieve a long-term effect, covalent grafting is required. Chemical modification yields a relatively homogenous repartition of the peptide on the surface, as a monolayer, and improve the stability over time. For that purpose, a wide range of organic functions can be introduced on PDMS in a few steps. However, only a small number of bioorthogonal ligation reactions have been used so far to conjugate peptides on the material surface. There are still a lot of possibilities to explore digging into the 'click' reactions tool-box, for peptide chemists.

Grafting densities obtained by covalent methods are much lower than those obtained by adsorption. They typically range from one to one hundred picomole per cm^2 depending on the anchoring chemistry and the peptide used. Roughly, it corresponds to a monomolecular layer of peptide on the PDMS surface. Higher covalent grafting densities can be expected (e.g. above 500 pmol/ cm^2), if the peptide is not grafted directly on PDMS but on a brush-like polymeric structure grafting from the PDMS.[180,181] Besides reported post-functionalization approaches, an alternative one-step strategy can be considered to produce peptide modified PDMS. The first requirement is the synthesis of silylated peptide monomers. Depending on the nature, the position, and the number of silyl groups within the peptide sequence, different peptide-polymer geometries have already been obtained[191,192], when silylated peptide are used as the only monomers. Moreover, methyldihydroxysilane-modified peptides could also be copolymerized with dimethyldichlorosilane (Me_2SiCl_2) to get peptide-functionalized silicone oils with a PDMS-like backbone (Figure 36, Direct Synthesis).[193] Beyond a single bioactive peptide, copolymerization with other silylated polymers like PEG, fluorophores, drugs, could be considered to afford multifunctional PDMS-based materials with unprecedented properties.

References annotation:

[157] °: Two different ways of PDMS functionalization are presented, leading to either covalent or non-covalent attachment of an enzyme, the Trypsin. Acrylic acid is used as linker, grafted by UV activation and either activated by ECD/NHS chemistry or modified by PDDA (Poly(diallyldimethylammonium chloride)).

[165] °: A direct grafting of an antimicrobial peptide is described, using a simple activation of the PDMS by oxygen plasma. The main point is the use of silylated peptides, without any linker or further activation.

[176] °: Two types of UV light activation of PDMS are described. Authors present the direct activation of PDMS surface and the activation through a photo-initiator (i.e. benzophenone).

[178] °: UV light activation of azido groups is presented here. Upon irradiation one side of the hetero-bi functional spacer is converted into nitrene functions, which are able to react with PDMS methyl groups.

[183] °: The synthesis of vinyl functionalized PDMSs by copolymerization with a vinyl silane are presented. The resulting vinyl PDMS are reacted with N-ter cysteinyl-peptides.

[194] °: Another copolymerization method is the use of classic silane monomers, with acrylate-based monomers with a cross-linker bearing both silane and acrylate functions. The epoxy modified PDMS surface is then coupled to small glycine peptides.

[187] °: This is the only example of hydroxyl-modified PDMSs obtained by microwave plasma polymerization of allyl alcohols. After activation with tresyl chloride, modified PDMS are reacted with the free N-ter of peptides.

Chapter 2: Development of silylated peptides synthesis by hydrosilylation

Chapter 2: Development of silylated peptides synthesis by hydrosilylation.

As explained in Chapter 1, we defined hybrid silylated peptides as peptide sequences displaying at least one silane group linked by a C-Si bond to the peptide. Hybrid silylated peptides can be obtained from alkoxysilanes or chlorosilanes (i.e. Si-OR or Si-Cl respectively) precursors whose hydrolysis affords hydroxysilane. Such compounds can condense with other silylated partners to get siloxane (Si-O-Si) bonds in chemoselective conditions, compatibles with other biomolecules including protein. These hybrid precursors are particularly attractive for direct surface functionalization avoiding the use of multistep reactions. As example, they can be covalently attached by condensation to hydroxyl activated surfaces (SiOH) such as silica glass[184,195–197] or silica nanoparticles[198,199] but also metal oxides (e.g. TiO_2[200]) or activated silicone.[141,165,183,188] As example, NPs can be modified by grafting of silylated compound[198] or directly functionalized (one pot synthesis) by mixing all precursors during the NPs preparation.[199] Besides, silylated peptides may react together in soft conditions, eventually in the presence of other silylated species (e.g. drugs, biopolymers, probes) to get novel peptide-based materials and architectures. For instance, hydrogels can be obtained by hydrolysis and polycondensation (sol-gel process) of multi-silylated peptides alone[201,202] or mixed with other hybrid biomolecules such as PEG moiety. The final material will have the peptide biological properties as well as the mechanical properties of the hydrogel optimized by the ratio of hybrid precursors.

In fact, the final structure of the material obtained from these hybrid precursors depends on the type of silane used (e.g. $SiMe_2Cl$, $SiMeCl_2$, $SiCl_3$, $SiMe_2OEt$, $SiMeOEt_2$, $Si(OEt)_3$) and the number of silane groups available on the precursor part. For example, a hybrid compound with just one dimethylalkoxysilyl group can only dimerize. However, with two dimethyl alkoxysilane functions, it would be able to condense into a linear chain forming a silicone based polymer. The formation of silicone based polymer is also the result of the condensation of one methyl dialkoxysilane function, leading to comb-like polymer. Finally, 3D networks like hydrogels, are obtained from the condensation of a blocks bearing one or several trialkoxysilane moieties (Figure 39).
In the nomenclature, there are three different class, M, D and T in function of the number of alkoxy groups borne by the silicon. Besides, a number indicates the degree of condensation, 0 being the non-condensed state. So, the fully condensed states are M^1, D^2 or T^3 (Figure 39).

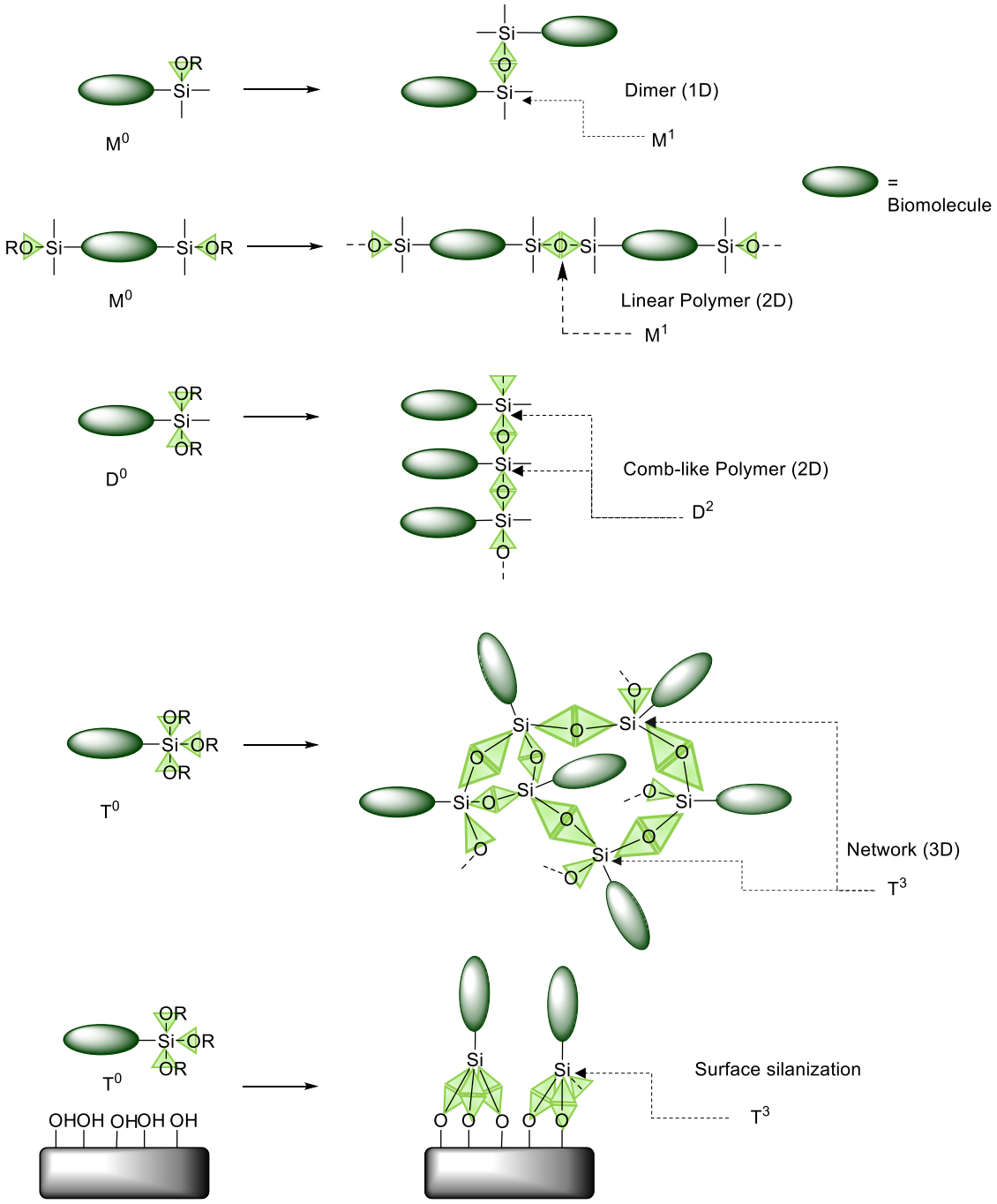

Figure 39. Different types of materials obtained from the condensation of hybrid biomolecules.

In this PhD work, we planned to prepare directly linear PDMS functionalized with silylated biomolecules by copolymerization. These hybrid macromonomers needed to be silylated in order to be able to copolymerize by condensation with dichlorodimethylsilane and so lead to linear polymer (D^2) (Figure 39).

Before material synthesis, the first challenge was to prepare the hybrid peptides. Peptide synthesis is well described in the literature, either on solid support or in solution by diverse strategies (e.g. Fmoc/tBu, Boc/Bzl, Z/tBu…) using various types of N-ter, C-ter and side chains protecting groups and resin-linkers. Thus, the most delicate point was the introduction of the silyl group at a desired position within the sequence.

Many types of reactions can be envisioned to attach a silylated reagent to a biomolecule. However, commercially available isocyanate reagents are probably the most popular. First, they are readily available with various silyl groups e.g. ($SiMe_2Cl$, $SiMeCl_2$, $SiCl_3$, $SiMe_2OEt$, $SiMeOEt_2$, $Si(OEt)_3$), second they react easily with free amino groups (e.g. N-terminus or Lys side chain of a peptide, Figure 40).

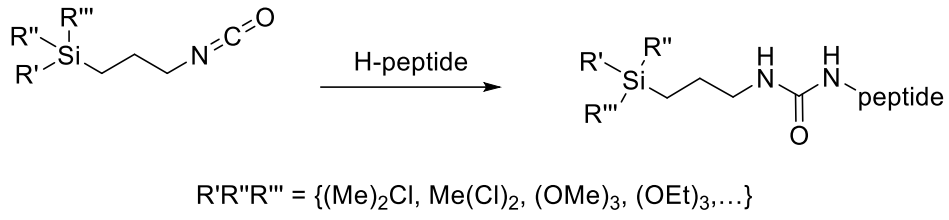

$R'R''R''' = \{(Me)_2Cl, Me(Cl)_2, (OMe)_3, (OEt)_3,\ldots\}$

Figure 40. Peptide silylation by reaction between N-ter amino group and isocyanate.

On the other hand, these convenient reagents present several drawbacks. First, they impose the addition of a five atoms long spacer between the reactive function of the biomolecule (e.g. the free amine) and the silicon atom. The spacer itself can be problematic, generating unwanted flexibility or distance between the bioactive sequence and the surface for example. In addition, introduction of supplementary urea function, which is undoubtedly involved in hydrogen bonds interactions, may modify the material structure in unwanted way. The use of isocyanate also requires synthetic caution. Indeed, isocyanates, being not chemoselective, may react with diverse functions of the peptides (i.e. other amines or alcohols groups). It means that protecting groups have to be placed on all other potential but unwanted anchoring points. Such protections have to be removed after the silylation, often by TFA treatment. In these conditions, it is not possible to keep intact the alkoxysilane or chlorosilane moieties, which hydrolyze into their corresponding silanols. Finally, in some cases when the silylation is done in the center of the peptide sequence, an orthogonal protection such an allyloxycarbonyl (Alloc) group has to be placed on the amine function in order to be later modified by the isocyanate.

To avoid all these drawbacks, we thought about another silylation strategy: the hydrosilylation of alkene containing peptides. This reaction could present a direct and customable method to obtain silylated compounds from an organosilane (RSiH) and an alkene, catalyzed by an electron-rich metal complex such as platinum complex.

Interestingly, this type of silylation does not imply a long spacer. Additionally, as it involves an unsaturated bond which is not normally present in peptides and proteins, it could proceed in a chemoselective way without requiring a panel of protecting groups on the reactive side chains of the amino acids. Moreover, this method does not add a urea function that could affect the structure and morphology of the subsequent material.

In this chapter, we will focus on the hydrosilylation of amino acids and peptides. This silylation method seemed promising to obtain silylated peptides in a straightforward way. Besides, it could be operated in chemoselective way during the peptide synthesis on solid support as long as an unsaturated bond (as side chain or end-group) was available. Taking into account all these considerations, we investigated the hydrosilylation of peptide sequences on solid support and in solution.

I. Hydrosilylation reaction

a. *Definition of hydrosilylation*

The hydrosilylation consist in the addition of an organosilane on an unsaturated group of an organic compound. Silane can be added to alkene, alkyne, aldehyde or ketone to yield alkyl silane, vinyl silane or silyl ethers and silyl esters respectively. The products of hydrosilylation reactions are organosilicon bearing an extra chain substituting the original proton (Figure 41). Various applications have been reached thanks to the hydrosilylation. It is the classic industrial way of the synthesis of polymers such as polydimethylsiloxane. It is also used for the depolymerization of some plastics, by reduction of ester function into the corresponding silylated alcohol [203] or used for the reduction of aldehyde and ketone.[204]

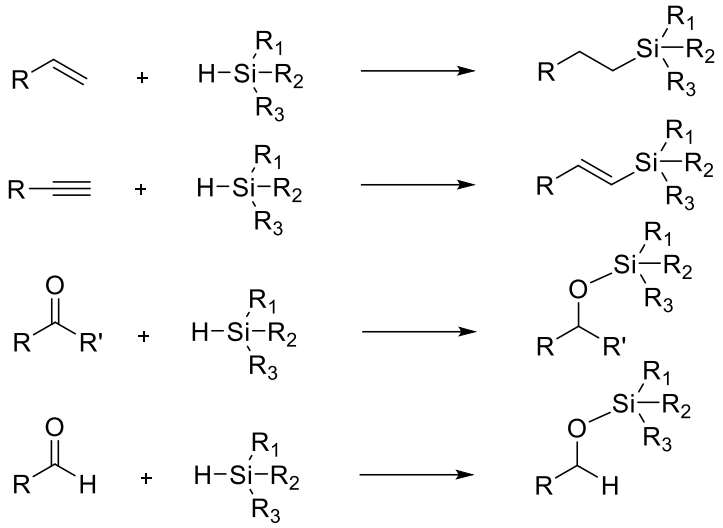

Figure 41. Hydrosilylation of common organic compounds.

The hydrosilylation requires a catalyst, which is generally an electron-rich transition metal complex: rhodium, platinum or nickel for example,[205] or Lewis acid[206] and organic bases such as trialkylamine.[207] The most common ones, both for research or and industrial purposes, are Platinum-based Karstedt's[208] and Speier's[209] catalysts (Figure 42).

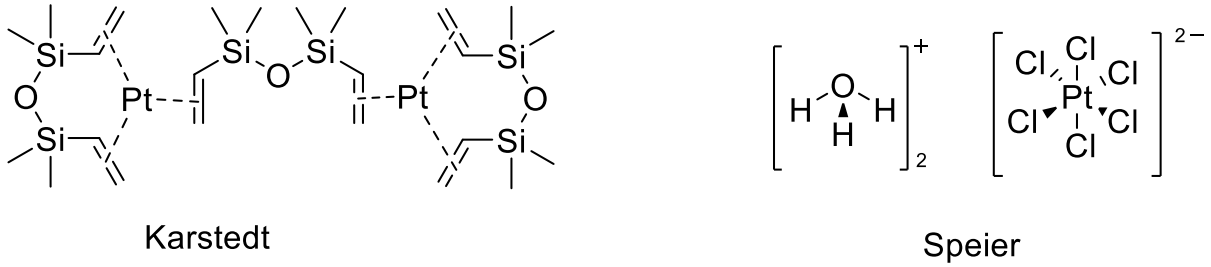

Figure 42. Karstedt's and Speier's catalysts.

Hydrosilylation mechanism is based on three components: the catalyst, the silane and the reactant (i.e unsaturated organic compound). The scope of the three components as well as the mechanism of the reaction have been the center of many studies. Indeed, organosilicons are highly valuable compounds for industrial applications such as water repellent coating or liquid silicone rubbers; it was of importance to enlarge the panel of substrates and to optimize the process to scale it up to the industrial level.

b. *Proposed mechanisms*

Several different mechanisms have been proposed for hydrosilylation depending on the reactivity of the metal complexes formed. The Chalk-Harrod mechanism (
Figure 43) is mainly an anti-Markovnikov addition, in which the intermediate metal complex includes a hydride (hydrogen bond to metal complex and so getting nucleophilic, basic or reducing properties), the organosilane and the alkene. After the bonding of the silane compound to the metal by an oxidative addition, the alkene insertion is done in this case directly on the metal complex. Then the final silylated compound is obtained by elimination. This kind of mechanism is favored by electron-rich transition metals, like platinum and rhodium.[205]

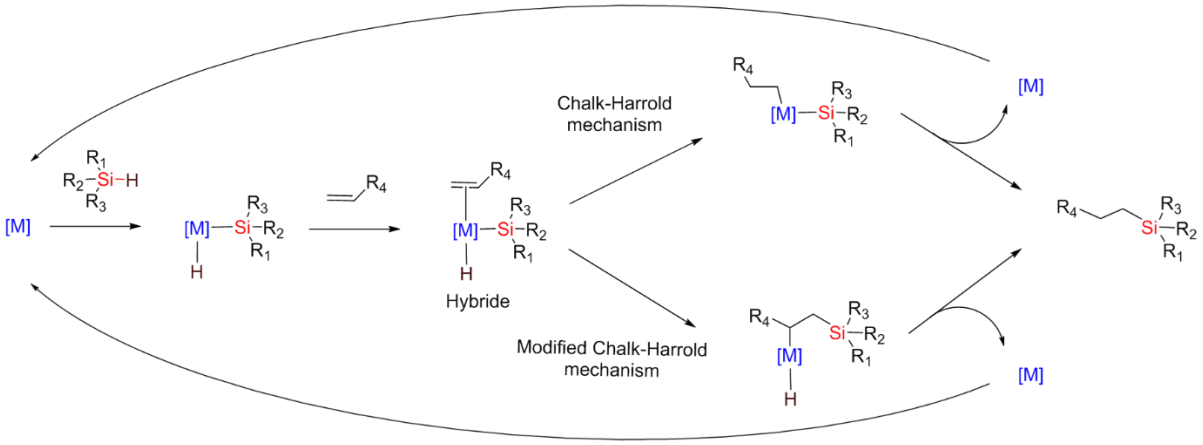

Figure 43. Chalk-Harrold and modified Chalk-Harrod mechanism.

In the modified Chalk-Harrold mechanism, the organosilane is also complexed to the metal in a first step and followed by the alkene, but here its insertion is done through the silane-metal complex bound. This intermediate metal complex is followed by a reduction/elimination by the alkene on the complex. It is more often applied to catalytic dehydrogenative silylation reactions.[210]

Hydrosilylation can be performed in various conditions of temperature, solvent and concentration. The classical solvents are non-polar solvents such as toluene or hexane for example.[211] However, it is not strictly reserved to them: other solvents, like dichloromethane and tetrahydrofuran, can be also found in the literature.[212,213] The hydrosilylation can be performed at room temperature or heated up to 100 °C. The more the reaction is heated up, the more it is efficient in term of conversion rate but at high temperature it may also lead to side reactions such as hydrogenation for example.[214]

c. *Catalysts*

The catalyst itself has been the object of numerous research.[215] As previously said, the most common ones are Karstedt and Speier's platinum-catalysts, widely used in the industry since the 50's and 70's (1973 for Karstedt and 1957 for Speier). Actually Karstedt catalyst is prepared from Speier's one.[216] The main advantage of Karstedt over Speier is its solubility. Indeed, Speier's catalyst is heterogeneous, used on silicon resin while Karstedt's one is dissolved into polydimethylsiloxane and then soluble in organic solvents. They are applied to the same type of hydrosilylation reactions. These two catalyst have a high turnover frequency (TOF), as well as a high selectivity. However, a new generation of platinum-based catalysts have been recently developed, more stable over moisture and light, such as N-heterocyclic carbene (NHC)-Pt complexes.[217–220] Other transition metals have proven good abilities to catalyze hydrosilylation such as: nickel,[210,221] manganese,[222] rhodium,[215 223] iridium[215] and rhenium.[215] They were discovered due to the industrial demand to decrease the catalyst and process prices. Indeed, these transition metal are cheaper than the Pt^0 even if its price have decreased in recent years.[224] It is worth noting that transition metals are not the only possibility for catalyzing hydrosilylation. Some non-metal catalyst have also been explored: radical initiators, tertiary amines and Lewis acids (e.g. borane catalyst $B(C_6F_5)_3$, $AlCl_3$, Bu_4PCl).[215] These Lewis acids catalysts enable a new approach for the insertion of the alkene : the H-Si bond is activated via η^1-coordination instead of the oxidative insertion described by Chalk-Harold.

d. *Unsaturated substrates, silanes and main applications*

In order to enlarge the scope of applications, diverse unsaturated substrates have been combined with different types of silane. The main substrates used for hydrosilylation are olefins, yielding an anti-Markovnikov silylation, reduction or even polymerization (
Figure 44).[205,225,226] A large panel of silanes and catalysts have been tested on them, from triethylsilane to phenyl-silane, triethoxysilane and even trichlorosilane, helping to get diverse hybrid molecules showing different

possibilities of silylation mechanism and reactivity.

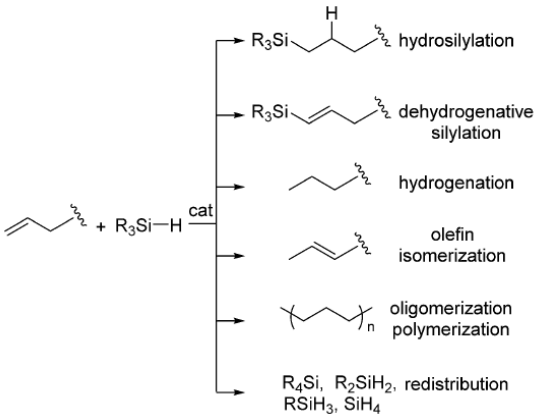

Figure 44. Results of hydrosilylation of olefins with a catalyst and a hydrosilane.[225]

Other substrates were also subjected to hydrosilylation: as polymers[203], fatty acids[227] or cyclohexene[228] for example. The polymers used as substrates are oxygenated plastics, polyesters or polycarbonates, depolymerized under iridium catalyst and mild hydrosilylation conditions, in order to lead to silyl esters or carbonates.[203] This example is presenting an efficient way to dispose plastics waste from bottle for example. The influence of the catalyst has been tested on the hydrosilylation of cyclohexene and allyl chloride by silyl chloride.[228] It finally proves that the catalyst has a role in the ratio of reduction observed after hydrosilylation.
Amino acids[229–231] have also been subject to hydrosilylation for diverse purposes. The amino acids silylation have been performed in the same research group. They developed a fast, direct and efficient method, catalyzed by platinum complex, to obtain silylated amino acids without losing the chirality of α-carbon. This method tolerates some N-ter and side chain protecting groups which is of prime importance for further coupling of the silylated amino acid (Figure 45).

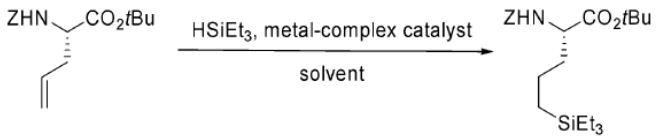

Figure 45. Synthesis of a triethylsilyl amino acid by hydrosilylation of Z-Allylgly-OtBu.[229]

However, this method has not been applied to chloro silane or alkoxysilane, besides, it has been developed on fully protected amino acid so the silane group have to be stable in the deprotection condition for further coupling. In our case, peptide coupling have to be done before the silylation since the chloro silane or alkoxysilane group can generate side reaction during coupling.
Then, two strategies for the synthesis of silylated peptide were proposed: either introduction of a silylated amino acid within the sequence, or direct silylation of the peptide (
Figure 46).[230] The peptide used as example is a tripeptide synthesized on solid support by SPPS. The hydrosilylation is done in dichloromethane, with Karstedt catalyst at 40 °C under microwave irradiations.

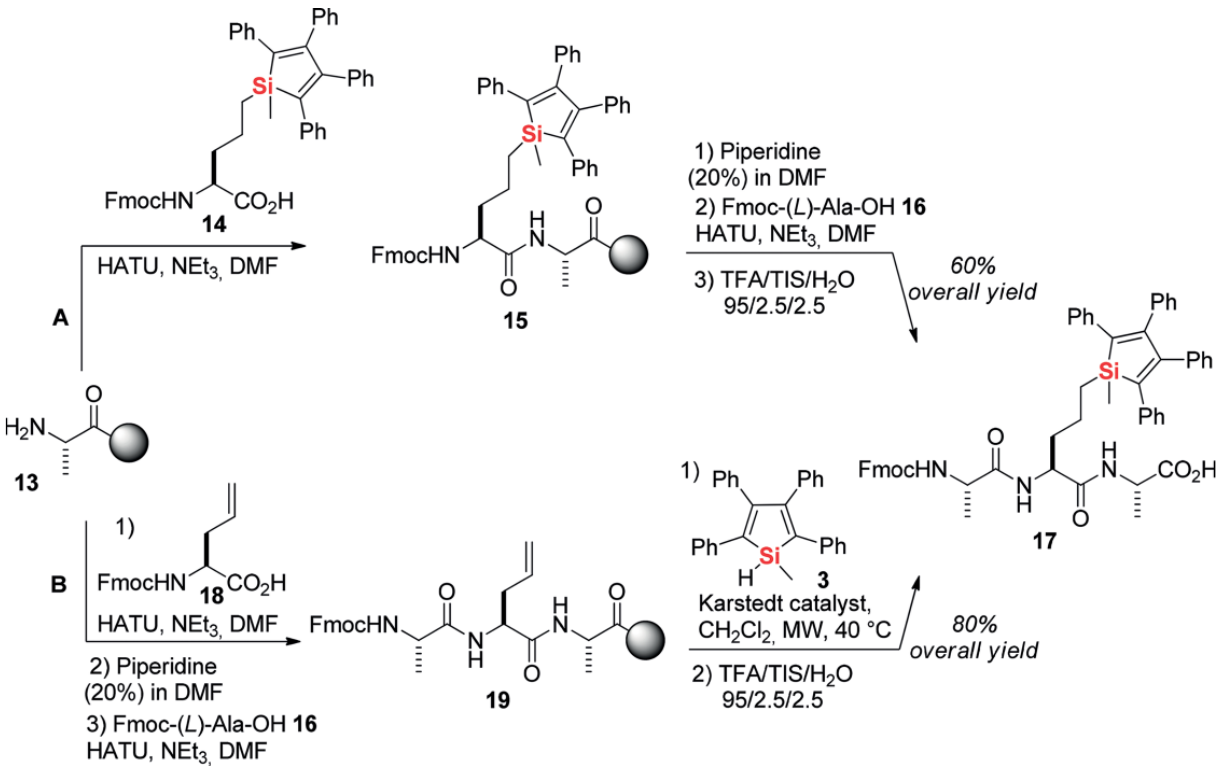

Figure 46. Two strategies developed for the synthesis of silylated peptide: either coupling of a silylated amino acid during the peptide synthesis or direct hydrosilylation of the peptide on solid support.[230]

However, this work was limited to triisopropylsilane and no chloro silane or alkoxysilane were used.

Hydrosilylation was also used to prepare pseudo-peptides, i.e. peptides with modified backbone. A regioselective hydrosilylation of enamide was developed for the direct synthesis of silicone-containing peptidomimetic analogues (Figure 47).[223]

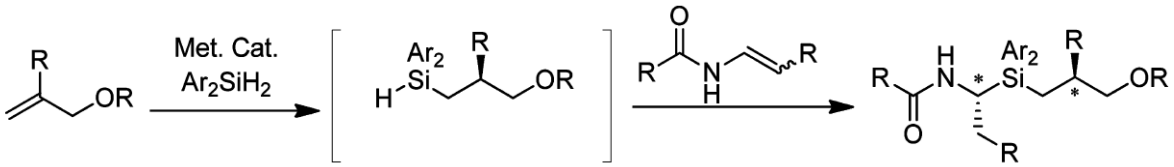

Figure 47. General pathway of synthesis of silicone containing peptidomimetic analog by sequential hydrosilylations.[223]

Such compounds were developed as enzyme inhibitors of angiotensin converting enzyme (ACE[232] or human neutrophil elastase (HNE) for example). The amide bond [CO-NH] present in natural R-Leu-Gly substrate was replaced by a silicon-containing bond R-Leuψ[Si(OH)$_2$-CH$_2$]Gly mimicking the transition state of the substrate. SiOH gave hydrogen binding to active site of the enzyme. Silicone-based peptidomimetics presented in Figure 48 turned out to be good inhibitors of HNE.

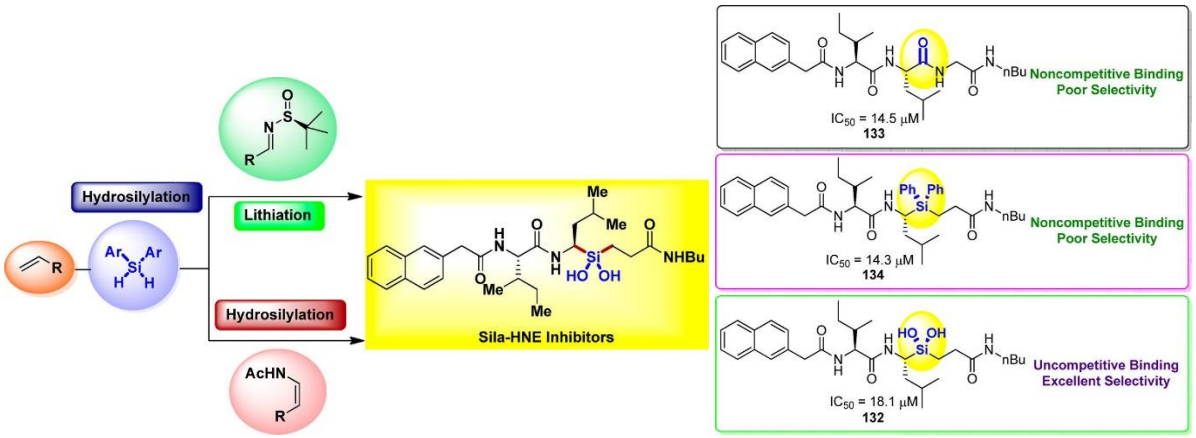

Figure 48. One pot, multicomponent synthesis of silicon-based peptidomimetic analogue.[232]

On the contrary of what was already described, we wanted to add a chlorosilane or an alkoxysilane either on one end of a peptide or one of its side chains. Ideally, our method had to be general enough to be applied on protected amino acids (which could be further incorporated within the course of peptide synthesis) or directly on an already prepared peptide containing at least one unsaturated bond either in solution (part II) or on solid support (part III). We first used chlorodimethyl silane ($HSiClMe_2$) as model silylating agent. The first attempts of hydrosilylation were performed in solution on Fmoc-protected amino acids bearing an allyl group, in particular Fmoc-AllylGly-OH and Fmoc-Lys(Alloc)-OH. Allylglycine (noted AllylGly) is a non proteinogenic amino acid bearing an allyl group on the α carbon of the glycine. In this study, it was used in (L) configuration. After determining the best experimental conditions, we tested this model on solid support along with other models compounds (Ac-Phe-AA-OH, Figure 49) and other silane reagents.

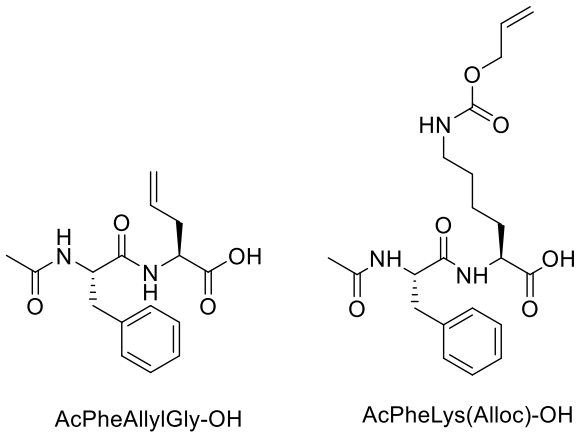

Figure 49. Dipeptide models used for hydrosilylation.

II. Optimization of the hydrosilylation process in solution

Dimethylchlorosilane was selected as first silylating agent to react with Fmoc-AllylGly-OH. Reaction with chlorodimethylsilane should afford dimethyl hydroxysilane derivatives, which may only form a single Si-O-Si bond, giving peptide dimers.[233] On the contrary of hybrid compounds presenting one dihydroxy or trihydroxysilane precursor, dimethylchlorosilane moiety limits the risk of unwanted premature polymerization (Figure 39).
We chose Karstedt's catalyst because of its well-known efficiency, its commercial availability, its reasonable cost (around 500 €/g of effective Pt^0) and its relative light and thermal stability over (from 20 to 200 °C). Several parameters were varied: the solvent, the duration, and the equivalents of silane and the substrate.
The presence of air and water is detrimental to the hydrosilylation reaction. In fact, the silane reagent can be easily hydrolyzed in contact with water to lead to condensed silanols. Thus the catalyst can be oxidized.
Consequently, two anhydrous solvents were used: DCM and chloroform thanks to their ability to solubilize amino acids or to swell resin beads used in SPPS. A precise concentration of the Fmoc-AllylGly-OH solution was fixed

($6.8.10^{-5}$ mol/L) and known numbers of equivalents of silane and catalyst were added. Microwave irradiation was used to heat the reaction at 50°C power was fixed at 150W. In order to do so, 10 mL tubes adapted to high pressure and able to be locked by septum cap were used. The tubes were filled up with anhydrous DCM containing 0.068mmol of amino acid with 5 mg of catalyst (0.010 equivalent related to Pt^0 quantity). Equivalents of dimethylchlorosilane were going from 10 to 20 and the duration from 1h to 15min.

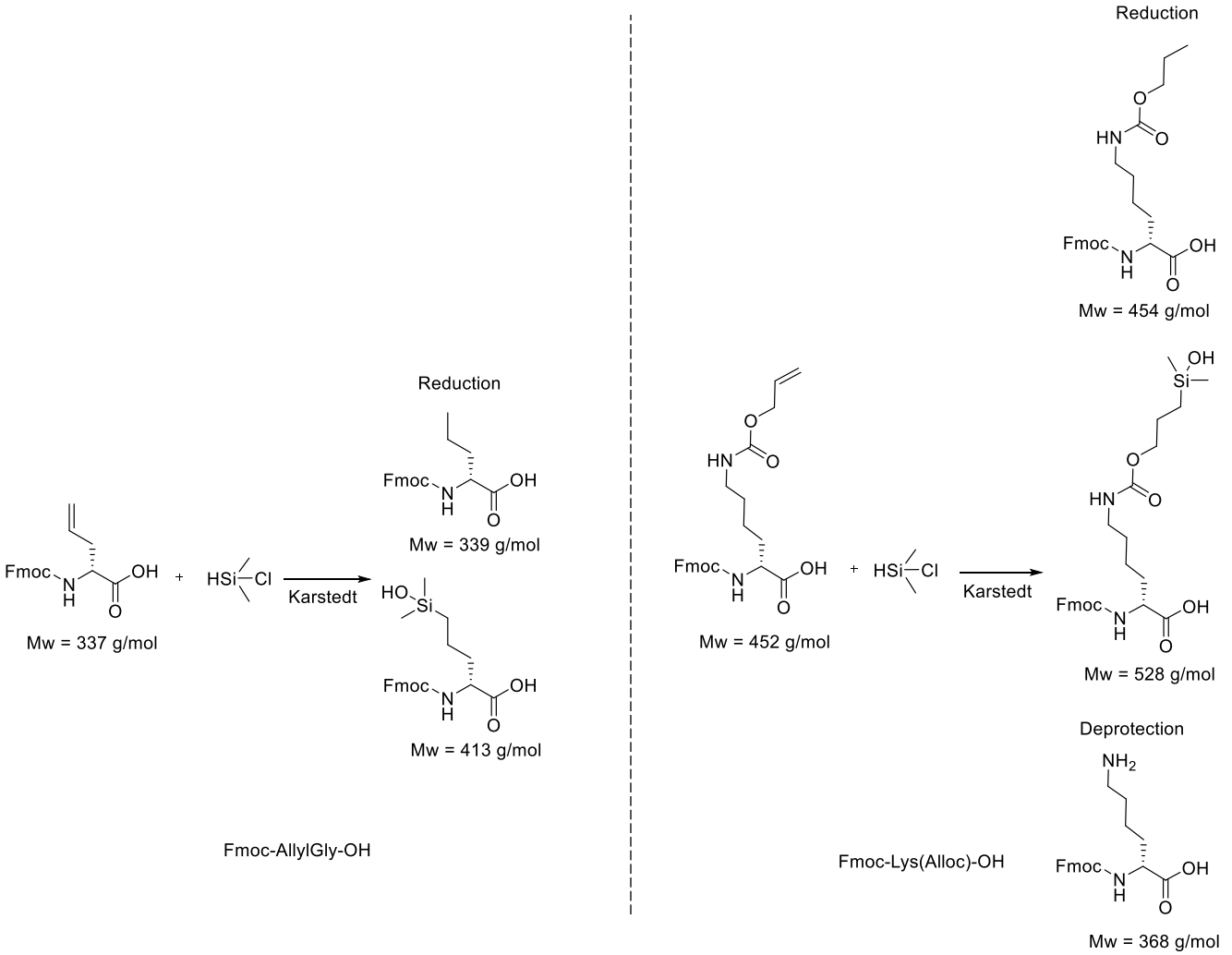

Figure 50. Hydrosilylation on Fmoc-AllylGly-OH and Fmoc-Lys(Alloc)-OH with $HSiMe_2Cl$ catalyzed by Karstedt catalyst. Side products identified.

Reaction mixtures were analysed by LC/MS to check the completion of the reaction. However, chlorosilanes species could not be detected as they are hydrolyzed during the preparation of the sample and the run performed in acetonitrile/water acidic (1‰ TFA) eluent system. It is worth noting that ethoxysilanes are more slowly hydrolyzed, but they are barely observed, except if they are injected immediately after their dissolution, and when short gradients (<3 min) are used for LC/MS analyses. Most of the time we only observed the silanols functions.
In mass spectrometry, we can expect to detect the m/z value of the protonated (e.g. $[R\text{-}SiMe_2OH+H]^+$) or cationized (e.g. $[R\text{-}SiMe_2OH+Na]^+$) silanol, with the presence of a strong siliconium ion (e.g. $[R\text{-}SiMe_2]^+$) coming from a water molecule loss from the protonated species. In our experiment, the expected hybrid amino acid is more hydrophilic than its allyl precursor. It elutes at a lower retention time when analyzed on reversed phases (RP), stationary phases used in HPLC (e.g. for Fmoc-AllylGly-OH, 1.70 min for the silylated compound over 1.72 min for the initial reactant and 1.76 min for its reduced version).
NB: all the reactions presented in this chapter, will be annotated by their original lab book ID.

Table 1. Results of hydrosilylation optimization in solution, heating by microwave irradiation at 50 °C and with 0.010 eq of Pt^0.

Reaction Id	Reactant	Solvent (Anhydrous)	$HSiMe_2Cl$ (eq)	Time (in min)	Composition % of the reaction [a]		
					Initial reactant	reduction	Silylation (polymerized)
JMA037	Fmoc-AllylGly-OH	DCM	20	30	0	12	88
JMA041	Fmoc-AllylGly-OH	DCM	20	15	5	9	16 (+70)
JMA042	Fmoc-AllylGly-OH	DCM	10	15	8	10	82
JMA043	Fmoc-AllylGly-OH	Chloroform	10	15	65	15	20
JMA039	Fmoc-Lys(Alloc)-OH	DCM	20	30	0	5	20 (+60) (+15% deprotection)

a: % were calculated by integration of peaks on UV spectrum at 214 nm

The silylation of Fmoc-AllylGly-OH proceeded quite well except for for the occurrence of a possible polymerization. (Table 1). 15 min and 10 equivalents of silane were sufficient to obtain 82% conversion of the Fmoc-AllylGly-OH into the silylated AA (**JMA042**).
Surprisingly, we noticed from **JMA042** and **JMA043** that the reaction in chloroform was less efficient: only 8% of initial reactant remained with DCM *vs* 65% in the chloroform in the same reactions conditions. This result is probably due to the non-polarity of the chloroform.
When the reaction was performed on Lys(Alloc), we noticed the partial deprotection of the Alloc (up to 15%, **JMA 039**). This is not surprising due to the recommended conditions of deprotection of Alloc. Indeed, in the literature, the removal of Alloc is operated with 0,1 equivalent of Pd^0 and 10 equivalent of phenylsilane ($PhSiH_3$) as the scavenger, for less than an hour.[234] So the action of Pt in solution with silane seemed to have the same effect even if it was less efficient than Pd^0 dedicated to Alloc removal.

On the LC/MS spectrum we could detect the deprotected Fmoc-Lys-OH (369 m/z, rt= 1.36 min), the silylated compound with a loss of water (528-17=511 m/z, rt= 1.84 min), a bit of reduced compound (455 m/z, rt= 1.88min). Oligomer species present a higher retention time than the monomers (i.e. 2.50, 2.67 and 280 min). Indeed, oligomerization may occur either during the hydrosilylation reaction (since the silane could have been hydrolyzed during the reaction by trace of water in the solvent) or in the sample vial even at pH ≈ 2 in water/acetonitrile (Figure 51).

In addition, a polymerization of the silane groups of the silylated amino acid was observed with the remaining non-reacted silane (Figure 52). The polymerization side product was obtained by poly-addition of the dimethylchlorosilane on the silanol function of the amino acid. Two options can be considered: either the silane function is turned into a silanol function by the presence of water and the heating process and then reacts on the silanol function of the silylated peptide by condensation; or the silane function is directly reacting on the silanol function of the silylated peptide. That can be explained by the very large excess of silane in solution (20eq), amplified by the fact that part of the Alloc was removed and not able to react anymore. Therefore, when operating hydrosilylation on solution, before any washing, the solvent was removed under vacuum leading to an increased concentration of silane.

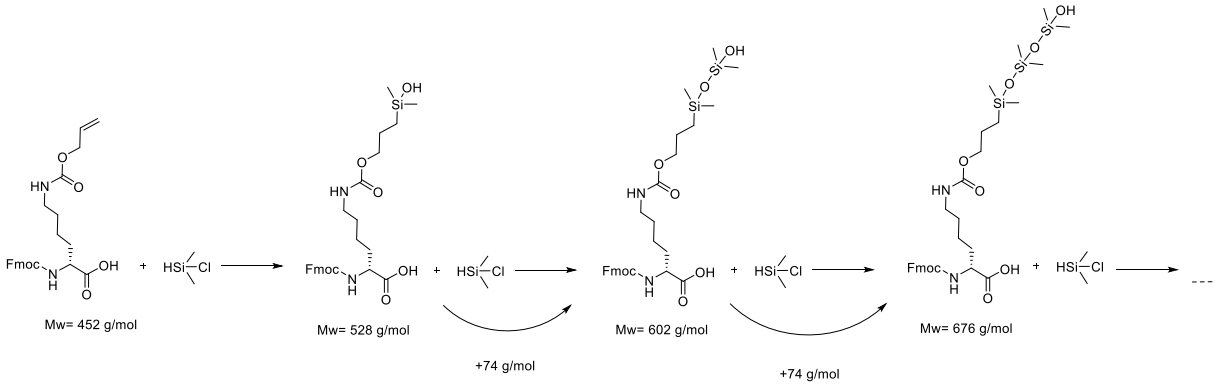

Figure 51. Polymerization of the $HSiMe_2Cl$ on FmocLys(Alloc)-OH.

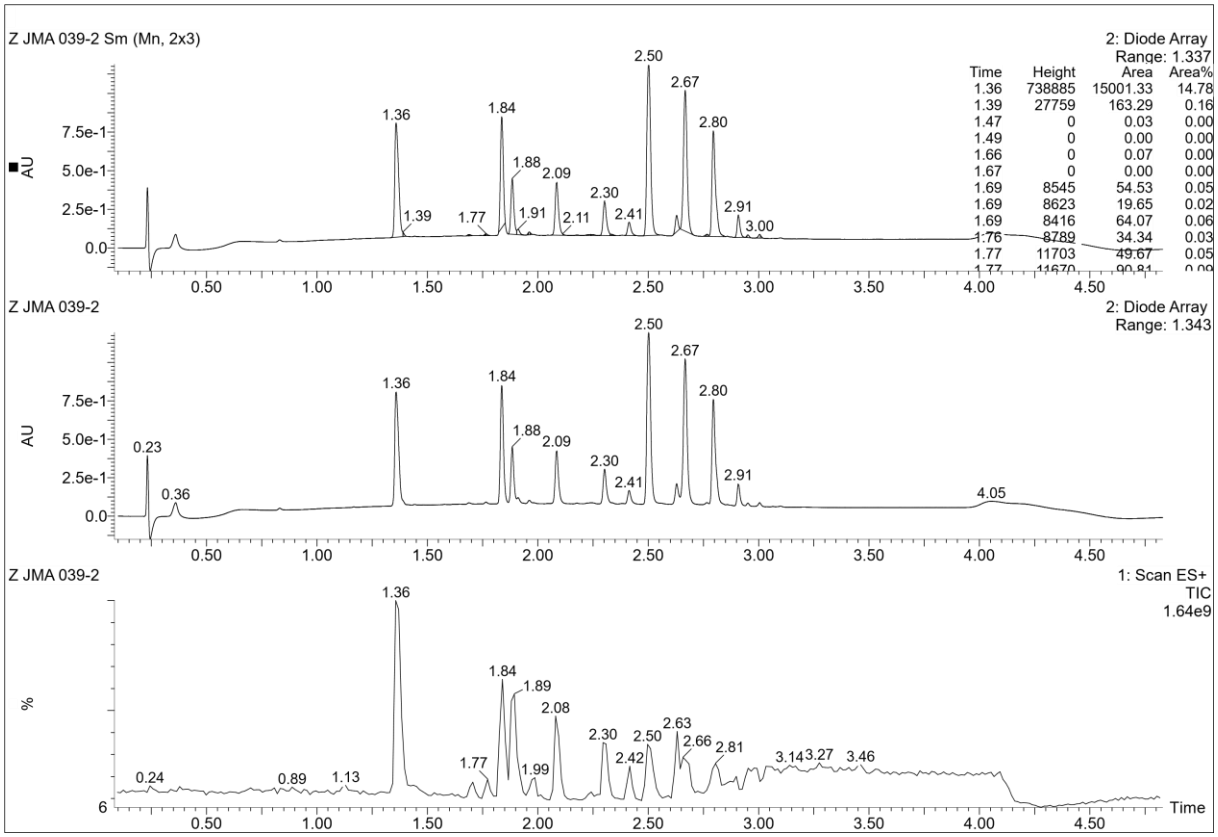

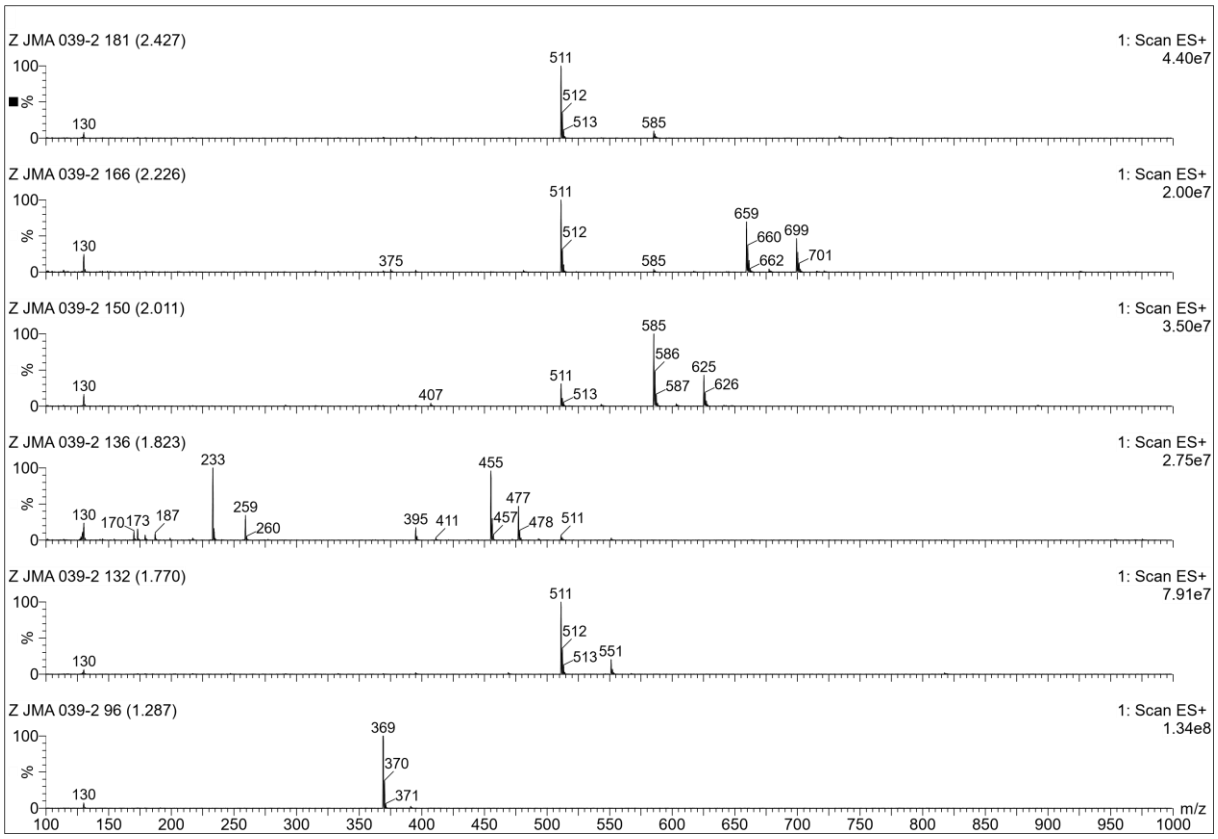

Figure 52. ESI + LC/MS of hydrosilylation on Fmoc-Lys(Alloc)-OH by $HSiMe_2Cl$ catalyzed by 0.010 eq of Pt^0, for 2h at 50 °C in anhydrous DCM; Top: chromatograms UV at 214nm and TIC, Bottom: MS spectra at 1.29, 1.77, 1.82, 2.01, 2.23 and 2.43 min.

The preliminary results obtained from hydrosilylation assays in solution were promising for AllylGlycine but highlighted some problems of deprotection of Alloc protected amino acids. Besides, in solution, washing and the storage of the product were more challenging as the concentration of the sample after reaction can lead to polymerization before the removal of the excess of silane. That is why the following assays were done on solid support.

III. Optimization of Hydrosilylation process on solid support

In order to be able to limit the polymerization of the $HSiMe_2Cl$ on the silylated amino acid, or the dimerization of the resulting silylated amino acid, the hydrosilylation was performed on solid support. The use of a solid support gave significant advantages: the stability over time if stored on the resin, the possibility to use high concentration of silane without favoring the polymerization between the silane and the silylated amino acid, and the ease of washing steps.

a. *Optimization of the reaction conditions on supported peptides containing AllylGlycine*

The Fmoc-Allylgly-OH substrate was coupled to RinkAmide AmphiSphere resin with 0.38 mmol/g loading (Figure 53). Rink amide linker is very common in SPPS and provides the final compound as a C-terminal amide. The AmphiSphere resin beads are amphiphilic, due to their composition (copolymer of PEG and PS). This matrix is superior to PS resin for the synthesis of long peptide as it allows both a good dispersion and swelling in organic solvent and less aggregation (i.e. hydrogen bond and hydrophobic interactions between peptide chains leading to a loss in coupling efficiency),[235] compared to pure PS resin.
However, AmphiSphere is quite hygroscopic and to avoid the unwanted presence of water, the resin was washed with anhydrous DCM then dried under vacuum before use. Therefore, we noticed that anhydrous DCM was better for washing than normal DCM, not only because it did not contain any water, but because classic DCM contained

amylene (2-methyl-2-butene) stabilizer. In presence of amylene, the Karstedt catalyst was totally quenched and unreactive. Consequently, anhydrous DCM was used for both hydrosilylation reaction and washing solvent. We used Karstedt's catalyst and chlorodimethylsilane at 30 equivalents, i.e. similar conditions used in solution. Duration and quantity of catalyst were decreased to a minimum.

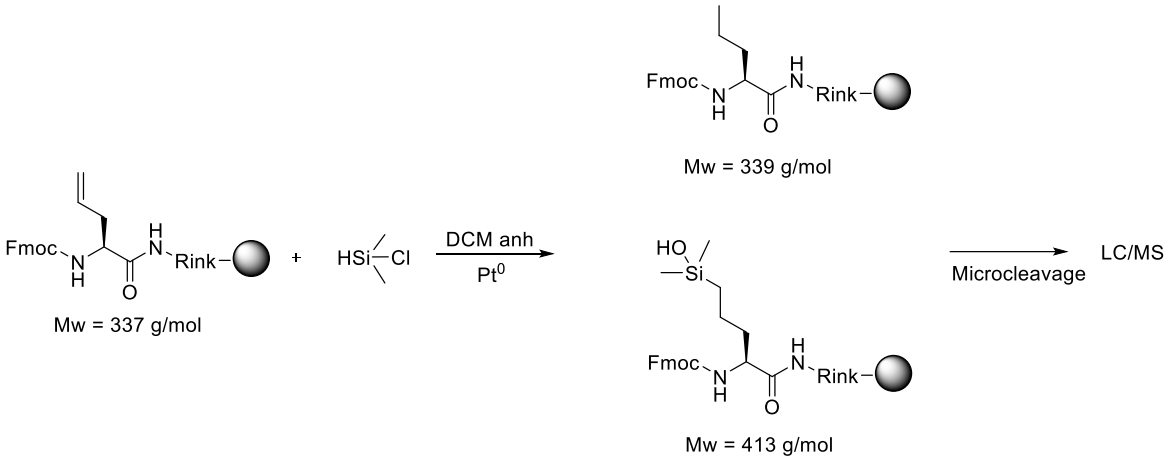

Figure 53. Hydrosilylation on FmocAllylGly-NH-Rink amide-AmphiSphere resin and its reduction

Table 2. Results of hydrosilylation on Fmoc-AllylGly-NH-Rink amide AmphiSphere resin with $HSiMe_2Cl$ and Karstedt catalyst in anhydrous DCM at 50 °C.

Reaction Id	Reactant	Eq in Pt^0	Eq in $HSiMe_2Cl$	Time (in min)	Composition %[a] of the reaction	
					Initial reactant	Silylated compound
JMA051	Fmoc-AllylGly-NH-●	0.010	30	720	0	100
JMA054	Fmoc-AllylGly-NH-●	0.010	30	240	14	86
JMA059	Fmoc-AllylGly-NH-●	0.005	30	240	2	98

●= Rink amide Amphisphere resin
a: % were calculated by integration of peaks on UV spectrum at 214 nm

After silylation, the supported compound was cleaved by TFA and analyzed by LC/MS. The retention times of starting FmocAllylGly-NH_2 and the associated silylated compound, Fmoc-((dimethylhydroxylsilyl)propane)Gly-OH but also the reduced side product Fmoc-propylGly-OH were very close (i.e rt= 1.67, 1.64 and 1.71 min, respectively) but we managed to calculate conversion %. Very high conversion was obtained ranging from 86 to 100 %. The reduced compound was not detected in these experiments. The results are then quite satisfying. So for the next step, the excess of silane will be optimized.

We also decide to change the model. As already explained, Fmoc protected derivatives of AllylGly, silylated and the reduced side product have very close retention time. To overcome this problem, we worked on AcPheAllylGlyNH_2 dipeptide (Figure 54). Indeed, the presence of the phenylalanine enabled UV detection while being less hydrophobic than the Fmoc group and thus allowed a better chromatographic separation of the starting material from the product and side products.
Silylation of supported AcPheAllylGlyNH_2 was tested with different quantities of silane and different durations. The results are presented in Table 3.

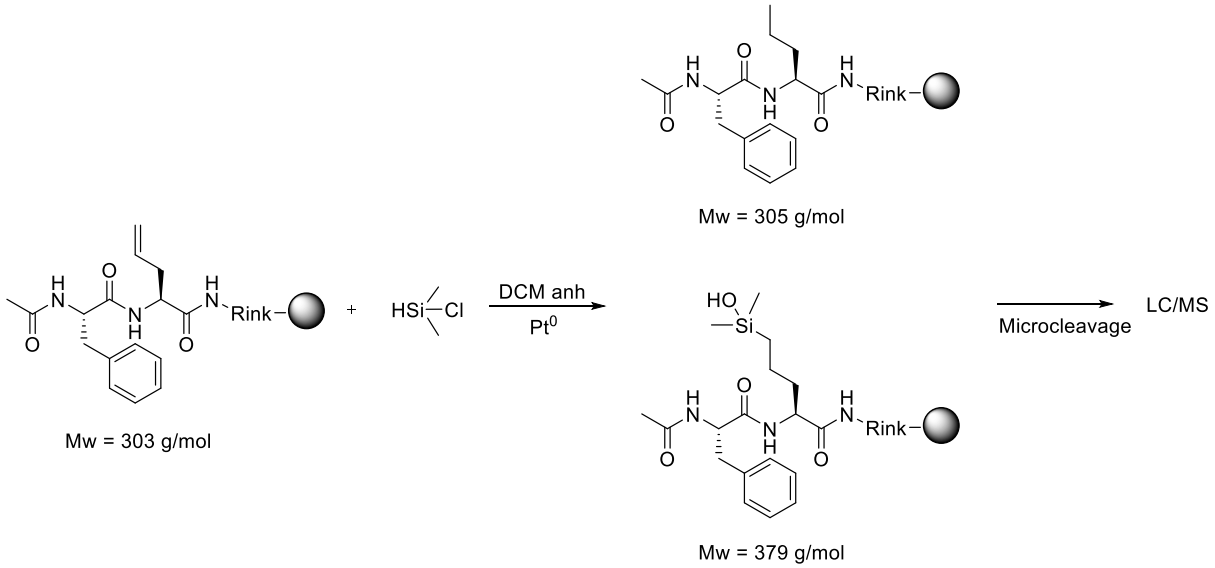

Figure 54. Hydrosilylation on AcPheAllylGly-NH-Rink amide AmphiSphere resin and its reduction.

Table 3. Results of hydrosilylation on AcPheAllylGly-NH-Rink amide AmphiSphere resin with $HSiMe_2Cl$ and Karstedt catalyst (0.005eq), in anhydrous DCM, at 50°C.

Reaction Id	Reactant	Eq in $HSiMe_2Cl$	Time (min)	Composition %[a] of the reaction		
				Initial reactant	reduced	silylated
JMA066	AcPheAllylGly-NH-●	30	240	0	8	92
JMA072	AcPheAllylGly-NH-●	20	120	0	5	95
JMA073	AcPheAllylGly-NH-●	10	120	7	10	83
JMA075	AcPheAllylGly-NH-●	10	60	100	0	0
JMA078	AcPheAllylGly-NH-●	20	60	0	3	97

●=Rink amide Amphisphere resin
a: % were calculated by integration of peaks on UV spectrum at 214 nm

We succeed to obtain up to 97% of the silylated compound with 20eq of silane and in 60 min (**JMA078**). A small amount of reduction (from 3 to 10%) was observed. A high conversion into silylated peptide was observed either for 120min with 10 eq of silane (**JMA073**) or for only 60 min using 20 eq of silane(**JMA078**). However, no silylation was observed with 10eq for 60min (**JMA075**). This can come either of a reaction problem as not reaction was observed at all (100% initial reactant) or with the quantity of silane, 60 min is not enough to event start the silylation.
Then, varying the ratio of silane at 20 or 30eq, we explored the ideal number of equivalents of catalyst (from 0.005 to 0.0025 eq of Pt^0) as well as the time (from 120 to 60 min) (Table 4). To add precise amount of catalyst, we prepared a stock solution of Karstedt catalyst (stabilized in polydimethylsiloxane in our case) in anhydrous DCM which was distributed as a precise volume.
The stock solution proved an efficient way to measure less than 5mg (less than 0.005 eq of Pt^0) with precision but we noticed that a loss of efficiency of the catalyst after 10 days, even if stored at 4°C under inert atmosphere. Thus, the catalyst solution was freshly prepared which unfortunately resulted in the waste of high quantity of catalyst.

Table 4. Results of hydrosilylation of AcPheAllylGly-NH-Rink amide AmphiSphere resin with $HSiMe_2Cl$ and in anhydrous DCM, at 50 °C.

Reaction Id	Reactant	Eq in Pt^0	Eq in $HSiMe_2Cl$	Time (min)	Composition %[a] of the reaction		
					Initial reactant	reduced	silylated
JMA077	AcPheAllylGly-NH-●	0.005	20	120	0	6	94
JMA080	AcPheAllylGly-NH-●	0.005 (100µL)	20	120	0	3	97
JMA097	AcPheAllylGly-NH-●	0.005	20	60	5	7	88
JMA095	AcPheAllylGly-NH-●	0.005 (100µL)	20	60	100	0	0
JMA096	AcPheAllylGly-NH-●	0.0025	20	60	100	0	0
JMA090	AcPheAllylGly-NH-●	0.0025 (50µL)	20	60	87	13	0
JMA101	AcPheAllylGly-NH-●	0.0025	30	60	100	0	0

●=Rink amide Amphisphere resin
a: % were calculated by integration of peaks on UV spectrum at 214 nm

The comparison of the direct use of Karstedt to the stock solution in the same conditions (0.005eq of Pt^0, 20eq of silane and 120min), respectively **JMA077** and **JMA080**, showed the same reactivity: 94% and 97% of silylated product obtained. Then the conditions were modified: mainly the time decreased to 60min and the eq of Pt^0 decreased to 0.0025.
We found that 0.0025 equivalent of Pt^0 was not enough to reach complete conversion of the substrate: 100% of initial reactant, either with 20 eq of silane (**JMA096**) or 30eq (**JMA101**); and 87% with the stock solution also at 0.0025eq along with 20 eq of silane (**JMA090**) but only reduction was observed. Therefore, 0.005 equivalent of Pt^0 was kept for the next experiments.
With 0.005 eq. of Pt^0 in 60 min, only 20 equivalents of silane were necessary to get up to 97% of conversion (**JMA078**). However, 3% of reduced compound was still present at the end. Therefore, we chose to go on with 30 equivalent and 120 min to make sure to reach completion.

b. *Hydrosilylation of supported peptides containing Lys(Alloc) and Glu(OAll)*

Optimal conditions were fixed at 30 equivalents of silane, 0.005 equivalent of Pt^0, 120 min at 50 °C in anhydrous DCM. We then studied the scope for the substrates by using other models. Lys(Alloc) and Glu(OAll) were incorporated in the dipetpide model: AcPhe(AA)-Rink amide AmphiSphere resin (Figure 15 and 16, respectively) and compared with previous results obtained with AllylGly. Two different silanes were tested on these new subtracts: $HSiMe_2Cl$ and $HSiMe(OEt)_2$.

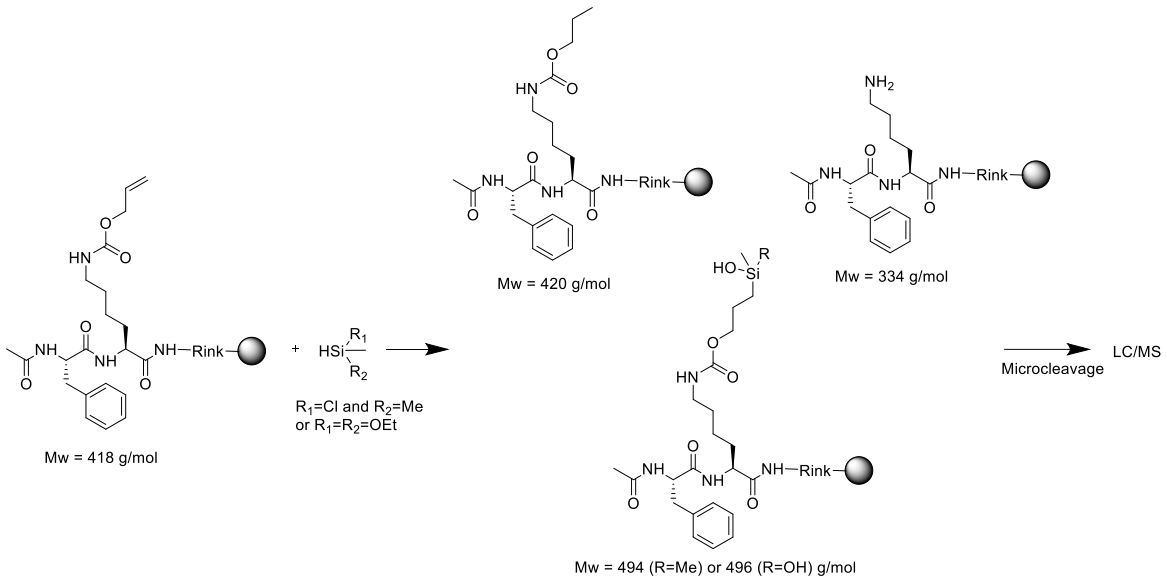

Figure 55. Hydrosilylation of AcPhe-Lys(Alloc)-NH-Rink amide Amphisphere resin and side products.

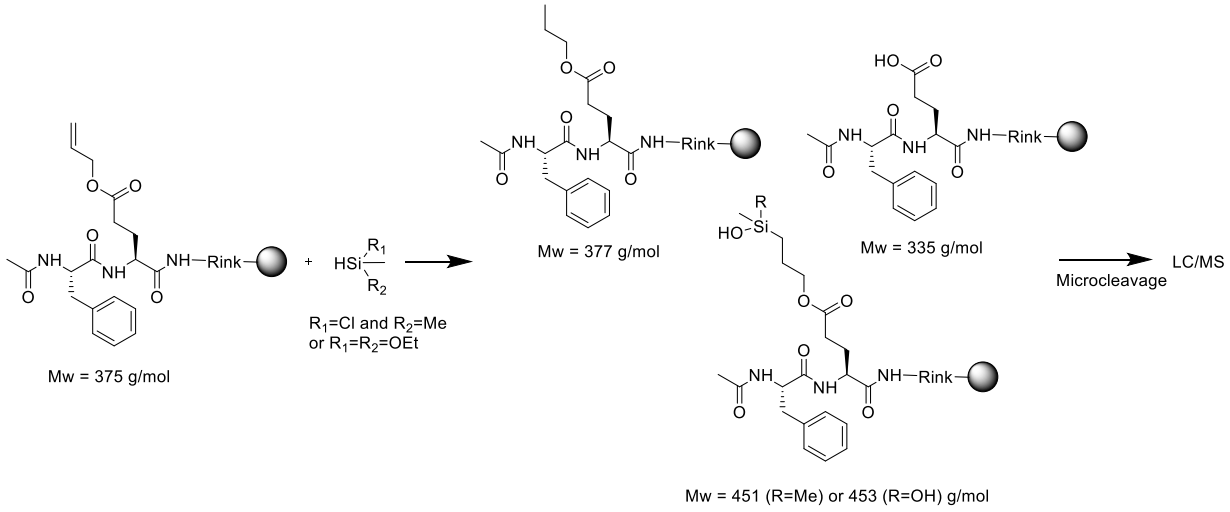

Figure 56. Hydrosilylation of AcPhe-Glu(OAll)-NH-Rink amide Amphisphere resin and side product.

Table 5. Results of hydrosilylation on various substrates, on an AmphiSphere resin and a RinkAmide linker, with 30 eq of silane during 120 min and in anhydrous DCM.

Reaction Id	Reactant	Eq in Pt^0	Silane	T° (°C)	Composition %[a] of the reaction			
					Initial reactant	reduction	silylation	deprotection
JMA111	AcPhe-Lys(Alloc)-NH-●	0.005	$HSiMe_2Cl$	50	90	0	0	10
JMA120	AcPhe-Lys(Alloc)-NH-●	0.010	$HSiMe(OEt)_2$	70	22	13	9	53
JMA112	AcPhe-Glu(OAll)-NH-●	0.005	$HSiMe_2Cl$	50	100	0	0	0
JMA121	AcPhe-Glu(OAll)-NH-●	0.010	$HSiMe(OEt)_2$	70	0	13	4	83

●=Rink amide Amphisphere resin

a: % were calculated by integration of peaks on UV spectrum at 214 nm

Hydrosilylation of Lys(Alloc) containing model with chlorodimethylsilane on support resulted in a complete failure

since 90% of the peptide did not react (**JMA111**). Moreover, we observed in partial deprotection of the Alloc (10%).
To improve the reaction, we increased the temperature to 70 °C instead of 50 °C. We also changed the silane and used diethoxymethylsilane, which enabled to heat at higher temperature due to its higher boiling point (95 °C for the diethoxymethylsilane compare to 35 °C for the chlorodimethylsilane). Since sealed reactors were used, the increase of the temperature should not cause any evaporation of the solvent (indeed, even if the pressure increased, no leak should be observed). We also added more catalyst (0.010 equivalent of Pt^0). The results were not conclusive as we actually catalyzed the deprotection and the reduction more than the hydrosilylation: we obtained 53% of deprotection, 13% of reduction and only 9% of silylated product (**JMA120**).
Results obtained with Glu(OAll) containing model (Table 5) were comparable to those obtained with Lys(Alloc). Once again, this model did not react with chlorodimethylsilane: 100% of initial peptide in this case (**JMA112**).
Diethoxymethylsilane used at 70 °C did not improve a lot the reaction. Only 4% of silylation was obtained, along with 13% of reduction and 83% of deprotection (**JMA121**). However, we can notice that even if we did not get a good conversion into silylated compound, the initial reactant has totally reacted this time.

c. *Hydrosilylation of supported AcPheAllylGly- with different silanes*

We turned our attention again on the initial supported model, AcPheAllylGlyNH-Rink amide AmphiSphere resin, to assay different silanes, during 2, 12 or 24h, to obtain different silylated compound. Six silanes were tested, bearing one, two or three ethoxy or chloro groups (

Figure 57, Table 6).

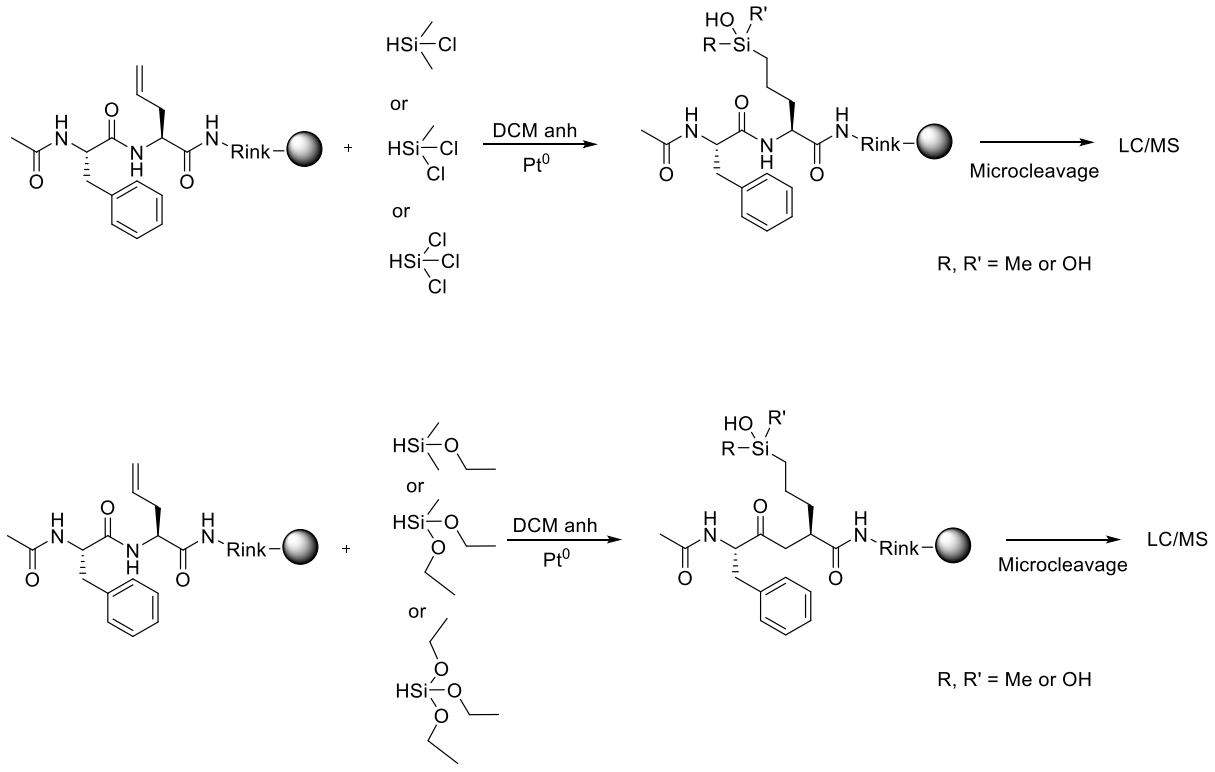

Figure 57. Hydrosilylation of AcPheAllylGly-NH-Rink amide Amphisphere resin with various silanes in optimized conditions: 30eq of silane, 0.005eq of Karstedt in anh. DCM at 50°C.

Noteworthy, we used for this set of experiment smaller reactor (6 mL instead of 10 mL) which could be filled up to the bottleneck with same amount of anhydrous solvent (6 mL) and substrate, avoiding any empty space where the volatile silanes could be ''trapped''.

Table 6. Results of hydrosilylation on AcPheAllylGly-NHRink amide Amphisphere resin, with 30 equivalents of silane, 0.005 eq Karstedt catalyst in 6mL of anhydrous DCM.

Reaction Id	Reactant	Silane	Time (h)	Composition %[a] of the reaction		
				Initial reactant	reduction	silylation
JMA241-1	AcPheAllylGly-NH-●	$HSiMe_2OEt$	2	65	13	22
JMA133	AcPheAllylGly-NH-●	$HSiMe_2OEt$	12	4	49	44
JMA136	AcPheAllylGly-NH-●	$HSiMe_2OEt$	24	1	40	58
JMA131	AcPheAllylGly-NH-●	$HSiMe(OEt)_2$	2	70	7	22
JMA134	AcPheAllylGly-NH-●	$HSiMe(OEt)_2$	12	3	31	63
JMA137	AcPheAllylGly-NH-●	$HSiMe(OEt)_2$	24	0	77	23
JMA132	AcPheAllylGly-NH-●	$HSi(OEt)_3$	2	57	39	3
JMA135	AcPheAllylGly-NH-●	$HSi(OEt)_3$	12	0	95	0
JMA139	AcPheAllylGly-NH-●	/	2	100	0	0
JMA316-3	AcPheAllylGly-NH-●	$HSiEt_3$	2	75	25	0

●=Rink amide Amphisphere resin
a: % were calculated by integration of peaks on UV spectrum at 214 nm

Overall, the side reaction of reduction of the alkene was observed in all the hydrosilylation attempts, ranging from 7 to 95%. In some cases, the presence of reduced compound was more important than the silylated one: up to 95% of reduction for **JMA135**, hydrosilylation attempt done with $HSi(OEt)_3$.
To understand how the reduction proceeded, a "blank hydrosilylation" was performed (**JMA139**). The resin was heated in solution with the catalyst but without any silane. As expected, no reaction was observed, meaning that the silane played a key role in the reduction process, probably as a source of hydrogen.
To follow the evolution of hydrosilylation conversion over the reduction one, the duration of the experiment has been increased from 2h to 12 or 24h (**JMA133, JMA134** and **JMA135** for 12h, and **JMA136** and **JMA 137** for 24h). In the case of the $HSiMe_2OEt$, it enabled better conversion: from 65 to 1% of initial reactant (between 2 and 24h). Thus, at 24h, the silylated product was the major compound compared to the reduced one (58% over 40%).
For $HSiMe(OEt)_2$, the 12h experiment (**JMA134**) gave better results than in 2h (**JMA131**), but it was not the case for a 24h treatment (**JMA137**). The difference between silylated and reduced compound was better at 12h (63% *vs* 31%) compared to 24h (23% *vs* 77%), both presenting a great reactivity since the initial reactant is totally or almost, converted. This was probably due to an experimental problem, a leak leading to presence of air and so water in the reactor, since once silylated the peptide cannot turn be reduced.
Finally, for the $HSi(OEt)_3$, reduction % increased from 39% to 95% with the time (12 to 24 hours) with no improvement on silylation. This is probably due to a lack of reactivity of the $HSi(OEt)_3$, enabling the reduction to take place instead of the silylation.
In addition, we evaluated several solvents (Table 7) to ensure that it did not play any role in the reduction side reaction. We showed again that anhydrous DCM was the best solvent even on solid support, compared to anhydrous THF or toluene, even if toluene would have enable heating at higher temperature (70°C). Indeed, the anhydrous DCM was the only solvent enabling the total conversion of the initial reactant. For both THF and toluene, there was still initial reactant after 24hours (35% for THF and 5% for Toluene, **JMA145 and 148**). Therefore, the increase of the temperature with anhydrous toluene seemed to favoring the reduction over the silylation: 5% of reduction at 50 °C (**JMA148**) vs 13% at 70 °C (**JMA158**).
So we kept anhydrous DCM at 50°C for the next experiments.

Table 7. Results of hydrosilylation on AcPheAllylGly-NHRink amide Amphisphere resin, with 30 equivalents of $HSiMe_2Cl$ and 0.005 eq Karstedt catalyst, in anhydrous solvent for 2h.

Reaction Id	Reactant	Solvent (anhydrous)	T° (°C)	Composition %[a] of the reaction		
				Initial reactant	reduction	silylation
JMA145	AcPheAllylGly-NH-●	THF	50	35	14	46
JMA146	AcPheAllylGly-NH-●	DCM	50	0	4	94
JMA148	AcPheAllylGly-NH-●	Toluene	50	5	5	85
JMA158	AcPheAllylGly-NH-●	Toluene	70	5	13	81

●=Rink amide Amphisphere resin
a: % were calculated by integration of peaks on UV spectrum at 214 nm

Different chloro silanes were also tested with different temperature and reaction times. For the 24h reaction, the experiment was done at RT° to minimize the leakage of these volatile silanes.

Table 8. Results of hydrosilylation on AcPheAllylGly-NHRink amide Amphisphere resin, with 30 equivalents of silane and 0.005 eq of Pt^0, in anhydrous DCM.

Reaction Id	Reactant	Silane	T° (°C)	Time in h	Composition %[a] of the reaction		
					Initial reactant	reduction	silylation
JMA146	AcPheAllylGly-NH-●	$HSiMe_2Cl$	50	2	0	4	94
JMA164	AcPheAllylGly-NH-●	$HSiMeCl_2$	50	2	33	39	0
JMA191	AcPheAllylGly-NH-●	$HSiMeCl_2$	RT°	24	0	58	32
JMA165	AcPheAllylGly-NH-●	$HSiCl_3$	50	2	95	0	0
JMA166	AcPheAllylGly-NH-●	$HSiCl_3$	RT°	24	19	75	0

●=Rink amide Amphisphere resin
a: % were calculated by integration of peaks on UV spectrum at 214 nm

Overall, the reduction was still the main product of these experiments (up to 58% after 24h for **JMA 191**). For the $HSiCl_3$, no silylation was observed even after 24h (**JMA166**), only more conversion into the reduced product. This last silane was more sensitive to air and has a low boiling point that made it difficult to handle and keep it non-hydrolyzed in a small reactor without any leak during 2h at 50 °C.
In the case of $HSiMeCl_2$, the 2h reaction (**JMA164**) probably encounters an experimental issue since no trace of silylation have been observed. However, the 24h reaction (**JMA191**) gave 32% of silylated compound and especially no trace of the initial reactant.

d. *Investigation of the reduction side reaction*

The reduction side reaction may be due to the presence of water which could act as hydrogen donor.[236] Even if the AmphiSphere resin was washed with anhydrous DCM and dried, it was possible that it still contained a little amount of water. To verify this hypothesis, we tried the same model but on PEG and PS-based resin beads. PEG resin was supposed to contain more water as a hydrophilic polymer. On the contrary, PS resin should contain less water that the AmphiSphere, which is a mix of both.

Table 9. Results of hydrosilylation on FmocAcPhePheAllylGly-linker-Resins with 30 equivalents of $HSiMe_2Cl$ and 0.005eq Karstedt catalyst, in anhydrous DCM at 50 °C for 2h.

Reaction Id	Reactant	Resine	Silane	Composition %[a] of the reaction		
				Initial reactant	reduction	silylation
JMA146	AcPheAllylGly-NH-●	AmphiSphere	$HSiMe_2Cl$	0	4	94
JMA197	AcPheAllylGly-NH-●	PEG	$HSiMe_2Cl$	95	0	4
JMA198	AcPheAllylGly-NH-●	PS	$HSiMe_2Cl$	82	0	8
JMA265-2	AcPheAllylGly-O-●	ChloroTrityl	$HSiMe_2Cl$			cleaved
JMA316-4	AcPheAllylGly-O-●	ChloroTrityl	$HSiMe_2OEt$	0 (100% hydrolysed)	0	0

●=Rink amide Amphisphere, PEG or PES resin
a: % were calculated by integration of peaks on UV spectrum at 214 nm

Surprisingly, we also observed almost no reaction (95% and 82% of initial reactant for PEG and PS resin respectively). For the PEG resin, this was probably due to the lack of solvatation in DCM. Indeed, PEG resin was highly hydrophilic, did not disperse in the reactor and stayed aggregated on the top of the solution. There was no dispersion problem of PS resin but the conversion was very low. This may be due to a too high loading of the resin. Indeed, the PS resin has a loading of 0.74 mmol/g vs 0.48 and 0.38 mmol/g for PEG and AmphiSphere respectively. It would mean that the hydrosilylation has a better yield with lower loading.
We also investigated the potential influence of the linker. Rink amide linker was replaced by 2-chloro chlorotrityl on PS resin. This linker is commonly used to get C-ter acid peptide. It is highly sensitive to acid treatment (only 1% solution of TFA is enough to cleave it, compared to a 100% solution of TFA required for RinkAmide cleavage).
As we anticipated, ChloroTrityl linker was prematurely cleaved during the hydrosilylation with $HSiMe_2Cl$ by the presence of HCl, due to the hydrolysis of the silane. The resin was turning red, which was an indication of the formation of a tertiary trityl carbocation. The solution issued from this test was analyzed as well, and there was trace of both silylated and non-silylated amino acid. The same hydrosilylation was done with ethoxydimethylsilane, which can not release any HCl in solution. This time no premature cleavage was observed but no reaction either.
We also studied the influence of the position of the alkene function on the amino acid model. To do so, several other dipeptide models (Figure *58*) were prepared on RinkAmide AmphiSphere resin : AcPheLys(propenoyl)-NH_2 and But-1-enoyl-PhePhe-NH_2), and 1-undeceneoyl-PhePhe-NH_2) (Figure 58).

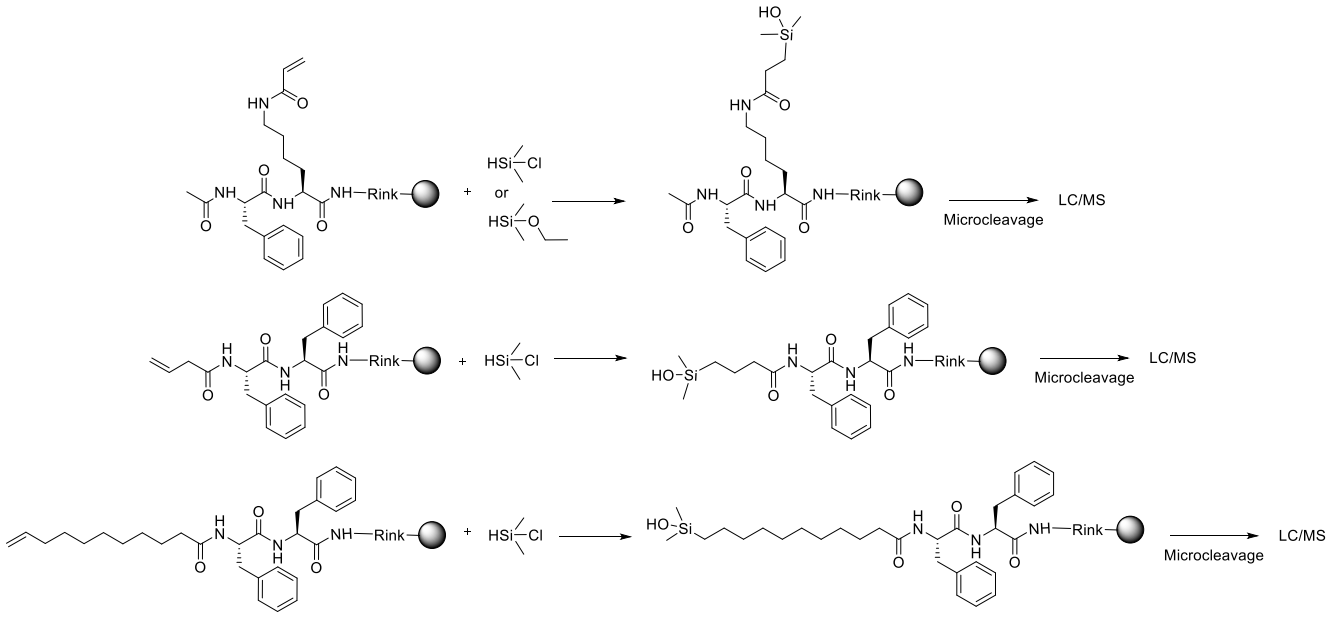

Figure 58. *H*ydrosilylation of different dipeptide models to understand the effect of the position of the alkene on the amino acid.

Table 10. Results of hydrosilylation on different substrates, on AmphiSphere resin with a RinkAmide linker, with 30 equivalents of silane and 0.005eq Karstedt catalyst, in anhydrous DCM at 50 °C.

Reaction Id	Reactant	Silane	Time (in h)	Composition %[a] of the reaction		
				Initial reactant	reduction	silylation
JMA146	AcPheAllylGly-NH-●	$HSiMe_2Cl$	2	0	4	94
JMA309-1	AcPheLys(propenoyl)-NH-●	$HSiMe_2Cl$	2	0	67	32
JMA309-2	AcPheLys(propenoyl)-NH-●	$HSiMe_2OEt$	2	0	65	35
JMA309-3	AcPheLys(propenoyl)-NH-●	$HSiMe_2OEt$	24	0	67	32
JMA301-1	But-1-enoyl-PhePhe-NH-●	$HSiMe_2Cl$	2	60	24	16
JMA301-2	1-undeceneoyl -PhePhe-NH-●	$HSiMe_2Cl$	2	92	6	2

●=Rink amide Amphisphere resin
a: % were calculated by integration of peaks on UV spectrum at 214 nm

The reactivity of AcPheLys(propenoyl)-NH_2 (**JMA309**) was good and no trace of initial peptide was found. However, in all the case, reduction occurred extensively, at least twice more than silylation (67% *vs* 32% respectively for the reduced and silylated compound; and 65 vs 35 the reduced and silylated compound) (
Table 10).
By comparing the two last experiments (**JMA 301-1** and **JMA 301-2**), it seemed that the closer to the peptide the alkene was, the more the reduction was observed. This also went with the reactivity: the 11-carbon long chain has a lower reactivity than the 4-carbon long chain: 92% of initial reactant vs 60%.

IV. Conclusion

The hydrosilylation method gave good results with the chlorodimethylsilane, used in solution or on solid support, mainly on AllylGly moiety. Unfortunately, reduction of the unsaturated alkene occurred for other silanes and on other subtract. We tried to understand which parameter is favoring the reduction over the silylation. First, the reactivity of the silane may play a role, the better the silane is reactive the less reduction should be observed. Then the subtract, and more precisely the alkene function position toward the peptide chain, is also influencing the competition: the closer the alkene is to the peptide, the more the reduction is observed.

The most interesting silanes in the context of the global PhD project were dichloromethylsilane or diethoxymethylsilane and triethoxysilane or trichlorosilane. Indeed, the two fists are of interest to prepare hybrid peptides macromonomers with hydroxyl or alkoxyl group on the silane function. These macromonomer could lead to the synthesis of PDMS-like polymers with peptide as pendant group on the siloxane backbone. The triethoxysilane or trichlorosilane derivatives are interesting for the grafting on silicone, glass or silica surface, forming 3 covalent bonds. They were also used to prepared hydrogels from hybrid polymers, oligosaccharides or collagen-peptides.

Unfortunately, hydrosilylation gave no good results in the later cases and could not replace the classical method, which uses isocyanate silylated derivatives. In order to favor hydrosilylation over unwanted reduction, some technical aspects could be improved (e.g. use of sealed reactors and other catalyst). This type of reaction should deserve some trial in a continuous flow system. Undoubtedly, a clear understanding of the reduction mechanism would be useful to avoid or limit it.

Chapter 3: Synthesis of hybrid macromonomers using silylated isocyanate

Chapter 3: Synthesis of hybrid macromonomers using silylated isocyanate

The aim of this chapter is to describe the hybrid silylated blocks, which were used for the design of new hybrid biomaterials. As explained in Chapter 1, different types of hybrid silylated blocks can be obtained depending on the way of silylation (i.e. the silylating reagents used) and on the type of silyl group. In this PhD thesis, we focused our attention on silicone-based polymers obtained by sol gel inorganic polymerization. Each hybrid monomer must be able to react with two others to elongate the polymeric backbone. Thus, we chose to polymerize hybrid blocks monosilylated with dihydroxysilane moiety. To do so, dichloromethylsilane or diethoxymethylsilane were used. Indeed, once hydrolysed, both the chloro and ethoxy groups are leading to silanols. To incorporate the silane function, silylated isocyanates were used to react with the selected biomolecules (i.e. isocyanatopropyl dichloromethylsilane and isocyanatopropyl diethoxymethylsilane).

We will first discuss the general strategy for the introduction of the silyl group on the bioorganic part, and then present all the blocks we prepared, divided in two parts: hybrid peptides and other hybrid biomolecules.

I. Hybrid macromonomers for the synthesis of hybrid materials

As already stated in Chapter 1, the hybrid molecules we used are composed of both an organic and an inorganic part, the latter containing one or several hydroxysilane group(s), or precursors of it (e.g. alkoxysilane, chlorosilane). Such hybrid biomolecules are of special interest for the surface functionalization of materials or the direct synthesis of novel biomaterials.

On one hand, the bio-organic part is responsible for the biological properties afforded to the resulting material and thus, imposes the final application. On the other hand, the silane moiety enables sol-gel inorganic polymerization.

The hybrid molecules designed in the frame of this PhD work are called ‘hybrid macromonomers’ as they will be polymerized to yield polymers and materials in a bottom-up approach. Compared to simple organosilanes such as APTES for example, they are relatively high MW molecules (> 500 g/mol).

The position of silane group within the hybrid macro-monomer has to be carefully chosen to preserve the biological properties of the organic part and orient it properly in the material. The type of the silane group plays also an important role and programs the geometry of the materials (Figure 61).

Another application of hybrid biomolecules is the surface functionalization of any type of metal oxide. In our laboratory, numerous examples were reported such as grafting on silica surface including Ordered Mesoporous Silica (OMS)[237] and silica NPs,[199] titanium surface,[200] glass.[189] They were also grafted on silicone, antibacterial catheters and wound healing dressings have been prepared this way.[141,165,181] The surface functionalization was done by dip coating[189,238] or incubation.[239] Noteworthy, a layer of silica can be first deposited on the material to enhance the covalent binding of the hybrid molecules.[200]

The topic of my PhD work is related to the direct synthesis of novel biomaterials instead of the functionalization of surface. Whatever the approach and the type of silane, the polymerization relies on sol-gel process, which is detailed in the following paragraph.

a. *Sol-gel process*

The sol-gel process have been discovered by M. Ebelmen[240,241] and T. Graham[242] by studying the hydrolysis of Tetraethyl orthosilicate (TEOS). They realized that the hydrolysis under acidic conditions was leading to silica material looking like glass. Since then, the sol-gel process has been widely explored and generally defined as the synthesis of oxide network from the inorganic polymerization of a precursor. The precursor is usually a metal alkoxide $M(OR)_n$ or a metal halide MX_n, (the metal being for example Si or Al). In this work, the metal is always Si and both ethoxy and chlorosilane were used leading to silanol functions once hydrolyzed: Si-OH.

The name of sol-gel came from the fact that the process undergoes a transition between a sol and a gel. The sol is a stable suspension in a liquid and the gel is a solid 3D network. The sol-gel process involves two types of reactions: first the hydrolysis then the condensation. The hydrolysis transforms alkoxysilanes (Si-OR) and halogenosilanes like chlorosilanes (Si-Cl) into silanols (Si-OH). The second step, the condensation, is forming siloxane bonds (Si-O-Si). There are two types of condensation: oxolation involves two silanol functions previously hydrolyzed, or alkoxolation which involves a silanol and an alkoxysilane (Si-OR) (Figure 59).

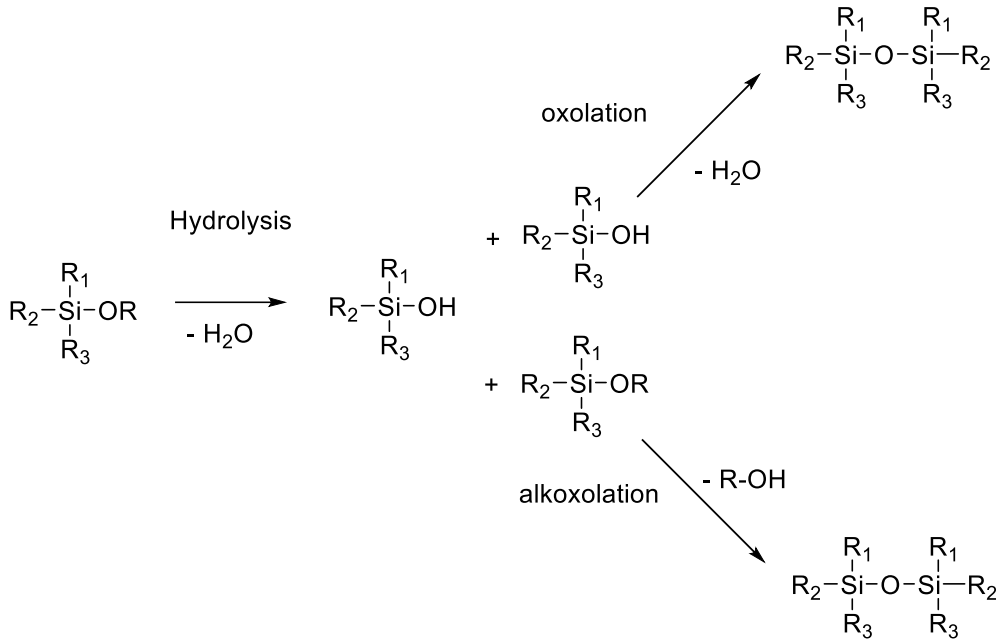

Figure 59. Two steps of sol-gel process: hydrolysis followed by oxolation or alkoxolation depending on the precursor.

Sol-gel process is usually performed in water and at ambient temperature and can be catalyzed both by acidic and basic conditions. Indeed, as shown on the Figure 60, at neutral pH the hydrolysis is really slow and so the sol-gel process cannot start, however as soon as the pH move away from the value 7, the hydrolysis rate increase. As shown on the following graph, there is no possible condensation at pH=2 however the hydrolysis is happening. This enable the storage of hydride molecule under the form of monomer and avoid any polymerization.

Alternatively, the condensation can be catalyzed by nucleophilic catalyst, which is of particular interest at pH 7. An example of catalyzer is the NaF, one of the most famous catalyzers for sol-gel. However, despite its high efficiency, NaF is toxic when used in too high concentration (>1.25%).[243]

The difference between these two types of precursors is into the speed of the hydrolysis and their stability. An alkoxysilane function is more stable than a silyl chloride one that will hydrolyze much faster.

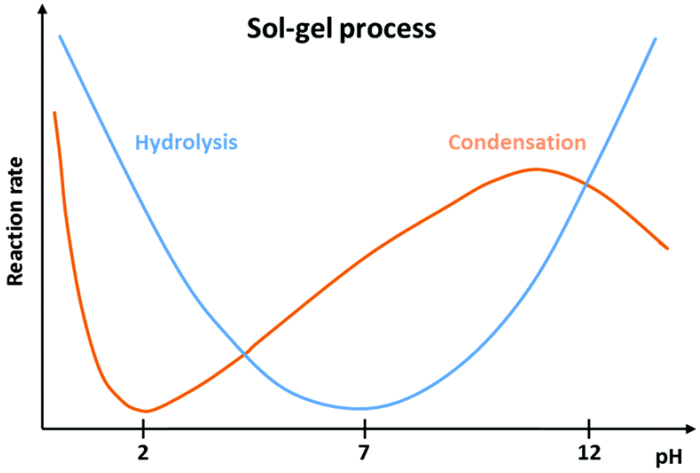

Figure 60. Evolution of the hydrolysis and condensation of TEOS in function of the pH.[244]

In the frame of this PhD, we mainly used the silyl chloride function as precursor and only once alkoxysilane function. This choice favors an acid catalysis. Indeed, the Si-Cl functions releases HCl upon hydrolysis, so decreasing the pH. Hydrolysis of SiCl is almost instantaneous in water-containing solution. Therefore, most of the macromonomer synthesized were purified in H_2O/ACN solution containing 1‰ TFA before being lyophilized. So most of the time they contain TFA salts that make the polymerization solution acidic once dissolved. As the precursor is turning quite fast into silanol, the condensation mechanism is probably oxolation.

b. *Type of silane moiety*

The choice of the precursor is determinant for the final material structure. Either alkoxysilane or silyl chloride function are leading to silanol after hydrolysis, so this is not the main factor about the final structure.

Actually, it is the number or resulting silanol functions that determines the final material structure (Figure 61). Indeed, with only one silanol function (M^0) the hybrid molecule has only one possibility: the dimerization (M^1). Then, with a dihydroxysilane group (D^0), the resulting material is a linear polymer (D^2). Finally, a precursor with trihydroxysilane (T^0) may yield a 3D network like a hydrogel (T^3). The condensation of a silylated precursor can also be performed on a surface. It is often called a silanization. An example at the bottom of Figure 61 shows the silanization with a trihydroxysilane.

Among other examples from our group, bioactive peptides were monosilylated by a dimethylhydroxysilane group and so leading to a dimerization.[245] The influence of the position of the silylation, and so the position of the dimerization bond, have been explored as well as the half-life of the dimer. Then other peptides were monosilylated by a methyldihydroxysilane group or bisilylated by a dimethylhydroxysilane group in order to create silicone based polymer with two different structures: linear or comb-like.[143,144] And finally, monosilylated or bisilylated peptide and PEG with a trihydroxysilane group have been proven able to form hybrid hydrogel with biological properties.[15,201,246]

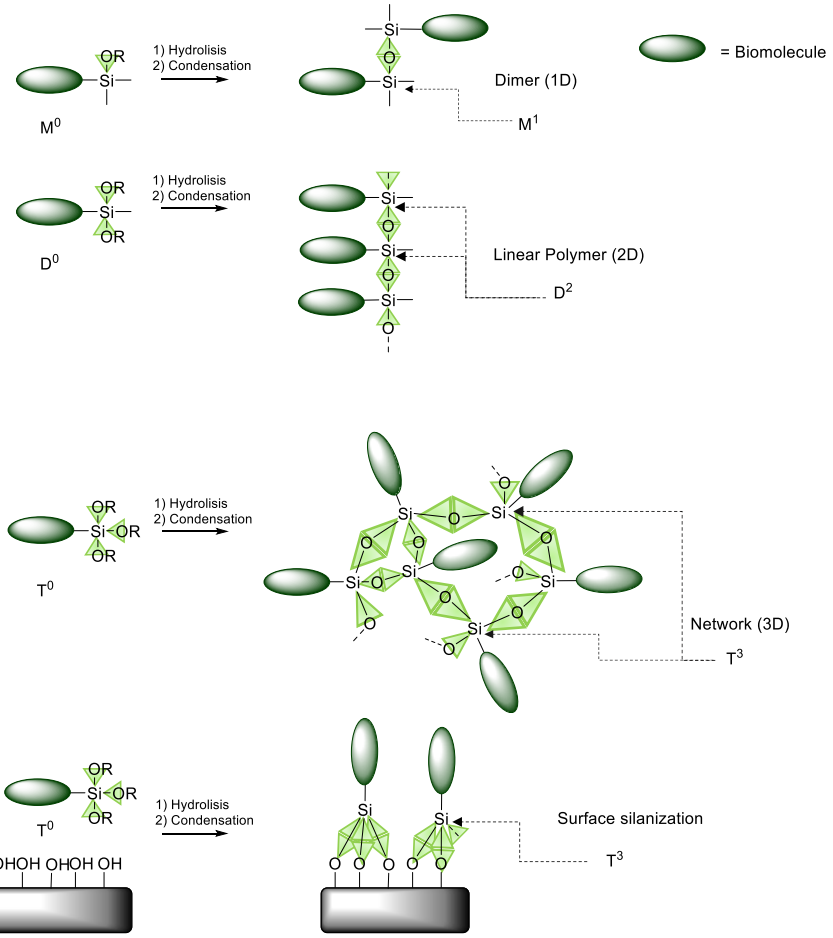

Figure 61. Type of material issued from hybrid biomolecule condensation.

In this PhD work, we focused our attention on the synthesis of macromonomers able to (co)polymerize with dichlorodimethylsilane (DCDMS) to yield multifunctional polymer chains. Such polymers were called 'silicone-based' polymers for their resemblance with PDMS, the monomers being separated by Si-O-Si bonds. Two options can be defined: either the macromonomer bears two dimethylhydroxysilane groups at each of his extremity for example, or it bears only one function dihydroxymethylsilane which is able to react twice. In the latter case, comb-like polymers, containing the biomolecule as pendant chain, can be obtained while the first option is enabling the biomolecule to be part of the backbone of the silicone based polymer (Figure 62). Several example of silylated peptide used as macromonomer for the synthesis of silicone based polymer have been described in our group.[143,144] Linear or cyclic peptide, from 2 to 5 amino acid long have been used for polymerization into peptide-modified silicone.

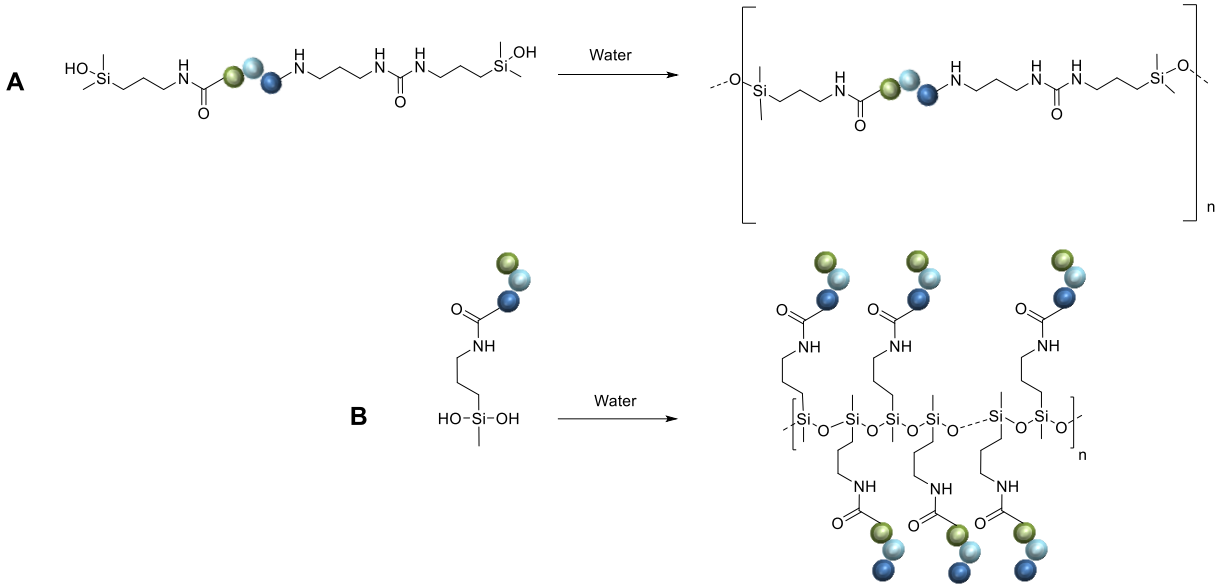

Figure 62. Two examples of polymerization of peptide-based macromonomer either A) bisilylated by dimethylhydroxysilane groups, or B) monosilylated by methyldihydroxysilane groups.[143,144]

As already stated in chapter 1, we chose the second option in this PhD work. More precisely, instead of having short homopolymers,[144] we investigated the copolymerization with DCDMS to get peptide-modified silicone (chapter 4) and also copolymerization of different macromonomers to get multifunctional materials (chapters 5 and 6).

c. *General considerations on the silylation of a biomolecule*

Different molecules were silylated to obtain the range of macromonomers needed for our work: drugs, peptides, PEG and dyes. Each of them plays an important role in the design of the different biomaterial.

The introduction of silyl group can be done in different ways. The silylation can be performed by hydrosilylation (Chapter 2) or by reacting commercially available silylation reagents with the biomolecule.

In this PhD work we chose to use isocyanate derivatives (e.g. isocyanatopropyl dichloromethylsilane). Isocyanate may react on amines, yielding to carbamide functions and on alcohol yielding carbamates.

The silylation is often the last step of the synthesis, simply because the silane group is relatively fragile and could hydrolyze and condense in the presence of water. This is difficult to avoid if repeated reactions or treatments are preformed after the introduction of the silyl group. Moreover, reaction with an isocyanate is not chemoselective. It implies that silylation of multifunctional molecule like a peptide, has to be done carefully: each side chain of amino acid that contains a reactive group able to react with the isocyanate has to be protected. This is particularly of importance for the N-terminus or for the Lys residue, which has a primary amine on its side chain. If such amines are not protected, the silylation will occur on different sites of the peptide and the polymerization will not lead the expected material structure. However, it is possible to play on the difference of reactivity between different groups to orient selectively the silylation. For example, if only one equivalent of the isocyanate is used, it will preferentially react with amine rather than alcohol.

In the case of peptide, silylation with an isocyanatopropyl reagent can be done either on solution or on solid support.

d. *Analyses and purification of hybrid macromonomers*

The stability of silylated biomolecule depends on the silane function. Silyl chloride functions turn almost immediately into silanol function in the presence of traces of water. We did not succeed to isolate their corresponding organocholrosilane, even the Et_2O precipitation is enough to hydrolyze them. On the contrary, it is possible to keep alkoxysilane functions intact if the biomolecule is conserved carefully under inert atmosphere. This point is important to notice because once hydrolyzed, even if the biomolecule is in powder form, it may condense leading to a solid and insoluble material which cannot be used anymore.

The only way to bring back a condensed silylated hybrid material into monomeric species is to treat it with a strong base, like NaOH. Hydroxide ions will depolymerize the network by breaking the siloxane bonds between hybrid monomers. To do so, the biomolecule has to be stable upon basic treatment and care should be taken to avoid side reaction like amide hydrolysis. After this depolymerization, HCl solution is added for neutralization. The hybrid monomer can be used immediately in the chosen conditions (pH, concentration). This type of treatment can be done several times but one has to remember that NaCl salts are generated and could interfere in the following steps of the material synthesis.

The stability of hybrid molecules is also to be taken into consideration for the analyses. For LC/MS analyses, hybrid molecules were solubilized into a H_2O/ACN (50/50) solution containing 1‰ TFA. In these conditions, hydrolysis of chloro or alkoxysilane occurs and only silanol species were detected on the spectrum. In contrast, NMR analyses (e.g. ^{1}H of ^{29}Si NMR) are performed in anhydrous solvent and alkoxysilane functions were detected while chlorosilane functions were not detected due to a fast hydrolysis.

As far as chromatography was concerned, hybrid silylated molecules may react with silica and so, can be covalently grafted on silica-based columns. Even in the case of reversed phase column like C_{18} grafted silica, residual silanol functions are available to react with the silylated biomolecules. Over the time and accentuated by the injection of basic solutions, depolymerization of the silica occurs, more and more silanol functions appears favoring the covalent binding of the hybrid molecules on the stationary phase. This is a serious problem for purification as a significant decrease of the yield was observed mainly due to a covalent capture of the silylated molecules in the preparative column. Moreover, the purifications were very detrimental for the semiprep C18 columns, which represent a rather expensive equipment.

To confront this issue, in this work, silylated molecules were preferentially analyzed and purified on a non-silica reversed-phase column: PLRP-S® column. These types of analytical or preparative column are made of styrene-divinylbenzene copolymer, and are dedicated to the chromatographic separation of small biomolecules. Their pore size goes from 10 to 400nm and they are adapted to usual solvents like water and acetonitrile. Besides, they tolerate wider pH range (i.e. from 2 to 14) than grafted silica columns, which suffers from depolymerization of the silica at basic pH or very acid pH.

Summing up, as soon as a biomolecule was silylated, we tried to perform the analyses in the same day, on an analytical PLRP-S column (4,6mm diameter, 150 or 50 mm length, 100 Å pore size, 5 µm particle) using a gradient of H_2O/ACN with 1‰ TFA (1.5mL/min over 6min). The purification was performed on a semi-preparative PLRP-S column (25 mm diameter, 150 mm length, 100 Å pore size, 8 µm particle) using the same type of gradient at 10 mL/min.

II. Synthesis of silylated peptides

a. *Solid phase peptide synthesis*

As explained, the silylation of hybrid peptides could be performed in solution or on solid support (SPPS). In any cases, the peptides were first prepared on solid support in Fmoc/tBu strategy.

SPPS strategy

The two major strategies for SPPS are Fmoc/tBu or Boc/Bzl refeering to the couple of "amine temporary protecting group/side chain protecting group". In Boc strategy, TFA treatment is necessary after each coupling step to remove the terbutyloxcarbonyl group and the side chains protections as well as the linker on the solid support are resistant to TFA but can be cleaved by strong acidic treatment like HF. We chose the Fmoc/tBu strategy which requires at each step the use of secondary amine solution (e.g. piperidine in DMF) to remove the fluorenylmethyloxicarbonyl (FMOC) protecting group. Normally, linker cleavage and side chains protecting group removal are done simultaneously by a TFA treatment. Noteworthy, some linkers (e.g. Sieber amide, Trityl) can be cleaved in mild acidic conditions (e.g. 1% TFA, TFE/AcOH/DCM 10/20/70) where TFA-labile side chain protecting groups are not affected. It is useful to synthesize protected peptides for further modifications like cyclisation or hydrosylilation. In addition, non-classical side-chain protecting groups, insensitive to TFA or piperidine such as Alloc for exemple, may afford a supplementary orthogonality useful to functionalize the peptide before its final cleavage form the support.

Fmoc protected amino acids

Some amino acids with reactive side chains requiers protecting groups which have to stay in place during the whole Fmoc/tBu SPPS to avoid side reactions. Moreover, the silylation of peptides was principally performed at the N-ter of the peptide thus, side chain protecting groups were also necessary to orient the silylation.

Side-chain protection is absolutely necessary with Lys that has a primary amine at the end of its side chain (e.g. with a Boc group). On the contrary, Arg side chain does not necessarily need to be protected in normal conditions. Indeed, the pKa of the guanidine function is around 13. It means that at pH 10, the Arg side chain is still protonated, avoiding any side reaction, even in the presence of an isocyanate reagent such as isocyanatopropyl dichloromethylsilane (IPDCMS). The main Fmoc derivatives used in this PhD thesis were: Fmoc-Arg(Pbf)-OH, Fmoc-Ahx-OH, Fmoc-Lys(Boc)-OH, Fmoc-His(Trt)-OH, Fmoc-Pro-OH, Fmoc-Ser(Trt)-OH, Fmoc-Asp(Trt)-OH, Fmoc-Gly-OH and Fmoc-βAla-OH. These usual amino acids are bearing classical side chain protections: tBu (tert-butyl), Pbf (2,2,4,6,7-Pentamethyldihydrobenzofuran-5-sulfonyl), Boc (ter-butoxycarboly) and Trt (Trityl). This side chain protecting groups are deprotected by TFA treatment. It is worth noting that we also used unusual Fmoc amino acids such as, Fmoc-Lys(Alloc)-OH, Fmoc-Lys(Mtt)-OH and Fmoc-Lys(ivDde). Their application will be explained in the context of their synthesis.

Resins and linkers

The choice of the resin matrix of the SPPS beads is mainly done in function of the peptide's size. For longer peptides (e.g. >15 amino acids), a PEG-based resin is preferred over PS because of its swelling properties which facilitates the accessibility of reagents and limits the aggregation phenomenon of anchored peptides.[247,248]

In this PhD work, we used Amphisphere (PEG/PS copolymer), a PS resin and ChemMatrix (100% PEG) of 200-400 mesh (≈0.1 mm diameter).

The linker is the position were the first amino acid is anchored, most of the time through its C-terminal carboxylic acid function. The choice of the linker depended partially on the C-ter function of the peptide after cleavage: either amide or carboxylic acid. Another factor was if we chose to remove or keep the aminoacids side chains protections after cleavage. In this work, Rink Amide and Sieber linkers were used for C-ter amide peptides and Trityl linker for the C-ter carboxylic acid peptidese (Figure 63). The anchorage of the first amino acid is adapted in function of the linker. For the RinkAmide and Sieber linkers, it is like a simple amino acid coupling (below). For the

Trityl linker, the carboxylate function of the Fmoc-AA-OH is activated by a base, DIEA in our case, and then is anchored to the resin by a nucleophile substitution of the chloro function.

After the anchorage of the first amino acid on Trityl linker, a capping step of non-reacted chloroTrityl functions was done by MeOH/DIEA solution (80/20; v/v) during 30min, in order to form methyl esters and avoid undesired reaction during SPPS followed by several washing of DCM (x2) and DMF (x3).

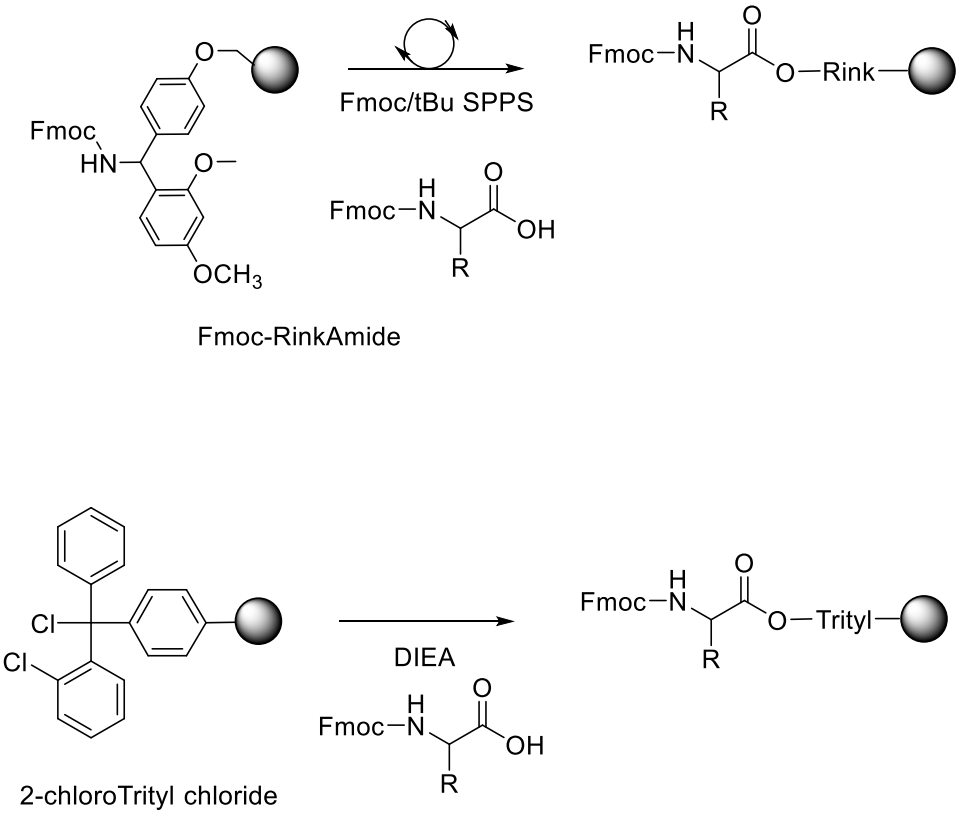

Figure 63. General scheme of the anchoring of an amino acid on Fmoc-RinkAmide and 2-chloroTrityl chloride resins.

SPPS Cycle of coupling and deprotection

We used uronim coupling reagent (i.e. 1-[Bis(dimethylamino)methylene]-1H-1,2,3-triazolo[4,5-b]pyridinium 3-oxide hexafluorophosphate, HATU) (Figure 64). Uronium are potent carboxylic acid activators but have to be used in equimolar amount related to the protected amino acid to avoid unwanted guanylation of the free N-terminal amine.[249] Coupling step are performed at basic pH to form the carboxylate and to keep the amine unprotonated. Tertiary amine N,N-Diisopropyléthylamine (DIEA) miscible in both DMF and DCM, was used in this PhD work.

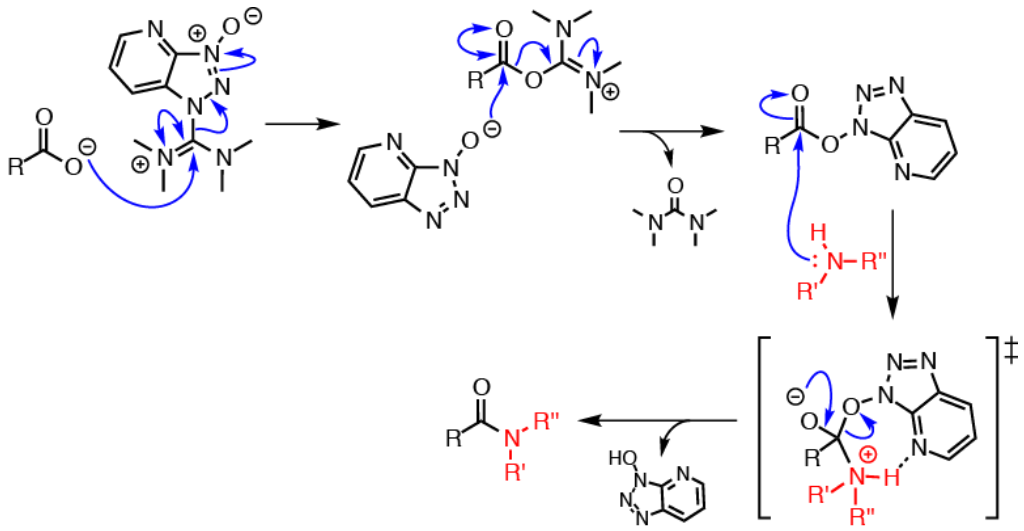

Figure 64. Mechanism of activation of the carboxylic acid function of amino acid by HATU in the presence of a tertiary amine used to form the carboxylate.

Amino acid coupling on solid support was performed with 1 eq of the resin poured in DMF. 6 eq of DIEA were added, followed by 3 eq of the Fmoc-AA-OH and finally 3 eq of HATU. The solution was stirred for at least 1h to form the amide bond between the activated Fmoc protected amino acid and the N-terminus amino group of the peptide immobilized on the solid support. Resin was washed three times with DMF. The Fmoc was deprotected by two successive DMF/piperidine (80/20; v/v) treatments of 20 min.

Cleavage

The cleavage of the peptide from the resin was performed during 2 hours, by acidic treatment: TFA/TIS/H_2O (98/1/1, v/v/v). TIS (Triisopropylsilane) with H_2O are used as a scavenger: to avoid side reactions during deprotection of peptides by reacting with the carbocation created by the side chain deprotections. After evaporation of the solvent under vacuum, the peptide was precipitated in Et_2O and washed three times with the same solvent.

The hybrid peptides prepared during this PhD work are summarized in Table 11.

Table 11. Silylated molecules of this PhD work

Compound #	Yield (in %)	Chapter	Formula
1	35	II.b	$Me(OH)_2Si-(CH_2)_3NHCO-AhxArgArg-NH_2$
2	45	II.c	$Me(OH)_2Si-(CH_2)_3NHCO-Lys_4His_4-NH_2$
3	40	II.c	$Me(OH)_2Si-(CH_2)_3NHCO-His_4-NH_2$
4	55	II.c	$Me(OH)_2Si-(CH_2)_3NHCO-Lys_4-NH_2$
5	30	II.d	$Me(OH)_2Si-(CH_2)_3NHCO-(\beta Ala)_4-GRGDSP-OH$
6	20	II.d	$Me(OH)_2Si-(CH_2)_3NHCO-NH-PEG-Ala(CF_3)-c[RGDfK]$,
7	n.d.	III.a	$Me(OH)_2Si-(CH_2)_3NHCO-NH-TMZ$
8	45	III.b	$Me(OH)_2Si-(CH_2)_3NHCO-NH-MTX$
9	40	III.b	$Me(OH)_2Si-(CH_2)_3NHCO-Phe(CF_3)-NH-MTX$
10	30	III.c	$Me(OH)_2Si-(CH_2)_3NHCO-BHD-CPT$
11	n.d.	III.d	$Me(OH)_2Si-(CH_2)_3NHCO-Lys-DOTA$
12	n.d.	III.d	$Me(OH)_2Si-(CH_2)_3NHCO-NH-(CH_2)-NH-DOTA\ GA$
13	85	III.e	$Me(OH)_2Si-(CH_2)_3NHCO-Florescein$
14	92	III.f	$Me(OH)_2Si-(CH_2)_3NHCO-NH-PEG-CONHCH_2F$

n.d.: non determined

b. *Hybrid antibacterial peptide **1***

The first hybrid peptide we prepared was based on the N-ter palmytoylated tripeptide PalmArgArgNH_2. This short amphipathic peptide demonstrated interesting antimicrobial properties, probably by disrupting bacteria membrane in a carpet-like mechanism, forming pores.[189] A silylated analogue was designed ($Me(OH)_2Si$-$(CH_2)_3$NHCO AhxArgArg-NH_2 compound **1**), in which the palm chain was replaced by silylated amino hexanoic acid. It has been used to functionalize silicone catheters but also silicone dressings.[165]

For the synthesis of the peptidic part of compound **1**, a Fmoc-Sieber PS resin has been chosen. Sieber linker allowed the cleavage of the peptide in mild acid conditions (i.e. 1% TFA in DCM) without the removal of the Pbf groups on the side chain of the Arginine residues (Figure 65). It allowed the recovery of Pbf-protected peptide, soluble in organic solvents and easily purified by RP-preparative HPLC. Indeed, Pbf groups are providing a better UV visibility of the peptide by HPLC and LC/MS. Besides, such protecting groups increased the hydrophobicity of the peptide, preventing it to get out of the purification column in the injection peak and thus greatly improving final compound purity.

The cleavage was performed in DCM/TFA (99/1, v/v) for 2h at room temperature, under stirring. After evaporation of the solvent and precipitation by Et_2O, the protected H-Ahx-Arg(Pbf)-Arg(Pbf)-NH_2 peptide was purified on preparative RP-HPLC equipped with a C_{18} reversed-phase column. The purified H-Ahx-Arg(Pbf)-Arg(Pbf)-NH_2 (1eq) was solubilized in anhydrous DMF. DIEA (6eq) and isocyanatopropyl dichloromethylsilane (1.2eq) were added to the mixture. The reaction was stirred for 1h under argon and the solvent was removed under reduced pressure. The hybrid monomer was then purified on preparative HPLC using a non-silica-based column PLRP-S. The resulting silylated peptide was bearing a dihydroxymethylsilane function instead of Si-Cl that has been hydrolyzed as soon as solubilized in water for the purification.

Finally, the Pbf groups were removed by TFA treatment, at room temperature for 2h. TFA was removed under vacuum and the deprotected hybrid peptide **1** was precipitated in Et_2O. It was then dissolved in H_2O/ACN/TFA (50/50/0.1, v/v/v), purified on preparative HPLC with PLRP-S column and finally lyophilized. The final yield was around 35%.

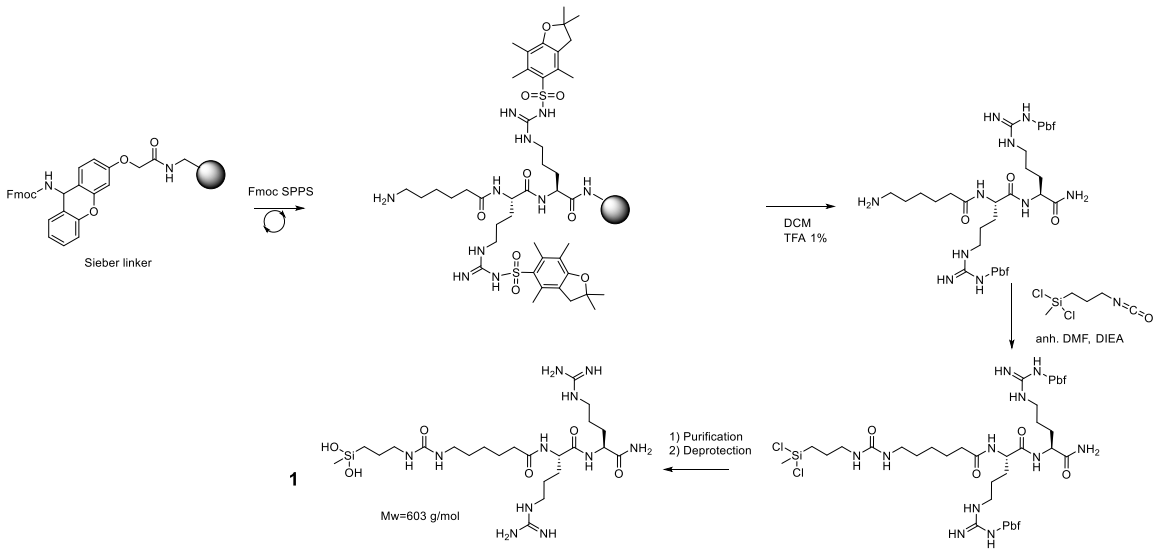

Figure 65. Synthesis and Silylation in solution of AhxArgArg-NH_2

On the ESI+ LC/MS chromatogram we identified the compound **1**: rt= 1.55min $[M+H]^+$ m/z 604, $[M+2H]^{2+}$ m/z 302.5; $[M+2H-H_2O]^{2+}$ m/z 293.5 (*Figure 66*).

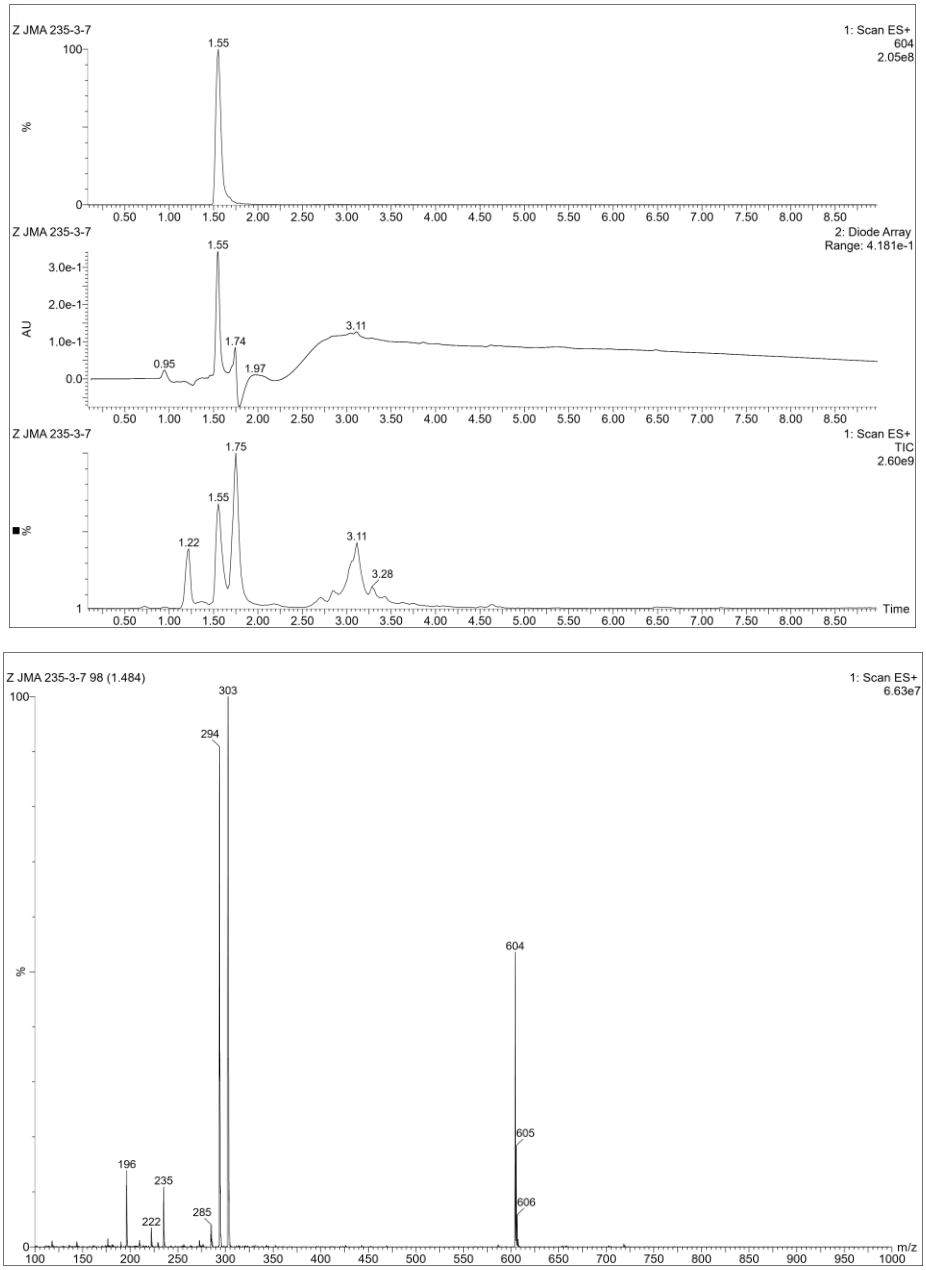

*Figure 66. ESI + LC/MS of compound **1** after purification, analyzed in H_2O/ACN (50/50) 1‰TFA on PLPR-S column. Top: chromatograms UV at 214nm and TIC, Bottom: MS spectrum at 1.55 min.*

c. *Hybrid peptides for polyplexes formation **2**, **3** and **4***

Three hybrid peptides ($Me(OH)_2Si$-$(CH_2)_3NHCO$-Lys_4His_4-NH_2, compound **2**, $Me(OH)_2Si$-$(CH_2)_3NHCO$-His_4-NH_2, compound **3** and $Me(OH)_2Si$-$(CH_2)_3NHCO$-Lys_4-NH_2, compound **4**) were designed to form polyplexes, i.e. complexes between polymers and oligonucleotides. His and Lys containing peptides have been described for the synthesis of vectors for small interfering RNA (siRNA).[250–253] Indeed, such cationic peptides are able to associate withsiRNAs, which are negatively charged. Lys is a well-known amino acid for the synthesis of polyplexes due to its a positive charge thanks to a primary amine function. In addition, His is known for its ability to cross membranes and escape endosomal capture, which is the second main quality for a siRNA vector. The vector has to form a complex with oligonucleotide, transport it to the cells and cross the membrane, and then release the siRNA inside the cell. The association of Lys and His helps both the complexation ad the membrane crossing. The His is also

helping for the release of the siRNA: thanks to the 'proton sponge' effect in the endosome. Indeed, the His residue is unprotonated at neutral pH. If the polyplex is absorbed via endocytosis, the pH lowers to 2-3 pH. The His residues are protonated and these allows them to cross/break the endosomal membrane and avoid entrapment.[254] Then due to the variation of pH, the peptide is changing its number of positive charges and is able to complex with counter ions from the cytoplasm. The siRNA is released slowly in the cytoplasm and free to get in contact with the genetic material. The importance of each amino acid in the synthesis of polyplexes will be detailed in chapter 6.

Compounds **2**, **3** and **4** were synthesized following the same protocol. Firstly, the peptide was synthesized by SPPS on a 2-chloroTrityl chloride (CTC) PS resin. This resin has been chosen in order to get a carboxylic acid function at the C-ter of each peptide.

Histidine imidazole ring is not reactive in the conditions of reaction with isocyanate. Indeed, imidazole ring is aromatic and none of the nitrogens can be easily modified. Thus, it was not necessary to keep it protected by a trityl during silylation.

For the silylation of Lys containing compounds, two options were possible here: either preforming a mild cleavage of the trityl linker to keep all the side chain protected and perform the silylation in solution, or doing the silylation directly on support. The first option allows a purification of the protected peptide before the silylation, knowing that another purification would probably be necessary after silylation.

The second option enables the use of excess of silane isocyanate, which can be washed afterward. This is not recommended in solution, as the silane precursor is then able to react again on itself. Indeed, once attached to the biomolecule, if the precursor is hydrolyzed into dihydroxymethylsinale in solution, as silanol function are available, the remaining silylation agent can react by sol-gel process creating siloxane bound with the silylated biomolecule. Then, the cleavage is done. As explained, the dichloromethylsilane is converted in dihydroxymethylsilane during the cleavage by traces of water in TFA. The silylated peptide is purified after this final step.

We chose the second option and the silylation of compounds **2**, **3** and **4** was performed on support.

After the last coupling and Fmoc-deprotection, the peptidyl resin was placed in anhydrous DMF. DIEA (6 eq) and isocyanatopropyl dichloromethylsilane (1.2 eq) were added to the mixture (Figure 67). The reaction was stirred overnight under argon atmosphere. The resin was then washed with DMF three times. The silylated peptide was cleaved from the resin by acidic treatment: 1h in TFA/TIS/H_2O (98/1/1, v/v/v). After evaporation of the solvent under vacuum, the hybrid peptide was precipitated in Et_2O. The hybrid macromonomer was finally purified on preparative HPLC using a non-silica column PLRP-S and lyophilized. The final yield of the synthesis was around 45% for **2**, 40% for **3** and 55% for **4**.

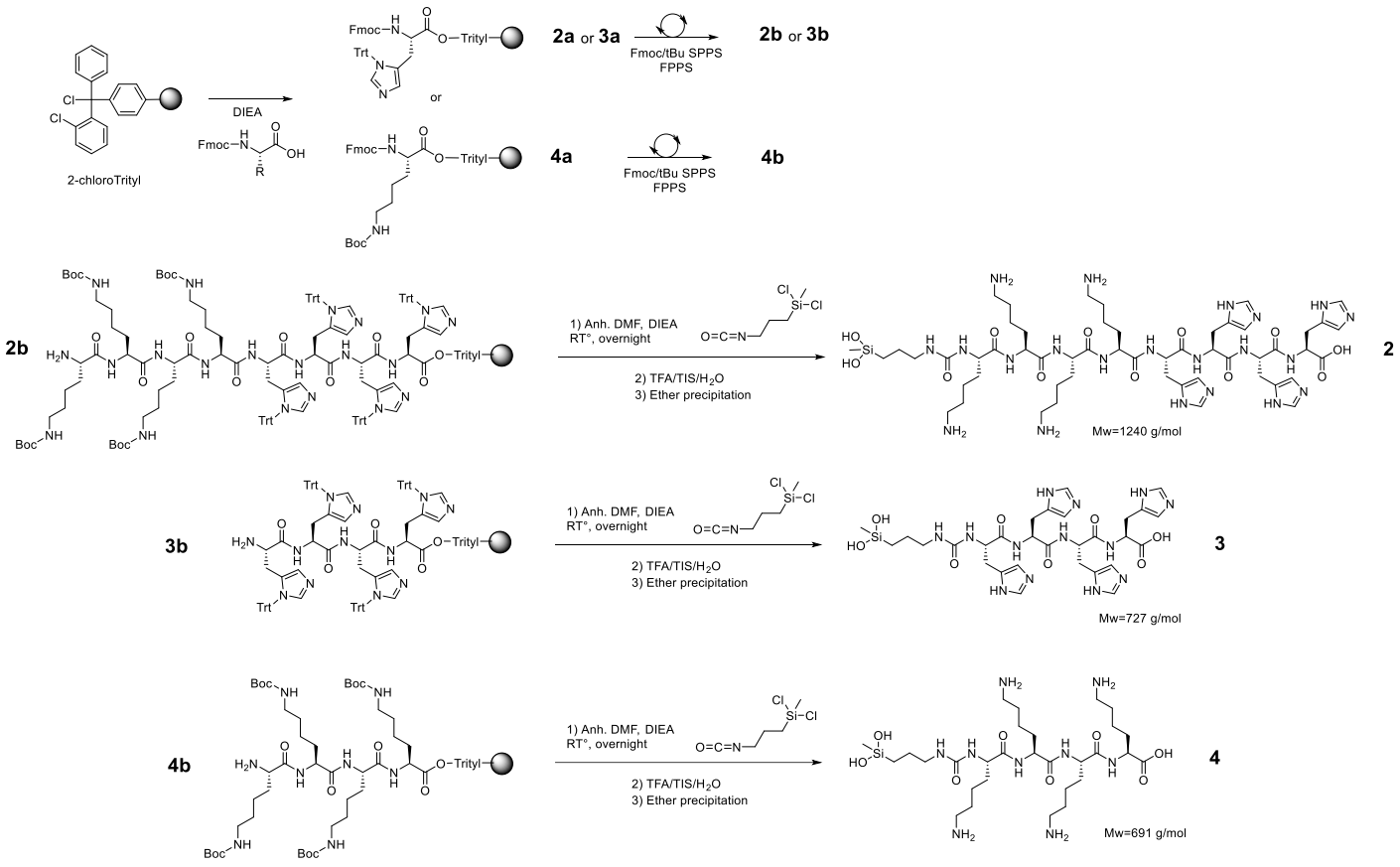

Figure 67. Silylation on support of peptide for polyplexes.

On the ESI+ LC/MS chromatogram we identified the compound **2**: rt= 0.27min $[M+H]^+$ m/z 1241; $[M+H]^{2+}$ m/z 621 (Figure 68).

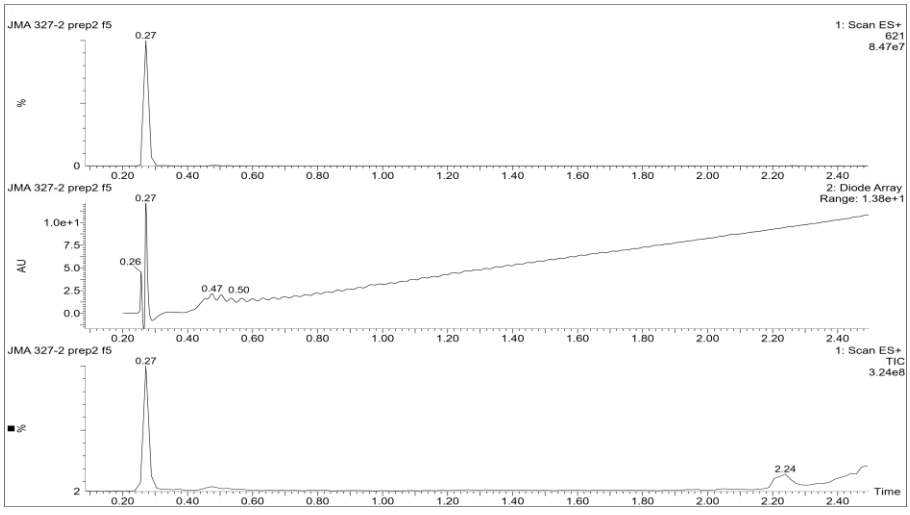

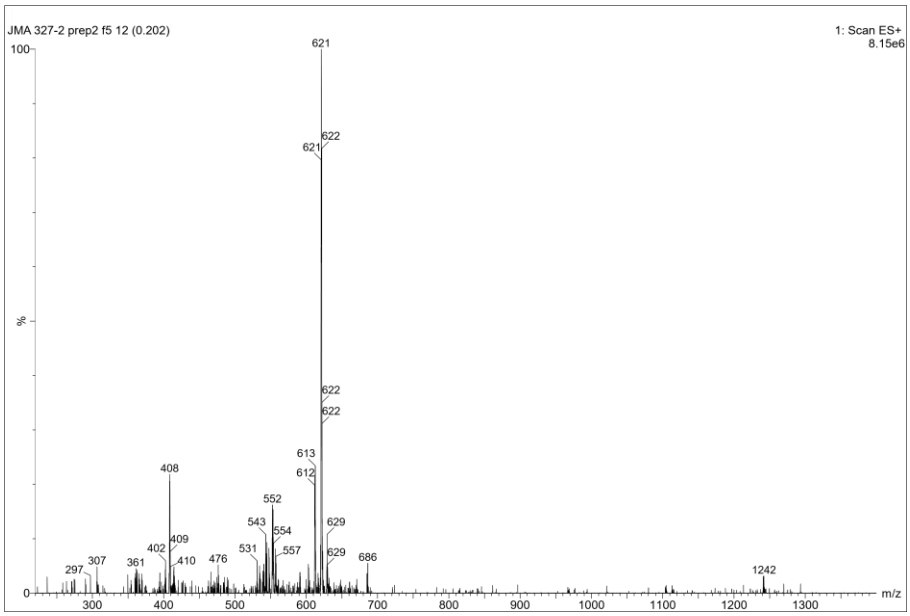

*Figure 68. ESI + LC/MS of compound **2** after purification, analyzed in H_2O/ACN (50/50) 1‰TFA on C_{18} grafted silica column. Top: chromatograms UV at 214nm and TIC, Bottom: MS spectrum at 0.20 min.*

d. *Hybrid RGD-based peptides **5** and **6***

The third type of hybrid peptide synthesized was based on the ArgGlyAsp (i.e. RGD) tripeptide motif. RGD is a motif found in fibronectin by E. Ruoslahti in 1970 and showed first attachment properties for the site of fibronectin, then other sites of recognitions have been found in other extracellular matrix.[255,256]

RGD-containing peptides have an interestingly high affinity for integrin receptors, especially $\alpha_V\beta_3$ integrins overexpressed on cancer cells. Integrins are transmembrane receptor composed of two parts: the α and the β.[257] These receptors are involved in the cell adhesion as they bind to extracellular matrix proteins, the fibronectin, thanks to their extracellular region. These integrin contains metal ions (Mn^{2+}, Ca^{2+} or Mg^{2+}), which strongly binds with RGD peptides through electrostatic interactions.[258,259]

RGD motif can be introduced as linear or cyclic peptides: the linear form as an agonist and the cyclic form as an antagonist of the integrin receptors.[260–263] It has been proven that the cyclic form, c[RGDfE] (with f being the d(Phe)), is more stable and more specific regarding $\alpha_{II}\beta_3$ integrin receptor.[264,265] Many materials have been functionalized with c[RGDfK] instead of c[RGDfE]: the substitution of the Glu by a Lys facilitates the conjugation of this peptide and its grafting.[266] Indeed, if a surface comprises activated carboxylic acid c[RGDfK] may react with it. The presence of both a Glu and a Asp in c[RGDfE] would have necessitated the temporary protection of the Asp.

As $\alpha_v\beta_3$ integrin receptors are overexpressed on cancer cells, RGD peptides are then ideal targeting agents for cancer cells either for diagnostic or drug delivery applications. Molecular imaging technologies (MIT) are based on the conjugation of a tracer (e.g. a dye, a radioelement) with a targeting agent to increase their sensibility in order to detect tumors at their early stage.[267] Thus, RGD peptides were coupled to a fluorescent dye or radio tracer (e.g. Cyanine 5.5, ^{18}F probe) to image cancer cells.[268–270] RGD peptides were also used for drug and gene delivery.[271,272] The drug-RGD conjugate accumulates preferentially on cancer cells and then, the drug cargo may cause the death of tumor cells.

A combination of these two applications is possible to get theranostic systems able to detect and treat cancer cells at the same time.

Finally, RGD peptides have shown great interest in tissue engineering.[273,274] Indeed, as fibronectin mimics, they can promote cell adhesion thus helping the colonization of materials by cells.[275] Consequently, they have been incorporated in many biomaterials, including hydrogels for cell encapsulation.[276,277]

We synthesized two different versions of hybrid RGD-based peptide, a linear one: $Me(OH)_2Si$-$(CH_2)_3NHCO$-$(\beta Ala)_4$-GRGDSP-OH, compound **5**, and c[RGDfK($Me(OH)_2Si$-$(CH_2)_3NHCO$-NH-PEG-Ala(CF_3))], compound **6**.

For the synthesis of compound **5** and **6**, a 2-CTC was chosen to obtain C-ter carboxylic acid functions (Figure 69).

In the case of compound **5**, the silylation was done in solution. TFA treatment released the peptide from the resin and removed all the side chains protecting groups. The deprotected side chains do not present any primary amine, and so the isocyanate (used in equimolar amount) only react at the N-terminus of the peptide chain (i.e. H-βAla). The purified peptide was solubilized in anhydrous DMF. DIEA (6 eq) and isocyanatopropyl dichloromethylsilane (1.2 eq) were added to the mixture. The reaction was stirred for 1h under argon. The solvent was evaporated under vacuum and the resulting silylated peptide precipitated in Et_2O. The hybrid macromonomer was finally purified again on preparative HPLC using a non-silica-based column PLRP-S and lyophilized. The final yield of the synthesis was around 30%.

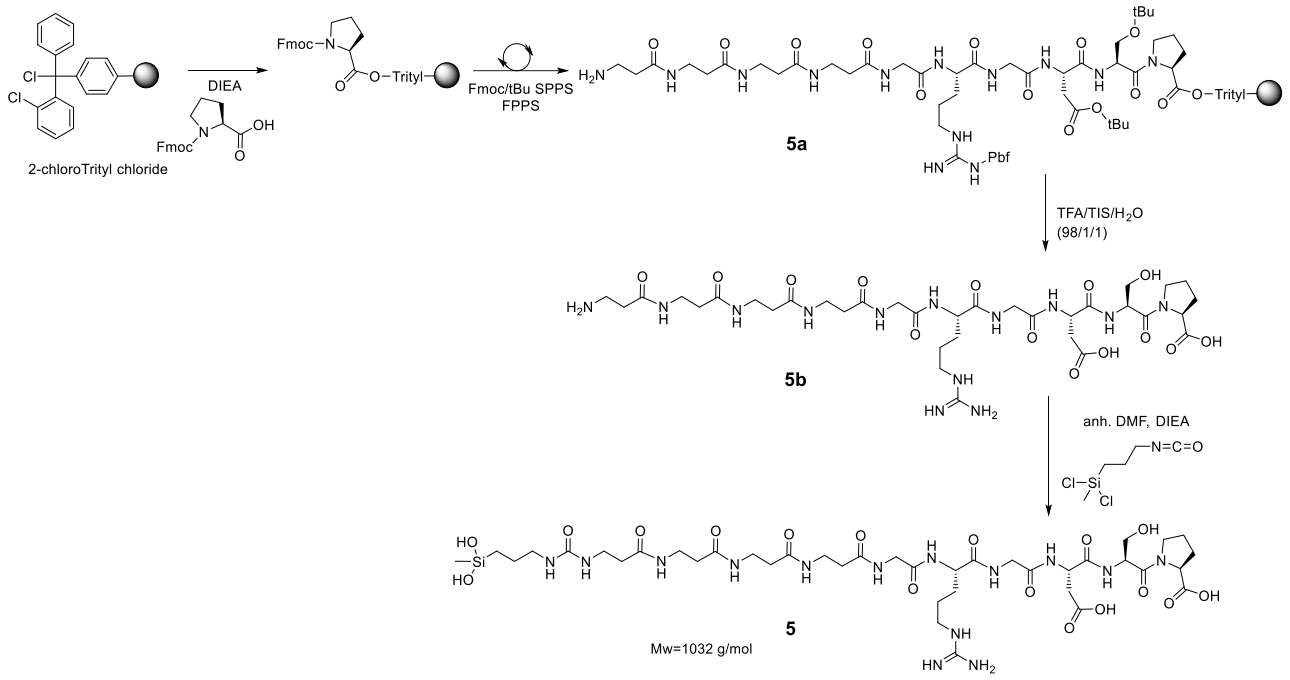

*Figure 69. Synthesis of hybrid peptide **5**.*

On the ESI+ LC/MS chromatogram, we identified the compound **5**: rt= 1.60min $[M+H]^+$ m/z 1034; $[M+H-H_2O]^{2+}$ m/z 500 (Figure 70).

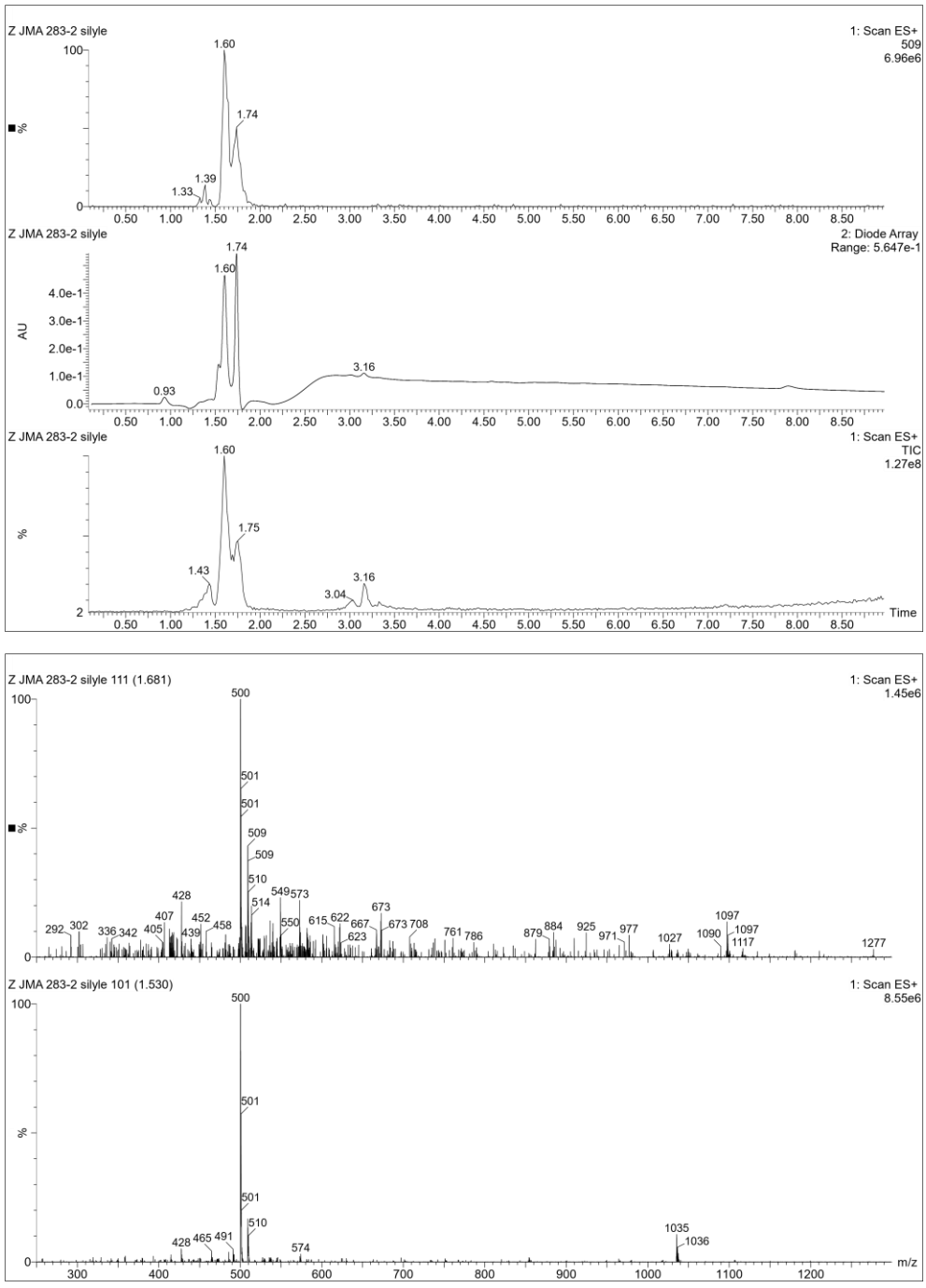

*Figure 70. ESI + LC/MS of compound **5** after purification, analyzed in H2O/ACN 1‰ TFA on PLRP-S column. Top: chromatograms UV at 214nm and TIC, Bottom: MS spectra at 1.60 and 1.74 min*

2-CTC PS resin was also used for the synthesis of compound **6**. However, the linker had a second role in this synthesis. In addition of generating a C-ter carboxylic acid function upon cleavage, this linker can be cleaved in mild conditions, to keep the side chain protecting groups. This is a key step for the N-ter C-ter cyclisation which is done in solution directly after the cleavage from the resin. Indeed, in order to avoid side reaction, only one primary amine function and one carboxylic acid function have to be free on the peptide. All the other side chain functions have to be protected. In addition, in order to avoid epimerization and so loss of specificity regarding the integrin, the cycle has to be formed in this order and no other: the reaction has to be done between the N-ter

amine of the Glu residue and the Gly, activated at its C-ter du to the fact that Gly residue is not a subject to epimerization.

The peptide was synthesized following classical Fmoc SPPS except the use of a non-usual side chain protection on the Lys: the ivDde. This protection is stable to TFA treatment and so to the cleavage of the peptide. Besides it enables a specific deprotection of the Lys without deprotecting the tBu and Pbf protection also present on the peptide during the synthesis. The peptide **6a** is cleaved with a DCM/TFE/AcOH (70/20/10, v/v/v) solution for 1h and then evaporated. Linear side chain protected peptide **6b** was precipitated in diethylether and the cyclisation was done in DMF, with DIEA (6eq) and HATU (1eq) at lower concentration than usual. Indeed, too high concentration of peptide can lead to side reaction such as intermolecular coupling and so dimerization or trimerization, etc. To avoid it, the peptide solution for the cyclisation has a concentration of peptide around 30 mM.

The solvent was then evaporated under vacuum and the cyclic, ivDde protected peptide **6b** was recovered by precipitation in Et_2O. The next step was the ivDde deprotection done by a 2%v hydrazine solution in DMF, which was monitored by LC/MS analysis.

The next step was the coupling of Fmoc-Ala(CF_3)-OH following classical amide coupling to yield compound **6c.** This fluorous amino acid will later enable the absolute quantification of this macromonomer into a polymer by ^{19}F NMR using Electronic Reference To access In vivo Concentrations (ERETIC) method.[278,279] The intensity of the ^{19}F NMR signal of the fluorine probe is compared to a standard curve made from TFA solution prepared in the same conditions as the NMR sample: same tube, same solvent, same volume. The known TFA concentration is giving a standard curve relating fluorous atom molar quantity to peak intensity in ^{19}F NMR.

Because of the role of this hybrid monomer played in the future application, the cyclic RGD peptide needed to be moved away from the silyl group. Consequently, a Boc-NH-PEG_{3000}-COOH was coupled to the primary amine of the fluorine probe by classic amide coupling to afford compound **6d**. The silylation was done in solution as previously leading to compound **6** (Figure 71). The final yield of the synthesis was around 20%.

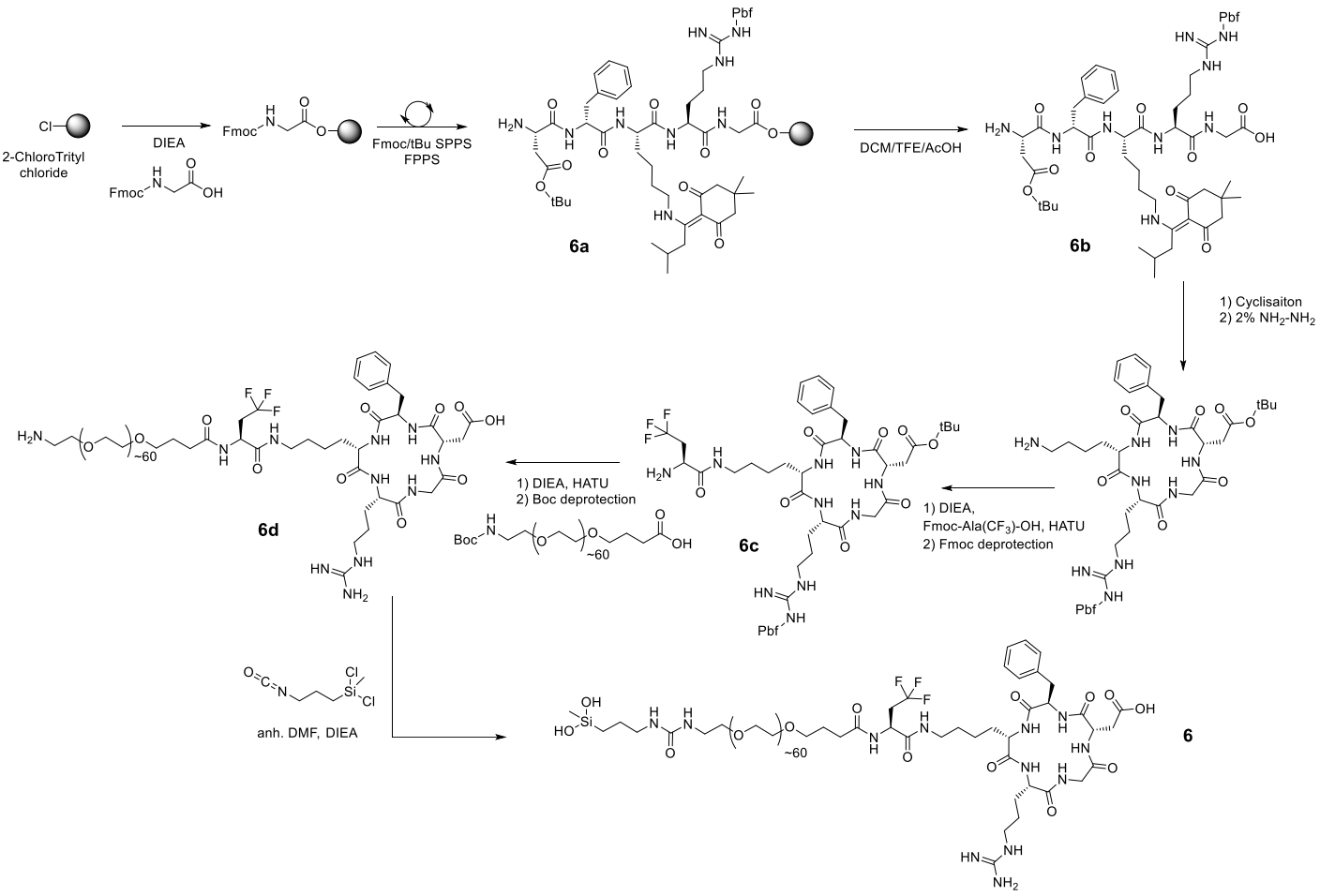

*Figure 71. Synthesis of hybrid peptide **6**.*

On the ESI+ LC/MS chromatogram we identified the compound **6c** before the Fmoc deprotection and after purification: rt= 2.31min $[M+H]^+$ m/z 1274 (Figure 72).

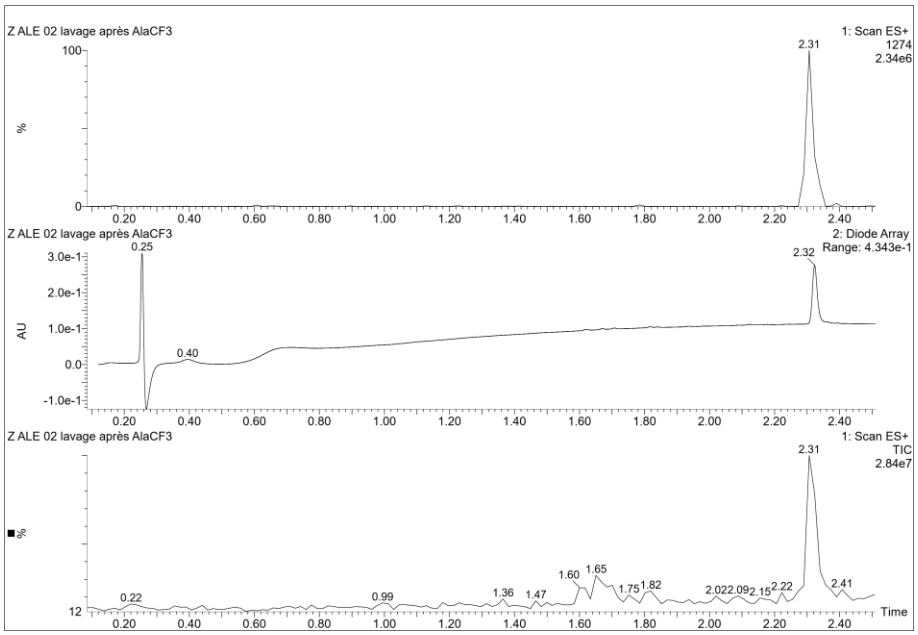

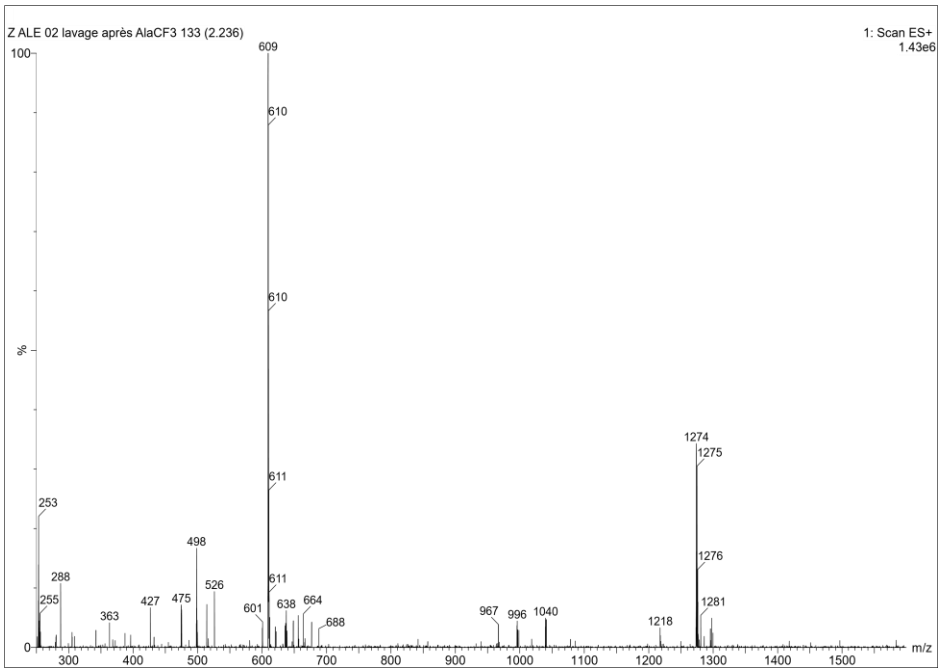

*Figure 72. ESI + LC/MS of compound **6c** before the Fmoc deprotection* and *after purification, analyzed in H_2O/ACN (50/50) 1‰TFA on C_{18} grafted silica column. Top: chromatograms UV at 214nm and TIC, Bottom: MS spectrum at 2.24 min.*

III. Synthesis of silylated drugs and organic molecules

As later presented in chapter 5 an ideal multifunctional material should present targeting agents (e.g. peptide ligands), but also drugs which could affect target cells. With the aim to prepare objects suitable for cancer therapy, we focus our attention on cytotoxic drugs already used for cancer treatment. Temozolomide, Methotrexate and Camptothecin were chosen as first examples of drugs to be silylated. In addition, and depending on the mode of action of these three drugs, they were modified by linkers designed to release the active moiety. Probes for imaging were also silylated: DOTA for PET and fluorescein for *in vitro* FACS experiments and fluorescent microscopy studies. At last, hybrid silylated PEG was also prepared as a way to tune the hydrophobic/hydrophilic balance of the materials but also as a stealth agent that should allow the polymers to avoid recognition by the immune system. In some cases, a fluorine probe was introduced for enabling quantification by ERETIC method as we did for compound **6**.

After a brief overview of the interest of each bioactive molecule and its potential application, the synthetic strategy, including the introduction of modifications, spacers and linkers, is presented here.

a. *Hybrid Temozolomide derivative **7***

Temozolomide (TMZ, 8-carbamoyl-3-methylimidazo[5,1-d]-1,2,3,5-tetrazin-4(3H)-one) is a drug which was marketed in 2000 by Schering Plough for the treatment of brain cancer.

TMZ is actually a prodrug: a biomolecule that needs a chemical reaction to be metabolized it into pharmacologically active drug after administration. This process helps to improve the bioavailability and to reduce side effects compared to the direct administration of active substance.

TMZ is an alkylating agent which belongs to the group of triazene derivatives that comprises several active prodrugs such as Dacarbazine or Mitozolomide.[280] Their characteristic is their decomposition in methyldiazonium cation (Figure 74).[281] At physiological pH, TMZ is subject to a base-catalyzed decomposition into monomethyl triazenoiimidazole carboxamide (MTIC) in the cytosol of the cell (Figure 73). MTIC is also rapidity degraded and turned into 5-aminoimidazole-4-carboxamide (AIC) and methyldiazominum cation (Figure 74). AIC is inactive but the methyldiazominum cation is highly toxic because it creates an alkylation of the guanine present in DNA sequence, at O^6 (6%) position and N^7(70%).[282] Although the O-alkylation happens less, it is the crucial one as it strongly affects the cell's time life. Indeed, the DNA is unable to repair the damage caused from the O-alkylation because the mismatch repair (MMR) mechanism does not work in this case. Indeed, the DNA cannot find a complementary base partner for the O^6-methylguanine. Finally, the DNA fragmentation is leading to the death of the cell.

It is worth noting that cells have developed a mechanism of resistance against such types of prodrugs via the methylguanine-DNA methyltransferase (MGMT). This enzyme is present in the nucleus of all living cells and, limits the action of TMZ by repairing the DNA damage caused by the O-alkylation. To overcome this problem some depletion molecule has been administrated in the same time than TMZ in order to inhibit the action of MGMT.[283,284]

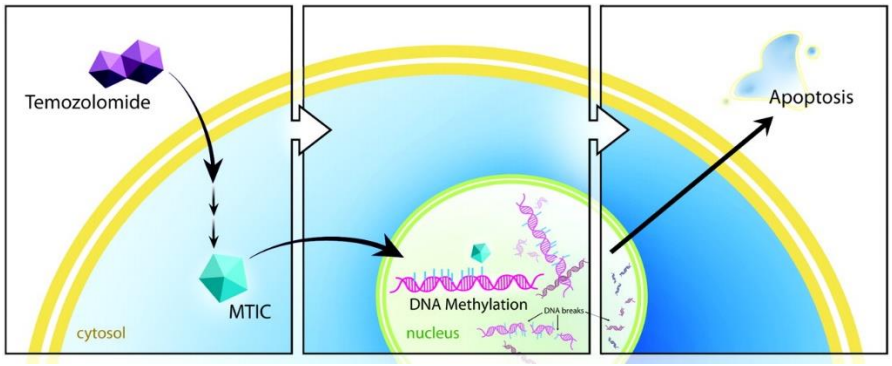

Figure 73. Proposed mechanism of action of TMZ in the cell.[285]

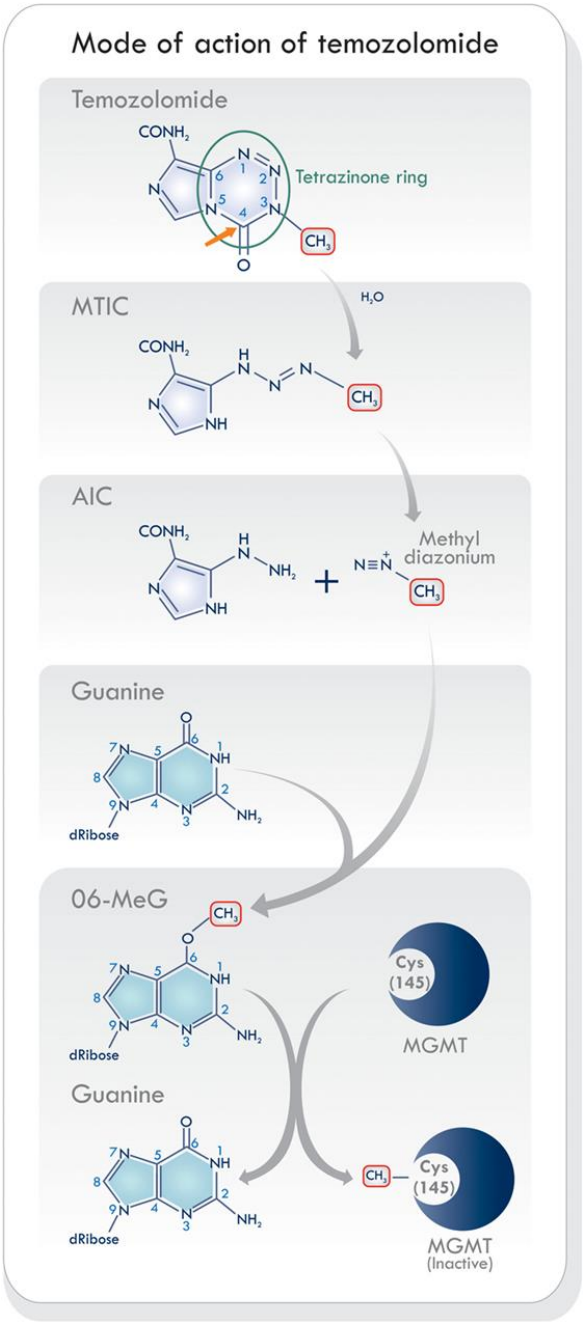

Figure 74. Mechanism of action of TMZ and its action on Guanine.[283]

We took profit of the pro-drug mechanism of TMZ to design the compound **7**, a silylated derivative of TMZ (Figure 75). Indeed, we did not modify any important part of the heterocycle required for the generation of the methyldiazonium. On the contrary, we inserted a silylated spacer at the amide position. For that purpose, we used a carboxylic acid derivative of the drug **7a** (3-Methyl-4-oxo-3,4-dihydroimidazo[5,1-d][1,2,3,5]tetrazine-8-carboxylic acid) which was coupled with a free primary amine of a N-Boc-1,3-diaminopropane spacer yielding compound **7b**. After the coupling, **7b** was extracted by ethyl acetate and washed several times by aqueous solution before being dried under $MgSO_4$.

Once purified, a TFA solution was used to remove the Boc-protecting group. Despite the acid treatment, the TMZ analog is not degraded as shown on Figure 74. This is due to the fact that the degradation is happening a physiological pH: TMZ is stable at pH<4.[280]

After precipitation as TFA salt, **7b** was reacted with isocyanatopropyl dichloromethylsilane (ICPDCMS) (1.2 eq) in anhydrous DMF in the presence of DIEA (6 eq) to remove the TFA salt. The hybrid drug, compound **7**, was precipitated in Et_2O and stored under argon atmosphere. This macromonomer has to be prepared freshly before any use for material synthesis as it cannot be hydrolyzed once condensed. Indeed, we use basic solution to hydrolyze condense macromonomer but TMZ is degraded at basic pH. The final yield was not determined as only a small part of it has been purified; the rest of it being degradated.

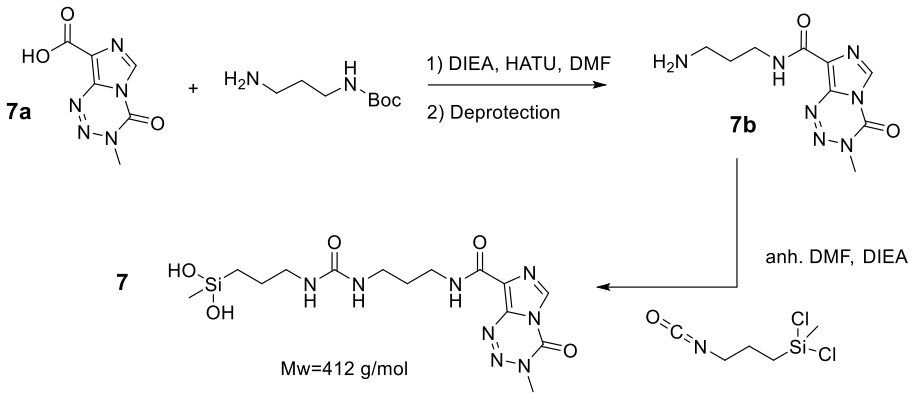

*Figure 75. Synthesis of compound **7**, silylated derivative of TMZ.*

b. *Hybrid Methotrexate derivatives **8** and **9***

Methotrexate (MTX) is used for the treatment of diverse cancers including breast, head or neck cancers, as well as autoimmune diseases and lymphocytic leukemia.[64,286] It was discovered in 1947 by Roy Hertz and marketed in 1950's.

MTX has actually a dual mode of action, being both a targeting agent and a drug. Indeed, MTX structure is very close to folic acid and shares the same ability to bind specific receptors overexpressed on membrane on cancer cells: folate transporter 1, also known as reduced folate carrier 1 (RFC1) and folate receptor (Figure 76).[287,288] This helps the MTX to go through the membrane of the cell. Once inside the cell, the MTX suffers an irreversible coupling of polyglutamate (i.e. 1 to 7 Glu moieties attached to MTX, catalyzed by folylpolyglutamate synthetase (FPGS), producing $MTX_{Glu(1-7)}$, Figure 77).[289] $MTX_{Glu(1-7)}$ inhibits several intracellular enzymes such as 5-aminoimidazole-4-carboxamide ribonucleotide transformylase (ATIC), involved in the inhibition of the action of adenosine and guanidine precursor; dihydrofolate reductase (DHFR) involved in the reduction of the folic acid; and thymidylate synthase (TS) involved in the inhibition of the synthesis of thymidine moieties. These multiple inhibition results in antiproliferative and anti-inflammatory effects.

The inhibition of DHFR enzyme confers to MTX the role of an antagonist of folic acid, and is also inducing an inhibition of proliferation of cancer cells.[287,290] MTX does not have irreversible side effects on healthy tissue on the contrary to malign cells that have a faster proliferation rate and are much more sensitive to this drug.

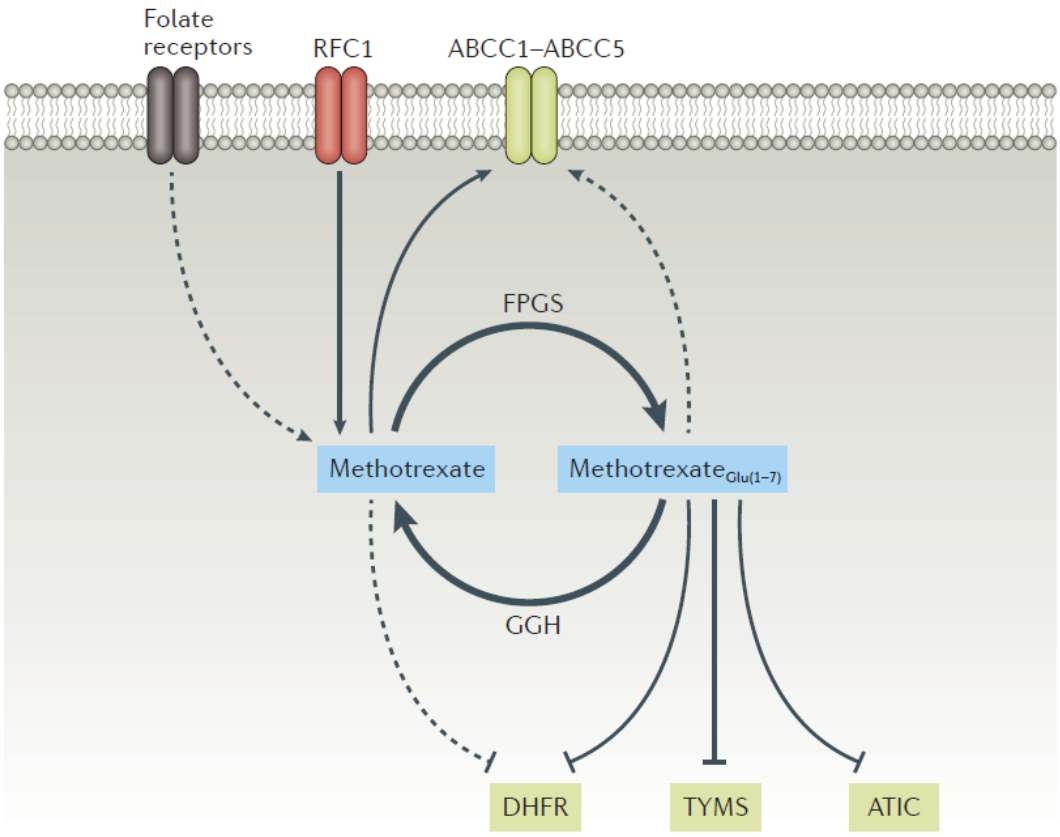

Figure 76. Mode of action of MTX inside the cell and its actions on ATIC, DHFR and TYMS.[287]

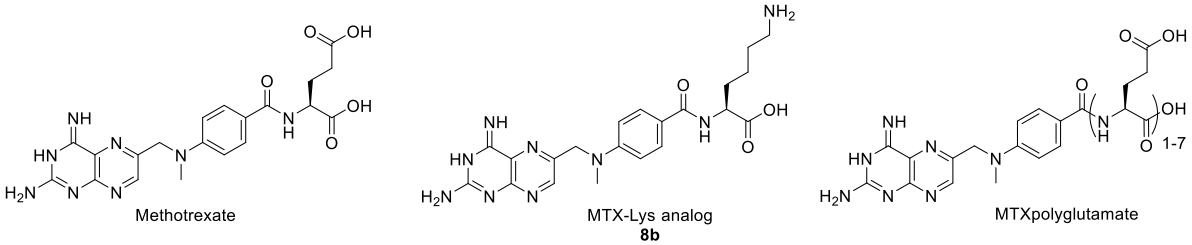

Figure 77. Comparison of the Methotrexate, the MTX analog and the MTX$_{Glu(1-7)}$.

MTX enter the cells through its interaction with reduced folate and folate receptors. It has been demonstrated that the heterocylic core was responsible for this interaction and that modification could be afforded at the Glutamic side without significate loss.[290] For example PAMAN dendritic polymer have been covalently modified in order to become nano carrier for MTX, Dextran have been conjugated to a peptide and then MTX in order to become a drug delivery system and dendritic chitosan was also modified at the Glu side to be able to load MTX moiety.[65,291,292]

On the basis of these data, we envisioned to add a spacer between the silane moiety and the drug on the Glutamic region of the molecule. For that, Glu was replaced by Lys and a spacer was installed at the side chain of Lys via an amide coupling. The precursor of MTX, compound **8a**, was used to prepare the lysine-containing analogue of MTX.

In addition, as the MTX core has to interact with cell surface, it had to be accessible on the corona of the NPs that we would have prepared. Thus, we chose a relatively long PEG spacer (3000 Da) presenting the MTX core at its extremity and the silane moiety at the other end (compound **8**). That would help the NPs to get to the cells.[293]

It is worth noting that, for a purpose of ERETIC ^{19}F NMR quantification, the fluorine-containing derivative of compound **8**, compound **9** was also prepared.

At last, the linker does need to be cleavable since we hypothesized that modified MTX conjugates will still be able to interact and inhibit their targets.

Compound **8** was synthesized on solid support and in solution. The first step was the anchoring of Fmoc-Lys(Alloc)-OH on a 2-CTC PS resin in DMF in the presence of DIEA. Then, after the removal of Fmoc protecting group by a DMF/piperidine solution (80/20; v/v), commercially available compound **8a** (4-[[(2,4-Diamino-6-pteridinyl)methyl]methylamino]benzoic acid) (1eq) was activated by HATU (1.5 eq) and DIEA (6 eq) in DMF during 15 min and coupled to the primary amine of the Lys anchored on solid support (1.5eq) overnight. This pre-activation was necessary because of the low reactivity of the benzoic acid function of the compound **8a**.

Without the pre-activation a guanilation, side reaction was observed on the Lys N-ter primary amine and so not all the compound **8a** were conjugated to the Lys moieties after the overnight reaction. Also, the compound **8a** was used in small default in order to maximize its conjugation and make sur all of it is attached to the solid support through the Lys moieties. This is why, after the next step, the Alloc deprotection, we cleaved this MTX derivate, compound **8b**, in order to be able to purify it before the coupling of the spacer, that will have to be done in solution.

The Alloc deprotection was carried out by Pd^0 Tetrakis (0.25eq) and phenylsilane(25 eq) for 30 min in DCM.[294] After this deprotection, the MTX-Lys derivative **8b** was cleaved from the support by a TFA treatment for 1h.

Boc-NH-PEG_{3000}-COOH was coupled with DIEA and HATU in DMF to **8b** yielding PEGylated compound **8c**. The silylation was done in solution using ICPDCMS (1.2 eq) in anhydrous DMF with DIEA (6 eq) for 1h at room temperature. The hybrid macromonomer **8**, was recovered after precipitation with a final yield of 45%.

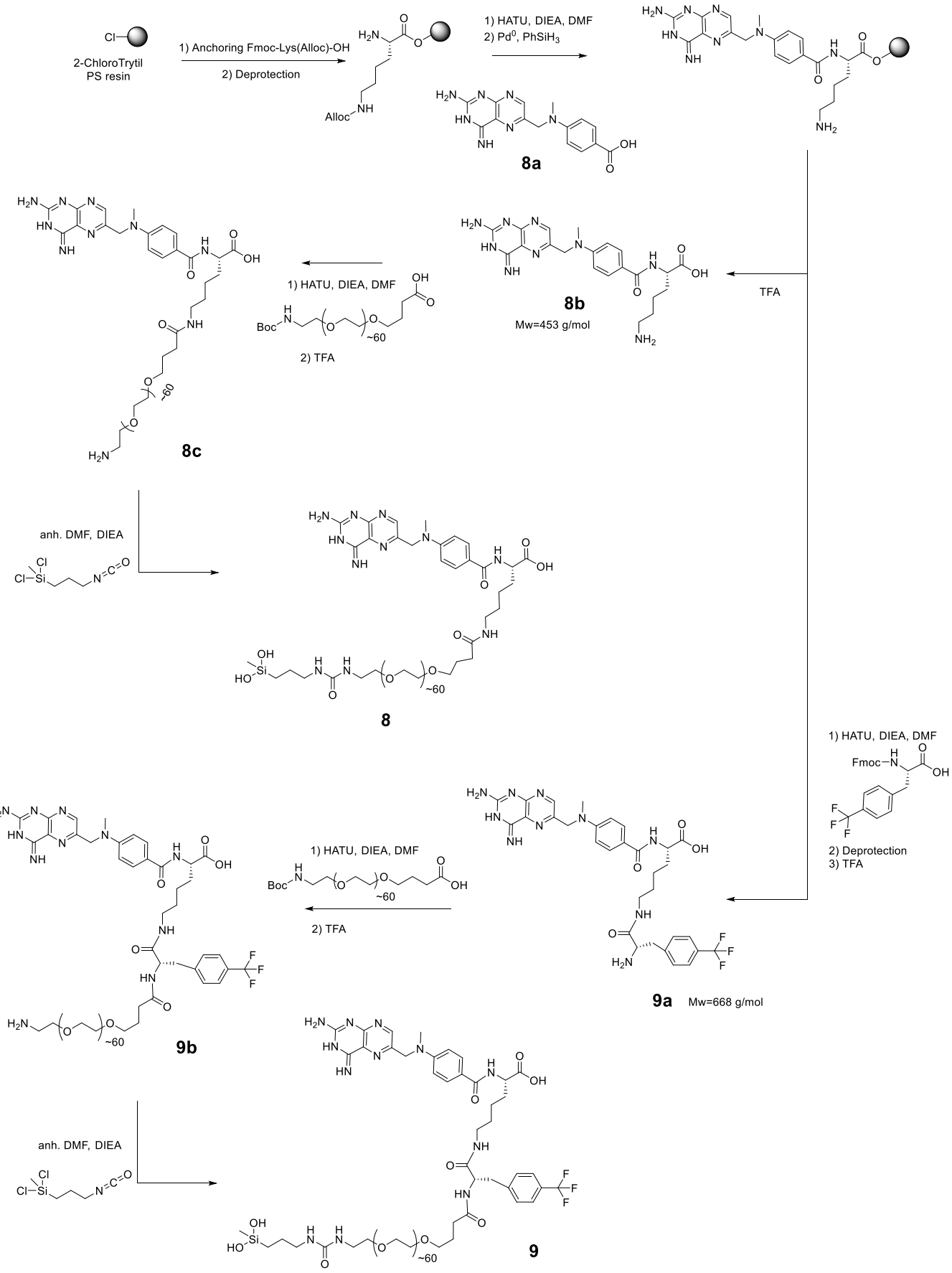

*Figure 78. Synthesis of compound **8** and **9**, silylated derivative of MTX.*

On the ESI+ LC/MS chromatogram we identified the compound **8b** after purification: rt= 0.70 min $[M+H]^+$ m/z 454 (Figure 79).

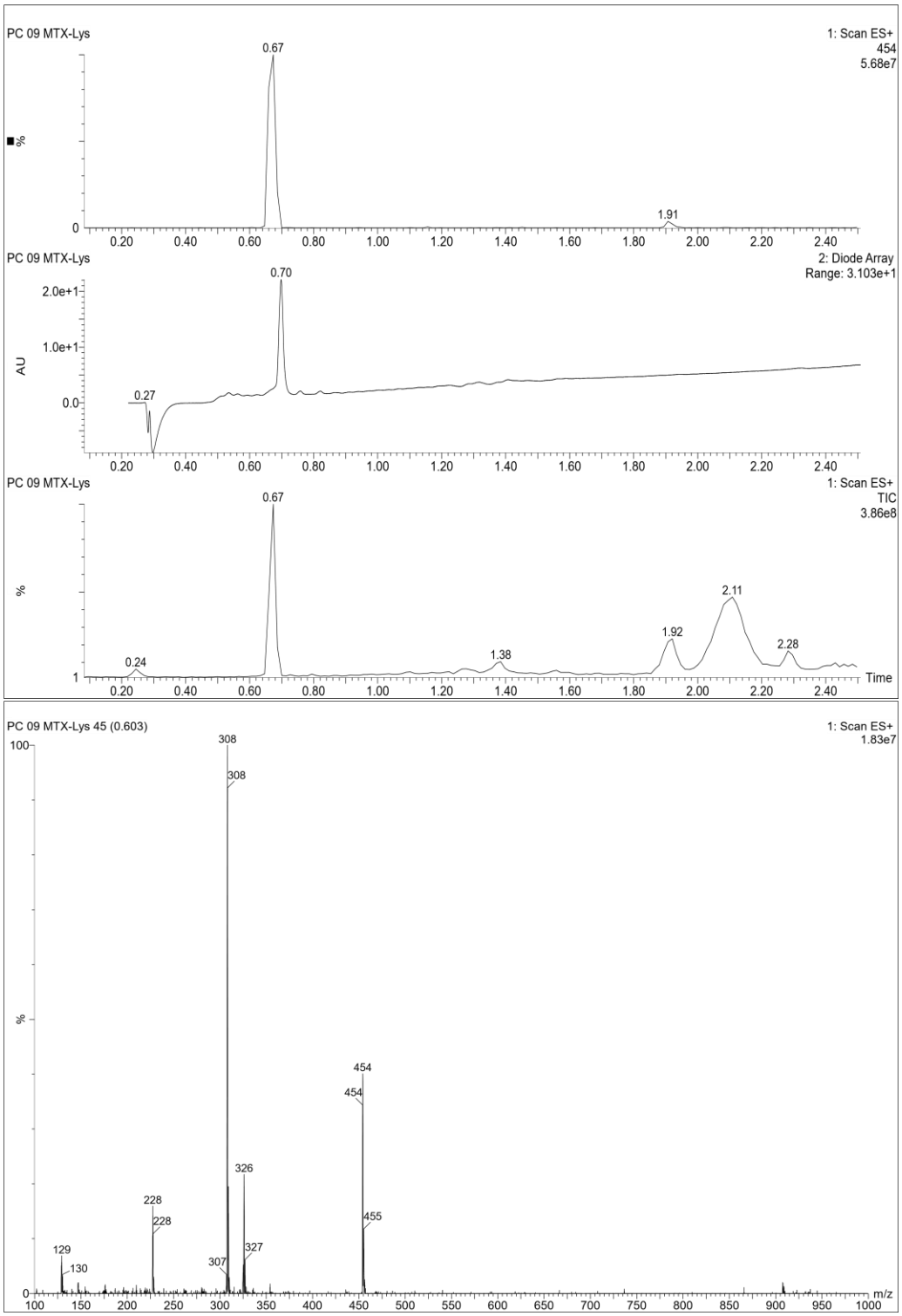

*Figure 79. ESI + LC/MS of compound **8b** after purification, analyzed in H_2O/ACN (50/50) 1 TFA ‰ on C_{18} grafted silica column. Top: chromatograms UV at 214nm and TIC, Bottom: MS spectrum at 0.70 min.*

On the ESI+ LC/MS chromatogram we identified the compound **9c** after purification: rt= 0.97 min $[M+H]^+$ m/z 670 (Figure 80).

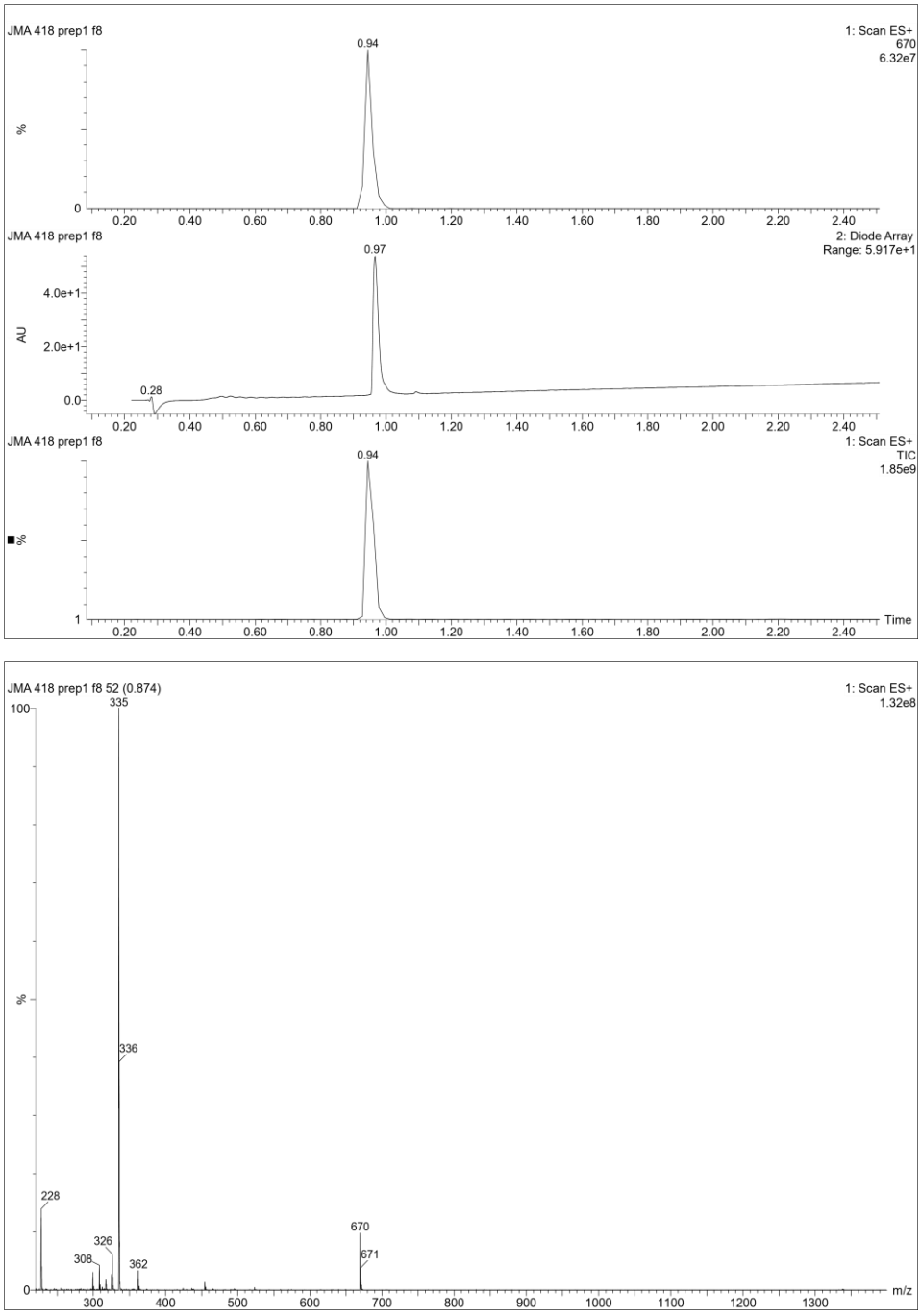

*Figure 80. ESI + LC/MS of compound **9a** after purification, analyzed in H_2O/ACN (50/50) 1‰ TFA on C18 grafted silica column. Top: chromatograms UV at 214nm and TIC, Bottom: MS spectrum at 0.97 min*

We first thought that the quantification of macromonomer **8** inside the multifunctional PDMS polymers would be possible by ^{1}H NRM. Unfortunately, proton signals were difficult to distinguish from those of hybrid c[RGD] compound **6**. This is why we finally prepared fluorinated compound **9** containing a H-(trifluoromethyl)-L-phenylalanine.

The synthesis was similar to the one of compound **8**, with one notable difference: Fmoc-Phe(CF_3)-OH was coupled to **8b** (HATU/DIEA) and deprotected before the cleavage and the coupling of BocNH-PEG_{3000}-COOH, which is more efficient in solution (Figure 78, bottom). The final yield of this reaction was around 40%.

c. *Hybrid Camptothecin derivative **10***

Camptothecin (CPT) was discovered by Monroe Wall in 1966 from natural extracts coming from the stem of camptotheca.[295] This drug have been proven effective against malignant tumor and able to block the action of topoisomerase 1 (Topo 1), an important enzyme involved in cell division. It is known as an efficient anti-cancer drug, active on ovarian, breast and colon cancers. It was marketed in 1995 in Europe.

CPT has several major drawbacks: it not soluble in water, has a low biocompatibility and is toxic to normal cells.[296] This led the researchers to synthesize analogues whose most of them were active on cancer cells. However, only two water-soluble analogues have been authorized for cancer treatment: Irinotecan and Topotecan (Figure 81).[297,298]

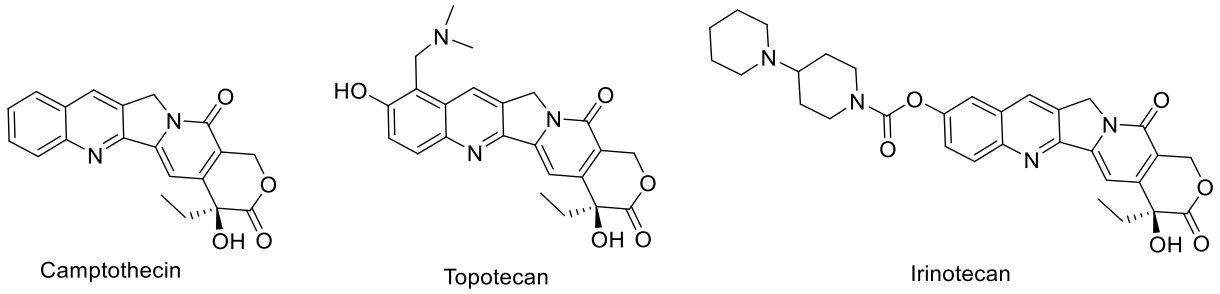

Figure 81. Comparison of Camptothecin and two of its water-soluble analogs.

The mode of action of CTP and its analogues been highlighted over the years. CPT enters the cell with the help of human P-glycoprotein (PGP) and human multidrug resistance protein 2 (MRP2) that play the role of transporter.[299] Once inside the cell, CPT binds to the Top1/DNA covalent complex involved in replication and transcription.[297] CPT needs the presence of both biomolecules to bind the complex, creating a tertiary complex. CPT is blocking the action of Top1 on the DNA, impairing replication and transcription and causing cell death. CPT has also an action on the RNA synthesis, suggesting that it may have another cellular target.[300]

On the contrary of MTX and TMZ, CPT has to be left unmodifed to exert its activity. That is why we plan to functionalize the active form of the drug with a traceless, self-immolative linker presenting the silyl group at one of its sides.[198] The chosen linker is the bis(2-hydroxyethyl) disulfide (BHD), a symmetric linker that can be conjugated twice through its hydroxyl groups (Figure 82). BHD is sensitive to reductive conditions, enabling the release of the drug in presence of gluthatione (GHS), an antioxidant biomolecule present in the cytosol that protects cells by regulating oxidation.

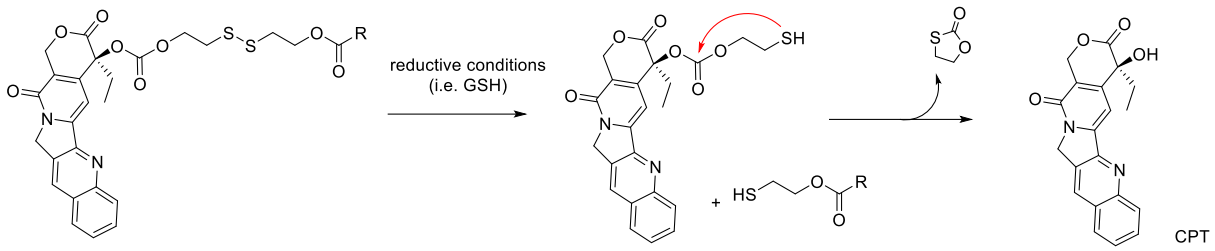

Figure 82. Glutathione mediated release of CPT from a conjugate (R) by reduction of the disulfide based a self immolative linker.

We proposed to link BHD and CPD hydroxyl groups via an carbonate, as shown in Xu et al.[198]; and the other side though a carbamate linkage formed by reacting alcohol of BHD with ICPDCMS (Figure 83).

A DCM solution of CPT (1eq) and 4-dimethylaminopyridine (DMAP) (3eq) was prepared under argon. Triphosgene (0.33 eq) was added to the mixture and stirred for 30 min at room temperature under argon to form activated carbamate **10a** which was not isolated. This solution was added dropwise to a solution of BHD (5 eq) in THF under argon. The objective here was to always keep the BHD linker in large excess to favor the mono addition of CTP on one side of the BHD and to avoid the formation of dimers. The mixture was stirred overnight.

The white precipitate, resulting from the activation by the triphosgene, was removed by filtration. The solution was extracted by ethyl acetate (EtOAc), washed three times by water and the solvent was evaporated under vacuum. CPT-BHD conjugate **10b** was purified by preparative RP-HPLC and lyophilized (45% yield).

The final step, i.e. silylation in solution, proved to be very difficult. Indeed, all the examples of silylations with isocyanate reagents in this PhD work were performed on amines, yielding urea bonds. Here, the nucleophile attacking isocyanate is the hydroxyl group of CMP, giving a carbamate bond. Alcohols are a way less reactive towards isocyanate than amines.

Several conditions have been tested with ICPDCMS and silylation was followed by LC/MS analyses of the crude, conversion percentage being calculated from integration of UV peaks on LC/MC chromatogram (Figure 84).

Dichloromethylsilane derivatives are highly sensitive to hydrolysis (even in dry conditions) and HCl is released in solution. That is why we normally use excess of DIEA (6 eq) to ensure that the pH is always basic favoring the nucleophilic attack on the isocyanate and the progress of the silylation reaction.

The silylation was performed in chloroform ($CHCl_3$) because of the solubility of both the CPT and the BHD. We choose to use trimethylamine (TEA) instead of DIEA because TEA have a better miscibility in the chloroform.

The first attempt was performed as usual, with isocyanatopropyl dichloromethylsilane and TEA in $CHCl_3$. The conversion rate was not as good as silylation on amine group: only 24% conversion was observed. The hydroxyl group probably needed activation, thanks to a catalyst, to be silylated.

Then we decide to use dibutyltin dilaurate (DBTDL) as catalyst. Indeed, it was already described, in Xu *et al*, [198] for the synthesis of CPT grafted silica NPs. This catalyst complexs first the hydroxyl and then the amine of the isocyanate, closing the two molecules.[301] Unfortunately, it gave no better results (20 % conversion). We heated the reaction at 60°C but it did not improve the conversion. Anhydrous chloroform was then used to limit the potential hydrolysis of the activated carbamate. In any case, no more than 15% conversion was obtained.

We hypothesized that, besides the low reactivity of the alcohol, the problem could come from the basic pH. Indeed, a well-known side reaction of CPT is the opening of the lactone cycle, forming a carboxylate and an alcohol.[302] This alcohol could compete with the ones of BHD linker[303] forming a intramolecular carbonate which may hydrolyze quickly.

To fix this problem, we chose use isocyanatopropyl diethoxymethylsilane (ICPDEMS) instead of ICPDCMS. This alkoxysilane reagent does not liberate any HCl thus, the pH should not change during the silylation and no more base is required. This should limit the opening of the lactone ring.

ICPDEMS was solubilized in $CHCl_3$. DBTDL catalyst (0.02 eq) was added and the mixture was heated up at 60°C, under argon. Interestingly, anhydrous $CHCl_3$ was not efficient as it was stabilized with 3% EtOH which corresponds to $3*10^{-1}$ mmol/mL. Considering that the concentration of **10a** was $4*10^{-3}$ mmol/mL, the EtOH is then not negligible since in excess and competes with CPT. The non-anhydrous $CHCl_3$ stabilized by amylenes was left on molecular-sieves to remove the water. It was then used for the reaction.

We finally obtained 64% conversion. The resulting silylated macromonomer **10** was obtained after purification. As expected, hydrolysis of alkoxysilane occurred during purification giving silanols.

The solvent was evaporated and hybrid compound **10** was solubilized into H_2O/ACN 1‰ TFA, purified on preparative RP-HPLC column and then lyophilized. The final yield of the synthesis is around 30%.

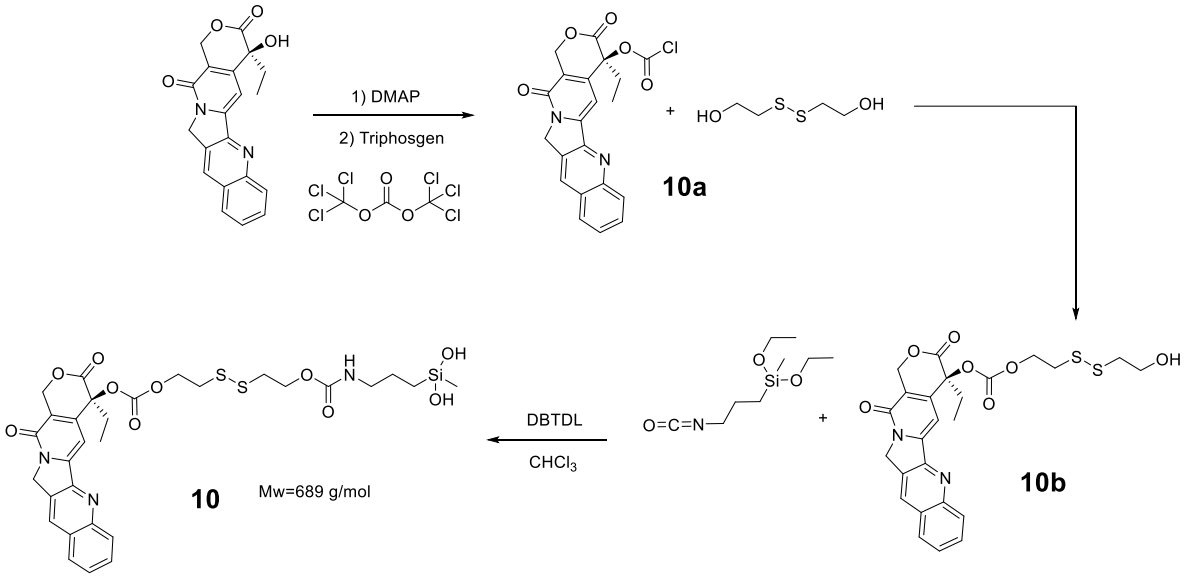

*Figure 83. Synthesis of hybrid compound **10**, silylated derivative of CPT.*

On the ESI+ LC/MS chromatogram we identified the compound **10** after purification: rt= 6.04 min $[M+H-H_2O]^+$ m/z 672 (Figure 84).

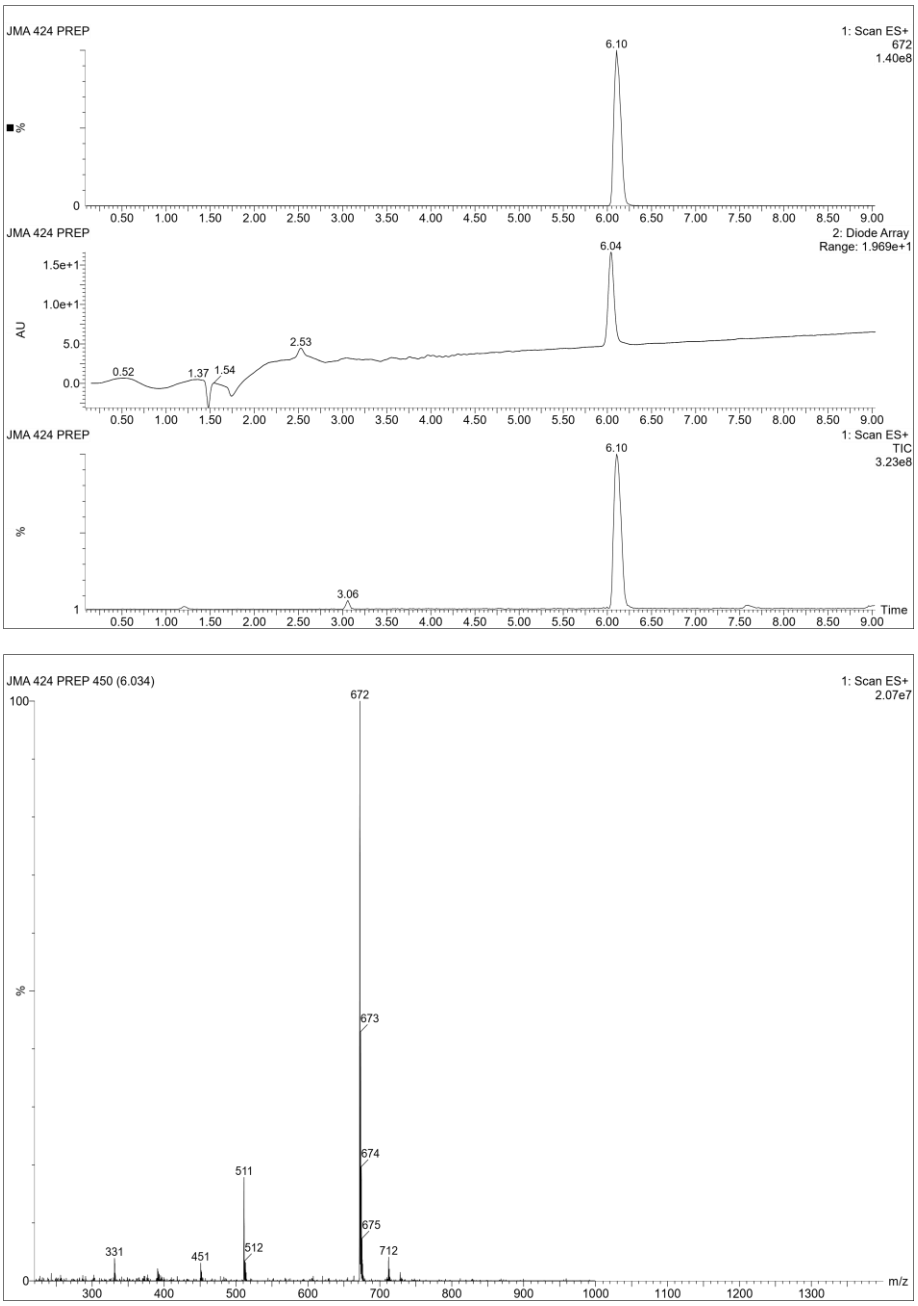

*Figure 84. ESI + LC/MS of compound **10** after purification, analyzed in H_2O/ACN (50/50) 1 TFA ‰ on PLRP-S column. Top: chromatograms UV at 214nm and TIC, Bottom: MS spectrum at 6.04 min*

d. *Hybrid Dota derivatives **11** and **12***

1,4,7,10-Tetraazacyclododecane-1,4,7,10-tetraacetic acid or DOTA is frequently used for the chelation of various metal cations such as ^{68}Ga. DOTA-Ga complexes are widely used in positron emission tomography (PET).[304,305] This technic enables the study of bodies by a non-invasive way and is widely utilized as diagnosis tool in oncology, neurology and cardiology. PET gives highly accurate images with the use of fluorine isotope (^{18}F), labelled on amino acids or biomolecule for example, however, gallium isotopes are now preferred due to their lower cost because they do not need the use of cyclotron. PET technic is based on the measurement of the emission of positron from a radioisotope (i.e. the tracer), with a gamma-camera (Figure 85).[306] Intravenous injection of this tracer is done a short time before the measurement.

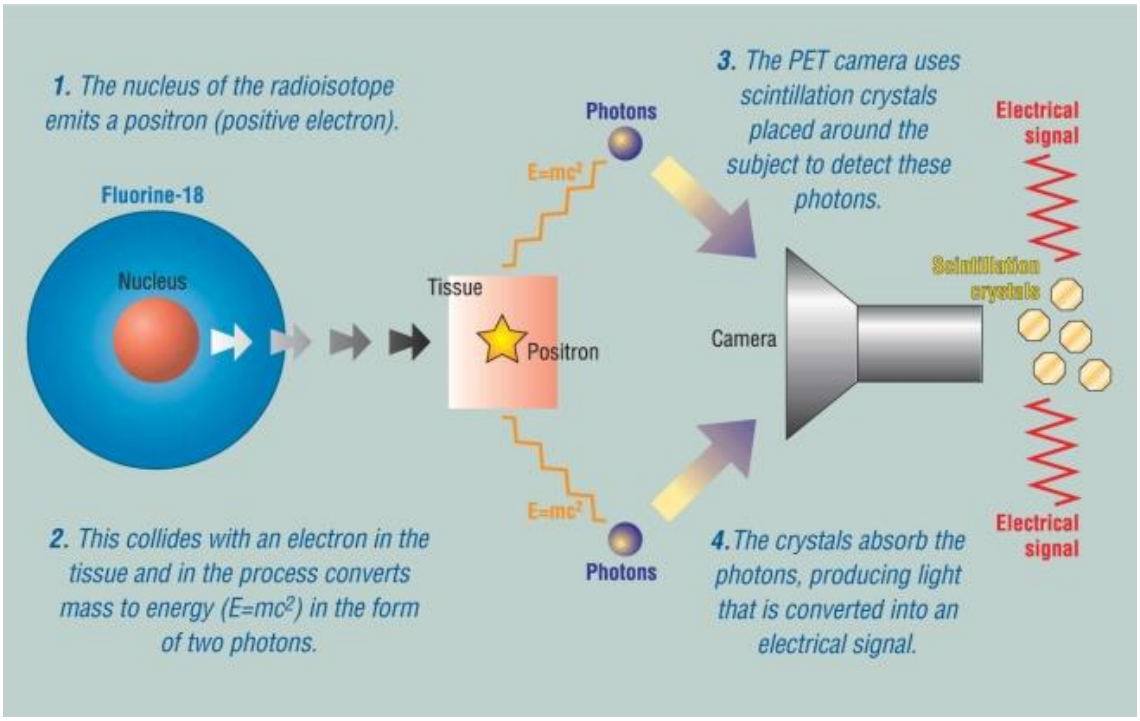

Figure 85. Principle of PET imaging.[306]

^{68}Ga proved to be useful for medicine and biology applications giving good quality PET images. In addition, the introduction of a chelator greatly simplifies the conjugation of GA to a ligand.[307–309] DOTA and NOTA (1,4,7-triazanonane-1,4,7-triyl)triacetic acid) are the most adapted ligands to chelate ^{68}Ga thanks to their cavity size. A lot on analogs have been described since, however DOTA stays the most used due to its availability and ease of synthesis and conjugation.[307]

We were interested by the synthesis of hybrid DOTA chelators to incorporate them in PDMS based copolymers. Such silylated compound would be able to bring imaging properties to PDMS based material or NPs after chelation of the ^{68}Ga that would have been done in a first time.[307] Combined with silylated drugs, the resulting multifunctional PDMS copolymers could be of interest for theranostics.

Two hybrid derivatives were prepared. The first one (compound **11**) was designed from DOTA (Figure 86). Commercially available DOTA(tBu)$_3$ (2-(4,7,10-tris(2-(tert-butoxy)-2-oxoethyl)-1,4,7,10-tetraazacyclododecan-1-yl)acetic acid, **11a**) was selected. This derivative has three of its carboxylic acid functions protected by terbutyl esters (OtBu), leaving only one function available for further modifications.

The second one (compound **12**) was based on the DOTA derivative DOTA GA (1,4,7,10- tetraazacyclododecane-1-glutaric acid 4,7,10-tetraacetic acid), presenting an interesting feature (Figure 86).[310] Indeed, thanks to its glutamic acid at the place of one of the four glycinyl moieties composing the DOTA, DOTAGA enabled the conjugation of the chelator via the side chain of Glu residue while keeping the four carboxylic acid functions available for optimal complexation of the ^{68}Ga.

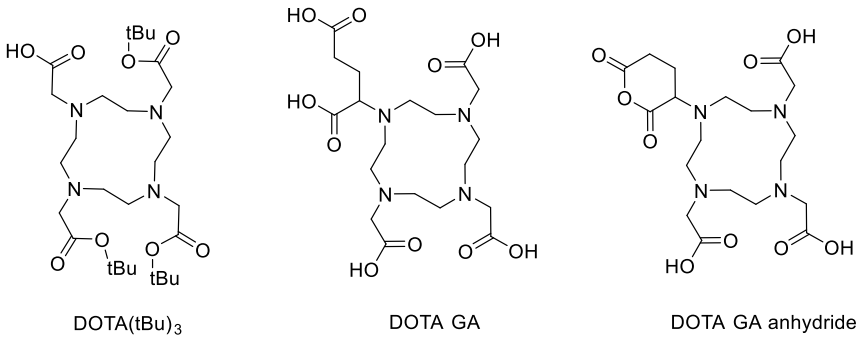

Figure 86. Comparison of three DOTA analogue: DOTA(tBU)$_3$, DOTA GA and DOTA GA anhydride.

The synthesis of compound **11** was performed on solid support (Figure 87). It enabled an easier removal of the possible non reacted DOTA (tBu)$_3$. First, Fmoc-Lys(Mtt)-OH (3eq) was anchored on RinkAmide PS resin using HATU/DIEA in DMF**.** Then the 4-methyltrityl (Mtt) protecting group was removed in mild conditions using only 1% TFA solution in DCM in the presence of 1% of triisopropylsilane as scavenger to neutralize the carbocations released. In these conditions, Rink amide linker was stable.

Several successive 2 minutes treatment of the resin with 1% TFA, 1% of triisopropylsilane in DCM solution were performed to release the Mtt group until the solution was transparent. Indeed, the presence of free Mtt gave a yellow color to the solution; thus it was easy to follow the end of the deprotection.

The N-ε of the lysine was reacted with DOTA(tBu)$_3$ activated by HATU/DIEA in DMF for 4h. After removal of Fmoc by DMF/piperidine solution, the silylation with ICPDCMS was performed directly on the resin in anhydrous DMF in the presence of DIEA, overnight under argon. The compound **11** is finally cleaved from the resin by TFA/TIS/H_2O (98/1/1, v/v/v) solution. The macromonomer was purified by preparative HPLC using a PLRP-S column, then lyophilized.

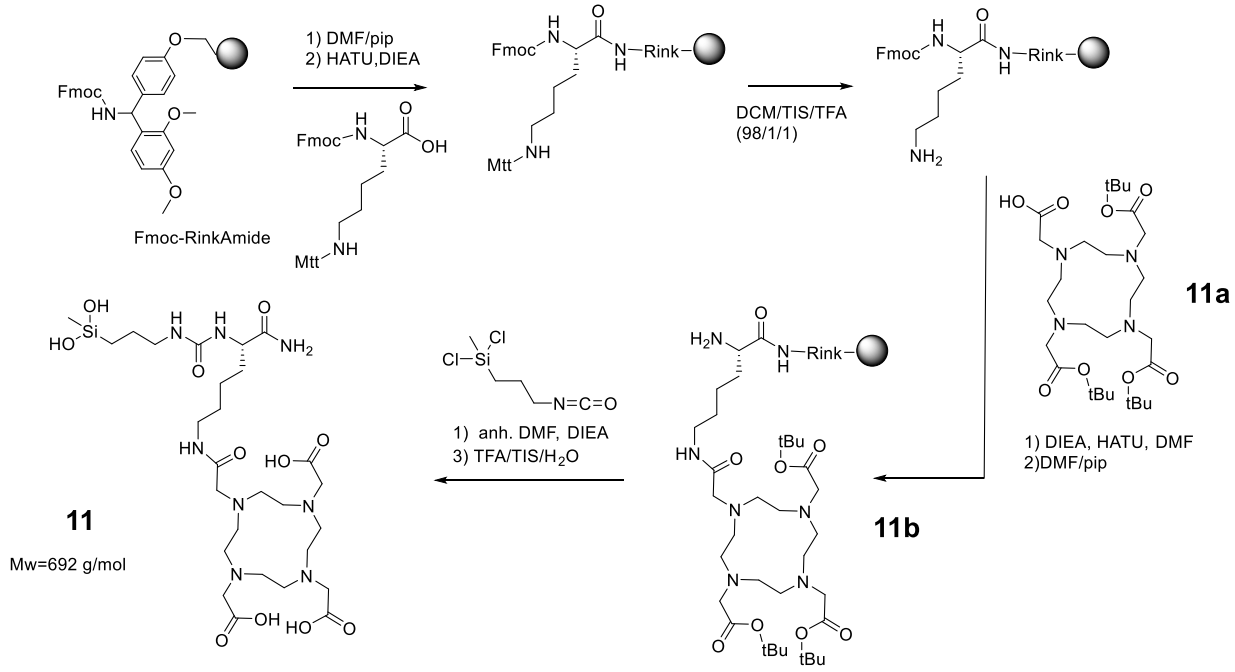

*Figure 87. Solid phase synthesis of hybrid compound **11**.*

On the ESI+ LC/MS chromatogram we identified the compound **11** after purification: rt= 0.61 min $[M+H]^+$ m/z 693 (Figure 88).

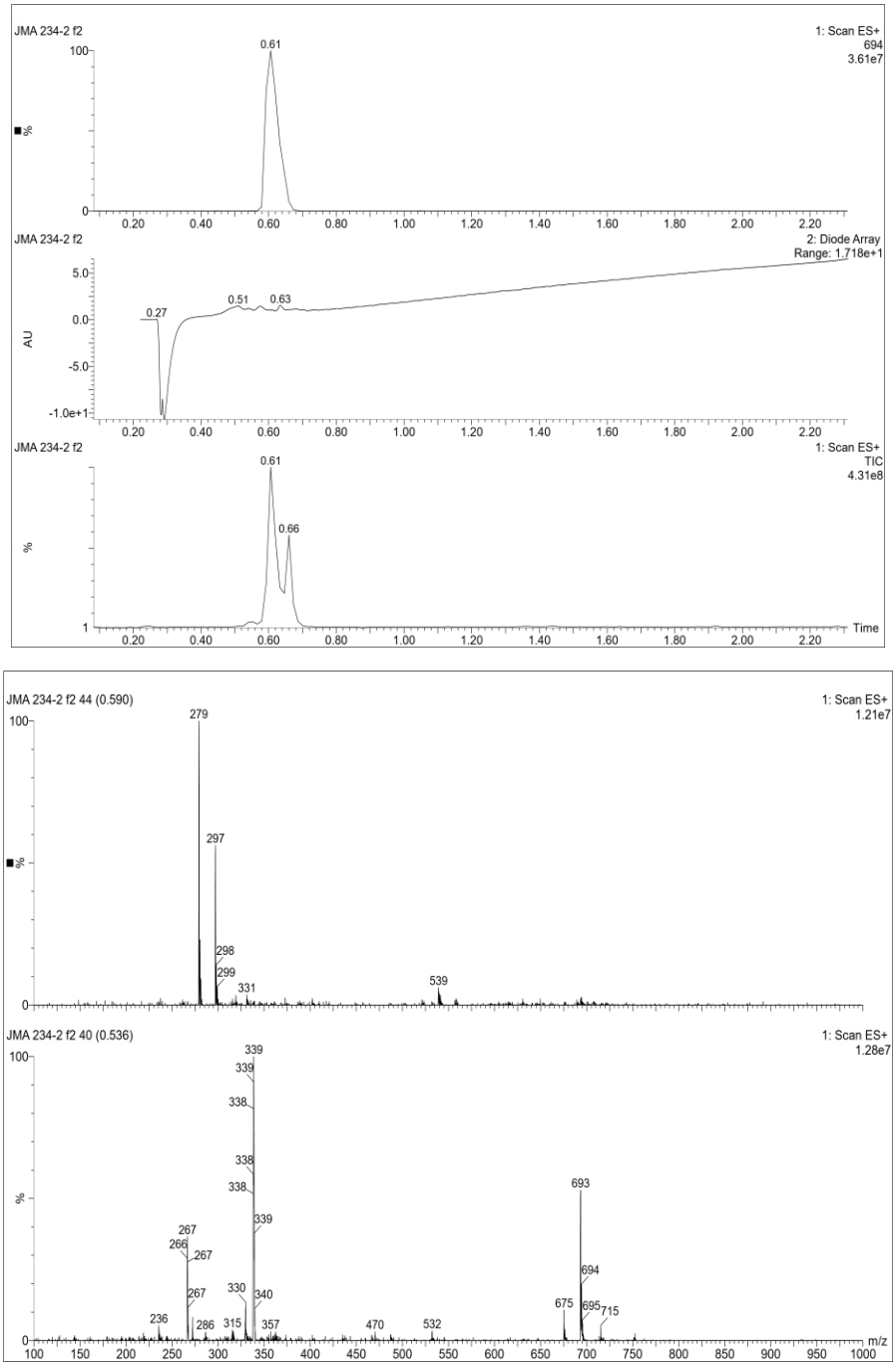

*Figure 88. ESI + LC/MS of compound **11** after purification, analyzed in H_2O/ACN 1‰ TFA on PLRP-S column. Top: chromatograms UV at 214nm and TIC, Bottom: MS spectra at 0.61 and 0.66 min*

12a was obtained from DOTAGA by reaction with acetic anhydride, yielding intramolecular carboxylic anhydride between the two carboxylic acid functions of the glutamic acid moiety.[310] The anhydride is sensitive to water and is rapidly hydrolyzed in less than one hour at room temperature. **12a** has to be opened by a nucleophile (i.e: a diamino spacer) to give the molecule **12b** which still present 4 carboxylic acid functions at suitable position to chelate the metal cation. Noteworthy, nucleophilic attack proceeds selectively on the carbonyl of the anhydride group to yields a single regioisomer.[305]

The synthesis of hybrid compound **12** had to be optimized and was not performed in the same way as compound **11**. Indeed, commercially available DOTAGA anhydride **12a** is not soluble in organic solvents, as it does not have any protecting group to mask the carboxylic acids functions. It is highly soluble in water, but easily hydrolyzed. Besides, the silylation needs anhydrous solvent, so water is not an option as solvent. The idea was then to first modify **12a** with an amine spacer on solid support in DMSO at 60 °C to avoid hydrolysis and being able to realize a coupling on the anhydride function (Figure 89). Then after cleavage, the resulting compound **12b** was soluble in organic solvent and so able to be silylated in anhydrous DMF.

First, a Fmoc mono protected diamine spacer, Fmoc-ethylenediamine, were anchored on a 2 CTC PS resin by nucleophilic substitution and the Fmoc was deprotected. The resulting resin was poured in DOTAGA anhydride DMSO solution heated at 80 °C overnight. At this temperature in DMSO, DOTAGA anhydride was slightly soluble (0.019 g/mL). Immobilized primary amine reacted with the anhydride to yield the supported intermediate **12b.** Interestingly, the fact that the reaction was performed on solid support greatly simplifies the work up and the removal of hydrolyzed DOTAGA anhydride side product. Indeed, any hydrolyzed DOTAGA cannot react anymore with the primary amine of the spacer and then stays in solution and is removed by washing the resin.

Supported intermediate **12b** is then cleaved from the resin by a TFA treatment for 1h. Compound **12c** obtained as TFA salt was silylated in solution by reacting with ICPDCMS (1.2 eq) in the presence of DIEA (6 eq) in anhydrous DMF for 1h. The hybrid macromonomer **12**, was purified by preparative HPLC using PLRP-S column and lyophilized.

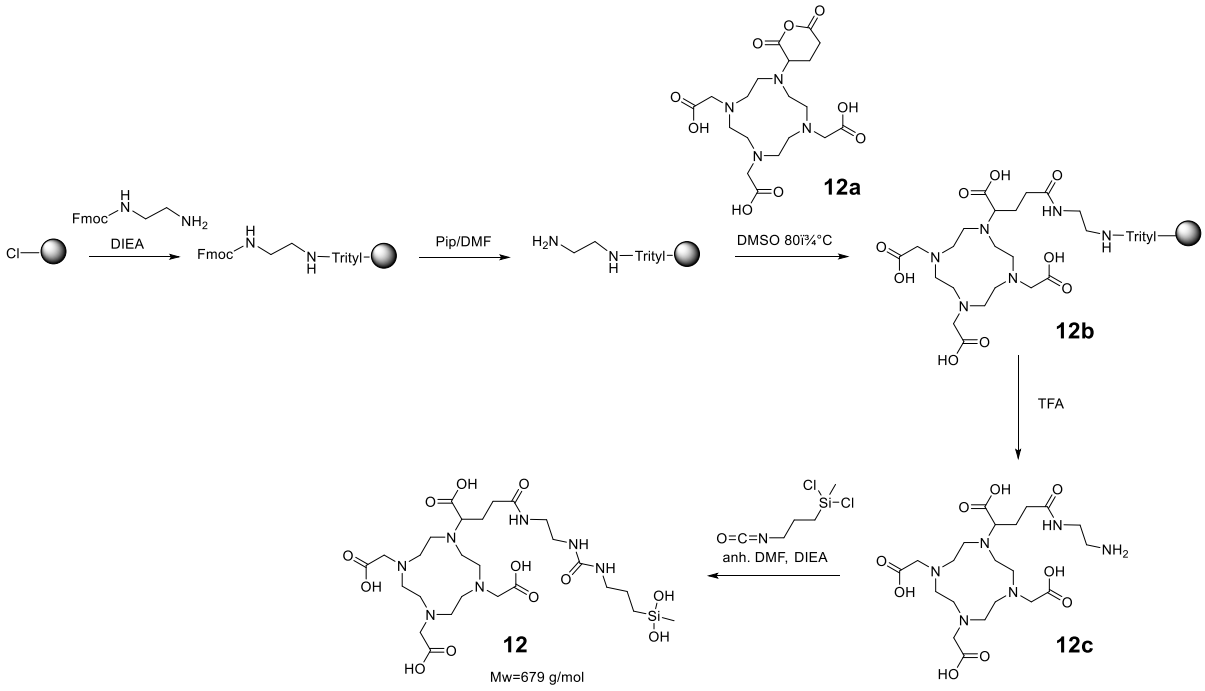

*Figure 89. Synthesis of compound **12**, silylated derivative of DOTAGA.*

On the ESI+ LC/MS chromatogram we identified the compound **12** after purification: rt= 1.51 min $[M+H-H_2O]^+$ m/z 662 (Figure 90).

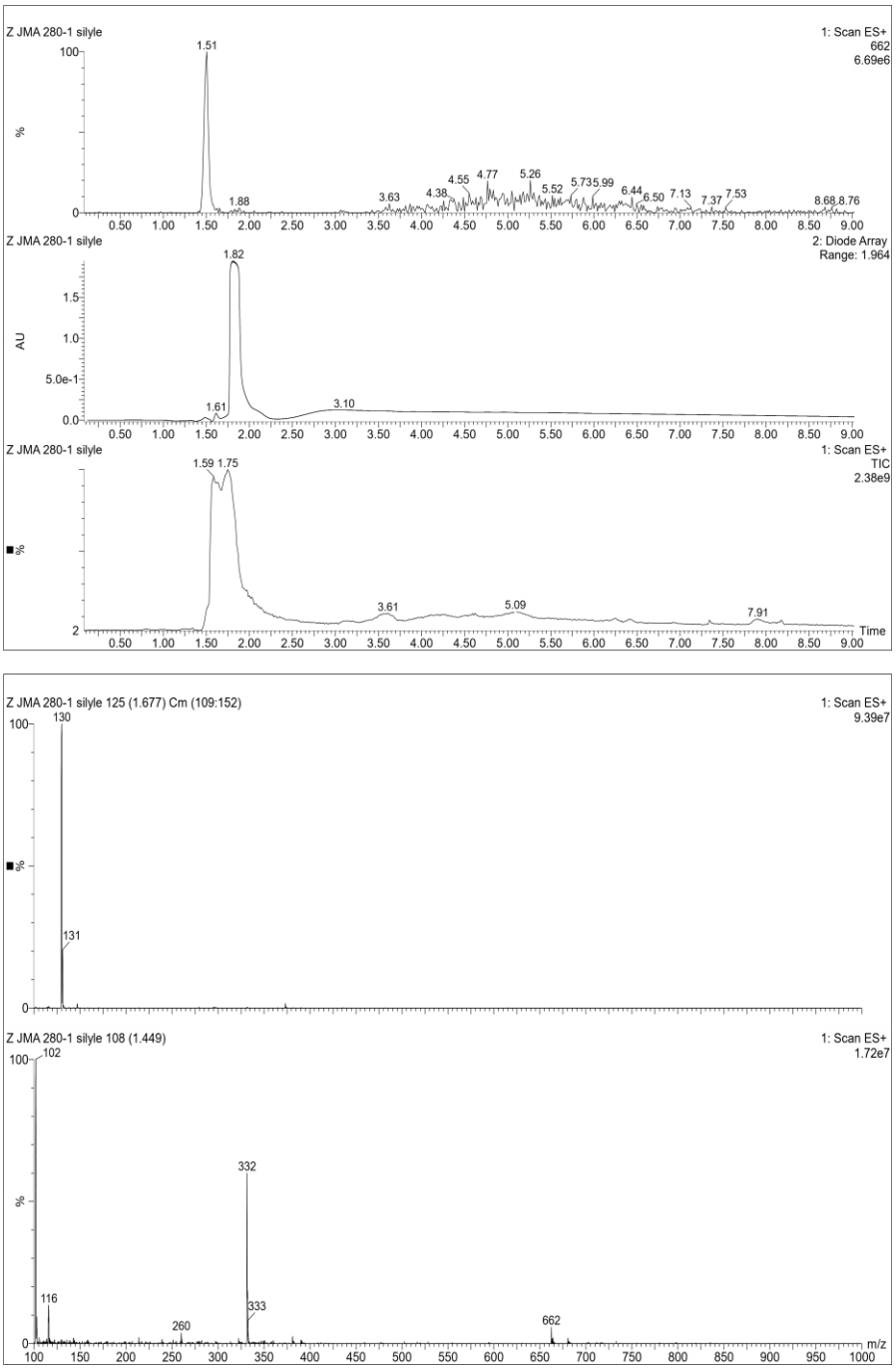

*Figure 90. ESI + LC/MS of compound **12** after purification, analyzed in H_2O/ACN (50/50) 1 ‰ TFA on PLRP-S column. Top: chromatograms UV at 214nm and TIC, Bottom: MS spectra at 1.51 and 1.75 min*

e. *Hybrid fluorescein **13***

Fluorescein[311,312] is a well-known dye with a high intensity emission peak around 520nm and an important molar adsorption coefficient (92,300cm^{-1}/M at 498 nm). A large number of analogs of the fluorescein have been described with various absorption and emission wavelengths for many applications. Very popular in biology, fluorescein is widely used for in vitro assays especially for FACS[313] and fluorescent microscopy such as confocal microscopy[314], as fluorescent probe. Fluorescein is often used for *in vivo* assay in neurosurgery and dermatology for example.[315]

Numerous derivatives of fluorescein have been designed, democratizing the use of this dye in biochemistry and biology. One of the most used in the highly reactive fluorescein-5-isothiocyanate (FITC). FITC shows an adsorption at 490 nm and an emission at 514 nm. It reacts rapidly and efficiently with amines, forming thio-urea bonds. We used FITC to prepare hybrid fluorescent compound **13** (Figure 91).

The hybrid fluorescein was incorporated into PDMS solid material (Chapter 4), as a model for the incorporation of a hybrid molecule in a copolymerized silicone. It was also incorporated it in PDMS NPs (chapter 5), in order to enable their imaging.

FITC (1eq) was solubilized in anhydrous DMF with DIEA (6eq). N-Boc-1,3-propanediamine (1.2 eq) was added to the solution to yield the protected intermediate **13a**. The mixture was flushed under argon, stirred for 1h at room temperature and finally concentrated in vacuum. The Boc protecting group was removed by TFA treatment for 2h at room temperature, and the TFA was removed in vacuum to give **13b** as TFA salt which was precipitated in Et_2O and recovered by centrifugation. **13b** was then solubilized in anhydrous DMF and the salts were neutralized by DIEA (6 eq). ICPDMCS (1.2 eq) was added. The mixture was stirred 1h at room temperature under argon. After concentration of the solvent, hybrid fluorescein derivative **13** was purified and lyophilized. The hybrid macromonomer was obtained with a final yield of 85%.

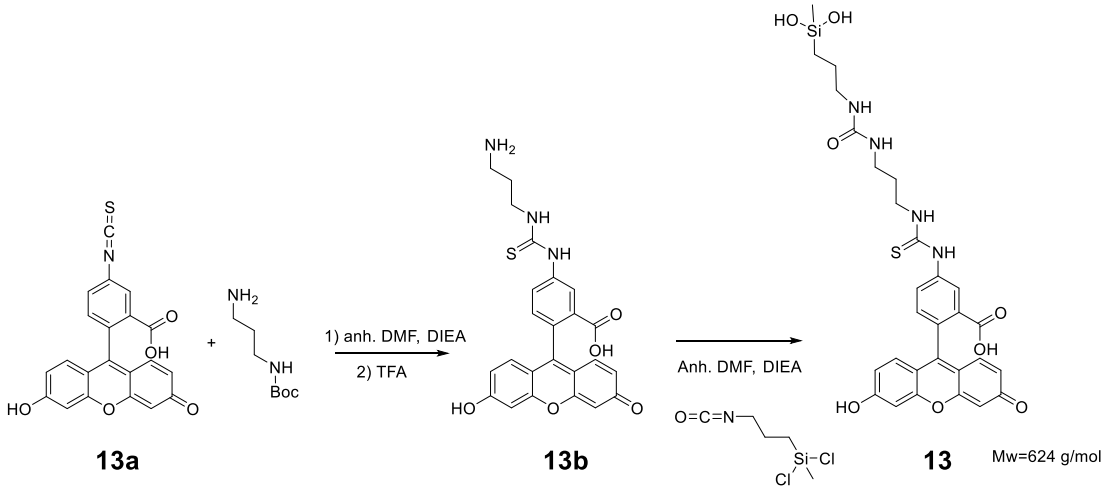

*Figure 91. Synthesis of hybrid fluorescein derivative **13**.*

On the ESI+ LC/MS chromatogram we identified the compound **11** after purification: rt= 1.16 min $[M+H]^+$ m/z 625 (Figure 92).

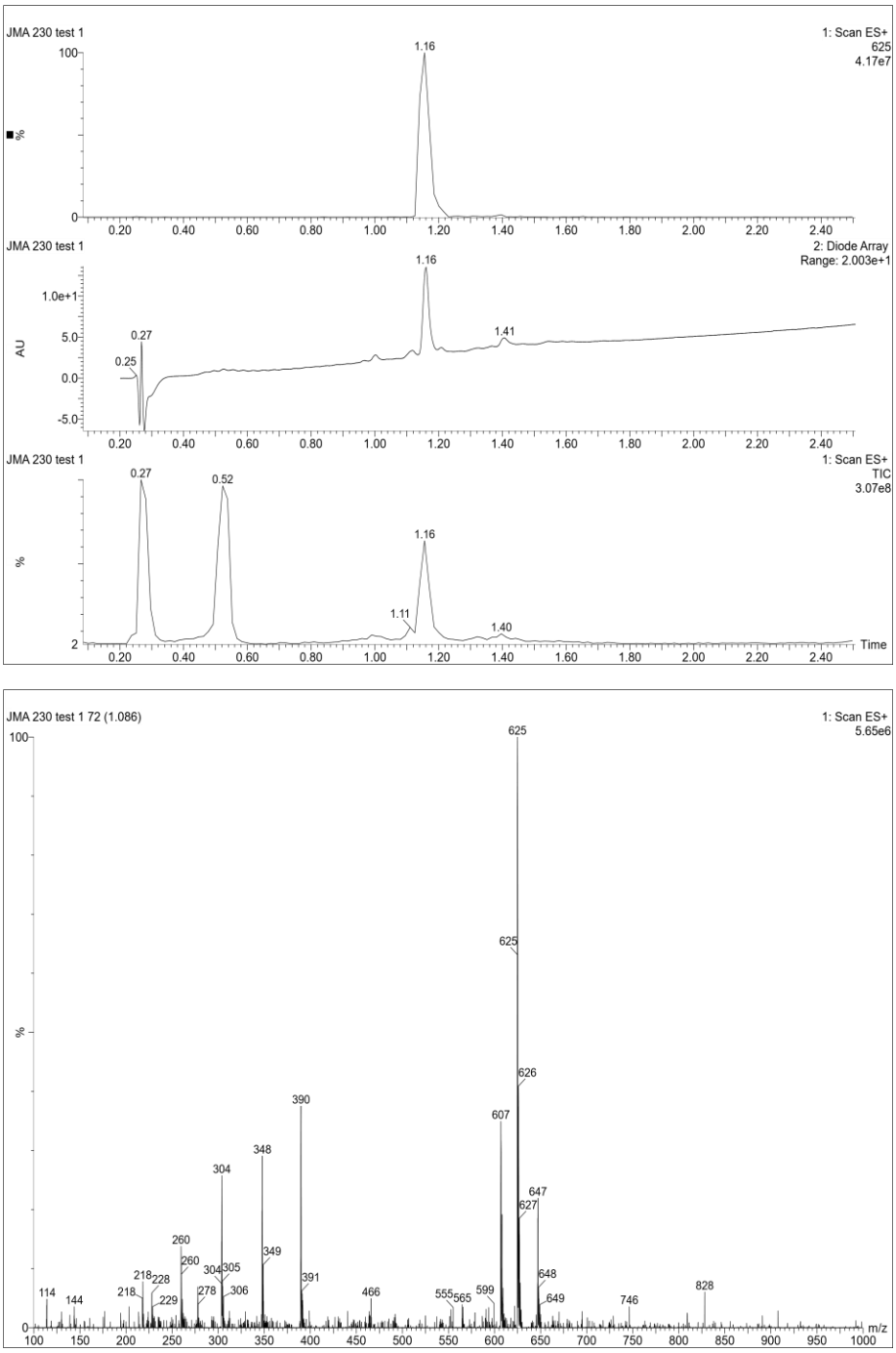

*Figure 92. ESI + LC/MS of compound **13** after purification, analyzed in H_2O/ACN (50/50) 1‰ TFA on PLRP-S column. Top: chromatograms UV at 214nm and TIC, Bottom: MS spectrum at 1.07 min*

f. *Hybrid PEG_{3000} (F-tagged) **14***

PEG_{3000} macromonomer **14** was used for the formation of PDMS NPs (chapter 5). It was supposed to bring hydrophilicity to the hydrophobic PDMS-based polymer backbone, turning it into an amphiphilic polymer. In addition, for vectorization purposes, PEG addition was thought to increase the stealth of NPs, helping them to improve their long-term blood circulation.[293] Besides NPs, PEG was used in numerous biological application especially to prepare coating for antifouling surfaces or drug delivery system by the synthesize of block-copolymers.[25,316–318]

We added a dihydroxymethylsilane to one end of the PEG_{3000}. In addition, as a purpose of quantification, a 2-Fluoroethylamine was introduced at the other extremity (Figure 93). As already explained, this probe was used for the detection of this macromonomer in ^{19}F NMR by ERETIC method giving one signal at -131ppm. To do that double modification, we used commercially available Boc-NH-PEG_{3000}-COOH to prepare compound **14**.

Boc-NH-PEG_{3000}-COOH was solubilized in DMF and activated by HATU/DIEA. 2-Fluoroethylamine was added to the solution and stirred 1h at room temperature yielding the intermediate **14a**. After evaporation, modified PEG was precipitated in Et_2O and washed three times with the same solvent. The Boc-deprotection was carried out by a TFA solution, at room temperature, stirred for 1h and then treated as previously described. **14b** was obtained as TFA salt and was silylated in solution with ICPDCMS as usual. Compound **14** was obtained after precipitation in Et_2O and filtration and used without another purification. No LC/MS analysis was performed of compound **14** since the polydispersity of the PEG_{3000} chain does not enable a clear LC/MS analysis. The global yield of this silylation is about 92%.

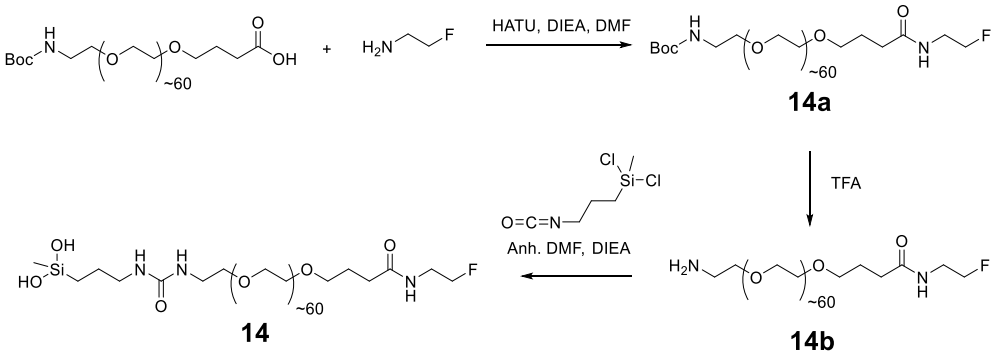

*Figure 93. Synthesis of hybrid PEG derivative **14***

Having all these building blocks in hand, we then proceeded to the syntheses and characterizations of various materials. In some cases, only one building block was used (e.g. for copolymerization with dichlorodimethylsilane), and in some other cases a combination of several buildings were copolymerized. Peptide-functionalized silicone material was presented in chapter 4 and multifunctional NPs for drug delivery or siRNA delivery were disclosed in chapter 5 and 6, respectively.

Chapter 4: Direct synthesis of peptide-modified silicone

NB: most of the work presented in this chapter constitutes a publication which is submitted:
Martin, Julie, Mohammad Wehbi, Cécile Echalier, Coline Pinese, Jean Martinez, Gilles Subra, et Ahmad Mehdi. « Direct synthesis of peptide-modified silicone. A new way for bioactive materials ». *Submitted*, 2019.

.

Chapter 4: Direct synthesis of peptide-modified silicone

As described in the first chapter of this manuscript, PDMS gathers numerous attractive characteristics (e.g. elasticity, stability, hydrophobicity and biocompatibility) that made it a very interesting material for biological application and in medical devices. However, it is inert and needs to be functionalized by biomolecules to acquire biological properties. As far as we know, only two ways have been explored, either direct adsorption of biomolecule onto the silicone surface or covalent immobilization (including copolymerization). All these approaches have been described in Chapter 1.

In this context, one of our main objective was to develop a third way by direct synthesis of a covalently functionalized silicone polymer. In this study, tow functional groups were selected i.e. a fluorophore or a peptide. This bottom-up approach relies on hybrid dichloromethyl silylated molecules (i.e. peptides, fluorophores) whose synthesis is described in chapters 2 and 3. An appropriate ratio of dichlorodimethylsilane (DCDMS) monomer is copolymerized with such hybrid macromonomers to yield a linear PDMS backbone, in which some methyl groups are substituted by pendant peptides (Figure 94). Noteworthy, comb like homopolymers of peptides were prepared in the same way[143,144] but only low short chains were obtained (15-25 repeats). In this PhD work, the copolymerization with DCDMS will give longer polymers whose properties will be expected to be closer from PDMS than polypeptides. Indeed, we hypothesized that a relatively low% of peptide (<5 mol% related to DCDMS) was necessary to give the desired bioactivity

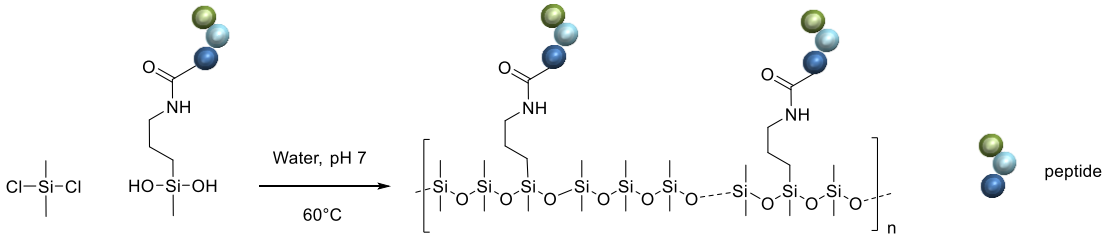

Figure 94. Scheme of copolymerization between DCDMS and hybrid silylated peptide.

Besides, the structure and state of the polymer depends on the required application. At ambient temperature, PDMS is in liquid state, the form of an oil. Oil state is adapted to several applications: it is a common surfactant applied to foam synthesis,[319] it can also be found as lubricant in mechanic[320] or, after cross-linking, as water repellent coating[321,322] and electrical protection.[323,324]

However, for most of bio applications especially for the fabrication of medical devices, polymers must be in solid state. In order to use PDMS as solid material (for an implant for example), linear chains have to be cross-linked. Several methods are used: free radical cross-linking with peroxide,[325] copolymerization with tetraethyl orthosilicate (TEOS)[326] or hydrosilylation catalyzed by platinum or ruthenium metals such as Karstedt's or Grubb's catalyst (see Figure 95).[327]

The hydrosilylation reaction is the same than the one we tried to develop in chapter 2 except it proceeds between vinyl and silane-modified silicone. This method is efficient to obtained a solid silicone-based material but require precaution about the use of metals that can be toxic when used in large amounts.

Even if Ruthenium catalysts have been described to be less toxic than Pd^0 ones, the quantity of metal used for the preparation of silicone materials has to be controlled and if possible removed. Thus, platinum catalyst are the

most used in industrial silicone synthesis since they are so far the most efficient.[215] In industrial process the Pt^0 quantity is limited to 4.5 ppm in the case of Dow Corning implant for example.[328]

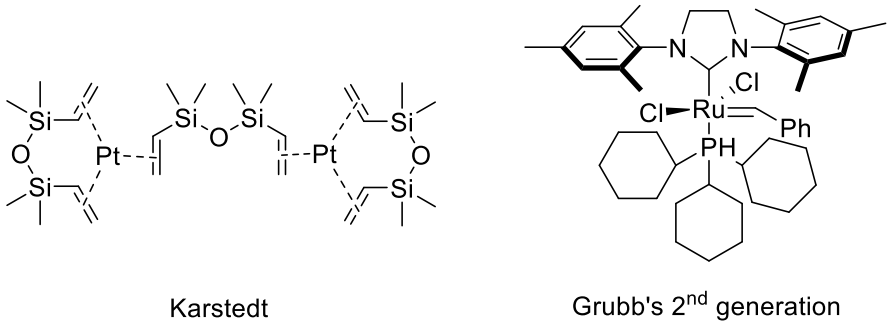

Figure 95. Hydrosilylation catalysts.

The second objective of this chapter was to prepare cross-linked silicone materials containing bioactive moieties from hybrid silicones oils obtained by our direct functionalization approach (Figure 96). Consequently, DCDMS and peptides macromonomers are also copolymerized with Si-Vinyl and Si-H monomers in order to obtain functionalized PDMS oils, able to cross-link by hydrosilylation.

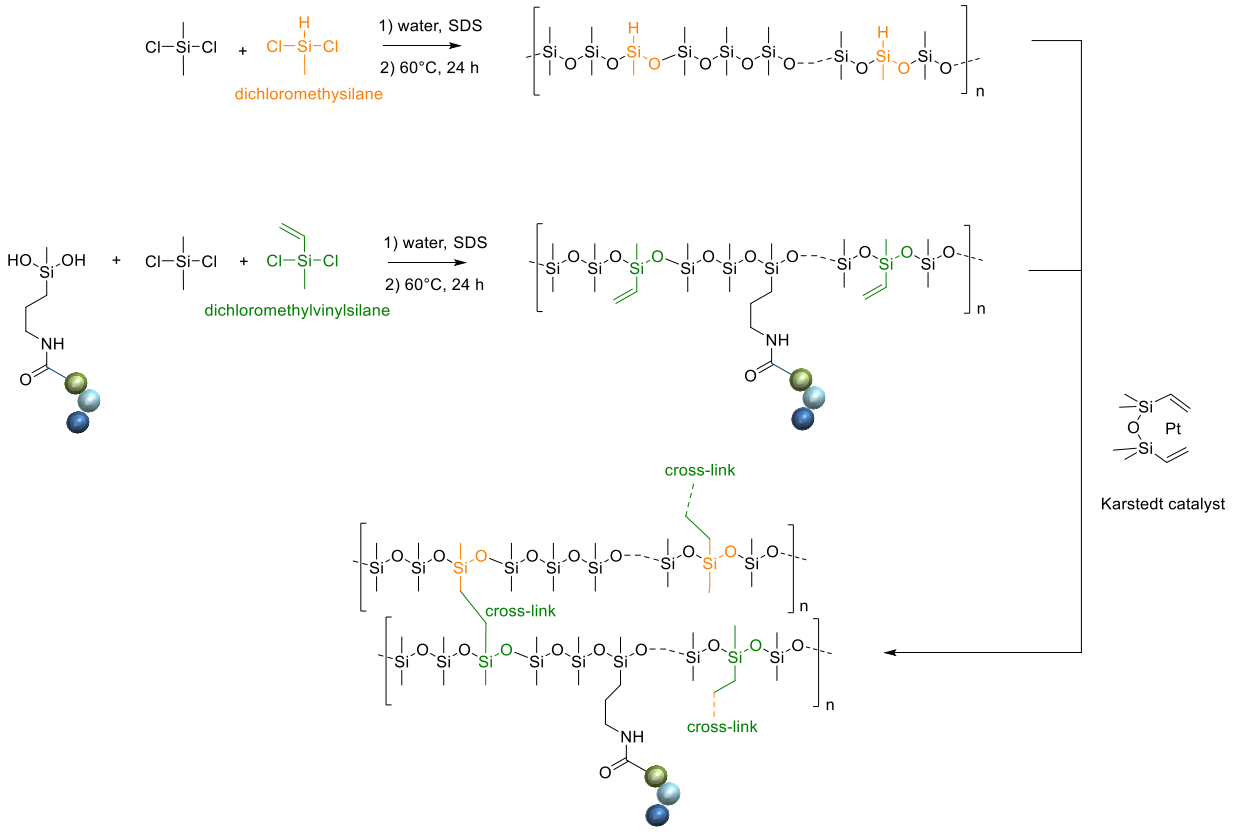

Figure 96. Scheme of general strategy of multifunctional PDMS synthesize followed by cross-linking by hydrosilylation.

We chose 3 macromonomers: hybrid fluorescein, hybrid Si-AhxArgArg and hybrid linear RGD, respectively compound **13**, **1** and **5** which each synthesized are detailer in chapter 3. From these two hybrid peptides, two

types of bioactive PDMS material were obtained: antibacterial and cell–adhesive. They were characterized by NMR (^{1}H and ^{29}Si), GPC, IR, Nano-Indentation and assayed for their biological properties.

An article presenting this work was submitted and it is included in the following pages. I contributed to it by performing the syntheses of the macromonomers, the PDMS oils and the PDMS corresponding materials. I also performed the GPC, ^{1}H and ^{29}Si NMR and IR analysis. I prepared all the samples for the NanoIdentation measurements and biological tests. I participated in the writing of the paper.

It is important to note that the numbering of the hybrid biomolecules does not fit with the chapter 3. Hybrid fluorescein **1** corresponds to compound **13**, hybrid peptide **2** to compound **1** and hybrid peptide **3** to compound **5.**

Direct synthesis of peptide-modified silicone. A new way for bioactive materials

Julie Martin,[a,b] Mohammad Wehbi,[a] Cécile Echalier,[a,b] Sylvie Hunger, [b] Audrey Bethry,[b] Xavier Garric,[b] Coline Pinese,[b] Jean Martinez,[b] Gilles Subra‡*[b] and Ahmad Mehdi‡*[a]

[a]ICGM Université de Montpellier, CNRS, ENSCM, Montpellier, France.

[b]IBMM Université de Montpellier, CNRS, ENSCM Montpellier, France.

ABSTRACT: A simple and efficient way to synthesize peptide-modified silicone materials is described. Silicone oils containing a chosen ratio of bioactive peptide sequences were prepared by acid-catalyzed co-polymerization of dichlorodimethylsilane, hybrid dichloromethyl peptidosilane and either Si-vinyl or Si-H functionalized monomers. Functionalized silicone oils were first obtained and then after hydrosilylation cross-linking, bioactive PDMS based materials were straightforward obtained. The introduction of an antibacterial peptide yields PDMS materials showing an interesting activity against *Staphylococcus Aureus*. In the same way, RGD ligands-containing PDMS demonstrated improved cell adhesion properties. This generic method was fully compatible with the stability of peptides and thus opened the way to the synthesis of a wide range of biologically active silicones.

Polydimethylsiloxane (PDMS), is a mixed organic/inorganic hydrophobic polymer displaying very interesting properties[1] such as high degree of oxygen permeability,[2] thermal and electrical resistance,[3] as well as being considered biocompatible.[4] Thanks to these features, it was used in many industrial applications such as antifoams, coatings, sealants and insulation. In the past decades, PDMS has been extensively adopted for the elaboration of microfluidic chips[5] that found useful applications in the fields of diagnostics, screening or biosensing.[6][7] Thanks to its biocompatibility, PDMS occupies an important position in the field of soft implantable biomedical devices.[8,9] As most synthetic polymers used in healthcare, PDMS is bio-inert i.e. it does not present any biological activity. For more complex therapeutics applications, these polymers have to be functionalized in order to obtain the chosen propertie(s) (e.g. targeting, cellular penetration, cellular adhesion, antimicrobial activity, better detection for imaging etc.). Moreover, the surface of PDMS is highly hydrophobic leading to unselective adsorption and subsequent denaturation of proteins.[10] Very early, simple chemical modifications (e.g. alkyl chains, cationic and anionic groups) of the hydrophobic native silicone surface have been used to improve its biocompatibility,[11] while more complex molecules such as sugar,[12] poly(L-lactic acid),[13] peptides and proteins[14,15] have been immobilized on PDMS to afford chosen bioactivities to the material. These modifications were performed by multi-step grafting chemistry, first introducing a functional group on the PDMS surface and then reacting with the molecule to be immobilized. Advantageously, our group showed recently that it was possible to graft peptides on silicone of medical devices in a single step by using hybrid bioorganic-inorganic molecules bearing an alkoxysilane group. This strategy was first applied to the modification of silicone catheter surfaces by antibacterial peptides to get an antibacterial material with high immediate efficiency by comparison to similar silver-embedded materials.[16] In the same way, bioactive peptides promoting wound-healing were successfully immobilized on silicone dressings.[17] These strategies concerned surface modification of bulk silicone by post-functionalization.

In contrast, direct strategies can be envisioned to offer peptide-containing silicone. We already reported on the polymerization of peptides using silane chemistry to get linear[18] and comb-like peptide-polymers assembled through Si-O-Si bonds.[19] However, these hybrid peptide polymers are limited to their modest polymerization degree (DP< 30) and, despite the similarities in their backbone; they did not display comparable physicochemical properties than PDMS.

Herein, we describe the direct synthesis of PDMS polymers incorporating bioactive peptides in a controlled ratio to get peptide-modified cross-linked PDMS (Figure **1**). We hypothesized that a low amount of bioactive peptide compared to silicone should be enough to induce a desired effect. To demonstrate that, we prepared two types of bioactive-PDMS with various molar % (0.01 to 10 mol%) of peptide. Taking into account the dramatic number of infections appearing subsequently to a medical device implantation[20], we chose to incorporate an antibacterial peptide. Alternatively, we prepared a silicone containing a derivative of fibronectin peptide sequence to improve the cell-adhesion properties of the material.

By contrast to post-grafted silicone, the modified PDMS materials present peptides homogenously distributed in the bulk. This will ensure the durability of the functionalization which cannot be altered by surface erosion or mechanical damage. This could afford durable and dedicated properties to implantable medical devices and general public healthcare devices such as nipples, lens, catheters etc. As an additional level of modularity, we propose a generic method based on the cross-linking of hybrid bioorganic-silicone oils which could be chosen and mixed in an appropriate ratio to get diverse peptide containing PDMS materials on-demand. Thus, the first step of our study was to optimize the synthesis of a hybrid PDMS polymeric oil.

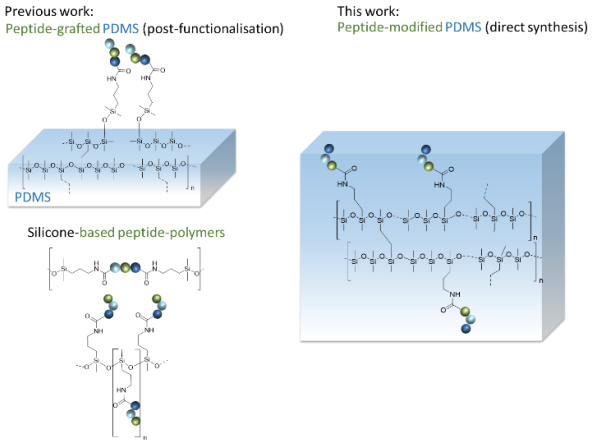

Figure 1. Different strategies using hybrid silane-peptides for the synthesis of peptide-containing silicone and polymers.

Different silicone oils were prepared. They are composed of three types of building-blocks. (i) Dichlorodimethylsilane (DCDMS), which will yield the main polymeric repeat of PDMS; (ii) dichloromethylsilane (DCMS) or dichloromethylvinylsilane (DCMVS), which are the siege of cross-linking between linear PDMS chains by hydrosylilation; (iii) hybrid building blocks displaying one dichloromethylsilane moiety and either a fluorescent dye (compound **1**) or a bioactive peptide sequence (compound **2** and **3)**. Fluorescent compound **1** was used to easily visualize the covalent incorporation of a hybrid building block with the PDMS chains. The hybrid peptide **2** is a cationic peptide, displaying two arginine residues and the hybrid peptide **3** is a linear peptide derived from fibronectin sequence (i.e. GRGDSP). The first one was selected for its antibacterial properties and the second one for its ability to enhance the cell adhesion.[21] **2** and **3** were first synthesized on solid support, using Rink amide or 2-Chloro chlorotrityl PS resin respectively. Peptide **3** was silylated on solid support while peptide **2** was cleaved, then silylated in solution, according to a well established procedure.[19]

The polymerization of dichlorosilyl blocks was performed using sodium dodecyl sulfate ([SDS]= 16.4 mM) as a surfactant in water at 60 °C. These experimental conditions were compatible with the stability of peptides. DSC hydrolyses in water producing dimethyldisilanol and hydrochloric acid, which catalyzes both hydrolysis and condensation processes. In these experimental conditions, three molecules of disilanols condensed into into hexamethylcyclotrisiloxane,[22] entering the core of SDS micelles. Acid-catalyzed hydrolysis induced both opening on the cycle and growing (Figure 2).

Non-functionalized PDMS (**P0**), PDMS functionalized with 1, 2.5, 5 and 10 mol% of DCMS (**P1**, **P3**, **P5** and **P7** respectively) and PDMS functionalized with 1, 2.5, 5 and 10 mol% of DCMVS (**P2**, **P4**, **P6** and **P8** respectively) were prepared using the procedure mentioned above (Table 1). The PDMS oils were recovered by 75 to 91% yields. Polymers were then characterized by size-exclusion chromatography (SEC) at a concentration of 10 mg/ml in chloroform ($CHCl_3$) (see Figure 1 in Supporting Information). The molar mass of the polymers ranged from 12600 (**P5**) to 28200 (**P8**). The introduction of the Si-H monomer yields shorter polymer lengths probably slowing down the polymerization whereas the introduction of Si-Vinyl has no effect on the size, except for the 10 mol% (**P8**) where the length is a little longer than the pristine PDMS. ^{29}Si NMR analyses of unfunctionalized PDMS showed a single peak at -22 ppm, corresponding to the siloxane $–(OSi(Me)_2)_n-$ whereas, several additional peaks were obtained for –OSi(RMe)- with R = H, Vinyl or peptide. Noteworthy, the ^{29}Si NMR confirmed the absence of any uncondensed monomer byproduct.

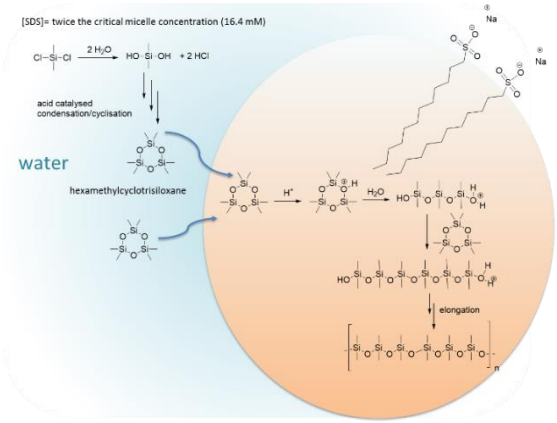

Figure 2. SDS promoted polymerization of dichlorodimethylsilane (DCDMS)

As a first examples of functionalization, we incorporated the hybrid fluorescein **1** at 0.01 or 0.1 mol% and hybrid peptide **2** and **3** at 0.01 to 10 mol% to get bioorganic PDMS-modified oils **P9** to **P20** (Table 1). These modified PDMS oils containing hybrid compound were prepared with the same protocol than **P2**, **P4**, **P6** and **P8** with DMCVS. At the low concentrations (0.01-0.1 mol%), it was not possible to detect the presence of the peptide in the copolymers by NMR while the incorporation of hybrid fluorescein at the same concentrations was clearly perceived by the color changes of **P9** and **P10** modified-PDMS oils, pale yellow (0.01% mol of compound **1**) to dark yellow (0.1% mol of compound **1**) respectively (Figure 4).

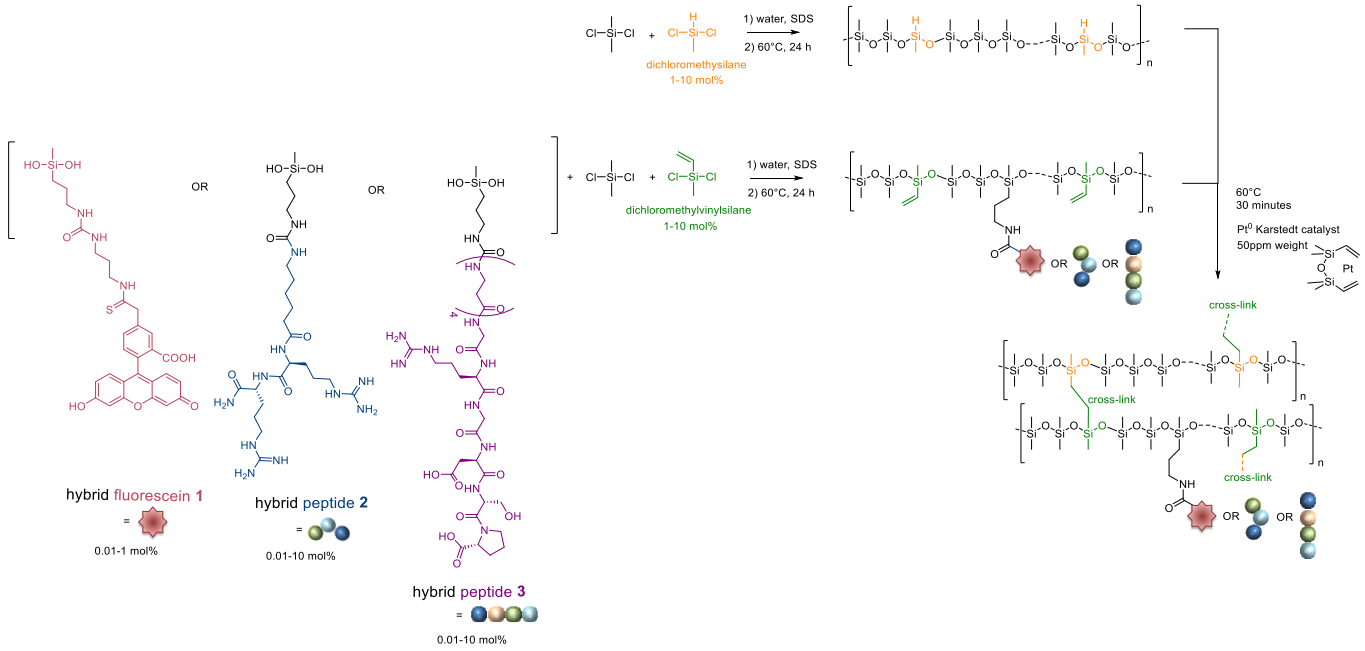

Figure 3. Direct synthesis of peptide-modified silicone (or fluorescent-silicone) by hydrosilylation-mediated cross-linking of functionalized silicone oils.

Table 1. Composition of different functional PDMS polymers

Polymer	**mol% of Silylated building blocks**							**Yield (%)**	**MW[a]**
	DCDMS	DCMS	DCMVS	Experimental %[b]	**1**	2	3		
P0	100	-	-	-	-	-	-	84	23100
P1	99	1	-	1	-	-	-	88	14800
P2	99	-	1	1.4	-	-	-	91	22200
P3	97.5	2.5	-	2.3	-	-	-	85	22500
P4	97.5	-	2.5	3.8	-	-	-	89	20200
P5	95	5	-	3.1	-	-	-	83	12600
P6	95	-	5	6.7	-	-	-	79	22100
P7	90	10	-	8.5	-	-	-	75	18600
P8	90	-	10	13	-	-	-	76	28200
P9	97.5	-	2.5	3.6	0.01	-	-	92	33500
P10	97.5	-	2.5	3.0	0.1	-	-	86	72900
P11	97.5	-	2.5	4.4	-	0.01	-	98	57400
P12	97.5	-	2.5	4.5	-	0.1	-	88	36000
P13	97.5	-	2.5	2.8	-	1	-	n.d.	60034
P14	97.5	-	2.5	2.3	-	5	-	n.d.	79301
P15	97.5	-	2.5	3.4	-	10	-	n.d.	61623

P16	97.5	-	2.5	2.5	-	-	0.01	n.d.	28990
P17	97.5	-	2.5	2.8	-	-	0.1	n.d.	28315
P18	97.5	-	2.5	3.0	-	-	1	n.d.	38284
P19	97.5	-	2.5	3.0	-	-	5	n.d.	70780
P20	97.5	-	2.5	2.3	-	-	10	n.d.	81601

[a] determined by SEC, [b] experimental percentage of DCMS and DCMVS determined by ^{1}H RMN integration, n.d. non determined due to the small quantity synthetized

Therefore, PDMS containing higher concentration of peptide were synthesized in order to detect both hybrid peptides **2** and **3** by ^{1}H NMR, and so prove their integration inside the silicone backbone (see Figure 7 in Supporting Information).

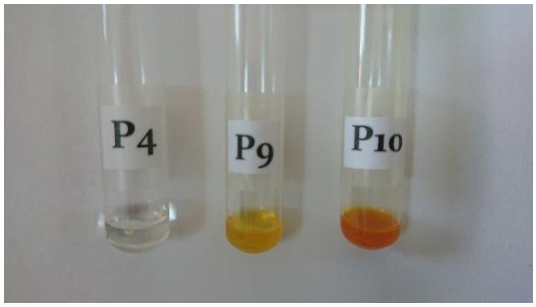

Figure 4. 2.5 mol% vinyl-PDMS oil **P4** (left), Fluorescein modified-PDMS oil **P9** (middle) and **P10** (right).

Having functionalized PDMS oils in hand, we set up the synthesis of silicone materials by cross-linking two modified PDMS displaying the same percentage of vinyl groups and Si-H functions (Figure 3). These functional PDMS materials, noted **M1** to **M16**, were obtained by hydrosilylation using the Karstedt's catalyst. The same amount of each complementary oils was mixed up with 50 ppm Kartsetdt's catalyst then spread into a glass slide and put in the oven at 60 °C for 30 min.

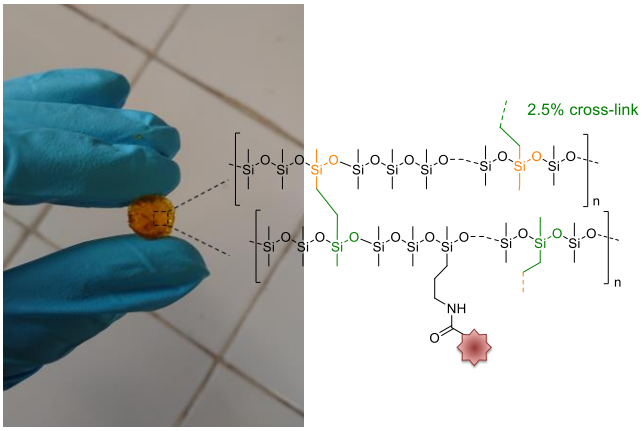

Figure 5. PDMS material **M6** (2.5% cross-linking, containing 0.5 mol% of hybrid fluorescein **1**) removed from a circular mold.

We have investigated the effect of crosslink's ratio (from 1% to 10%) on the mechanical properties of PDMS by nano indentation. We observed a linear progression of the indentation modulus of the materials obtained when the crosslinking amount was between 2.5 and 10%. Above 10% cross-linking, the material loses its elasticity and became more susceptible to break under pressure. On the contrary, below 2.5% cross-linking, no solid material was obtained and, characterization by indentation was not performed. Taking into account these results, we chose arbitrary the 2.5% for the following syntheses of hybrid silicone material containing peptide or fluorescein.

We then prepared peptide-modified-PDMS materials **M7** and **M8** containing respectively 0.005 mol% and 0.05 mol% of hybrid peptide **2**, from hybrid silicone oils. Si-H and peptide modified Si-Vinyl silicone oils were mixed and drop-casted on microscope glass slides (~2 cm²) in the presence of Karstedt's catalyst. After 30 min at 60 °C, the cross-linking is over and thin layers (~100 µm) 0f PDMS-based antibacterial were obtained. 3 samples were prepared for each material as well as a non-functionalized PDMS materials **M2** obtained from **P3** and **P4** PDMS oils (Table **2**).

M7 and **M8** were evaluated for antibacterial activity against the Staphylococcus aureus gram positive bacteria. This bacteria strain is responsible for many nosocomial infection and is commonly found on contaminated medical devices.[23,24] The antibacterial activity was investigated according to the ISO 22196 standard with minor modifications. 10µl of bacterial solution (105 CFU.mL^{-1}) was dropped on each sample and recovered with 1 cm² sterile glass coverslip. After 24 h at 37 °C, bacteria were detached from supports by washing and sonication. The viable bacteria in solution were spread on agar plates for CFU determination. The assay was performed in triplicate. The percentage of inhibition was calculated on the basis of the number of bacteria found on non-functionalized PDMS material (**M2**).

Table 2. Composition of different functional PDMS materials obtained from functionalized PMDS oils. [a]Average of 10 indentation modulus (E_{IT}) obtained by indents at 60µN and 100µN.

Material	Obtained from 50/50 mol%				
	V-PDMS	H-PDMS	Xlink %	E_{IT} (MPa) [a]	mol% peptide
M1	**P1**	**P2**	1	n.d.	0
M2	**P3**	**P4**	2.5	1.61	0
M3	**P5**	**P6**	5	2.66	0
M4	**P7**	**P8**	10	5.68	0
M5	**P3**	**P9**	2.5	3.09	0
M6	**P3**	**P10**	2.5	2.70	0
M7	**P3**	**P11**	2.5	1.49	0.005
M8	**P3**	**P12**	2.5	1.12	0.05
M9	**P3**	**P13**	2.5	0.26	0.5
M10	**P3**	**P14**	2.5	0.28	2.5
M11	**P3**	**P15**	2.5	0.18	5
M12	**P3**	**P16**	2.5	1.23	0.005

M13	**P3**	**P17**	2.5	0.35	0.05
M14	**P3**	**P18**	2.5	0.29	0.5
M15	**P3**	**P19**	2.5	1.12	2.5
M16	**P3**	**P20**	2.5	0.77	5

Results are reported in Figure **6**. The number of bacteria found on functionalized **M2** (over 580 000 bacteria/mm^2) was much higher than the number found on peptide-modified materials (110 000 - 180 000) which corresponded to a decrease of 70% and 81.5 % for **M7** and **M8** respectively. This result clearly demonstrated that the peptide kept its antibacterial properties when covalently linked on silicone, avoiding the bacterial adhesion on surfaces, and that only small amount of peptide is necessary to get an antibacterial activity.

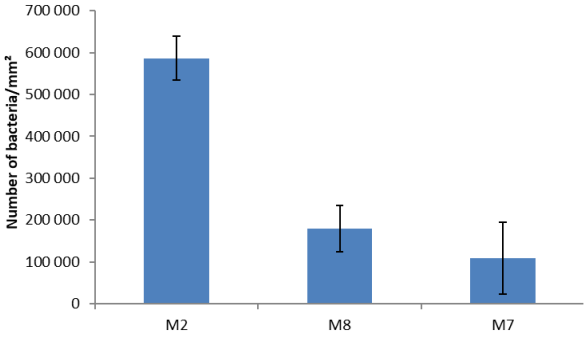

Figure 6. Antibacterial activity of silicone materials **M2**, **M7** and **M8** against *S. aureus* after 24 hours incubation.

Moreover, as the peptide is covalently immobilized on the polymer chains of the materials, one could expect a prolonged activity compared to a simple antibacterial incorporation. Such material with sustained antibacterial activity is particularly attractive for medical device conception such as catheter, laryngeal masks and septum.

We also prepared peptide **3**-modified-PDMS materials (**M12** to **M16** containing from 0.005 mol% to 5 mol% hybrid peptide **3**), from hybrid silicone oils. Si-H (**P3**) and peptide modified Si-Vinyl silicone oils (**P16**-**P20**) were mixed and drop-casted on glass coverslip (1 cm²), in the presence of Karstedt's catalyst. After 30 min at 60 °C, the cross-linking was complete and thin layers (~100 µm) 0f hybrid PDMS were obtained.

RGD-containing PDMS **M14**, **M15** and **M16** assayed for the adhesion of L929 fibroblasts and compared to non-functionalized PDMS materials **M2**. Highly favorable 'Treated for Cell Culture Polystyrene' (TCPS) was used as a positive control. L929 fibroblasts cells were deposited onto the different materials. After 4 h, PrestoBlue assay was performed. Cell adhesion was significantly higher on RGD-PDMS **M14** (0.5%) compared to control **M2** (control**)**. In addition, cell adhesion on **M14** was as good as the positive TCPS control witnessing the importance of the RGD peptide, which turned the PDMS into a surface suitable for proliferation. The cell adhesion was less interesting with **M15** and **M16** which yet incorporated more RGD peptides**, M16** being even less efficient than the silicone control, probably because of a too high density of peptides on the surface. Thus, the incorporation of 0.5 mol% of **3** was enough to promote fibroblast adhesion.

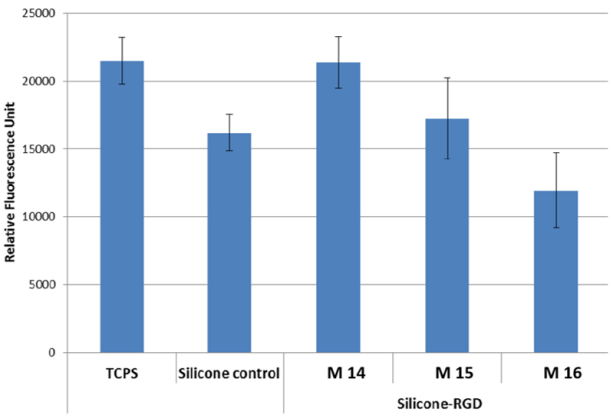

Figure 7. Fibroblast cell adhesion on silicone materials **M2**, **M14, M15** and **M16** after 4h incubation.

Several studies describing the modification of silicone with antibacterial peptides or cell-adhesion peptides have been reported in literature. [16,25–27] However and in strong contrast, the approach we reported here is completely different. Indeed, the bioactive peptides were covalently incorporated in the silicone oils before the preparation of PDMS materials. This strategy is highly generic as different oils can be mixed together and cross-linked, the peptide moiety being either carried by the vinyl-functionalized PDMS or by the Si-H functionalized PDMS. Moreover, different types of peptides can be introduced together for a synergistic effect. Combinations of bioactive moieties can be introduced on the same linear PDMS oil or on differently modified PDMS oils. In these first examples, we used a short cationic peptide and a 9-mer linear peptide to demonstrate how generic was the strategy. Hydrosilylation proceeded chemoselectively versus carboxylic acids, alcohols, amides, phenols and amines, enabling the reticulation of PDMS in the presence of unprotected peptides. This strategy opens the way to the design of any tailored bioactive silicone material by combination of the suitable bioactive silicone oils prepared with hybrid dichloromethylsilyl-biomolecules.

ASSOCIATED CONTENT

Supporting Information

Synthesis of hybrid fluorescein **1** and hybrid peptide **2** and **3**, characterization of PDMS oils by GPC, ^{1}H and ^{29}Si NMR analyses and IR, detailed protocol of antibacterial and cell adhesion assay, can be found in Supporting Information. This material is available free of charge via the Internet.

AUTHOR INFORMATION

Corresponding Author

ahmad.mehdi@umontpellier.fr
gilles.subra@umontpellier.fr

Author Contributions

‡These authors contributed equally.

ACKNOWLEDGMENT

Peptide syntheses were performed using the facilities of SynBio3 IBISA platform supported by ITMO cancer.

Cecile Echalier, PhD was partly supported by the ‘Chercheur d’Avenir’ grant from Conseil Régional Languedoc Roussillon awarded to Pr Gilles Subra.

REFERENCES

[1] M. J. Owen, in *Adv. Silicones Silicone-Modif. Mater.*, American Chemical Society, **2010**, pp. 13–18.

[2] N. A. Chekina, V. N. Pavlyuchenko, V. F. Danilichev, N. A. Ushakov, S. A. Novikov, S. S. Ivanchev, *Polym. Adv. Technol.* **2006**, *17*, 872–877.

[3] F. B. Madsen, L. Yu, A. E. Daugaard, S. Hvilsted, A. L. Skov, *RSC Adv.* **2015**, *5*, 10254–10259.

[4] J. N. Lee, X. Jiang, D. Ryan, G. M. Whitesides, *Langmuir ACS J. Surf. Colloids* **2004**, *20*, 11684–11691.

[5] P. N. Nge, C. I. Rogers, A. T. Woolley, *Chem. Rev.* **2013**, *113*, 2550–2583.

[6] R. Zhang, H.-Q. Gong, X. D. Zeng, C. C. Sze, *Anal. Bioanal. Chem.* **2013**, *405*, 4277–4282.

[7] M. J. Carroll, L. E. Stopfer, P. K. Kreeger, *Chem. Commun.* **2014**, *50*, 5279–5281.

[8] J. C. Salamone, A. B. Salamone, K. Swindle-Reilly, K. X.-C. Leung, R. E. McMahon, *Regen. Biomater.* **2016**, *3*, 127–128.

[9] S. Bhatt, J. Pulpytel, F. Arefi-Khonsari, *Surf. Innov.* **2015**, *3*, 63–83.

[10] V. Bartzoka, M. R. McDermott, M. A. Brook, *Adv. Mater.* **1999**, *11*, 257–259.

[11] J. H. Silver, J. C. Lin, F. Lim, V. A. Tegoulia, M. K. Chaudhury, S. L. Cooper, *Biomaterials* **1999**, *20*, 1533–1543.

[12] K. Beppu, Y. Kaneko, J. Kadokawa, H. Mori, T. Nishikawa, *Polym. J.* **2007**, *39*, 1065–1070.

[13] H. Maeda, T. Kasuga, *J. Biomed. Mater. Res. A* **2008**, *85*, 742–746.

[14] H. Chen, M. A. Brook, H. D. Sheardown, Y. Chen, B. Klenkler, *Bioconjug. Chem.* **2006**, *17*, 21–28.

[15] D. R. Calabrese, B. Wenning, J. A. Finlay, M. E. Callow, J. A. Callow, D. Fischer, C. K. Ober, *Polym. Adv. Technol.* **n.d.**, *26*, 829–836.

[16] C. Pinese, S. Jebors, C. Echalier, P. Licznar-Fajardo, X. Garric, V. Humblot, C. Calers, J. Martinez, A. Mehdi, G. Subra, *Adv. Healthc. Mater.* **2016**, *5*, 3067–3073.

[17] C. Pinese, S. Jebors, P. Emmanuel Stoebner, V. Humblot, P. Verdié, L. Causse, X. Garric, H. Taillades, J. Martinez, A. Mehdi, et al., *Mater. Today Chem.* **2017**, *4*, 73–83.

[18] S. Jebors, J. Ciccione, S. Al-Halifa, B. Nottelet, C. Enjalbal, C. M’Kadmi, M. Amblard, A. Mehdi, J. Martinez, G. Subra, *Angew. Chem. Int. Ed.* **2015**, *54*, 3778–3782.

[19] S. Jebors, C. Pinese, B. Nottelet, K. Parra, M. Amblard, A. Mehdi, J. Martinez, G. Subra, *J. Pept. Sci.* **2015**, *21*, 243–247.

[20] R. O. Darouiche, *N. Engl. J. Med.* **2004**, *350*, 1422–1429.

[21] N. Masurier, J.-B. Tissot, D. Boukhriss, S. Jebors, C. Pinese, P. Verdie, M. Amblard, A. Mehdi, J. Martinez, V. Humblot, et al., *J. Mater. Chem. B* **2018**, DOI 10.1039/C8TB00051D.

[22] G. Palaprat, F. Ganachaud, *Comptes Rendus Chim.* **2003**, *6*, 1385–1392.

[23] R. O. Darouiche, *Clin. Infect. Dis.* **2001**, *33*, 1567–1572.

[24] L. García-Aparicio, E. Blázquez-Gómez, O. Martin, L. Krauel, I. de Haro, J. Rodó, *Actas Urol. Esp.* **2015**, *39*, 53–56.

[25] K. D. Prijck, N. D. Smet, M. Rymarczyk-Machal, G. V. Driessche, B. Devreese, T. Coenye, E. Schacht, H. J. Nelis, *Biofouling* **2010**, *26*, 269–275.

[26] K. Lim, R. R. Y. Chua, R. Saravanan, A. Basu, B. Mishra, P. A. Tambyah, B. Ho, S. S. J. Leong, *ACS Appl. Mater. Interfaces* **2013**, *5*, 6412–6422.

[27] B. Mishra, A. Basu, R. R. Y. Chua, R. Saravanan, P. A. Tambyah, B. Ho, M. W. Chang, S. S. J. Leong, *J. Mater. Chem. B* **2014**, *2*, 1706–1716.

Chapter 5: Synthesis of multifunctional PDMS-Nanoparticles

Chapter 5: Synthesis of multifunctional PDMS-Nanoparticles

I. Introduction

Nanoparticles (NPs) are nano-objects defined mainly by their size, from 1 to 200 nm in one dimension. They can be classified by their shape, properties or composition. According to their composition, they can be sorted into three different groups: organic, inorganic or hybrid, for particles combining an inorganic and an organic part.[329] Organic NPs are divided in three main structures: micelles, vesicles or dendrimeric structures.[330] Micelles are constituted of amphiphilic molecules, such as surfactants or block copolymers with hydrophilic and hydrophobic parts, that self-assembles together to form a NP, often following a core-shell organization. One specific type of micelles is the polymersome (or polymeric micelles).[331] Polymeric micelles are obtained from amphiphilic polymer, usually block-copolymer with a hydrophilic part and a hydrophobic one.[332,333] In function of the nature of the solvent, organic or aqueous media, one part will constitute the core of the polymeric micelles and the other one the shell.

Vesicles, the result of self-assembly of lipids, usually form hollow spheres. Surfactants and most of lipids, are amphipathic molecules, containing polar head and non-polar tail, that may self-assemble into diverse structures in water. In addition, one specific type of vesicle is the liposomes. Liposomes are vesicles made of phospholipids.[334,335] Phospholipids are composed of two parts: a hydrophilic one, the head, and a hydrophobic one, the tail. The tail is usually made of two aliphatic chain and the head of a polar phosphate group.

The structure they adopt depends on the size of each part of the molecule: head *vs* tail. If the head is bigger than the tail, it will lead to micelles or liposomes, if they are equal to planar bilayer and if the head is smaller than the tail, inverted micelles are observed (Figure 97).

Dendrimers are hyper branched macromolecules usually symmetric with a well-controlled structure that forms NPs of selected size.[336] Dendrimers generate their own type of NPs, with cavities in-between their branches and well-defined number of active groups, at the end of the branches.

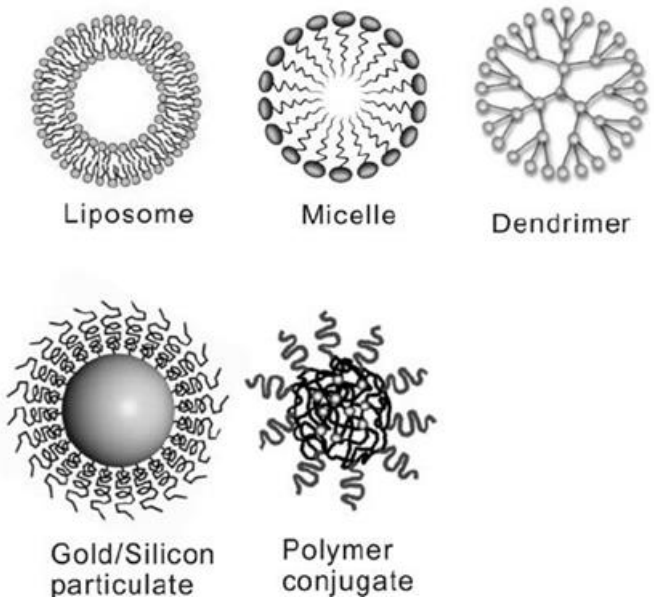

Figure 97. Various types of NPs described in the literature. (Adapted from[337])

Whatever their types, most of the NPs can be prepared following two different approaches: either by top-down (from bulk to NPs) or bottom-up (form atoms to NPs) approach, the later giving generally a better control on the size distribution of the particles.[335] Applications of the NPs are numerous and diverse and are depending on their composition, their shape and especially their size which is a very important parameter impacting on the NPs properties.[332,338–340] For example, the shape of gold NPs, whether they are cubic or spherical, directly impacts their action on the immunological responses of cells.[340] NPs were notably developed in microelectronics,[341] in cosmetics formulation,[342] in medicine as drug delivery systems,[343] but also in energy especially in the composition of solar cells,[344] in catalysis systems[345] and even in food industry.[346]
Due to their small size enabling them to circulate in the blood stream while limiting renal clearance, and the fact that such a single object may gather several functions, NPs are particularly attractive tools for biomedical applications for diagnosis and/or treatment, acting as delivery systems (e.g. drugs, genes) or imaging agents. It is the principles of 'magic bullet' developed in Figure 98 (i.e. a single object gathering several functions. The ligands present on the 'magic bullet' can be either peptides, proteins, antibodies or even small molecules.[347] They can be grafted directly on the NPs or through a spacer such as PEG. PEG moiety is bringing more visibility to the ligand toward receptors, besides it helps the NPs to get a better furtivity in blood vessel.[348]

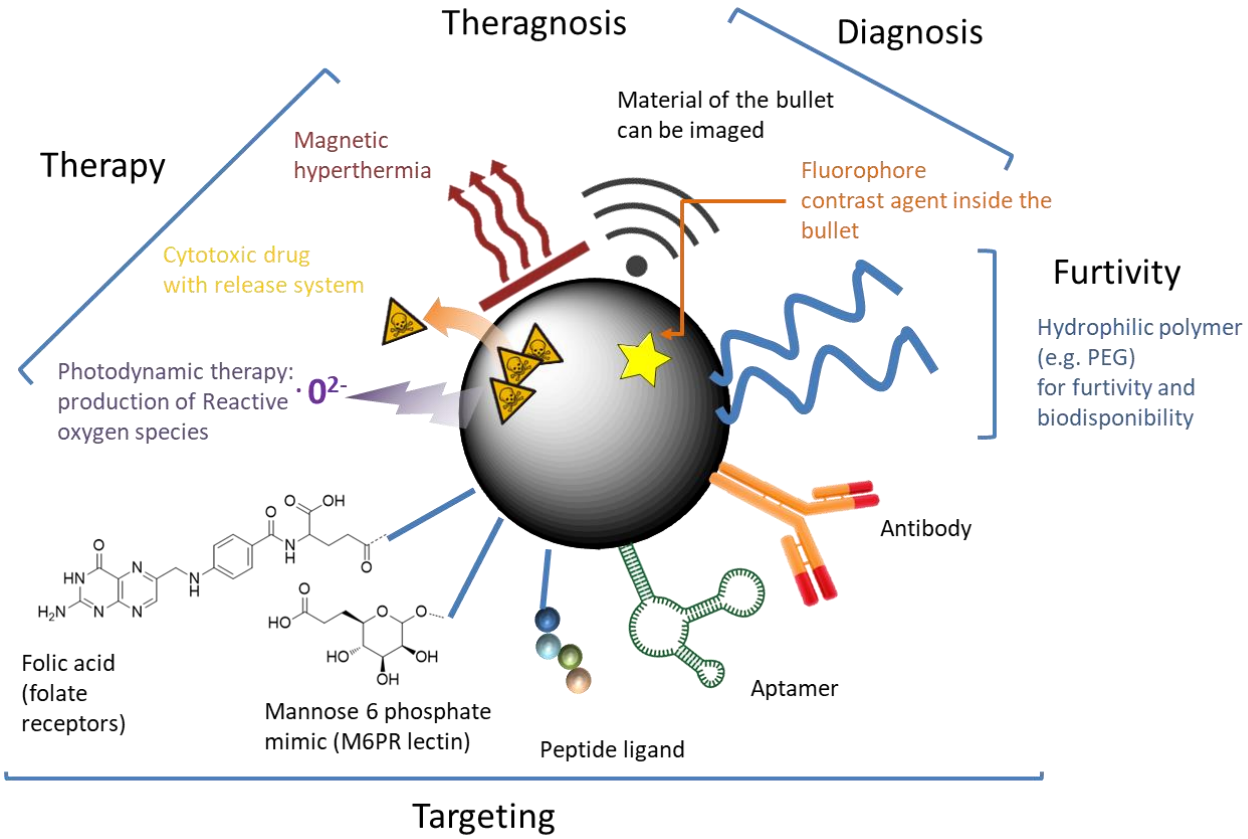

Figure 98. Magic Bullet for theranostic applications

Obviously, NPs used *in vivo* have to be biocompatible but must also present specific properties linked to the application. For example, in the case of drug delivery system, the NPs must be able to load a drug, either non-covalently or covalently. In the latter case, they may release the drug by responding to a stimulis such as pH, reductive media or UV light. Most of the time, drugs are cytotoxic molecules used in chemotherapy.[349,350] In this context, it is highly important that NPs reach the selected cells on the targeted organ. For that, the NPs need to

be as selective as possible. Thus, the NPs can be decorated by ligands, which recognize special features of the selected cells, such as over expressed receptors, to enhance the targeting properties.

Other decorations can be added to the system to earn new abilities, like triggered linkers for the release of covalently-attached drug or zwitterionic molecules for example,[351] favoring the interaction with the drug in the case of the non-covalent loading. In order to let them target the receptors at the surface of the selected cells, ligands have to be at the surface of the particles and should remain accessible. The linker is placed between the drug and the anchor point on the surface or inside the particles. It can be sensitive to the variation of pH if based on acid-labile function, to reduction if it contains disulfide bond for example, or to UV light like *ortho*-nitrobenzyl or phenacyl ester derivatives.[352]

NPs present an additional advantage for cancer therapy due to so-called enhanced permeability and retention effect (EPR). EPR is an universal concept to target solid tumors, explaining why NPs for cancer therapy with an optimal size range helps them to penetrate the tumor tissues and stay in them at the same time.[353,354]

Solid tumors cells have an anatomy and a physiopathology different from normal tissue: they have a higher vascular density, larger gaps between the endothelium cells which enable a selective extravasation through the blood vessel.[355] This gap is bigger than in normal tissues due to the vascularity permeability needed to provision nutriment and oxygen for the tumor growth. This vascularity permeability also favors the passage of NPs of adapted size. Once passed the blood vessel of the solid tumor, NPs are accumulated, hence the retention aspect, at high concentration and for a long time (>100h).[356] In order to benefit from EPR effect, the NPs have some constraints of size. On one hand, NPs that are smaller than 10 nm are too small mainly because they are filtered by the kidney or by the lymphatic system from normal tissue. On the other hand, NPs bigger than 200 nm have no chances to get through any vessels. The optimal size range according to the EPR is from 50 to 150 nm.[357,358] Indeed, tumors are creating opening big enough to let NPs bigger than 50 nm going through, while they are impermeable to normal vessel. However, they have to stay smaller than 150 nm approximatively, in order to be able to cross tumor vessel and then being accumulated in the tumor (Figure 99).

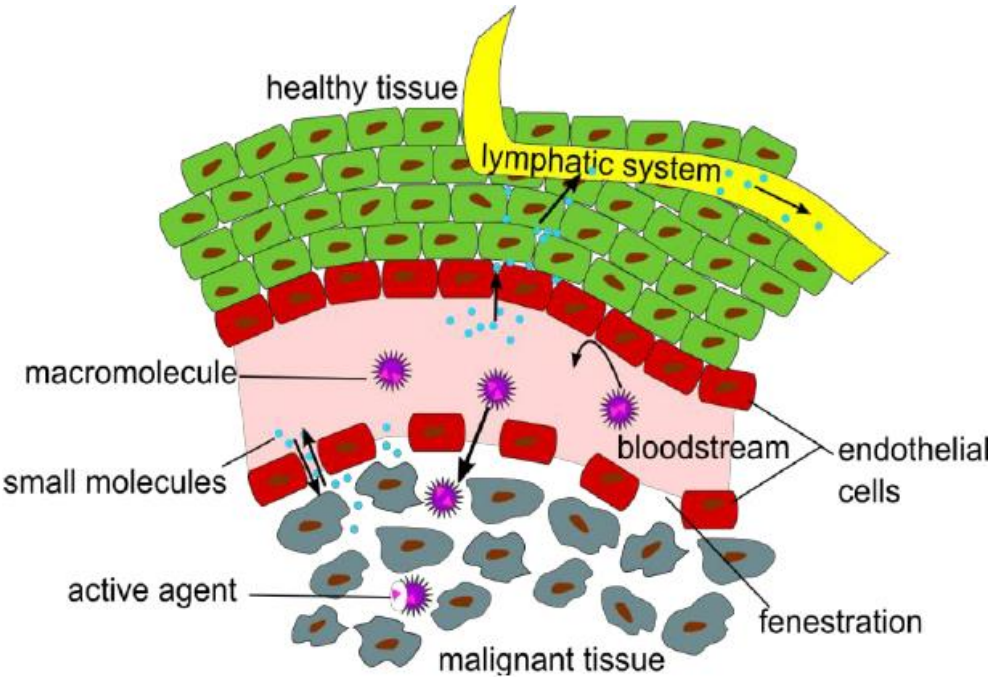

Figure 99. EPR effect on the blood vessels near tumor cells .[358]

It is worth noting that selectivity to tumor cells can be further enhanced thanks to specific ligands targeting overexpressed receptors.

In this context, our goal was to develop a new family of multifunctional particles that could be decorated by any combination of targeting ligand, probes and drugs. Such particles will be prepared by a bottom-up approach based on the combination of hybrid blocks. We focus our attention on polydimethylsiloxane (PDMS) backbone functionalized with pendant relevant bioactive moieties. The main part of the work was first to establish the proof of concept of multifunctional PDMS-NPs. Potential biological applications are numerous but, as a preliminary study, we designed particles that could be useful for cancer therapy or diagnosis. 50-150 nm diameter particles should be ideal to benefit from EPR effect.

Diverse silylated macromonomers were synthesized and then copolymerized with dichlorodimethylsilane to get an amphiphilic polymer using sol-gel method. Indeed, the silicone backbone (i.e. dimethylsiloxane) is by definition highly hydrophobic, and due to the addition of more hydrophilic silylated monomers, an amphiphilic polymer would be obtained.

Biomolecules of interest, such as peptides or hydrophilic drugs, could play the role of hydrophilic parts but we also investigate the introduction of silylated polyethylene glycol (PEG) as hydrophilic macromonomers.

We made the hypothesis that such amphiphilic comb-like polymer chain could assemble to yield polymeric particles.[318,359,360] For example, a block copolymer composed of PEG and PLA (polylactic acid), one of the most common combination, is able to self-assemble into micelles which can be used as a drug delivery system.[361] Indeed, the formation of polymeric NPs is based on the self-assembly of amphiphilic polymers dispersed in a solvent, water most of the time. By playing on the hydrophilic/hydrophobic balance (i.e. backbone chain length vs hydrophilicity of pendant groups) it should be possible to modulate the characteristics of the particles, such as their size and shape, in order to match the application wanted (

Figure 100). In our case, the polymer composition is either a statistical polymer or a block copolymer, the topology is alike a graft polymer and finally the self-assembly is leading to micelles.

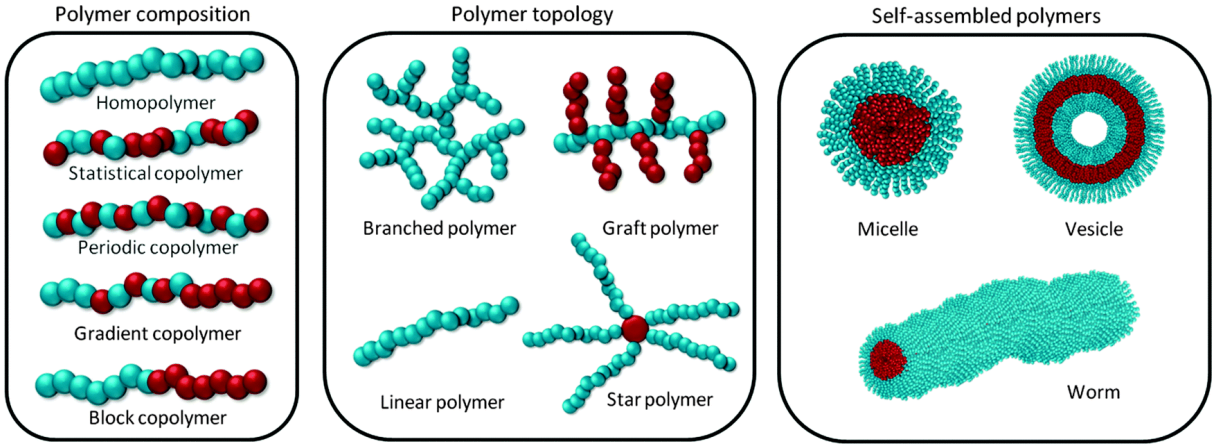

Figure 100. Different possibilities of polymer composition, structure and self-assembly.[362]

The first milestone will be the definition of an optimal composition of functional PDMS allowing the formation of particles. In a first attempt, we will study the behavior of PDMS in water and its propensity to form particles (part II). Then, we will investigate PEG-PDMS particles (see part III). After finding the optimized composition, functionalized NPs will be prepared by adding desired silylated biomolecule of interest during the polymerization. It could be ligands to target receptors overexpressed in cancer cells or cytotoxic drugs. In the

latter case, a cleavable linker will be placed between the drug and the silyl group to enable the release of the molecule (part IV).
First, pristine PDMS have been synthesized to test some parameters of the polymerization and preparation of NPs. The presence or not of the surfactant, the stability of the NPs formation over sonication and lyophilization will be first studied.

NB: all the reactions presented in this chapter, will be annotated by their original lab book ID.

II. Synthesis and characterization of PDMS-NPs

a. Synthesis of PDMS

Our goal was to obtain approximatively 50-150 nm diameter PDMS NPs. We wanted to verify if the size of the PDMS polymer chain would have an impact on the diameter of the particles. Two methods of preparation of PDMS chains were investigated from polymerization of dichlorodimethylsilane (DCDMS) monomers. The first one is described in chapter 4 and involves a surfactant, the sodium dodecyl sulfate (SDS) enabling the elongation of the silicone chain inside the SDS micelles formed in water. Afterwards, an extraction step is necessary to separate the surfactant from the polymer. Chloroform is used as extracting solvent, in which PDMS is completely soluble but not the SDS. Then several washing with water are sufficient to remove the remaining SDS. Finally, the PMDS solution is dried under $MgSO_4$, filtered and concentrated by evaporation of the organic solvent under vacuum. The second mode of polymerization is operated without any surfactant in order to facilitate the extraction of the resulting PDMS (IIII.a.2).

1. Synthesis of PDMS with surfactant

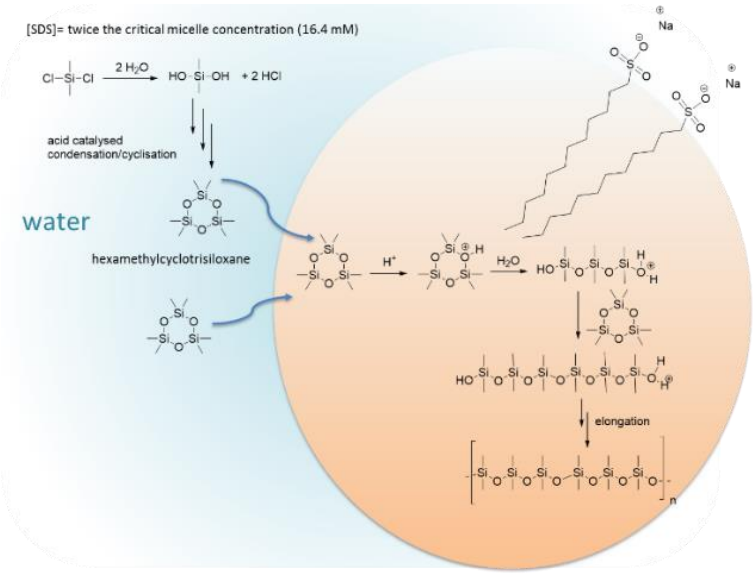

Figure 101. Polymerization of DCDMS in water with the use of SDS surfactant.

The PDMS synthesis is based on three steps: the hydrolysis of its monomer, i.e. the dichlorodimethylsilane, the formation of hexamethylcyclotrisiloxane[363] and finally the ring-opening of leading to the growing of the PDMS chain in the surfactant micelles (Figure 101, chapter 4).

We studied the length of the PDMS chains as a function of polymerization time using GPC. Eight different polymerization reactions were performed simultaneously in the same conditions (concentration of DCDMS and SDS, volume of solvent, temperature and type of reactor) and were stopped at different time: $P_{248\text{-}x}$, x corresponding to the number of hours. PDMS was extracted and finally analyzed by GPC to obtain its molecular mass in number (Mn) and in weight (Mw) (Figure 102 and Figure 103) and its polydispersity index (Đ), Đ=Mw/Mn. The yield was calculated by comparing the theoretical and experimental polymer weight obtained (Figure 104). Mn gives the average molar mass of the polymer, while Mw gives a distribution of the molar mass: it gives the molar mass the most represented in the batch. Then, the Đ is expresses the diversity of the molar mass: the more the Đ is close to 1, the more the polymer chains have a molar mass close to each other and so a narrower peak on size exclusion chromatography analyses.

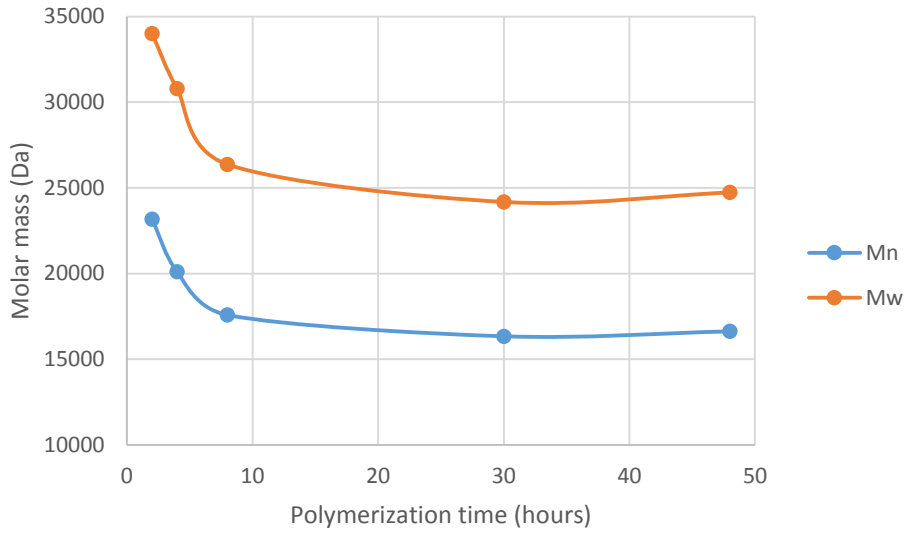

Figure 102. Evolution of the molar mass of PDMS in function of the polymerization time, analyzed by SEC in THF.

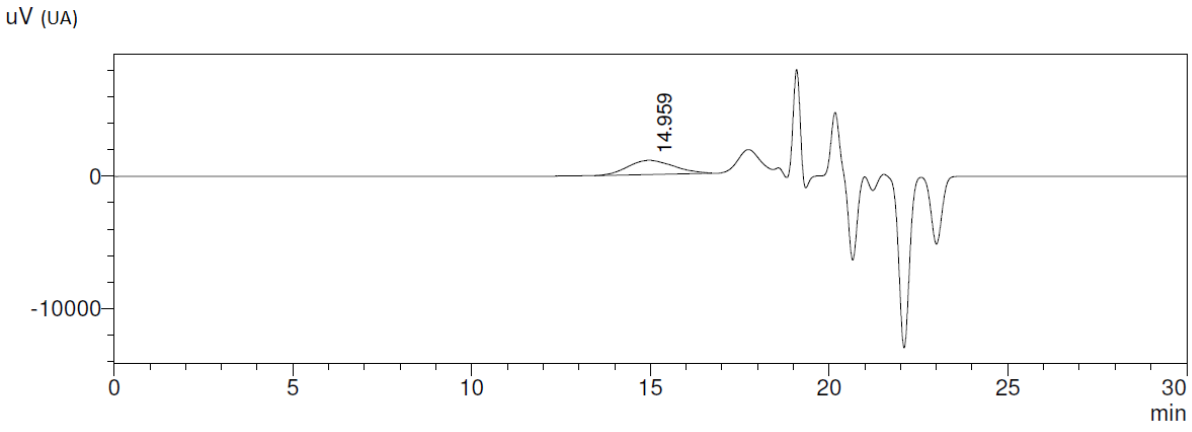

Figure 103. GPC chromatogram (THF, 1ml/min, 30 °C) of a 5 mg/mL solution of a PDMS obtained by polymerization of DCMDS during 8 hours, filtered with a PTFE 0.45 µm.

Unexpectedly, increasing polymerization time (i.e. from one to four hours), resulted in lower molar mass, either in number and in weight, and so shorter PDMS chains: Mn goes from 23.2 kDa for **$P_{248\text{-}1}$** to 17.6 kDa for **$P_{248\text{-}8}$**, corresponding to approximatively 300 and 230 synthons respectively (Figure 102). One explanation could be that the dichlorodimethylsilane monomers are reacting all together from the beginning and then the polymer is rearranging in more thermodinamicaly stable smaller chains over time.

Figure 103 shows a typical GPC chromatogram of a PDMS in chloroform. The first peak is the one corresponding to the polymer while the others are due to the solvent. It is then the first peak that is integrated and compared to the PDMS standard curve also preformed in chloroform.

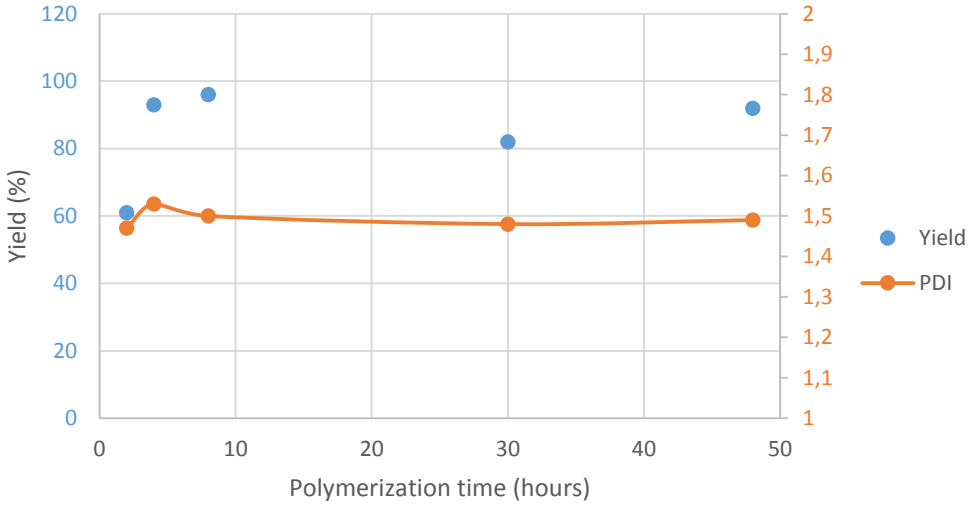

Figure 104. Evolution of the yield and the polydispersity of the PDMS as function of the time.

Then, the Đ curve showed that smaller values are obtained with a longer polymerization time. Small Đ values are associated to low polydispersity meaning that the PDMS chain sizes are slightly more homogeneous after 8h, Đ=1.5 for $\mathbf{P_{248\text{-}8}}$, than after 1h, Đ=1.63 for $\mathbf{P_{248\text{-}1}}$. The polymer weight and the yield were stable after 8h of polymerization, so we chose this duration as minimal polymerization time for further experiments.

2. *Synthesis of PDMS without surfactant*

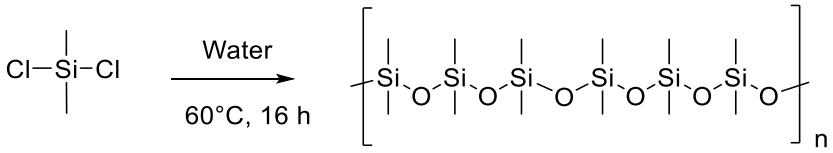

Figure 105. Polymerization of DCDMS without surfactant.

To simplify the process, the use of the surfactant can be questioned. Indeed, the SDS stays between the two phases, organic and aqueous, during the extraction of the PDMS by chloroform. This step could be even more critical with PDMS functionalized with amphiphilic parts. Two polymer have been synthesized simultaneously in the same conditions except for the presence or not of SDS: respectively, $\mathbf{P_{252\text{-}1}}$ and $\mathbf{P_{252\text{-}2}}$.

The PDMS synthesis was essayed without any surfactant (Figure 105). THF and chloroform were tested for the GPC analysis to compare them. Previously, only THF was used for GPC but it seemed that the reflection indices (RI) of the THF was too close to the one of PDMS, i.e. they are iso-refractive. We switched to chloroform for further analyses. As expected, the size obtained from GPC (whatever the solvent used) was more than two times higher with SDS than without SDS (i.e. 37.8 kD and Mw= 14.8 kDa, for $\mathbf{P_{252\text{-}1}}$ and $\mathbf{P_{252\text{-}2}}$ respectively). Advantageously, washing steps were simpler and easier since no surfactant (which stayed in between the two phases during the extraction had to be washed from the polymer).
However, we still had to determine if the mode of synthesis (with or without surfacant) would have an influence on the preparation of the particles and in particular on their sizes.

b. Preparation and characterization of PDMS NPs

We first prepared NPs from pristine PDMS (PDMS NPs) as reference to observe the differences of behavior with the ones obtained with modified PDMS (e.g. PEG-PDMS NPs) and to assess the influence and importance of the modifications. Unmodified PDMS is completely hydrophobic, so the formation of NPs will be different from the ones obtained with more hydrophilic, modified PDMS. Nevertheless, these preliminary studies on PDMS NPs allowed us to try different methods and treatments, to test the self-assembly of pristine PDMS into NPs and to optimize their characterization by Dynamic Light Scatering (DLS).

The first step was to find the appropriate solvent allowing the formation of NPs. In addition, the solvent had to be compatible with the final application. As already stated, our final aim was to get particles suitable for cancer targeting. Thus, water (at pH 7) seemed a good choice as solvent for the formation of particles. Phosphate-buffered saline (PBS, pH 7.4) widely used in cell culture, was also tested.

Of course, pristine silicone polymer is not soluble in aqueous media. Dispersion of pure PDMS, $\mathbf{P_{248}}$: synthesized with SDS during 16h in water was tested. As expected, placing PDMS directly in water resulted in a floating material (see Figure 106).

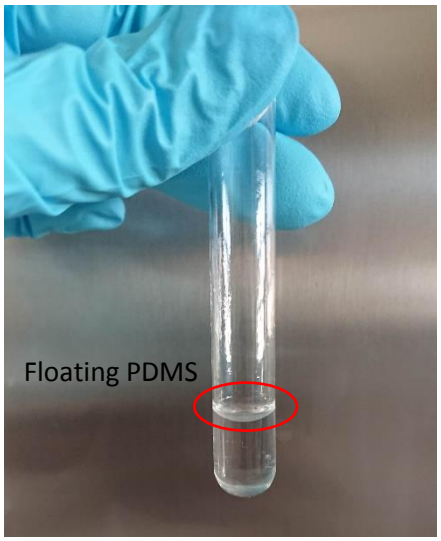

Figure 106. Picture of PDMS $\boldsymbol{P_{248}}$ floating over water in a hemolysis tube.

Alternatively, we proposed to solubilize $\mathbf{P_{248}}$ in an organic solvent before nanoprecipitation in water. We dissolved the PDMS in a small amount of THF (e.g. ≈10 mg in 50 µl), then 1950 µl of water were added to obtain different concentrations. The solution was sonicated and vortexed (for ~5min) to get particles dispersed in water (Table 12, Figure 107).

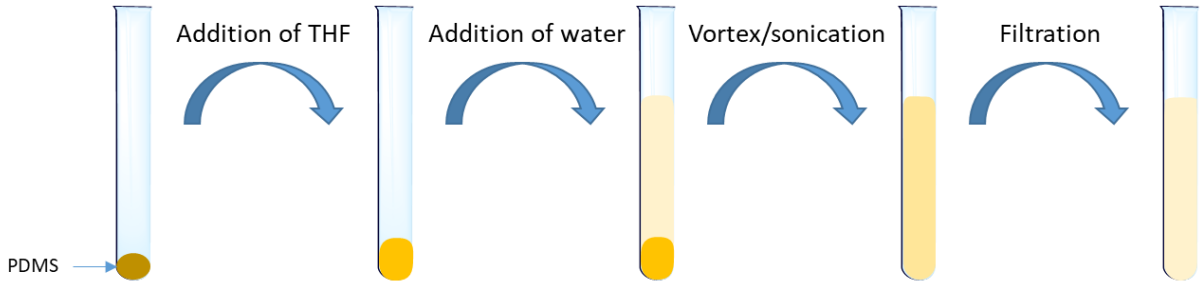

Figure 107. PMDS NPs preparation protocol.

We were able to test several conditions to check the stability of these kinds of dispersion by analyzing the resulting solution by DLS. The concentration, the initial amount of THF, the sonication/vortex duration and the use of the freeze drier were investigated (Table 12).

Table 12. DLS analysis on NPs formed from P_{248}, PDMS synthesized with SDS

Sample	Organic solvent (µL)		Aqueous solvent (µL)		[PDMS] (mg/mL)	Treatment	Size (nm)[a]
NP_{248-1}	THF	50	H_2O	1950	5	None	207 and 618
NP_{248-2}	THF	50	H_2O	1950	1	Dilution	500 to 800
NP_{248-3}	THF	50	H_2O	1950	0.5	Dilution	500
NP_{248-4}	THF	50	H_2O	1950	5	Sonication (5min)	180 and 700
NP_{248-5}	THF	200	H_2O	1950	5	More initial THF	180 and 645
NP_{248-6}	THF	50 (+100)	H_2O	1950	5	Addition of THF	250
NP_{248-7}	THF	50	H_2O	1950	5	Lyophilisation	130 and 740
NP_{248-8}	THF	50	PBS	1950	5	PBS instead of water	900
NP_{248-9}	EtOH	50	H_2O	1950	5	EtOH instead of THF	300
NP_{248-10}	DMSO	50	H_2O	1950	5	DMSO instead of THF	70 to 650
NP_{248-11}	THF	50	H_2O	1950	5	Ultraturax (12*1000rpm, 5min)	891
NP_{248-12}	THF	50	H_2O	1950	5	Ultraturax (18*1000rpm, 5min)	162 and 851
NP_{248-13}	THF	50	H_2O	1950	5	Ultraturax (24*1000rpm, 5min)	128 and 732
NP_{248-14}	THF	50	H_2O	1950	5	Ultraturax (24*1000rpm, 10min)	123 and 900
NP_{248-15}	THF	50	H_2O	1950	5	Filtration (0.45µm)	180
NP_{258}	THF	50	H_2O	1950	5	Polymerization without SDS	179 and 698

[a] NPs diameter size obtained by DLS

The DLS measurements were recorded on VASCO™ nanoparticle size analyzer which had the advantage to reduce constraints due to sample preparation as no filtration were required neither the use of a plastic cuvette.

Influence of the concentration and sonication

For the first attempt, **NP_{248-1}** particles obtained were quite polydispersed (from 200nm to 800nm). When diluting this solution 5 or 10 times in water leading to 1 and 0.5 mg/mL respectively, **NP_{248-2}** and **NP_{248-3}** were obtained. Their polydispersity decreased, with a final population centered around of 500nm (Figure 108). Alternatively, sonication was performed after the dispersion at 5mg/mL (**NP_{248-4}**). It also helped to get a narrower polydispersity even if two different populations appeared, the population 1 around 180 nm and the population 2 around 700 nm (Figure 109).

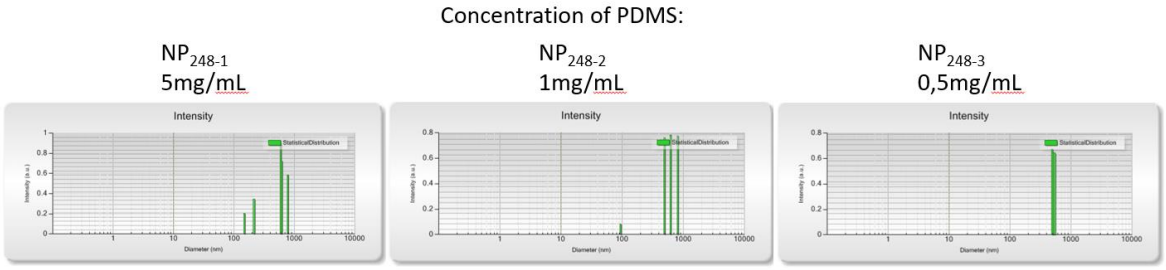

Figure 108. Dilution effect on the size of the PDMS-NP by DLS measurement in intensity.

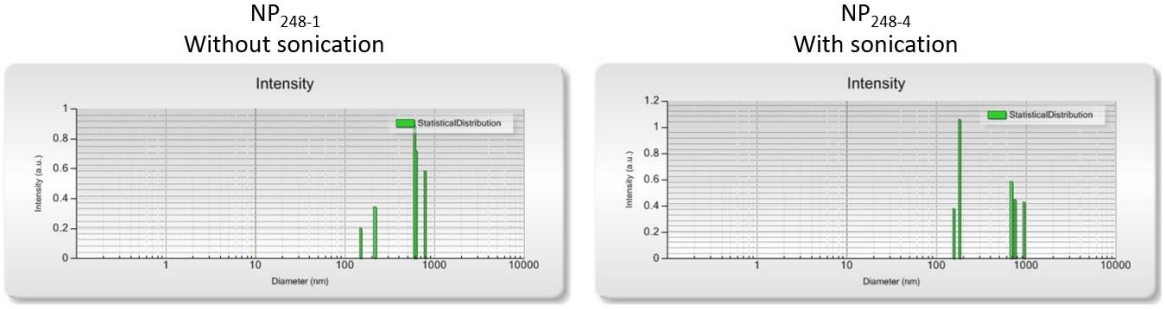

Figure 109. Effect of the sonication on the size of PDMS NPs by DLS measurement in intensity.

Influence of the addition of THF

The influence of the amount of initial THF on the polydispersity was also tested. We noted that using more THF (200 µL instead of 50µL, sample **NP$_{248\text{-}5}$** and **NP$_{248\text{-}1}$** respectively) led to an increase of the population of bigger particles (645 nm) over the smaller (180 nm). The addition of 100 µL of THF in the 2 mL solution of **NP$_{248\text{-}1}$** was also tried (Sample **NP$_{248\text{-}6}$**): firstly, 50µL of THF containing the PDMS was precipitated into 1.950 mL of water (**NP$_{248\text{-}5}$**), and then, 100 µL of THF was added to the solution (**NP$_{248\text{-}6}$**). We wanted to check if the THF would go inside the NP and make it grow. Interestingly, we obtained almost monodispersed NPs centered around 250 nm (Figure 110).

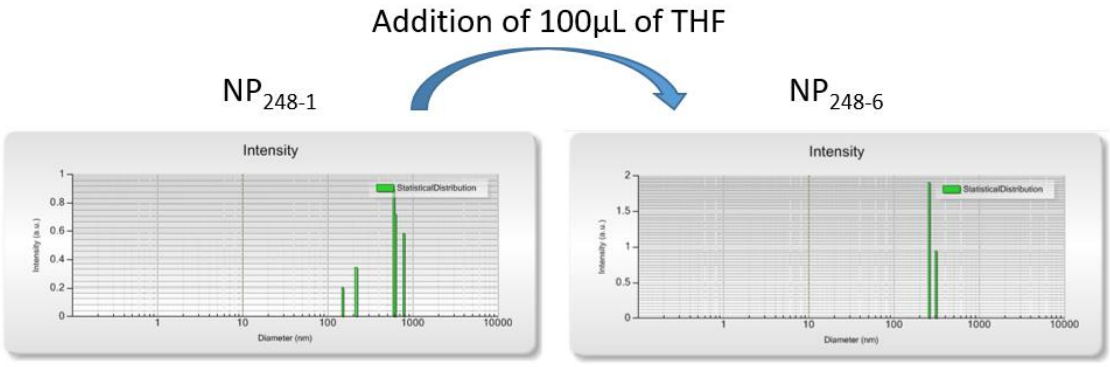

Figure 110. Effect of the addition of 100 µL of THF on PDMS-NPs by DLS measurement in intensity.

Influence of freeze-drying

A new suspension was prepared following **NP$_{248\text{-}1}$** protocol and then freeze dried to check the stability after lyophilization: Lyophilized particles were then dispersed again in THF then water (as the initial dispersion). **NP$_{248\text{-}7}$** were obtained as two well defined populations (130 nm and 740 nm) (Figure 111).

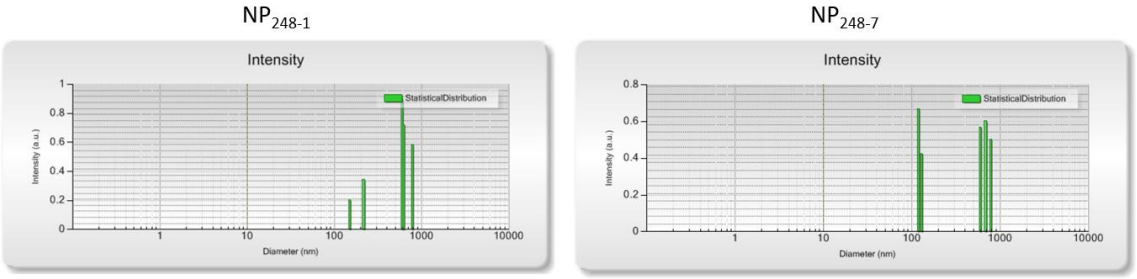

Figure 111. Effect of the lyophilization on PDMS-NPs by DLS measurement in intensity.

Influence of solvent

The nature of the solvent was investigated as well. Instead of 50 µL of THF in 1.950 mL of water, each solvent, organic and aqueous, have been changed alternatively keeping the same proportions. THF was replaced by ethanol or DMSO and water was replaced by PBS (**NP_{248-9}**, **NP_{248-10}** and **NP_{248-8}** respectively). EtOH in water gave mostly only one population around 300 nm plus two really less represented populations at 200 nm and 700 nm. DMSO in water gave a higher polydispersity (from 70nm to 650 nm, including NPs at 300 nm as well). THF in PBS gave only one population at 900 nm, probably due to aggregation favored by the high concentration of salts presents in the PBS.

According to the results, the initial solvents (i.e. THF in water) seemed to be the best option.

Influence of homogenizer

In order to get preferentially a monodispersed, smaller population of NPs (population 1), we treated the solution with a homogenizer device: the Ultra Turrax® which was supposed to give a better dispersion of PDMS NPs in water. This dispersion was performed in the same condition than **NP_{248-1}** (dissolved in THF then precipitated in water) at different speeds (12, 18 and 24.10^3 rpm) and different durations (5 or 10 min). Unfortunately, this method did not change the NPs size significantly (Table 12, NP_{248-11} compared to **NP_{248-14}**). However, compared to **NP_{248-7}** obtained without Ultra Turrax®, the two populations have smaller polydispersity: they are more separated from each other and more defined. We observed a small decrease of the size of population 1 (from 180 nm to 125 nm) and an increase of the size the population 2 (from 700 nm to 950 nm).

Summing up, the best results in term of size and polydispersity were obtained from **NP_{248-7}** obtained by nanoprecipitation of PDMS solubilized in THF and then lyophilized. Therefore, to obtain only the population 1 centered around 130 nm we removed the bigger particles (over 500 nm) by filtration on 0.45µM H-PTFE filter. We obtained a good dispersion around 180 nm by DLS.

Influence of the polymer size

Having determined the optimal mode of preparation, we checked the influence of the PDMS chain size on the diameter of the NPs.

DLS measurement of NPs obtained from PMDS synthesized without SDS (14.8 kDa MW) were compared to those obtained from PDMS synthesized with SDS (37.8 kDa); **NP_{258}** and **NP_{248-1}** respectively. Interestingly, the polymer chain size did not have a significate influence on the NPs size neither on the distribution of populations. We obtained two populations at 179 and 698 nm instead of 207 and 618 nm for **NP_{258}** and **NP_{248-1}** respectively. This assay comforted us in our choice to get rid of SDS during the synthesis of polymers. Therefore, for the following syntheses, we decided to work without any surfactant, allowing easier washing and extraction and so avoiding any contamination as SDS contaminations.

III. Synthesis of PEG-PDMS NPs

a. Synthesis and characterization of PEG-PDMS

We showed that PDMS polymers, solubilized in THF, are able to form particles by nanoprecipitation in water. However, we wanted to investigate amphiphilic particles, which would include PEG chains as hydrophilic component. PEG is a well-known hydrophilic polymer, widely used for biological and biomedical applications. Noteworthy, PEG had been already used for the preparation of NPs from block copolymers as hyaluronic acid-*b*-PEG[316,364] or PEG-*b*-PLA (polylactic acid).[25] In the bottom-up strategy we disclose here, we had to prepare a PEG chain bearing a methyldichlorosilane group at one of its extremities. This monosilylated PEG_{3000} (called Si-PEG-F, compound **14**), had to be copolymerized with DCDMS (Figure 112). Macromonomer **14** includes a fluor atom at one of its ends to be used as probe for ^{19}F ERETIC NMR quantification[199] (chapter 3). A fluoro amino ethyl moiety was introduced at the carboxylic acid function of the PEG_{3000}; the other side was devoted to the reaction of anime with ICPDCMS.

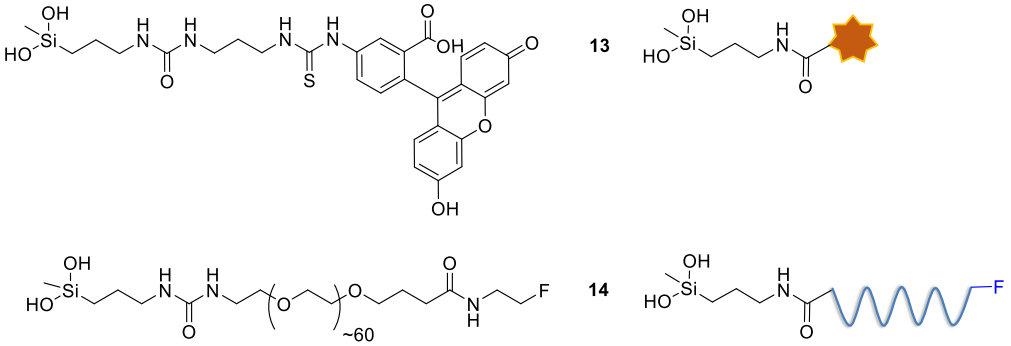

*Figure 112. (Macro)monomers **13** and **14**, Si-Fluorescein and Si-PEG-F.*

We assumed that a molar ratio of 0.5 mol% to 2 mol% of silylated PEG **14** was suitable to get amphiphilic polymer. These molar ratios were calculated comparing the molar quantity of $–Si(Me)_2-O-$ synthon to –Si(Me)PEG-O synthon. Such molar ratio corresponds to a weight ratio of 18 w% to 46 w% of PEG over the whole polymer and then should be enough to get an amphiphilic polymer. It also corresponds to 5 to 20 PEG chain(s) for each PDMS polymer chain of 1000 SiO units of length. This ratio of PEG towards the whole polymer is in agreement with examples from the literature: approximatively from 2 to 45 w%.[348,365,366]

In order to get the ideal size of NPs from these copolymer (i.e. from 50 to 150 nm to take profit of EPR effect), the mol% of compound **14** related to DCDMS have been varied from 0.5 mol% to 2 mol%. We assumed that going above 2 mol% of compound **14** was not necessary. Indeed, as already discussed in the previous paragraph, 2 mol% of PEG_{3000} monomer correspond to 46 weight% in the final polymer, yielding an equilibrated balance between hydrophilic and hydrophobic part of the PEG-PDMS polymer.

Another functional silylated monomer was introduced during the PDMS polymerization: a hybrid fluorescein derivative[367,367–370] (compound **13**) obtained by reaction of FITC (fluorescein isothiocyanate) with a diamine spacer and then isocyanatepropyl dichloromethylsilane (its synthesis was described in chapter 3). Thanks to the presence of fluorescein in the polymer, we could expect to facilitate the visualization of the particles by confocal microscopy, and eventually witness their internalization inside the cells when bioassays will be performed. We fixed the fluorescein ratio to 0.1 mol%, corresponding to 1 fluorescein for polymer chain of 1000 SiO units of length. This relatively low quantity should not have a big impact on the polymer and will be sufficient to detect the particles by fluorescent microscopy.

We also investigated two different ways of polymerization to highlight the influence of the polymer structure on the resulting NPs size and shape. The way A consisted in a direct polymerization of all monomers at the same time in order to get a statistical repartition of each monomer in the multifunctional fluorescein-PEG-PDMS. On the other end, the way B consisted in the synthesis of a multifunctional PEG-PDMS block copolymer by synthesizing first the silicone part with DMDCS and adding the hybrids monomers (i.e. compounds **13** and **14**) afterwards (Figure 113).

Interestingly, all the monomers were soluble in water. Thus, we used the same protocol than the one used for PDMS NPs (II.b), i.e. polymerization of DCDMS or silylated monomers in water at 60 °C for 24h without any surfactant. For the way A, all monomers reacted together during 24h. For the way B, DCDMS was polymerized alone for 16h then the other macromonomers were added to the mixture for another 8h period. Both strategies are following the same washing steps: extraction by chloroform, washing with water three times, drying by $MgSO_4$ and evaporation of the chloroform.

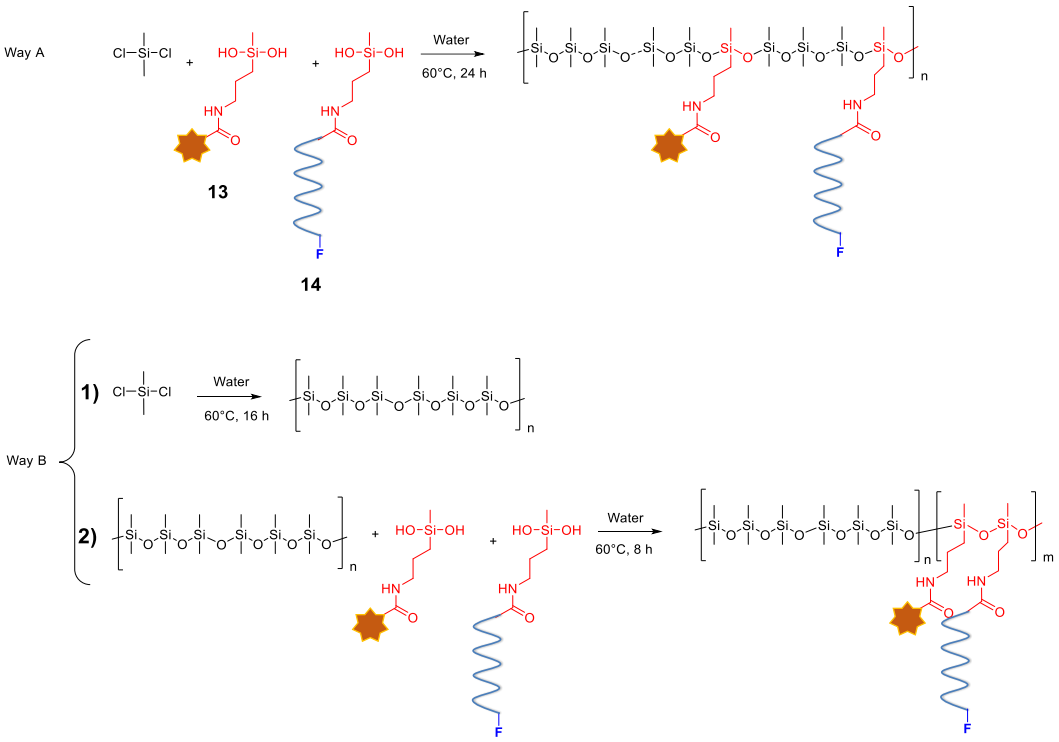

*Figure 113. Copolymerization of dichlorodimethylsilane with silylated PEG macromonomer **14**, fluorescein monomer **13** by two different ways: A) statistical copolymerization; B) block copolymerization.*

The influence of the polymerization strategy was determined by GPC and ^{19}F NMR quantification. This quantification would decipher which method gives the highest incorporation of PEG macromonomer closest to the theoretical molar%, in the functional PDMS chain. The quantification of PEG amount in the PEG-PDMS has also been done with ^{1}H-NMR. To do so, peaks due to PEG chains, two protons of two CH_2 function at 3.35 and 3.55 ppm on ^{1}H NMR, were integrated and compared to the integration of the peak at 0 ppm due to the three protons on CH_3-Si-O signal (Figure 114). The ratio between this two integration is then compared to the theoretical ratio (from the theoretical mol% of compound **14**) and so the experimental mol% of this compound is obtained.

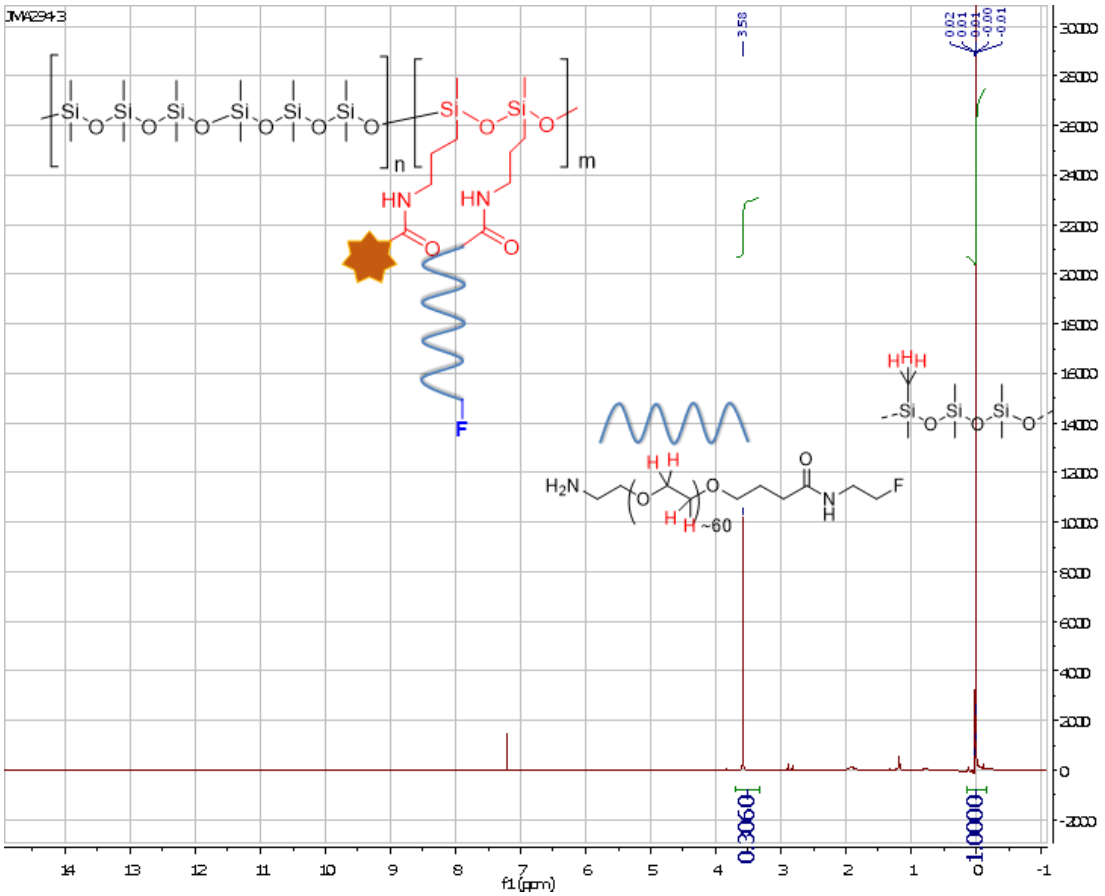

*Figure 114. ^{1}H NMR spectrum of **$P_{294\text{-}B}$** and PEG mol% quantification.*

At the same time, GPC was performed on each polymer which proved to be soluble in chloroform. As previously, GPC was operated in chloroform and the resulting chromatograms were compared to PDMS standards curves obtained from commercial PDMS with precise molecular mass. It is important to point out that the use of PDMS standards has its limits: it is adapted for slightly modified PDMS but is certainly less accurate when the PDMS modifications differs too much from pristine PDMS.

The overall yield of the syntheses of polymers was difficult to obtain due to the small quantity synthesized and the high loss during washing and drying with $MgSO_4$ (approximatively 50 % recovered). Indeed, and as expected theses polymers proved to be amphiphilic, and were more difficult to isolate from the aqueous phase than PDMS. When we skipped the drying step on $MgSO_4$, the yield was still not possible to determine, due, this time, to the presence of water. We could approximate the yield around at least 50% thanks to the quantity recovered after every wahsing. To get a reliable idea of the yield, the polymerizations should be scaled-up. At this point of the work, we focused our attention on the determination of the optimal percentage of PEG in the PEG-PDMS to get NPs. All the results obtained are reported in Table 13.

*Table 13. Characterization of macromonomer **13** and **14** containing PDMS.*

Samples	Theoretical	Experimental mol% [a]		Experimental mol% [b]		Mw (kDa)[c]	
	mol%	Way A	Way B	Way A	Way B	Way A	Way B
P_{293}: Fluorescein-PEG-PDMS	1	1.92	0.80	0.48	0.34	14.0	63.9
P_{294}: Fluorescein-PEG-PDMS	0.5	1.59	0.75	0..25	0.5	15.7	51.7
P_{295}: PEG-PDMS	1	2.35	0.79	0.59	0.46	19.8	60.7

a: obtained by ^{19}F NMR
b: obtained by ^{1}H NMR
c: obtained by GPC in chloroform

As showed in Table 13, the way A (i.e. statistical polymerization in one step) gave a higher content of PEG monomer than the way B (i.e. bloc polymerization in two steps, one pot). Indeed, we obtained 1.92 mol% for **P_{293}**, and 1.59 mol% for **P_{294}** which are both above the theoretical value: 1 mol% and 0.5 mol% respectively. Of course, the overall amount of Si-PEG could not have really increased; it was the amount of DCDMS polymerized which decreased. The presence of Si-PEG monomer at the beginning of the reaction was probably disturbing the DCDMS polymerization. One explanation could be that when copolymerizing with Si-PEG, the forming polymer is staying in solution instead of getting precipitated at the surface where most of the polymerized DCDMS are. Indeed, we previously showed that DCDMS polymerized really fast (Figure 102) and the resulting insoluble PDMS floated on the top of water solution.
In comparison, the way B yielded longer polymer chains (approximatively 4 time longer) and an incorporation of PEG closest to theoretical value (0.8 mol% vs 1 mol% theoretical for **P_{293}** and 0.75mol% vs 0.5mol% theoretical for **P_{294}**). The PEG macromonomers were adding themselves quite easily at the end of an already existing PDMS chain.
The syntheses of polymers with 1 mol% of PEG were repeated without fluorescent monomer **13,** to make sure it did not alter the polymerization. As expected, the Mw obtained by GPC and the mol% of PEG determined by ^{19}F NMR were in the same range: 15.7 kDa and 2.35% for way A and 60.7 kDa and 0.79% for way B.

b. Preparation and characterization of PEG-PDMS NPs

PEG-PDMS **NP_{293}, NP_{294}, NP_{295}**, have been prepared from polymers **P_{293}, P_{294}** and **P_{295}** respectively. They have been differentiated in function of the way of polymerization, way A or B, and will be furtherly annotated **$NP_{xxx\text{-}A\ or\ B}$**. Two methods of NPs preparation have been investigated: first by Method 1 (II.b), solubilization in THF (10 mg/50 µL) and then nanoprecipitation in water to get a 5 mg/mL final concentration). Alternatively, we tested a direct nanoprecipitation of the polymer into water with the help of sonication for 5min (Method 2, II.b) with the same final concentration: 5 mg/mL. Noteworthy this method of preparation was not possible with full PDMS polymers and yielded insoluble material on the top of the aqueous media. In contrast, the hydrophilicity of PEG chains allowed the dispersion of the PEG-PDMS polymers and the formation of particles.

Table 14. Size measurement by DLS of NPs formed by methods 1 or 2 (both at 5 mg/mL) and from two ways of polymerization of the PEG-PDMS (way A or B).

Samples	Theoretical PEG mol%	NPs size (in nm)[a]			
		Method 1		Method 2	
		Population 1	Population 2	Population 1	Population 2
$NP_{293\text{-}A}$	1	157	467 to 933	134	851
$NP_{293\text{-}B}$	1	141	676	128	977
$NP_{294\text{-}A}$	0.5	134	562	147 and 281	776
$NP_{294\text{-}B}$	0.5	154	933	134	851
$NP_{295\text{-}A}$	1	162	977	147	323
$NP_{295\text{-}B}$	1	112	513	154	708

a: determined by DLS

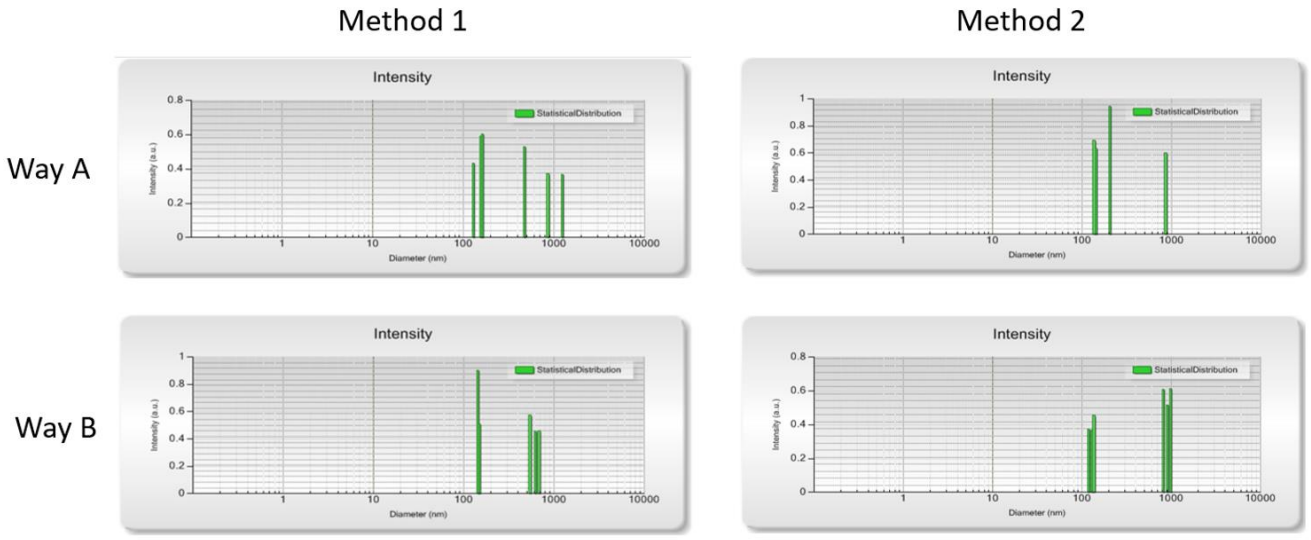

Figure 115. DLS measurement in intensity of P_{293} (1mol% of PEG) obtained by two ways of polymerization (A and B) and two methods of preparation (1 and 2)

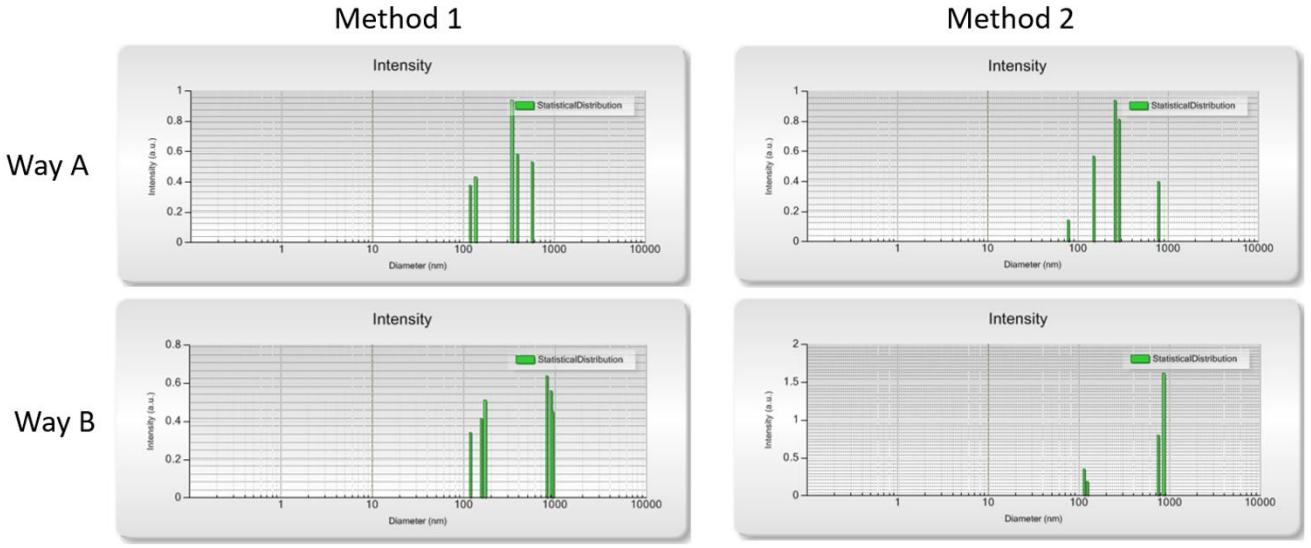

Figure 116. DLS measurement in intensity of P_{294} (0.5 mol% of PEG) obtained by two ways of polymerization (A and B) and two methods of preparation (1 and 2)

Influence of the mol% of PEG

DLS analyses of **P_{293}** and **P_{294}** (prepared with 1 mol% and 0.5 mol%. of PEG, respectively) showed that two populations are still present (at ~140 nm and ~900 nm)(Figure 115 and Figure 116). Population 2 was big enough to be filtered, over a 0.45 µm H-PTFE filter.

Influence of the method of preparation

Noteworthy, particles obtained by method 2 displayed a narrower polydispersity for each population, except for one sample: **$P_{294\text{-}A}$**. This method was favoring the 130 nm population which was the most interesting for biological assays. In addition, the method 2 is simpler and avoid the use of organic solvent.

Influence of the concentration

To limit the occurrence of population 2 in PEG-PDMS NPs which probably resulted from aggregation, the concentration was decreased to 1mg/mL instead of 5 mg/mL. Indeed, the 5 mg/mL solution is a little turbid, so maybe too concentrated (Figure 118). Once the concentration decreased to 1 mg/mL, the population of bigger particles was not decreasing, but the solution was limpid and the two populations were narrower according to the DLS analysis (Figure 117).

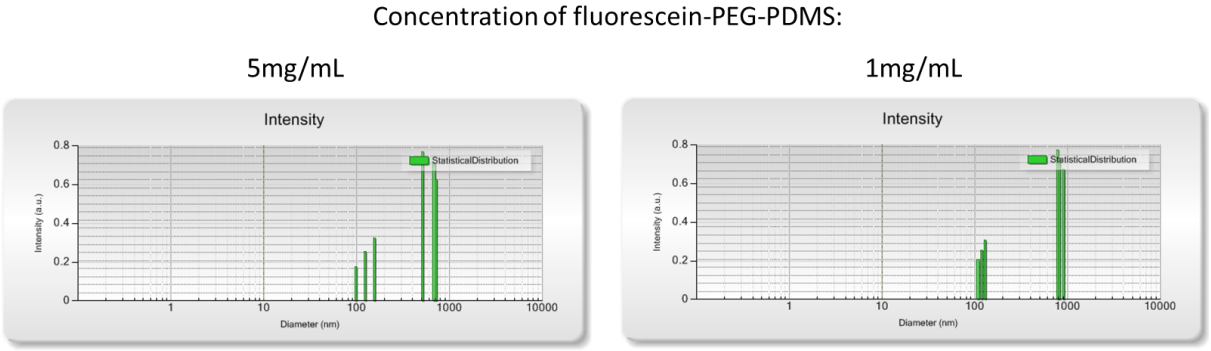

*Figure 117. Comparison of **$NP_{295\text{-}B}$**, at two concentrations and by method 2, by DLS measurement in intensity*

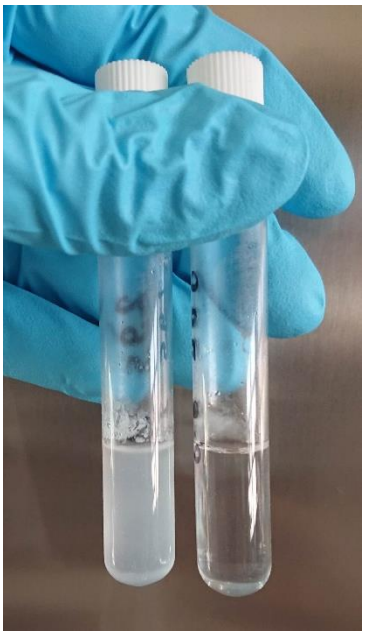

*Figure 118. Picture of **$NP_{295\text{-}B}$** at 5 mg/mL (left) and 1 mg/mL (right) in hemolysis tubes.*

Influence of the concentration: one-pot polymerization / NP formation

As a control experiment, we also performed a one-pot polymerization / NP formation at 1mg/ml. Indeed, the polymerization was normally performed at 40mg/mL of PEG-PDMS in water, which was too high to be able to form NPs. We copolymerized 1 mol% of compound **14** with DCDMS (introduced at the same time, way A) to get a final concentration of 1 mg/mL (**P_{342}**). Noteworthy, after 16 hours of reaction, the medium remained limpid. The polymerization solution was then filtrated and analyzed by Nanoparticle Tracking Analysis (NTA) to get the size and the number of NPs.
NTA is based on a microscope lens combined to a laser and a camera that films the circulating solution thanks to a fixed flow. Then a tracking software is analyzing the NPs, giving their size and number in a given volume, thus enabling to calculate the concentration. This method is adapted to monodispersed NPs with a size from 10 to 1000 nm approximatively. To give accurate values, the concentration of the NPs has to be around 10^8 NPs/mL.

Interstingly, NTA analysis of **P_{342}** showed that NPs were directly formed during the polymerization and with a average size of 96.1 nm, comparable to **$NP_{295\text{-}B}$** obtained by two steps method (Figure 119). Despite being attractive and simple, this one pot method was not be keep for the next syntheses since no prior characterization of the polymer can be done. Indeed NPs were obtained in a dilute solution and would have to be concentrated and extracted to analyse the polymer afterwards whihch would have complicated our study. Nevertheless, we showed that polymerization in water could afford directly NPs of interesting size if the concentration is low enough.

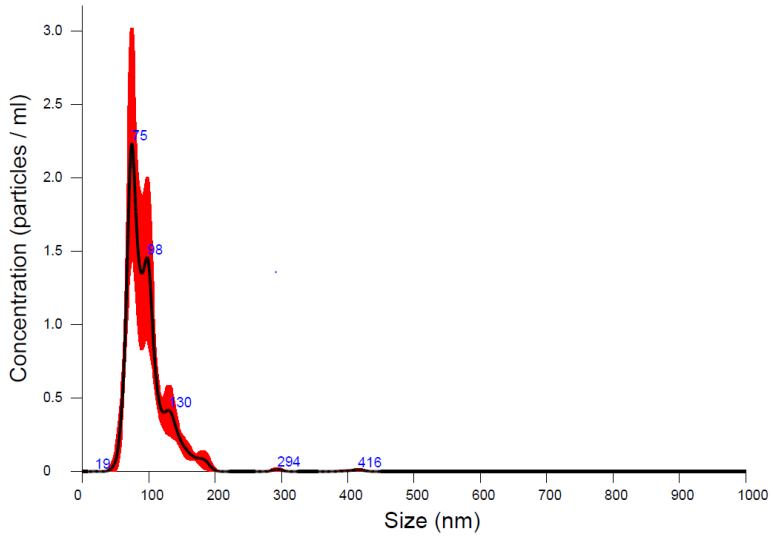

*Figure 119. NTA analysis of direct polymerization/NPs preparation: **P_{342}***

Summing up, the best option to obtain two well-defined populations and favoring small particles (population 1 centered around 130 nm) was to synthesize the polymer by the way B (diblock strategy) and to disperse it by the method 2, directly into water. Filtration on a 0.45 µm H-PTFE filter removed the population 2 of sample (<450 nm) to recover only the population 1 of small NPs (Figure 120).

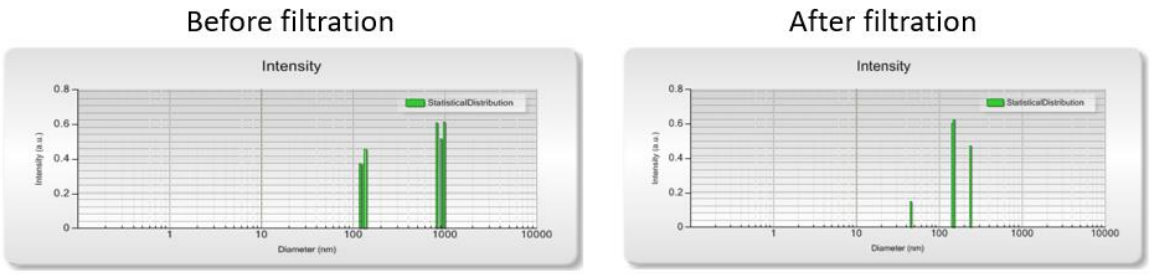

Figure 120. Comparison of $NP_{293\text{-}B}$, before and after filtration with a 0.45µm H-PTFE filter, by DLS measurement in intensity.

Determination of the NPs concentration

It is interesting to estimate the number of polymer chains which formed one NP, in particular to have an idea about the number of bioactive compounds displayed by each single particle in biological assays. To calculate that, it is necessary to know the number of NPs in solution. Indeed, dividing the known weight of polymer used for the preparation of the NPs by the number of particle would give us the weight of polymer per particle. From this value, we could deduce the number of each macromonomer constituting the NPs. DLS measurement are not able to count the NPs in solution. So we turned our attention to the NTA device. We applied this method the **$NP_{293\text{-}B}$**. We optimized a protocol in order to be able to get a precise weight of polymer involved in the formation of NPs, event after filtration.

We used a 0.94 mg/mL of **$P_{293\text{-}B}$** to prepare NPs. NTA gave a **$NP_{293\text{-}B}$** concentration of 5.6 10^8 NPs/mL, which means that each NPs is weighting $1.7*10^{-9}$ mg. As the molar mass of one synthon of compound **14** is 3262 g/mol and it is incorporated in the polymer at 0.80 mol%, we can determine the w% of compound **14** in the polymer: it represents 25 w% of the polymer. Then, we can calculate mg_{PEG}/NPs: $0.25*1.7*10^{-9}$ mg=$4.2*10^{-10}$mg of PEG/NPs. From this results, the mole quantity of PEG/NPs is extracted: $1.2*10^{-13}$ $mmol_{PEG}$/NPs and finally, by the Avogadro number, we can have the number of PEG moiety by NPs: $7.4*10^7$ PEG moieties by NPs.
The same calculation for the fluorescein, compound **13** can be done and gives $9*10^6$ fluorescein moieties by NPs.
In the same idea, as the Mn of the polymer is 26372 Da (obtained by chloroform GPC), we can deduce that there is $6.4*10^{-17}$ mol of polymer per NPs and so approximatively $3.8*10^7$ polymer chain per NPs. This means that there are approximatively two chains of PEG par chain of polymer.

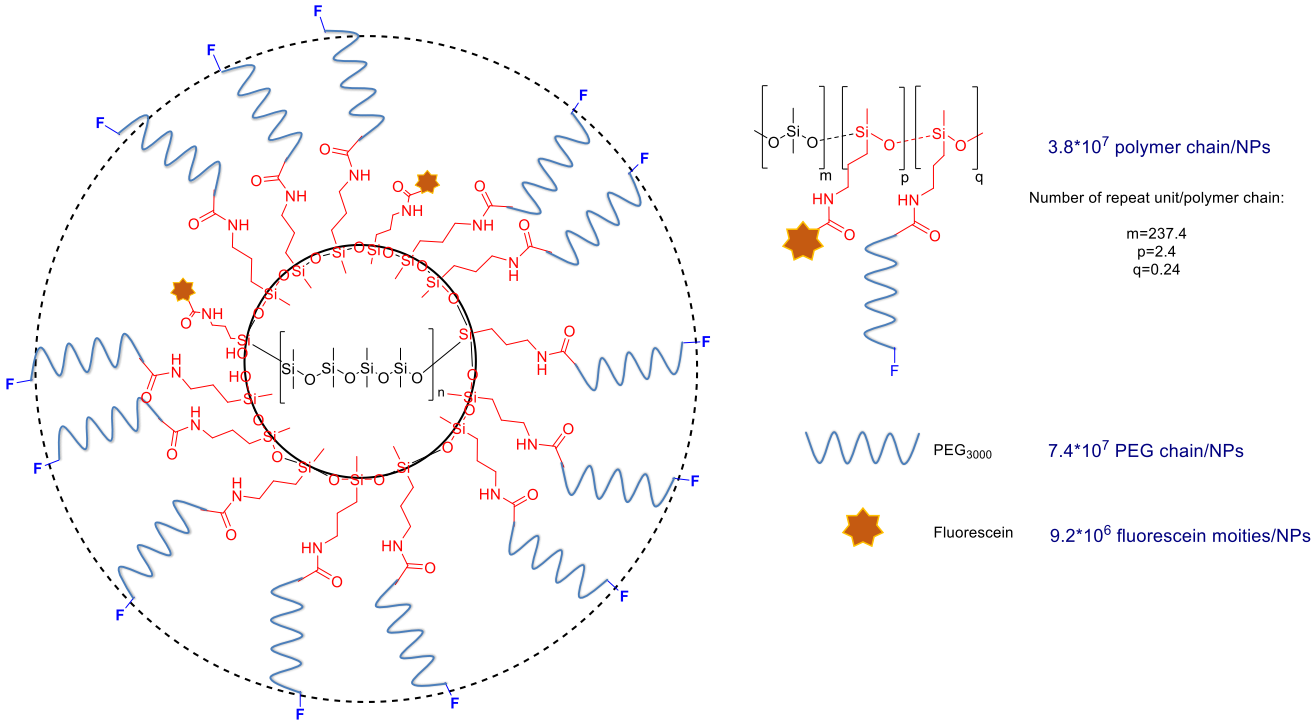

Figure 121. Schematic representation of the organization of Fluorescein-PEG-PDMS NPs.

IV. Synthesis cRGD PEG-PDMS NPs

For the preparation of PDMS NPs, we fixed the quantity of compound **14** (Si-PEG_{3000}-F macromonomer) to 1 mol%. The next step was the integration of an active biomolecule to get biological properties. As a first example, we chose a silylated analogue of the cyclic RGD peptide (noted cRGD). The main steps of the synthesis of this hybrid macromonomer were detailed in chapter 3 as well as its mode of action regarding its binding to the integrin $\alpha_v\beta_3$ receptors, over expressed on cancer cells surface.

a. Design and synthesis of hybrid cRGD macromonomer

Different geometries could be considered to position the ligand on the polymer chain. If we had opted for the direct silylation of c[RGDfK] via the side chain of the Lysine residue, the ligand would have been placed close to the backbone. We hypothesized that in this situation, the pendant PEG_{3000} chains used for the NPs formation (~160 Å), could mask it, preventing it to recognize the receptors.

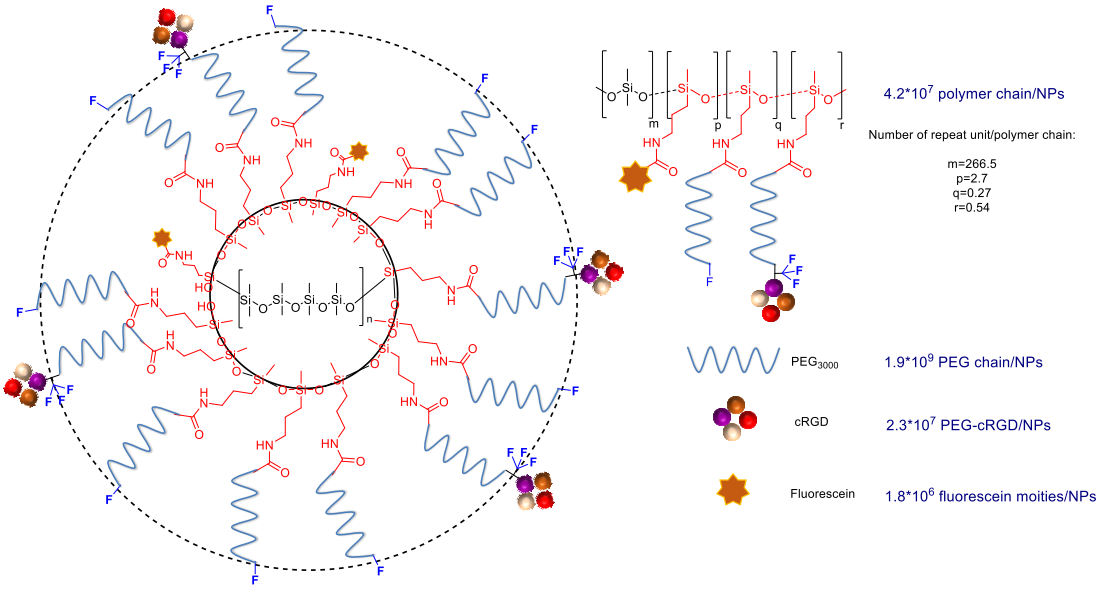

Figure 122. Schematic representation of the Fluorescein-cRGD-PEG-PDMS NPs.

Consequently, we placed the cRGD ligand at the end of PEG_{3000} chain to keep its availability for the cells receptors (compound **6,** Figure 123). As a purpose of quantification by ^{19}F NMR, we also insert a 3,3,3-trifluoro-alanine as a spacer between the PEG chain and the cRGD. Trifluoro alanine gives a different signal (singlet at -64 ppm) compared to the fluorethylamine coupled at the end of PEG_{3000} **14** (singlet at -131 ppm). So, two different peaks will be detected in the ^{19}F NMR spectra, allowing absolute quantification of each monomer in the same polymer chain. The synthesis of compound **6** is detailed in chapter 3.

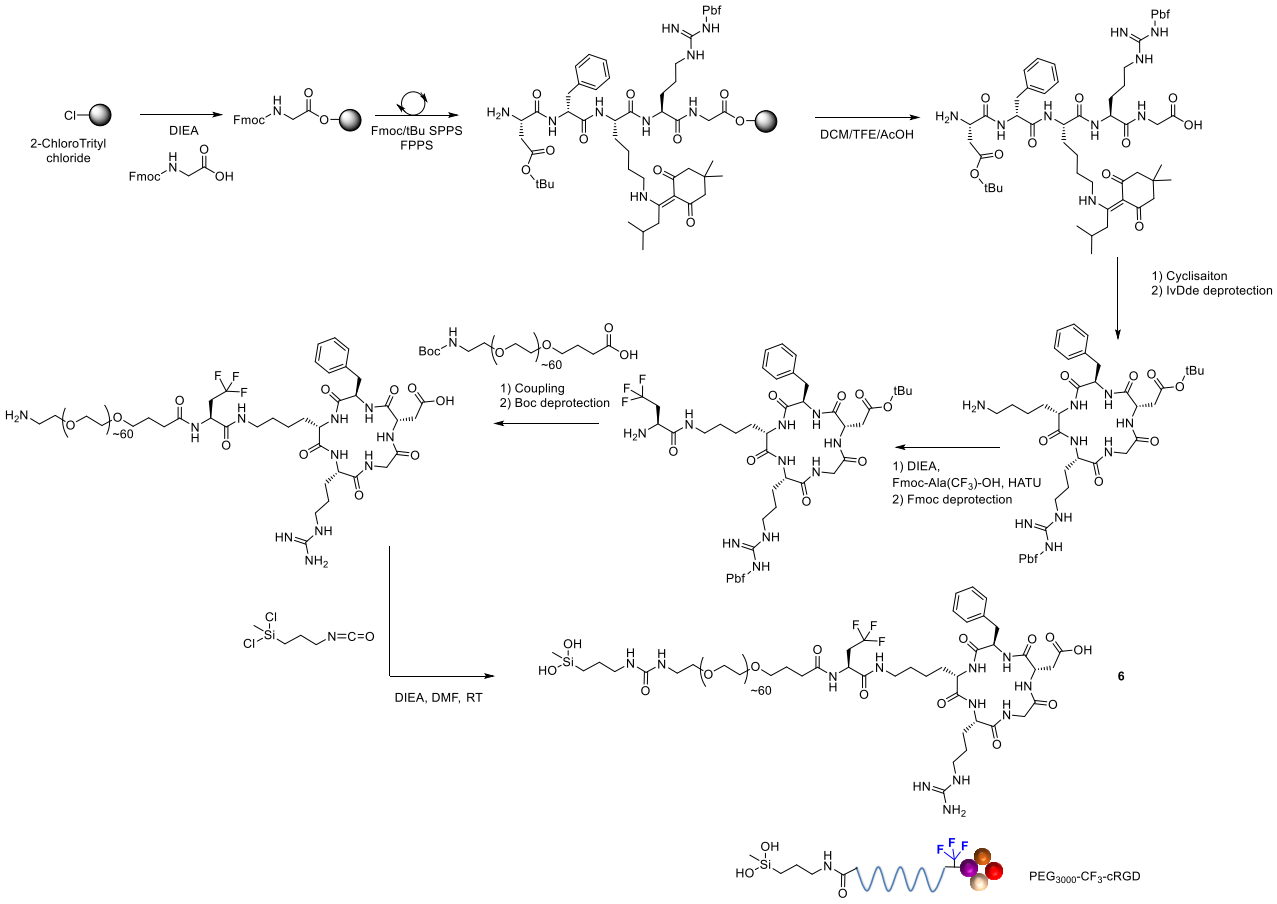

*Figure 123. Synthesis of macromonomer **6**, Si-PEG-CF_3-cRGD.*

b. Synthesis and characterization of fluorescein-cRGD-PEG-PDMS

Macromonomer **6**, Si-PEG-CF_3-cRGD, was copolymerized with hybrid PEG **14**, hybrid fluorescein **13** and DCDMS (Figure 124). We kept the total concentration of PEGylated monomers to 1 mol%. Three different polymers were prepared: $\mathbf{P_{296}}$, $\mathbf{P_{347}}$ and $\mathbf{P_{352}}$ with different quantities of **6** in the polymer. $\mathbf{P_{296}}$ contained only 0.2 mol% of macromonomer **6**, and 0.8 mol% of macromonomer **14**. On the other hand, $\mathbf{P_{347}}$ was prepared only with 1mol% of macromonomer **6**. At last, $\mathbf{P_{352}}$ was prepared with 0.5 mol% of both macromonomer **6** and **14**. The synthesis was done followig way A, all monomers added in the same time and let polymerized in water for 24h at 60 °C in order to get the highest integration of each macromonomers in the resulting PDMS. The resulst are presented in Table 15.

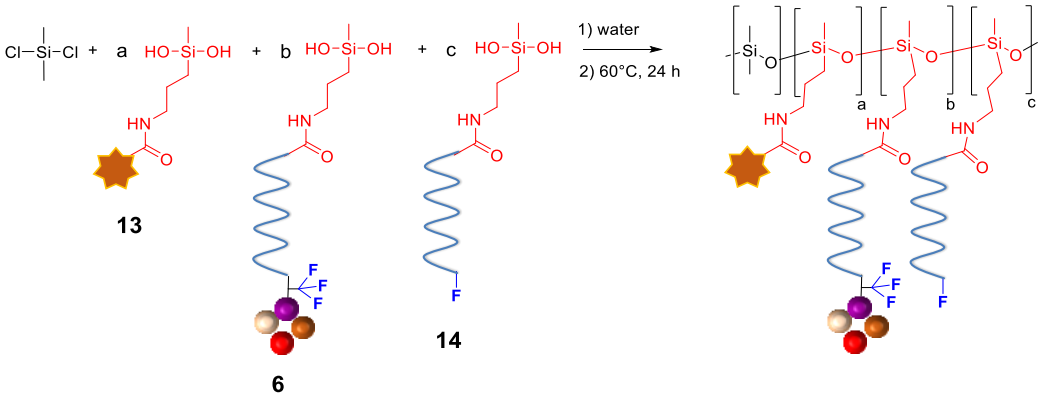

*Figure 124. Copolymerization of DCDMS with macromonomers **6** and **14** and compound **13**.*

Table 15. Characterization of fluorescein-cRGD-PEG-PDMS.

Samples	Si-PEG-F mol%		Si-PEG-CF_3-cRGD mol%		Global Si-PEG mol%		Mw (in kDa)[c]
	Theoretical	Experimental[a]	Theoretical	Experimental[a]	Theoretical	Experimental[b]	
$P_{293\text{-}A}$: PEG-PDMS	1	1.92	0	0	1	0.48	14.0
$P_{296\text{-}A}$: cRGD-PEG-PDMS	0.8	1.67	0.2	n.d.	1	0.42	29.7
$P_{352\text{-}A}$: cRGD-PEG-PDMS	0.5	0.38	0.5	0.12	1	0.72	43.6
$P_{347\text{-}A}$: cRGD-PEG-PDMS	0	0	1	0.76	1	0.81	98.7

a: Determined by ^{19}F NMR
b: obtained by ^{1}H NMR
c: Determined by chloroform GPC
n.d.: Non determined

The polymers were characterized by NMR (^{19}F and ^{1}H) and by GPC. As expected, we got a high percentage of incorporation of the PEG macromonomer in $\mathbf{P_{296\text{-}A}}$: 1.67 mol% instead of 0.8 mol% theoretically. This correlated with the results obtained with $\mathbf{P_{293}}$ and $\mathbf{P_{294}}$ synthesized by the way A.
Noteworthy, the Mw of $\mathbf{P_{296\text{-}A}}$ was 29.7 kDa compared to 63.9 kDa for $\mathbf{P_{293\text{-}B}}$ obtained exclusively with 1 mol% of **14**. It was still higher than the Mw of $\mathbf{P_{252\text{-}2}}$ (14.8 kDa for 100 % PDMS) obtained by the same method. Once more,

these values of Mw were estimated by GPC, using as standard a curve obtained from pristine PDMS. Our polymers should have a very similar behavior in the GPC column.
If we assumed that the Mw are relevant, it would mean that there is ~0.54 cRGD in average on each polymer chain. Indeed, the average molar mass of one repeat unit in **P_{296}** is 110 g/mol calculated from the pondered contribution of each macromonomer. Knowing that the polymer had a Mw=29.7 kDa, there is ~270 SiO units in the polymer and so, 0.2 % of 140 lead to ~0.54 cRGD units.

c. Preparation and characterization of fluorescein-cRGD-PEG-PDMS NPs

The preparation of the **$NP_{296\text{-}A}$**, **$NP_{347\text{-}A}$** and **$NP_{352\text{-}A}$** done following the method 2: direct nanoprecipitation in water at 1mg/mL, followed by 5min sonication and filtration with 0.45 µm H-PTFE filter. The results are presented in Table 16.

Table 16. Size measurement by DLS, NTA and zeta potential of Fluorescein-cRGD-PEG-PDMS NPs.

Samples	Theoretical Si-PEG-F mol%	Theoretical Si-PEG-CF_3-cRGD mol%	NPs size by DLS (in nm)		NPs size by NTA (in nm)	Zeta potential (in mV)
			Population 1	Population 2		
$NP_{293\text{-}A}$	1	0	134	851	69.2	-12
$NP_{296\text{-}A}$	0.8	0.2	162	776	75.4	-5
$NP_{352\text{-}A}$	0.5	0.5	102		77.7	0
$NP_{347\text{-}A}$	0	1	180		93.7	-3

The DLS analyses showed two populations for each sample, in the same range than the one obtained with **$NP_{293\text{-}A}$**: population 1 around at 170 nm and a population 2 above than 700 nm. The incorporation of compound **6**, PEG-CF_3-cRGD, in the PEG-PDMS did not seem to disturb the formation of NPs. These results were also validated by NTA.
As expected, the size calculated by NTA were in each case smaller than the one obtained by DLS: for example, the diameter of **$NP_{293\text{-}A}$** was 69.2nm by NTA instead of 134 nm by DLS. It is worth noting here that a slight increase of the NPs size was observed when more PEG-CF_3-cRGD was incorporated in the polymer: from 75.4 nm to 93.7 nm for 0.2 to 1mol % of compound **6**, respectively.
We also analyzed this sample by Transmission Electron Microscopy (TEM). Thus, some drop of the solution of **$NP_{296\text{-}A}$** have been disposed over a TEM grid and then let drying. The TEM image gives NPs and an idea of their size: from 60 to 80 nm plus one at 260 nm approximatively. This corresponds to the NTA analysis results (75.4 nm).

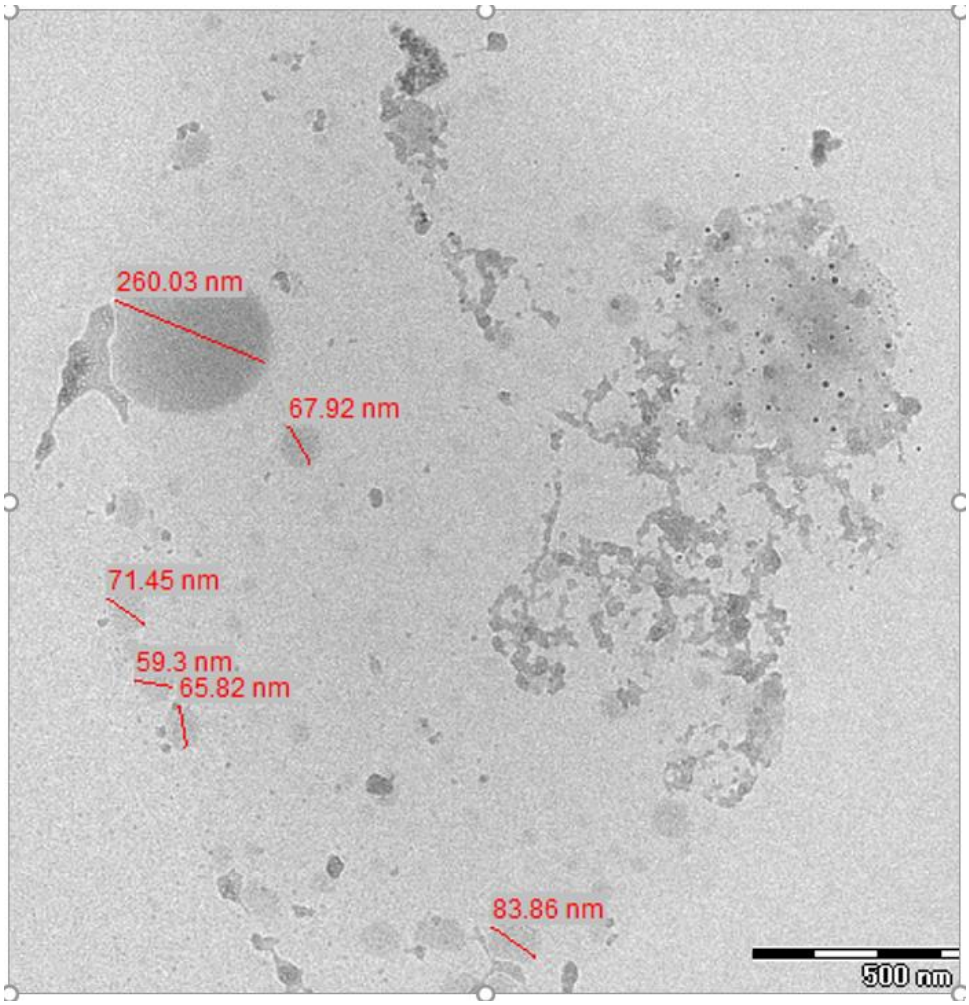

Figure 125. TEM image of ***NP$_{296-A}$***

By the same calculation used with **NP$_{293-A}$**, the NTA results enabled us to determine the quantity of PEG, fluorescein, cRGD moieties and polymer chain par NPs: $1.9*10^8$ PEG moieties per NPs, $9.6*10^7$ fluorescein moieties per NPs, $2.3*10^7$ cRGD moieties per NPs and $4.2*10^7$ polymer chain per NPs (Figure 122). There is also approximatively 5 compounds **14** and 0.5 compound **6** par polymer chain.
We could also deduce the concentration of cRGD: we obtained $9.0*10^{-3}$ mmol/L of cRGD in the solution.

The zeta potential of all samples has also been measured by a Nanosizer apparatus with an adapted cuvette: wearing two electrodes in contact with the solution. Except for **NP$_{352}$**, the zeta potential decreased with the increase of PEG-CF_3-cRGD in the NP: from -12.0 mV to -2.6 mV for 0 to 1 mol% of compound **6** respectively. This may be due to the presence of the peptide ligand containing one arginine residue which brought some positive charges able to neutralize the negative charges already present on the PEG-PDMS NPs.

d. Preliminary binding assays

Fluorescence activated cell-sorting (FACS) is a device highly used in biology and biochemistry to determine the binding affinity of fluorescent NPs towards cells. It is made of a flow cytometry device that counts and characterize cells or NPs in function of their fluorescence or optic properties (Figure 126).[371] The affinity between cells and NPs results in a modification of their fluorescence, for example, and so the FACS is able to highlight this

difference. FACS devices are able to analyze hundreds of fluorescent NPs at the same time and sort them in several sub populations.

FACS analysis were performed on **NP_{296}** by the team of Dr. Jean-Luc Coll: "Cancer targets and Experimental therapeutics" at Institute of Advanced Bioscience (IAB) in Grenoble. This assay should highlight the binding properties of the cRGD-containing NPs. Non functionalized 1 mol% PEG-PDMS NPs, **$NP_{293\text{-}A}$**, were used as negative control.

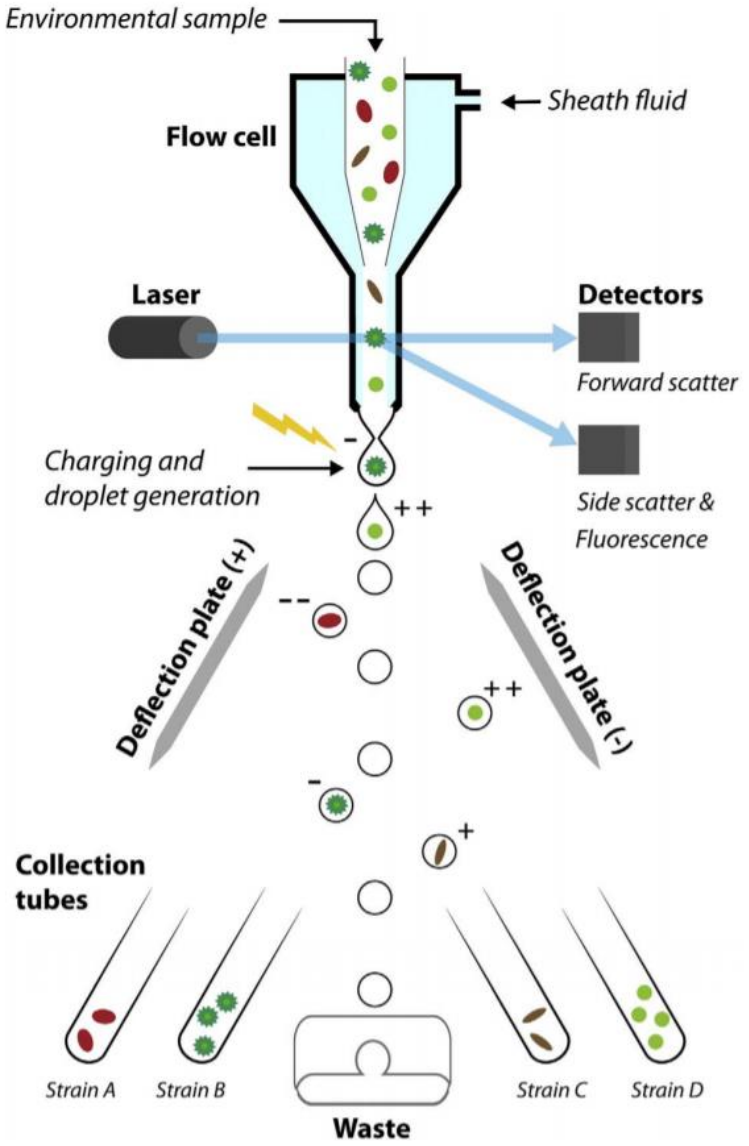

Figure 126. General scheme of the principle of FACS.[371]

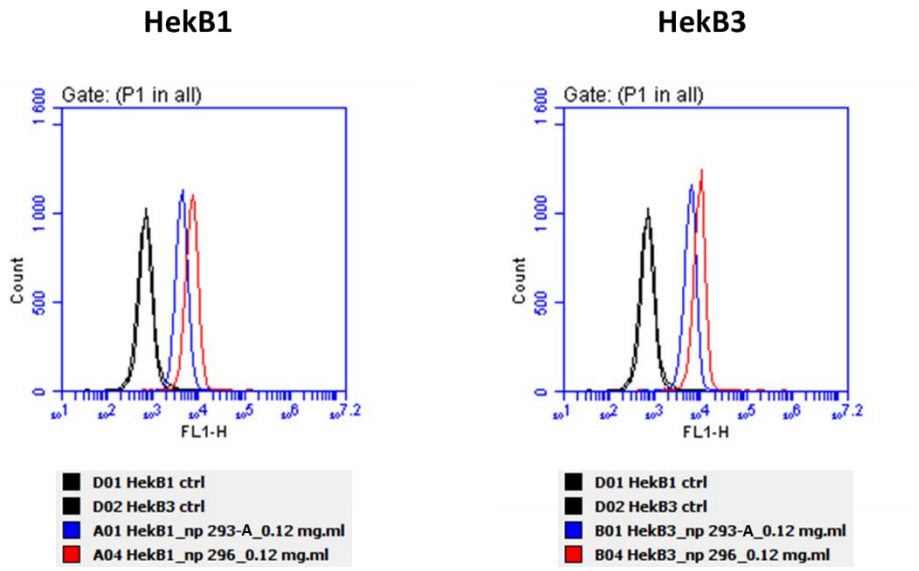

Figure 127. FACS results on $NP_{293\text{-}A}$ and NP_{296} on two cells lines: HeKβ1 and Hekβ3 (overexpressing $\alpha_v\beta_3$ integrin receptor) after 30min of incubation at 37 °C, and at 12 mg/mL of NPs.

Both types of NPs were incubated with two different cell lines: Hekβ_1 and Hekβ_3. The second cell line overexpresses the integrin specific to the cRGD peptide, $\alpha_v\beta_3$. The fluorescence intensity is then measured by the FACS in order to determine the bonding affinity between the NPs and the cell line. If the bonding of the NPs is specific to the integrin, a difference should be visible between the two assays.

Unfortunately, we were not able to see any significant difference between **NP_{296}** and **$NP_{293\text{-}A}$** (Figure 127). Indeed, both type of NPs seems to bind with the same affinity with the cells line: if one of the two type of NPs were more selective towards the cell line, the peak associated in the FACS graph results would be displaced to the right. However, in this case, the two peaks, blue and red, are approximatively at the same intensity whether the NPs is wearing cRGD or not, and whether the cell lines are overexpressing $\alpha_v\beta_3$ or not. The bonding is then not specific and the NPs are not specific either.

Several explanations could be proposed. The PEG chain could be arranged into so called 'mushroom' conformation, burying the cRDG ligand within the polymer chains and masking for the receptors. It cannot also exclude that the core of the NPs may not be composed of PDMS only but also PEG, and the peptide ligands could be inside the NPs rather than at the corona. Finally, the amount of this bioactive monomer is maybe too low for all the NPs to get enough cRDG.
Additional FACS experiments will be performed on **NP_{347}**, which contains a higher quantity of cRGD (0.76 mol% of compound **6** according to ^{29}Si NMR). We will know if our hypothesis about the too low amount of binding ligand could be comforted.

V. Synthesis of drug-based PEG-PDMS NPs

Our ultimate aim was to obtain multifunctional NPs targeting cells but also able to deliver a drug at the appropriate site. These particles could be defined as smart drug delivery system (SDDS) combining several properties including targeting, loading of the drug, crossing of membrane cell and release of the cargo.
The first point, targeting, is theoretically given by the size of the particle (EPR effect) but also the presence of ligands.

The crossing through the membrane cell could be done by many possibilities. Two mains pathways can be distinguished: direct penetration or endocytic pathways (Figure 128). The direct penetration followed three methods: diffusion through the membrane, permeation helped by ligands such as cell penetrating peptide[185,372–374] or pore formation on the membrane. The endocytic pathway is creating an endosome when the NPs is passing through the membrane that will have to be degradated latter.

The NPs were interacting with the membrane and then taken up by the cell by different manners in function of the receptors targeted by the NPs.

In our case, we may hypothesize that the PDMS NPs will follow an endocytotic pathway, in particular the Clathrin dependent way since we disposed ligand with affinity to the cell membrane receptors.

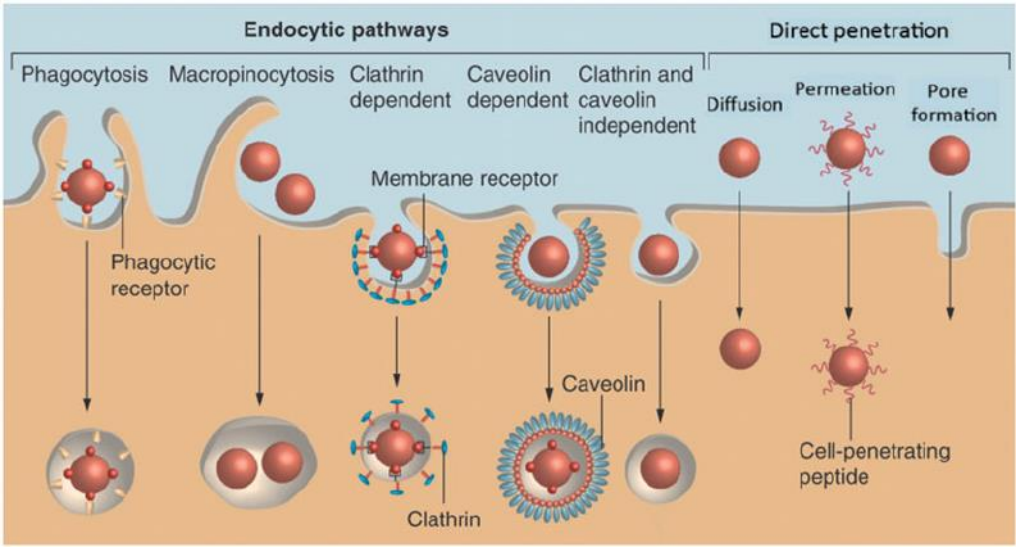

Figure 128. Different possibility for a NP to cross a cell membrane.[375]

Once the targeting ability fixed, the drug has to be loaded in the NPs. Covalent immobilization relies on a chemical bound between the drug and a part of the NP while non-covalent method is based on interactions e.g. hydrophobic,[376] electrostatic,[377] hydrogen bonding[378] or steric immobilization.[379]

For our project, we chose a covalent system which we found easier to implement with a bottom up approach. The drug will be attached covalently to the polymer which will form the NPs afterwards. The main advantage is that the drug will not leak from the particle during its circulation. However, a dedicated cleavable linker has to be designed to release the drug when necessary. The stimuli responsive linker has to be used for the attachment of the drug. It can be triggered by the acidic pH of the cytoplasm (pH=5.5), by the presence of a reducer or by UV light activation. This kind of activation should preferentially happen inside the cells to get the drug released in the right place and to avoid any premature leakage. If the drug is a pro-drug, the active moiety can be released from the pro-drug inside the cells, thus avoiding the use of a cleavable linker (e.g. Temozolomide).[380,381]

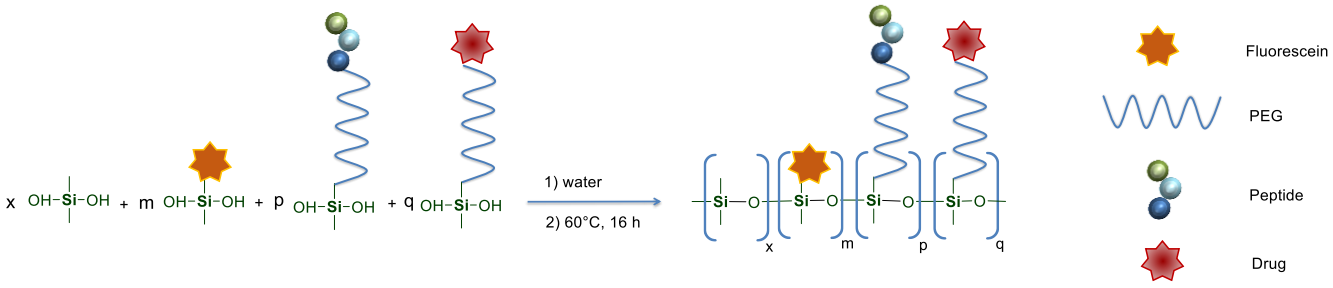

Figure 129. Four components, drug-containing functional PDMS polymerization.

a. Description of drug-linker associations used

Several drugs were silylated in order to incorporate them inside the PDMS polymer which will form the NPs. Their syntheses were described in Chapter 3.

Some of them did not need any active linker, it is the case of Temozolomide (TMZ). TMZ is a prodrug, it is not active before the administration and turns into a biologically active molecule by a chemical transformation. Indeed, this drug undergoes hydrolysis inside the cells triggered by the higher pH (pH>7). Then a highly biologically active compound is released: the methyl diazonium methylating agent (Figure 74).[283] This type a drug are prodrugs, they are not active before the administration, and then by a chemical transformation, it turns into a biologically active molecule. As the cleavage of the active part of the TMZ is due to pH variation, the drug did not have to be placed at the extremity of a PEG chain and did not need either a cleavable linker. The drug was modified in order to react with the dichloromethysilanepropyl isocyanate leading to the macromonomer compound **7** (Figure 130).

The case of methotrexate (MTX) is different, first because the MTX has a dual activity: it is both a ligand and an active drug. Its ligand properties imposed that we placed it at the end of a PEG chain, like we did for hybrid cRGD. Indeed, it had to be available to target folate receptor and especially the folate transporter (RFC1) a the surface of cancer cells helping the NPs to go through the membrane.[287] Then, once inside the cells, we expected that MTX would be transform into the polyglutamate analog and so be active intracellularly. Consequently, as TMZ we made the hypothesis that TMX would not need any cleavable linker. The MTX was then coupled with PEG_{3000} as linker and silylated to lead to compound **8**.

On the contrary, a cleavable linker was required for camptothecin (CPT). Indeed, the unmodified drug is required to exert its activity inside the cell. We chose a linker sensitive to reductive conditions based on a disulfide bond. This linker, bis(2-hydroxyethyl)disulfide, is cleaved by reduction, mediated by glutathione for example, and then undergoes a rearrangement which releases unmodified CPT (

Figure 131).[198] The CPT does not have any ligand properties so PEG chain are not needed. Consequently, a cleavable linker was coupled to the CPT and it was silylated by isocyanatopropyl diethoxymethysilane to obtain compound **10** (Figure 130).

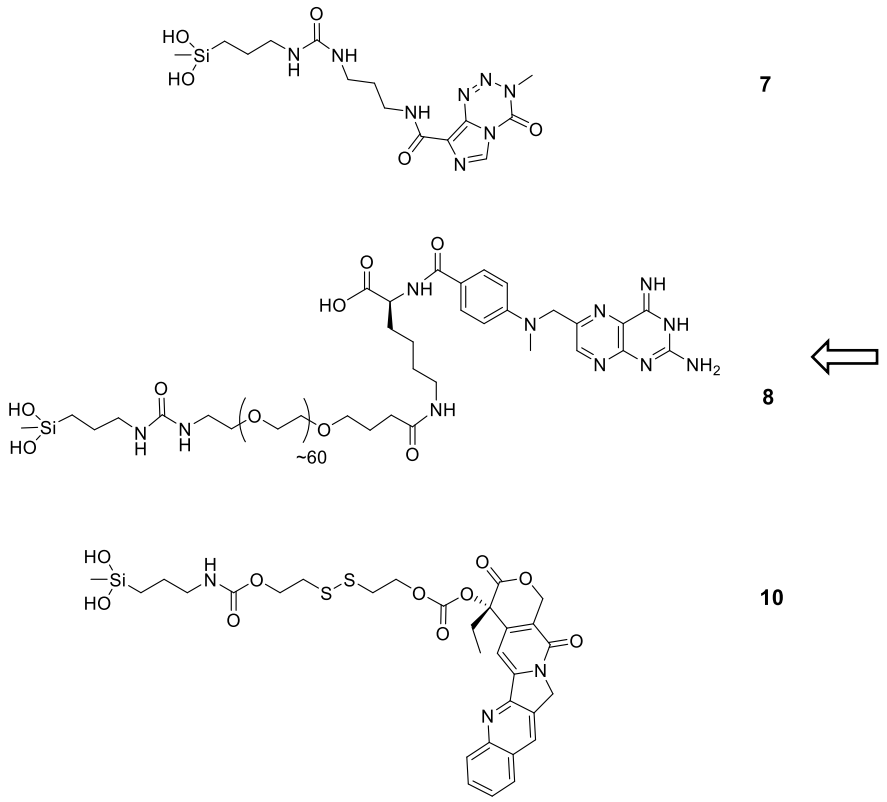

*Figure 130. Hybrid drugs macromonomer **7**, **8** and **10**.*

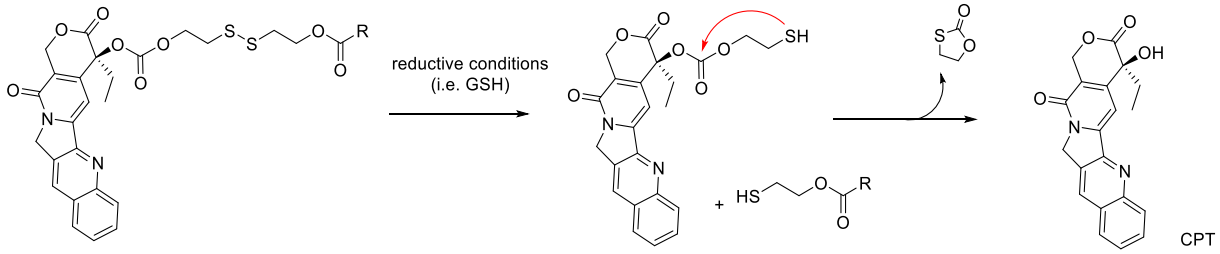

Figure 131. Release of CPT by reduction of the disulfide based linker with glutathione.

b. Synthesis and characterization of drug-containing PEG-PDMS

Once the hybrids macromonomers have been synthesized, we copolymerized them with DCDMS to get multifunctional PDMS and then to form NPs from it. As previously tested with cRGD macromonomer **6**, a total of 1 mol% of PEGylated macromonomers (combination of **6, 8 and 14**) was used for the polymerization. The other silylated drugs have not been used for the synthesis multifunctional PDMS yet. The optimization of the protocol has been done with compound **8,** and once biological assay are giving good results, the other drugs will be tested as well.

So far, four different polymers have been synthesized to perform preliminary biological assays of affinity and toxicity: a negative control with neither the ligand neither the drug (**$P_{293\text{-}A}$**), a MTX/cRGD containing PDMS (**$P_{364\text{-}A}$**), a cRGD containing PDMS (**$P_{352\text{-}A}$**) and a MTX containing PMDS (**$P_{403\text{-}A}$**) (Figure 132).

The first MTX macromonomer **8** did not wear any fluorous probe as we thought that ^{1}H NMR would be sufficient for its quantification in the multifunctional PDMS. Indeed, the quantification of macromonomer **14** and/or **6** was theoretically possible by ERETIC ^{19}F NMR and the quantification of overall PEG content (**6+8+14**) was possible by ^{1}H NMR. Thus, the mol% of macromonomer **8** could be obtained by subtracting the quantity of PEGylated

macromonomers **6** and **14** to total PEG quantity. To overcome this problem, the MTX macromonomer **9** bearing a CF_3 derivate of Phenylalanine was synthesized to be quantified by ERETIC ^{19}F RMN (Figure 133).
All the characterizations, GPC and NMR (^{1}H and ^{19}F), of the polymers were presented in Table 17.

Table 17. Characterization of multifunctional PDMS containing macromonomer 6, 8, 13 and/or 14.

Samples	Si-PEG-F mol% 14		Si-PEG-CF_3-cRGD mol% 6		Si-PEG-MTX mol% 8 or 9		Mw (in kDa)[b]
	Theoretical	Experimental[a]	Theoretical	Experimental[a]	Theoretical	Experimental[a]	
$P_{293\text{-}A}$ PEG-PDMS	1	1.92	-	-	-	-	14.0
$P_{364\text{-}A}$: MTX-cRGD -PEG-PDMS	-	-	0.5	n.d.	0.5	n.d.	34.3
$P_{352\text{-}A}$: cRGD-PEG-PDMS	0.5	0.44	0.5	0.14	-	-	43.6
$P_{403\text{-}A}$: MTX-PEG-PDMS	0.5	n.d.	-	-	0.5	n.d.	n.d.
$P_{426\text{-}A}$: MTX-Phe(CF_3)-cRGD-PEG-PDMS	-	-	0.5	0.39	0.5	0.28	n.d.

a: Determined by ^{19}F NMR
b: Determined by chloroform GPC
n.d.: Non determined

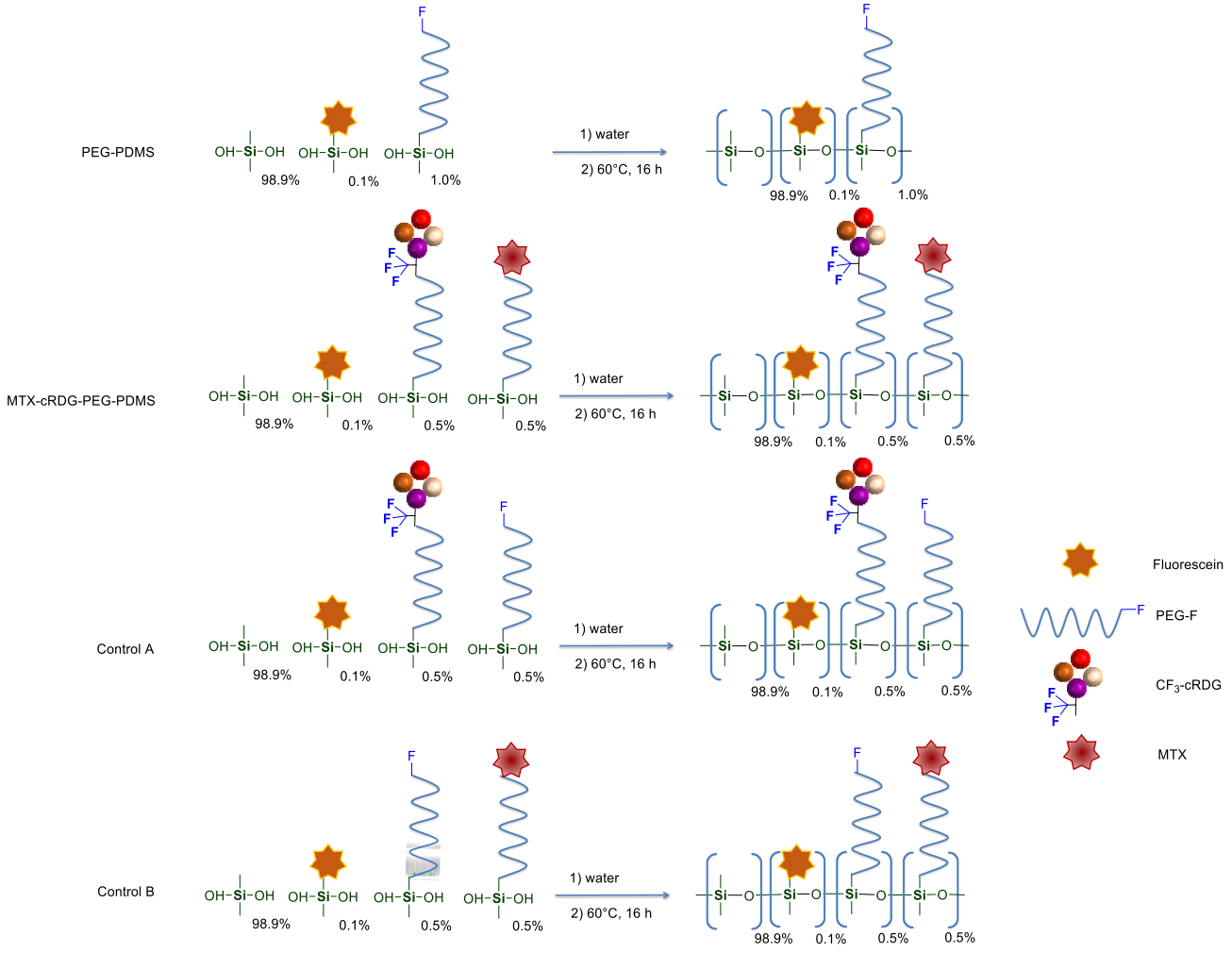

Figure 132. Schematic syntheses of MTX and cRGD containing PEG-PDMS.

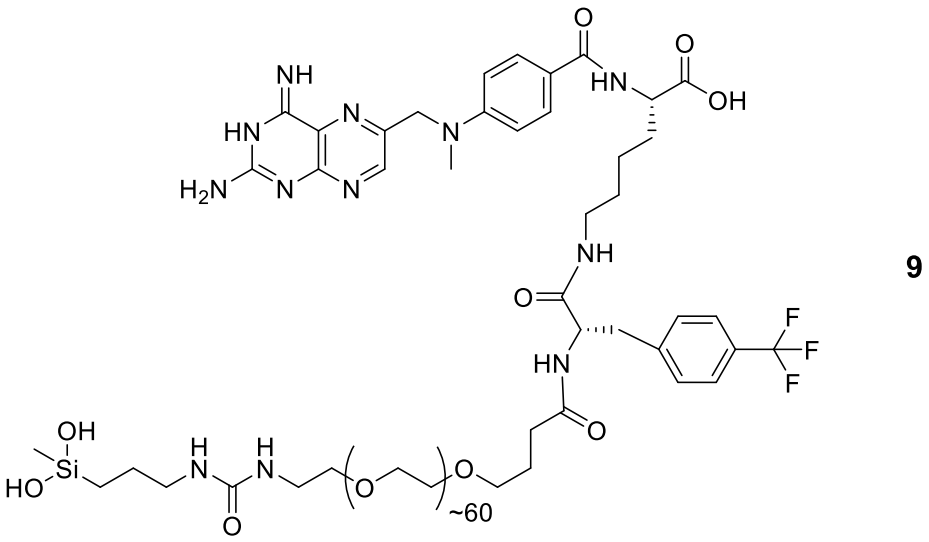

9

*Figure 133. Scheme of macromonomer **9**, Si-PEG-Phe(CF_3)-MTX.*

^{19}F NRM analyses showed that macromonomers **6** and **8** (or **9)** were incorporated in amount smaller than theoretical maximum molar quantities: 0.14 mol% of **6** instead of 0.5 mol% for $\mathbf{P_{352\text{-}A}}$; 0.39 mol% of **6** and 0.28 mol% of **9** instead of 0.5 mol% each for P_{426}. On the contrary, the mol% of **14** was quite close to the theoretical value: 0.44 mol% instead of 0.5 mol% for $\mathbf{P_{352\text{-}A}}$, and even higher for $\mathbf{P_{293\text{-}A}}$ with 1.92 mol% instead of 1 mol%. Overall, the mol% obtained were in an acceptable range, close enough to the theoretical values.
According to GPC analyses, the polymers were 2-3 times longer than simple PEG-PDMS ($\mathbf{P_{293\text{-}A}}$) with higher Mw: 34.3 kDa for $\mathbf{P_{364}}$ and 43.6 kDa for $\mathbf{P_{352\text{-}A}}$ instead of 14.0 kDa for $\mathbf{P_{293\text{-}A}}$.

c. Preparation and characterization of drug-containing PEG-PDMS NPs

The preparation of NPs from the previous multifunctional PDMS were done by method 2: direct precipitation in water at 1 mg/mL, followed by 5 min sonication and filtration with 0.45 µm H-PTFE filter.

Table 18. Size measurement by DLS and NTA, and zeta potential of drug containing PEG-PDMS NPs

Samples	Theoretical Si-PEG-F mol%	Theoretical Si-PEG-CF_3-cRGD mol%	Theoretical Si-PEG-MTX mol%	NPs size by DLS (in nm) Population 1	PDI	NPs size by NTA (in nm)	Zeta potential (in mV)
$\mathbf{NP_{293\text{-}A}}$	1	0	0	101.7	0.180	69.2	-12
$\mathbf{NP_{364\text{-}A}}$	0	0.5	0.5	160.1	0.226	110.7	0
$\mathbf{NP_{352\text{-}A}}$	0.5	0.5	0	115.6	0.212	85.3	0
$\mathbf{NP_{403\text{-}A}}$	0.5	0	0.5	136.9	0.172	115.8	0
$\mathbf{NP_{426\text{-}A}}$	0	0.5	0.5	n.d.	n.d.	n.d.	0

n.d.: Non determined

The size of the NPs was in the same range than PEG-PDMS or cRGD-PEG-PDMS NPs from 100 nm to 140 nm. It seemed that the incorporation of MTX (hybrid compounds **8** or **9**), increased the size of the NPs. This was confirmed by DLS and NTA which were in good agreement. As example, diameters determined by DLS were 160 nm and 137 nm for $\mathbf{NP_{364\text{-}A}}$ and $\mathbf{NP_{403\text{-}A}}$, containing each 0.5 mol% of **8**, *vs* 102 nm and 116 nm for $\mathbf{NP_{293\text{-}A}}$ and $\mathbf{NP_{352\text{-}A}}$, which did not contain compound **8**.
The composition of the polymers did not have an important impact of the resulting zeta potential. The only parameter influencing the potential seems to be the quantity of Si-PEG-F, compound **14.** Each NPs containing

less than 0.5 mol% of **14** have a zeta potential close to 0 mV while the PEG-PDMS, **$NP_{293\text{-}A}$**, displayed a -12.0 mV potential.

Since a filtration step was needed for the preparation of monodisperse NPs solution, we wanted to check if the final composition of the NPs was affected by the filtration. Indeed, it could have taken apart polymer chains containing silylated drugs since they are less hydrophilic. This point is really important for any biological assay: we need to make sure that the mol% of drug in NPs solution is not decreased by the filtration step. To do so, an ERETIC quantification was done before and after NPs preparation and filtration. Hopefully, the quantity of compounds **6** (PEG) and **9** (MTX) in **P_{326}** was actually higher after filtration. This can be explained by the fact that pure PDMS chain are highly hydrophobic. So if there was some pure PDMS resulting from the polymerization **P_{326}**, they were probably removed by the filtration, and consequently giving a quantity of compound **6** and **9** higher than in the original polymer relatively to the global polymer weight.

VI. Preliminary biological assays: cytotoxicity efficiency

In order to prove the activity of the drug-containing PEG-PDMS NPs, preliminary cell viability assays have been performed on cancer cells. It was the first step to determine the efficiency of these NPs as drug delivery system. Further tests would have to be done afterwards, in particular the assessment of the toxicity towards normal cells.

In this first attempt we wanted to determine the activity of the MTX-cRGD-PEG-PDMS NPs, **$NP_{364\text{-}A}$**. To make sure that the observed activity of these NPs will be due to the presence of MTX, control NPs without MTX were prepared from **P_{352}**, cRGD-PEG-PDMS (negative control). MTX is not a fully cytotoxic agent but it inhibits the proliferation of several cancer cells lines, including A375 human melanoma cell line.

The neutral red uptake (NRU) assay is based on the ability of viable cells to take up the vital dye neutral red after the 72h incubation. It penetrates the membranes of living cells by nonionic passive diffusion and concentrates in the lysosomes.[382]

$NP_{364\text{-}A}$ were assayed *in vitro* on human melanoma metastatic cancer cells A375 cells compared to free compound **8b** (MTX-Lys analog) and negative control **$NP_{352\text{-}A}$**, containing cRDG but not MTX. The inhibition of proliferation was determined after subtracting the baseline proliferation.

$NP_{364\text{-}A}$ were prepared to get a final concentration up to 292 µM of MTX moiety. The toxicity was found to be concentration-dependent after 72h. The compound **8b** and **$NP_{364\text{-}A}$** both fit the logistic regression by the activity on A375 human melanoma cell line (Figure 134). In this activity, calculations were established for the concentrations of MTX per nanoparticles and correlated to the **$NP_{364\text{-}A}$** mass concentration. Morphological investigations by light microscopy also witnessed the antiproliferative activity.

These preliminary results showed **$NP_{364\text{-}A}$** were more active than control **$NP_{352\text{-}A}$** (Figure 134). Indeed, **$NP_{364\text{-}A}$** slowed down the proliferation of cancer cells whereas **$NP_{352\text{-}A}$** did not.

Control **$NP_{352\text{-}A}$**, without MTX, did not induce any signficative growth inhibition until 97 µM of compound **14** (replacing compound **8** in the polymer composition) and their effect was comparable to the negative control group without any treatment. In addition, at the highest concentration (292 µM), MTX loaded **$NP_{364\text{-}A}$** induced 27,2% cell proliferation inhibition while control **$NP_{352\text{-}A}$** gave only 8,5 % cell proliferation inhibition.

However, when comparing free compound **8b** and **$NP_{364\text{-}A}$** at equal concentration of MTX, the free drug had an activity more than 10 times higher than the coalvently bound MTX. GI_{50} values (concentrations giving 50% of growth inhibition) were 6,077 ± 0,871 µM (n=2) and 83,69 ± 9,39 (n=2) for the free and NP-bound MTX, respectively.

Despite being very premininary, our results opened perspectives to use of the MTX-cRGD-PEG-PDMS NPs for cancer treatment.

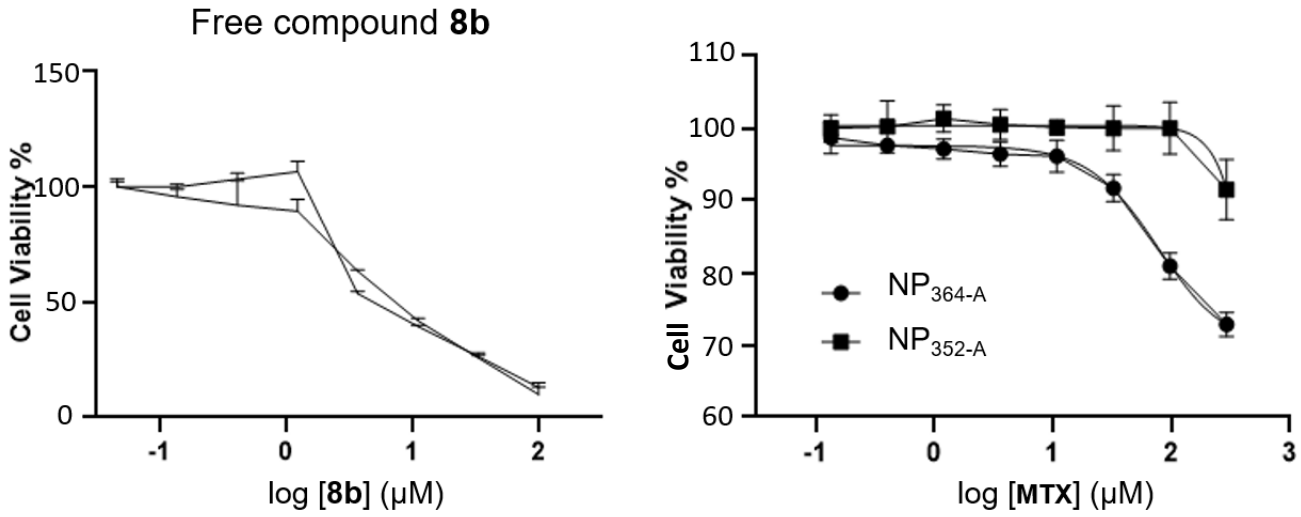

*Figure 134. Cell viability curves for left: compound **8b** free; right: **$NP_{352\text{-}A}$** and **$NP_{364\text{-}A}$**.*

However, the activity was not as high as expected and could be imporved. This may be due to various parameters: the ability of the NPs to cross the cell membrane, the availability of the drug at the corona of the NPs or the variation of affinity of the drug towards receptor since it has been covalently modified to be attached on the PEG moiety.

To understand and overcome this limits, over type association between MTX and the NPs could be investigated (e.g. cleavable linker, non covalent association). Also, other drugs such as the camptothecin could be introduced in NPs, either in the core of the PEG-PDMS NPs (i.e. attached directly to the polysiloxane backbone); or at the end of a PEG chain. We could expect CPT-NPs to be more active as IC_{50} of free CPT is higher than free MTX (IC_{50}=0.013 µM for CPT on A375 human melanoma cell line).

Chapter 6: Synthesis of peptide-PDMS polyplexes

Chapter 6: Synthesis of peptide-PDMS polyplexes

I. Introduction

a. Basics of SiRNA transfection

Numerous diseases are related to the expression of a specific protein, which can be a normal protein overexpressed in certain pathologies, a mutated or misfolded pathological protein or a protein from a pathogen.

The treatment of such diseases can be difficult with small molecule drugs; presenting specific and toxicity issues. Alternatively, instead of curing the diseases by fighting the resulting symptoms, it has been proposed to stop the synthesis of the pathogenic protein by inhibiting their transcription. This kind of treatment is called gene therapy.

There are several gene inhibition strategies. The first one relies on deoxyribonucleic acid (DNA). DNA is found in the nucleus of cells and is composed of a double strand: the sense and the anti-sense strand. These two strands are paired together following a precise sequence of nucleic acid (cytosine (C), guanine (G), adenine (A) or thymine (T)) with anionic phosphodiester backbone. The DNA codes the synthesis of protein thanks to its anti-sense strand via a translation/transcription mechanism (Figure 135). The DNA is first translated into messenger ribonucleic acid (mRNA) thanks RNA polymerase.

The transcription (oligonucleotide -> other type of oligonucleotide) is the first step of the gene expression, corresponding to the lecture of the DNA by RNA polymerase leading to the production of RNA, a double stranded helix formed on nucleic acids (G uracil (U), A, and C). This key step of the protein synthesis is operated into the nucleus. Then, once transcription of the DNA is done, the mRNA is read by a ribosome in the cytoplasm which starts the ribosomal synthesis of protein: it is the translation (oligonucleotide -> peptide) step. SiRNA-based gene therapy can act just before this step by stopping the translation and so the protein production.

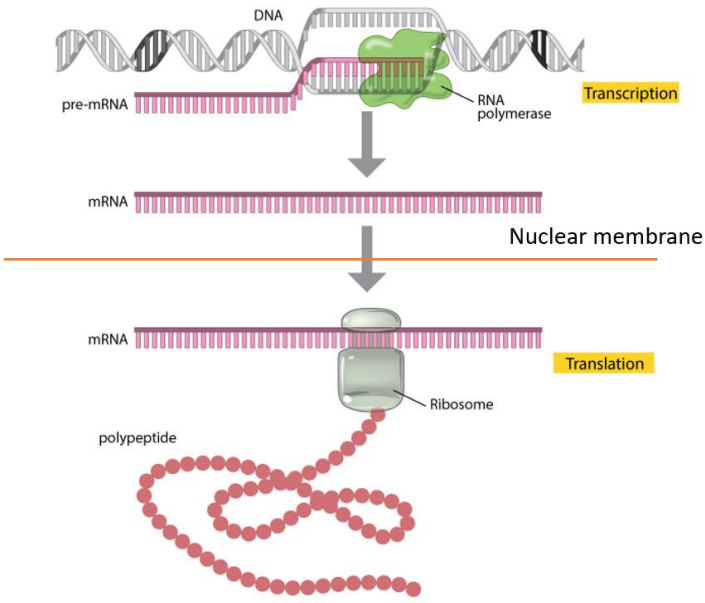

Figure 135. Transcription and translation steps of DNA.(adapted from[383])

DNA was first used for gene inhibition: by edition of the DNA sequence, instead of performing transcription, the modified DNA block the mRNA synthesis and so the protein associated. However, it suffered important drawbacks including the requirement of a relatively important size to be efficient in gene silencing and the need to bring it to the nucleus.[384] As an improvement of DNA-based gene inhibition, small interfering RNA (siRNA) strategies have emerged.[385] This technic is based on the knock-down (i.e. the silencing) of the selected gene) but not its erasure from the gene pool of the living organism. As DNA, SiRNA is also made of a double strand of nucleic acids with anionic phosphodiester backbone. However, some notable differences can be pointed out: the size, the stability and the endosomal release. The DNA is way longer than the siRNA: up to several kilo of base pair of nucleic acids vs only 21-23 for the siRNA. DNA is also more stable than the siRNA, however, siRNA can be easily chemically synthesized and stabilized by some chemical modifications. Finally, the release is done in the cytoplasm for the siRNA while the DNA needs a transport to the nucleus. Overall, siRNA is presenting the advantages of its small size and its ease of chemical synthesis that make it easy to manipulate.

The principle of siRNA action is based on transcription/translation step of the DNA (Figure 136). SiRNA was discovered in 1990 by accident since it was originally designed to over express the chalcone synthase by genetic addition but finally induced its complete silencing.[386] Its discoverers introduced the notion of co-suppression: inhibition of both the original and introduced gene. SiRNA is constituted by ribonucleic acids assembling either of a double-stranded helix or single one (which is less stable). Its mechanism has been clearly described since its discovery and be worth a Nobel prized for its discovery for Fire and Mello in 2006.[387]

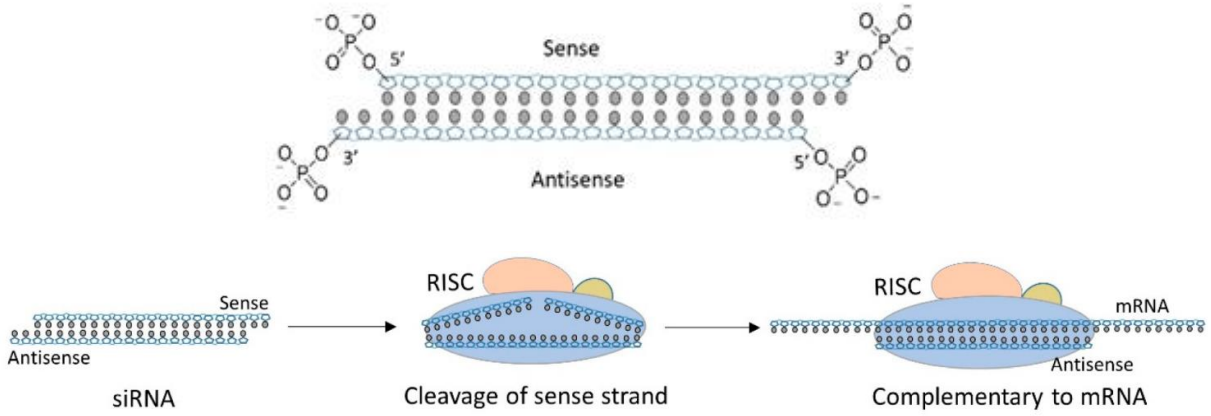

Figure 136. Structure of siRNA and the cleavage of its sense strand by the RISC complex.[388]

Once in the cytoplasm of the cell, the double stranded siRNA is associated with a protein complex, RISC (RNA Induced Silencing Complex), which cleaves it smaller fragment and then evacuates the "passenger" strand. Then the "guide" strand is performing a scan of different mRNA is operated until one strand of mRNA matches with the single guide strand of siRNA by base paring. Once linked, the siRNA is cleaving the selected mRNA strand and so stopping the associated protein synthesis.[389]

Two siRNA analogs were also described for RNA interference (RNAi): small hairpin RNA (shRNA)[390] and micro RNA (miRNA). They are both longer than the siRNA and need a transcription step before the interference with mRNA in the RISC.[391,392] However, they will not be detailed here since we are focusing on the siRNA.

All of these versions of RNAi share the same drawbacks that impair their use as therapeutic tools: they may have toxic effects in inducing an immune response when they accumulate outside the membrane cells. Thus being

negatively charged, they have difficulties to cross the cell membrane and they have a short half-life due to degradation by serum nucleases.

In order to avoid most of these problems, siRNA has to be transported by a vector. Two main categories of vectors can be defined: viral or non-viral. The viral vectors comprise several types of virus like retrovirus or adenovirus. The main advantages of the viral vector are their high efficiency to cross the cell membrane. Viral siRNA vectors were commercialized as Gendicine® in 2003 and Glybera® in 2012. However, in term of biosafety, the viral vectors may have represented a danger, especially immunogenicity, and this is why non-viral vectors were developed.

The transfection efficiency of the non-viral vectors is usually not as good as the viral ones, in term of membrane cell penetration, but they can be chemically modified to enhance their properties. Non-viral vectors for siRNA can be sorted in two categories: covalent conjugates and complexes.

Several types of biomolecules have been conjugated to siRNA. The conjugation is done either at one end of the guide (or "sense") strand of the siRNA, or at the 3' extremity of the "passenger" (or "antisense"), through the phosphorylated group, in order not to disturb the activity of the guide (or "sense") strand.[254] It goes from to lipids[393] (e.g. cholesterol[394]) to peptides for example.[395] As already explained, they confer stability and/or targeting properties to the resulting bioconjugate, helping the transport of siRNA inside the cell and bring it to the RISC complex.

The second approach for non-viral vectors relies on the non-covalent complexation with a vector. An ideal non-viral non-covalent siRNA vector has to tackle three main challenges: complexation, transport through the cell membrane and release in the cell.

Complexation

The complexation between siRNA and its vector is based on electrostatic interactions. Indeed, the siRNA is negatively charged because of the phosphodiester groups linking each nucleotide base of the strand (Figure 136); and the vectors present numerous positive charges to form ionic interactions with the siRNA.

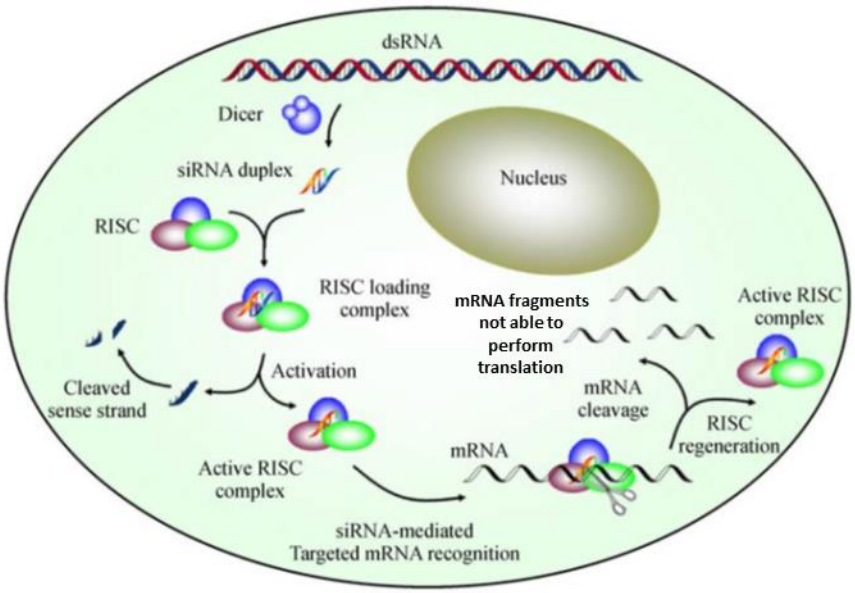

Figure 137. Mode of action of the siRNA/vector complex.(adapted from[396])

Crossing the membrane

Transport of siRNA through the cytoplasmic membrane can be performed with or without the help of membrane receptor ligands (Figure 137). In most of the cases, the siRNA-vector complex is taken up by endosomes (i.e vesicles made from the cell membrane and goes into the cytoplasm).

Endosomal escape

The release of the siRNA from the vector inside the cell in order to let it meet the RISC depends on two parameters: the dissociation of the siRNA from the vector and the escape from the endosome. One proposed mechanism of endosomal escape is the “proton-sponge effect”.

The polyplexes enter the cell through an endosome. On the endosome membrane, an ATPase proton pump introduces protons in the endosome once in the cell. The increase of the proton concentration make the pH drop to 5.5 and so induce a protonation of the polymer of the polyplexes which displays buffer properties. Then, these protons being captured by the polymer, other protons enter the endosome to keep the pH to 5.5. Consequently, chloride counter ions enter in order to keep the electro neutrality in the endosomal vesicles. This flow of chloride is raising the osmotic pressure: water is filling-up the vesicles resulting in their swelling and lysis.

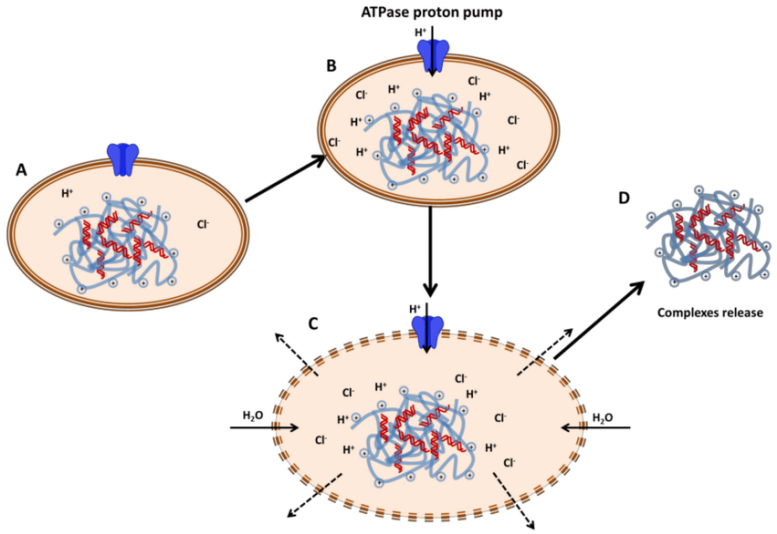

Figure 138. “proton-sponge effect” mechanism: A) siRNA-vector complexes trapped in endosome; B) ATPase proton pump introduces protons in the endosome inducing protonation of the polymer; C) chloride ions enter the endosome to counterbalance the free proton and D) the endosome is breaking due to water flow, caused by osmotic pressure.[397]

Dissociation

After endosomal escape, the final step for the vector is the dissociation from the siRNA, to let it complex with the RISC and then operating its gene silencing process. The dissociation can be triggered by the degradation of the vector, due the endosomal conditions (pH, reducing conditions by glutathione present in the cytoplasm) or simply by diminution of the stability of the complexes provoked by the change of its protonated state. Once in the cytoplasm, the polymer vector can be protonated and complexed with ions of the cytoplasm. The release of the siRNA is done slowly in the cytoplasm in function if its stability, and especially if no modification have been done on the polymer.[398]

b. Types of non-viral vectors for siRNA transfection

Three different generation of non-viral vectors marked the evolution of the research in this field.

1st generation: cationic system

The 1st generation consist in cationic systems able to from complex with the negatively charged siRNA. Different natures of vector emerged as cationic lipids[399] or cationic polymers.[400,401] Cationic lipids form liposomes and then complex with siRNA: such association is called lipoplexes. Liposomes display a good affinity with the cell membrane compared to polymer vectors.

The complex formed between a cationic polymer and a siRNA is a polyplexe. They usually showed a good transfection ability, at least in vitro. The most classical ones are PEI (polyethylenimine)[400], PLL (poly-L-Lysine),[402] chitosan[403], cyclodextrine derivatives[404] or dendrimers (like polyamidoamine (PAMAM)).[405,406]

2nd generation: PEGylated system

The second generation of non-viral vectors is based on the first ones improved with PEG chains. The addition of PEG on the vectors, either polyplexes or lipoplexes, contributes to a better hydrophilicity and stability *in vivo*, and stealth during circulation in the body. However, these PEGylated systems are often less efficient compared to the first generation, mainly because they are less internalized.[407,408]

3rd generation: targeting system

The third generation includes a targeting system in the vector. Ligands binding to surface receptors of target cells such as RGD or folic acid are grafted on or copolymerized within the polymeric vector before the siRNA complexation. Beside targeting, ligands contribute to an active internalization once in contact with cell membrane receptors.

Polyplexes are usually resulting in 100 to 300 nm NPs, depending on the size of the polymer used for the complexation. In addition, the zeta potential of these NPs is an important parameter. In order to get a stable polyplexes the zeta potential of the NP has to be positive; it is usually around +20 to +30 mV. Finally, the complex formed is generally quite stable over the time, except for the acidification that create a dissociation and so the release of the siRNA.

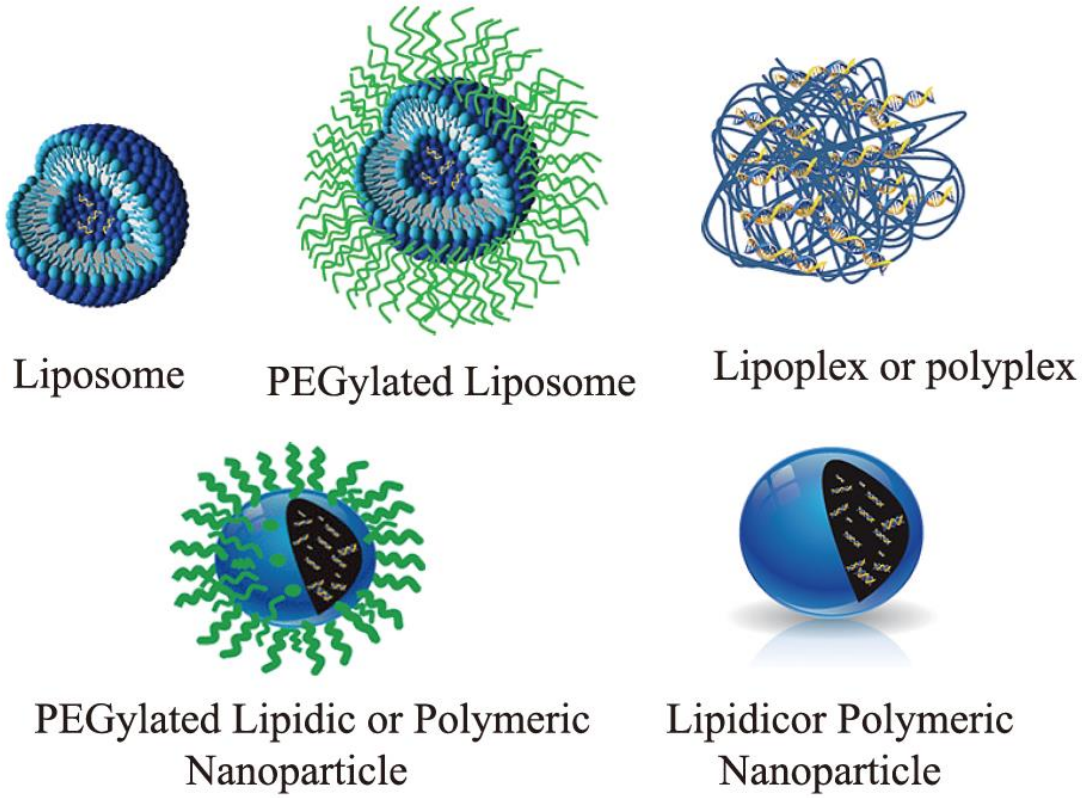

Figure 139. Non-viral vectors used for siRNA complexation.(adapted from [409])

c. *Peptide-based polyplexes*

As already stated, polyplexes are mainly based on electropositive charged polymers, like PEI or pLL. But homopolymers of lysine, as linear chains for example, were also used for the same job.[251,410] Besides such simple homopolymers, well-defined peptide sequences have been investigated as a new family of non-viral vectors. In particular, cationic cell penetrating peptides (CPP) which have already proven their ability to cross the cell membranes taking with them various cargo, have been combined with siRNA to give peptide-based polyplexes.[372,373] The ability to cross cell membrane for such complexes can be optimized by playing on the number and the position of positives charges and the nature of the cationic amino acid used in the sequences (e.g. Lys, Arg, His). Several CCP have been re-designed for siRNA transfection showing promising results both in term of complexation and internalization, such as WRAP peptide[252] or histidine/lysine containing peptides.[253,411–416]

The combined use of both Lys and His residues presents several interesting features. First, cationic poly(Lys,His) peptide-based polymers easily complex negatively charged siRNA. Second, these systems are particularly efficient to promote endosomal escape via the proton sponge effect. Indeed, the pKa of Lys and His side chains are respectively 10 and 6. It means that at cytosolic pH 7.4, lysines are protoned while histidines are not. Once in the endosome, pH drops to 5.5 inducing the capture of more protons, initiating the proton-sponge mediated lysis of the endosome. In addition, these systems are experiencing endosomal escape due to proton sponge effect and have the ability to release the cargo once inside the cell thanks to a variable pKa due to the combined presence of Lys and His (pKa of 10 for the polyLys and around 6 for the poly His and 6.5 the polyLysHis).[253,411–416]

His and Lys residues can be introduced in different ways on a polymeric vector. The first example described an acrylate-based polymer functionalized with pLL and HisLys polypeptides. Two strategies are presented (Figure

140): in the first one, the polyLys and polyHis moieties are copolymerized with the N-(2-Hydroxypropyl)methacrylamide (HPMA) in order to lead to block copolymer with an acrylate backbone. In the second strategy, the acrylate polymer is polymerized in a first step by copolymerization of HPMA and pyridyl disulfide methacrylamide (PDSMA). Then in a second step, the acrylate modified polyLys is copolymerized at the end of the acrylate polymer, and by a third step, the cystein modified polyHis is grafted as a pendant chain by disulfide bond formation. The second strategy enable to formation of a cleavable polyHis pendant chain.

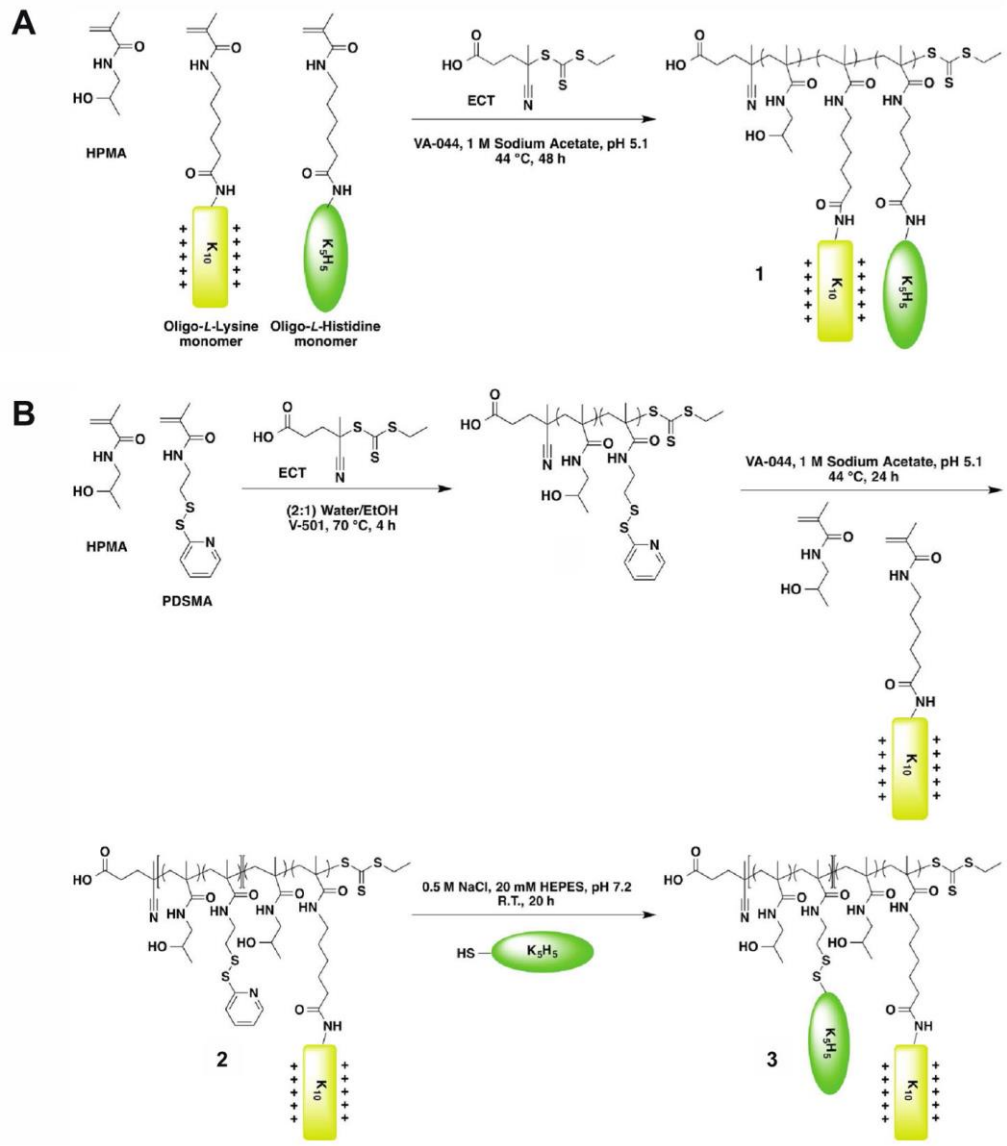

Figure 140. Two different strategies for the synthesis of acrylate-based pLL and polyHis modified polymers for the design of polyplexes.[413]

The length, the type of structure (i.e. copolymer with peptide/polymer pendant chain cleavable or not), the zeta potential and the morphology of all of these polymers were investigated to study their impact on complexation and transfection.

In the case of these block copolymer, the morphology plays the determinant role. For example, rod-like NPs seems to accumulated in the endosome and so the delivery of the carriage is slower.[412] The size of the pendant polyLysine chain had also an influence on the complexation and transfection efficiency: the complexation increasing with the length while the transfection efficiency decreased. In contrast, the type of polymer structure, alternative or block copolymer, did not influence significativelly the complexation nor the transfection.[411]

The ratio between His and Lys residues in these systems has to be necessarily high (i.e. up to 40 times more His block than Lys block) to favor the endosomal escape compared to the same polymers obtained with Lys alone.[413]

The second type of HisLys polymers described in literature is based on a pLL functionalized by His moieties.[415] Two structures were presented: either a block copolymer of His and Lys or a pLL grafted by a polyHis as pendant chain. In both cases, the His moieties are incorporated at 30 mol%. The branched structure has shown better complexation and induced less hemolysis than the linear copolymer, for the same quantity of His residue. Thus, the presence of His in the polypeptide, especially the polyHis pendant chain, helped to get a better transfection than the pristine pLL.

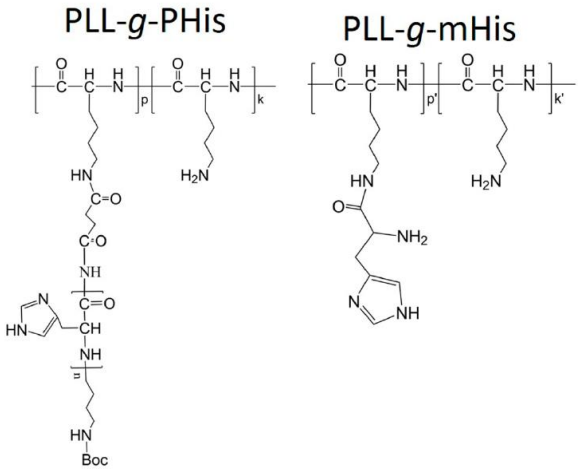

Figure 141. Two structures of acrylate-based Lys and His modified polymers for the design of polyplexes.[415]

The third type of HisLys polymer is a linear polymer obtained by oxidative polymerization of decapeptides of type –CysLys$_x$His$_y$Cys-OH (Figure 142, with x+y=8) used as macromonomers.[253] Except, for H-CysLys$_8$Cys-OH and H-CysHis$_8$Cys-OH, the polypeptides have a fixed ratio of 4 Lys and 4 His disposed either alternatively or by pairs or quartets in the sequence.

Interestingly, once in the cytosol after escaping from endosomes, the reductive conditions cleave the disulfide bonds, inducing the de-polymerization and the subsequent release of the siRNA. The complexation and release efficiency of each polymer were studied as well as the resulting pKa of the polypeptide based polymer obtained. As long as 4 His residues are present in the sequence, along with Lys residues, the final pKa is close to 6 (i.e. the His pKa). The pKa is an important parameter since it is one of the major factor of the dissociation once in the cytoplasm. Finally, the best sequence was determined as H-CysK$_4$H$_4$Cys-OH (Figure 142).

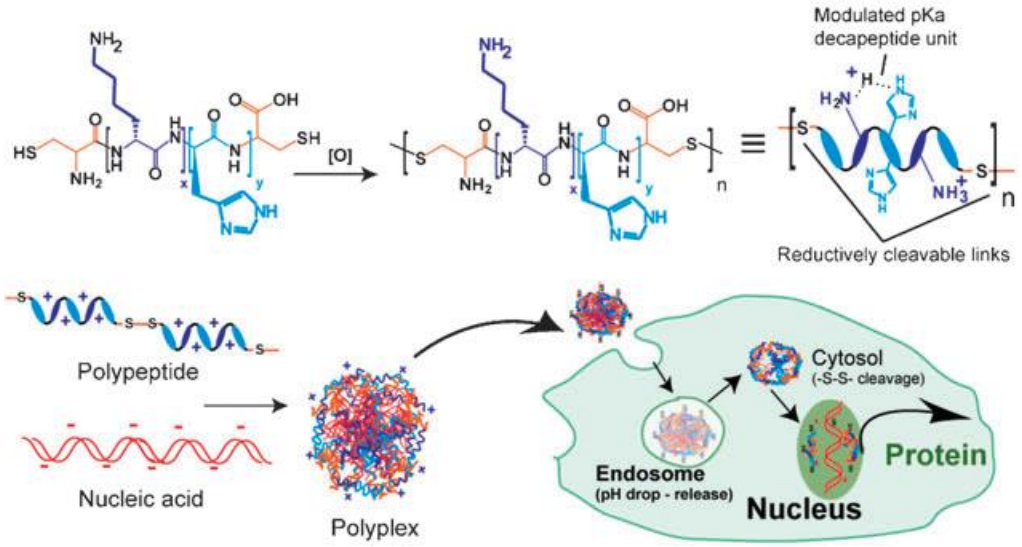

Figure 142. Polymerization of H-Cys[LysHis]$_4$Cys-OH leading to a polypeptide able to form a polyplex.[253]

All the above cited examples of peptide-based polyplexes were obtained in two steps: first the multi-step syntheses of the vector (either by grafting a polyHis on a pLL for example)[415] and then, the complexation with siRNA.

In this context, we took inspiration of the studies about His/Lys peptide-based polyplexes but we followed a different approach. We aimed at preparing polyplexes with PDMS-based peptide polymers and, advantageously, forming the complex in a single step by using sol-gel inorganic polymerization in the presence of siRNA.

d. Our strategy to prepare peptide-PDMS polyplexes

According to the studies presented previously, it has been proven that pLL was efficient for complexation but presented a better transfection efficiency when completed by His residues. Addition of His was also more efficient as branched polyHis block as pendant chain.[413] From the studies of Nasanit et al.,[253] we saw that an equal ratio between Lys and His within a linear polypeptide chain was the best option.[253] In the case of branched polymers the ratio was different, a large excess of the polyHis branch was necessary over polyLys branch (up to 40 times more).[413]

We decided to prepare comb-like structures with pendant peptide His/Lys containing chains, disposed on a polysiloxane backbone. They will be obtained by using hybrid dichloromethylsilyl-hybrid peptides able to complex with siRNA.

Two approaches were evaluated. The first one (Figure 143, top) relies on the preparation of His/Lys containing peptide-PDMS nanoparticles using the same strategy as the one described in chapter 5 (II. Synthesis of His/Lys peptide-PEG-PDMS NPs) including $SiMe_2Cl_2$ and silylated PEG compound **14**. Such particles could be mixed with siRNA, to form polyplexes. Noteworthy, combining an oligonucleotide with already-prepared NPs is a strategy that has been already disclosed. For example, we may cite polyalkylcyanoacrylate NPs[417] and poly(2-dimethyl amino)ethyl methacrylate) (pDMAEMA) sunflower-like NPs.[418] The preparation of such NPs is detailed in the part II of this chapter and the polyplexes formation is described in part c.

More interestingly, we also envision a modular alternative strategy (Figure 143, bottom) to prepare polymer/peptide-polyplexes. Instead of using free peptides to interact with siRNA[250,251,419] or instead of synthesizing polymers presenting peptides sequences and mix them with siRNA afterwards,[420,421] we planned to

use the well-defined silylated peptide macromonomers which could polymerize in water the presence of siRNA to form polyplexes in a single step. We hoped that a higher complexation rate could be achieved this way and that the polyplex will be more stable than the one obtained with non-polymerized peptides sequences. Ideally, we wanted to investigate if the siRNA could act as a template for the polymerization of peptide macromonomers, yielding peptide-polymers with higher molar mass and narrower polydispersity. This second strategy is presented in the part III of this chapter.

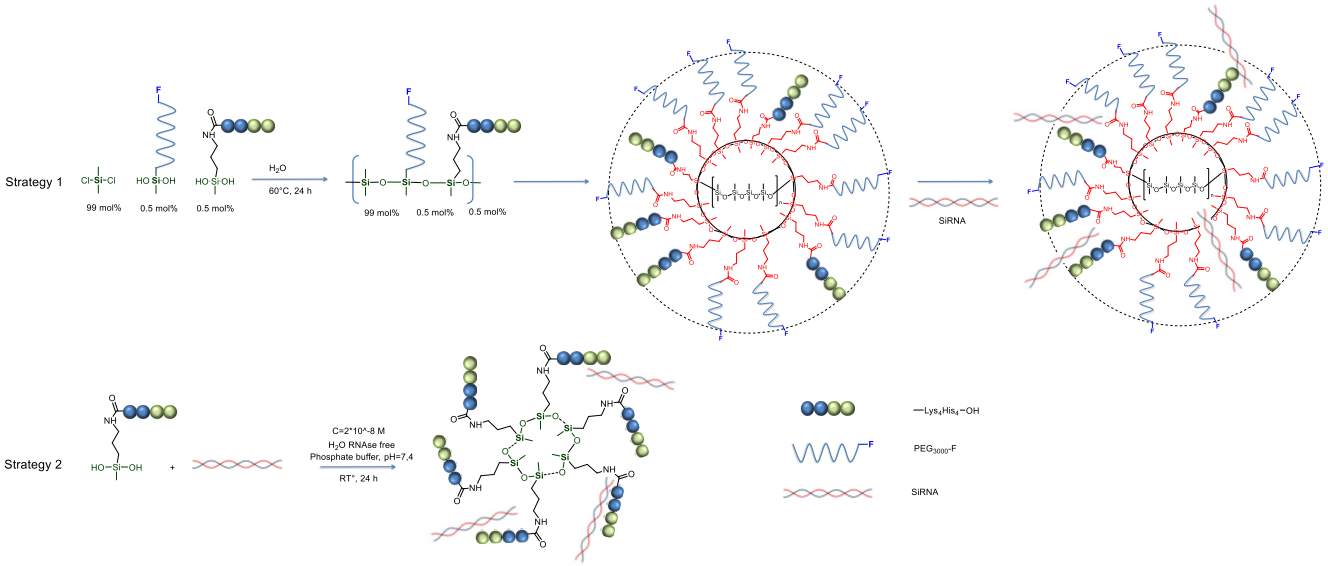

Figure 143. Strategies of preparation of polyplexes from hybrid silicone-based peptide polymers.

NB: all the reactions presented in this chapter, will be annotated by their original lab book ID.

II. Synthesis of His/Lys peptide-PEG-PDMS NPs

a. *Synthesis of His and Lys containing hybrid peptides*

The first step consisted in the syntheses of dihydroxysilyl macromonomers needed for the preparation of peptide-based PDMS. The silylation of peptides was developed in chapter 3. In order to incorporate the peptide macromonomer into silicone polymer, the hybrid peptide needed two hydroxyl group on the silane function to be able to give two Si-O-Si bonds. This is why we used dichloromethylsilanepropyl isocyanate as silylating agent.[144]

As a peptide sequence, we chose K_4H_4 peptide which was already linearly polymerized via disulfide bonds to get a polymer suitable for transfection.[253] As already discussed, the imidazole rings of His would affect the global pKa of the polymer (decreasing the pH down to pH≈6.5) and should enhance the endosomal escape.

We decided to investigate a comb-like geometry, with pendant peptidyl moieties on a PDMS backbone. This geometry would be similar to the example explained previously in the copolymerization of HPMA with acrylate modified polyLys and polyHis.[413] So in order to get a similar branched structure, we prepared the K_4H_4 peptide macromonomer (Figure 145, compound **2**) silylated at its N-terminus (i.e. at the extremity of the four-Lysine repeat).

Instead of using acrylate modification at each end of the peptide to perform a RAFT copolymerization, we applied a sol-gel process for the polymerization and so a silylation on the peptide. We choose to perform a monosilylation with two hydroxy group on one silane function at one extremity of the peptide, and to copolymerize it with DCMDS to get a comb-like polymer with peptide pendant chains and silicone backbone

(Figure 144). However, we chose to work with the K_4H_4 sequence presented by Nasanit et al. (i.e. the oxidative polymerization of Cys-residues) but to change the polymer linear structure.

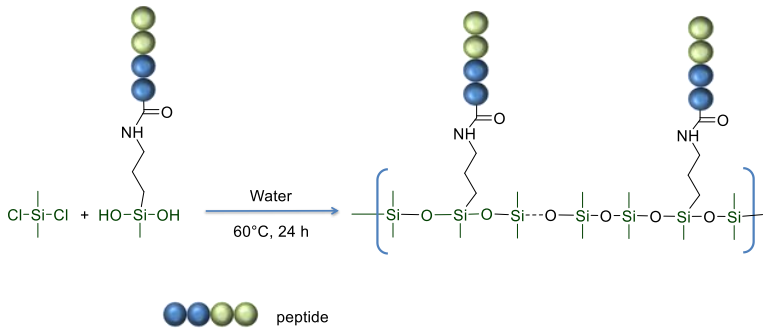

Figure 144. Comb-like copolymer synthesized by condensation of DCDMS and a dihydroxymethylsilylated peptide.

Alternatively, silylated tetrapeptides containing only His or only Lys residues were prepared (compounds **3** and **4**, respectively). We planned to use these two different hybrid peptide macromonomers at different ratios (i.e. 40/60/, 50/50 and 60/40) for the polymerization to obtain comb-like peptide copolymers alternating randomly His_4 or Lys_4 pendant chains. This experiment could have highlighted the role of each part of the peptide (His or Lys part), showing for example, if the His-peptide is more complexed to the siRNA than the Lys one.

On the contrary to hybrid peptides described in chapter 3; hybrid silylated peptides **2**, **3** and **4** were synthesized entirely on solid support (Figure 145).

2 Chloro chlorotrityl PS resin was used to obtain C-terminus carboxylic acid peptide after cleavage. Lysine and histidine side chains remained protected by Boc or Trt groups respectively, thus avoiding unwanted modification during silylation at the N-terminus of supported compounds **2b**, **3b** or **4b** performed with isocyanatopropyl dichloromethylsilane (ICPDCMS). Once the silylation was done on the resin beads, the hybrid peptides were then cleaved by an acidic treatment, TFA/TIS/$H_2$0 (98/1/1) and the side chains were deprotected in the same operation. Finally, hybrid peptides were precipitated in Et_2O, dried under vacuum and stored under inert atmosphere at 4°C.

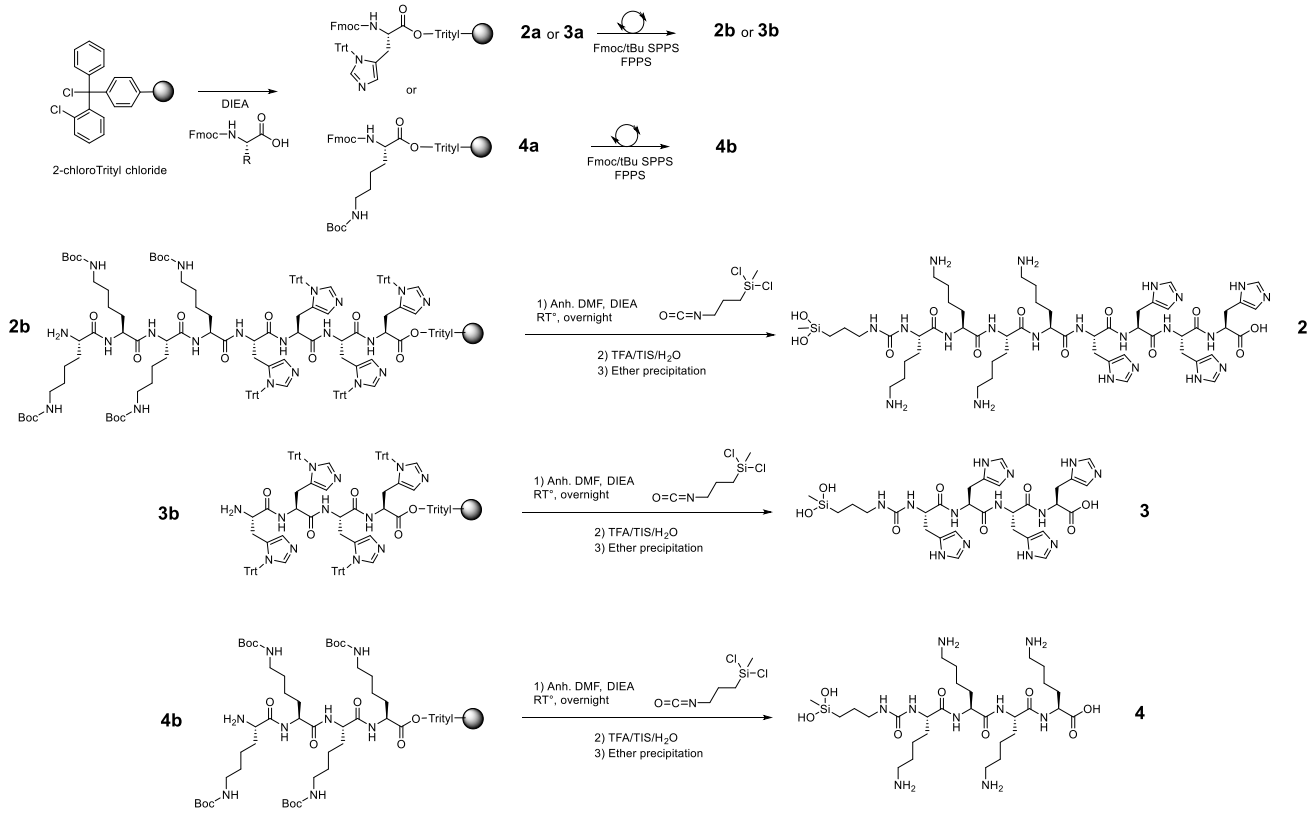

*Figure 145. Syntheses of hybrid peptides **2**, **3** and **4** on solid support*

The resulting compounds **2**, **3** and **4** were analyzed by LC/MS on a reversed-phase C_{18} grafted silica column. As example, the LC/MS of compound **2** is presented in Figure 146. The sample was prepared in H_2O/ACN (50/50) 1‰ TFA. As the peptides are highly hydrophilic, they elute at almost the same retention time as the injection peak, at 0.26min for the injection peak vs 0.27min for the peptide. We detected the expected monoprotonated ion 1242 m/z in the peak at 0.27min.

The exact molar mass of the silylated peptide is 1239.68 g/mol which would correspond to a monoprotonated ion $[M+H]^+$ 1242 m/z. We could mainly see the di-charged species $[M+2H]^{2+}$ on the spectrum: 621 m/z. In addition, the ionization of the siloxane function is leading to a water molecule loss, corresponding to 1222m/z, and so the di-charged species were observed at 612 m/z (Figure 146).

This LC/MS analysis confirmed the presence of the compound 2 with high purity (>95%) after purification and a final yield of 68% (Figure 146).

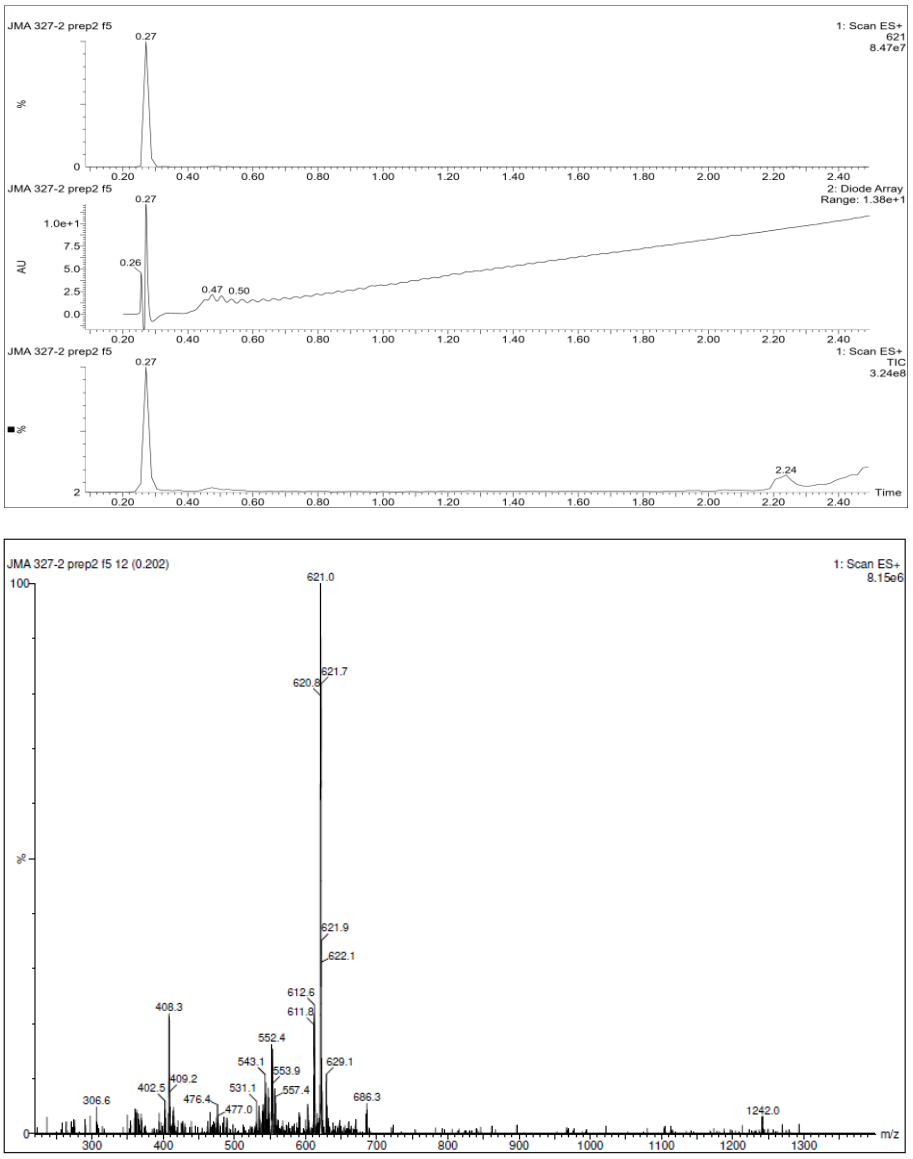

Figure 146. ESI + LC/MS of compound 2 Top: chromatograms UV at 214nm and TIC, Bottom: MS spectrum at 0.27 min.

b. *Synthesis and characterization of Lys/His containing peptide-PDMS polymers and NPs*

Once the peptide macromonomers synthesized, functional PDMS could be prepared as described in chapter 5. The silylated peptide **2**, or a combination of **3** and **4**, was incorporated in the PDMS chain along with dichloromethylsilylated PEG_{3000} (compound **14**) and DCDMS.

The use of PEG to functionalize polyplexes was already described. Indeed, PEG chains provide to a kind of shield to the polyplexes formed, which prevents premature leak of the cargo,[374,422] and brings furtivity.[423–425] The PEG chains of polyplexes were modified with linkers to be released either before passing the membrane (e.g. with peptide substrates cleaved by matrix metalloprotease-2), or in the cytoplasm (e.g. with disulfide bridges cleaved by reduction).[407,426,427]

We already determined in the chapter 5 that the best PEG-PDMS NPs were obtained when PEG_{3000} macromonomers **14** were included at 0.5-1 mol%, (i.e. 18-33 w%) related to silicone content (chapter 5, **NP_{293}** and **NP_{294}**). Including between 1 and 2 mol% (i.e. 33-46 w%) of PEG lead to a polymer too hydrophilic to be

soluble in water and too hydrophobic to be soluble in organic solvent. Over 2 mol% of PEG would results in a water soluble polymer.

We decided to keep the 'hydrophilic ratio' to 33 w%. It implied that 67 w% of DCDMS, turning into a dimethylsilyl (DMS) group, was used to prepare the peptide polymer (Figure 147):

$$\frac{w\%(peptide) + w\%(PEG)}{w\%(peptide) + w\%(PEG) + w\%(DMS)} \approx 33w\%$$

We choose to add only 0.5 mol% (i.e. 18 w%) of hybrid PEG **14**, to leave room for the peptide into the multifunctional PDMS.

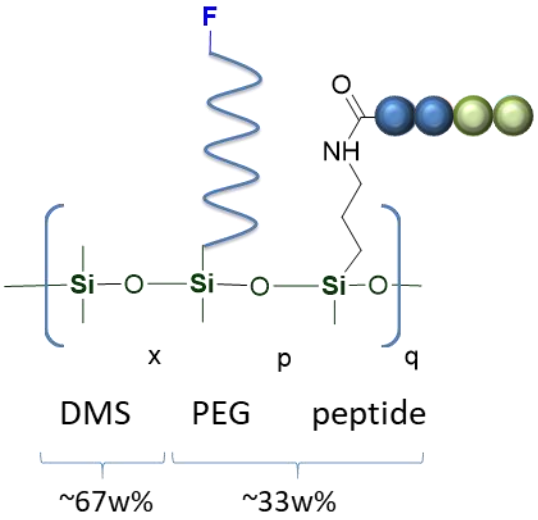

Figure 147. General composition of peptide-PEG-PDMS as example for the composition calculation.

Several quantities of hybrid peptide **2** were tested (0.5, 0.75 and 1 mol%) as well as two polymerization methods (Figure 148): the direct polymerization (way A, chapter 5 page 159) or the diblock strategy (way B, chapter 5 page 159).

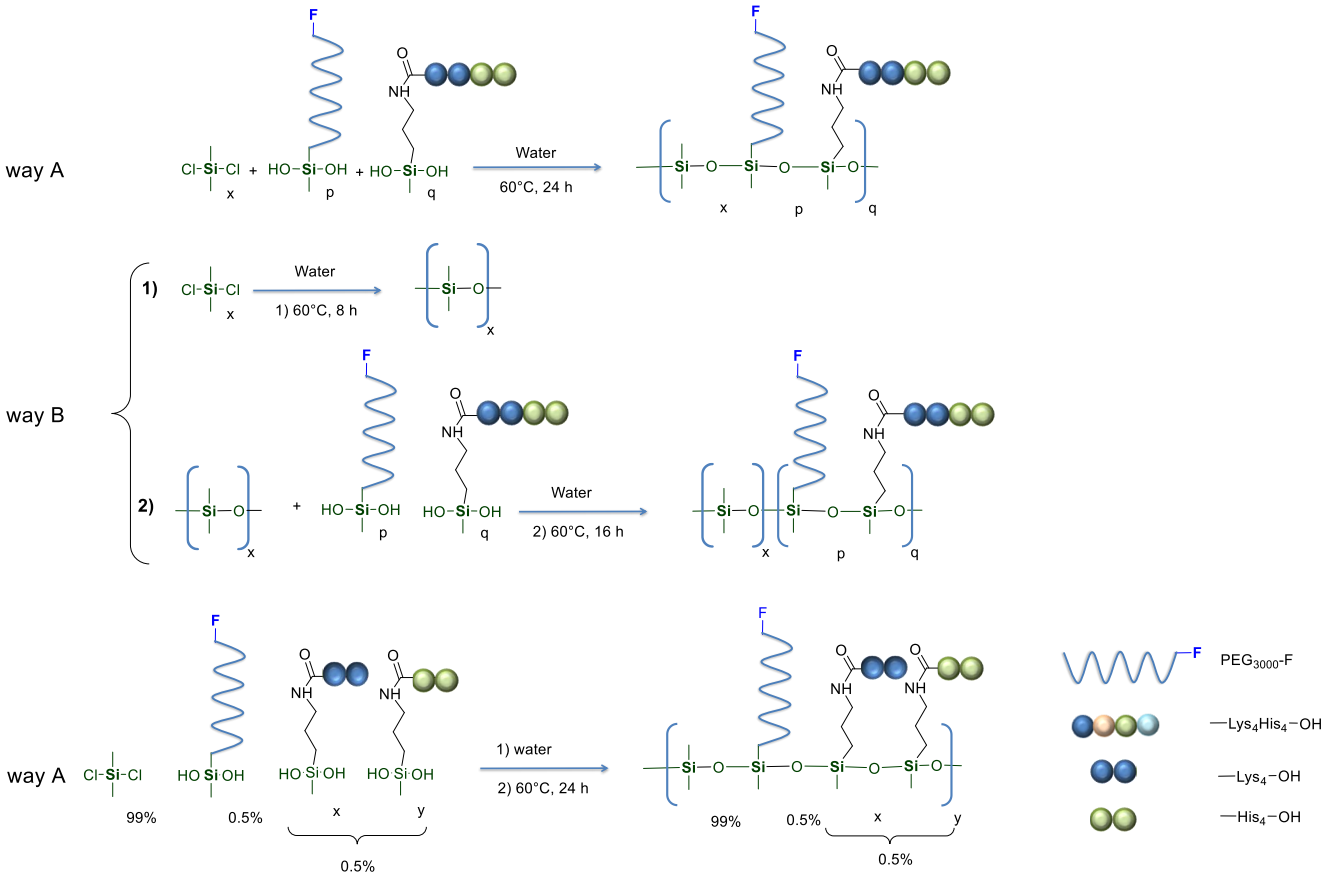

Figure 148. Syntheses of peptide-PEG-PDMS for polyplexes formation

Table 19. Summary of Peptide-PEG-PDMS synthesized and their hydrophilic balance.

Reaction Id	-O-Si(Me)-PEG-F		-O-Si(Me)-K_4H_4		-O-Si(Me)$_2$		Way	mol% of PEG-F[a]	mol% of PEG-F[b]	Mw (kDa)[c]
	mol%	w%	mol%	w%	mol%	w%				
P_{334-A}	0.50%	16%	0.75%	9%	98.75%	75%	A	n.d.	n.d.	n.d.
P_{334-B}	0.50%	16%	0.75%	9%	98.75%	75%	B	n.d.	n.d.	n.d.
P_{335-A}	0.50%	17%	0.50%	6%	99.00%	77%	A	0.26	0.61	36.9
P_{335-B}	0.50%	17%	0.50%	6%	99.00%	77%	B	0.10	0.29	60.5
P_{336}	0.00%	0%	1.00%	14%	99.00%	86%	A	n.d.	n.d.	n.d.
P_{337-A}	0.50%	16%	1.00%	12%	98.50%	73%	A	n.d.	n.d.	n.d.
P_{337-B}	0.50%	16%	1.00%	12%	98.50%	73%	B	n.d.	n.d.	n.d.

Reaction Id	-O-Si(Me)-PEG-F		-O-Si(Me)-K_4		-O-Si(Me)-H_4		-O-Si(Me)$_2$		Way	mol% of PEG-F[a]	mol% of PEG-F[b]	Mw (kDa)[c]
	mol%	w%	mol%	w%	mol%	w%	mol%	w%				
P_{349}	0.50%	16%	0.20%	3%	0.30%	6%	99.00%	75%	A	0.41	0.50	27.9
P_{350}	0.50%	16%	0.25%	4%	0.25%	4%	99.00%	75%	A	0.49	0.53	34.4
P_{351}	0.50%	16%	0.30%	6%	0.20%	3%	99.00%	75%	A	0.44	0.32	21.9

a: determined by ERETIC method by ^{19}F NMR; b: determined by ^{1}H NMR; c: determined by GPC performed in chloroform; n.d.: non determined

Briefly, for the way A, monomers were mixed together in water at 60 °C for 24h. For the way B, DCDMS was first polymerized in water for 16h at 60 °C and then other hybrid monomers are added for 8h at 60 °C. The reactions were done on small scale: a total of 2 mmol of monomers are poured in 5mL of water to get a theoretical amount

of ≈200 mg of polymer. At the end of the polymerization, polymers are extracted by chloroform, washed by water, dried and finally concentrated.

Peptide-PEG-PDMS **P_{334}**, **P_{336}** and **P_{337}** could not be isolated. They precipitated in between the aqueous and organic phase. The extraction of the resulting polymer was then not possible with chloroform. However, they were no soluble in water either. Despite numerous attempts, we did not manage to find appropriate solvent (e.g. acetate buffer, THF, chloroform) to characterize them by GPC or NMR. On the contrary, peptide polymer **P_{335}** was isolated and characterized by GPC in chloroform and by ^{1}H and ^{19}F NMR. The ERETIC method revealed that the way B led to lower incorporation of Si-PEG-F macromonomer compound **14** (0.26 *vs* 0.10 mol% for way A and B, respectively). The way A was preferred for the following syntheses.

Three other polymers **P_{349}**, **P_{350}** and **P_{351}** have been synthesized using combinations (40/60, 50/50 and 60/40 of the macromonomers **3** and **4** (
Table 19). The quantity of PEG was also fixed at 0.5 mol%, as previously, and the total amount of silylated peptide representing 0.5mol%, in order to be able to compare them to P335 prepared with compound 2. These three polymers have also been characterized by GPC in chloroform and by 1H and 19F NMR.
First, we observed that 0.5 mol% of Si-PEG-F and 0.5mol% of hybrid peptide (compound **2** alone or **3**+**4**) was the maximum possible % to obtain chloroform-soluble peptide-PEG-PDMS. It represented 25 w% of 'hydrophilic' monomers. The peptides were probably too hydrophilic to be incorporated in a high percentage in the PDMS chain while keeping the possibility to extract the multifunctional PDMS in chloroform.

We noticed that **$P_{335\text{-}A}$** and **$P_{335\text{-}B}$** are both in the same range of Mw than **$P_{294\text{-}A}$** and **$P_{294\text{-}B}$**, respectively (PEG-PDMS with 0.5 mol% theoretical quantity of compound **14**, **chapter 5**). Indeed, the polymer size (Mw), **$P_{294\text{-}2}$** and **$P_{294\text{-}3}$** was in 15.7 and 51.7 kDa respectively. This was comparable to Mw of **$P_{335\text{-}A}$** and **$P_{335\text{-}B}$**: 36.9 and 60.5 kDa respectively. This confirmed that the way B lead to higher molar mass of polymer, at least twice higher.

The experimental quantity of compound **14** have been determined by both ^{29}Si (ERETIC method) and ^{1}H NMR. The ^{1}H NMR quantification was done by the same way than in the chapter 5: by comparison of the theoretical ratio of the peak integration of the PEG chain and the peak integration of the methylsilyl group. The quantification of the peptides could not be performed this way since they do not have high intensity peaks, compared to the ones resulting from the PEG chain (3.5 ppm) and the ones from the methyl silyl group (0 ppm).

The experimental mol% of compound **14,** was in coherency with the results obtained with **$P_{294\text{-}A}$** and **$P_{294\text{-}B}$**: the way A is leading to higher content than the way B, in both ^{29}Si (ERETIC method) and ^{1}H NMR. However, probably due to the presence of impurity, the ERETIC method gave half of the expected quantity: 0.26 mol% and 0.10 mol% instead of 0.5 mol% theoretically for **$P_{335\text{-}A}$** and **$P_{335\text{-}B}$** respectively. Indeed, this method is based on a precise weight of the polymer, so the presence of impurity in the polymer affect directly the result since the weight take in account the polymer plus the possible impurities. However, the ^{1}H NMR quantification was based on relative comparison of the integration of PEG chain peak and methyl silyl peak. No precise weighting of the polymer was required to get the ^{1}H NMR spectrum and so the quantification may be closer to the reality: 0.61 mol% and 0.29 mol% for **$P_{335\text{-}A}$** and **$P_{335\text{-}B}$** respectively, which means twice the ERETIC method results.

P_{349}, **P_{350}** and **P_{351}** were characterized by GPC, ^{29}Si (ERETIC method) and ^{1}H NMR. The Mw determined by GPC analysis (Figure 149) were coherent and in the same range for **$P_{294\text{-}A}$** and **$P_{335\text{-}A}$** (15.7 and 36.9 kDa respectively) both polymerized by the same way A. Also, the experiment mol% of compound **14** determined by ERETIC method gave results really close to the theoretical quantity (0.5 mol%): 0.41, 0.49 and 0.44 mol% for **P_{349}**, **P_{350}** and **P_{351}** respectively. This proved that the polymers have been efficiently washed since no impurity seemed to alter the quantification. The incorporation of compound **14** was done with high yield. These results were confirmed by the ^{1}H NMR quantification: 0.50, 0.53 and 0.32 mol% for **P_{349}**, **P_{350}** and **P_{351}** respectively.

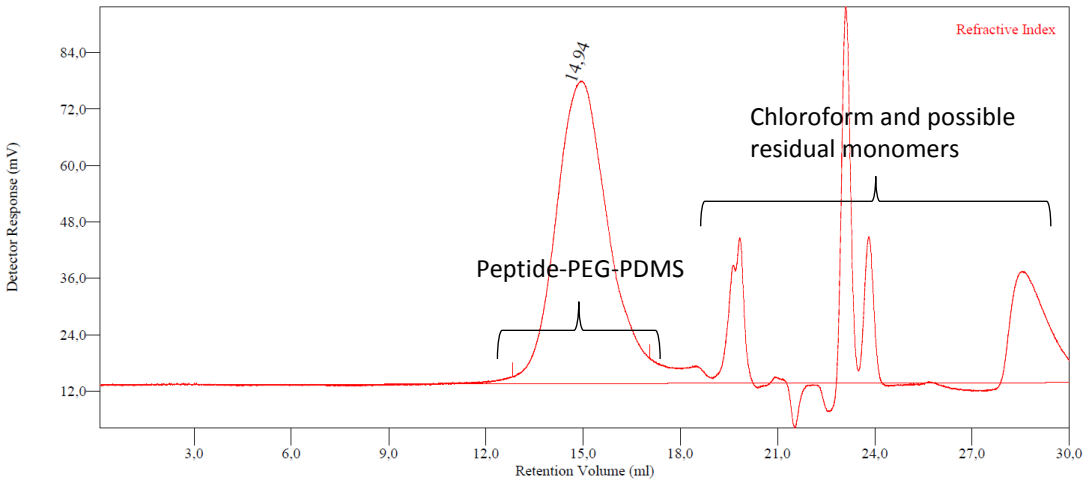

*Figure 149. GPC chromatogram (Chloroform, 1ml/min, 30°C) of a 5mg/mL solution of a peptide-PEG-PDMS **P_{350}**, filtered with a PTFE 0.45µm filter.*

Summing up, we determined suitable compositions of peptide-PEG-PDMS obtained by way A. They gave polymer chain lengths comparable to PEG-PDMS obtained in chapter 5 (15.7 kDA for 0.5 mol% of compound **14,** and 14.0 kDa for 1 mol% of compound **14**). The yield of incorporation of the compound **14** was around 50% for **P_{335}** and around 90% for **P_{349}** **P_{350}** and **P_{351}**. As we got peptide-PEG-PDMS with size and composition close to what we were looking for, the next step was the preparation of NPs as previously done in chapter 5.

c. *Preparation of His/Lys peptide PEG PDMS NPs*

Following previously established protocol (chapter 5), NPs from polymers **$P_{335\text{-}A}$** and **$P_{335\text{-}B}$** (synthesized following by methods A and B respectively) were prepared. They have been formed into water with a 1mg/mL concentration of polymer, agitated by vortex and sonicated for 5min. The resulting NPs were analyzed by both DLS and NTA, to get the size, shape, and concentration of NPs formed, and by zeta potential (Table 20).

Table 20. Peptide-PEG-PDMS NPs characterization

Sample	mol% of –O-Si(Me)-PEG-F		Polymer size by GPC (in kDa) [b]	NPs size by DLS (in nm)	Zeta potential (in mV)	NPs size by NTA (in nm)
	Theoretical	Experimental [a]				
$NP_{335\text{-}A}$	0.5	0.26	36.9	129 and 472	-35	70,1
$NP_{335\text{-}A}$	0.5	0.1	60.5	138 and 786	-40	80,9

a: Experimental percentage obtained by ERETIC method by ^{19}F NMR; b: GPC performed in chloroform

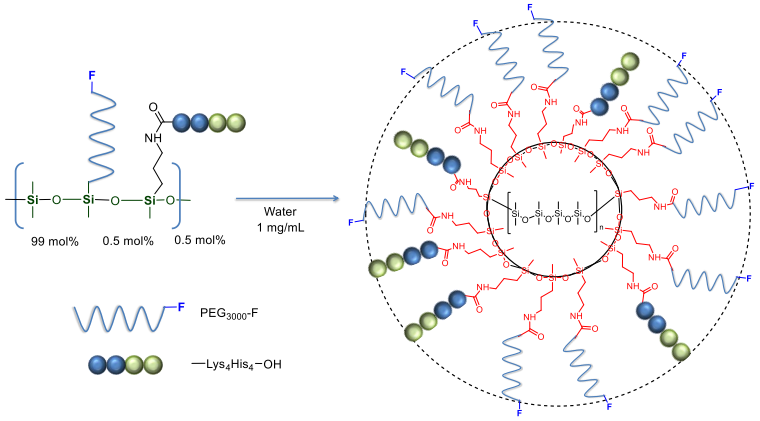

Figure 150. Preparation of $NP_{335\text{-}A}$ and $NP_{335\text{-}B}$.

One of the main characteristic of a good candidate as a vector is its cationic properties to be able to complex the negatively charged siRNA. Unfortunately, in our case, despite the cationic peptides, **$NP_{335\text{-}A}$** and **$NP_{335\text{-}B}$** showed a negative zeta potential. This could be due to the presence of PEG chain which may mask the basic groups from the exterior of the corona. We then tried to prepare the same types of polymers without the PEG macromonomers, only using DCDMS and hybrid peptide **2** (1 mol%). Polymer **P 336** was soluble neither in water nor chloroform, and so no NPs could be prepared from it.

Summing up, even if NPs were of acceptable size and shapes (i.e. round particles around 100nm), the negative zeta potential was a major brake to prepare polyplexes.

III. Direct synthesis of His/Lys-polysiloxane polyplexes with siRNA

To overcome the zeta potential problem encountered with peptide-PEG-PDMS NPs and the solubility problem observed for peptide-PEG-PDMS **P_{336}**, we decided to get rid of DCDMS and hybrid PEG and to use exclusively hybrid peptide **2** to form the functional polymer (Figure 152). This idea opened the possibility of an *in situ* polymerization/complexation to form polyplexes in one pot.

We also wanted to compare such direct preparation with the complexation of siRNA with a pre-formed peptide-polymer (Figure 153).

a. *Synthesis of His/Lys-polysiloxane siRNA polyplexes: pre-polymerization method*

The silylated peptide **2**, was dissolved in water (at 5.10^{-2} mol/L) and polymerized for 24h in RNAse free water at pH7.4 at room temperature. The resulting polymer was characterized by DLS and zeta potential (Table 21). Polymer **P_{327}** formed NPs around 197 nm, but with a wide polydisperisty: PDI=0.45. On the contrary of **$NP_{335\text{-}A}$** and **$NP_{335\text{-}B}$**, and as expected, the zeta potential measurement was clearly positive: +25mV.

Table 21. Characterizations of His/Lys-polysiloxane and its self-assembly into NPs.

Sample	Polymer size by GPC (in kDa)[a]	NPs size by DLS (in nm)	PDI associated with DLS	Zeta potential (in mV)
P_{327}	n.d.	~197	0.45	+25

a: GPC performed in acetate buffer at pH 4.6
n.d.: non-determined

This *preformed* peptide His/Lys-polysiloxane have been characterized by DLS, zeta potential but also Transmission electron microscopy (TEM) to get images of the resulting structure. Indeed, the DLS is showing NPs around 197 nm so we wanted to check if they were possible to be seen by TEM.

The images of **P_{327}** are showing NPs around 150 nm, so coherent to DLS results. Therefore, we can notice an original organization of the polymer that suggest an auto-assembly while the polymer is growing. Some NPs are able to be distinguish and then linker by polymer chain probably.

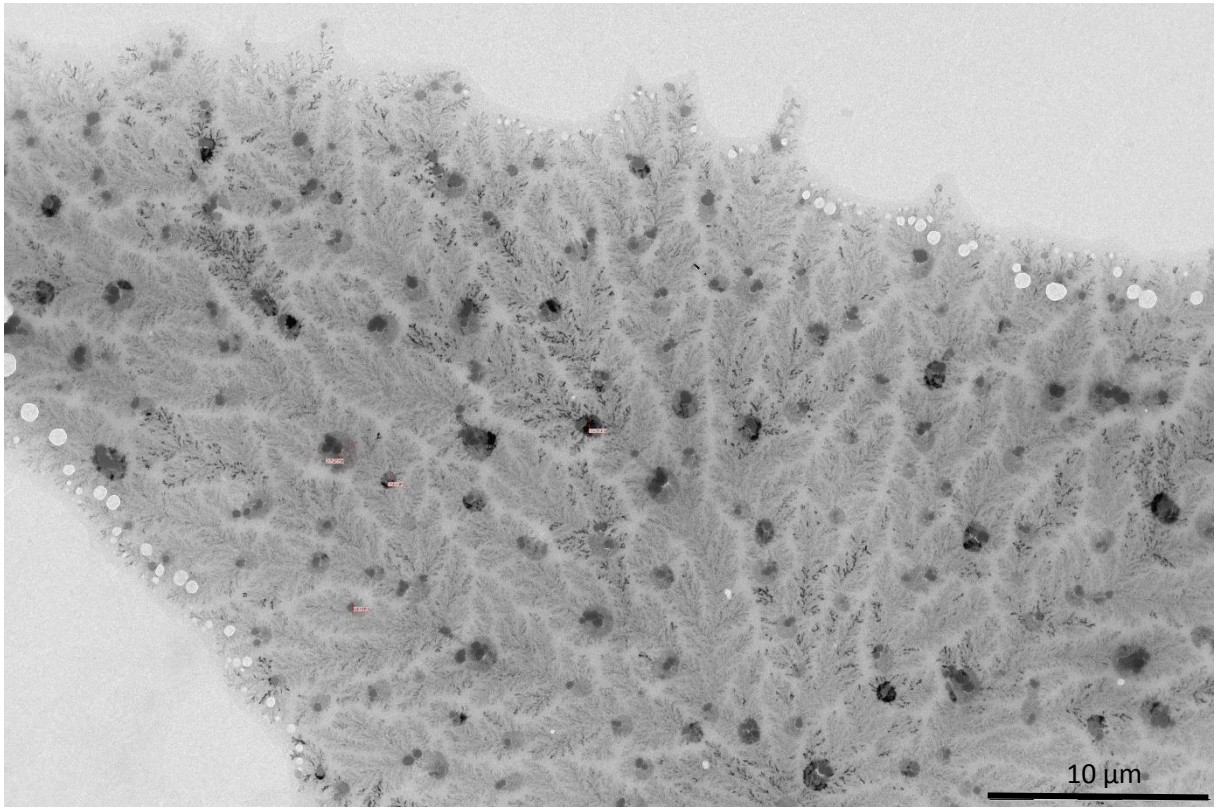

*Figure 151. TEM image of the preformed polymerization of compound **2** forming His/Lys-polysiloxane.*

The NPs formed from $\mathbf{P_{327}}$ were mixed with siRNA to prepare polyplexes. To measure the ability to complex with siRNA, agarose gel electrophoresis (AGE) experiments were performed, with various ratios of NPs/siRNA (Figure 152).

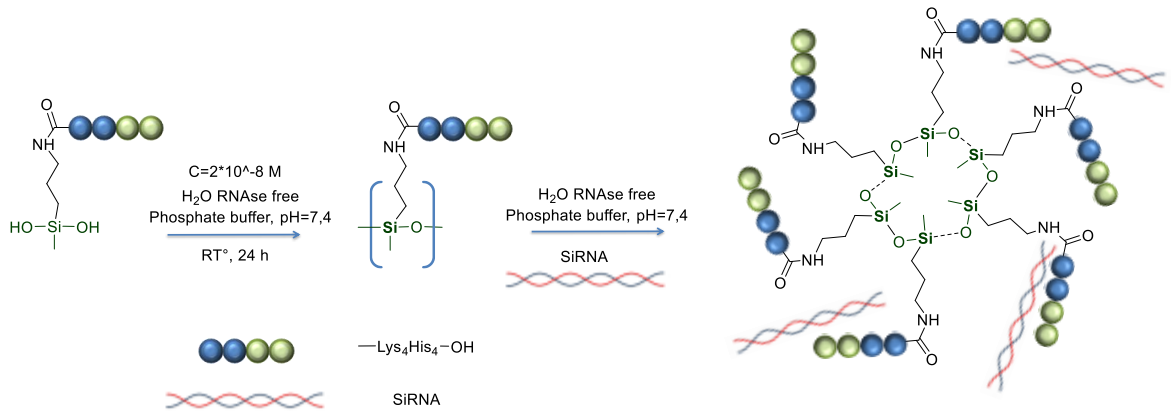

Figure 152. Synthesis of His/Lys-polysiloxane siRNA polyplexes: pre-polymerization method.

b. *Synthesis of His/Lys-polysiloxane siRNA polyplexes: in situ method*

In contrast to the 2-steps method, we tried a direct one-pot synthesis of the polyplexe by polymerizing the peptide in presence of the siRNA (Figure 153). Noteworthy, as the SiRNA is sensitive to elevated temperature, the polymerization was performed at room temperature during 24 hours, instead of 60 °C. Hybrid peptide **2** was dissolved in RNAse free water, at pH 7.4, at 5.10^{-2} mol/L and then mixed with siRNA at various ratio.

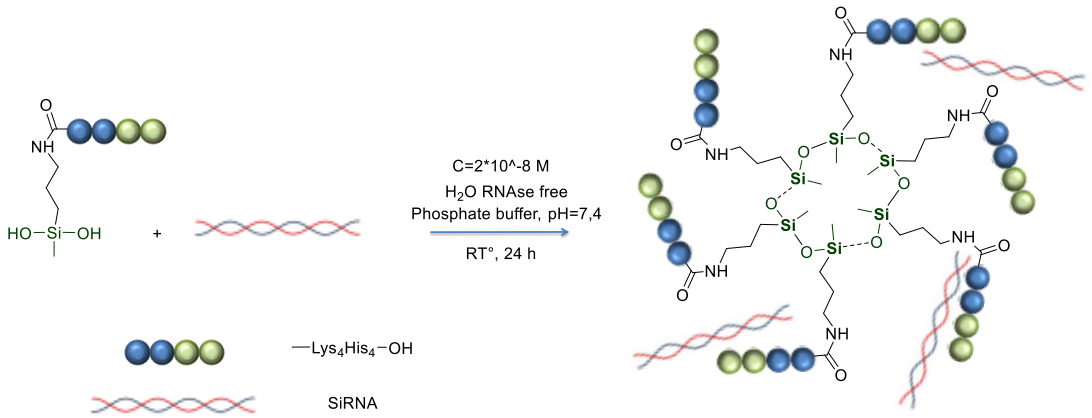

Figure 153. Synthesis of silicone-based peptide polymer polyplexes: in situ method.

At pH 7.4, we considered 4 positives charges on compound **2:** one from each Lys side chain. Indeed, the pKa of Lys side chain is 10, meaning that primary amines were protonated, which was not the case for imidazoles (pKa = 6.5).

This number of positive charges was necessary to calculate the N/P ratio between the peptide and the siRNA. The N/P terminology corresponds to the ratio of the quantity of amine (N) present in the vector, over the quantity of phosphate (P) related to the siRNA.

The siRNA had 21 negative charges on each strand due to phosphate groups for a total of 42 negative charges. We varied the N/P ratio from 2 to 40 to prepare polyplexes. A ratio of 2 meant that there were twice more positive charges than negative one. Since the peptide had 4 positive charges and the siRNA 21 negative charge par strand so 42 in total, a ratio N/P=2 corresponded to 21 peptide sequences for one siRNA double strand moiety.

c. *Polyplexes characterization*

Polyplexes were characterized by agarose gel electrophoresis (AGE) using a 2 w% agarose gel, at 50 V for 30 min.[428–430] An agarose gel with several normalized wells is placed in an electrophoresis tank cover by a Tris/Borate/EDTA (TBE) buffer then an electric courant in going from one side to another. As soon as an electric courant is applied to the gel, the siRNA goes from the well in direction of the positive electrode of the tank.

In our case, we placed a certain quantity of siRNA and polymeric vectors (obtained either as *preformed* polymers or from the *in situ* polymerization), as well as GelRed, (i.e. 5,5'-(6,22-dioxo-11,14,17-trioxa-7,21-diazaheptacosane-1,27-diyl)bis(3,8-diamino-6-phenylphenanthridin-5-ium) iodide), a fluorophore which intercalates with the base pair of the siRNA, making the non-complexed siRNA visible under UV lamp at 312 nm. On the contrary, the siRNA trapped in a polyplex was no more accessible form intercalant and should not be detected, preventing also the siRNA from migrating. Moreover, the overall charge of a polyplex should be slightly positive due to the excess of polymer.

As reference, the first well was filled up with a DNA ladder, composed of double-stranded DNA fragments with known Mw. This ladder was useful to verify that the spots observed on the gel correspond to the Mw expected for free siRNA (i.e around 13,300 Mw). Two negative controls were added: siRNA alone and peptide-polymeric material alone. Each different N/P ratio occupied a well.

At the end of the migration, the gel was revealed under UV (312 nm) and a picture was taken. The ideal N/P for complexation was determined for the well in which no free SiRNA was detected.

We compared the polyplexes formed by the two methods (*in situ* polymerization or *preformed* polymerization), with N/P ratio from 2 to 40. AGE showed that the *in situ* method enable a much better complexation than the two step method using pre-formed NPs (Figure 154). Indeed, complexation was nearly completed at N/P = 20 for the *in situ* method and was not achieved even at N/P=40 for the *preformed* method. Moreover, at such ratio for the *preformed* method, a degradation of the siRNA was observed, witnessed by the enlargement and the blurriness of the spot.

The *in situ* method was chosen for the following experiments.

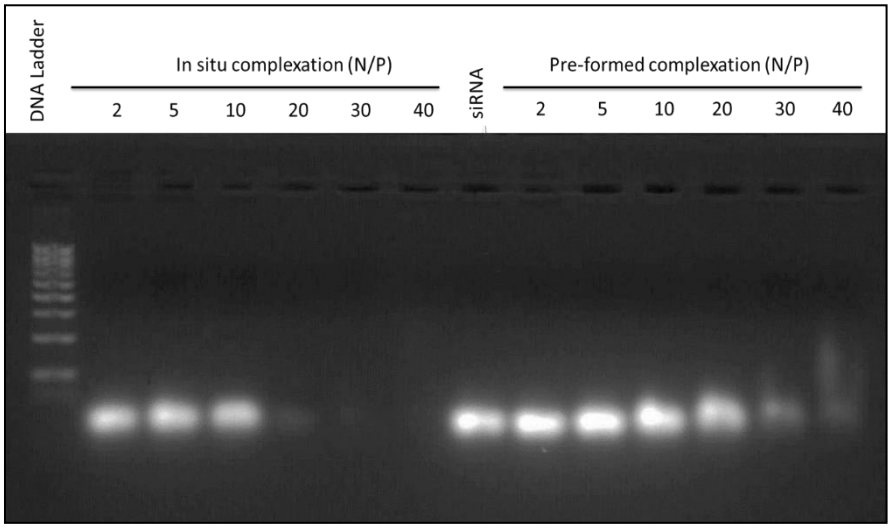

Figure 154. AGE results of siRNA binding by two different methods: in situ and preformed polymer.

We then tried to observe the shape and the size of the objects formed by *in situ* complexation. We were pleased to observe by TEM spherical objects from ~100 to 170 nm (Figure 155). This size is probably underestimated due to the drying step of the TEM grid sample preparation. Indeed, the sample **$NP_{248\text{-}20}$** had an average size of 220 nm by DLS measurement vs 130 nm by TEM images analysis. On the contrary, the size obtained by DLS may be overestimated due to the hydrodynamic radius taken in account.

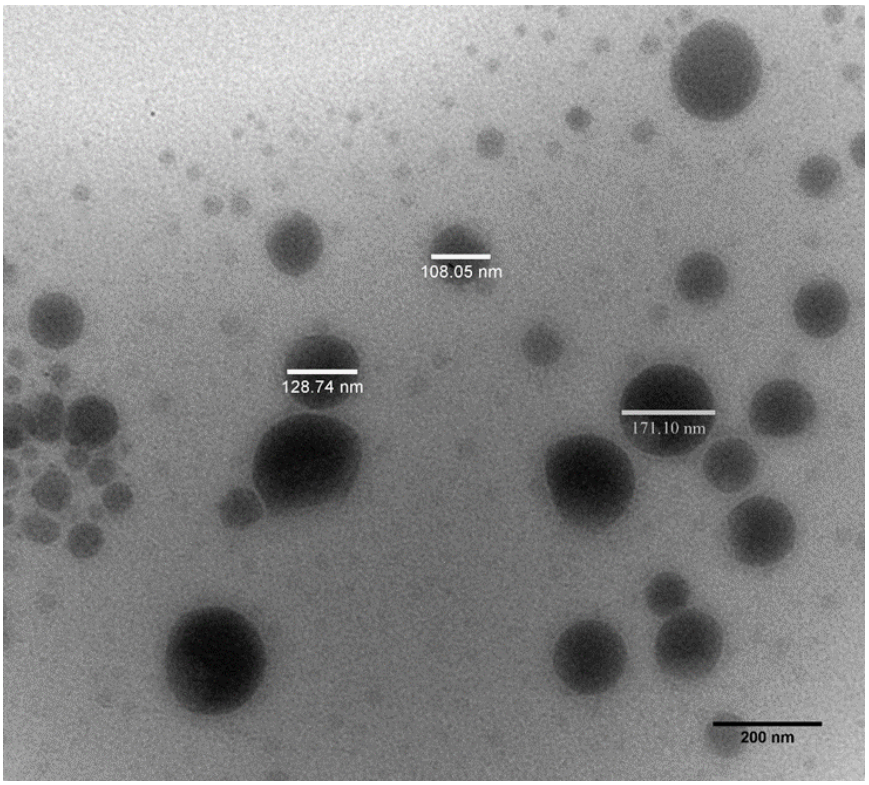

Figure 155. TEM image of ***NP$_{428-20}$*** *polyplexe at N/P=20 obtained by in situ polymerization*

The size of these polyplexes was also determined by DLS. The DLS results were in agreement with the TEM observation and showed no big difference between the different ratios. It indicated diameters around 220nm, quite close to the size of previous NPs obtained from the '*preformed* method' without any siRNA: 197 nm. These results suggested that the siRNA was no disturbing the formation of NPs during the polymerization.

Table 22. DLS measurement of different ratio of polypeptides in the polyplexes obtained by in situ polymerization.

Samples	N/P ratio	NPs size by DLS (in nm)	PDI[a]
NP_{428-20}	20	216,66 ±11,96	0,179 ± 0,086
NP_{428-30}	30	225,5	0,172
NP_{428-40}	40	233,1	0,215

At this point, we showed that hybrid peptide **2**, forming His/Lys-polysiloxane, was able to form polyplexes at N/P 20 ratio which correspond to 210 peptides for a single chain of siRNA.

One important question was to know if the polymerization had an impact or not on the formation of the particles. To decipher that behavior, we synthesized a control hybrid peptide which was not able to polymerize. Hybrid peptide **2bis** (Figure 156) was prepared in the same way than **2** except that by silylation was performed with isocyanatopropyl trimethylsilane. Consequently, **2bis** did not have any silanol group; the trimethylsilane function being not reactive.

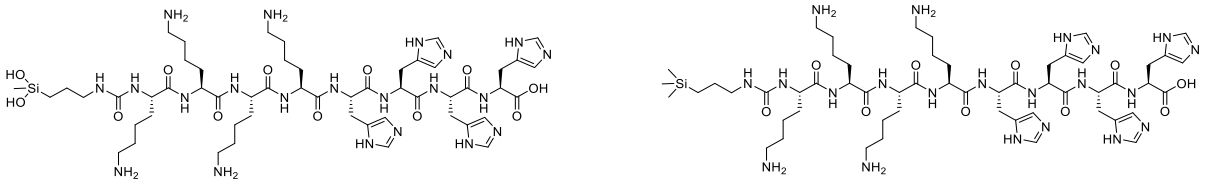

*Figure 156. Scheme of the compound **2** and the analogue control (non polymerizable, non reactif), **2bis.***

We prepared in parallel polyplexes either with **2** or **2b** at different N/P ratios by *in situ* method. AGE analyses results were clear: the peptide **2b** was not able to polymerize and was not able to form any complex with the siRNA even at high N/P ratio (Figure 157). (Noteworthy, in this experiment, we obtained a better complexation of siRNA from N/P ratio of 10 with compound **2**.)

This result was the prouf the polymer is required to form polyplexes. Taken together with the bad results obtained with the *preformed* polymerization method, this observation also suggests that polymerization could occur in thigh association with the siRNA and that the genetic material could behave as a template for the peptide polymerization. This could be verified by comparison between the size of peptide polymers polymerized with and without siRNA.

Indeed, the size of the polymer chain issued from the *preformed* method (polymerization of the compound **2** without siRNA) are about to be determined by GPC and ^{29}Si NMR The same characterizations should be done with the polymer issued of the polymerization *in situ* (polymerization in presence of siRNA), in order to be able to compare them and so highlight the role of the siRNA in the polymerization: either leading to higher or smaller polymer chain length. However, to do so, the siRNA needs to be extracted from the polymer formed *in situ* to make sure it does not alter the characterizations. These experiments are still to be done.

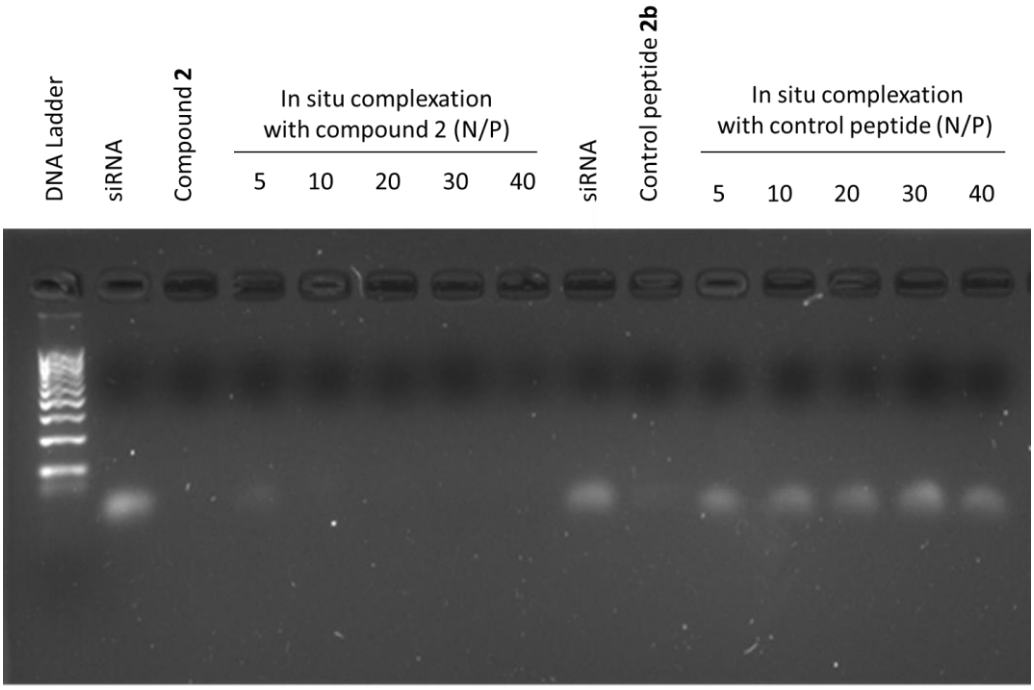

*Figure 157. AGE of siRNA binding with hybrid dihydroxysilyl peptide **2** and hybrid trimethylsilyl peptide control **2b**.*

IV. Polyplexes stability assays

Forming polyplexes is just the first step. In one hand, polyplexes should be stable enough to protect the siRNA during its circulation before reaching its target. In the other hand, as already explained, dissociation should happen to release the siRNA in the cytosol. If the vector present too strong binding affinity with the siRNA is will be never released at its destination.

To perform stability assays, a polyanionic biopolymer was used as competitor of the siRNA: the heparin (Figure 158).[384,431] The presence of heparin was supposed to disturb the polyplex formed with peptide polymer obtained by *in situ* method. The peptide-polymer could preferably form another complex with the heparin instead of forming a polyplex with the siRNA.

The heparin was either added directly during the polymerization of the compound **2** in presence of siRNA, so creating a direct competition (method 1); or added after the formation of the polyplexe (24h after the polymerization of **2** in presence of siRNA) (method 2). Heparin was added in several quantities from 0 to 40 eq. of heparin on the N/P=20 polyplexes formed with compound **2**.

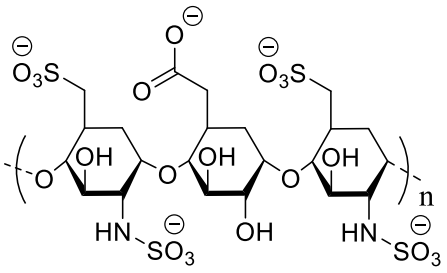

Figure 158. Heparin structure in solution.

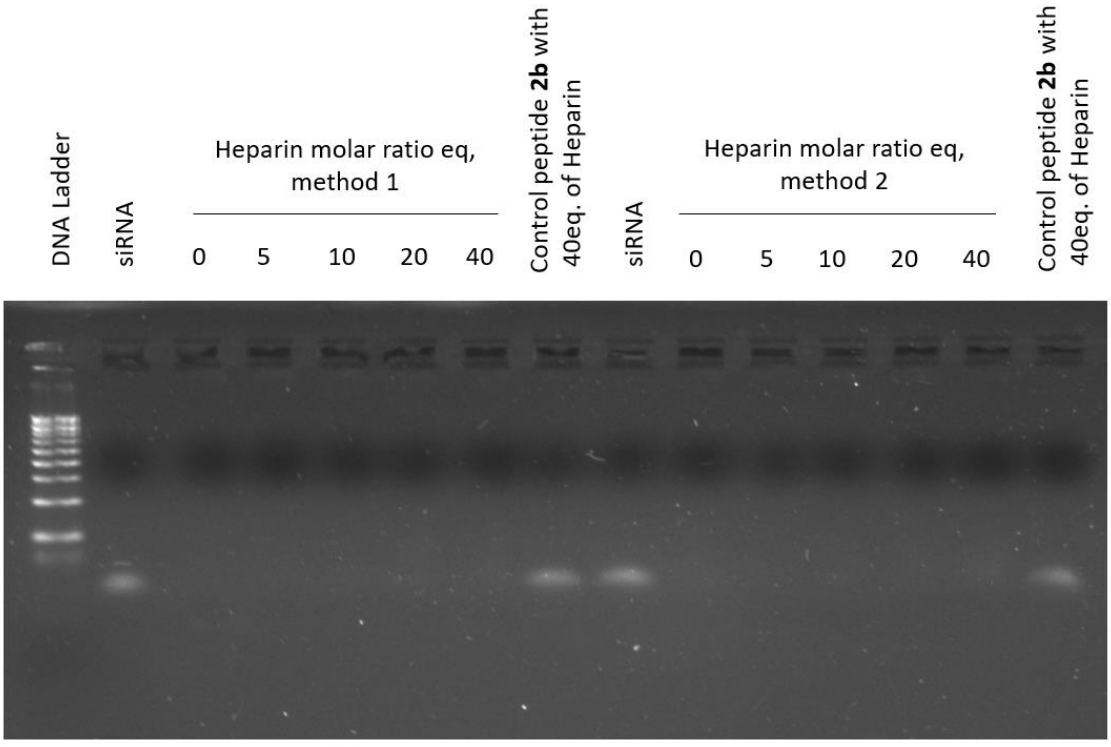

Figure 159. AGE dissociation essays on polyplexes by in situ method, with different ratio of heparin and by two methods: direct addition of heparin during the in situ polymerization, method 1; or i) formation of the polyplexes in situ for 24h, ii) addition of heparin 150min before the AGE, method 2.

The results were highly surprising as no dissociation was observed. In any case, the siRNA remained trapped in the polyplexe (

Figure 159). That is both a good and a bad news: our polyplexes are really stable, but are probably too stable to release efficiently the siRNA in the cytosol.

Several experiments are ongoing: first we want to prove the templating effect of the siRNA on the polymerization. To do so we need to separate the siRNA form the His/Lys-polysiloxane polymerized *in situ* to perform a GPC analysis, in order to compare the size of the polymer formed with and without the presence of siRNA during the polymerization.

Then, we need to fix the release issue. If we do not succeed to find a proper way to release the siRNA from the *in situ* formed polyplexes, some modification will have to be done on the polyplexes to decrease their stability. To do so, the silylated peptide could be modified. One possibility is to perform a silylation by hydroxydimethylsilane group at each extremity to lead to a linear polymer which could not be as efficient as the comb-like one to complex siRNA. We could also use different ratio of compound **3** and **4** or we could copolymerize it with other silylated, less cationic peptides having less affinity with the siRNA. Finally, the introduction of cleavable sequences between the peptide sequence and the silane group, e.g. disulfide bridges for example, could help the release of the siRNA.

Conclusion and Perspectives

Conclusion and Perspectives

One of the objectives of this PhD was to set up a new method for the preparation of hybrid silylated molecules. We imagined in **chapter 2** a strategy based on hydrosilylation of an unsaturated bond to obtain silylated peptides on solid support. Theoretically orthogonal, this strategy was attractive. Unfortunately, the scope of the reaction was not as wide as we expected and only chlorodimethylsilane were successfully introduced on double bonds, especially on AllylGly moiety. This was due to the unwanted reduction of the unsaturated bond happening when the silane was not reactive enough and so making the side reaction reactivity equivalent or even higher than the hydrosilylation one. Nevertheless, we proposed that this side reaction could be diminished by limiting the presence of water, and the yield could be improved by changing the nature of the catalyzer; either other Pt-based catalyst, like NHC-Pt complex, or other metal-based catalyst such as Ruthenium for example.

We prepared different types of hybrid blocks, including peptides, drugs and dyes. It is worth noting that, due to time constraints, some of the hybrid silylated biomolecules presented in **chapter 3** have not been used yet for the synthesis of hybrid materials. For example, DOTA hybrid were particularly difficult to synthesize due to the solubility constrains and the hydrolysis of the DOTA GA anhydride derivative. This hybrid block will be of high interest to prepare NPs for MRI imaging. Also, two other drugs, camptothecin and methotrexate, could be incorporated in the design of drug delivery systems including silicone-based NPs or silica NPs. Besides the panel of building block presented in **chapter 3**, it could be of interest to silylate new categories of biomolecules including biopolymers, such as chitosan for example. Indeed, new hybrid hydrogel could be designed from such silylated biopolymer.

The **chapter 4** showed the first example of direct synthesis of bioactive PDMS material using a bottom-up strategy. The copolymerization of DCDMS with peptide hybrid macromonomers for the design of peptide-PDMS materials, in opposition to the grafting method described until now. The variation of the quantity of functionalized silane monomers, Si-Vinyl and Si-H, enabled the modulation of the stiffness of the resulting PDMS material by hydrosilylation. Therefore, the quantity of peptide macromonomer also modulated the biological properties of the materials.

We also showed that it was possible to prepare hybrid PDMS NPs. The **chapter 5** disclosed the optimization of the protocol and the polymer composition, to get PEG-PDMS NPs with a reproducible size and shape. The hydrophilic/hydrophobic balance of the polymer was the key point of theses syntheses. Once the optimization done, the composition modified to afford biological properties: first targeting (with the cRGD as a ligand) and then cytotoxicity (with MTX as drug). Unfortunately, we could not prove the benefit of cRGD ligands on PDMS NPs as no specific binding was showed compared to control particles. The quantity of cRGD must be probably increased. The preliminary biological test, of cell viability, showed a validation of the activity drug-modified NPs. Even if so far the activity of the drug containing NPs is not as good as the free drug, we got a proof of concept so further assays will be done.

In the same way, theranostic NPs could also be synthesized by combining DOTA hybrid chelator with hybrid drugs and targeting ligands. Du to time constraints hybrid camptothecin and temozolomide were not included in the preparation of NPs. Drug-PDMS NPs will be synthesized an evaluated on cancer cell lines in collaboration with “Oncopharmacotoxicologie cellulaire et moléculaire” team of IBMM and IAB in Grenoble. The release of the drug from the PDMS NPs will also be studied. It is worth noting that the hybrid blocks we prepared could be used directly for the preparation of multifunctional silica NPs. Indeed, hybrid biomolecule could be grafted on surface or well defined silica NPs or introduced in the core during the Stoebner process of formation of NPs.

The last part of the PhD, the **chapter 6**, was dedicated to explore the possibility to form polyplexes between cationic peptide-polymers and siRNA. We established a proof of concept. We first synthesized NPs based on the

sample protocol then the previous chapter by replacing drug macromonomer by His and Lys-rich hybrid peptide, keeping the PEG macromonomer to get the NPs. But, the polymerization of the His_4Lys_4 peptide macromonomer alone showed better complexation results than the PDMS NPs, especially when involved in a *in situ* complexation/polymerization in presence of siRNA which yielded very stable polyplexes. Noteworthy, a control trimethylsilyl peptide macromonomer was unable to form complex with siRNA, meaning that the polymerization was needed to create polyplexes.

Surprisingly, the polyplexes prepared from an *in* situ method have a strong affinity with the siRNA and could not be separated by heparin. This result is very interesting as far as stability of polyplexes is concerned. However, it is an issue for the release and the dissociation of the genetic material. Thus, to prove the impact of the presence of siRNA during the polymerization of the peptide macromonomer, and so highlight its possible templating effect, we need to find a method the extracte the siRNA from the *in situ* complex.

First, we plan to make some supplementary dissociation experiments (e.g. chemical degradation of siRNA by use of strongly acidic conditions, used of dextran sulfate instead of heparin). In addition, several improvements could be envisioned. First, the selected peptide can be silylated at each of its extremities in order to lead to a linear polymer rather than the comb-like structure we obtained. The affinity with the siRNA could be significantly different. Then, various ratio of the Lys_4 or His_4 hybrid peptides could be tested for complexation with siRNA and the stability of the resulting polyplexes could be evaluated. Last, we could also introduce a proportion of less efficient peptide for complexation, containing a small proportion of non-charged or anionic residues.

References

(1) Martin, J.; Martinez, J.; Mehdi, A.; Subra, G. Silicone Grafted Bioactive Peptides and Their Applications. *Curr. Opin. Chem. Biol.* **2019**, *52*, 125–135. https://doi.org/10.1016/j.cbpa.2019.06.012.
(2) Deming, T. J. Synthetic Polypeptides for Biomedical Applications. *Prog. Polym. Sci.* **2007**, *32* (8), 858–875. https://doi.org/10.1016/j.progpolymsci.2007.05.010.
(3) Kanasty, R.; Dorkin, J. R.; Vegas, A.; Anderson, D. Delivery Materials for SiRNA Therapeutics. *Nat. Mater.* **2013**, *12* (11), 967. https://doi.org/10.1038/nmat3765.
(4) Waterhouse, S. H.; Gerrard, J. A. Amyloid Fibrils in Bionanotechnology. *Aust. J. Chem.* **2004**, *57* (6), 519–523. https://doi.org/10.1071/ch04070.
(5) Hoffman, A. S.; Stayton, P. S. Bioconjugates of Smart Polymers and Proteins: Synthesis and Applications. *Macromol. Symp.* **2004**, *207* (1), 139–152. https://doi.org/10.1002/masy.200450314.
(6) Klok, H.-A. Biological–Synthetic Hybrid Block Copolymers: Combining the Best from Two Worlds. *J. Polym. Sci. Part Polym. Chem.* **2005**, *43* (1), 1–17. https://doi.org/10.1002/pola.20527.
(7) Harris, J. M.; Chess, R. B. Effect of Pegylation on Pharmaceuticals. *Nat. Rev. Drug Discov.* **2003**, *2* (3), 214–221. https://doi.org/10.1038/nrd1033.
(8) Rösler, A.; Klok, H.-A.; Hamley, I. W.; Castelletto, V.; Mykhaylyk, O. O. Nanoscale Structure of Poly(Ethylene Glycol) Hybrid Block Copolymers Containing Amphiphilic β-Strand Peptide Sequences. *Biomacromolecules* **2003**, *4* (4), 859–863. https://doi.org/10.1021/bm034058s.
(9) Shi, J.; Votruba, A. R.; Farokhzad, O. C.; Langer, R. Nanotechnology in Drug Delivery and Tissue Engineering: From Discovery to Applications. *Nano Lett.* **2010**, *10* (9), 3223–3230. https://doi.org/10.1021/nl102184c.
(10) Bae, Y.; Nishiyama, N.; Fukushima, S.; Koyama, H.; Yasuhiro, M.; Kataoka, K. Preparation and Biological Characterization of Polymeric Micelle Drug Carriers with Intracellular PH-Triggered Drug Release Property: Tumor Permeability, Controlled Subcellular Drug Distribution, and Enhanced in Vivo Antitumor Efficacy. *Bioconjug. Chem.* **2005**, *16* (1), 122–130. https://doi.org/10.1021/bc0498166.
(11) Brem, H.; Gabikian, P. Biodegradable Polymer Implants to Treat Brain Tumors. *J. Controlled Release* **2001**, *74* (1), 63–67. https://doi.org/10.1016/S0168-3659(01)00311-X.
(12) Pichavant, L.; J. López-González, M.; Favereaux, A.; Héroguez, V. Thermosensitive Polynorbornene Poly(Ethylene Oxide) Nanoparticles Loaded with OligoDNAs: An Innovative Approach for Acting on Cancer-Associated Pain. *Polym. Chem.* **2018**, *9* (3), 362–371. https://doi.org/10.1039/C7PY01889D.
(13) Lee, E. S.; Na, K.; Bae, Y. H. Doxorubicin Loaded PH-Sensitive Polymeric Micelles for Reversal of Resistant MCF-7 Tumor. *J. Controlled Release* **2005**, *103* (2), 405–418. https://doi.org/10.1016/j.jconrel.2004.12.018.
(14) Mout, R.; F. Moyano, D.; Rana, S.; M. Rotello, V. Surface Functionalization of Nanoparticles for Nanomedicine. *Chem. Soc. Rev.* **2012**, *41* (7), 2539–2544. https://doi.org/10.1039/C2CS15294K.
(15) Echalier, C.; Levato, R.; A. Mateos-Timoneda, M.; Castaño, O.; Déjean, S.; Garric, X.; Pinese, C.; Noël, D.; Engel, E.; Martinez, J.; et al. Modular Bioink for 3D Printing of Biocompatible Hydrogels: Sol–Gel Polymerization of Hybrid Peptides and Polymers. *RSC Adv.* **2017**, *7* (20), 12231–12235. https://doi.org/10.1039/C6RA28540F.
(16) Khan, F.; Tanaka, M.; Ahmad, S. R. Fabrication of Polymeric Biomaterials: A Strategy for Tissue Engineering and Medical Devices. *J. Mater. Chem. B* **2015**, *3* (42), 8224–8249. https://doi.org/10.1039/C5TB01370D.
(17) Goddard, J. M.; Hotchkiss, J. H. Polymer Surface Modification for the Attachment of Bioactive Compounds. *Prog. Polym. Sci.* **2007**, *32* (7), 698–725. https://doi.org/10.1016/j.progpolymsci.2007.04.002.
(18) Moy, V.; Florin, E.; Gaub, H. Intermolecular Forces and Energies between Ligands and Receptors. *Science* **1994**, *266* (5183), 257–259. https://doi.org/10.1126/science.7939660.
(19) Hwang, I.-T.; Kim, D.-K.; Jung, C.-H.; Lee, J.-S.; Choi, J.-H.; Nho, Y.-C.; Suh, D.-H.; Shin, K. Patterned Immobilization of Biomolecules on a Polymer Surface Functionalized by Radiation Grafting. *J. Nanosci. Nanotechnol.* **2011**, *11* (5), 4562–4566. https://doi.org/10.1166/jnn.2011.3643.
(20) Jiang, H.; Xu, F.-J. Biomolecule-Functionalized Polymer Brushes. *Chem. Soc. Rev.* **2013**, *42* (8), 3394. https://doi.org/10.1039/c2cs35453e.
(21) Robson Marsden, H.; Kros, A. Polymer-Peptide Block Copolymers – An Overview and Assessment of

Synthesis Methods. *Macromol. Biosci.* **2009**, *9* (10), 939–951. https://doi.org/10.1002/mabi.200900057.
(22) Wilson, P. Synthesis and Applications of Protein/Peptide-Polymer Conjugates. *Macromol. Chem. Phys.* **2017**, *218* (9), n/a-n/a. https://doi.org/10.1002/macp.201600595.
(23) A. Paik, B.; R. Mane, S.; Jia, X.; L. Kiick, K. Responsive Hybrid (Poly)Peptide–Polymer Conjugates. *J. Mater. Chem. B* **2017**, *5* (42), 8274–8288. https://doi.org/10.1039/C7TB02199B.
(24) Samad, A. A.; Bethry, A.; Koziolová, E.; Netopilík, M.; Etrych, T.; Bakkour, Y.; Coudane, J.; Omar, F. E.; Nottelet, B. PCL–PEG Graft Copolymers with Tunable Amphiphilicity as Efficient Drug Delivery Systems. *J. Mater. Chem. B* **2016**, *4* (37), 6228–6239. https://doi.org/10.1039/C6TB01841F.
(25) Otsuka, H.; Nagasaki, Y.; Kataoka, K. PEGylated Nanoparticles for Biological and Pharmaceutical Applications. *Adv. Drug Deliv. Rev.* **2003**, *55* (3), 403–419. https://doi.org/10.1016/S0169-409X(02)00226-0.
(26) Chawla, K.; Lee, S.; Lee, B. P.; Dalsin, J. L.; Messersmith, P. B.; Spencer, N. D. A Novel Low-Friction Surface for Biomedical Applications: Modification of Poly(Dimethylsiloxane) (PDMS) with Polyethylene Glycol(PEG)-DOPA-Lysine. *J. Biomed. Mater. Res. A* **2009**, *90A* (3), 742–749. https://doi.org/10.1002/jbm.a.32141.
(27) Harris, J. M.; Chess, R. B. Effect of Pegylation on Pharmaceuticals. *Nat. Rev. Drug Discov.* **2003**, *2* (3), 214–221. https://doi.org/10.1038/nrd1033.
(28) Ahangaran, F.; Navarchian, A. H.; Picchioni, F. Material Encapsulation in Poly(Methyl Methacrylate) Shell: A Review. *J. Appl. Polym. Sci.* **2019**, *136* (41), 48039. https://doi.org/10.1002/app.48039.
(29) Teeka, P.; Chaiyasat, A.; Chaiyasat, P. Preparation of Poly (Methyl Methacrylate) Microcapsule with Encapsulated Jasmine Oil. *Energy Procedia* **2014**, *56*, 181–186. https://doi.org/10.1016/j.egypro.2014.07.147.
(30) Lasprilla, A. J. R.; Martinez, G. A. R.; Lunelli, B. H.; Jardini, A. L.; Filho, R. M. Poly-Lactic Acid Synthesis for Application in Biomedical Devices — A Review. *Biotechnol. Adv.* **2012**, *30* (1), 321–328. https://doi.org/10.1016/j.biotechadv.2011.06.019.
(31) Bhatt, S.; Pulpytel, J.; Arefi-Khonsari, F. Low and Atmospheric Plasma Polymerisation of Nanocoatings for Bio-Applications. *Surf. Innov.* **2015**, *3* (2), 63–83. https://doi.org/10.1680/sufi.14.00008.
(32) Vlassov, S.; Oras, S.; Antsov, M.; Sosnin, I.; Polyakov, B.; Shutka, A.; Krauchanka, M. Yu.; Dorogin, L. M. Adhesion and Mechanical Properties of PDMS-Based Materials Probed with AFM: A Review. *Rev. Adv. Mater. Sci.* **2018**, *56* (1), 62–78. https://doi.org/10.1515/rams-2018-0038.
(33) Wolf, M. P.; Salieb-Beugelaar, G. B.; Hunziker, P. PDMS with Designer Functionalities—Properties, Modifications Strategies, and Applications. *Prog. Polym. Sci.* **2018**, *83*, 97–134. https://doi.org/10.1016/j.progpolymsci.2018.06.001.
(34) Eduok, U.; Faye, O.; Szpunar, J. Recent Developments and Applications of Protective Silicone Coatings: A Review of PDMS Functional Materials. *Prog. Org. Coat.* **2017**, *111*, 124–163. https://doi.org/10.1016/j.porgcoat.2017.05.012.
(35) Luo, Q.; Lin, Y.-X.; Yang, P.-P.; Wang, Y.; Qi, G.-B.; Qiao, Z.-Y.; Li, B.-N.; Zhang, K.; Zhang, J.-P.; Wang, L.; et al. A Self-Destructive Nanosweeper That Captures and Clears Amyloid β-Peptides. *Nat. Commun.* **2018**, *9* (1), 1802. https://doi.org/10.1038/s41467-018-04255-z.
(36) Novelli, F.; De Santis, S.; Diociaiuti, M.; Giordano, C.; Morosetti, S.; Punzi, P.; Sciubba, F.; Viali, V.; Masci, G.; Scipioni, A. Curcumin Loaded Nanocarriers Obtained by Self-Assembly of a Linear d,l-Octapeptide-Poly(Ethylene Glycol) Conjugate. *Eur. Polym. J.* **2018**, *98*, 28–38. https://doi.org/10.1016/j.eurpolymj.2017.11.010.
(37) Singh, A.; Corvelli, M.; Unterman, S. A.; Wepasnick, K. A.; McDonnell, P.; Elisseeff, J. H. Enhanced Lubrication on Tissue and Biomaterial Surfaces through Peptide-Mediated Binding of Hyaluronic Acid. *Nat. Mater.* **2014**, *13* (10), 988–995. https://doi.org/10.1038/nmat4048.
(38) Kao, W. J.; Hubbell, J. A. Murine Macrophage Behavior on Peptide-Grafted Polyethyleneglycol-Containing Networks. *Biotechnol. Bioeng.* **1998**, *59* (1), 2–9. https://doi.org/10.1002/(SICI)1097-0290(19980705)59:1<2::AID-BIT2>3.0.CO;2-G.
(39) Remmler, D.; Schwaar, T.; Pickhardt, M.; Donth, C.; Mandelkow, E.; Weller, M. G.; Börner, H. G. On the Way to Precision Formulation Additives: 2D-Screening to Select Solubilizers with Tailored Host and Release Capabilities. *J. Controlled Release* **2018**, *285*, 96–105.

https://doi.org/10.1016/j.jconrel.2018.06.032.
(40) Cheng, D.-B.; Yang, P.-P.; Cong, Y.; Liu, F.-H.; Qiao, Z.-Y.; Wang, H. One-Pot Synthesis of PH-Responsive Hyperbranched Polymer–Peptide Conjugates with Enhanced Stability and Loading Efficiency for Combined Cancer Therapy. *Polym. Chem.* **2017**, *8* (16), 2462–2471. https://doi.org/10.1039/C7PY00101K.
(41) Samsoninkova, V.; L. Venkatareddy, N.; Wagermaier, W.; Dallmann, A.; G. Börner, H. Precision Compatibilizers for Composites: In-between Self-Aggregation, Surfaces Recognition and Interface Stabilization. *Soft Matter* **2018**, *14* (11), 1992–1995. https://doi.org/10.1039/C7SM02518A.
(42) Rho, J. Y.; Brendel, J. C.; MacFarlane, L. R.; Mansfield, E. D. H.; Peltier, R.; Rogers, S.; Hartlieb, M.; Perrier, S. Probing the Dynamic Nature of Self-Assembling Cyclic Peptide–Polymer Nanotubes in Solution and in Mammalian Cells. *Adv. Funct. Mater.* **2018**, *28* (24), 1704569. https://doi.org/10.1002/adfm.201704569.
(43) Sallam, S.; Dolog, I.; Paik, B. A.; Jia, X.; Kiick, K. L.; Wesdemiotis, C. Sequence and Conformational Analysis of Peptide–Polymer Bioconjugates by Multidimensional Mass Spectrometry. *Biomacromolecules* **2018**, *19* (5), 1498–1507. https://doi.org/10.1021/acs.biomac.7b01694.
(44) Sun, Y.; Liu, H.; Cheng, L.; Zhu, S.; Cai, C.; Yang, T.; Yang, L.; Ding, P. Thiol Michael Addition Reaction: A Facile Tool for Introducing Peptides into Polymer-Based Gene Delivery Systems. *Polym. Int.* **2018**, *67* (1), 25–31. https://doi.org/10.1002/pi.5490.
(45) Donahoe, C. D.; Cohen, T. L.; Li, W.; Nguyen, P. K.; Fortner, J. D.; Mitra, R. D.; Elbert, D. L. Ultralow Protein Adsorbing Coatings from Clickable PEG Nanogel Solutions: Benefits of Attachment under Salt-Induced Phase Separation Conditions and Comparison with PEG/Albumin Nanogel Coatings. *Langmuir* **2013**, *29* (12), 4128–4139. https://doi.org/10.1021/la3051115.
(46) Chandna, P.; Khandare, J. J.; Ber, E.; Rodriguez-Rodriguez, L.; Minko, T. Multifunctional Tumor-Targeted Polymer-Peptide-Drug Delivery System for Treatment of Primary and Metastatic Cancers. *Pharm. Res.* **2010**, *27* (11), 2296–2306. https://doi.org/10.1007/s11095-010-0235-2.
(47) Wang, J.; Zaidi, S. S. A.; Hasnain, A.; Guo, J.; Ren, X.; Xia, S.; Zhang, W.; Feng, Y. Multitargeting Peptide-Functionalized Star-Shaped Copolymers with Comblike Structure and a POSS-Core To Effectively Transfect Endothelial Cells. *ACS Biomater. Sci. Eng.* **2018**, *4* (6), 2155–2168. https://doi.org/10.1021/acsbiomaterials.8b00235.
(48) Sethuraman, V. A.; Bae, Y. H. TAT Peptide-Based Micelle System for Potential Active Targeting of Anti-Cancer Agents to Acidic Solid Tumors. *J. Controlled Release* **2007**, *118* (2), 216–224. https://doi.org/10.1016/j.jconrel.2006.12.008.
(49) Baker, L. M. S.; Baker, P. R. S.; Golin-Bisello, F.; Schopfer, F. J.; Fink, M.; Woodcock, S. R.; Branchaud, B. P.; Radi, R.; Freeman, B. A. Nitro-Fatty Acid Reaction with Glutathione and Cysteine: KINETIC ANALYSIS OF THIOL ALKYLATION BY A MICHAEL ADDITION REACTION. *J. Biol. Chem.* **2007**, *282* (42), 31085–31093. https://doi.org/10.1074/jbc.M704085200.
(50) Jing, P.; Rudra, J. S.; Herr, A. B.; Collier, J. H. Self-Assembling Peptide-Polymer Hydrogels Designed From the Coiled Coil Region of Fibrin. *Biomacromolecules* **2008**, *9* (9), 2438–2446. https://doi.org/10.1021/bm800459v.
(51) Zhao, T.; Sellers, D. L.; Cheng, Y.; Horner, P. J.; Pun, S. H. Tunable, Injectable Hydrogels Based on Peptide-Cross-Linked, Cyclized Polymer Nanoparticles for Neural Progenitor Cell Delivery. *Biomacromolecules* **2017**, *18* (9), 2723–2731. https://doi.org/10.1021/acs.biomac.7b00510.
(52) Tsurkan, M. V.; Chwalek, K.; Prokoph, S.; Zieris, A.; Levental, K. R.; Freudenberg, U.; Werner, C. Defined Polymer–Peptide Conjugates to Form Cell-Instructive StarPEG–Heparin Matrices In Situ. *Adv. Mater.* **2013**, *25* (18), 2606–2610. https://doi.org/10.1002/adma.201300691.
(53) Riahi, N.; Liberelle, B.; Henry, O.; De Crescenzo, G. Impact of RGD Amount in Dextran-Based Hydrogels for Cell Delivery. *Carbohydr. Polym.* **2017**, *161* (Supplement C), 219–227. https://doi.org/10.1016/j.carbpol.2017.01.002.
(54) Li, J.; Yu, Y.; Myungwoong, K.; Li, K.; Mikhail, J.; Zhang, L.; Chang, C.-C.; Gersappe, D.; Simon, M.; Ober, C.; et al. Manipulation of Cell Adhesion and Dynamics Using RGD Functionalized Polymers. *J. Mater. Chem. B* **2017**, *5* (31), 6307–6316. https://doi.org/10.1039/C7TB01209H.
(55) Kumar, P.; Takayesu, A.; Abbasi, U.; Kalathottukaren, M. T.; Abbina, S.; Kizhakkedathu, J. N.; Straus, S.

K. Antimicrobial Peptide–Polymer Conjugates with High Activity: Influence of Polymer Molecular Weight and Peptide Sequence on Antimicrobial Activity, Proteolysis, and Biocompatibility. *ACS Appl. Mater. Interfaces* **2017**, *9* (43), 37575–37586. https://doi.org/10.1021/acsami.7b09471.

(56) Danial, M.; Tran, C. M.-N.; Young, P. G.; Perrier, S.; Jolliffe, K. A. Janus Cyclic Peptide–Polymer Nanotubes. *Nat. Commun.* **2013**, *4*, 2780. https://doi.org/10.1038/ncomms3780.

(57) Lowe, A. B. Thiol-Yne 'Click'/Coupling Chemistry and Recent Applications in Polymer and Materials Synthesis and Modification. *Polymer* **2014**, *55* (22), 5517–5549. https://doi.org/10.1016/j.polymer.2014.08.015.

(58) Pan, Z.; Kang, X.; Zeng, Y.; Zhang, W.; Peng, H.; Wang, J.; Huang, W.; Wang, H.; Shen, Y.; Huang, Y. A Mannosylated PEI–CPP Hybrid for TRAIL Gene Targeting Delivery for Colorectal Cancer Therapy. *Polym. Chem.* **2017**, *8* (35), 5275–5285. https://doi.org/10.1039/C7PY00882A.

(59) Anwar, N.; Rix, A.; Lederle, W.; C. Kuehne, A. J. RGD-Decorated Conjugated Polymer Particles as Fluorescent Biomedical Probes Prepared by Sonogashira Dispersion Polymerization. *Chem. Commun.* **2015**, *51* (45), 9358–9361. https://doi.org/10.1039/C4CC10092A.

(60) Dawson, P. E.; Muir, T. W.; Clark-Lewis, I.; Kent, S. B. H. Synthesis of Proteins by Native Chemical Ligation. *Sci. New Ser.* **1994**, *266* (5186), 776–779.

(61) Ali Shah, M. I.; Xu, Z.-Y.; Liu, L.; Jiang, Y.-Y.; Shi, J. Mechanism for the Enhanced Reactivity of 4-Mercaptoprolyl Thioesters in Native Chemical Ligation. *RSC Adv.* **2016**, *6* (72), 68312–68321. https://doi.org/10.1039/C6RA13793H.

(62) Isahak, N.; Gody, G.; R. Malins, L.; J. Mitchell, N.; J. Payne, R.; Perrier, S. Single Addition of an Allylamine Monomer Enables Access to End-Functionalized RAFT Polymers for Native Chemical Ligation. *Chem. Commun.* **2016**, *52* (88), 12952–12955. https://doi.org/10.1039/C6CC06010B.

(63) Min, L.; Liu, M.; Liu, L.; Rao, Z.; Zhu, C.; Fan, L. Enzymatic Synthesis of Quaternary Ammonium Chitosan-Silk Fibroin Peptide Copolymer and Its Characterization. *Int. J. Biol. Macromol.* **2018**, *109*, 1125–1131. https://doi.org/10.1016/j.ijbiomac.2017.11.108.

(64) Chau, Y.; Padera, R. F.; Dang, N. M.; Langer, R. Antitumor Efficacy of a Novel Polymer–Peptide–Drug Conjugate in Human Tumor Xenograft Models. *Int. J. Cancer* **2006**, *118* (6), 1519–1526. https://doi.org/10.1002/ijc.21495.

(65) Chau, Y.; Tan, F. E.; Langer, R. Synthesis and Characterization of Dextran−Peptide−Methotrexate Conjugates for Tumor Targeting via Mediation by Matrix Metalloproteinase II and Matrix Metalloproteinase IX. *Bioconjug. Chem.* **2004**, *15* (4), 931–941. https://doi.org/10.1021/bc0499174.

(66) Larnaudie, S. C.; Brendel, J. C.; Romero-Canelón, I.; Sanchez-Cano, C.; Catrouillet, S.; Sanchis, J.; Coverdale, J. P. C.; Song, J.-I.; Habtemariam, A.; Sadler, P. J.; et al. Cyclic Peptide–Polymer Nanotubes as Efficient and Highly Potent Drug Delivery Systems for Organometallic Anticancer Complexes. *Biomacromolecules* **2018**, *19* (1), 239–247. https://doi.org/10.1021/acs.biomac.7b01491.

(67) Larnaudie, S. C.; Sanchis, J.; Nguyen, T.-H.; Peltier, R.; Catrouillet, S.; Brendel, J. C.; Porter, C. J. H.; Jolliffe, K. A.; Perrier, S. Cyclic Peptide-Poly(HPMA) Nanotubes as Drug Delivery Vectors: In Vitro Assessment, Pharmacokinetics and Biodistribution. *Biomaterials* **2018**, *178*, 570–582. https://doi.org/10.1016/j.biomaterials.2018.03.047.

(68) Mitra, A.; Nan, A.; Papadimitriou, J. C.; Ghandehari, H.; Line, B. R. Polymer-Peptide Conjugates for Angiogenesis Targeted Tumor Radiotherapy. *Nucl. Med. Biol.* **2006**, *33* (1), 43–52. https://doi.org/10.1016/j.nucmedbio.2005.09.005.

(69) Line, B. R.; Mitra, A.; Nan, A.; Ghandehari, H. Targeting Tumor Angiogenesis: Comparison of Peptide and Polymer-Peptide Conjugates. *J. Nucl. Med.* **2005**, *46* (9), 1552–1560.

(70) Elsner, C.; Ernst, C.; Buchmeiser, M. R. Miniaturized Biocatalysis on Polyacrylate-Based Capillary Monoliths. *J. Appl. Polym. Sci.* **2011**, *119* (3), 1450–1458. https://doi.org/10.1002/app.32657.

(71) Kızılbey, K.; Mansuroğlu, B.; Derman, S.; Mustafaeva Akdeste, Z. An *In Vivo* Study: Adjuvant Activity of Poly-n-Vinyl-2-Pyrrolidone-Co-Acrylic Acid on Immune Responses against Melanoma Synthetic Peptide. *Bioengineered* **2018**, *9* (1), 134–143. https://doi.org/10.1080/21655979.2017.1373529.

(72) Aveyard, J.; W. Bradley, J.; McKay, K.; McBride, F.; Donaghy, D.; Raval, R.; A. D'Sa, R. Linker-Free Covalent Immobilization of Nisin Using Atmospheric Pressure Plasma Induced Grafting. *J. Mater. Chem. B* **2017**, *5* (13), 2500–2510. https://doi.org/10.1039/C7TB00113D.

(73) Zhang, C.; Zhang, L.; Zhang, Y.; Sun, N.; Jiang, S.; Fujihara, T. J.; Sun, Y. Development of Antithrombotic Nanoconjugate Blocking Integrin A2β1-Collagen Interactions. *Sci. Rep.* **2016**, *6*, 26292. https://doi.org/10.1038/srep26292.

(74) Velander, W. H.; Madurawe, R. D.; Subramanian, A.; Kumar, G.; Sinai-Zingde, G.; Riffle, J. S.; Orthner, C. L. Polyoxazoline-Peptide Adducts That Retain Antibody Avidity. *Biotechnol. Bioeng.* **1992**, *39* (10), 1024–1030. https://doi.org/10.1002/bit.260391006.

(75) Linhardt, A.; König, M.; Schöfberger, W.; Brüggemann, O.; Andrianov, A. K.; Teasdale, I. Biodegradable Polyphosphazene Based Peptide-Polymer Hybrids. *Polymers* **2016**, *8* (4), 161. https://doi.org/10.3390/polym8040161.

(76) Echalier, C.; Valot, L.; Martinez, J.; Mehdi, A.; Subra, G. Chemical Cross-Linking Methods for Cell Encapsulation in Hydrogels. *Mater. Today Commun.* **2019**, 100536. https://doi.org/10.1016/j.mtcomm.2019.05.012.

(77) Chapman, R.; A. Jolliffe, K.; Perrier, S. Modular Design for the Controlled Production of Polymeric Nanotubes from Polymer / Peptide Conjugates. *Polym. Chem.* **2011**, *2* (9), 1956–1963. https://doi.org/10.1039/C1PY00202C.

(78) Chapman, R.; Jolliffe, K. A.; Perrier, S. Synthesis of Self-Assembling Cyclic Peptide-Polymer Conjugates Using Click Chemistry. *Aust. J. Chem.* **2010**, *63* (8), 1169. https://doi.org/10.1071/CH10128.

(79) Koh, M. L.; Jolliffe, K. A.; Perrier, S. Hierarchical Assembly of Branched Supramolecular Polymers from (Cyclic Peptide)–Polymer Conjugates. *Biomacromolecules* **2014**, *15* (11), 4002–4011. https://doi.org/10.1021/bm501062d.

(80) Koh, M. L.; FitzGerald, P. A.; Warr, G. G.; Jolliffe, K. A.; Perrier, S. Study of (Cyclic Peptide)–Polymer Conjugate Assemblies by Small-Angle Neutron Scattering. *Chem. – Eur. J.* **2016**, *22* (51), 18419–18428. https://doi.org/10.1002/chem.201603091.

(81) Selegård, R.; Aronsson, C.; Brommesson, C.; Dånmark, S.; Aili, D. Folding Driven Self-Assembly of a Stimuli-Responsive Peptide-Hyaluronan Hybrid Hydrogel. *Sci. Rep.* **2017**, *7* (1), 7013. https://doi.org/10.1038/s41598-017-06457-9.

(82) Canalle, L. A.; van der Knaap, M.; Overhand, M.; van Hest, J. C. M. A Comparison of Triazole-Forming Bioconjugation Techniques for Constructing Comb-Shaped Peptide–Polymer Bioconjugates. *Macromol. Rapid Commun.* **2011**, *32* (2), 203–208. https://doi.org/10.1002/marc.201000507.

(83) Karandish, F.; Froberg, J.; Borowicz, P.; Wilkinson, J. C.; Choi, Y.; Mallik, S. Peptide-Targeted, Stimuli-Responsive Polymersomes for Delivering a Cancer Stemness Inhibitor to Cancer Stem Cell Microtumors. *Colloids Surf. B Biointerfaces* **2018**, *163*, 225–235. https://doi.org/10.1016/j.colsurfb.2017.12.036.

(84) Bose, A.; Jana, S.; Saha, A.; Mandal, T. K. Amphiphilic Polypeptide-Polyoxazoline Graft Copolymer Conjugate with Tunable Thermoresponsiveness: Synthesis and Self-Assembly into Various Micellar Structures in Aqueous and Nonaqueous Media. *Polymer* **2017**, *110*, 12–24. https://doi.org/10.1016/j.polymer.2016.12.068.

(85) Luxenhofer, R.; López-García, M.; Frank, A.; Jordan, R. First Poly(2-Oxazoline)-Peptide Conjugate for Targeted Radionuclide Cancer Therapy. 3.

(86) Bolley, J.; Guenin, E.; Lievre, N.; Lecouvey, M.; Soussan, M.; Lalatonne, Y.; Motte, L. Carbodiimide versus Click Chemistry for Nanoparticle Surface Functionalization: A Comparative Study for the Elaboration of Multimodal Superparamagnetic Nanoparticles Targeting Avβ3 Integrins. *Langmuir* **2013**, *29* (47), 14639–14647. https://doi.org/10.1021/la403245h.

(87) Chelushkin, P. S.; Leko, M. V.; Dorosh, M. Y.; Burov, S. V. Oxime Ligation in Acetic Acid: Efficient Synthesis of Aminooxy-Peptide Conjugates: Oxime Ligation in Acetic Acid: Rapid Conjugation of Aminooxy-Peptides. *J. Pept. Sci.* **2017**, *23* (1), 13–15. https://doi.org/10.1002/psc.2931.

(88) Collins, J.; Wallis, S. J.; Simula, A.; Whittaker, M. R.; McIntosh, M. P.; Wilson, P.; Davis, T. P.; Haddleton, D. M.; Kempe, K. Comb Poly(Oligo(2-Ethyl-2-Oxazoline)Methacrylate)-Peptide Conjugates Prepared by Aqueous Cu(0)-Mediated Polymerization and Reductive Amination. *Macromol. Rapid Commun.* **2017**, *38* (2). https://doi.org/10.1002/marc.201600534.

(89) Shipp, D. A. Reversible-Deactivation Radical Polymerizations. *Polym. Rev.* **2011**, *51* (2), 99–103. https://doi.org/10.1080/15583724.2011.566406.

(90) Ran, J.; Wu, L.; Zhang, Z.; Xu, T. Atom Transfer Radical Polymerization (ATRP): A Versatile and Forceful

Tool for Functional Membranes. *Prog. Polym. Sci.* **2014**, *39* (1), 124–144. https://doi.org/10.1016/j.progpolymsci.2013.09.001.

(91) Mei, Y.; Beers, K. L.; Byrd, H. C. M.; VanderHart, D. L.; Washburn, N. R. Solid-Phase ATRP Synthesis of Peptide−Polymer Hybrids. *J. Am. Chem. Soc.* **2004**, *126* (11), 3472–3476. https://doi.org/10.1021/ja039583d.

(92) Rettig, H.; Krause, E.; Börner, H. G. Atom Transfer Radical Polymerization with Polypeptide Initiators: A General Approach to Block Copolymers of Sequence-Defined Polypeptides and Synthetic Polymers. *Macromol. Rapid Commun.* **2004**, *25* (13), 1251–1256. https://doi.org/10.1002/marc.200400140.

(93) Ayres, L.; Hans, P.; Adams, J.; Löwik, D. W. P. M.; van Hest, J. C. M. Peptide–Polymer Vesicles Prepared by Atom Transfer Radical Polymerization. *J. Polym. Sci. Part Polym. Chem.* **2005**, *43* (24), 6355–6366. https://doi.org/10.1002/pola.21107.

(94) Loschonsky, S.; Couet, J.; Biesalski, M. Synthesis of Peptide/Polymer Conjugates by Solution ATRP of Butylacrylate Using an Initiator-Modified Cyclic D-Alt-L-Peptide. *Macromol. Rapid Commun.* **2008**, *29* (4), 309–315. https://doi.org/10.1002/marc.200700700.

(95) Reyhani, A.; McKenzie, T. G.; Fu, Q.; Qiao, G. G. Redox-Initiated Reversible Addition–Fragmentation Chain Transfer (RAFT) Polymerization. *Aust. J. Chem.* **2019**, *72* (7), 479–489. https://doi.org/10.1071/CH19109.

(96) Hentschel, J.; Bleek, K.; Ernst, O.; Lutz, J.-F.; Börner, H. G. Easy Access to Bioactive Peptide−Polymer Conjugates via RAFT. *Macromolecules* **2008**, *41* (4), 1073–1075. https://doi.org/10.1021/ma8000934.

(97) Larnaudie, S. C.; Brendel, J. C.; Jolliffe, K. A.; Perrier, S. PH-Responsive, Amphiphilic Core–Shell Supramolecular Polymer Brushes from Cyclic Peptide–Polymer Conjugates. *ACS Macro Lett.* **2017**, *6* (12), 1347–1351. https://doi.org/10.1021/acsmacrolett.7b00728.

(98) Chen, C.; Kong, F.; Wei, X.; H. Thang, S. Syntheses and Effectiveness of Functional Peptide-Based RAFT Agents. *Chem. Commun.* **2017**, *53* (78), 10776–10779. https://doi.org/10.1039/C7CC05316A.

(99) Sciannamea, V.; Jérôme, R.; Detrembleur, C. In-Situ Nitroxide-Mediated Radical Polymerization (NMP) Processes: Their Understanding and Optimization. *Chem. Rev.* **2008**, *108* (3), 1104–1126. https://doi.org/10.1021/cr0680540.

(100) L. Becker, M.; Liu, J.; L. Wooley, K. Peptide - Polymer Bioconjugates : Hybrid Block Copolymers Generated via Living Radical Polymerizations from Resin-Supported Peptides. *Chem. Commun.* **2003**, *0* (2), 180–181. https://doi.org/10.1039/B209557B.

(101) Becker, M. L.; Liu, J.; Wooley, K. L. Functionalized Micellar Assemblies Prepared via Block Copolymers Synthesized by Living Free Radical Polymerization upon Peptide-Loaded Resins. *Biomacromolecules* **2005**, *6* (1), 220–228. https://doi.org/10.1021/bm049551y.

(102) Lowe, A. B.; Sumerlin, B. S.; McCormick, C. L. The Direct Polymerization of 2-Methacryloxyethyl Glucoside via Aqueous Reversible Addition-Fragmentation Chain Transfer (RAFT) Polymerization. *Polymer* **2003**, *44* (22), 6761–6765. https://doi.org/10.1016/j.polymer.2003.08.039.

(103) Albertin, L.; Stenzel, M. H.; Barner-Kowollik, C.; Foster, L. J. R.; Davis, T. P. Well-Defined Diblock Glycopolymers from RAFT Polymerization in Homogeneous Aqueous Medium. *Macromolecules* **2005**, *38* (22), 9075–9084. https://doi.org/10.1021/ma051310a.

(104) Bernard, J.; Hao, X.; Davis, T. P.; Barner-Kowollik, C.; Stenzel, M. H. Synthesis of Various Glycopolymer Architectures via RAFT Polymerization: From Block Copolymers to Stars. *Biomacromolecules* **2006**, *7* (1), 232–238. https://doi.org/10.1021/bm0506086.

(105) Albertin, L.; Kohlert, C.; Stenzel, M.; Foster, L. J. R.; Davis, T. P. Chemoenzymatic Synthesis of Narrow-Polydispersity Glycopolymers: Poly(6- *O* -Vinyladipoyl- D -Glucopyranose). *Biomacromolecules* **2004**, *5* (2), 255–260. https://doi.org/10.1021/bm034199u.

(106) Spijker, H. J.; van Delft, F. L.; van Hest, J. C. M. Atom Transfer Radical Polymerization of Adenine, Thymine, Cytosine, and Guanine Nucleobase Monomers. *Macromolecules* **2007**, *40* (1), 12–18. https://doi.org/10.1021/ma061808s.

(107) Spijker, H. J.; Dirks, A. J.; Hest, J. C. M. van. Synthesis and Assembly Behavior of Nucleobase-Functionalized Block Copolymers. *J. Polym. Sci. Part Polym. Chem.* **2006**, *44* (13), 4242–4250. https://doi.org/10.1002/pola.21529.

(108) Spijker, H. J.; Dirks, A. (Ton) J.; van Hest, J. C. M. Unusual Rate Enhancement in the Thymine Assisted

ATRP Process of Adenine Monomers. *Polymer* **2005**, *46* (19), 8528–8535. https://doi.org/10.1016/j.polymer.2005.02.127.
(109) Lutz, J.-F.; Börner, H. G. Modern Trends in Polymer Bioconjugates Design. *Prog. Polym. Sci.* **2008**, *33* (1), 1–39. https://doi.org/10.1016/j.progpolymsci.2007.07.005.
(110) Ayres, L.; Vos, M. R. J.; Adams, P. J. H. M.; Shklyarevskiy, I. O.; van Hest, J. C. M. Elastin-Based Side-Chain Polymers Synthesized by ATRP. *Macromolecules* **2003**, *36* (16), 5967–5973. https://doi.org/10.1021/ma025727h.
(111) Wu, K.; Yang, J.; Koňák, Č.; Kopečková, P.; Kopeček, J. Novel Synthesis of HPMA Copolymers Containing Peptide Grafts and Their Self-Assembly Into Hybrid Hydrogels. *Macromol. Chem. Phys.* **2008**, *209* (5), 467–475. https://doi.org/10.1002/macp.200700486.
(112) Ladmiral, V.; Charlot, A.; Semsarilar, M.; P. Armes, S. Synthesis and Characterization of Poly(Amino Acid Methacrylate)-Stabilized Diblock Copolymer Nano-Objects. *Polym. Chem.* **2015**, *6* (10), 1805–1816. https://doi.org/10.1039/C4PY01556H.
(113) Das, D.; Gerboth, D.; Postma, A.; Srinivasan, S.; Kern, H.; Chen, J.; Ratner, D. M.; Stayton, P. S.; Convertine, A. J. Synthesis of Zwitterionic, Hydrophobic, and Amphiphilic Polymers via RAFT Polymerization Induced Self-Assembly (PISA) in Acetic Acid. *Polym. Chem.* **2016**, *7* (39), 6133–6143. https://doi.org/10.1039/C6PY01172A.
(114) Bauri, K.; Narayanan, A.; Haldar, U.; De, P. Polymerization-Induced Self-Assembly Driving Chiral Nanostructured Materials. *Polym. Chem.* **2015**, *6* (34), 6152–6162. https://doi.org/10.1039/C5PY00919G.
(115) Ahmed, M. Peptides, Polypeptides and Peptide–Polymer Hybrids as Nucleic Acid Carriers. *Biomater. Sci.* **2017**, *5* (11), 2188–2211. https://doi.org/10.1039/C7BM00584A.
(116) Shi, J.; Schellinger, J. G.; Pun, S. H. Engineering Biodegradable and Multifunctional Peptide-Based Polymers for Gene Delivery. *J. Biol. Eng.* **2013**, *7*, 25. https://doi.org/10.1186/1754-1611-7-25.
(117) Jebors, S.; Enjalbal, C.; Amblard, M.; Subra, G.; Mehdi, A.; Martinez, J. Switchable Polymer-Grafted Mesoporous Silica's: From Polyesters to Polyamides Biosilica Hybrid Materials. *Tetrahedron* **2013**, *69* (36), 7670–7674.
(118) Kricheldorf, H. R. Polypeptides and 100 Years of Chemistry of α-Amino Acid N-Carboxyanhydrides. *Angew. Chem. Int. Ed.* **2006**, *45* (35), 5752–5784. https://doi.org/10.1002/anie.200600693.
(119) Hadjichristidis, N.; Iatrou, H.; Pitsikalis, M.; Sakellariou, G. Synthesis of Well-Defined Polypeptide-Based Materials via the Ring-Opening Polymerization of α-Amino Acid N-Carboxyanhydrides. *Chem. Rev.* **2009**, *109* (11), 5528–5578. https://doi.org/10.1021/cr900049t.
(120) Koga, T.; Taguchi, K.; Kobuke, Y.; Kinoshita, T.; Higuchi, M. Structural Regulation of a Peptide-Conjugated Graft Copolymer: A Simple Model for Amyloid Formation. *Chem. – Eur. J.* **2003**, *9* (5), 1146–1156. https://doi.org/10.1002/chem.200390132.
(121) Subra, G.; Mehdi, A.; Enjalbal, C.; Amblard, M.; Brunel, L.; Corriu, R.; Martinez, J. Functionalised Mesoporous Silica: A Good Opportunity for Controlled Peptide Oligomerisation. *J. Mater. Chem.* **2011**, *21* (17), 6321–6326. https://doi.org/10.1039/C0JM04492J.
(122) Verdie, P.; Ronga, L.; Cristau, M.; Amblard, M.; Cantel, S.; Enjalbal, C.; Puget, K.; Martinez, J.; Subra, G. Oxyfold: A Simple and Efficient Solid-Supported Reagent for Disulfide Bond Formation. *Chem.- Asian J.* **2011**, *6* (9), 2382–2389.
(123) Maeda, K.; Kamiya, N.; Yashima, E. Poly(Phenylacetylene)s Bearing a Peptide Pendant: Helical Conformational Changes of the Polymer Backbone Stimulated by the Pendant Conformational Change. *Chem. – Eur. J.* **2004**, *10* (16), 4000–4010. https://doi.org/10.1002/chem.200400315.
(124) Sanda, F.; Gao, G.; Masuda, T. Helical Polymer Carrying Helical Grafts from Peptide-Based Acetylene Macromonomers: Synthesis. *Macromol. Biosci.* **2004**, *4* (6), 570–574. https://doi.org/10.1002/mabi.200400019.
(125) Audouin, F.; Knoop, R. J. I.; Huang, J.; Heise, A. Star Polymers by Cross-Linking of Linear Poly(Benzyl-L-Glutamate) Macromonomers via Free-Radical and RAFT Polymerization. A Simple Route toward Peptide-Stabilized Nanoparticles. *J. Polym. Sci. Part Polym. Chem.* **2010**, *48* (20), 4602–4610. https://doi.org/10.1002/pola.24258.
(126) Zhao, J.; Dong, Z.; Cui, H.; Jin, H.; Wang, C. Nanoengineered Peptide-Grafted Hyperbranched Polymers

for Killing of Bacteria Monitored in Real Time via Intrinsic Aggregation-Induced Emission. *ACS Appl. Mater. Interfaces* **2018**, *10* (49), 42058–42067. https://doi.org/10.1021/acsami.8b15921.

(127) Cesana, S.; Auernheimer, J.; Jordan, R.; Kessler, H.; Nuyken, O. First Poly(2-Oxazoline)s with Pendant Amino Groups. *Macromol. Chem. Phys.* **2006**, *207* (2), 183–192. https://doi.org/10.1002/macp.200500495.

(128) Hoogenboom, R. Poly(2-Oxazoline)s: A Polymer Class with Numerous Potential Applications. *Angew. Chem. Int. Ed.* **2009**, *48* (43), 7978–7994. https://doi.org/10.1002/anie.200901607.

(129) Tsutsumiuchi, K.; Aoi, K.; Okada, M. Synthesis of Polyoxazoline−(Glyco)Peptide Block Copolymers by Ring-Opening Polymerization of (Sugar-Substituted) α-Amino Acid N-Carboxyanhydrides with Polyoxazoline Macroinitiators. *Macromolecules* **1997**, *30* (14), 4013–4017. https://doi.org/10.1021/ma970086p.

(130) Tsutsumiuchi, K.; Aoi, K.; Okada, M. Synthesis of Novel Glycopeptide-Polyoxazoline Block Copolymers by Direct Coupling between Living Anionic and Cationic Polymerization Systems. *Macromol. Rapid Commun.* **1995**, *16* (10), 749–755. https://doi.org/10.1002/marc.1995.030161007.

(131) Enomoto, H.; Nottelet, B.; Al Halifa, S.; Enjalbal, C.; Dupré, M.; Tailhades, J.; Coudane, J.; Subra, G.; Martinez, J.; Amblard, M. Synthesis of Peptide -Grafted Comb Polypeptides via Polymerisation of NCA-Peptides. *Chem. Commun.* **2013**, *49* (4), 409–411. https://doi.org/10.1039/C2CC37597D.

(132) Biagini, S. C. G.; Gareth Davies, R.; Gibson, V. C.; Giles, M. R.; Marshall, E. L.; North, M. Ruthenium Initiated Ring Opening Metathesis Polymerisation of Amino-Acid and -Ester Functionalised Norbornenes and a Highly Selective Chain-End Functionalisation Reaction Using Molecular Oxygen. *Polymer* **2001**, *42* (15), 6669–6671. https://doi.org/10.1016/S0032-3861(01)00146-X.

(133) Kammeyer, J. K.; Blum, A. P.; Adamiak, L.; Hahn, M. E.; Gianneschi, N. C. Polymerization of Protecting-Group-Free Peptides via ROMP. *Polym. Chem.* **2013**, *41*, 3929–3933. https://doi.org/10.1039/C3PY00526G.

(134) Wang, Z.; Li, Y.; Huang, Y.; P. Thompson, M.; M. LeGuyader, C. L.; Sahu, S.; C. Gianneschi, N. Enzyme-Regulated Topology of a Cyclic Peptide Brush Polymer for Tuning Assembly. *Chem. Commun.* **2015**, *51* (96), 17108–17111. https://doi.org/10.1039/C5CC05653E.

(135) Biagini, S. C. G.; Parry, A. L. Investigation into the ROMP Copolymerization of Peptide- and PEG-Functionalized Norbornene Derivatives. *J. Polym. Sci. Part Polym. Chem.* **2007**, *45* (15), 3178–3190. https://doi.org/10.1002/pola.22068.

(136) Blum, A. P.; Kammeyer, J. K.; Gianneschi, N. C. Activating Peptides for Cellular Uptake via Polymerization into High Density Brushes †Electronic Supplementary Information (ESI) Available: Full Experimental Details and Additional Figures Are Provided. See DOI: 10.1039/C5sc03417e Click Here for Additional Data File. *Chem. Sci.* **2016**, *7* (2), 989–994. https://doi.org/10.1039/c5sc03417e.

(137) Chien, M.-P.; Rush, A. M.; Thompson, M. P.; Gianneschi, N. C. Programmable Shape-Shifting Micelles. *Angew. Chem. Int. Ed.* **2010**, *49* (30), 5076–5080. https://doi.org/10.1002/anie.201000265.

(138) Wright, D. B.; Touve, M. A.; Adamiak, L.; Gianneschi, N. C. ROMPISA: Ring-Opening Metathesis Polymerization-Induced Self-Assembly. *ACS Macro Lett.* **2017**, *6* (9), 925–929. https://doi.org/10.1021/acsmacrolett.7b00408.

(139) Martinez, J.; Mehdi, A.; Subra, G.; Jebors, S. Process for Preparation of Bioorganic Nylon Polymers and Their Use as Antibacterial Material. WO/2017/098018, June 16, 2017.

(140) Nishimura, S.; Higashi, N.; Koga, T. Facile Synthesis of Multiblock Copolymers Containing Sequence-Controlled Peptides and Well-Defined Vinyl Polymers by Nitroxide-Mediated Polymerization. *Chem. – Eur. J.* **2017**, *23* (60), 15050–15058. https://doi.org/10.1002/chem.201703655.

(141) Pinese, C.; Jebors, S.; Emmanuel Stoebner, P.; Humblot, V.; Verdié, P.; Causse, L.; Garric, X.; Taillades, H.; Martinez, J.; Mehdi, A.; et al. Bioactive Peptides Grafted Silicone Dressings: A Simple and Specific Method. *Mater. Today Chem.* **2017**, *4*, 73–83. https://doi.org/10.1016/j.mtchem.2017.02.007.

(142) Masurier, N.; Tissot, J.-B.; Boukhriss, D.; Jebors, S.; Pinese, C.; Verdie, P.; Amblard, M.; Mehdi, A.; Martinez, J.; Humblot, V.; et al. Site-Specific Grafting on Titanium Surfaces with Hybrid Temporin Antibacterial Peptides. *J. Mater. Chem. B* **2018**. https://doi.org/10.1039/C8TB00051D.

(143) Jebors, S.; Ciccione, J.; Al-Halifa, S.; Nottelet, B.; Enjalbal, C.; M'Kadmi, C.; Amblard, M.; Mehdi, A.; Martinez, J.; Subra, G. A New Way to Silicone-Based Peptide Polymers. *Angew. Chem. Int. Ed.* **2015**, *54*

(12), 3778–3782. https://doi.org/10.1002/anie.201411065.
(144) Jebors, S.; Pinese, C.; Nottelet, B.; Parra, K.; Amblard, M.; Mehdi, A.; Martinez, J.; Subra, G. Turning Peptides in Comb Silicone Polymers. *J. Pept. Sci.* **2015**, *21* (3), 243–247. https://doi.org/10.1002/psc.2757.
(145) B. Madsen, F.; Yu, L.; E. Daugaard, A.; Hvilsted, S.; L. Skov, A. A New Soft Dielectric Silicone Elastomer Matrix with High Mechanical Integrity and Low Losses. *RSC Adv.* **2015**, *5* (14), 10254–10259. https://doi.org/10.1039/C4RA13511C.
(146) Chekina, N. A.; Pavlyuchenko, V. N.; Danilichev, V. F.; Ushakov, N. A.; Novikov, S. A.; Ivanchev, S. S. A New Polymeric Silicone Hydrogel for Medical Applications: Synthesis and Properties. *Polym. Adv. Technol.* **2006**, *17* (11–12), 872–877. https://doi.org/10.1002/pat.820.
(147) Owen, M. J. Properties and Applications of Silicones. In *Advances in Silicones and Silicone-Modified Materials*; ACS Symposium Series; American Chemical Society, 2010; Vol. 1051, pp 13–18. https://doi.org/10.1021/bk-2010-1051.ch002.
(148) Lee, J. N.; Jiang, X.; Ryan, D.; Whitesides, G. M. Compatibility of Mammalian Cells on Surfaces of Poly(Dimethylsiloxane). *Langmuir* **2004**, *20* (26), 11684–11691. https://doi.org/10.1021/la048562+.
(149) Moretto, H.-H.; Schulze, M.; Wagner, G. Silicones. In *Ullmann's Encyclopedia of Industrial Chemistry*; Wiley-VCH Verlag GmbH & Co. KGaA, Ed.; Wiley-VCH Verlag GmbH & Co. KGaA: Weinheim, Germany, 2000. https://doi.org/10.1002/14356007.a24_057.
(150) Liu, Y.; Zhang, L.; Wu, W.; Zhao, M.; Wang, W. Restraining Non-Specific Adsorption of Protein Using Parylene C-Caulked Polydimethylsiloxane. *Biomicrofluidics* **2016**, *10* (2). https://doi.org/10.1063/1.4946870.
(151) Brash, J. L. Exploiting the Current Paradigm of Blood–Material Interactions for the Rational Design of Blood-Compatible Materials. *J. Biomater. Sci. Polym. Ed.* **2000**, *11* (11), 1135–1146. https://doi.org/10.1163/156856200744237.
(152) Jońca, J.; Tukaj, C.; Werel, W.; Mizerska, U.; Fortuniak, W.; Chojnowski, J. Bacterial Membranes Are the Target for Antimicrobial Polysiloxane-Methacrylate Copolymer. *J. Mater. Sci. Mater. Med.* **2016**, *27* (3), 55. https://doi.org/10.1007/s10856-016-5669-6.
(153) Hu, S.; Ren, X.; Bachman, M.; Sims, C. E.; Li, G. P.; Allbritton, N. Cross-Linked Coatings for Electrophoretic Separations in Poly(Dimethylsiloxane) Microchannels. *ELECTROPHORESIS* **2003**, *24* (21), 3679–3688. https://doi.org/10.1002/elps.200305592.
(154) Feng, J.-J.; Wang, A.-J.; Fan, J.; Xu, J.-J.; Chen, H.-Y. Hydrophilic Biopolymer Grafted on Poly(Dimethylsiloxane) Surface for Microchip Electrophoresis. *Anal. Chim. Acta* **2010**, *658* (1), 75–80. https://doi.org/10.1016/j.aca.2009.10.052.
(155) Alauzun, J. G.; Young, S.; D'Souza, R.; Liu, L.; Brook, M. A.; Sheardown, H. D. Biocompatible, Hyaluronic Acid Modified Silicone Elastomers. *Biomaterials* **2010**, *31* (13), 3471–3478. https://doi.org/10.1016/j.biomaterials.2010.01.069.
(156) Keranov, I.; Vladkova, T.; Minchev, M.; Kostadinova, A.; Altankov, G. Preparation, Characterization, and Cellular Interactions of Collagen-Immobilized PDMS Surfaces. *J. Appl. Polym. Sci.* **2008**, *110* (1), 321–330. https://doi.org/10.1002/app.28630.
(157) Wu, H.; Zhai, J.; Tian, Y.; Lu, H.; Wang, X.; Jia, W.; Liu, B.; Yang, P.; Xu, Y.; Wang, H. Microfluidic Enzymatic-Reactors for Peptide Mapping: Strategy, Characterization, and Performance. *Lab. Chip* **2004**, *4* (6), 588–597. https://doi.org/10.1039/B408222B.
(158) Yu, X.; Xiao, J.; Dang, F. Surface Modification of Poly(Dimethylsiloxane) Using Ionic Complementary Peptides to Minimize Nonspecific Protein Adsorption. *Langmuir* **2015**, *31* (21), 5891–5898. https://doi.org/10.1021/acs.langmuir.5b01085.
(159) Wang, D.; Oleschuk, R. D.; Horton, J. H. Surface Modification of Poly(Dimethylsiloxane) with a Perfluorinated Alkoxysilane for Selectivity toward Fluorous Tagged Peptides. *Langmuir* **2008**, *24* (3), 1080–1086. https://doi.org/10.1021/la702038t.
(160) Wang, D.; Douma, M.; Swift, B.; Oleschuk, R. D.; Horton, J. H. The Adsorption of Globular Proteins onto a Fluorinated PDMS Surface. *J. Colloid Interface Sci.* **2009**, *331* (1), 90–97. https://doi.org/10.1016/j.jcis.2008.11.010.
(161) Mishra, G.; Bhattacharyya, S.; Bhatia, V.; Ateeq, B.; Sharma, A.; Sivakumar, S. Direct Intranuclear

Anticancer Drug Delivery via Polydimethylsiloxane Nanoparticles: In Vitro and in Vivo Xenograft Studies. *ACS Appl. Mater. Interfaces* **2017**, *9* (40), 34625–34633. https://doi.org/10.1021/acsami.7b08806.

(162) Wu, D.; Zhao, B.; Dai, Z.; Qin, J.; Lin, B. Grafting Epoxy-Modified Hydrophilic Polymers onto Poly(Dimethylsiloxane) Microfluidic Chip to Resist Nonspecific Protein Adsorption. *Lab. Chip* **2006**, *6* (7), 942–947. https://doi.org/10.1039/B600765A.

(163) Wu, D.; Qin, J.; Lin, B. Self-Assembled Epoxy-Modified Polymer Coating on a Poly(Dimethylsiloxane) Microchip for EOF Inhibition and Biopolymers Separation. *Lab. Chip* **2007**, *7* (11), 1490–1496. https://doi.org/10.1039/B708877A.

(164) Yeh, S.-B.; Chen, C.-S.; Chen, W.-Y.; Huang, C.-J. Modification of Silicone Elastomer with Zwitterionic Silane for Durable Antifouling Properties. *Langmuir* **2014**, *30* (38), 11386–11393. https://doi.org/10.1021/la502486e.

(165) Pinese, C.; Jebors, S.; Echalier, C.; Licznar-Fajardo, P.; Garric, X.; Humblot, V.; Calers, C.; Martinez, J.; Mehdi, A.; Subra, G. Simple and Specific Grafting of Antibacterial Peptides on Silicone Catheters. *Adv. Healthc. Mater.* **2016**, *5* (23), 3067–3073. https://doi.org/10.1002/adhm.201600757.

(166) Pinese, C.; Jebors, S.; Stoebner, P. E.; Humblot, V.; Verdié, P.; Causse, L.; Garric, X.; Taillades, H.; Martinez, J.; Mehdi, A.; et al. Bioactive Peptides Grafted Silicone Dressings: A Simple and Specific Method. *Mater. Today Chem.* **2017**, *4*, 73–83. https://doi.org/10.1016/j.mtchem.2017.02.007.

(167) Boateng, S.; Lateef, S. S.; Crot, C.; Motlagh, D.; Desai, T.; Samarel, A. M.; Russell, B.; Hanley, L. Peptides Bound to Silicone Membranes and 3D Microfabrication for Cardiac Cell Culture. *Adv. Mater.* **2002**, *14* (6), 461–463. https://doi.org/10.1002/1521-4095(20020318)14:6<461::AID-ADMA461>3.0.CO;2-S.

(168) Lateef, S. S.; Boateng, S.; Hartman, T. J.; Crot, C. A.; Russell, B.; Hanley, L. GRGDSP Peptide-Bound Silicone Membranes Withstand Mechanical Flexing in Vitro and Display Enhanced Fibroblast Adhesion. *Biomaterials* **2002**, *23* (15), 3159–3168.

(169) Sui, G.; Wang, J.; Lee, C.-C.; Lu, W.; Lee, S. P.; Leyton, J. V.; Wu, A. M.; Tseng, H.-R. Solution-Phase Surface Modification in Intact Poly(Dimethylsiloxane) Microfluidic Channels. *Anal. Chem.* **2006**, *78* (15), 5543–5551. https://doi.org/10.1021/ac060605z.

(170) Makamba, H.; Kim, J. H.; Lim, K.; Park, N.; Hahn, J. H. Surface Modification of Poly(Dimethylsiloxane) Microchannels. *ELECTROPHORESIS* **2003**, *24* (21), 3607–3619. https://doi.org/10.1002/elps.200305627.

(171) Bowden, N.; Huck, W. T. S.; Paul, K. E.; Whitesides, G. M. The Controlled Formation of Ordered, Sinusoidal Structures by Plasma Oxidation of an Elastomeric Polymer. *Appl. Phys. Lett.* **1999**, *75* (17), 2557–2559. https://doi.org/10.1063/1.125076.

(172) Chen, H.; Brook, M. A.; Sheardown, H. D.; Chen, Y.; Klenkler, B. Generic Bioaffinity Silicone Surfaces. *Bioconjug. Chem.* **2006**, *17* (1), 21–28. https://doi.org/10.1021/bc050174b.

(173) Mikhail, A. S.; Jones, K. S.; Sheardown, H. Dendrimer-Grafted Cell Adhesion Peptide–Modified PDMS. *Biotechnol. Prog.* **2008**, *24* (4), 938–944. https://doi.org/10.1002/btpr.5.

(174) Mikhail, A. S.; Ranger, J. J.; Liu, L.; Longenecker, R.; Thompson, D. B.; Sheardown, H. D.; Brook, M. A. Rapid and Efficient Assembly of Functional Silicone Surfaces Protected by PEG: Cell Adhesion to Peptide-Modified PDMS. *J. Biomater. Sci. Polym. Ed.* **2010**, *21* (6–7), 821–842. https://doi.org/10.1163/156856209X445311.

(175) Ferreira, P.; Carvalho, Á.; Correia, T. R.; Antunes, B. P.; Correia, I. J.; Alves, P. Functionalization of Polydimethylsiloxane Membranes to Be Used in the Production of Voice Prostheses. *Sci. Technol. Adv. Mater.* **2013**, *14* (5), 055006. https://doi.org/10.1088/1468-6996/14/5/055006.

(176) Prijck, K. D.; Smet, N. D.; Rymarczyk-Machal, M.; Driessche, G. V.; Devreese, B.; Coenye, T.; Schacht, E.; Nelis, H. J. *Candida Albicans* Biofilm Formation on Peptide Functionalized Polydimethylsiloxane. *Biofouling* **2010**, *26* (3), 269–275. https://doi.org/10.1080/08927010903501908.

(177) Smet, N. D.; Rymarczyk-Machal, M.; Schacht, E. Modification of Polydimethylsiloxane Surfaces Using Benzophenone. *J. Biomater. Sci. Polym. Ed.* **2009**, *20* (14), 2039–2053. https://doi.org/10.1163/156856208X397901.

(178) Li, B.; Chen, J.; Wang, J. H.-C. RGD Peptide-Conjugated Poly(Dimethylsiloxane) Promotes Adhesion, Proliferation, and Collagen Secretion of Human Fibroblasts. *J. Biomed. Mater. Res. A* **2006**, *79* (4), 989–998. https://doi.org/10.1002/jbm.a.30847.

(179) Vladkova, T. G.; Keranov, I. L.; Dineff, P. D.; Youroukov, S. Y.; Avramova, I. A.; Krasteva, N.; Altankov, G.

P. Plasma Based Ar+ Beam Assisted Poly(Dimethylsiloxane) Surface Modification. *Nucl. Instrum. Methods Phys. Res. Sect. B Beam Interact. Mater. At.* **2005**, *236* (1), 552–562. https://doi.org/10.1016/j.nimb.2005.04.040.

(180) Lim, K.; Chua, R. R. Y.; Saravanan, R.; Basu, A.; Mishra, B.; Tambyah, P. A.; Ho, B.; Leong, S. S. J. Immobilization Studies of an Engineered Arginine–Tryptophan-Rich Peptide on a Silicone Surface with Antimicrobial and Antibiofilm Activity. *ACS Appl. Mater. Interfaces* **2013**, *5* (13), 6412–6422. https://doi.org/10.1021/am401629p.

(181) Mishra, B.; Basu, A.; Chua, R. R. Y.; Saravanan, R.; Tambyah, P. A.; Ho, B.; Chang, M. W.; Leong, S. S. J. Site Specific Immobilization of a Potent Antimicrobial Peptide onto Silicone Catheters: Evaluation against Urinary Tract Infection Pathogens. *J. Mater. Chem. B* **2014**, *2* (12), 1706–1716. https://doi.org/10.1039/C3TB21300E.

(182) Rambarran, T.; Gonzaga, F.; Brook, M. A. Generic, Metal-Free Cross-Linking and Modification of Silicone Elastomers Using Click Ligation. *Macromolecules* **2012**, *45* (5), 2276–2285. https://doi.org/10.1021/ma202785x.

(183) Calabrese, D. R.; Wenning, B.; Finlay, J. A.; Callow, M. E.; Callow, J. A.; Fischer, D.; Ober, C. K. Amphiphilic Oligopeptides Grafted to PDMS-Based Diblock Copolymers for Use in Antifouling and Fouling Release Coatings. *Polym. Adv. Technol.* **2015**, *26* (7), 829–836. https://doi.org/10.1002/pat.3515.

(184) Akers, P. W.; Dingley, A. J.; Swift, S.; Nelson, A. R. J.; Martin, J.; McGillivray, D. J. Using Neutron Reflectometry to Characterize Antimicrobial Protein Surface Coatings. *J. Phys. Chem. B* **2017**, *121* (24), 5908–5916. https://doi.org/10.1021/acs.jpcb.7b02886.

(185) Rytkönen, J.; Arukuusk, P.; Xu, W.; Kurrikoff, K.; Langel, Ü.; Lehto, V.-P.; Närvänen, A. Porous Silicon–Cell Penetrating Peptide Hybrid Nanocarrier for Intracellular Delivery of Oligonucleotides. *Mol. Pharm.* **2014**, *11* (2), 382–390. https://doi.org/10.1021/mp4002624.

(186) Maurice, V.; Slostowski, C.; Herlin-Boime, N.; Carrot, G. Polymer-Grafted Silicon Nanoparticles Obtained Either via Peptide Bonding or Click Chemistry. *Macromol. Chem. Phys. 213* (23), 2498–2503. https://doi.org/10.1002/macp.201200326.

(187) Aucoin, L.; Griffith, C. M.; Pleizier, G.; Deslandes, Y.; Sheardown, H. Interactions of Corneal Epithelial Cells and Surfaces Modified with Cell Adhesion Peptide Combinations. *J. Biomater. Sci. Polym. Ed.* **2002**, *13* (4), 447–462. https://doi.org/10.1163/156856202320253956.

(188) Lim, K.; Chua, R. R. Y.; Bow, H.; Tambyah, P. A.; Hadinoto, K.; Leong, S. S. J. Development of a Catheter Functionalized by a Polydopamine Peptide Coating with Antimicrobial and Antibiofilm Properties. *Acta Biomater.* **2015**, *15*, 127–138. https://doi.org/10.1016/j.actbio.2014.12.015.

(189) Jebors, S.; Cecillon, S.; Faye, C.; Enjalbal, C.; Amblard, M.; Mehdi, A.; Subra, G.; Martinez, J. From Protected Trialkoxysilyl-Peptide Building Blocks to Bioorganic–Silica Hybrid Materials. *J. Mater. Chem. B* **2013**, *1* (47), 6510–6515. https://doi.org/10.1039/C3TB21326A.

(190) Echalier, C.; Kalistratova, A.; Ciccione, J.; Lebrun, A.; Legrand, B.; Naydenova, E.; Gagne, D.; Fehrentz, J.-A.; Marie, J.; Amblard, M.; et al. Selective Homodimerization of Unprotected Peptides Using Hybrid Hydroxydimethylsilane Derivatives. *RSC Adv.* **2016**, *6* (39), 32905–32914. https://doi.org/10.1039/C6RA06075G.

(191) Jebors, S.; Ciccione, J.; Al-Halifa, S.; Nottelet, B.; Enjalbal, C.; M'Kadmi, C.; Amblard, M.; Mehdi, A.; Martinez, J.; Subra, G. A New Way to Silicone-Based Peptide Polymers. *Angew. Chem. Int. Ed.* **2015**, *54* (12), 3778–3782. https://doi.org/10.1002/anie.201411065.

(192) Jebors, S.; Pinese, C.; Nottelet, B.; Parra, K.; Amblard, M.; Mehdi, A.; Martinez, J.; Subra, G. Turning Peptides in Comb Silicone Polymers. *J. Pept. Sci.* **2015**, *21* (3), 243–247. https://doi.org/10.1002/psc.2757.

(193) Martin, J.; Wehbi, M.; Echalier, C.; Pinese, C.; Martinez, J.; Subra, G.; Mehdi, A. Direct Synthesis of Peptide-Modified Silicone. A New Way for Bioactive Materials. *Submitted*. 2019.

(194) Xu, C.; He, R.; Xie, B.; Ismail, M.; Yao, C.; Luan, J.; Li, X. Improved Protein Resistance of Silicone Hydrogels by Grafting Short Peptides for Ophthalmological Application. *Int. J. Polym. Mater. Polym. Biomater.* **2017**, *66* (12), 618–625. https://doi.org/10.1080/00914037.2016.1252356.

(195) Godoy-Gallardo, M.; Mas-Moruno, C.; Yu, K.; Manero, J. M.; Gil, F. J.; Kizhakkedathu, J. N.; Rodriguez, D. Antibacterial Properties of HLf1–11 Peptide onto Titanium Surfaces: A Comparison Study Between

Silanization and Surface Initiated Polymerization. *Biomacromolecules* **2015**, *16* (2), 483–496. https://doi.org/10.1021/bm501528x.

(196) Ammar, M.; Smadja, C.; Phuong Ly, G. T.; Tandjigora, D.; Vigneron, J.; Etcheberry, A.; Taverna, M.; Dufour-Gergam, E. Chemical Engineering of Self-Assembled Alzheimer's Peptide on a Silanized Silicon Surface. *Langmuir* **2014**, *30* (20), 5863–5872. https://doi.org/10.1021/la500695y.

(197) Boccafoschi, F.; Fusaro, L.; Cannas, M. 15 - Immobilization of Peptides on Cardiovascular Stent. In *Functionalised Cardiovascular Stents*; Wall, J. G., Podbielska, H., Wawrzyńska, M., Eds.; Woodhead Publishing, 2018; pp 305–318. https://doi.org/10.1016/B978-0-08-100496-8.00016-0.

(198) Xu, Z.; Liu, S.; Kang, Y.; Wang, M. Glutathione- and PH-Responsive Nonporous Silica Prodrug Nanoparticles for Controlled Release and Cancer Therapy. *Nanoscale* **2015**, *7* (13), 5859–5868. https://doi.org/10.1039/C5NR00297D.

(199) Ciccione, J.; Jia, T.; Coll, J.-L.; Parra, K.; Amblard, M.; Jebors, S.; Martinez, J.; Mehdi, A.; Subra, G. Unambiguous and Controlled One-Pot Synthesis of Multifunctional Silica Nanoparticles. *Chem. Mater.* **2016**, *28* (3), 885–889. https://doi.org/10.1021/acs.chemmater.5b04398.

(200) Masurier, N.; Tissot, J.-B.; Boukhriss, D.; Jebors, S.; Pinese, C.; Verdié, P.; Amblard, M.; Mehdi, A.; Martinez, J.; Humblot, V.; et al. Site-Specific Grafting on Titanium Surfaces with Hybrid Temporin Antibacterial Peptides. *J. Mater. Chem. B* **2018**, *6* (12), 1782–1790. https://doi.org/10.1039/C8TB00051D.

(201) Echalier, C.; Jebors, S.; Laconde, G.; Brunel, L.; Verdié, P.; Causse, L.; Bethry, A.; Legrand, B.; Van Den Berghe, H.; Garric, X.; et al. Sol–Gel Synthesis of Collagen-Inspired Peptide Hydrogel. *Mater. Today* **2017**, *20* (2), 59–66. https://doi.org/10.1016/j.mattod.2017.02.001.

(202) Echalier, C.; Pinese, C.; Garric, X.; Van Den Berghe, H.; Jumas Bilak, E.; Martinez, J.; Mehdi, A.; Subra, G. Easy Synthesis of Tunable Hybrid Bioactive Hydrogels. *Chem. Mater.* **2016**, *28* (5), 1261–1265. https://doi.org/10.1021/acs.chemmater.5b04881.

(203) Monsigny, L.; Berthet, J.-C.; Cantat, T. Depolymerization of Waste Plastics to Monomers and Chemicals Using a Hydrosilylation Strategy Facilitated by Brookhart's Iridium(III) Catalyst. *ACS Sustain. Chem. Eng.* **2018**, *6* (8), 10481–10488. https://doi.org/10.1021/acssuschemeng.8b01842.

(204) Zhao, X.-X.; Zhang, P.; Guo, Z.-X. K_2CO_3-Activated Hydrosilylation: From Redistribution of Polymethylhydrosiloxane to Selectively Reduction of Aldehydes and Ketones. *ChemistrySelect* **2017**, *2* (25), 7670–7677. https://doi.org/10.1002/slct.201701592.

(205) Chalk, A. J.; Harrod, J. F. Homogeneous Catalysis. II. The Mechanism of the Hydrosilation of Olefins Catalyzed by Group VIII Metal Complexes1. *J. Am. Chem. Soc.* **1965**, *87* (1), 16–21. https://doi.org/10.1021/ja01079a004.

(206) Zheng, H.-J.; Chen, W.-B.; Wu, Z.-J.; Deng, J.-G.; Lin, W.-Q.; Yuan, W.-C.; Zhang, X.-M. Highly Enantioselective Synthesis of β-Amino Acid Derivatives by the Lewis Base Catalyzed Hydrosilylation of β-Enamino Esters. *Chem. - Eur. J.* **2008**, *14* (32), 9864–9867. https://doi.org/10.1002/chem.200801582.

(207) Addis, D.; Zhou, S.; Das, S.; Junge, K.; Kosslick, H.; Harloff, J.; Lund, H.; Schulz, A.; Beller, M. Hydrosilylation of Ketones: From Metal-Organic Frameworks to Simple Base Catalysts. *Chem. - Asian J.* **2010**, *5* (11), 2341–2345. https://doi.org/10.1002/asia.201000427.

(208) Karstedt, B. Platinum Complexes of Unsaturated Siloxanes and Platinum Containing Organopolysiloxanes. US3775452 (A), November 27, 1973.

(209) Speier, J. L.; Webster, J. A.; Barnes, G. H. The Addition of Silicon Hydrides to Olefinic Double Bonds. Part II. The Use of Group VIII Metal Catalysts. *J. Am. Chem. Soc.* **1957**, *79* (4), 974–979. https://doi.org/10.1021/ja01561a054.

(210) Pappas, I.; Treacy, S.; Chirik, P. J. Alkene Hydrosilylation Using Tertiary Silanes with α-Diimine Nickel Catalysts. Redox-Active Ligands Promote a Distinct Mechanistic Pathway from Platinum Catalysts. *ACS Catal.* **2016**, *6* (7), 4105–4109. https://doi.org/10.1021/acscatal.6b01134.

(211) Chung, D.; Kim, T. G. Solvent Effect on the Hydrosilylation Reactions for the Synthesis of Polydimethylsiloxane Grafted with Polyoxyethylene Catalyzed by Speier's Catalyst. 6.

(212) Zeng, J. Y.; Hsieh, M.-H.; Lee, H. M. Rhodium Complexes of PCNHCP: Oxidative Addition of Dichloromethane and Catalytic Hydrosilylation of Alkynes Affording (E)-Alkenylsilanes. *J. Organomet. Chem.* **2005**, *690* (24–25), 5662–5671. https://doi.org/10.1016/j.jorganchem.2005.07.025.

(213) Trost, B. M.; Ball, Z. T. Alkyne Hydrosilylation Catalyzed by a Cationic Ruthenium Complex: Efficient and General Trans Addition. *J. Am. Chem. Soc.* **2005**, *127* (50), 17644–17655. https://doi.org/10.1021/ja0528580.
(214) Sellinger, A.; Laine, R. M.; Chu, V.; Viney, C. Palladium- and Platinum-Catalyzed Coupling Reactions of Allyloxy Aromatics with Hydridosilanes and Hydridosiloxanes: Novel Liquid Crystalline/Organosilane Materials. *J. Polym. Sci. Part Polym. Chem.* **1994**, *32* (16), 3069–3089. https://doi.org/10.1002/pola.1994.080321608.
(215) Hofmann, R.; Vlatković, M. Z.; Wiesbrock, F. Fifty Years of Hydrosilylation in Polymer Science: A Review of Current Trends of Low-Cost Transition-Metal and Metal-Free Catalysts, Non-Thermally Triggered Hydrosilylation Reactions, and Industrial Applications. In *Polymers*; 2017. https://doi.org/10.3390/polym9100534.
(216) Lappert, M. F.; Scott, F. P. A. The Reaction Pathway from Speier's to Karstedt's Hydrosilylation Catalyst. *J. Organomet. Chem.* **1995**, *492* (2), C11–C13. https://doi.org/10.1016/0022-328X(94)05359-J.
(217) Berthon-Gelloz, G.; Buisine, O.; Brière, J.-F.; Michaud, G.; Stérin, S.; Mignani, G.; Tinant, B.; Declercq, J.-P.; Chapon, D.; Markó, I. E. Synthetic and Structural Studies of NHC–Pt(Dvtms) Complexes and Their Application as Alkene Hydrosilylation Catalysts (NHC=N-Heterocyclic Carbene, Dvtms=divinyltetramethylsiloxane). *J. Organomet. Chem.* **2005**, *690* (24), 6156–6168. https://doi.org/10.1016/j.jorganchem.2005.08.020.
(218) Markó, I. E.; Stérin, S.; Buisine, O.; Berthon, G.; Michaud, G.; Tinant, B.; Declercq, J.-P. Highly Active and Selective Platinum(0)-Carbene Complexes. Efficient, Catalytic Hydrosilylation of Functionalised Olefins. *Adv. Synth. Catal.* **2004**, *346* (12), 1429–1434. https://doi.org/10.1002/adsc.200404048.
(219) Buisine, O.; Berthon-Gelloz, G.; Brière, J.-F.; Stérin, S.; Mignani, G.; Branlard, P.; Tinant, B.; Declercq, J.-P.; Markó, I. E. Second Generation N-Heterocyclic Carbene–Pt(0) Complexes as Efficient Catalysts for the Hydrosilylation of Alkenes. *Chem. Commun.* **2005**, *0* (30), 3856–3858. https://doi.org/10.1039/B506369H.
(220) Markó, I. E.; Stérin, S.; Buisine, O.; Mignani, G.; Branlard, P.; Tinant, B.; Declercq, J.-P. Selective and Efficient Platinum(0)-Carbene Complexes As Hydrosilylation Catalysts. *Science* **2002**, *298* (5591), 204–206. https://doi.org/10.1126/science.1073338.
(221) Li, Q.; Ji, S.; Li, M.; Duan, X. Pt-Ni Alloy Catalysts for Highly Selective Anti-Markovnikov Alkene Hydrosilylation. *Sci. China Mater.* **2018**, *61* (10), 1339–1344. https://doi.org/10.1007/s40843-018-9282-1.
(222) Yang, X.; Wang, C. Manganese-Catalyzed Hydrosilylation Reactions. *Chem. – Asian J.* **2018**, *13* (17), 2307–2315. https://doi.org/10.1002/asia.201800618.
(223) Min, G. K.; Skrydstrup, T. Regioselective Rh(I)-Catalyzed Sequential Hydrosilylation toward the Assembly of Silicon-Based Peptidomimetic Analogues. *J. Org. Chem.* **2012**, *77* (14), 5894–5906. https://doi.org/10.1021/jo300904z.
(224) Commodities: Latest Platinum Price & Chart /markets/platinum.aspx (accessed Aug 27, 2019).
(225) Nakajima, Y.; Shimada, S. Hydrosilylation Reaction of Olefins: Recent Advances and Perspectives. *RSC Adv.* **2015**, *5* (26), 20603–20616. https://doi.org/10.1039/C4RA17281G.
(226) Jakobsson, K.; Chu, T.; Nikonov, G. I. Hydrosilylation of Olefins Catalyzed by Well-Defined Cationic Aluminum Complexes: Lewis Acid versus Insertion Mechanisms. *ACS Catal.* **2016**, *6* (11), 7350–7356. https://doi.org/10.1021/acscatal.6b01694.
(227) El Kadib, A.; Katir, N.; Castel, A.; Delpech, F.; Rivière, P. Hydrosilylation of Unsaturated Fatty Acid N-Phenyl Amides. *Appl. Organomet. Chem.* **2007**, *21* (7), 590–594. https://doi.org/10.1002/aoc.1240.
(228) Belyakova, Z. V.; Chernyshev, E. A.; Storozhenko, P. A.; Knyazev, S. P.; Turkel'taub, G. N.; Parshina, E. V.; Kisin, A. V. Hydrosilylation of Cyclohexene and Allyl Chloride with Trichloro-, Dichloro(Methyl)-, and Chlorodimethylsilanes in the Presence of Pt(0) Complexes. *Russ. J. Gen. Chem.* **2006**, *76* (6), 925–930. https://doi.org/10.1134/S1070363206060120.
(229) Marchand, D.; Martinez, J.; Cavelier, F. Straightforward Synthesis of Chiral Silylated Amino Acids through Hydrosilylation. *Eur. J. Org. Chem.* **2008**, *2008* (18), 3107–3112. https://doi.org/10.1002/ejoc.200800066.
(230) Arribat, M.; Rémond, E.; Richeter, S.; Gerbier, P.; Clément, S.; Cavelier, F. Silole Amino Acids with

Aggregation-Induced Emission Features Synthesized by Hydrosilylation. *Eur. J. Org. Chem.* **2019**, *2019* (12), 2275–2281. https://doi.org/10.1002/ejoc.201801869.

(231) Cavelier, F.; Marchand, D.; Martinez, J. α,A'-Disubstituted Amino Acids with Silylated Side Chains as Lipophilic Building Blocks for the Synthesis of Peptaibol Analogues. *Chem. Biodivers.* **2008**, *5* (7), 1279–1287. https://doi.org/10.1002/cbdv.200890114.

(232) Min, G. K.; Hernández, D.; Skrydstrup, T. Efficient Routes to Carbon–Silicon Bond Formation for the Synthesis of Silicon-Containing Peptides and Azasilaheterocycles. *Acc. Chem. Res.* **2013**, *46* (2), 457–470. https://doi.org/10.1021/ar300200h.

(233) Echalier, C.; Kalistratova, A.; Ciccione, J.; Lebrun, A.; Legrand, B.; Naydenova, E.; Gagne, D.; Fehrentz, J.-A.; Marie, J.; Amblard, M.; et al. Selective Homodimerization of Unprotected Peptides Using Hybrid Hydroxydimethylsilane Derivatives. *RSC Adv.* **2016**, *6* (39), 32905–32914. https://doi.org/10.1039/C6RA06075G.

(234) Isidro-Llobet, A.; Álvarez, M.; Albericio, F. Amino Acid-Protecting Groups. *Chem. Rev.* **2009**, *109* (6), 2455–2504. https://doi.org/10.1021/cr800323s.

(235) Chan, W.; White, P. *Fmoc Solid Phase Peptide Synthesis: A Practical Approach*; Oxford University Press, 1999.

(236) Shin, H.; Moon, B. Careful Investigation of the Hydrosilylation of Olefins at Poly(Ethylene Glycol) Chain Ends and Development of a New Silyl Hydride to Avoid Side Reactions. *J. Polym. Sci. Part Polym. Chem.* **2018**, *56* (5), 527–536. https://doi.org/10.1002/pola.28924.

(237) Jebors, S.; Enjalbal, C.; Amblard, M.; Mehdi, A.; Subra, G.; Martinez, J. Bioorganic Hybrid OMS by Straightforward Grafting of Trialkoxysilyl Peptides. *J. Mater. Chem. B* **2013**, *1* (23), 2921–2925. https://doi.org/10.1039/C3TB20122H.

(238) Dou, B.; Wang, Y.; Zhang, T.; Meng, G.; Shao, Y.; Lin, X.; Wang, F. Electrochemically Assisted Silanization Treatment of an Aluminum Alloy under Oxygen Pressure for Corrosion Protection. *New J. Chem.* **2018**, *42* (12), 9771–9782. https://doi.org/10.1039/C8NJ00043C.

(239) Massia, S. P.; Holecko, M. M.; Ehteshami, G. R. In Vitro Assessment of Bioactive Coatings for Neural Implant Applications. *J. Biomed. Mater. Res. A* **2004**, *68A* (1), 177–186. https://doi.org/10.1002/jbm.a.20009.

(240) Ebelmen, M. M. Recherches Sur Les Combinaisons Des Acides Boriques et Siliciques Avec Les Éthers. *Ann Chim Phys* **1846**, *16*, 129.

(241) Ebelmen, M. Sur L'hyalite Artificielle et L'hydrophane. *C R Acad Sci* **1847**, *25*, 854.

(242) Graham, T. On the Properties of Silicic Acid and Other Analogous Colloidal Substances. *J Chem Soc* **1864**, *17*, 318–327.

(243) Morpurgo, M.; Teoli, D.; Pignatto, M.; Attrezzi, M.; Spadaro, F.; Realdon, N. The Effect of Na2CO3, NaF and NH4OH on the Stability and Release Behavior of Sol–Gel Derived Silica Xerogels Embedded with Bioactive Compounds. *Acta Biomater.* **2010**, *6* (6), 2246–2253. https://doi.org/10.1016/j.actbio.2009.12.021.

(244) Montheil, T.; Echalier, C.; Martinez, J.; Subra, G.; Mehdi, A. Inorganic Polymerization: An Attractive Route to Biocompatible Hybrid Hydrogels. *J. Mater. Chem. B* **2018**, *6* (21), 3434–3448. https://doi.org/10.1039/C8TB00456K.

(245) Echalier, C.; Kalistratova, A.; Ciccione, J.; Lebrun, A.; Legrand, B.; Naydenova, E.; Gagne, D.; Fehrentz, J.-A.; Marie, J.; Amblard, M.; et al. Selective Homodimerization of Unprotected Peptides Using Hybrid Hydroxydimethylsilane Derivatives. *RSC Adv.* **2016**, *6* (39), 32905–32914. https://doi.org/10.1039/C6RA06075G.

(246) Echalier, C.; Pinese, C.; Garric, X.; Van Den Berghe, H.; Jumas Bilak, E.; Martinez, J.; Mehdi, A.; Subra, G. Easy Synthesis of Tunable Hybrid Bioactive Hydrogels. *Chem. Mater.* **2016**, *28* (5), 1261–1265. https://doi.org/10.1021/acs.chemmater.5b04881.

(247) Boll, E.; Drobecq, H.; Ollivier, N.; Raibaut, L.; Desmet, R.; Vicogne, J.; Melnyk, O. A Novel PEG-Based Solid Support Enables the Synthesis of >50 Amino-Acid Peptide Thioesters and the Total Synthesis of a Functional SUMO-1 Peptide Conjugate. *Chem. Sci.* **2014**, *5* (5), 2017–2022. https://doi.org/10.1039/C3SC53509F.

(248) García-Ramos, Y.; Paradís-Bas, M.; Tulla-Puche, J.; Albericio, F. ChemMatrix® for Complex Peptides and

Combinatorial Chemistry. *J. Pept. Sci.* **2010**, *16* (12), 675–678. https://doi.org/10.1002/psc.1282.
(249) Hachmann, J.; Lebl, M. Search for Optimal Coupling Reagent in Multiple Peptide Synthesizer. *Pept. Sci.* **2006**, *84* (3), 340–347. https://doi.org/10.1002/bip.20482.
(250) Li, W.; Wang, D.; Shi, X.; Li, J.; Ma, Y.; Wang, Y.; Li, T.; Zhang, J.; Zhao, R.; Yu, Z.; et al. A SiRNA-Induced Peptide Co-Assembly System as a Peptide-Based SiRNA Nanocarrier for Cancer Therapy. *Mater. Horiz.* **2018**, *5* (4), 745–752. https://doi.org/10.1039/C8MH00392K.
(251) Chen, B.; Xu, W.; Pan, R.; Chen, P. Design and Characterization of a New Peptide Vector for Short Interfering RNA Delivery. *J. Nanobiotechnology* **2015**, *13* (1), 39. https://doi.org/10.1186/s12951-015-0098-0.
(252) Konate, K.; Dussot, M.; Aldrian, G.; Vaissière, A.; Viguier, V.; Neira, I. F.; Couillaud, F.; Vivès, E.; Boisguerin, P.; Deshayes, S. Peptide-Based Nanoparticles to Rapidly and Efficiently "Wrap 'n Roll" SiRNA into Cells. *Bioconjug. Chem.* **2019**, *30* (3), 592–603. https://doi.org/10.1021/acs.bioconjchem.8b00776.
(253) Nasanit, R.; Iqbal, P.; Soliman, M.; Spencer, N.; Allen, S.; C. Davies, M.; S. Briggs, S.; W. Seymour, L.; A. Preece, J.; Alexander, C. Combination Dual Responsive Polypeptide Vectors for Enhanced Gene Delivery. *Mol. Biosyst.* **2008**, *4* (7), 741–745. https://doi.org/10.1039/B803262A.
(254) Khalil, I. A.; Yamada, Y.; Harashima, H. Optimization of SiRNA Delivery to Target Sites: Issues and Future Directions. *Expert Opin. Drug Deliv.* **2018**, *15* (11), 1053–1065. https://doi.org/10.1080/17425247.2018.1520836.
(255) Pierschbacher, M. D.; Ruoslahti, E. Variants of the Cell Recognition Site of Fibronectin That Retain Attachment-Promoting Activity. *Proc. Natl. Acad. Sci.* **1984**, *81* (19), 5985–5988. https://doi.org/10.1073/pnas.81.19.5985.
(256) Ruoslahti, E.; Pierschbacher, M. D. New Perspectives in Cell Adhesion: RGD and Integrins. *Science* **1987**, *238* (4826), 491–497. https://doi.org/10.1126/science.2821619.
(257) Humphries, J. D. Integrin Ligands at a Glance. *J. Cell Sci.* **2006**, *119* (19), 3901–3903. https://doi.org/10.1242/jcs.03098.
(258) Yu, Y. P.; Wang, Q.; Liu, Y. C.; Xie, Y. Molecular Basis for the Targeted Binding of RGD-Containing Peptide to Integrin AVβ3. *Biomaterials* **2014**, *35* (5), 1667–1675. https://doi.org/10.1016/j.biomaterials.2013.10.072.
(259) Xiong, J.-P.; Stehle, T.; Goodman, S. L.; Arnaout, M. A. Integrins, Cations and Ligands: Making the Connection. *J. Thromb. Haemost.* **2003**, *1* (7), 1642–1654. https://doi.org/10.1046/j.1538-7836.2003.00277.x.
(260) Villard, V.; Kalyuzhniy, O.; Riccio, O.; Potekhin, S.; Melnik, T. N.; Kajava, A. V.; Rüegg, C.; Corradin, G. Synthetic RGD-Containing α-Helical Coiled Coil Peptides Promote Integrin-Dependent Cell Adhesion. *J. Pept. Sci.* **2006**, *12* (3), 206–212. https://doi.org/10.1002/psc.707.
(261) Schaffner, P.; Dard, M. M. Structure and Function of RGD Peptides Involved in Bone Biology. *Cell. Mol. Life Sci. CMLS* **2003**, *60* (1), 119–132. https://doi.org/10.1007/s000180300008.
(262) Kapp, T. G.; Rechenmacher, F.; Neubauer, S.; Maltsev, O. V.; Cavalcanti-Adam, E. A.; Zarka, R.; Reuning, U.; Notni, J.; Wester, H.-J.; Mas-Moruno, C.; et al. A Comprehensive Evaluation of the Activity and Selectivity Profile of Ligands for RGD-Binding Integrins. *Sci. Rep.* **2017**, *7*, 39805. https://doi.org/10.1038/srep39805.
(263) Haubner, R.; Gratias, R.; Diefenbach, B.; Goodman, S. L.; Jonczyk, A.; Kessler, H. Structural and Functional Aspects of RGD-Containing Cyclic Pentapeptides as Highly Potent and Selective Integrin $\alpha_V\beta_3$ Antagonists. *J. Am. Chem. Soc.* **1996**, *118* (32), 7461–7472. https://doi.org/10.1021/ja9603721.
(264) Thumshirn, G.; Hersel, U.; Goodman, S. L.; Kessler, H. Multimeric Cyclic RGD Peptides as Potential Tools for Tumor Targeting: Solid-Phase Peptide Synthesis and Chemoselective Oxime Ligation. *Chem. – Eur. J.* **2003**, *9* (12), 2717–2725. https://doi.org/10.1002/chem.200204304.
(265) Pierschbacher, M. D.; Ruoslahti, E. Cell Attachment Activity of Fibronectin Can Be Duplicated by Small Synthetic Fragments of the Molecule. *Nature* **1984**, *309* (5963), 30–33. https://doi.org/10.1038/309030a0.
(266) Fu, S.; Xu, X.; Ma, Y.; Zhang, S.; Zhang, S. RGD Peptide-Based Non-Viral Gene Delivery Vectors Targeting Integrin Avβ3 for Cancer Therapy. *J. Drug Target.* **2019**, *27* (1), 1–11. https://doi.org/10.1080/1061186X.2018.1455841.

(267) Sun, X.; Niu, G.; Yan, Y.; Yang, M.; Chen, K.; Ma, Y.; Chan, N.; Shen, B.; Chen, X. Phage Display-Derived Peptides for Osteosarcoma Imaging. *Clin. Cancer Res. Off. J. Am. Assoc. Cancer Res.* **2010**, *16* (16), 4268–4277. https://doi.org/10.1158/1078-0432.CCR-10-0968.

(268) Kwon, S.; Ke, S.; Houston, J. P.; Wang, W.; Wu, Q.; Li, C.; Sevick-Muraca, E. M. Imaging Dose-Dependent Pharmacokinetics of an RGD-Fluorescent Dye Conjugate Targeted to Avβ3 Receptor Expressed in Kaposi's Sarcoma. *Mol. Imaging* **2005**, *4* (2), 15353500200505104. https://doi.org/10.1162/15353500200505103.

(269) Glaser, M.; Morrison, M.; Solbakken, M.; Arukwe, J.; Karlsen, H.; Wiggen, U.; Champion, S.; Kindberg, G. M.; Cuthbertson, A. Radiosynthesis and Biodistribution of Cyclic RGD Peptides Conjugated with Novel [18F]Fluorinated Aldehyde-Containing Prosthetic Groups. *Bioconjug. Chem.* **2008**, *19* (4), 951–957. https://doi.org/10.1021/bc700472w.

(270) Cai, H.; Conti, P. S. RGD-Based PET Tracers for Imaging Receptor Integrin Avβ3 Expression. *J. Label. Compd. Radiopharm.* **2013**, *56* (5), 264–279. https://doi.org/10.1002/jlcr.2999.

(271) Chen, X.; Plasencia, C.; Hou, Y.; Neamati, N. Synthesis and Biological Evaluation of Dimeric RGD Peptide−Paclitaxel Conjugate as a Model for Integrin-Targeted Drug Delivery. *J. Med. Chem.* **2005**, *48* (4), 1098–1106. https://doi.org/10.1021/jm049165z.

(272) Wang, F.; Chen, L.; Zhang, R.; Chen, Z.; Zhu, L. RGD Peptide Conjugated Liposomal Drug Delivery System for Enhance Therapeutic Efficacy in Treating Bone Metastasis from Prostate Cancer. *J. Controlled Release* **2014**, *196*, 222–233. https://doi.org/10.1016/j.jconrel.2014.10.012.

(273) Asati, S.; Pandey, V.; Soni, V. RGD Peptide as a Targeting Moiety for Theranostic Purpose: An Update Study. *Int. J. Pept. Res. Ther.* **2019**, *25* (1), 49–65. https://doi.org/10.1007/s10989-018-9728-3.

(274) Huettner, N.; Dargaville, T. R.; Forget, A. Discovering Cell-Adhesion Peptides in Tissue Engineering: Beyond RGD. *Trends Biotechnol.* **2018**, *36* (4), 372–383. https://doi.org/10.1016/j.tibtech.2018.01.008.

(275) Jao, D.; Mou, X.; Hu, X. Tissue Regeneration: A Silk Road. *J. Funct. Biomater.* **2016**, *7* (3). https://doi.org/10.3390/jfb7030022.

(276) Burdick, J. A.; Anseth, K. S. Photoencapsulation of Osteoblasts in Injectable RGD-Modified PEG Hydrogels for Bone Tissue Engineering. *Biomaterials* **2002**, *23* (22), 4315–4323. https://doi.org/10.1016/S0142-9612(02)00176-X.

(277) Weber, L. M.; Hayda, K. N.; Haskins, K.; Anseth, K. S. The Effects of Cell–Matrix Interactions on Encapsulated β-Cell Function within Hydrogels Functionalized with Matrix-Derived Adhesive Peptides. *Biomaterials* **2007**, *28* (19), 3004–3011. https://doi.org/10.1016/j.biomaterials.2007.03.005.

(278) Do, N. M.; Olivier, M. A.; Salisbury, J. J.; Wager, C. B. Application of Quantitative ^{19} F and ^{1} H NMR for Reaction Monitoring and In Situ Yield Determinations for an Early Stage Pharmaceutical Candidate. *Anal. Chem.* **2011**, *83* (22), 8766–8771. https://doi.org/10.1021/ac202287y.

(279) Akoka, S.; Barantin, L.; Trierweiler, M. Concentration Measurement by Proton NMR Using the ERETIC Method. *Anal. Chem.* **1999**, *71* (13), 2554–2557. https://doi.org/10.1021/ac981422i.

(280) Marchesi, F.; Turriziani, M.; Tortorelli, G.; Avvisati, G.; Torino, F.; De Vecchis, L. Triazene Compounds: Mechanism of Action and Related DNA Repair Systems. *Pharmacol. Res.* **2007**, *56* (4), 275–287. https://doi.org/10.1016/j.phrs.2007.08.003.

(281) Whitelaw, B. C. How and When to Use Temozolomide to Treat Aggressive Pituitary Tumours. *Endocr. Relat. Cancer* **2019**, *26* (9), R545–R552. https://doi.org/10.1530/ERC-19-0083.

(282) Todd, A.; Groundwater, P. W.; Gill, J. H. *Anticancer Therapeutics: From Drug Discovery to Clinical Applications*; John Wiley & Sons, 2018.

(283) Syro, L. V.; Rotondo, F.; Camargo, M.; Ortiz, L. D.; Serna, C. A.; Kovacs, K. Temozolomide and Pituitary Tumors: Current Understanding, Unresolved Issues, and Future Directions. *Front. Endocrinol.* **2018**, *9*. https://doi.org/10.3389/fendo.2018.00318.

(284) Fan, C.-H.; Liu, W.-L.; Cao, H.; Wen, C.; Chen, L.; Jiang, G. O6-Methylguanine DNA Methyltransferase as a Promising Target for the Treatment of Temozolomide-Resistant Gliomas. *Cell Death Dis.* **2013**, *4* (10), e876. https://doi.org/10.1038/cddis.2013.388.

(285) Wesolowski, J. R.; Rajdev, P.; Mukherji, S. K. Temozolomide (Temodar). *Am. J. Neuroradiol.* **2010**, *31* (8), 1383–1384. https://doi.org/10.3174/ajnr.A2170.

(286) Cipriani, P.; Ruscitti, P.; Carubbi, F.; Liakouli, V.; Giacomelli, R. Methotrexate: An Old New Drug in

Autoimmune Disease. *Expert Rev. Clin. Immunol.* **2014**, *10* (11), 1519–1530. https://doi.org/10.1586/1744666X.2014.962996.

(287) Brown, P. M.; Pratt, A. G.; Isaacs, J. D. Mechanism of Action of Methotrexate in Rheumatoid Arthritis, and the Search for Biomarkers. *Nat. Rev. Rheumatol.* **2016**, *12* (12), 731–742. https://doi.org/10.1038/nrrheum.2016.175.

(288) Fernández, M.; Javaid, F.; Chudasama, V. Advances in Targeting the Folate Receptor in the Treatment/Imaging of Cancers. *Chem. Sci.* **2018**, *9* (4), 790–810. https://doi.org/10.1039/C7SC04004K.

(289) Dervieux, T.; Furst, D.; Lein, D. O.; Capps, R.; Smith, K.; Walsh, M.; Kremer, J. Polyglutamation of Methotrexate with Common Polymorphisms in Reduced Folate Carrier, Aminoimidazole Carboxamide Ribonucleotide Transformylase, and Thymidylate Synthase Are Associated with Methotrexate Effects in Rheumatoid Arthritis. *Arthritis Rheum.* **2004**, *50* (9), 2766–2774. https://doi.org/10.1002/art.20460.

(290) Wong, P. T.; Choi, S. K. Mechanisms and Implications of Dual-Acting Methotrexate in Folate-Targeted Nanotherapeutic Delivery., Mechanisms and Implications of Dual-Acting Methotrexate in Folate-Targeted Nanotherapeutic Delivery. *Int. J. Mol. Sci. Int. J. Mol. Sci.* **2015**, *16, 16* (1, 1), 1772, 1772–1790. https://doi.org/10.3390/ijms16011772, 10.3390/ijms16011772.

(291) Kukowska-Latallo, J. F.; Candido, K. A.; Cao, Z.; Nigavekar, S. S.; Majoros, I. J.; Thomas, T. P.; Balogh, L. P.; Khan, M. K.; Baker, J. R. Nanoparticle Targeting of Anticancer Drug Improves Therapeutic Response in Animal Model of Human Epithelial Cancer. *Cancer Res.* **2005**, *65* (12), 5317–5324. https://doi.org/10.1158/0008-5472.CAN-04-3921.

(292) Rahimi, M.; D. Safa, K.; Alizadeh, E.; Salehi, R. Dendritic Chitosan as a Magnetic and Biocompatible Nanocarrier for the Simultaneous Delivery of Doxorubicin and Methotrexate to MCF-7 Cell Line. *New J. Chem.* **2017**, *41* (8), 3177–3189. https://doi.org/10.1039/C6NJ04107H.

(293) Cheng, W.; Nie, J.; Xu, L.; Liang, C.; Peng, Y.; Liu, G.; Wang, T.; Mei, L.; Huang, L.; Zeng, X. PH-Sensitive Delivery Vehicle Based on Folic Acid-Conjugated Polydopamine-Modified Mesoporous Silica Nanoparticles for Targeted Cancer Therapy. *ACS Appl. Mater. Interfaces* **2017**, *9* (22), 18462–18473. https://doi.org/10.1021/acsami.7b02457.

(294) Beugelmans, R.; Neuville, L.; Bois-Choussy, M.; Chastanet, J.; Zhu, J. Palladium Catalyzed Reductive Deprotection of Alloc: Transprotection and Peptide Bond Formation. *Tetrahedron Lett.* **1995**, *36* (18), 3129–3132. https://doi.org/10.1016/0040-4039(95)00449-M.

(295) Wall, M. E.; Wani, M. C.; Cook, C. E.; Palmer, K. H.; McPhail, A. T.; Sim, G. A. Plant Antitumor Agents. I. The Isolation and Structure of Camptothecin, a Novel Alkaloidal Leukemia and Tumor Inhibitor from Camptotheca Acuminata1,2. *J. Am. Chem. Soc.* **1966**, *88* (16), 3888–3890. https://doi.org/10.1021/ja00968a057.

(296) Wen, Y.; Wang, Y.; Liu, X.; Zhang, W.; Xiong, X.; Han, Z.; Liang, X. Camptothecin-Based Nanodrug Delivery Systems. *Cancer Biol. Med.* **2017**, *14* (4), 363–370. https://doi.org/10.20892/j.issn.2095-3941.2017.0099.

(297) Li, F.; Jiang, T.; Li, Q.; Ling, X. Camptothecin (CPT) and Its Derivatives Are Known to Target Topoisomerase I (Top1) as Their Mechanism of Action: Did We Miss Something in CPT Analogue Molecular Targets for Treating Human Disease Such as Cancer? *Am. J. Cancer Res.* **2017**, *7* (12), 2350–2394.

(298) Lazareva, N. F.; Baryshok, V. P.; Lazarev, I. M. Silicon-Containing Analogs of Camptothecin as Anticancer Agents. *Arch. Pharm. (Weinheim)* **2018**, *351* (1), 1700297. https://doi.org/10.1002/ardp.201700297.

(299) Lalloo, A. K.; Luo, F. R.; Guo, A.; Paranjpe, P. V.; Lee, S.-H.; Vyas, V.; Rubin, E.; Sinko, P. J. Membrane Transport of Camptothecin: Facilitation by Human P-Glycoprotein (ABCB1) and Multidrug Resistance Protein 2 (ABCC2). *BMC Med.* **2004**, *2* (1), 16. https://doi.org/10.1186/1741-7015-2-16.

(300) Capranico, G.; Ferri, F.; Fogli, M. V.; Russo, A.; Lotito, L.; Baranello, L. The Effects of Camptothecin on RNA Polymerase II Transcription: Roles of DNA Topoisomerase I. *Biochimie* **2007**, *89* (4), 482–489. https://doi.org/10.1016/j.biochi.2007.01.001.

(301) Niyogi, S.; Sarkar, S.; Adhikari, B. Catalytic Activity of DBTDL in Polyurethane Formation. 4.

(302) Chourpa, I.; Riou, J.-F.; Millot, J.-M.; Pommier, Y.; Manfait, M. Modulation in Kinetics of Lactone Ring Hydrolysis of Camptothecins upon Interaction with Topoisomerase I Cleavage Sites on DNA. *Biochemistry* **1998**, *37* (20), 7284–7291. https://doi.org/10.1021/bi972902r.

(303) Chourpa, I.; Millot, J.-M.; Sockalingum, G. D.; Riou, J.-F.; Manfait, M. Kinetics of Lactone Hydrolysis in

Antitumor Drugs of Camptothecin Series as Studied by Fluorescence Spectroscopy. *Biochim. Biophys. Acta BBA - Gen. Subj.* **1998**, *1379* (3), 353–366. https://doi.org/10.1016/S0304-4165(97)00115-3.

(304) Chilla, S. N. M.; Henoumont, C.; Elst, L. V.; Muller, R. N.; Laurent, S. Importance of DOTA Derivatives in Bimodal Imaging. *Isr. J. Chem.* **2017**, *57* (9), 800–808. https://doi.org/10.1002/ijch.201700024.

(305) Moreau, M.; Raguin, O.; Vrigneaud, J.-M.; Collin, B.; Bernhard, C.; Tizon, X.; Boschetti, F.; Duchamp, O.; Brunotte, F.; Denat, F. DOTAGA-Trastuzumab. A New Antibody Conjugate Targeting HER2/Neu Antigen for Diagnostic Purposes. *Bioconjug. Chem.* **2012**, *23* (6), 1181–1188. https://doi.org/10.1021/bc200680x.

(306) *Positron Emission Tomography: Basic Science and Clinical Practice*; Valk, P. E., Ed.; Springer: London ; New York, 2003.

(307) Kilian, K. 68Ga-DOTA and Analogs: Current Status and Future Perspectives. *Rep. Pract. Oncol. Radiother.* **2014**, *19*, S13–S21. https://doi.org/10.1016/j.rpor.2014.04.016.

(308) Velikyan, I. 68Ga-Based Radiopharmaceuticals: Production and Application Relationship. *Molecules* **2015**, *20* (7), 12913–12943. https://doi.org/10.3390/molecules200712913.

(309) Velikyan, I. Prospective of ^{68} Ga-Radiopharmaceutical Development. *Theranostics* **2014**, *4* (1), 47–80. https://doi.org/10.7150/thno.7447.

(310) Bernhard, C.; Moreau, M.; Lhenry, D.; Goze, C.; Boschetti, F.; Rousselin, Y.; Brunotte, F.; Denat, F. DOTAGA-Anhydride: A Valuable Building Block for the Preparation of DOTA-like Chelating Agents. *Chem. Weinh. Bergstr. Ger.* **2012**, *18* (25), 7834–7841. https://doi.org/10.1002/chem.201200132.

(311) Yan, F.; Fan, K.; Bai, Z.; Zhang, R.; Zu, F.; Xu, J.; Li, X. Fluorescein Applications as Fluorescent Probes for the Detection of Analytes. *TrAC Trends Anal. Chem.* **2017**, *97*, 15–35. https://doi.org/10.1016/j.trac.2017.08.013.

(312) Cavallo, C.; De Laurentis, C.; Vetrano, I. G.; Falco, J.; Broggi, M.; Schiariti, M.; Ferroli, P.; Acerbi, F. The Utilization of Fluorescein in Brain Tumor Surgery: A Systematic Review. *J. Neurosurg. Sci.* **2018**, *62* (6), 690–703. https://doi.org/10.23736/S0390-5616.18.04480-6.

(313) Lanier, L. L.; Warner, N. L. Paraformaldehyde Fixation of Hematopoietic Cells for Quantitative Flow Cytometry (FACS) Analysis. *J. Immunol. Methods* **1981**, *47* (1), 25–30. https://doi.org/10.1016/0022-1759(81)90253-2.

(314) Wallace, M. B.; Meining, A.; Canto, M. I.; Fockens, P.; Miehlke, S.; Roesch, T.; Lightdale, C. J.; Pohl, H.; Carr-Locke, D.; Löhr, M.; et al. The Safety of Intravenous Fluorescein for Confocal Laser Endomicroscopy in the Gastrointestinal Tract. *Aliment. Pharmacol. Ther.* **2010**, *31* (5), 548–552. https://doi.org/10.1111/j.1365-2036.2009.04207.x.

(315) Robertson, T. A.; Bunel, F.; Roberts, M. S. Fluorescein Derivatives in Intravital Fluorescence Imaging. *Cells* **2013**, *2* (3), 591–606. https://doi.org/10.3390/cells2030591.

(316) Cho, H.-J.; Yoon, I.-S.; Yoon, H. Y.; Koo, H.; Jin, Y.-J.; Ko, S.-H.; Shim, J.-S.; Kim, K.; Kwon, I. C.; Kim, D.-D. Polyethylene Glycol-Conjugated Hyaluronic Acid-Ceramide Self-Assembled Nanoparticles for Targeted Delivery of Doxorubicin. *Biomaterials* **2012**, *33* (4), 1190–1200. https://doi.org/10.1016/j.biomaterials.2011.10.064.

(317) Roberts, M. J.; Bentley, M. D.; Harris, J. M. Chemistry for Peptide and Protein PEGylation. *Adv. Drug Deliv. Rev.* **2002**, *54* (4), 459–476. https://doi.org/10.1016/S0169-409X(02)00022-4.

(318) Rösler, A.; Vandermeulen, G. W. M.; Klok, H.-A. Advanced Drug Delivery Devices via Self-Assembly of Amphiphilic Block Copolymers. *Adv. Drug Deliv. Rev.* **2012**, *64*, 270–279. https://doi.org/10.1016/j.addr.2012.09.026.

(319) Höfer, R.; Jost, F.; Schwuger, M. J.; Scharf, R.; Geke, J.; Kresse, J.; Lingmann, H.; Veitenhansl, R.; Erwied, W. Foams and Foam Control https://onlinelibrary.wiley.com/doi/abs/10.1002/14356007.a11_465 (accessed Aug 13, 2019). https://doi.org/10.1002/14356007.a11_465.

(320) Wilson, W. R. D.; Huang, X. B. Viscoplastic Behavior of a Silicone Oil in a Metalforming Inlet Zone. *J. Tribol.* **1989**, *111* (4), 585–590. https://doi.org/10.1115/1.3261981.

(321) Arianpour, F.; Farzaneh, M.; Kulinich, S. A. Hydrophobic and Ice-Retarding Properties of Doped Silicone Rubber Coatings. *Appl. Surf. Sci.* **2013**, *265*, 546–552. https://doi.org/10.1016/j.apsusc.2012.11.042.

(322) Kobayashi, H.; Tateishi, M.; Masatomi, T. Silicone Resin Composition for Water Repellent Coating. US7019069B2, March 28, 2006.

(323) Wong, C. P. High Performance Silicone Gel as IC Device Chip Protection. *MRS Online Proc. Libr. Arch.* **1987**, *108*. https://doi.org/10.1557/PROC-108-175.
(324) Horikoshi, J.; Kimura, T. RTV Silicone Rubber Composition for Electric and Electronic Part Protection, Circuit Boards, Silver Electrodes, and Silver Chip Resistors. US7553901B2, June 30, 2009.
(325) Mani, S. Fundamentals aspects of crosslinking control of PDMS rubber at high temperatures using TEMPO nitroxide. 127.
(326) Kaffashi, A.; Jannesari, A.; Ranjbar, Z. Silicone Fouling-Release Coatings: Effects of the Molecular Weight of Poly(Dimethylsiloxane) and Tetraethyl Orthosilicate on the Magnitude of Pseudobarnacle Adhesion Strength. *Biofouling* **2012**, *28* (7), 729–741. https://doi.org/10.1080/08927014.2012.702342.
(327) Lewis, L.; Stein, J.; Gao, Y.; Colborn, R.; Hutchins, G. Platinum Catalysts Used in the Silicones Industry: Their Synthesis and Activity in Hydrosilylation. *Platin. Met Rev* **1997**, *41*.
(328) Bondurant, S.; Ernster, V.; Herdman, R. *Implant Catalogue*; National Academies Press (US), 1999.
(329) Tyagi, S. Nanoparticles – An Overview of Classification and Applications; 2016.
(330) Romero, G.; Moya, S. E. Chapter 4 - Synthesis of Organic Nanoparticles. In *Frontiers of Nanoscience*; de la Fuente, J. M., Grazu, V., Eds.; Nanobiotechnology; Elsevier, 2012; Vol. 4, pp 115–141. https://doi.org/10.1016/B978-0-12-415769-9.00004-2.
(331) Huang, J.; Bonduelle, C.; Thévenot, J.; Lecommandoux, S.; Heise, A. Biologically Active Polymersomes from Amphiphilic Glycopeptides. *J. Am. Chem. Soc.* **2012**, *134* (1), 119–122. https://doi.org/10.1021/ja209676p.
(332) Carlsen, A.; Lecommandoux, S. Self-Assembly of Polypeptide-Based Block Copolymer Amphiphiles. *Curr. Opin. Colloid Interface Sci.* **2009**, *14* (5), 329–339. https://doi.org/10.1016/j.cocis.2009.04.007.
(333) Klok, H.-A.; Langenwalter, J. F.; Lecommandoux, S. Self-Assembly of Peptide-Based Diblock Oligomers. *Macromolecules* **2000**, *33* (21), 7819–7826. https://doi.org/10.1021/ma0009606.
(334) Hasan, S. A Review on Nanoparticles: Their Synthesis and Types. **2015**, *4*, 4.
(335) Ealia, S. A. M.; Saravanakumar, M. P. A Review on the Classification, Characterisation, Synthesis of Nanoparticles and Their Application. *IOP Conf. Ser. Mater. Sci. Eng.* **2017**, *263*, 032019. https://doi.org/10.1088/1757-899X/263/3/032019.
(336) Klajnert, B.; Bryszewska, M. Dendrimers: Properties and Applications. **2001**, *48*, 10.
(337) Wang, Q. NANOPARTICLES FOR APPLICATIONS IN DRUG DELIVERY; 2014; pp 159–196. https://doi.org/10.13140/RG.2.1.3200.7203.
(338) Gao, K.; Jiang, X. Influence of Particle Size on Transport of Methotrexate across Blood Brain Barrier by Polysorbate 80-Coated Polybutylcyanoacrylate Nanoparticles. *Int. J. Pharm.* **2006**, *310* (1–2), 213–219. https://doi.org/10.1016/j.ijpharm.2005.11.040.
(339) Li Bassi, A.; Cattaneo, D.; Russo, V.; Bottani, C. E.; Barborini, E.; Mazza, T.; Piseri, P.; Milani, P.; Ernst, F. O.; Wegner, K.; et al. Raman Spectroscopy Characterization of Titania Nanoparticles Produced by Flame Pyrolysis: The Influence of Size and Stoichiometry. *J. Appl. Phys.* **2005**, *98* (7), 074305. https://doi.org/10.1063/1.2061894.
(340) Niikura, K.; Matsunaga, T.; Suzuki, T.; Kobayashi, S.; Yamaguchi, H.; Orba, Y.; Kawaguchi, A.; Hasegawa, H.; Kajino, K.; Ninomiya, T.; et al. Gold Nanoparticles as a Vaccine Platform: Influence of Size and Shape on Immunological Responses *in Vitro* and *in Vivo*. *ACS Nano* **2013**, *7* (5), 3926–3938. https://doi.org/10.1021/nn3057005.
(341) Matsui, I. Nanoparticles for Electronic Device Applications: A Brief Review. *J. Chem. Eng. Jpn. - J CHEM ENG JPN* **2005**, *38*, 535–546. https://doi.org/10.1252/jcej.38.535.
(342) W Wiechers, J.; Musee, N. Engineered Inorganic Nanoparticles and Cosmetics: Facts, Issues, Knowledge Gaps and Challenges. *J. Biomed. Nanotechnol.* **2010**, *6*, 408–431. https://doi.org/10.1166/jbn.2010.1143.
(343) Doane, T. L.; Burda, C. The Unique Role of Nanoparticles in Nanomedicine: Imaging, Drug Delivery and Therapy. *Chem. Soc. Rev.* **2012**, *41* (7), 2885–2911. https://doi.org/10.1039/c2cs15260f.
(344) Manaktala, S.; M Singh, K.; Professor, A. NANOTECHNOLOGY FOR ENERGY APPLICATIONS 1; 2016.
(345) Sharma, N.; Ojha, H.; Bharadwaj, A.; Pathak, D. P.; Sharma, R. K. Preparation and Catalytic Applications of Nanomaterials: A Review. *RSC Adv.* **2015**, *5* (66), 53381–53403. https://doi.org/10.1039/C5RA06778B.

(346) Kumar, R.; Lal, S. Synthesis of Organic Nanoparticles and Their Applications in Drug Delivery and Food Nanotechnology: A Review. *J. Nanomater. Mol. Nanotechnol.* **2014**, *3*. https://doi.org/10.4172/2324-8777.1000150.
(347) Sercombe, L.; Veerati, T.; Moheimani, F.; Wu, S. Y.; Sood, A. K.; Hua, S. Advances and Challenges of Liposome Assisted Drug Delivery. *Front. Pharmacol.* **2015**, *6*. https://doi.org/10.3389/fphar.2015.00286.
(348) Cęlakmak, İ. A Review of Poly(Ethylene Oxide)-Based Block Copolymers. *J. Macromol. Sci. Part A* **1995**, *32* (sup7), 1113–1122. https://doi.org/10.1080/10601329508019152.
(349) Bao, G.; Mitragotri, S.; Tong, S. Multifunctional Nanoparticles for Drug Delivery and Molecular Imaging. *Annu. Rev. Biomed. Eng.* **2013**, *15*, 253–282. https://doi.org/10.1146/annurev-bioeng-071812-152409.
(350) Charrueau, C.; Zandanel, C. Drug Delivery by Polymer Nanoparticles: The Challenge of Controlled Release and Evaluation. In *Polymer Nanoparticles for Nanomedicines: A Guide for their Design, Preparation and Development*; Vauthier, C., Ponchel, G., Eds.; Springer International Publishing: Cham, 2016; pp 439–503. https://doi.org/10.1007/978-3-319-41421-8_14.
(351) Doane, T.; Burda, C. Nanoparticle Mediated Non-Covalent Drug Delivery. *Adv. Drug Deliv. Rev.* **2013**, *65* (5), 607–621. https://doi.org/10.1016/j.addr.2012.05.012.
(352) Leriche, G.; Chisholm, L.; Wagner, A. Cleavable Linkers in Chemical Biology. *Bioorg. Med. Chem.* **2012**, *20* (2), 571–582. https://doi.org/10.1016/j.bmc.2011.07.048.
(353) Stylianopoulos, T. EPR-Effect: Utilizing Size-Dependent Nanoparticle Delivery to Solid Tumors. *Ther. Deliv.* **2013**, *4* (4), 421–423. https://doi.org/10.4155/tde.13.8.
(354) Maeda, H. Polymer Therapeutics and the EPR Effect. *J. Drug Target.* **2017**, *25* (9–10), 781–785. https://doi.org/10.1080/1061186X.2017.1365878.
(355) Fang, J.; Nakamura, H.; Maeda, H. The EPR Effect: Unique Features of Tumor Blood Vessels for Drug Delivery, Factors Involved, and Limitations and Augmentation of the Effect. *Adv. Drug Deliv. Rev.* **2011**, *63* (3), 136–151. https://doi.org/10.1016/j.addr.2010.04.009.
(356) Maeda, H.; Wu, J.; Sawa, T.; Matsumura, Y.; Hori, K. Tumor Vascular Permeability and the EPR Effect in Macromolecular Therapeutics: A Review. *J. Controlled Release* **2000**, *65* (1–2), 271–284. https://doi.org/10.1016/S0168-3659(99)00248-5.
(357) Danhier, F. To Exploit the Tumor Microenvironment: Since the EPR Effect Fails in the Clinic, What Is the Future of Nanomedicine? *J. Controlled Release* **2016**, *244*, 108–121. https://doi.org/10.1016/j.jconrel.2016.11.015.
(358) Stockhofe, K.; Postema, J.; Schieferstein, H.; Ross, T. Radiolabeling of Nanoparticles and Polymers for PET Imaging. *Pharmaceuticals* **2014**, *7* (4), 392–418. https://doi.org/10.3390/ph7040392.
(359) Klaikherd, A.; Nagamani, C.; Thayumanavan, S. Multi-Stimuli Sensitive Amphiphilic Block Copolymer Assemblies. *J. Am. Chem. Soc.* **2009**, *131* (13), 4830–4838. https://doi.org/10.1021/ja809475a.
(360) Rijpkema, S. J.; Toebes, B. J.; Maas, M. N.; de Kler, N. R. M.; Wilson, D. A. Designing Molecular Building Blocks for Functional Polymersomes. *Isr. J. Chem.* **2019**. https://doi.org/10.1002/ijch.201900039.
(361) Wang, J.; Li, S.; Han, Y.; Guan, J.; Chung, S.; Wang, C.; Li, D. Poly(Ethylene Glycol)–Polylactide Micelles for Cancer Therapy. *Front. Pharmacol.* **2018**, *9*. https://doi.org/10.3389/fphar.2018.00202.
(362) Rinkenauer, A. C.; Schubert, S.; Traeger, A.; Schubert, U. S. The Influence of Polymer Architecture on in Vitro PDNA Transfection. *J. Mater. Chem. B* **2015**, *3* (38), 7477–7493. https://doi.org/10.1039/C5TB00782H.
(363) Palaprat, G.; Ganachaud, F. Synthesis of Polydimethylsiloxane Microemulsions by Self-Catalyzed Hydrolysis/Condensation of Dichlorodimethylsilane. *Comptes Rendus Chim.* **2003**, *6* (11), 1385–1392. https://doi.org/10.1016/j.crci.2003.09.002.
(364) Choi, K. Y.; Min, K. H.; Yoon, H. Y.; Kim, K.; Park, J. H.; Kwon, I. C.; Choi, K.; Jeong, S. Y. PEGylation of Hyaluronic Acid Nanoparticles Improves Tumor Targetability in Vivo. *Biomaterials* **2011**, *32* (7), 1880–1889. https://doi.org/10.1016/j.biomaterials.2010.11.010.
(365) Kutikov, A. B.; Song, J. Biodegradable PEG-Based Amphiphilic Block Copolymers for Tissue Engineering Applications. *ACS Biomater. Sci. Eng.* **2015**, *1* (7), 463–480. https://doi.org/10.1021/acsbiomaterials.5b00122.
(366) Hu, Y.; Jiang, X.; Ding, Y.; Zhang, L.; Yang, C.; Zhang, J.; Chen, J.; Yang, Y. Preparation and Drug Release

Behaviors of Nimodipine-Loaded Poly(Caprolactone)–Poly(Ethylene Oxide)–Polylactide Amphiphilic Copolymer Nanoparticles. *Biomaterials* **2003**, *24* (13), 2395–2404. https://doi.org/10.1016/S0142-9612(03)00021-8.

(367) Gref, R.; Lück, M.; Quellec, P.; Marchand, M.; Dellacherie, E.; Harnisch, S.; Blunk, T.; Müller, R. H. 'Stealth' Corona-Core Nanoparticles Surface Modified by Polyethylene Glycol (PEG): Influences of the Corona (PEG Chain Length and Surface Density) and of the Core Composition on Phagocytic Uptake and Plasma Protein Adsorption. *Colloids Surf. B Biointerfaces* **2000**, *18* (3–4), 301–313. https://doi.org/10.1016/S0927-7765(99)00156-3.

(368) Hickey, J. W.; Santos, J. L.; Williford, J.-M.; Mao, H.-Q. Control of Polymeric Nanoparticle Size to Improve Therapeutic Delivery. *J. Control. Release Off. J. Control. Release Soc.* **2015**, *219*, 536–547. https://doi.org/10.1016/j.jconrel.2015.10.006.

(369) Nagavarma, B. V. N.; Yadav, H.; Ayaz, A.; S. Vasudha, L.; G. Shivakumar, H. Different Techniques for Preparation of Polymeric Nanoparticles- A Review. *Asian J. Pharm. Clin. Res.* **2012**, *5*, 16–23.

(370) Rao, J. P.; Geckeler, K. E. Polymer Nanoparticles: Preparation Techniques and Size-Control Parameters. *Prog. Polym. Sci.* **2011**, *36* (7), 887–913. https://doi.org/10.1016/j.progpolymsci.2011.01.001.

(371) Pereira, H.; Schulze, P. S. C.; Schüler, L. M.; Santos, T.; Barreira, L.; Varela, J. Fluorescence Activated Cell-Sorting Principles and Applications in Microalgal Biotechnology. *Algal Res.* **2018**, *30*, 113–120. https://doi.org/10.1016/j.algal.2017.12.013.

(372) Heitz, F.; Morris, M. C.; Divita, G. Twenty Years of Cell-Penetrating Peptides: From Molecular Mechanisms to Therapeutics. *Br. J. Pharmacol.* **2009**, *157* (2), 195–206. https://doi.org/10.1111/j.1476-5381.2009.00057.x.

(373) Vaissière, A.; Aldrian, G.; Konate, K.; Lindberg, M. F.; Jourdan, C.; Telmar, A.; Seisel, Q.; Fernandez, F.; Viguier, V.; Genevois, C.; et al. A Retro-Inverso Cell-Penetrating Peptide for SiRNA Delivery. *J. Nanobiotechnology* **2017**, *15* (1), 34. https://doi.org/10.1186/s12951-017-0269-2.

(374) Veiman, K.-L.; Künnapuu, K.; Lehto, T.; Kiisholts, K.; Pärn, K.; Langel, Ü.; Kurrikoff, K. PEG Shielded MMP Sensitive CPPs for Efficient and Tumor Specific Gene Delivery in Vivo. *J. Control. Release Off. J. Control. Release Soc.* **2015**, *209*, 238–247. https://doi.org/10.1016/j.jconrel.2015.04.038.

(375) Akash, M. S. H.; Rehman, K.; Chen, S. Polymeric-Based Particulate Systems for Delivery of Therapeutic Proteins. *Pharm. Dev. Technol.* **2016**, *21* (3), 367–378. https://doi.org/10.3109/10837450.2014.999785.

(376) Kim, C. K.; Ghosh, P.; Pagliuca, C.; Zhu, Z.-J.; Menichetti, S.; Rotello, V. M. Entrapment of Hydrophobic Drugs in Nanoparticle Monolayers with Efficient Release into Cancer Cells. *J. Am. Chem. Soc.* **2009**, *131* (4), 1360–1361. https://doi.org/10.1021/ja808137c.

(377) Manju, S.; Sreenivasan, K. Enhanced Drug Loading on Magnetic Nanoparticles by Layer-by-Layer Assembly Using Drug Conjugates: Blood Compatibility Evaluation and Targeted Drug Delivery in Cancer Cells. *Langmuir* **2011**, *27* (23), 14489–14496. https://doi.org/10.1021/la202470k.

(378) Kim, B.-S.; Park, S. W.; Hammond, P. T. Hydrogen-Bonding Layer-by-Layer-Assembled Biodegradable Polymeric Micelles as Drug Delivery Vehicles from Surfaces. *ACS Nano* **2008**, *2* (2), 386–392. https://doi.org/10.1021/nn700408z.

(379) Kester, M.; Heakal, Y.; Fox, T.; Sharma, A.; Robertson, G. P.; Morgan, T. T.; Altinoğlu, E. İ.; Tabaković, A.; Parette, M. R.; Rouse, S. M.; et al. Calcium Phosphate Nanocomposite Particles for In Vitro Imaging and Encapsulated Chemotherapeutic Drug Delivery to Cancer Cells. *Nano Lett.* **2008**, *8* (12), 4116–4121. https://doi.org/10.1021/nl802098g.

(380) Vinciguerra, D.; Denis, S.; Mougin, J.; Jacobs, M.; Guillaneuf, Y.; Mura, S.; Couvreur, P.; Nicolas, J. A Facile Route to Heterotelechelic Polymer Prodrug Nanoparticles for Imaging, Drug Delivery and Combination Therapy. *J. Controlled Release* **2018**, *286*, 425–438. https://doi.org/10.1016/j.jconrel.2018.08.013.

(381) Vinciguerra, D.; Jacobs, M.; Denis, S.; Mougin, J.; Guillaneuf, Y.; Lazzari, G.; Zhu, C.; Mura, S.; Couvreur, P.; Nicolas, J. Heterotelechelic Polymer Prodrug Nanoparticles: Adaptability to Different Drug Combinations and Influence of the Dual Functionalization on the Cytotoxicity. *J. Controlled Release* **2019**, *295*, 223–236. https://doi.org/10.1016/j.jconrel.2018.12.047.

(382) Repetto, G.; del Peso, A.; Zurita, J. L. Neutral Red Uptake Assay for the Estimation of Cell Viability/Cytotoxicity. *Nat. Protoc.* **2008**, *3* (7), 1125–1131. https://doi.org/10.1038/nprot.2008.75.

(383) Clancy, S. Translation: DNA to MRNA to Protein. *Nat. Educ.* **2008**, *1*, 101.

(384) Scholz, C.; Wagner, E. Therapeutic Plasmid DNA versus SiRNA Delivery: Common and Different Tasks for Synthetic Carriers. *J. Controlled Release* **2012**, *161* (2), 554–565. https://doi.org/10.1016/j.jconrel.2011.11.014.

(385) Dana, H.; Chalbatani, G. M.; Mahmoodzadeh, H.; Karimloo, R.; Rezaiean, O.; Moradzadeh, A.; Mehmandoost, N.; Moazzen, F.; Mazraeh, A.; Marmari, V.; et al. Molecular Mechanisms and Biological Functions of SiRNA. *Int. J. Biomed. Sci. IJBS* **2017**, *13* (2), 48–57.

(386) Napoli, C.; Lemieux, C.; Jorgensen, R. Introduction of a Chimeric Chalcone Synthase Gene into Petunia Results in Reversible Co-Suppression of Homologous Genes in Trans. *Plant Cell* **1990**, *2* (4), 279–289.

(387) Fire, A.; Xu, S.; Montgomery, M. K.; Kostas, S. A.; Driver, S. E.; Mello, C. C. Potent and Specific Genetic Interference by Double-Stranded RNA in Caenorhabditis Elegans. *Nature* **1998**, *391* (6669), 806–811. https://doi.org/10.1038/35888.

(388) Tai, W. Current Aspects of SiRNA Bioconjugate for In Vitro and In Vivo Delivery. *Molecules* **2019**, *24* (12), 2211. https://doi.org/10.3390/molecules24122211.

(389) Gaglione, M.; Mercurio, M. E.; Potenza, N.; Mosca, N.; Russo, A.; Novellino, E.; Cosconati, S.; Messere, A. Synthesis and Gene Silencing Properties of SiRNAs Containing Terminal Amide Linkages. *BioMed Res. Int.* **2014**, *2014*. https://doi.org/10.1155/2014/901617.

(390) Moore, C. B.; Guthrie, E. H.; Huang, M. T.-H.; Taxman, D. J. Short Hairpin RNA (ShRNA): Design, Delivery, and Assessment of Gene Knockdown. *Methods Mol. Biol. Clifton NJ* **2010**, *629*, 141–158. https://doi.org/10.1007/978-1-60761-657-3_10.

(391) Lord, C. J.; Martin, S. A.; Ashworth, A. RNA Interference Screening Demystified. *J. Clin. Pathol.* **2009**, *62* (3), 195–200. https://doi.org/10.1136/jcp.2008.058735.

(392) Torrecilla, J.; Rodríguez-Gascón, A.; Solinís, M. Á.; del Pozo-Rodríguez, A. Lipid Nanoparticles as Carriers for RNAi against Viral Infections: Current Status and Future Perspectives. *BioMed Res. Int.* **2014**, *2014*, 1–17. https://doi.org/10.1155/2014/161794.

(393) Lorenz, C.; Hadwiger, P.; John, M.; Vornlocher, H.-P.; Unverzagt, C. Steroid and Lipid Conjugates of SiRNAs to Enhance Cellular Uptake and Gene Silencing in Liver Cells. *Bioorg. Med. Chem. Lett.* **2004**, *14* (19), 4975–4977. https://doi.org/10.1016/j.bmcl.2004.07.018.

(394) Soutschek, J.; Akinc, A.; Bramlage, B.; Charisse, K.; Constien, R.; Donoghue, M.; Elbashir, S.; Geick, A.; Hadwiger, P.; Harborth, J.; et al. Therapeutic Silencing of an Endogenous Gene by Systemic Administration of Modified SiRNAs. *Nature* **2004**, *432* (7014), 173–178. https://doi.org/10.1038/nature03121.

(395) Choi, S. W.; Lee, S. H.; Mok, H.; Park, T. G. Multifunctional SiRNA Delivery System: Polyelectrolyte Complex Micelles of Six-Arm PEG Conjugate of SiRNA and Cell Penetrating Peptide with Crosslinked Fusogenic Peptide. *Biotechnol. Prog.* **2010**, *26* (1), 57–63. https://doi.org/10.1002/btpr.310.

(396) Cao, Y.; Liu, X.; Peng, L. Molecular Engineering of Dendrimer Nanovectors for SiRNA Delivery and Gene Silencing. *Front. Chem. Sci. Eng.* **2017**, *11* (4), 663–675. https://doi.org/10.1007/s11705-017-1623-5.

(397) Santos-Carballal, B.; Fernández Fernández, E.; Goycoolea, F. Chitosan in Non-Viral Gene Delivery: Role of Structure, Characterization Methods, and Insights in Cancer and Rare Diseases Therapies. *Polymers* **2018**, *10* (4), 444. https://doi.org/10.3390/polym10040444.

(398) Tros de Ilarduya, C.; Sun, Y.; Düzgüneş, N. Gene Delivery by Lipoplexes and Polyplexes. *Eur. J. Pharm. Sci.* **2010**, *40* (3), 159–170. https://doi.org/10.1016/j.ejps.2010.03.019.

(399) Felgner, P. L.; Gadek, T. R.; Holm, M.; Roman, R.; Chan, H. W.; Wenz, M.; Northrop, J. P.; Ringold, G. M.; Danielsen, M. Lipofection: A Highly Efficient, Lipid-Mediated DNA-Transfection Procedure. *Proc. Natl. Acad. Sci. U. S. A.* **1987**, *84* (21), 7413–7417. https://doi.org/10.1073/pnas.84.21.7413.

(400) Boussif, O.; Lezoualc'h, F.; Zanta, M. A.; Mergny, M. D.; Scherman, D.; Demeneix, B.; Behr, J. P. A Versatile Vector for Gene and Oligonucleotide Transfer into Cells in Culture and in Vivo: Polyethylenimine. *Proc. Natl. Acad. Sci. U. S. A.* **1995**, *92* (16), 7297–7301. https://doi.org/10.1073/pnas.92.16.7297.

(401) Samal, S. K.; Dash, M.; Vlierberghe, S. V.; Kaplan, D. L.; Chiellini, E.; Blitterswijk, C. van; Moroni, L.; Dubruel, P. Cationic Polymers and Their Therapeutic Potential. *Chem. Soc. Rev.* **2012**, *41* (21), 7147–7194. https://doi.org/10.1039/C2CS35094G.

(402) Matsumoto, S.; Christie, R. J.; Nishiyama, N.; Miyata, K.; Ishii, A.; Oba, M.; Koyama, H.; Yamasaki, Y.;

Kataoka, K. Environment-Responsive Block Copolymer Micelles with a Disulfide Cross-Linked Core for Enhanced SiRNA Delivery. *Biomacromolecules* **2009**, *10* (1), 119–127. https://doi.org/10.1021/bm800985e.

(403) Katas, H.; Alpar, H. O. Development and Characterisation of Chitosan Nanoparticles for SiRNA Delivery. *J. Controlled Release* **2006**, *115* (2), 216–225. https://doi.org/10.1016/j.jconrel.2006.07.021.

(404) O'Mahony, A. M.; Godinho, B. M. D. C.; Ogier, J.; Devocelle, M.; Darcy, R.; Cryan, J. F.; O'Driscoll, C. M. Click-Modified Cyclodextrins as Nonviral Vectors for Neuronal SiRNA Delivery. *ACS Chem. Neurosci.* **2012**, *3* (10), 744–752. https://doi.org/10.1021/cn3000372.

(405) Kesharwani, P.; Banerjee, S.; Gupta, U.; Mohd Amin, M. C. I.; Padhye, S.; Sarkar, F. H.; Iyer, A. K. PAMAM Dendrimers as Promising Nanocarriers for RNAi Therapeutics. *Mater. Today* **2015**, *18* (10), 565–572. https://doi.org/10.1016/j.mattod.2015.06.003.

(406) Wu, J.; Huang, W.; He, Z. Dendrimers as Carriers for siRNA Delivery and Gene Silencing: A Review https://www.hindawi.com/journals/tswj/2013/630654/ (accessed Aug 13, 2019). https://doi.org/10.1155/2013/630654.

(407) Li, J.; Ge, Z.; Liu, S. PEG-Sheddable Polyplex Micelles as Smart Gene Carriers Based on MMP-Cleavable Peptide-Linked Block Copolymers. *Chem. Commun.* **2013**, *49* (62), 6974–6976. https://doi.org/10.1039/C3CC43576H.

(408) Kleemann, E.; Neu, M.; Jekel, N.; Fink, L.; Schmehl, T.; Gessler, T.; Seeger, W.; Kissel, T. Nano-Carriers for DNA Delivery to the Lung Based upon a TAT-Derived Peptide Covalently Coupled to PEG–PEI. *J. Controlled Release* **2005**, *109* (1), 299–316. https://doi.org/10.1016/j.jconrel.2005.09.036.

(409) Youngren-Ortiz, S. R.; Gandhi, N. S.; España-Serrano, L.; Chougule, M. B. Aerosol Delivery of SiRNA to the Lungs. Part 2: Nanocarrier-Based Delivery Systems. *KONA Powder Part. J.* **2017**, *34* (0), 44–69. https://doi.org/10.14356/kona.2017005.

(410) Kwoh, D. Y.; Coffin, C. C.; Lollo, C. P.; Jovenal, J.; Banaszczyk, M. G.; Mullen, P.; Phillips, A.; Amini, A.; Fabrycki, J.; Bartholomew, R. M.; et al. Stabilization of Poly-L-Lysine/DNA Polyplexes for in Vivo Gene Delivery to the Liver. *Biochim. Biophys. Acta* **1999**, *1444* (2), 171–190. https://doi.org/10.1016/s0167-4781(98)00274-7.

(411) Shi, J.; Choi, J. L.; Chou, B.; Johnson, R. N.; Schellinger, J. G.; Pun, S. H. Effect of Polyplex Morphology on Cellular Uptake, Intracellular Trafficking, and Transgene Expression. *ACS Nano* **2013**, *7* (12). https://doi.org/10.1021/nn403069n.

(412) Shi, J.; Schellinger, J. G.; Pun, S. H. Engineering Biodegradable and Multifunctional Peptide-Based Polymers for Gene Delivery. *J. Biol. Eng.* **2013**, *7*, 25. https://doi.org/10.1186/1754-1611-7-25.

(413) Shi, J.; Schellinger, J. G.; Johnson, R. N.; Choi, J. L.; Chou, B.; Anghel, E. L.; Pun, S. H. Influence of Histidine Incorporation on Buffer Capacity and Gene Transfection Efficiency of HPMA-Co-Oligolysine Brush Polymers. *Biomacromolecules* **2013**, *14* (6), 1961–1970. https://doi.org/10.1021/bm400342f.

(414) Soliman, M.; Nasanit, R.; Abulateefeh, S. R.; Allen, S.; Davies, M. C.; Briggs, S. S.; Seymour, L. W.; Preece, J. A.; Grabowska, A. M.; Watson, S. A.; et al. Multicomponent Synthetic Polymers with Viral-Mimetic Chemistry for Nucleic Acid Delivery. *Mol. Pharm.* **2012**, *9* (1), 1–13. https://doi.org/10.1021/mp200108q.

(415) Hwang, H. S.; Hu, J.; Na, K.; Bae, Y. H. Role of Polymeric Endosomolytic Agents in Gene Transfection: A Comparative Study of Poly(l-Lysine) Grafted with Monomeric l-Histidine Analogue and Poly(l-Histidine). *Biomacromolecules* **2014**, *15* (10), 3577–3586. https://doi.org/10.1021/bm500843r.

(416) Leng, Q.; Kahn, J.; Zhu, J.; Scaria, P.; Mixson, J. Needle-like Morphology of H2K4b Polyplexes Associated with Increases in Transfection in Vitro. *Cancer Ther.* **2007**, *5B*, 193–202.

(417) Balland, O.; Saison-Behmoaras, T.; Garestier, T.; Hélène, C. Nanoparticles as Carriers for Antisense Oligonucleotides. In *Targeting of Drugs 5: Strategies for Oligonucleotide and Gene Delivery in Therapy*; Gregoriadis, G., McCormack, B., Eds.; NATO ASI Series; Springer US: Boston, MA, 1996; pp 131–142. https://doi.org/10.1007/978-1-4615-6405-8_14.

(418) Cheng, Y.; Wei, H.; Tan, J.-K. Y.; Peeler, D. J.; Maris, D. O.; Sellers, D. L.; Horner, P. J.; Pun, S. H. Nano-Sized Sunflower Polycations as Effective Gene Transfer Vehicles. *Small Weinh. Bergstr. Ger.* **2016**, *12* (20), 2750–2758. https://doi.org/10.1002/smll.201502930.

(419) EL Andaloussi, S.; Lehto, T.; Mäger, I.; Rosenthal-Aizman, K.; Oprea, I. I.; Simonson, O. E.; Sork, H.; Ezzat,

K.; Copolovici, D. M.; Kurrikoff, K.; et al. Design of a Peptide-Based Vector, PepFect6, for Efficient Delivery of SiRNA in Cell Culture and Systemically in Vivo. *Nucleic Acids Res.* **2011**, *39* (9), 3972–3987. https://doi.org/10.1093/nar/gkq1299.

(420) Kasai, H.; Inoue, K.; Imamura, K.; Yuvienco, C.; Montclare, J. K.; Yamano, S. Efficient SiRNA Delivery and Gene Silencing Using a Lipopolypeptide Hybrid Vector Mediated by a Caveolae-Mediated and Temperature-Dependent Endocytic Pathway. *J. Nanobiotechnology* **2019**, *17*. https://doi.org/10.1186/s12951-019-0444-8.

(421) Qu, X.; Hu, Y.; Wang, H.; Song, H.; Young, M.; Xu, F.; Liu, Y.; Cheng, G. Biomimetic Dextran–Peptide Vectors for Efficient and Safe SiRNA Delivery. *ACS Appl. Bio Mater.* **2019**, *2* (4), 1456–1463. https://doi.org/10.1021/acsabm.8b00714.

(422) Li, J.; Ge, Z.; Liu, S. PEG-Sheddable Polyplex Micelles as Smart Gene Carriers Based on MMP-Cleavable Peptide-Linked Block Copolymers. *Chem. Commun. Camb. Engl.* **2013**, *49* (62), 6974–6976. https://doi.org/10.1039/c3cc43576h.

(423) Li, Y.; Kröger, M.; Liu, W. K. Endocytosis of PEGylated Nanoparticles Accompanied by Structural and Free Energy Changes of the Grafted Polyethylene Glycol. *Biomaterials* **2014**, *35* (30), 8467–8478. https://doi.org/10.1016/j.biomaterials.2014.06.032.

(424) Jokerst, J. V.; Lobovkina, T.; Zare, R. N.; Gambhir, S. S. Nanoparticle PEGylation for Imaging and Therapy. *Nanomed.* **2011**, *6* (4), 715–728. https://doi.org/10.2217/nnm.11.19.

(425) Suk, J. S.; Xu, Q.; Kim, N.; Hanes, J.; Ensign, L. M. PEGylation as a Strategy for Improving Nanoparticle-Based Drug and Gene Delivery. *Adv. Drug Deliv. Rev.* **2016**, *99* (Pt A), 28–51. https://doi.org/10.1016/j.addr.2015.09.012.

(426) Ping, Y.; Hu, Q.; Tang, G.; Li, J. FGFR-Targeted Gene Delivery Mediated by Supramolecular Assembly between β-Cyclodextrin-Crosslinked PEI and Redox-Sensitive PEG. *Biomaterials* **2013**, *34* (27), 6482–6494. https://doi.org/10.1016/j.biomaterials.2013.03.071.

(427) Veiman, K.-L.; Künnapuu, K.; Lehto, T.; Kiisholts, K.; Pärn, K.; Langel, Ü.; Kurrikoff, K. PEG Shielded MMP Sensitive CPPs for Efficient and Tumor Specific Gene Delivery in Vivo. *J. Controlled Release* **2015**, *209*, 238–247. https://doi.org/10.1016/j.jconrel.2015.04.038.

(428) Chen, P.; Chen, B.; Pan, R.; Askhatova, D. Effective Small Interfering RNA Delivery in Vitro via a New Stearylated Cationic Peptide. *Int. J. Nanomedicine* **2015**, 3303. https://doi.org/10.2147/IJN.S79306.

(429) Jafari, M.; Xu, W.; Pan, R.; Sweeting, C. M.; Karunaratne, D. N.; Chen, P. Serum Stability and Physicochemical Characterization of a Novel Amphipathic Peptide C6M1 for SiRNA Delivery. *PLoS ONE* **2014**, *9* (5), e97797. https://doi.org/10.1371/journal.pone.0097797.

(430) Wu. The Investigation of Polymer-SiRNA Nanoparticle for Gene Therapy of Gastric Cancer in Vitro. *Int. J. Nanomedicine* **2010**, 129. https://doi.org/10.2147/IJN.S8503.

(431) Danielsen, S.; Maurstad, G.; Stokke, B. T. DNA-Polycation Complexation and Polyplex Stability in the Presence of Competing Polyanions. *Biopolymers* **2005**, *77* (2), 86–97. https://doi.org/10.1002/bip.20170.

Experimental Section

Experimental section

Table of content

Table of Figures

Chapter 2

LC/MS analyses

Samples for LC/MS analyses were prepared in an ACN/H_2O (50/50, v/v) mixture containing 1‰ TFA. The LC/MS system consisted of a Waters Alliance 2695 HPLC coupled to a Water Micromass ZQ spectrometer (electrospray ionization mode, ESI+).

Analysis of non-silylated compounds were carried out by HPLC using a Phenomenex Onyx, 25 x 4.6 mm reversed-phase column. A flow rate of 3 mL/min and a gradient of (0-100)% B over 2.5 min were used. Eluent A: water/0.1% HCO_2H; eluent B: acetonitrile/0.1% HCO_2H.

Analysis of silylated compounds were carried out by HPLC using a PLRP-S®, 25 x 4.6 mm reversed-phase column. A flow rate of 3 mL/min and a gradient of (5-100)% B over 9 min were used. Eluent A: water/0.1% HCO_2H; eluent B: acetonitrile/0.1% HCO_2H.

UV detection was performed at 214 nm. Electrospray mass spectra were acquired at a solvent flow rate of 200 µL/min. Nitrogen was used for both the nebulizing and drying gas. The data were obtained in a scan mode ranging from 100 to 1000 m/z or 250 to 1500 m/z to in 0.7 sec intervals. All measurements were performed in the positive ion mode.

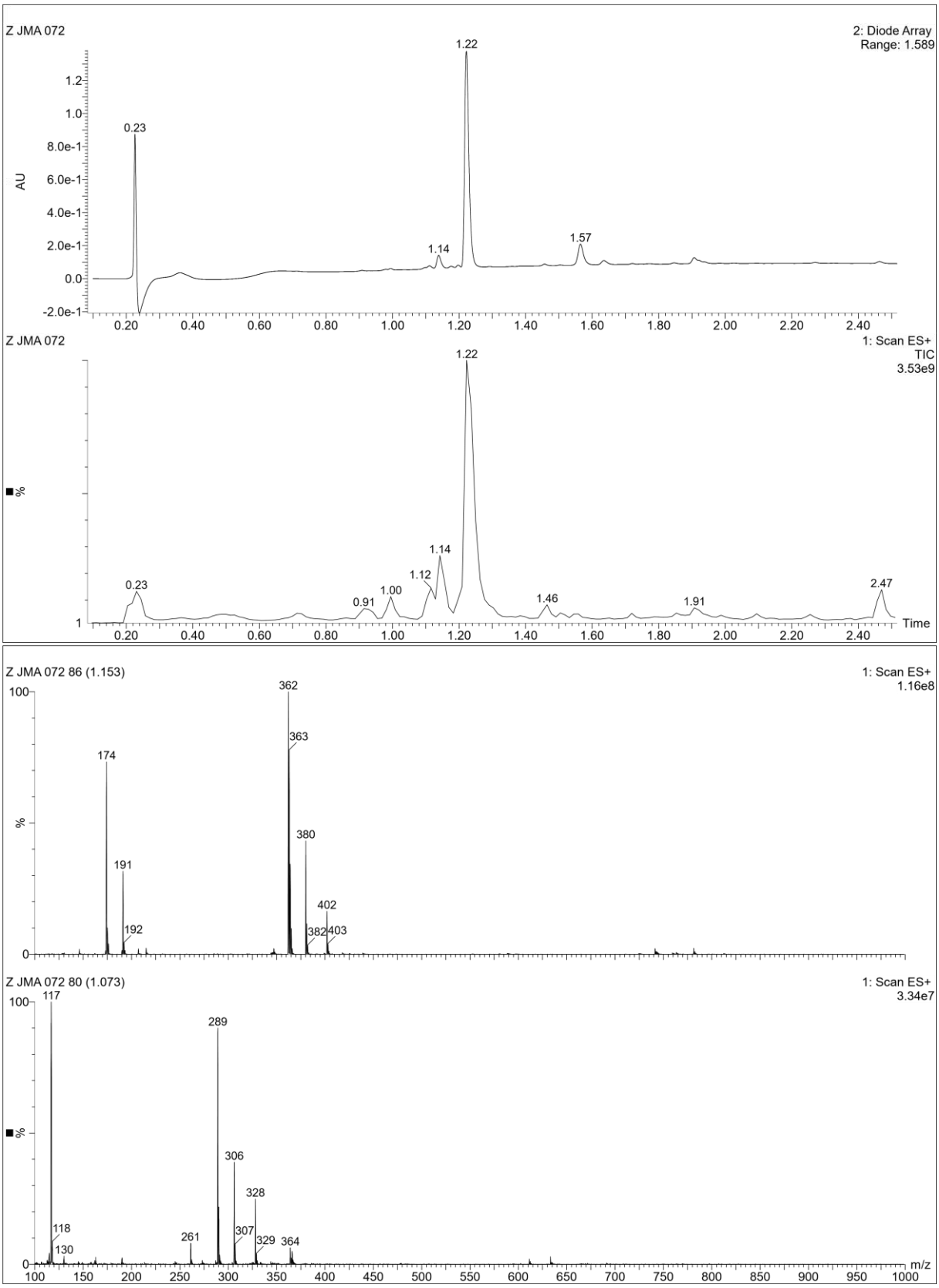

*Figure 1. ESI + LC/MS of hydrosilylation on AcPheAllylGly-resin with 20 eq of $HSiMe_2Cl$ and Karstedt catalyst (0.005eq), in anhydrous DCM, at 50°C, for 120 min, **JMA072**. Top: chromatograms UV at 214nm and TIC, Bottom: MS spectra at 1.14 and 1.22 min.*

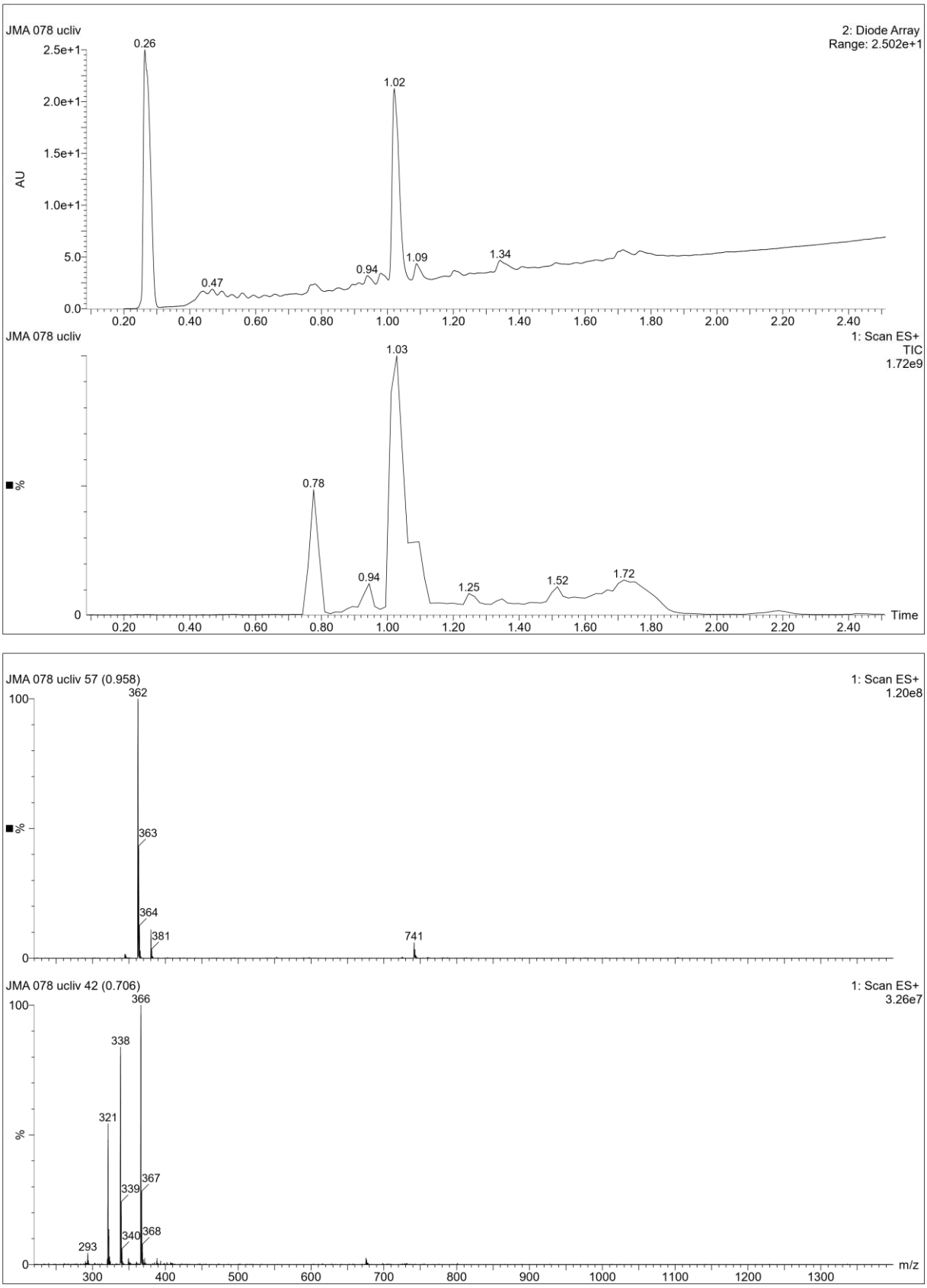

*Figure 2. ESI + LC/MS of hydrosilylation on AcPheAllylGly-resin with 20 eq of HSiMe2Cl and Karstedt catalyst (0.005eq), in anhydrous DCM, at 50°C, for 60 min, **JMA078**. Top: chromatograms UV at 214nm and TIC, Bottom: MS spectra at 0.78 and 1.03 min.*

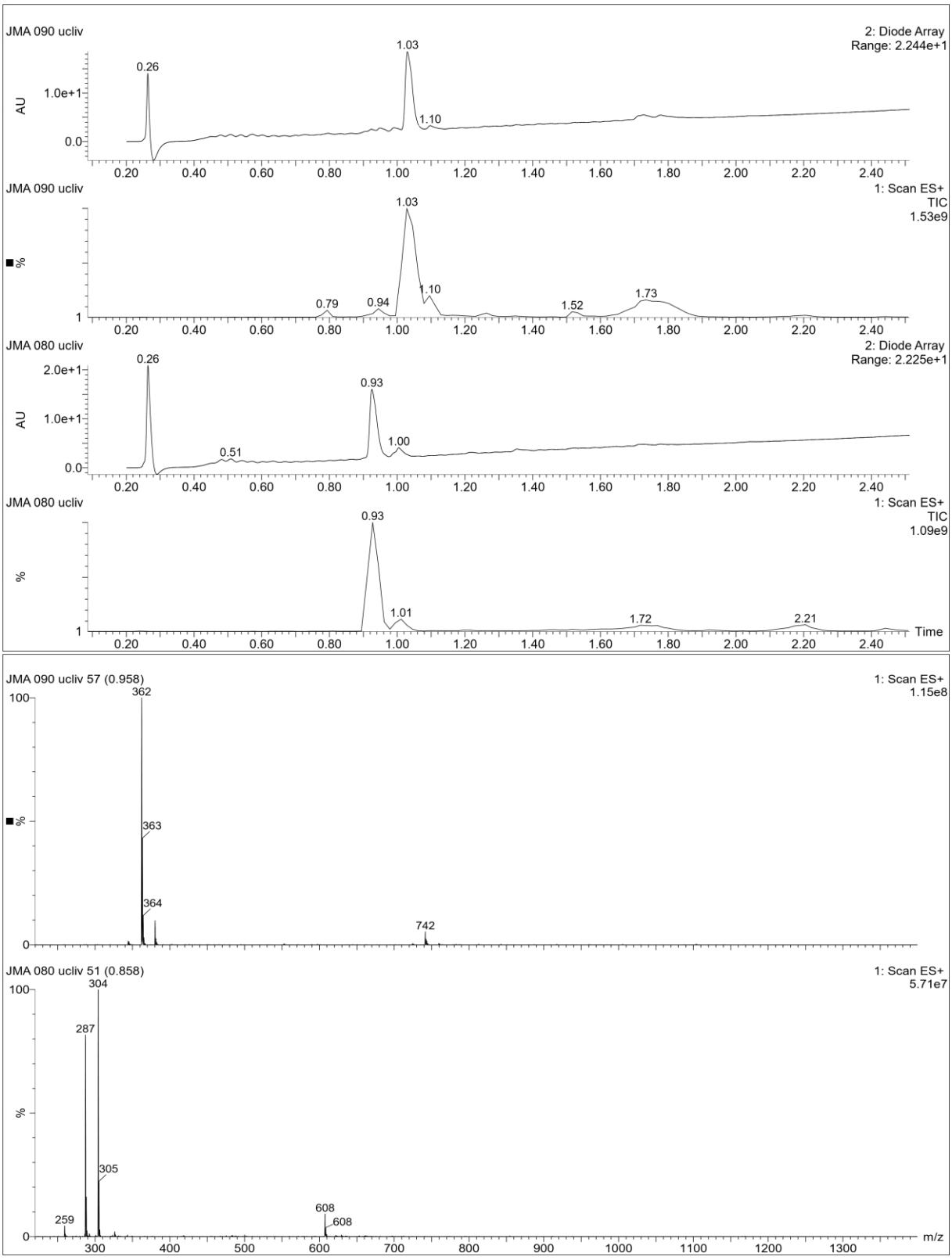

*Figure 3. ESI + LC/MS of hydrosilylation on AcPheAllylGly-resin with 20 eq of HSiMe2Cl in anhydrous DCM, at 50°C, with Karstedt catalyst (0.005eq) for 120 min, **JMA080** and with Karstedt catalyst (0.0025eq) for 60 min, **JMA090**. Top: chromatograms UV at 214nm and TIC, Bottom: MS spectra at 0.93 and 1.03 min for **JMA080** and **JMA090** respectively.*

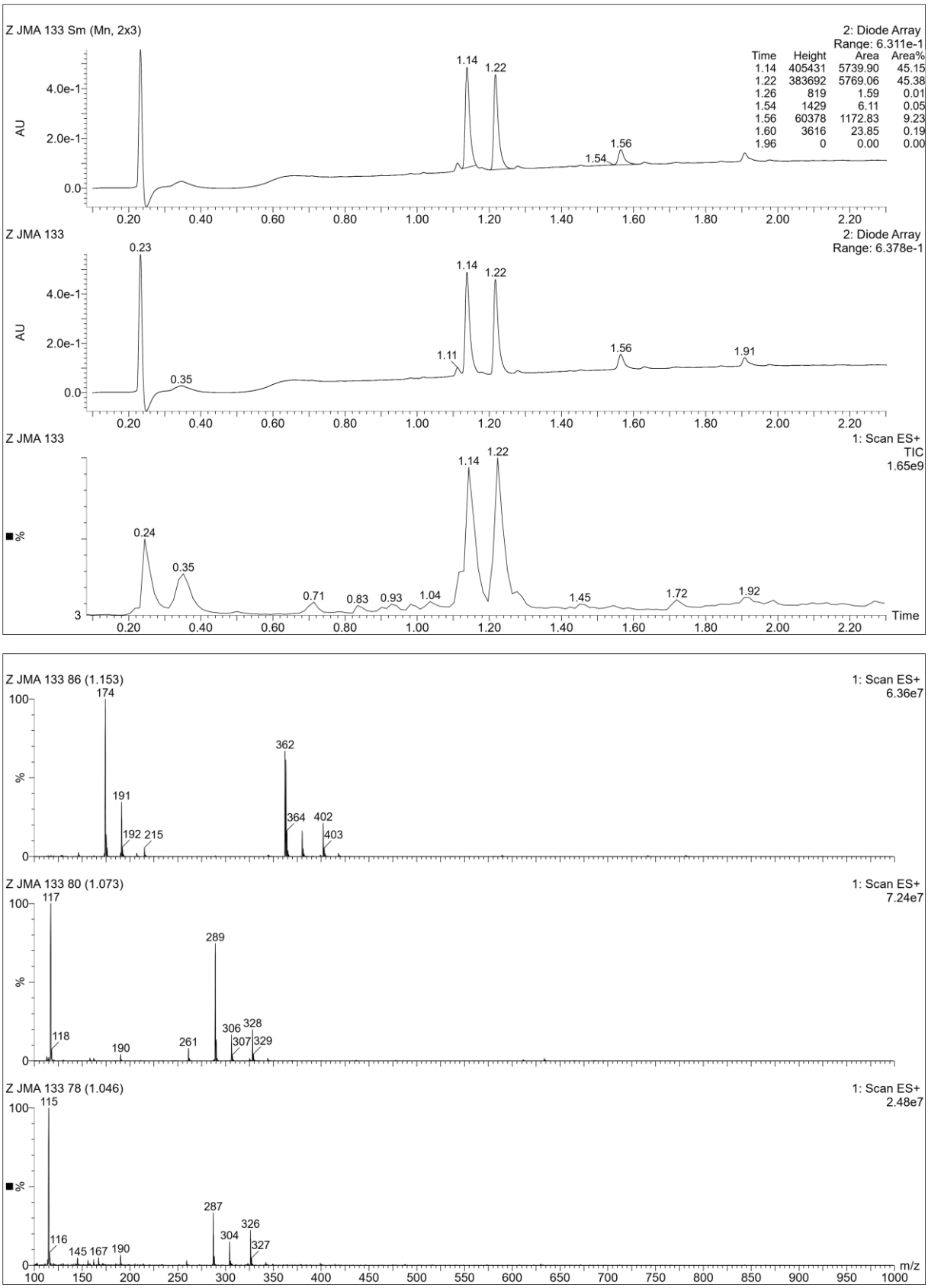

*Figure 4. ESI + LC/MS of hydrosilylation on AcPheAllylGly-NHRink amide Amphishere resin, with 30 equivalents of $HSiMe_2OEt$, 0.005 eq Karstedt catalyst in 5mL of anhydrous DCM, for 12h, **JMA 133**. Top: chromatograms UV at 214nm and TIC, Bottom: MS spectra at 1.11, 1.14 and 1.22 min.*

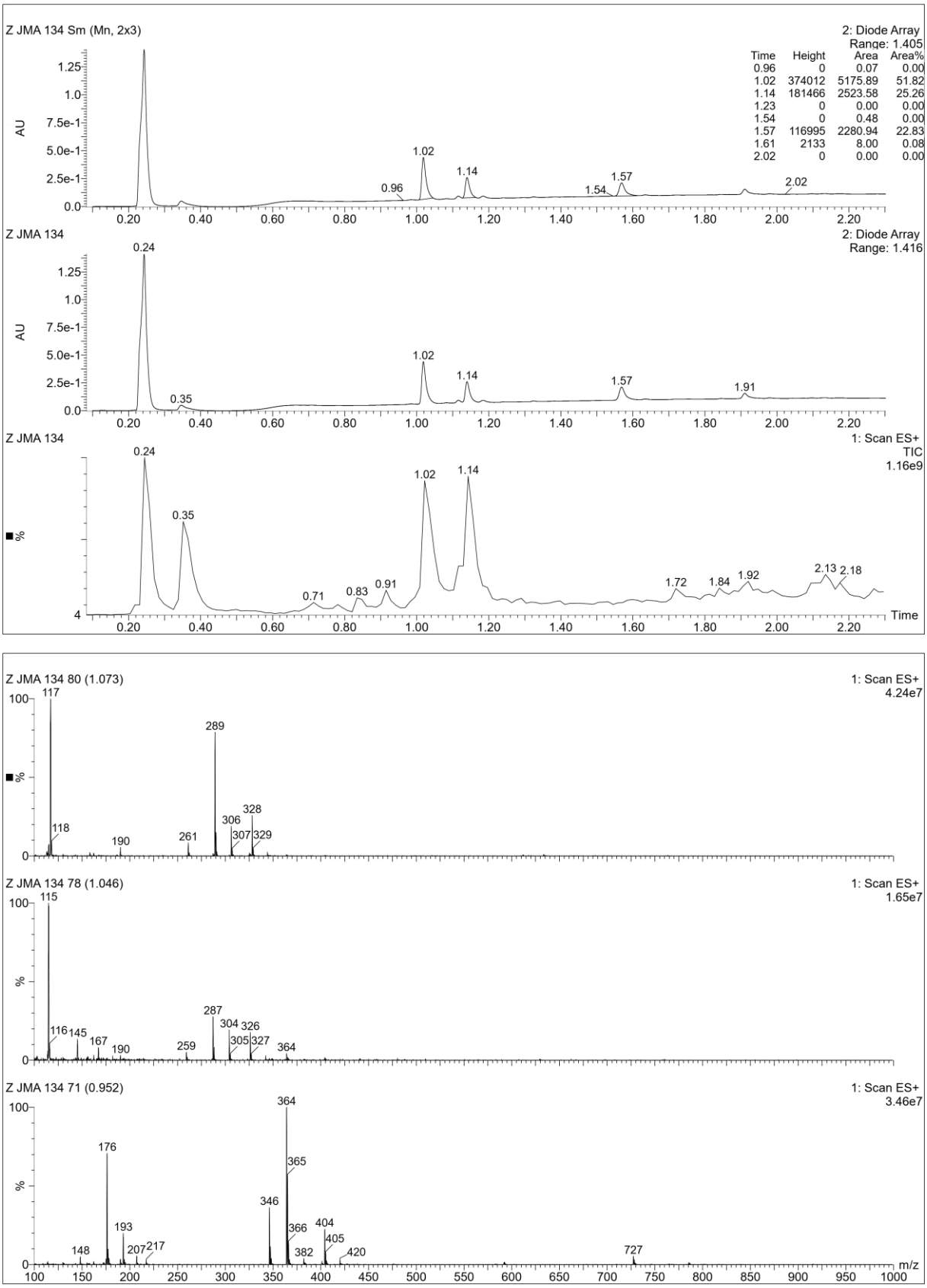

*Figure 5. ESI + LC/MS of hydrosilylation on AcPheAllylGly-NHRink amide Amphishere resin, with 30 equivalents of $HSiMe(OEt)_2$, 0.005 eq Karstedt catalyst in 5mL of anhydrous DCM, for 12h, **JMA 134**. Top: chromatograms UV at 214nm and TIC, Bottom: MS spectra at 1.02, 1.12 and 1.14 min.*

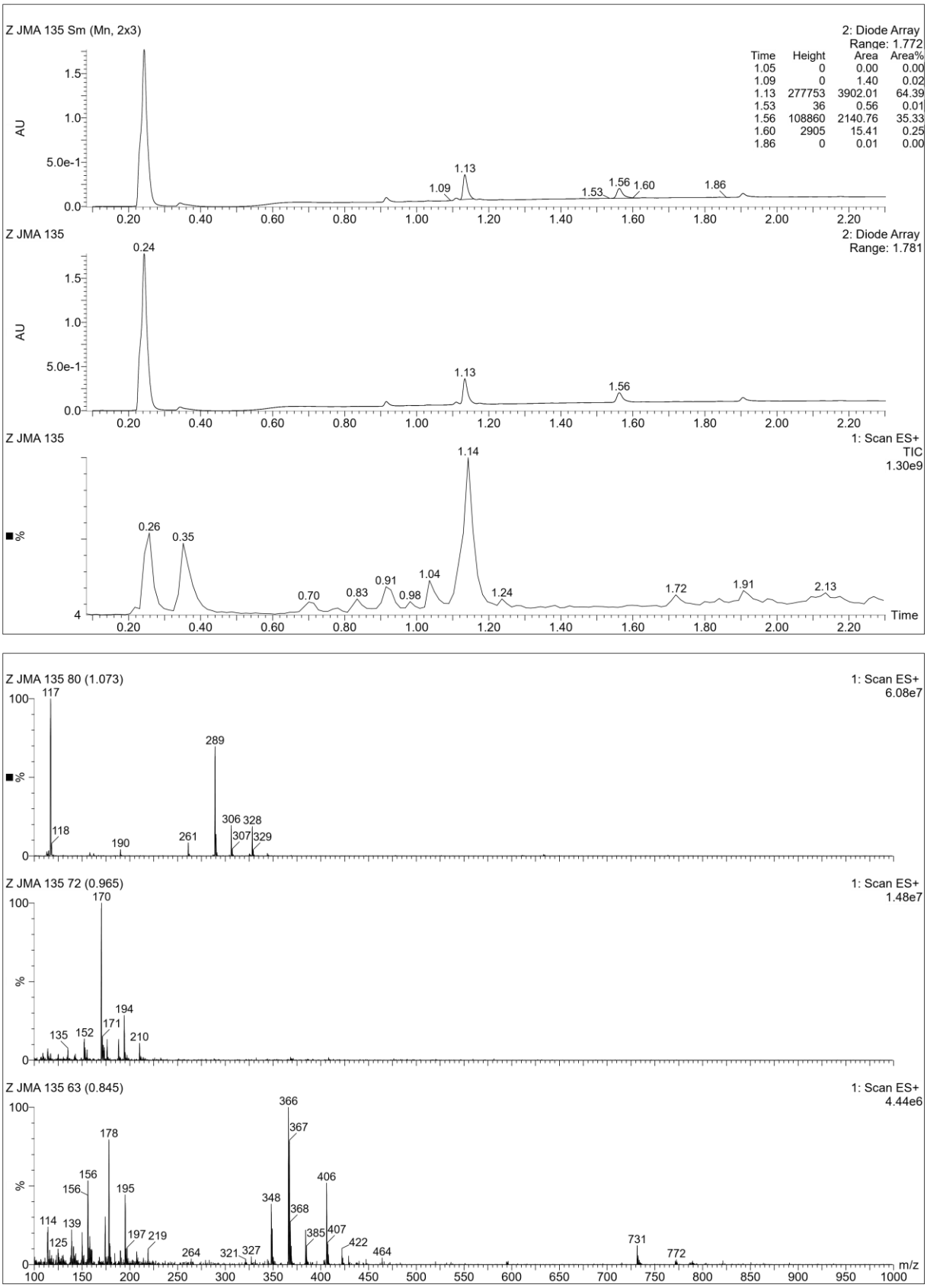

*Figure 6. ESI + LC/MS of hydrosilylation on AcPheAllylGly-NHRink amide Amphishere resin, with 30 equivalents of His(OEt)$_3$, 0.005 eq Karstedt catalyst in 5mL of anhydrous DCM, for 12h, **JMA 135**. Top: chromatograms UV at 214nm and TIC, Bottom: MS spectra at 0.91, 1.04 and 1.14 min*

Chapter 3

Estimation of amino acid loading

The resin was treated with 20% piperidine/DMF (2 x 3 mL, 3 min) and 50 µL of the combined deprotection solution was diluted to 10 mL using 20% piperidine/DMF in a volumetric flask. The UV absorbance of the resulting solution was measured (λ = 301 nm, ε = 7800 M-1 cm-1) to estimate the amount of amino acid loaded onto the resin.

LC/MS analyses

Samples for LC/MS analyses were prepared in an ACN/H_2O (50/50, v/v) mixture containing 1‰ TFA. The LC/MS system consisted of a Waters Alliance 2695 HPLC coupled to a Water Micromass ZQ spectrometer (electrospray ionization mode, ESI+).

Analysis of non-silylated compounds were carried out by HPLC using a Phenomenex Onyx, 25 x 4.6 mm reversed-phase column. A flow rate of 3 mL/min and a gradient of (0-100)% B over 2.5 min were used. Eluent A: water/0.1% HCO_2H; eluent B: acetonitrile/0.1% HCO_2H.

Analysis of silylated compounds were carried out by HPLC using a PLRP-S®, 25 x 4.6 mm reversed-phase column. A flow rate of 3 mL/min and a gradient of (5-100)% B over 9 min were used. Eluent A: water/0.1% HCO_2H; eluent B: acetonitrile/0.1% HCO_2H.

UV detection was performed at 214 nm. Electrospray mass spectra were acquired at a solvent flow rate of 200 µL/min. Nitrogen was used for both the nebulizing and drying gas. The data were obtained in a scan mode ranging from 100 to 1000 m/z or 250 to 1500 m/z to in 0.7 sec intervals. High Resolution Mass Spectrometric analyses were performed with a time of flight (TOF) mass spectrometer fitted with an Electrospray Ionization source. All measurements were performed in the positive ion mode.

NMR analyses

^{1}H and ^{29}Si NMR spectra were recorded at room temperature in deuterated solvents on a Bruker AMX/400 spectrometer operating at 500 and 79 MHz respectively. Chemical shifts (δ) are reported in parts per million using residual non-deuterated solvents as internal references ($CHCl_3$ in $CDCl_3$, δH = 7.26 ppm)

^{29}Si NMR spectrum of all the hybrid compound synthesized was conducted on a 400MHz Bruker NMR spectrometer. The samples were prepared in CDCl3 (50 mg/mL) at r.t.

^{1}H NMR spectrum of all the hybrid compound synthesized have been operated on a 500 MHz Bruker NMR spectrometer. All samples were prepared in $CDCl_3$ (30 mg/mL) at r.t.

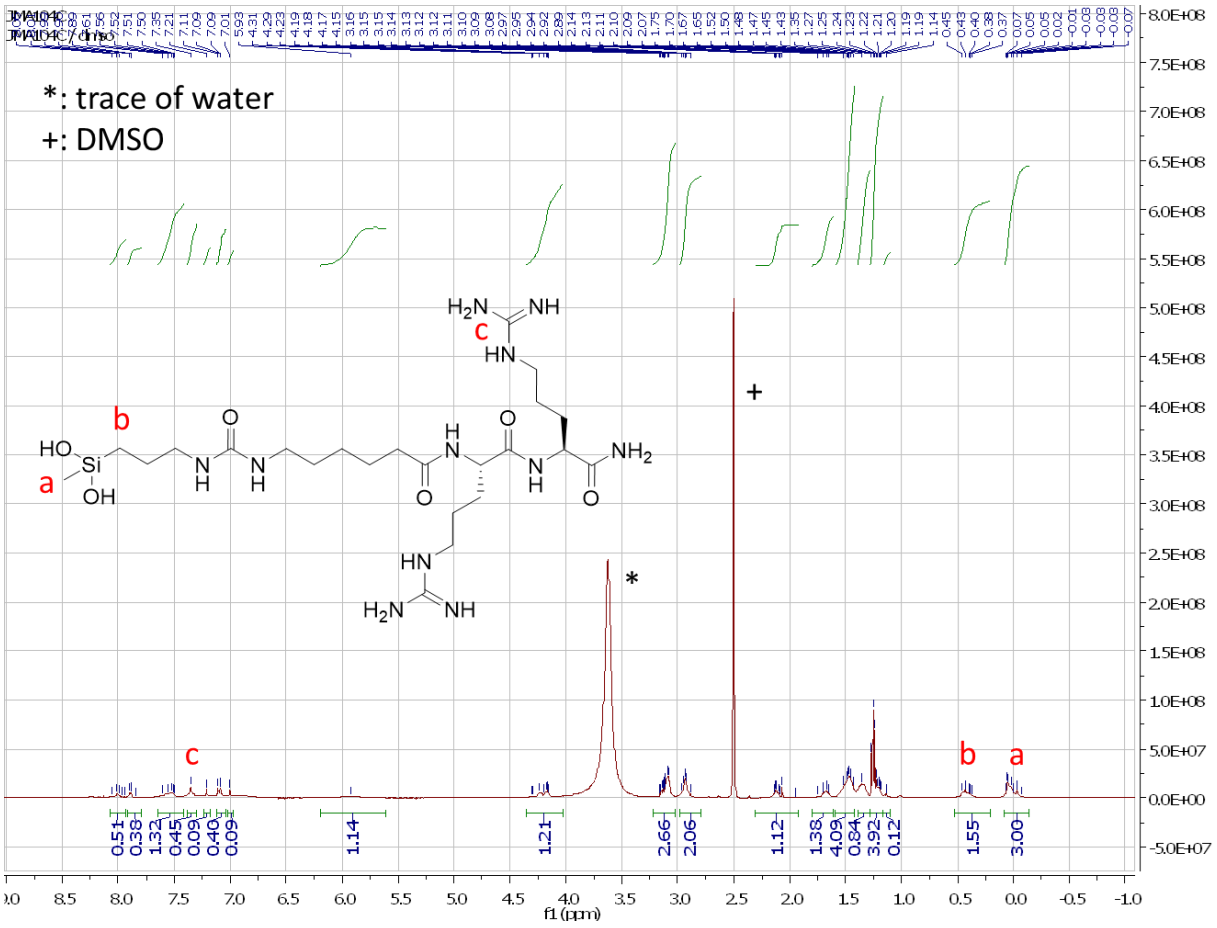

*Figure 7. ^{1}H NMR spectrum of compound **1**.*

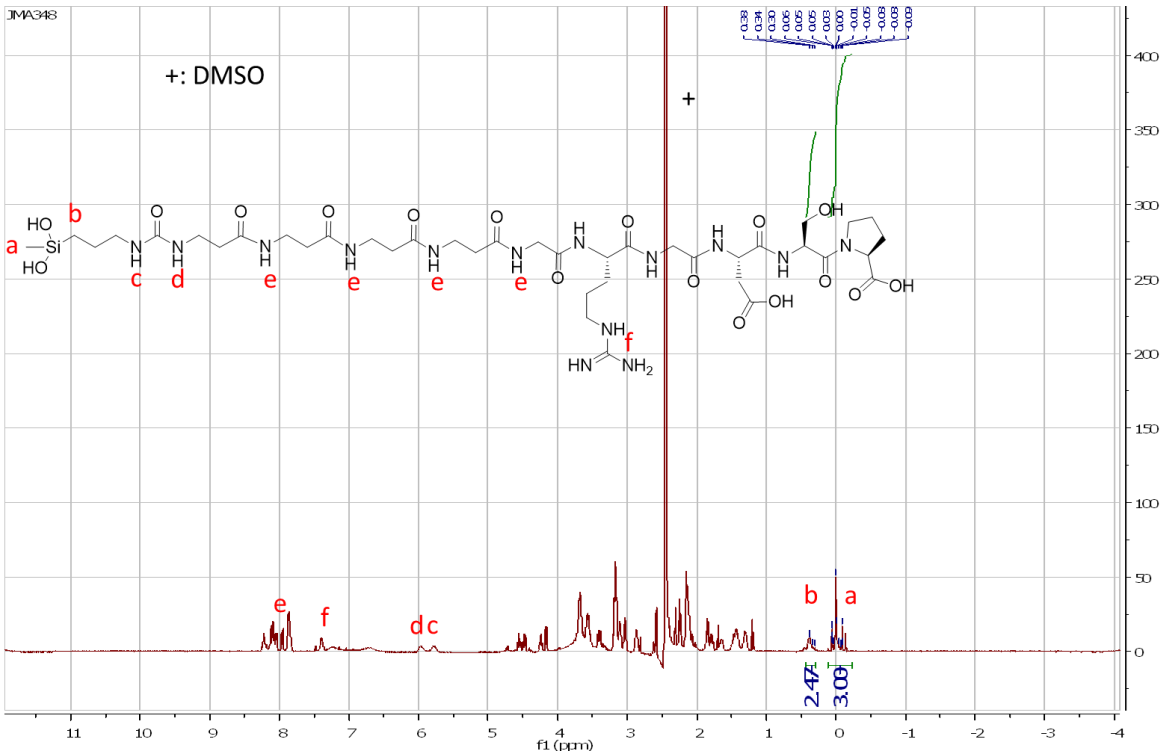

*Figure 8. ^{1}H NMR spectrum of compound **5**.*

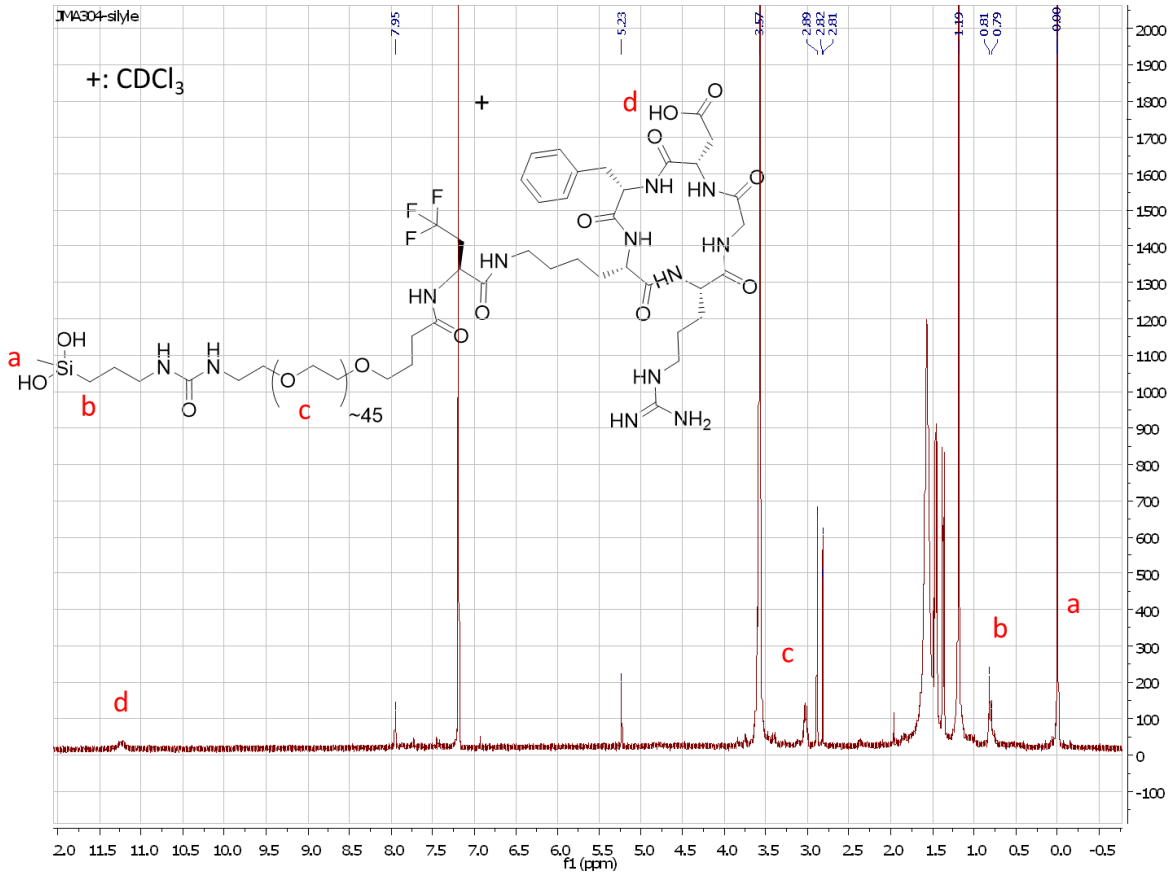

*Figure 9. ^{1}H NMR spectrum of compound **6**.*

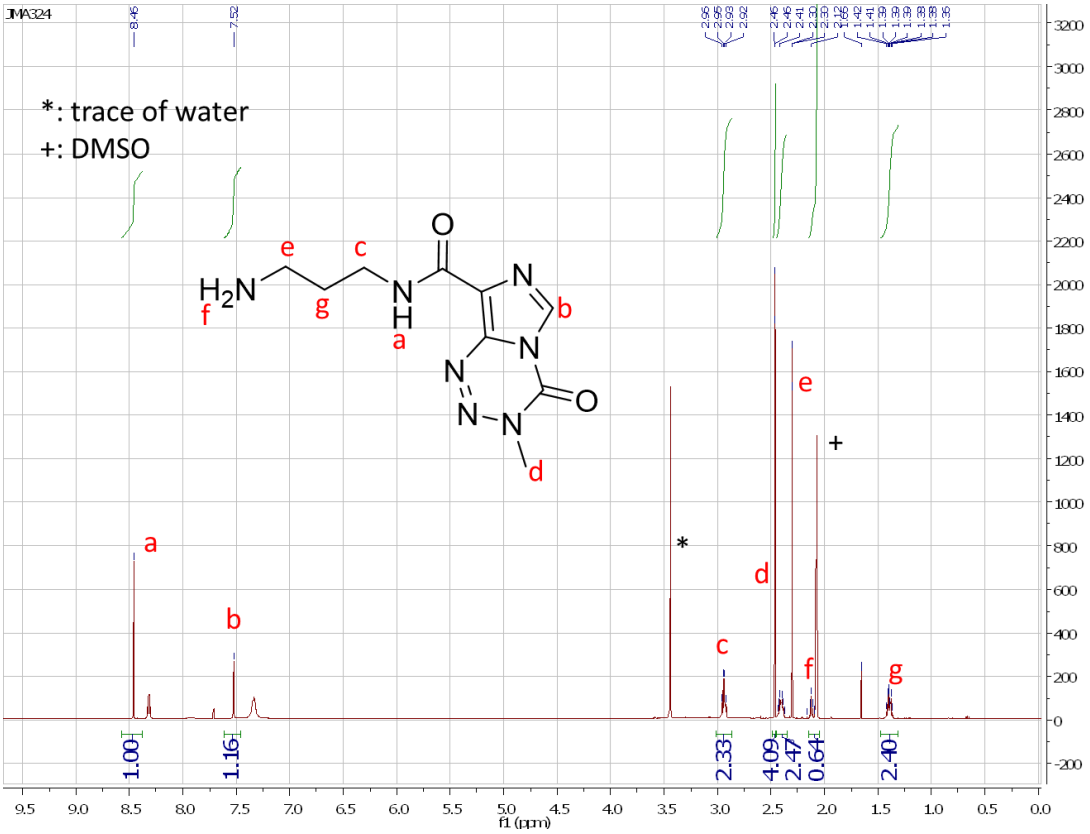

*Figure 10. ^{1}H NMR spectrum of compound **7b**.*

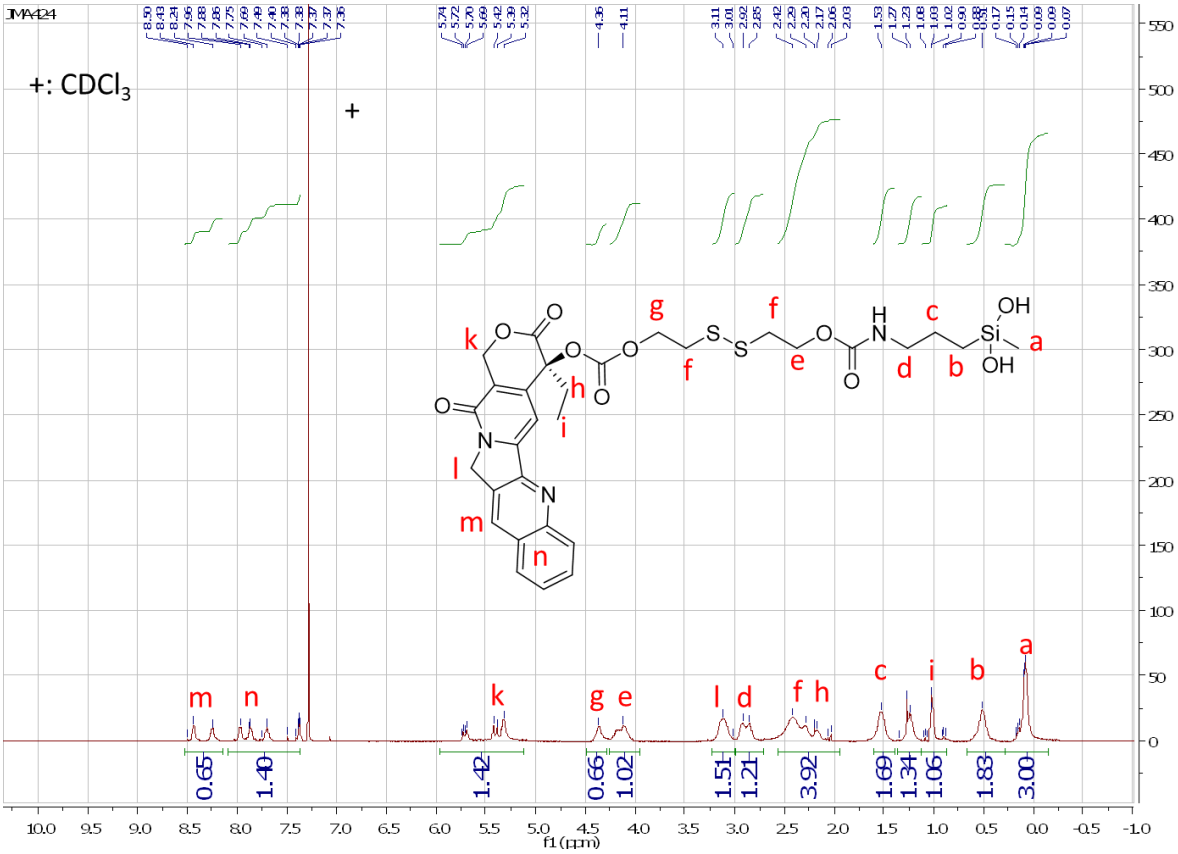

*Figure 11. ^{1}H NMR spectrum of compound **10**.*

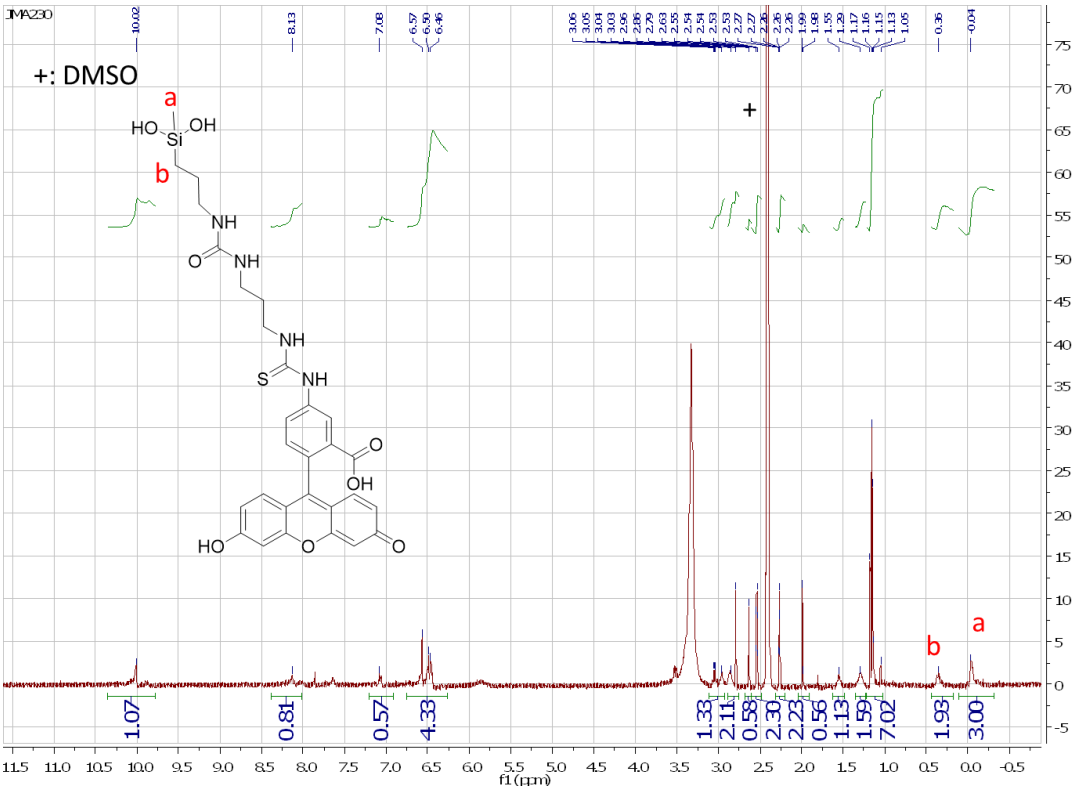

*Figure 12. ^{1}H NMR spectrum of compound **13**.*

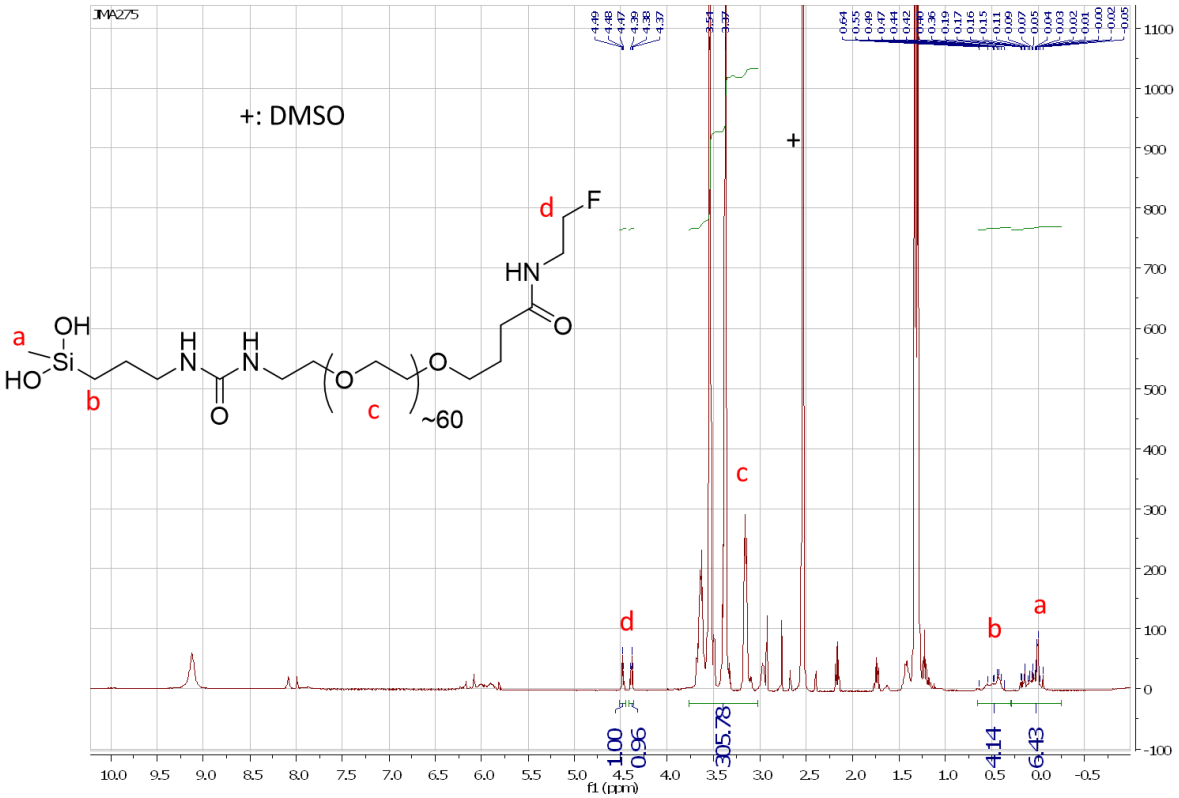

*Figure 13. [1]H NMR spectrum of compound **14.***

Chapter 4

NB: most of the work presented in this chapter constitutes the supporting information of a publication which is submitted: Martin, Julie, Mohammad Wehbi, Cécile Echalier, Coline Pinese, Jean Martinez, Gilles Subra, et Ahmad Mehdi. « Direct synthesis of peptide-modified silicone. A new way for bioactive materials ». *Submitted*, 2019.

Abbreviations

ACN, acetonitrile; Ahx, ε-aminohexanoic acid; CHCl3, Chloroforme; DCM, dichloromethane; DIEA, diisopropylethylamine; DMF, N-N'-dimethylformamide; Fmoc, fluorenylmethoxycarbonyl; FITC, Fluorescein-5-isothiocyanate; HATU, 1-[Bis(dimethylamino)methylene]-1H-1,2,3-triazolo[4,5-b]pyridinium 3-oxid hexafluorophosphate; HPLC, high performance liquid chromatography; LC/MS, tandem liquid chromatography/ mass spectrometry; n. d., non determined; NMR, nuclear magnetic resonance; Pbf, 2,2,4,6,7-pentamethyldihydrobenzofuran-5-sulfonyl; PS, polystyrene; RT, room temperature; SPPS, solid phase peptide synthesis; TFA, trifluoroacetic acid; TIS, triisopropylsilane. Other abbreviations used were those recommended by the IUPAC-IUB Commission (Eur. J. Biochem. 1984, 138, 9-37).

LC/MS analyses

Samples for LC/MS analyses were prepared in an ACN/H_2O (50/50, v/v) mixture containing 1‰ TFA. The LC/MS system consisted of a Waters Alliance 2695 HPLC coupled to a Water Micromass ZQ spectrometer (electrospray ionization mode, ESI+).

Analysis of non-silylated compounds were carried out by HPLC using a Phenomenex Onyx, 25 x 4.6 mm reversed-phase column. A flow rate of 3 mL/min and a gradient of (0-100)% B over 2.5 min were used. Eluent A: water/0.1% HCO_2H; eluent B: acetonitrile/0.1% HCO_2H.

Analysis of silylated compounds were carried out by HPLC using a PLRP-S®, 25 x 4.6 mm reversed-phase column. A flow rate of 3 mL/min and a gradient of (5-100)% B over 9 min were used. Eluent A: water/0.1% HCO_2H; eluent B: acetonitrile/0.1% HCO_2H.

UV detection was performed at 214 nm. Electrospray mass spectra were acquired at a solvent flow rate of 200 µL/min. Nitrogen was used for both the nebulizing and drying gas. The data were obtained in a scan mode ranging from 100 to 1000 m/z or 250 to 1500 m/z to in 0.7 sec intervals. High Resolution Mass Spectrometric analyses were performed with a time of flight (TOF) mass spectrometer fitted with an Electrospray Ionization source. All measurements were performed in the positive ion mode.

NMR analyses

^{1}H and ^{29}Si NMR spectra were recorded at room temperature in deuterated solvents on a Bruker AMX/400 spectrometer operating at 500 and 79 MHz respectively. Chemical shifts (δ) are reported in parts per million using residual non-deuterated solvents as internal references ($CHCl_3$ in $CDCl_3$, δH = 7.26 ppm)

Hybrid monomers synthesis

*Hybrid Fluorescein **1***

Fluorescein-5-isothiocyanate (FITC) (120 mg, 0.3 mmol) was solubilized into anhydrous DMF. DIEA (100 µL, 1.8 mmol) was added and then N-Boc-1,3-propanediamine (62 µL, 0.36 mmol). The mixture was flushed under argon, stirred for 1h at r.t. and finally concentrated *in vacuo*. The Boc protecting group was removed by TFA treatment for 2h at r.t., and the TFA was removed *in vacuo*. The hybrid fluorescein was precipitated in Et_2O and recovered by centrifugation. The product was then solubilized in anhydrous DMF. DIEA (500 µL, 2.4 mmol) and isocyanatopropyl dichloromethylsilane (80 µL, 0.36 mmol) were added. The mixture was flushed by argon and stirred 1h at r.t. After concentration of the solvent *in vacuo*, the product was purified by a PLRP-S column and lyophilized.

*Peptide **2** synthesis*

Fmoc-Sieber PS resin (0.88 mmol/g, 1eq) was placed in a solid-phase peptide synthesis syringe. The Fmoc group was removed by two successive DMF-piperidine (80:20; v/v) treatments (2 x 20min). Fmoc-Arg(Pbf)-OH (3 eq) was anchored to the resin in the presence of DIEA (6 eq) and HATU (3 eq) in DMF for 1h stirred at 450 rpm/min. Resin was then washed 3 times using DMF. The Fmoc group was removed from Fmoc-Arg(Pbf)-Sieber-resin as previously described. 3 washing steps (DMF) were performed at the end of deprotection. The following amino acids, Fmoc-Arg(Pbf)-OH then Fmoc-Ahx-OH, were coupled and deprotected using the same protocol.

*Peptide **2** cleavage and silylation*

Sieber linker allowed the cleavage of the peptide without the removal of the Pbf on the side chain of the Arginine residue. It allowed the recovery of Pbf-protected peptide, soluble in organic solvents and easily purified by RP-preparative HPLC. The cleavage was performed in DCM/TFA (99/1, v/v) for 2h at room temperature, under stirring. After concentration of the solvent and precipitation by Et_2OH, the H-Ahx-Arg(Pbf)-Arg(Pbf)-NH_2 peptide was purified on preparative RP-HPLC equipped with a C_{18} reversed-phase column. The purified H-Ahx-Arg(Pbf)-Arg(Pbf)-NH_2 (600 mg, 0.6 mmol) was solubilized in anhydrous DMF. DIEA (600 µL, 3.6 mmol) and isocyanatopropyl dichloromethylsilane (160 µL, 0.7 mmol) were added to the mixture. The reaction was stirred for 1h under argon atmosphere, and the solvent was removed *in vacuo*. The hybrid monomer was then purified on preparative HPLC using a non-silica-based column PLRP-S, and finally the Pbf groups were removed by TFA treatment, at room temperature for 2h. TFA was removed *in vacuo* and the deprotected hybrid peptide **2** was precipitated in Et_2OH. The monomer was then dissolved in H_2O/ACN/TFA (50/50/0.1, v/v/v) and finally lyophilized.

*Hybrid Peptide **3** synthesis*

2-chloroTrityl PS resin (1,60 mmol/g, 1eq) was placed in a solid-phase peptide synthesis syringe. Fmoc-Pro-OH (3 eq) was anchored to the resin in the presence of DIEA (6 eq) in DMF, stirred overnight at 450 rpm/min. A capping of non-reacted chloroTrityl function were done by MeOH/DIEA solution (80:20; v/v) during 30min. Several washed by DCM (x2) and DMF (x3) were operated. The Fmoc group was removed by two successive DMF-piperidine (80:20; v/v) treatments (2 x 20min). 3 washing steps (DMF) were performed at the end of deprotection. Following amino acids, Fmoc-AA-OH (3 eq) were coupled to the previous amino acid, Fmoc-deprotected, in the presence of DIEA (6 eq) and HATU (3 eq) in DMF for 1h stirred at 450 rpm/min. Resin was then washed 3 times using DMF. The operations are repeated for the next amino acids.

After the last coupling and Fmoc-deprotection, the peptide-resin was placed in anhydrous DMF. DIEA (6eq) and isocyanatopropyl dichloromethylsilane (1.2eq) were added to the mixture. The reaction was stirred overnight under argon atmosphere. The resin was then washed with DMF three times. The silylated peptide was cleaved from the resin by acidic treatment: 1h in TFA/TIS/H_2O (98/1/1). After

evaporation of the solvent under vacuum, the hybrid peptide was precipitated in Et_2OH three times. The hybrid monomer was finally purified on preparative HPLC using a non-silica-based column PLRP-S and lyophilized.

GPC analyses

The molecular weight of the polymer was determined using Gel permeation chromatography (GPC). The analysis was performed on a Waters GPC system consisting of a PLgel Mixed C-5µm-2*300m column, a pump and a UV detector. CHCl3 was used as the eluent at flow rate of 1ml/min at 25°C and samples prepared at 10mg/mL and filtered with PTFE 0.45µm filters.

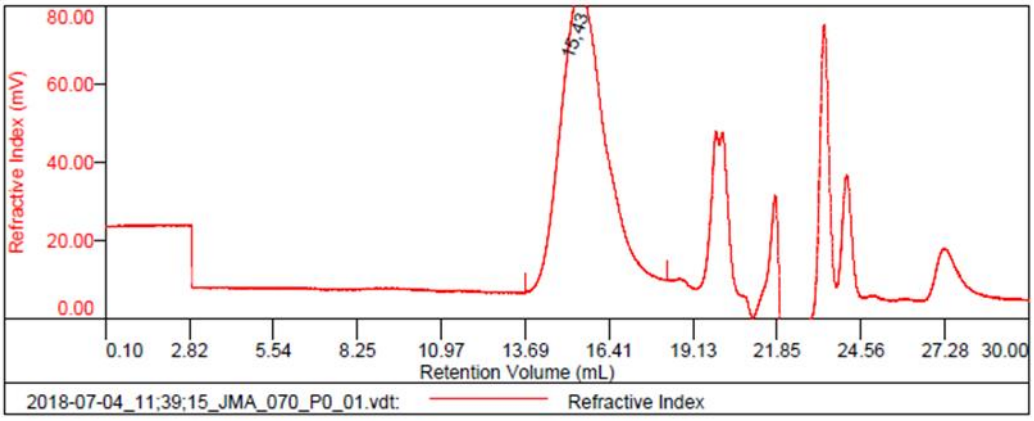

Figure 14. GPC analyses spectrum of the P0 PDMS oil.

^{29}Si NMR characterization

^{29}Si NMR spectrum of PDMS oil was conducted on a 400MHz Bruker NMR spectrometer. The sample was prepared in CDCl3 (50 mg/mL) at r.t. Si NMR of natural PDMS showed a single peak at -22 ppm in ^{29}Si NMR, which corresponded to Si of PDMS. The occurrence of a single peak confirmed the absence of any uncondensed by-product. In the case of modified PDMS, the NMR showed other peaks due to the presence of –O-Si(Me)R, R=H or Vinyl.

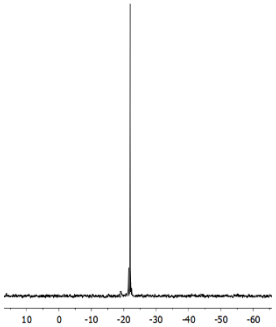

Figure 15. ^{29}Si NMR spectrum of the natural PDMS oil, P0

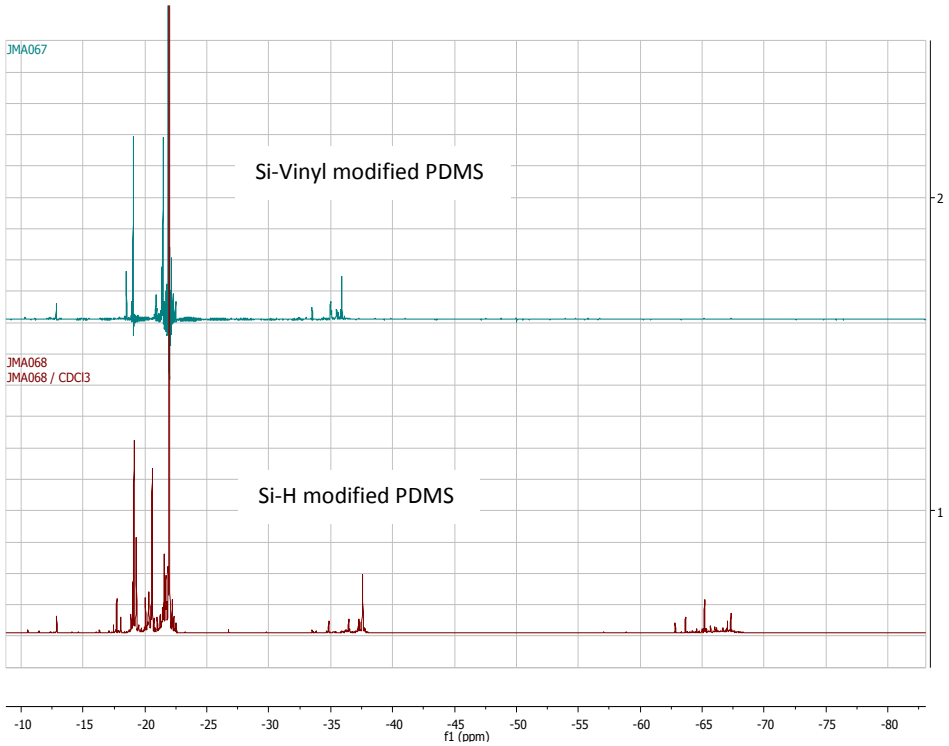

Figure 16. ^{29}Si NMR spectrum of Si-Vinyl and Si-H modified silicone, at 10 mol%

^{1}H NMR characterization

^{1}H NMR spectrum of all the PDMS synthesized have been operated on a 500 MHz Bruker NMR spectrometer. All samples were prepared in $CDCl_3$ (30 mg/mL) at r.t. Each spectrum showed a solvent peak at 7.27 ppm plus traces of the SDS surfactant at at 3.57, 1.49, 1.19 and 0.81 ppm. The Si-CH_3 created a signal around 0 ppm. Then the Si-H peak is present at 4.62 ppm and the Si-vinyl around 5.87 ppm (Figures 3 and 4). The integration of these two peaks allowed the quantification of the experimental quantity of the functional monomers, Si-H and Si-vinyl, incorporated into the PDMS chains (Figure 5).

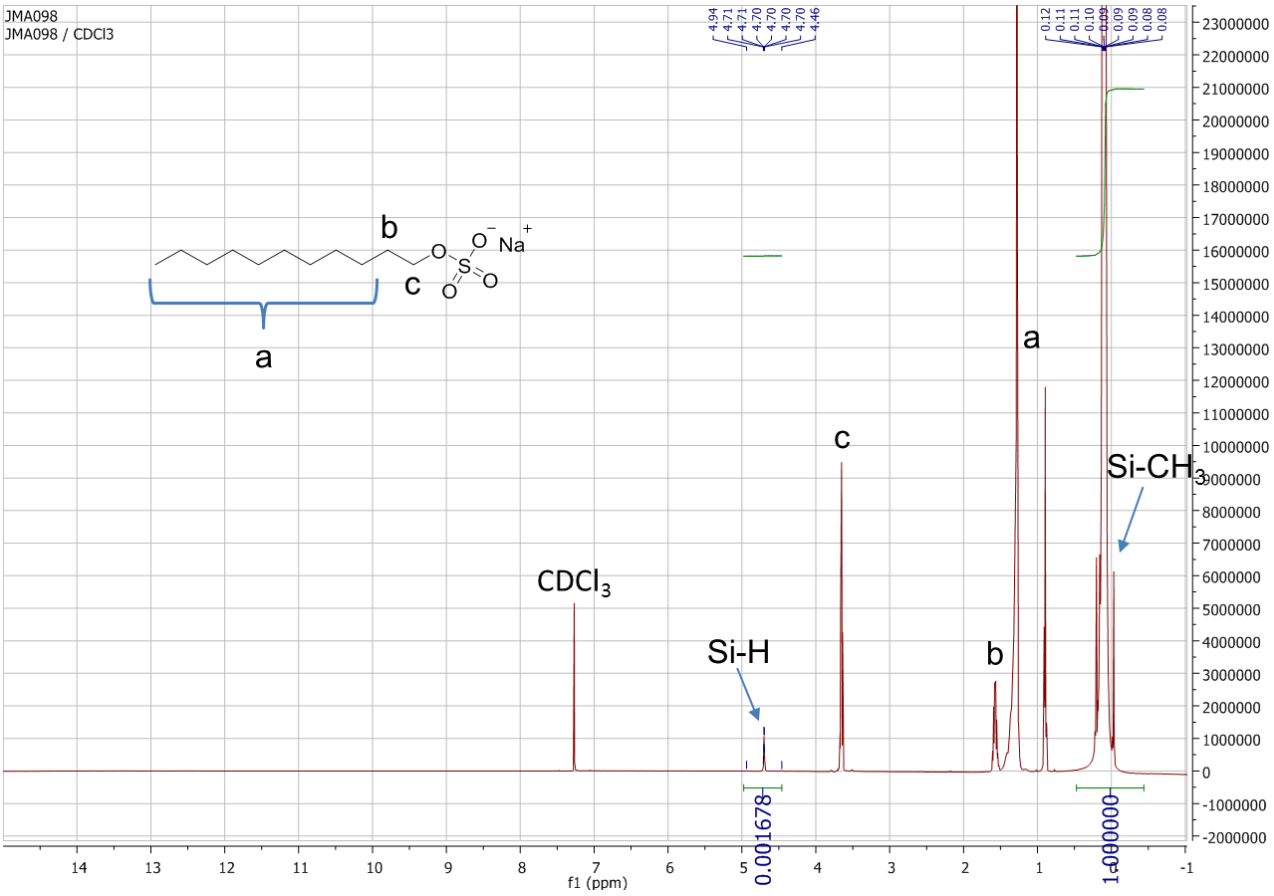

Figure 17. ^{1}H NMR spectrum of Si-H modified PDMS oil

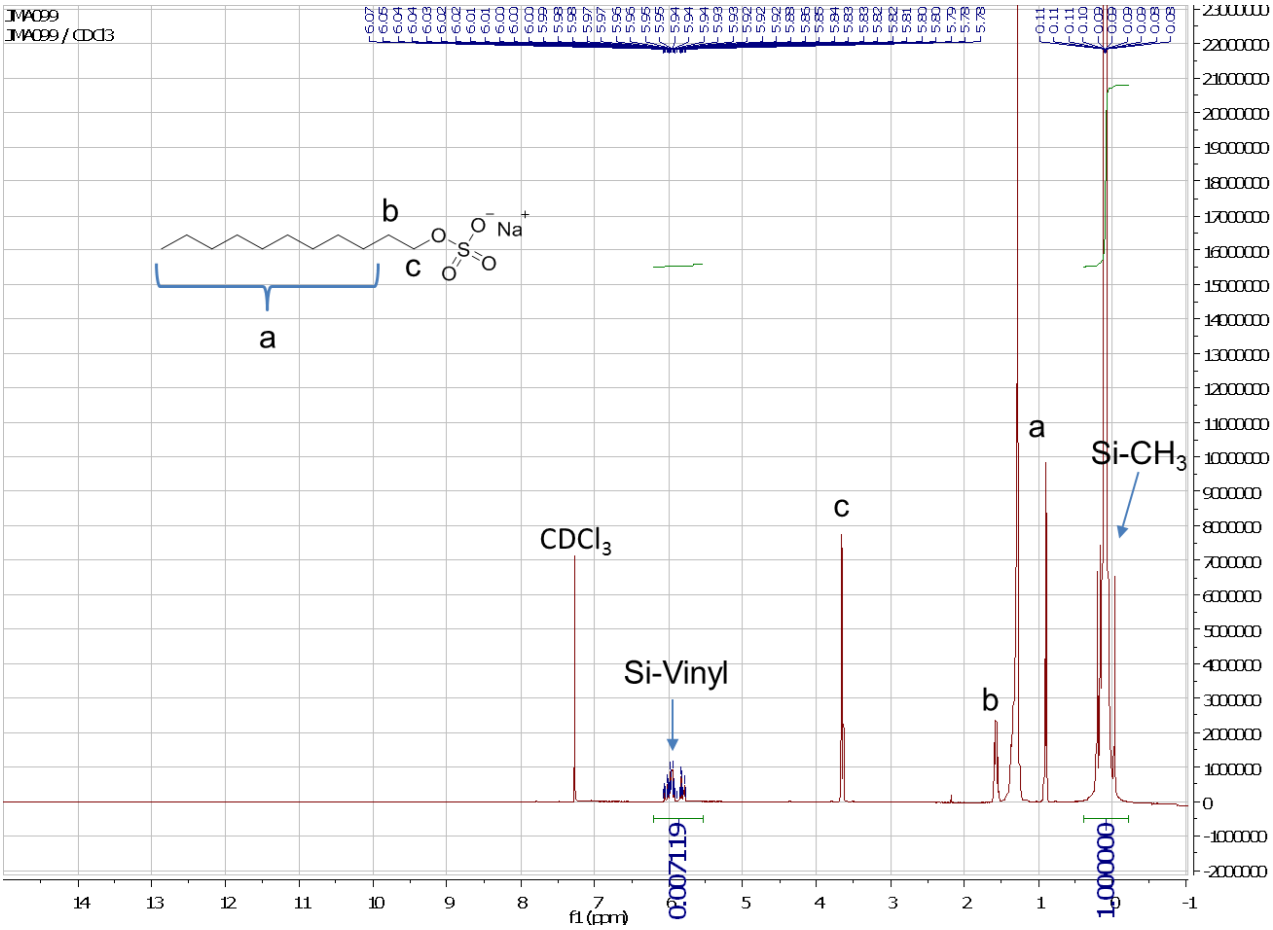

Figure 18. ^{1}H NMR spectrum of Si-Vinyl modified PDMS oil

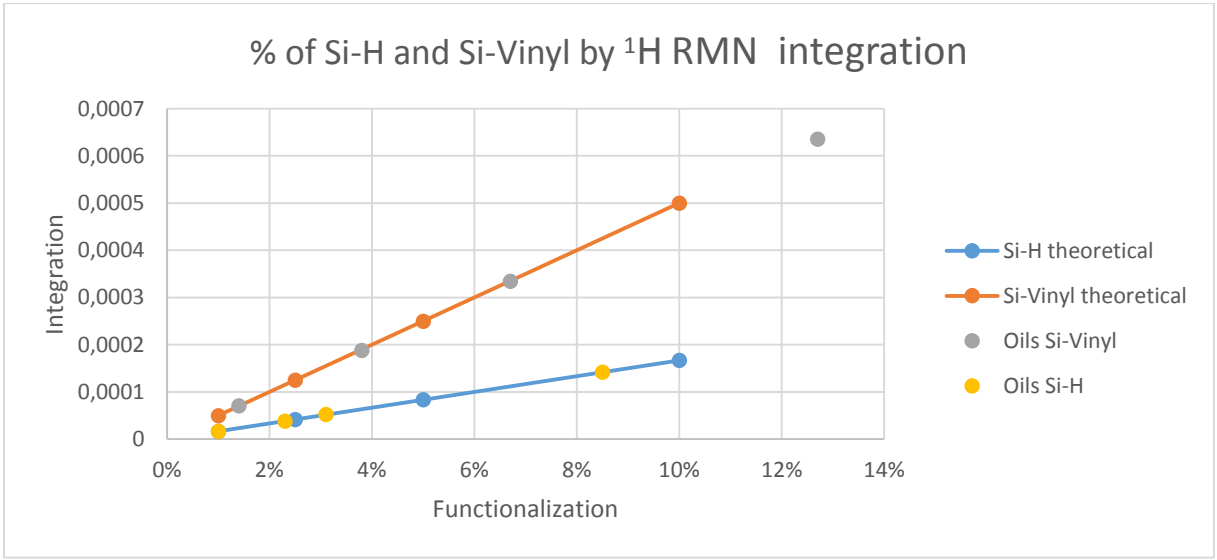

Figure 19. Experimental percentage of functional monomer, Si-H and Si-Vinyl, into PDMS oils by integration of ^{1}H NMR spectrum

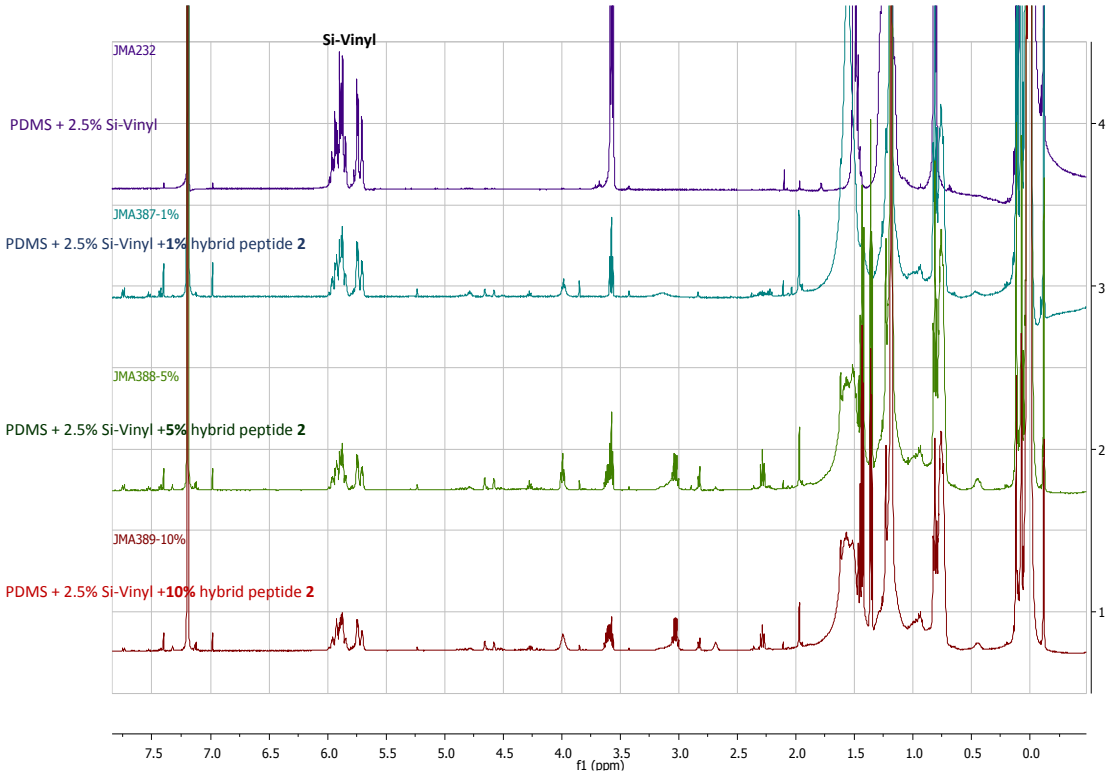

Figure 20. Evolution of hybrid peptide 2 peaks on ^{1}H NMR in function of mol%

Infra-Red characterization

Infra-Red analyses have been performed on each PDMS oil and every PDMS material. They have been realized on a FI-IR spectrometer with a Spectrum Two™ system from Perkin Elmer. Samples were simply put on the diamond, and analyzed at R.T. The comparison between the different percentages of Si-H and Si-vinyl functionalization's showed quite clearly the increase of the specific peak on the spectrum. Indeed, the wave number at 910 cm^{-1} was specific to Si-H, and the one at 530 cm^{-1} specific to Si-vinyl[1,2]. On the spectrum of the resulting material (10 mol% functionalization), none of these specific wave numbers showed a peak, which indicated that the cross-linking was total (Figure 6).

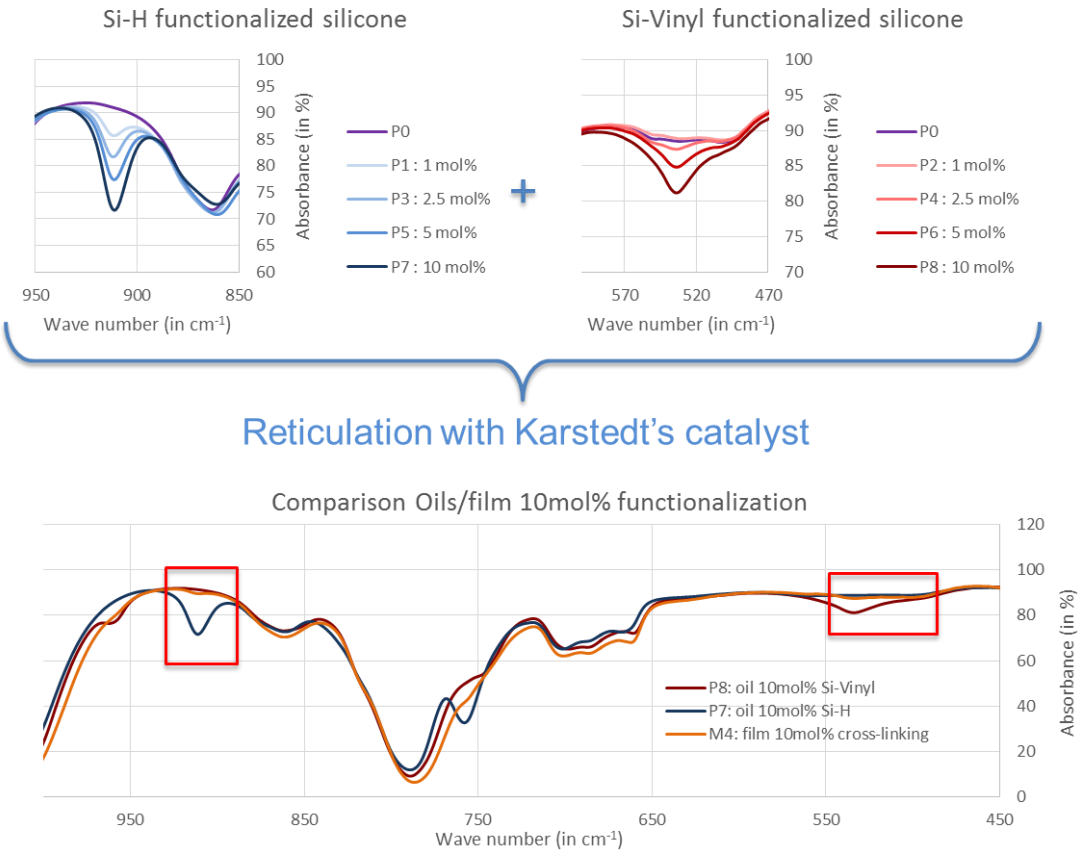

Figure 21. Comparison of IR characterization of each functional PDMS oil, and 10 mol% modified oils P8 and P9 with the PDMS material associated, M4

Nano-indentation

The indentation modulus (E_{IT}) of each PDMS material was determined by nano-indentation equipped with a Berkovich tip and using Oliver and Pharr method for data analysis. 5 indents were performed at 60 µN and 5 at 100 µN on each films. An average indentation modulus is then calculated, showing that the evolution of the indentation modulus in function of the cross-linking percentage is linear (Figure 7). Thanks to the model line associated, experimental cross-linking percentage of hybrid PDMS material were determined and compared to the corresponding natural PDMS material (Table 1).

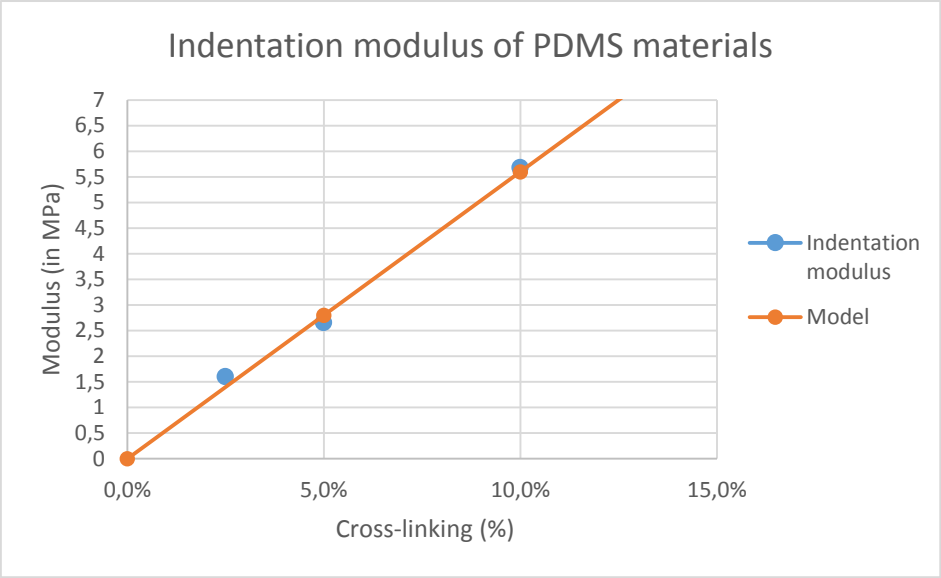

Figure 22. Evolution of the Indentation modulus of PDMS material with different cross-linking percentage: 2.5%, 5% and 10%, respectively M2, M3 and M4

Table 1. Experimental cross-linking of hybrid PDMS material

Material	Experimental Cross-linking (%)	Hybrid monomer (mol%)	Hybrid macromonomer
M2	2.9	0	/
M5	5.5	0.005	Hybrid Fluorescein **1**
M6	4.8	0.05	
M7	2.7	0.005	
M8	3.3	0.05	
M9	0.5	0.5	Hybrid Peptide **2**
M10	0.5	2.5	
M11	0.3	5	
M12	2.2	0.005	
M13	0.6	0.05	
M14	0.5	0.5	Hybrid Peptide **3**
M15	2.0	2.5	
M16	1.4	5	

Antibacterial assays

The Staphylococcus aureus solution was adjusted to 105 CFU.mL^{-1} in trypticase soja medium. 10µl of bacterial solution were dropped on samples and recovered with 1 cm² sterile glass coverslip. After 24 h at 37 °C, bacteria were detached from supports by washing with 3 mL sterile saline solution, and sonicated for 3 min. The viable bacteria in solution were then serially diluted (1/100, 1/1000 and 1/10 000), and 100-µL aliquots were spread on gelose trypticase soja plates for CFU determination. The assay was performed in triplicate. The percentage of inhibition was calculated according to the bacterial number on surfaces without peptide (**M2**).

Cell adhesion assays

Adhesion properties of peptide 3-modified-PDMS materials were measured on L929 mouse fibroblasts cultured. After UV-C exposition at 0.120 J/cm² for 2x28 seconds, peptide 3-modified-PDMS materials deposed on glass slides were placed in a 24-well cell culture plate in quintuplicates. $8{,}6.10^4$ cells in 80 µL of culture medium were added on top of hybrid PDMS material. Cells were allowed to adhere for 4h at 37 °C. Then, all the wells were washed with DPBS and PrestoBlue (1 mL of a 10% (v/v) solution of PrestoBlue, Molecular 29 probes by life technologies, in the culture medium) was added. The plate was incubated for 1h. Then 200 µL of each well were transferred to a 96 well black plate for fluorescence reading (λexcitation = 535 nm, λemission = 615 nm). Cell observation after 4h adhesion and 1h incubation with Prestoblue solution.

References

(1) Launer, P. J.; Arkles, B. Infrared Analysis of Organosilicon Compounds. *Silicone Compd. Regist. Rev.* **1987**, *100*.

(2) Ou, D. L.; Seddon, A. B. Near- and Mid-Infrared Spectroscopy of Sol–Gel Derived Ormosils: Vinyl and Phenyl Silicates. *J. Non-Cryst. Solids* **1997**, *210* (2), 187–203. https://doi.org/10.1016/S0022-3093(96)00585-6.

Chapter 5

NMR analyses

^{1}H and ^{29}Si NMR spectra were recorded at room temperature in deuterated solvents on a Bruker AMX/400 spectrometer operating at 500 and 79 MHz respectively. Chemical shifts (δ) are reported in parts per million using residual non-deuterated solvents as internal references ($CHCl_3$ in $CDCl_3$, δH = 7.26 ppm)

^{29}Si NMR spectrum of all the polymer synthesized was conducted on a 400MHz Bruker NMR spectrometer. The samples were prepared in CDCl3 (50 mg/mL) at r.t.

^{1}H NMR spectrum of all the polymer synthesized have been operated on a 500 MHz Bruker NMR spectrometer. All samples were prepared in $CDCl_3$ (30 mg/mL) at r.t.

^{19}F NMR quantification by ERETIC method have been operated on a 400MHz Bruker NMR spectrometer. The sample were prepared in $CDCl_3$ (10mg/mL) at r.t.

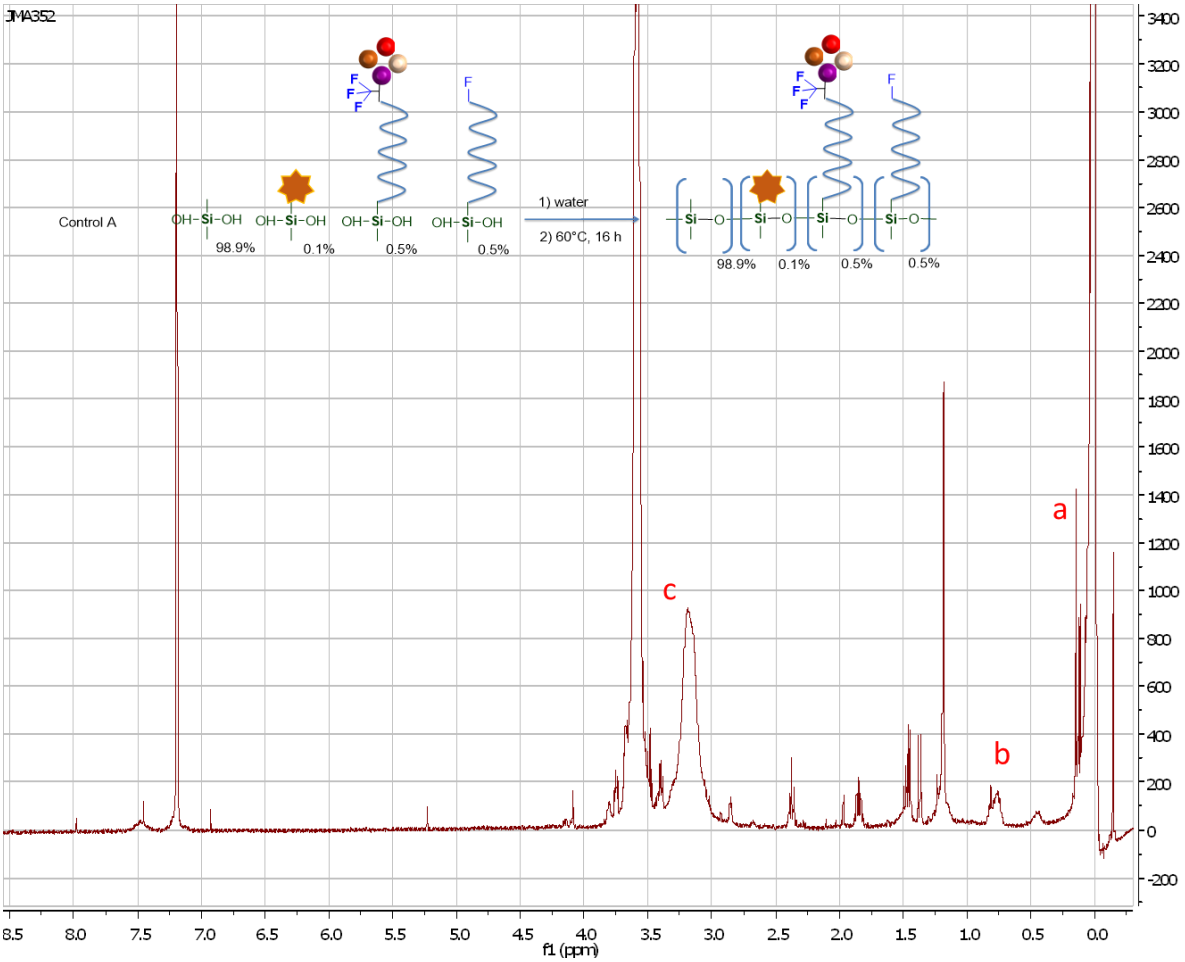

*Figure 23. ^{1}H NMR spectrum of **P_{352}**, a: methyl silyl group, b: CH_2-Si and c: PEG chain.*

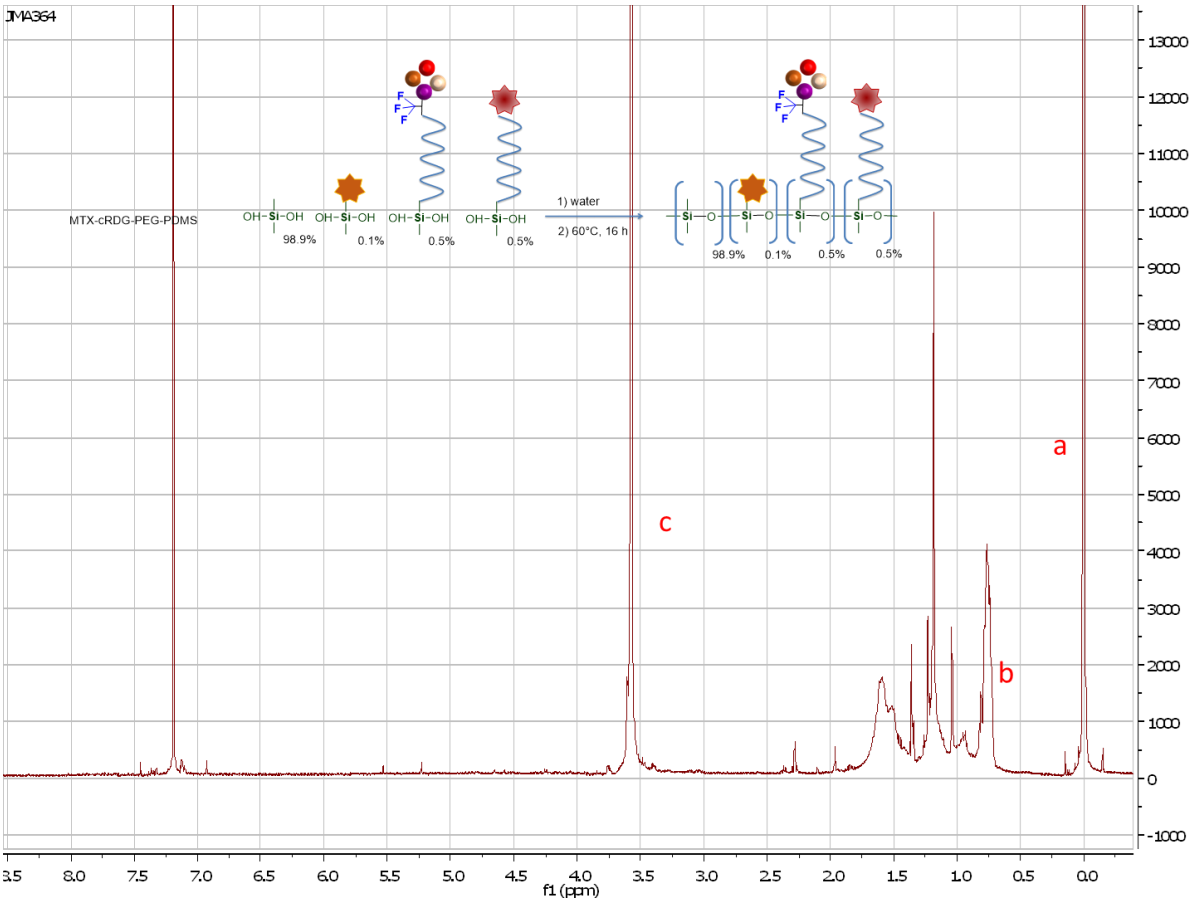

*Figure 24. [1]H NMR spectrum of **P364**, a: methyl silyl group, b: CH_2-Si and c: PEG chain.*

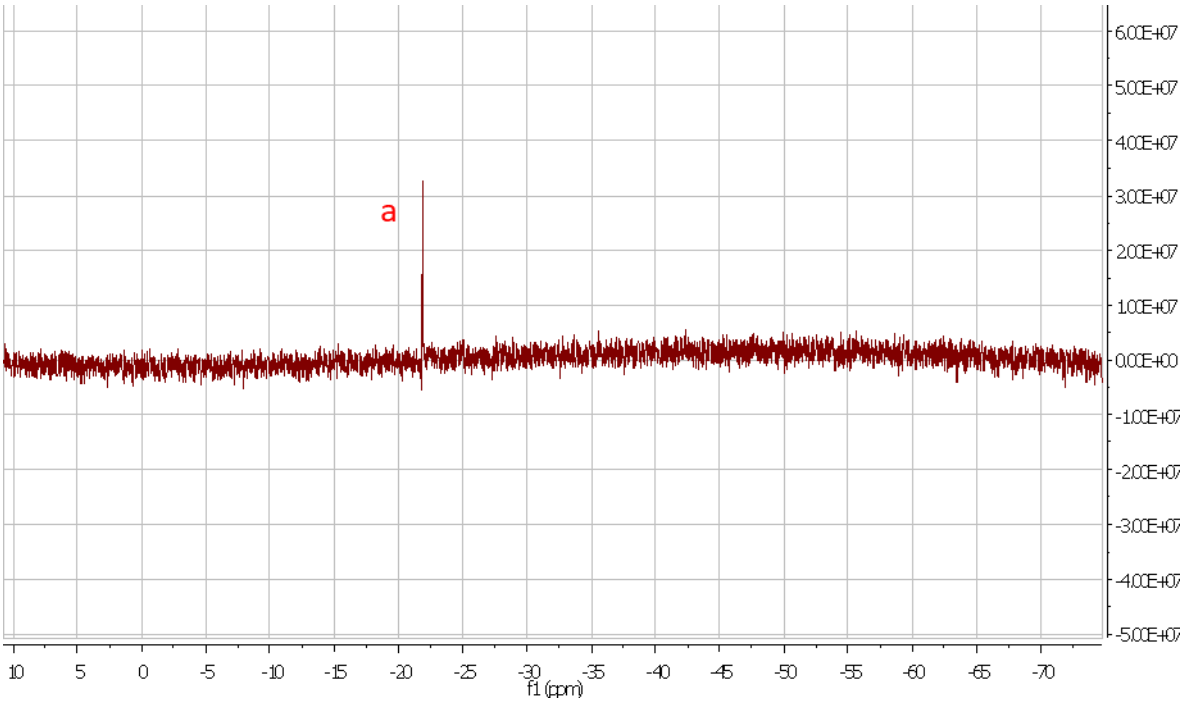

Figure 25. [29]Si NMR spectrum of P364, a: methyl silyl group.

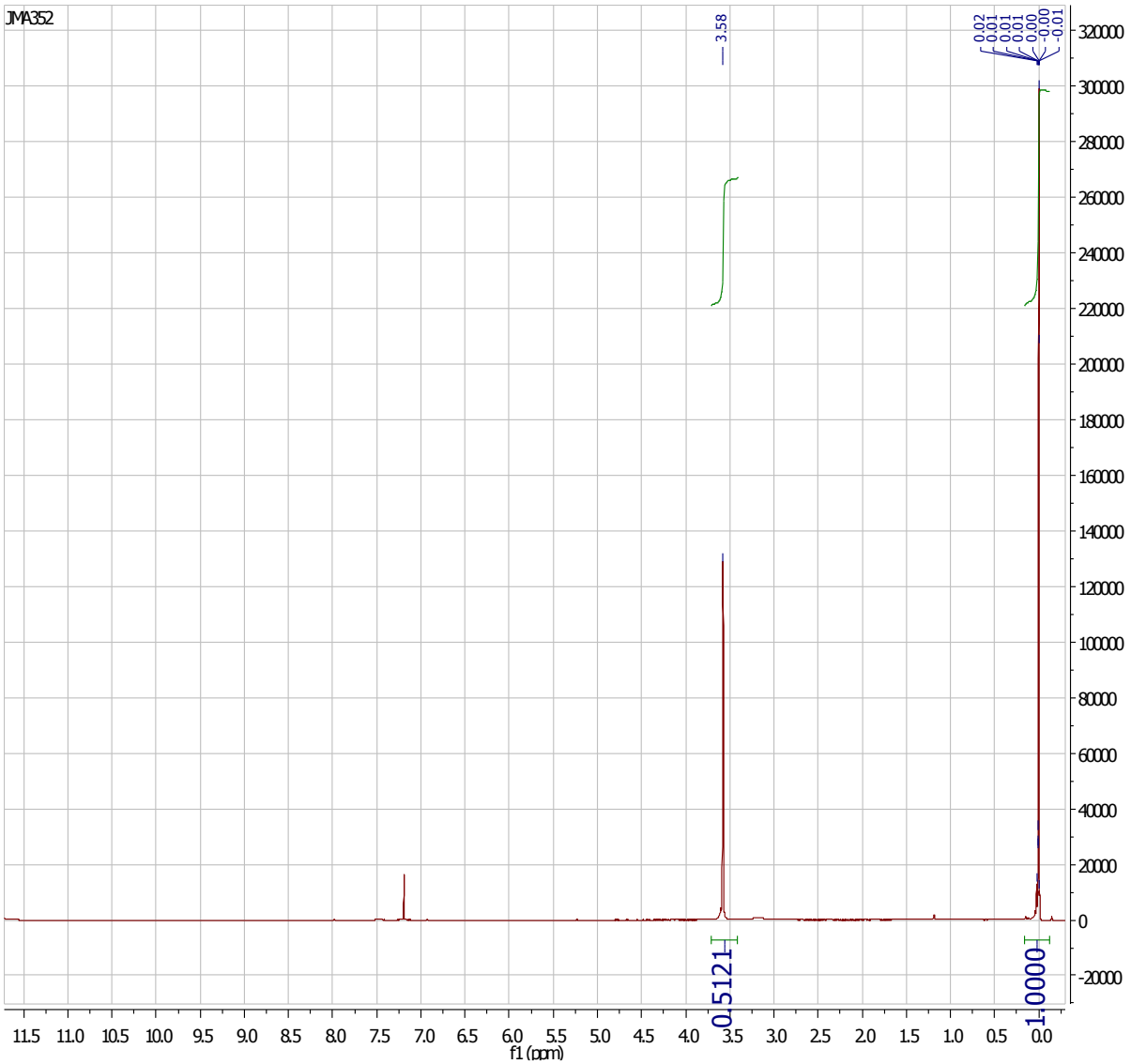

Figure 26. ^{1}H NMR spectrum and quantification of PEG chain by integration comparison of $P_{352\text{-}A}$.

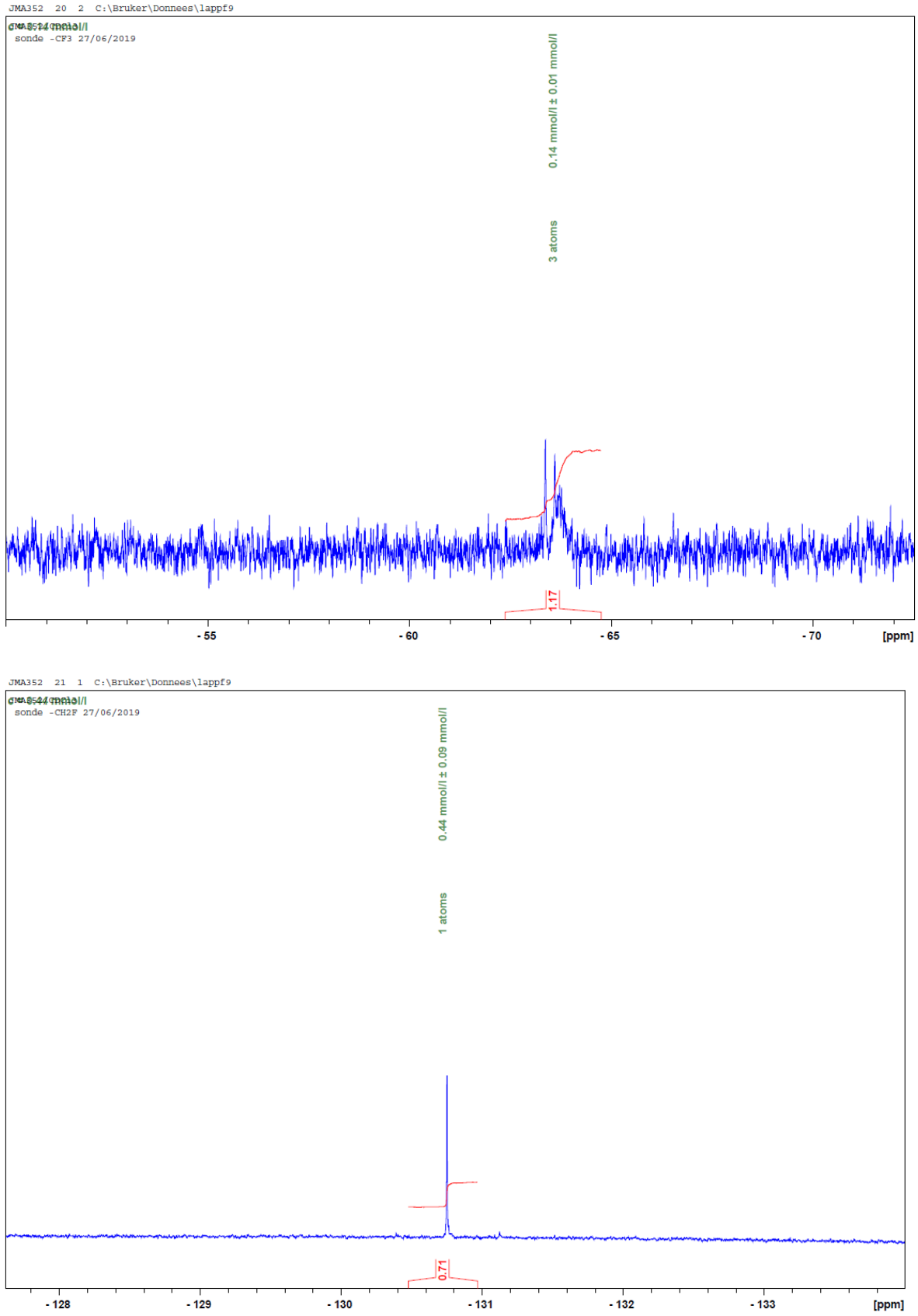

Figure 27. ^{19}F NMR quantification by ERETIC method of ***$P_{352\text{-}A}$***.

GPC analyses

The molecular weight of the polymer was determined using Gel permeation chromatography (GPC). The analysis was performed on a Waters GPC system consisting of a PLgel Mixed C-5µm-2*300m column, a pump and a UV detector. CHCl3 was used as the eluent at flow rate of 1ml/min at 25°C and samples prepared at 10mg/mL and filtered with PTFE 0.45µm filters.

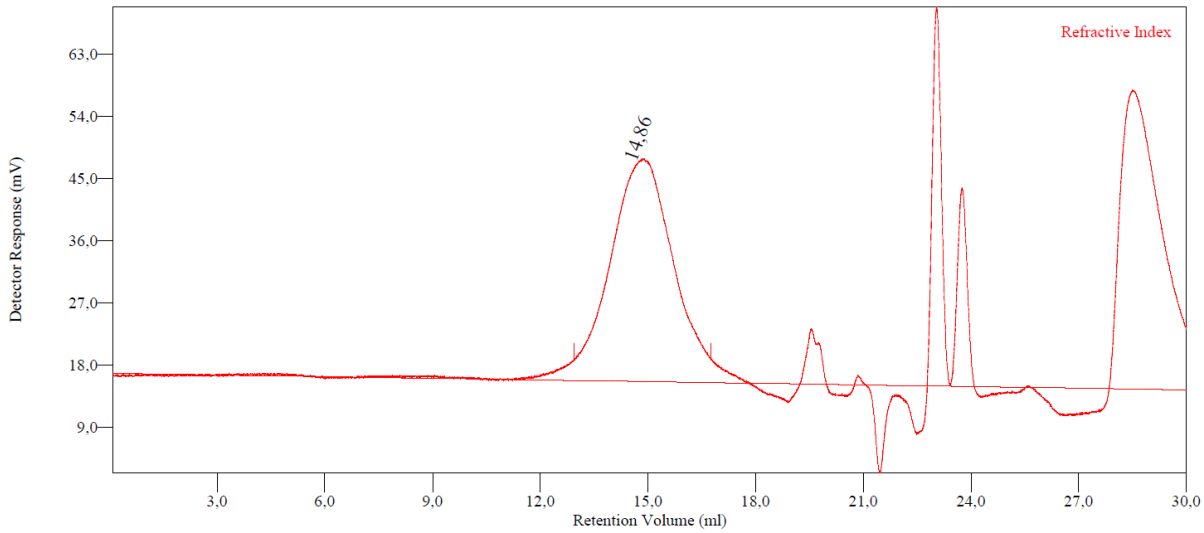

Figure 28. GPC chromatograms of $P_{352\text{-}A}$.

Repeat unit number calculation

The average number of repeat unit in a polymer chain is calculated from the molecular weight in number (Mn). An average molecular weight of one repeat unit is calculated taking in account the composition of the polymer: from the different percentage of each macromonomer associated with their molecular weight. Then the molecular weight in number (Mn) is divided by this average molecular weight of one repeat unit, leading to the average number of repeat unit per polymer chain. Finally, to get the repeat unit number of a specific macromonomer, its molecular percentage is applied to the global number of repeat unit.

Protocol NTA preparation sample

The polymer is precisely weighted between 2 and 5 mg in a tared hemolysis tube. The adapted volume of water is then added in the tube to get a final concentration of 1 mg/mL. Vortex and especially ultra-sons are applied in order to get it completely dispersed.

Then, the solution if filtered in a new tared hemolysis tube by a 0.45µm H-PTFE filter. The first hemolysis tube is freeze-dried in the lyophilizator to take away the rest of water. Once dried, it is finally weighted to get the amount of polymer that stayed stuck in it by subtraction of the tared weight of the tube. The exact quantity of polymer in solution in then determined by subtraction of the quantity stayed in the first tube. to get the amount of polymer which stayed stuck in the first tube.

NTA analysis

NTA measurements were obtained from NanoSight NS300, at 25°C, with a 405 nm laser (Blue405 laser). Video tracking of the samples was captured with a sCMOS camera, fixed at level 16, and treated by NanoSight software NTA 3.2 Dev Build 3.2.16. Each measurement is based on three 30s video. The final concentration has to be between 10^6 and 10^9 NPs/mL and around 50 NPs/frame to give accurate results. Samples are diluted from 1/100 to 1/2.

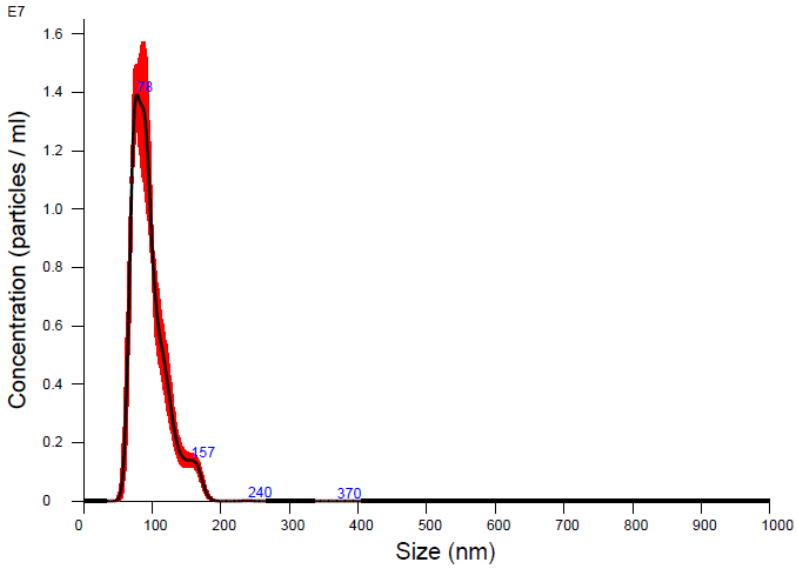

Figure 29. NTA measurment of ***$NP_{352\text{-}A}$*** *in water, diluted at 1/10.*

DLS and zeta potential analysis

The DLS measurement recorded on VASCO™ nanoparticle size and Zetasizer NanoZS. In both case analyses were performed at 25°C with 1mL of sample with a 657 nm laser. For the Zetasizer, a 1mL plastic cuvette was used. Three acquisitions of one minute per sample was captured to yield an average and standard deviation. A blank was calculated using the viscosity and reflective index of water. For the zeta potential, electrode cuvettes were used and the results are based on Electrophoretic Light Scattering.

TEM analysis

The TEM images are issued from a TEM 120 kV with various enlargement. Samples were prepared on water then disposed on adapted grid and let dried for at least 4h at room temperature.

Chapter 6

LC/MS analyses

Samples for LC/MS analyses were prepared in an ACN/H_2O (50/50, v/v) mixture containing 0.1% TFA. The LC/MS system consisted of a Waters Alliance 2695 HPLC coupled to a Water Micromass ZQ spectrometer (electrospray ionization mode, ESI+).

Analysis of non-silylated compounds were carried out by HPLC using a Phenomenex Onyx, 25 x 4.6 mm reversed-phase column. A flow rate of 3 mL/min and a gradient of (0-100)% B over 2.5 min were used. Eluent A: water/0.1% HCO2H; eluent B: acetonitrile/0.1% HCO2H.

Analysis of silylated compounds were carried out by HPLC using a PLRP-S®, 25 x 4.6 mm reversed-phase column. A flow rate of 3 mL/min and a gradient of (5-100)% B over 9 min were used. Eluent A: water/0.1% HCO_2H; eluent B: acetonitrile/0.1% HCO_2H.

UV detection was performed at 214 nm. Electrospray mass spectra were acquired at a solvent flow rate of 200 µL/min. Nitrogen was used for both the nebulizing and drying gas. The data were obtained in a scan mode ranging from 100 to 1000 m/z or 250 to 1500 m/z to in 0.7 sec intervals. All measurements were performed in the positive ion mode.

NMR analyses

^{1}H and ^{29}Si NMR spectra were recorded at room temperature in deuterated solvents on a Bruker AMX/400 spectrometer operating at 500 and 79 MHz respectively. Chemical shifts (δ) are reported in parts per million using residual non-deuterated solvents as internal references ($CHCl_3$ in $CDCl_3$, δH = 7.26 ppm)

^{29}Si NMR spectrum of all the polymer synthesized was conducted on a 400MHz Bruker NMR spectrometer. The samples were prepared in CDCl3 (50 mg/mL) at r.t.

^{1}H NMR spectrum of all the polymer synthesized have been operated on a 500 MHz Bruker NMR spectrometer. All samples were prepared in $CDCl_3$ (30 mg/mL) at r.t.

^{19}F NMR quantification by ERETIC method have been operated on a 400MHz Bruker NMR spectrometer. The sample were prepared in $CDCl_3$ (10mg/mL) at r.t.

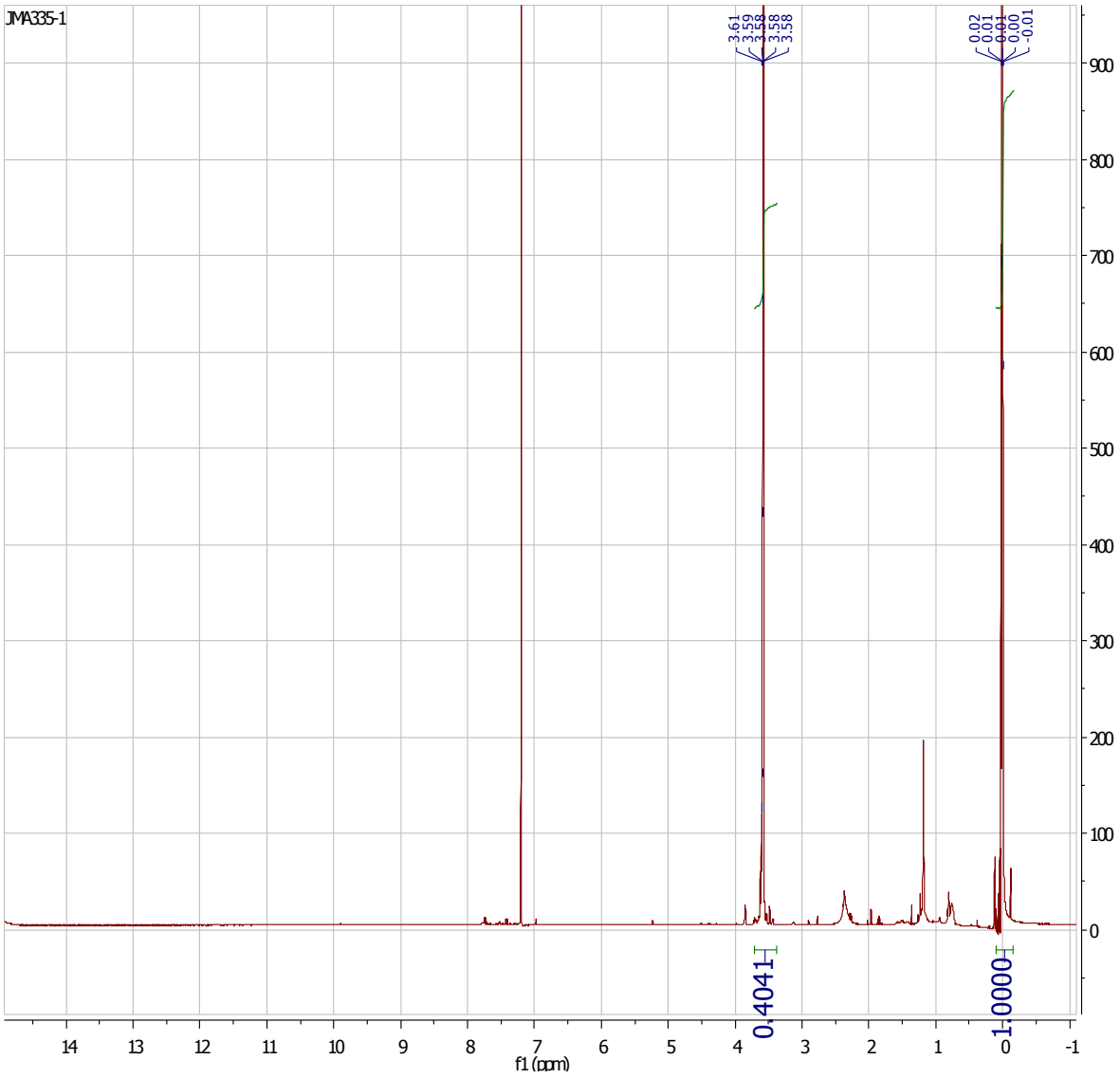

Figure 30. ^{1}H NMR spectrum and quantification of PEG chain by integration comparison of $P_{335\text{-}A}$.

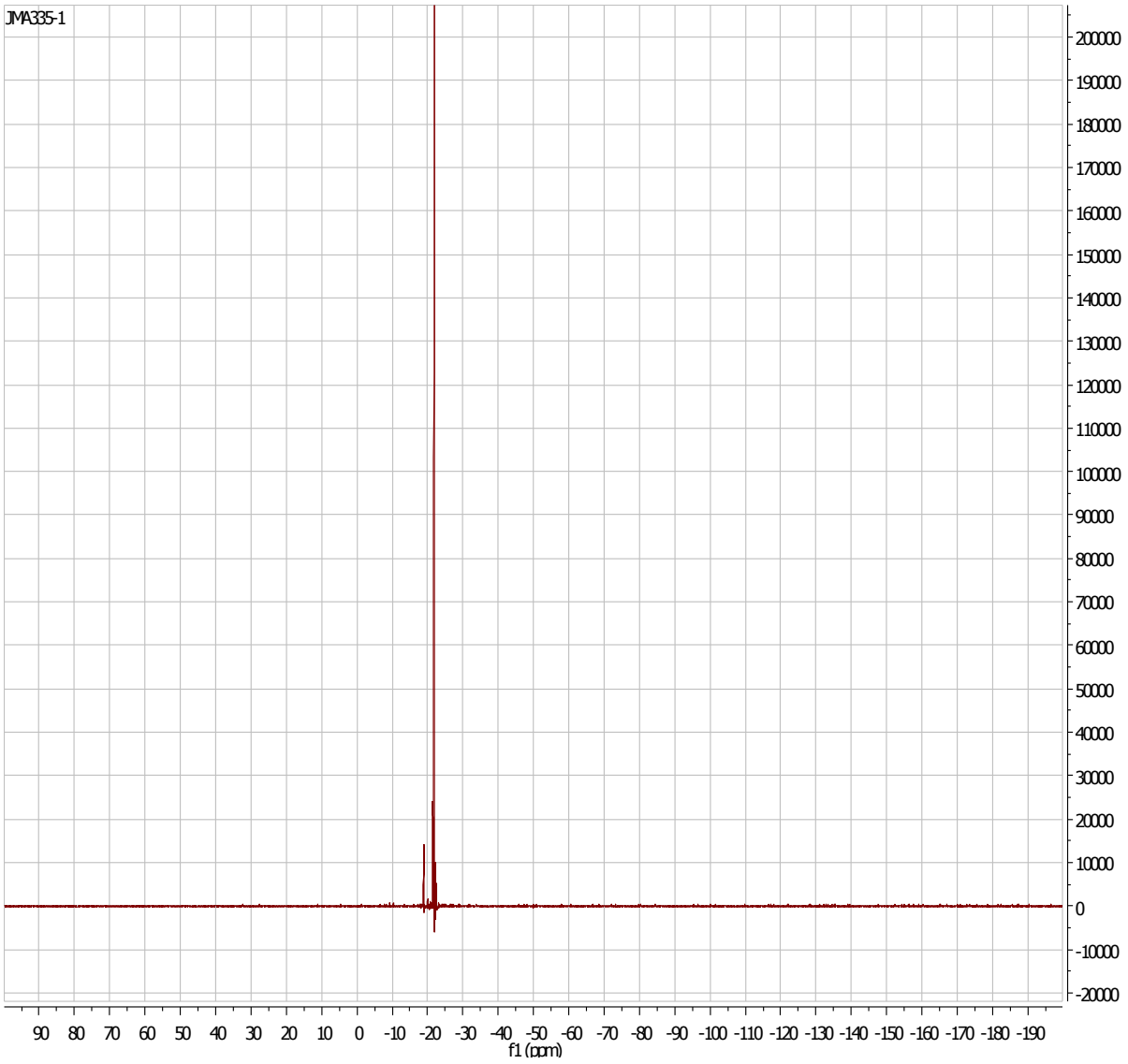

Figure 31. ^{29}Si NMR spectrum of $\boldsymbol{P_{335\text{-}A}}$

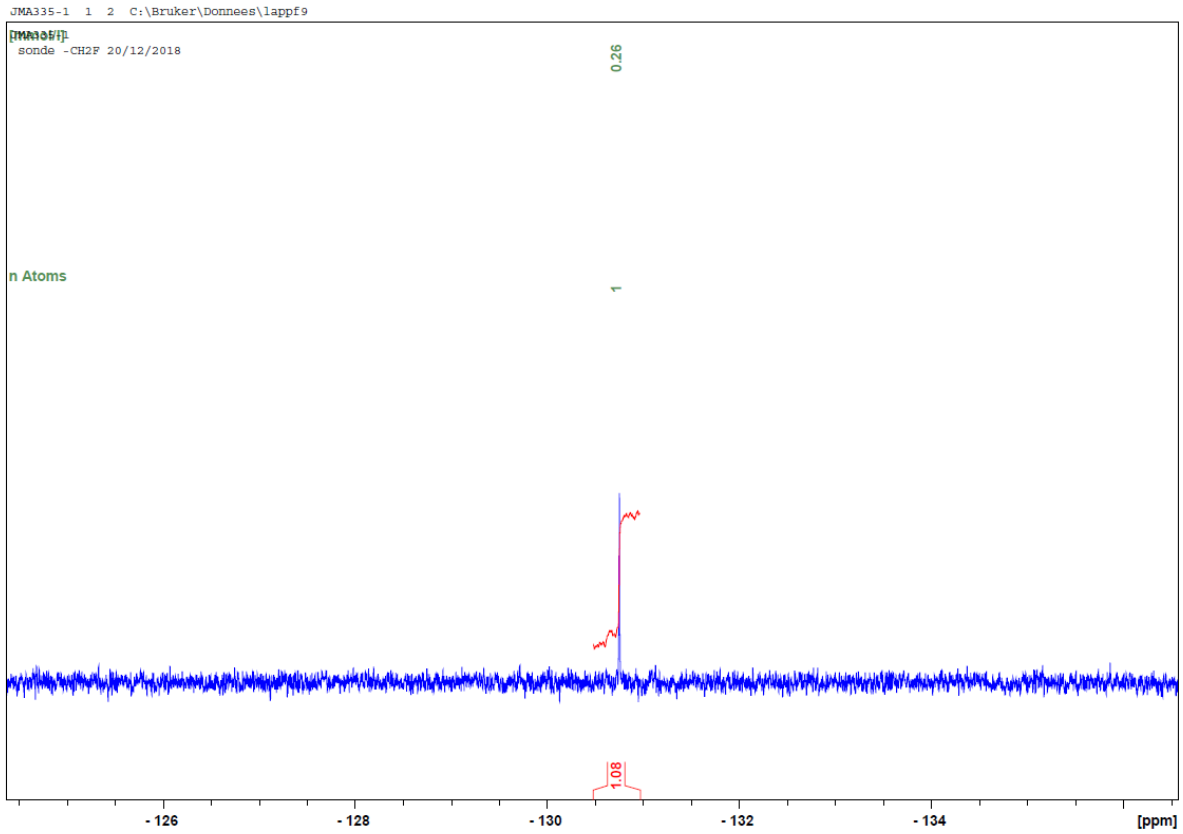

Figure 32. ^{19}F NMR quantification by ERETIC method of ***$P_{335\text{-}A}$***.

GPC analyses

The molecular weight of the polymer was determined using Gel permeation chromatography (GPC). The analysis was performed on a Waters GPC system consisting of a PLgel Mixed C-5µm-2*300m column, a pump and a UV detector. CHCl3 was used as the eluent at flow rate of 1ml/min at 25°C and samples prepared at 10mg/mL and filtered with PTFE 0.45µm filters.

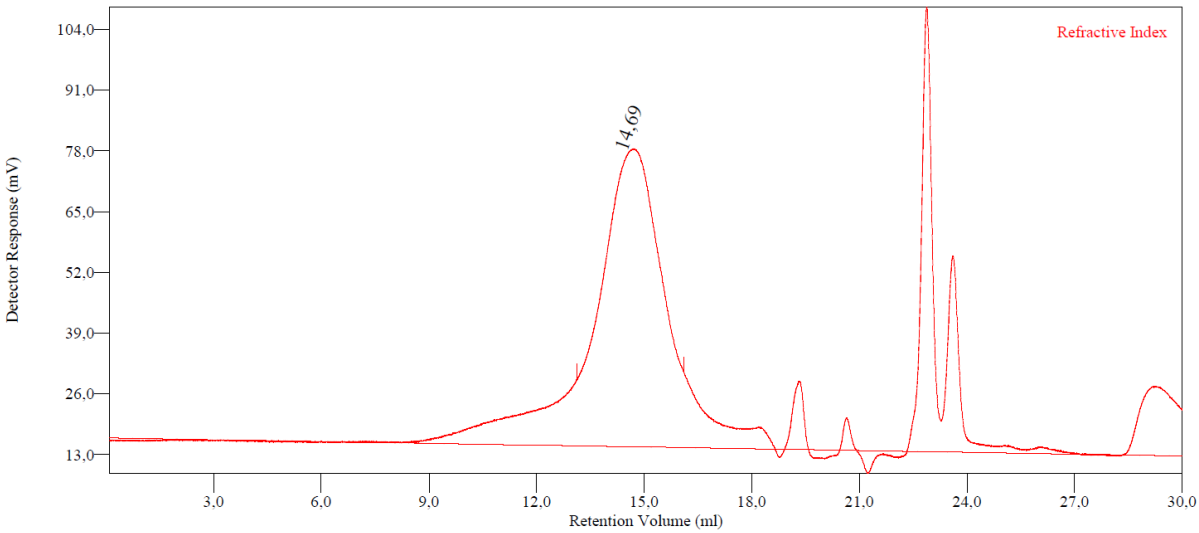

Figure 33.GPC chromatogram of method of ***$P_{335\text{-}A}$***.

Protocol NTA preparation sample

The polymer is precisely weighted between 2 and 5 mg in a tared hemolysis tube. The adapted volume of water is then added in the tube to get a final concentration of 1 mg/mL. Vortex and especially ultrasons are applied in order to get it completely dispersed.

Then, the solution if filtered in a new tared hemolysis tube by a 0.45µm H-PTFE filter. The first hemolysis tube is freeze-dried in the lyophilizator to take away the rest of water. Once dried, it is finally weighted to get the amount of polymer that stayed stuck in it by subtraction of the tared weight of the tube. The exact quantity of polymer in solution in then determined by subtraction of the quantity stayed in the first tube. to get the amount of polymer which stayed stuck in the first tube.

NTA analysis

NTA measurements were obtained from NanoSight NS300, at 25°C, with a 405 nm laser (Blue405 laser). Video tracking of the samples was captured with a sCMOS camera, fixed at level 16, and treated by NanoSight software NTA 3.2 Dev Build 3.2.16. Each measurement is based on three 30s video. The final concentration has to be between 10^6 and 10^9 NPs/mL and around 50 NPs/frame to give accurate results. Samples are diluted from 1/100 to 1/2.

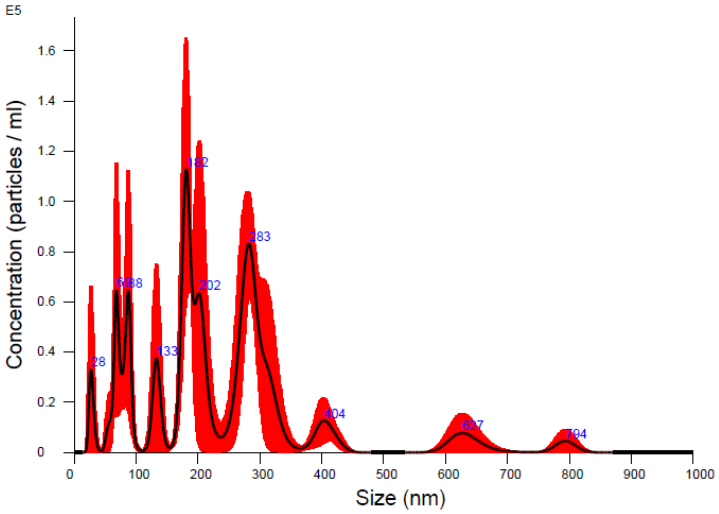

*Figure 34. NTA measurement of **NP$_{428\text{-}20}$**, in water, diluted 1/5.*

DLS and zeta potential analysis

The DLS measurement recorded on VASCO™ nanoparticle size and Zetasizer NanoZS. In both case analyses were performed at 25°C with 1mL of sample with a 657 nm laser. For the Zetasizer, a 1mL plastic cuvette was used. Three acquisitions of one minute per sample was captured to yield an average and standard deviation. A blank was calculated using the viscosity and reflective index of water. For the zeta potential, electrode cuvettes were used and the results are based on Electrophoretic Light Scattering.

TEM analysis

The TEM images are issued from a TEM 120 kV with various enlargement. Samples were prepared on water then disposed on adapted grid and let dried for at least 4h at room temperature.

Gel Retardation Assay

Agarose gel (2 % w/v, (Ultrapure™, Agarose 1000, Invitrogen) was loaded with 10 µL of *in situ* formed and pre-formed complexes in RNase-free water at different si- K_4H_4 peptide/siRNA ratios (N/P 5, 10, 20, and 40) with a fixed amount of siRNA (0,25 µM final concentration). A DNA ladder, composed of double-stranded DNA fragments with known base pairs number was used as a control to verify that the spots observed on the gel correspond to free siRNA. The electrophoresis was performed in a vertical gel electrophoresis apparatus (Invitrogen Novex Mini-Cell system). at 50 V until the migration has been confirmed then decreased to 50 V running for 30 mins. To visualize the SiRNA by UV detection, the agarose gel was stained with 0.05 µL GelRed (Interfine Chemicals) per ml agarose gel. The images were recorded after 160 msec exposure by Vilber Lourmat Infinity Vx2 (Fisher Scientific, Hampton, USA). The signal intensities were quantified after background subtraction using Image J software (gel plotting analysis). Each band intensity is then normalized to the band intensity of the siRNA alone (= 100%): Relative fluorescence (%) = fluorescence intensity (condition x)/fluorescence intensity (siRNA alone) x 100.

Additionally, the loading capacity of siRNA quantitatively determined also by Image J. Normalizing with the highest band intensity and calculated as %siRNA load per polymer weight as:

$$Loading\ Capacity\ \left(\frac{\%}{w}\right) = \frac{(100 - \ siRNA\ \%\ intensity\ by\ gel\ electrophoresis\ quantification)}{Polymer\ weight}$$

Stability: Polyanion competition assay

To evaluate the stability of the polyplex, si- K_4H_4 peptide: siRNA and control complexes (complexes with $Si(Me)_3$ -silylated K_4H_4 peptide) were prepared at N/P ratio of 20 and measured using a polyanion competition assay as previously described (41). Heparin (sodium salt, Sigma-Aldrich) was added at the corresponding molar equivalents (0.1, 0.5, 1, 2, 5 or 10 eq.) of the siRNA concentration, mixed and incubated further 10 mins at room temperature. Ten microliters of each sample, corresponding to 0,25 µM ofsiRNA, was then analyzed by electrophoresis on agarose gel (2% wt/vol) as previously described. As a control, $Si(Me)_3$- silylated K_4H_4 peptide was used to determine the stability in the case of non-complexation.

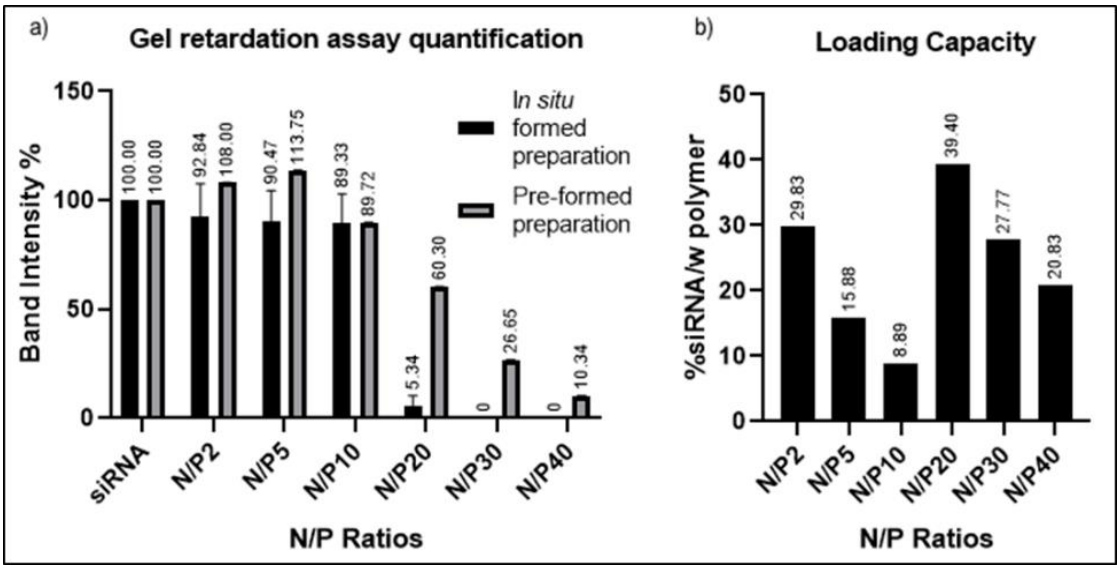

Figure 35. Quantification of siRNA bands on agarose gel retardation assay (n=3) b) Loading capacity based on quantification of band intensity.

Abstract:

The purpose of this PhD work was the design and synthesis of new hybrid biomaterials based on a polysiloxane backbone. To do so, several biomolecules were silylated, in order to be incorporated in a multifunctional silicone backbone by a bottom-up strategy. Indeed, in contrast to post-grafting approaches, we set up the direct copolymerization of hybrid biomolecule macromonomers presenting a methyldihydroxysilyl moiety, with the dichlorodimethylsilane (DCDMS). Different types of biomolecules have been silylated: peptides, drugs and imaging probes, each of them affording specific properties to the final bioorganic silicone material. Three main applications are described: (i) the design and synthesis of bioactive PDMS cross-linked materials, (ii) silicone-based nanoparticules (NPs) and (iii) silicone-based polyplexes. PDMS materials with biological properties, either antimicrobial or cell adhesion, were obtained by copolymerization of hybrid peptide macromonomer with DCDMS, vinyl and silane reagents followed by hydrosilylation. Silicone-based NPs resulted from the introduction of several hydrophilic macromonomers at 0.5 to 1 mol% compared to DCDMS. Hybrid peptide ligands targeting cancer cell receptors, PEG and a drug model (Methotrexate) were prepared and copolymerized. At last, we investigated the preparation of siRNA polyplexes involving LysHis-based hybrid peptide macromonomers by an in situ polymerization method.

Key words: peptides, hybrid macromonomers, sol-gel, PDMS, nanoparticles, polyplexes

Résumé :

Les travaux de recherches de cette thèse concernent la conception et la synthèse de nouveaux matériaux hybrides basés sur un squelette polysiloxane. Pour cela, plusieurs molécules ont été silylées dans le but d'être incorporées dans une chaine de silicone multifonctionnel. En effet, au contraire des approches de post-greffages, nous avons mis au point une copolymérisation directe de ces macromonomères hybrides présentant une fonction methyldihydroxysilane avec du dichlorodimethylsilane (DCDMS). Plusieurs types de biomolécules ont été silylées : peptides, médicaments, sondes pour l'imagerie, chacune de ces molécules apportant des propriétés particulières au matériau final. Trois principales applications sont présentées : (i) la synthèse directe de film de silicone réticulés bioactifs, (ii) la préparation de nanoparticules (NPs) de silicone multifunctionnel (iii) ou des polyplexes. Des films de PDMS bioactifs (antibactériens ou promouvant l'adhésion cellulaire) réticulés ont été obtenus par copolymérisation de macromonomères hybrides peptidiques avec du DCMS et des monomères silane ou vinyl silane permettant une réticulation par hydrosilylation. Les NPs de silicone hybride sont issues de l'introduction de plusieurs macromonomères hydrophiles de 0.5 à 1mol% par rapport au DCDMS. Des ligands peptidiques ciblant les cellules cancéreuses, du PEG et du méthotrexate, tous trois silylés, ont été préparés et copolymérisés. Enfin, nous présentons les résultats préliminaires obtenus pour la préparation de polyplexes de siRNA basés sur la polymérisation in situ de peptides hybrides possédant des séquences riches en histidine et lysine.

Mots clés : peptides, macromonomères hybrides, sol-gel, PDMS, nanoparticules, polyplexes